

Timescales of continental subduction:  
Constraints from ultrahigh-pressure  
metapelites in the Western Gneiss  
Region, Norway

Thesis submitted in accordance with the requirements of the University of Adelaide for  
an Honours Degree in Geology

Samantha Nicole March  
November 2020



THE UNIVERSITY  
*of* ADELAIDE

## **TIMESCALES OF CONTINENTAL SUBDUCTION: CONSTRAINTS FROM ULTRAHIGH-PRESSURE METAPELITES IN THE WESTERN GNEISS REGION, NORWAY**

### **ULTRAHIGH-PRESSURE METAPELITES IN THE WGR**

#### **ABSTRACT**

The Western Gneiss Region (WGR), Norway is an archetypal continental ultrahigh-pressure (U)HP terrane with an extensive metamorphic history, recording the subduction and subsequent exhumation of continental crust to depths exceeding 120 km. The vast bulk of past work within the WGR has focused on mafic eclogites. In this study, data from rare garnet-kyanite metapelites in (UHP) domains of the WGR is presented. U–Pb geochronology and trace element compositions in zircon, monazite, apatite and rutile were acquired, and  $P$ – $T$  conditions were calculated by mineral equilibria forward modelling and Zr-in-rutile thermometry. The Ulsteinvik metapelite prograde path traverses through ~600–710 °C and ~11–14 kbar. Minimum peak conditions are ~750 °C and ~2.9 GPa in an inferred garnet-kyanite-coesite-omphacite-muscovite-rutile-quartz-H<sub>2</sub>O assemblage. Plagioclase-biotite-quartz intergrowths developed after omphacite-phengite-rutile breakdown on the early retrograde path, followed by cordierite-spinel-plagioclase symplectites after garnet-kyanite-biotite, defining a retrograde  $P$ – $T$  point at ~740 °C and ~7 kbar. Late Ordovician-Early Silurian (~470–440 Ma) zircon and rutile age data in Ulsteinvik pre-dates the major Scandian UHP subduction episode in the WGR, interpreted as recording early Caledonian subduction within the Blåhø nappe. Monazite and apatite U–Pb geochronology and trace element data suggest exhumation occurred at ~400 Ma. The Fjørtoft metapelite is a constituent of the Blåhø nappe. Minimum peak  $P$ – $T$  conditions are ~1.8 GPa and ~750 °C, with poor peak mineral fidelity attributed to extensive retrograde deformation. Negative Eu anomalies in ~423 Ma monazite suggest retrograde conditions were reached by ~423 Ma. Ulsteinvik and Fjørtoft may have experienced pre-Scandian subduction together within the Blåhø nappe but record dissimilar histories after this. Two potential scenarios are presented: (1) Ulsteinvik resided within the mantle for 20 million-years longer than Fjørtoft during Scandian subduction, or (2), the samples were exhumed at different times during pre-Scandian subduction of the Blåhø nappe.

#### **KEYWORDS**

Metapelite, subduction, ultrahigh-pressure, Western Gneiss Region, U–Pb geochronology,  $P$ – $T$  pseudosection

## TABLE OF CONTENTS

Timescales of continental subduction: constraints from ultrahigh-pressure metapelites in the Western Gneiss Region, Norway.....	i
Ultrahigh-pressure metapelites in the WGR.....	i
Abstract.....	i
Keywords.....	i
List of Figures and Tables .....	3
Introduction .....	4
Geological Background .....	7
Overview of the Western Gneiss Region .....	7
Metamorphism of the Western Gneiss Region.....	9
Past geochronological work in Nordøyane and Sørøyane.....	12
Samples.....	12
Methods .....	18
Whole-rock geochemistry.....	18
Electron Probe Micro Analyses (EPMA) .....	18
LA–ICP–MS: Geochronology.....	19
LA–ICP–MS: Trace elements .....	20
Mineral equilibria forward modelling .....	20
Results .....	21
Petrography.....	21
WGC2019J-25B .....	21
WGC2019J-31A.....	22
Mineral chemistry.....	23
Garnet .....	23
Plagioclase.....	25
K-Feldspar .....	25
Spinel.....	25
Biotite .....	25
Cordierite.....	27
Ilmenite.....	27
Zircon U–Pb geochronology and trace elements.....	27
WGC2019J-25B .....	28
WGC2019J-31A.....	31
Monazite U–Pb geochronology and trace elements .....	31

WGC2019J-25B & WGC2019A-3.....	32
WGC2019J-31A .....	32
Apatite U–Pb geochronology and trace elements.....	36
WGC2019J-25B & WGC2019A-3.....	36
Rutile U–Pb geochronology .....	38
WGC2019J-25B .....	38
WGC2019J-31A.....	39
Zr-in-rutile thermometry.....	39
Mineral equilibria forward modelling .....	40
WGC2019J-25B .....	40
WGC2019J-31A .....	43
Discussion.....	45
Interpretation of U–Pb geochronology and trace elements .....	45
Pressure–temperature conditions during metamorphism .....	50
Tectonic implications for the Caledonian evolution of the Western Gneiss Region.....	53
Conclusion.....	56
Acknowledgments .....	57
References .....	58
Appendix 1: Whole-rock geochemistry.....	67
Appendix 2: Extended EPMA methods and results .....	68
Appendix 3A: Extended LA–ICP–MS methods .....	73
Appendix 3B: LA–ICP–MS garnet results.....	78
Appendix 3C: LA–ICP–MS zircon results.....	92
Appendix 3C: LA–ICP–MS monazite results .....	198
Appendix 3D: LA–ICP–MS apatite results .....	235
Appendix 3E: LA–ICP–MS rutile results.....	258
Appendix 3F: LA–ICP–MS biotite and k-feldspar results .....	268
Appendix 4A: Extended mineral equilibria forward modelling methods .....	271
Appendix 4B: Extended mineral equilibria forward modelling results.....	273



## LIST OF FIGURES AND TABLES

Figure 1: Geologic map of the Western Gneiss Region, Norway. ....	6
Figure 2: Field photos from sample locations. ....	11
Figure 3: Photomicrographs from this study. ....	22
Figure 4: Garnet EPMA and LA–ICP–MS elemental maps and traverse data. ....	26
Figure 5: EPMA elemental maps for WGC2019J-25B reaction textures. ....	27
Figure 6: Zircon SEM-CL metamorphic zoning. ....	28
Figure 7: Zircon concordia plots and cumulative probability distribution plots. ....	29
Figure 8: Zircon REE spiderplots. ....	30
Figure 9: Monazite concordia plots. ....	33
Figure 10: Monazite thin section scan and cumulative probability distribution plot. ....	34
Figure 11: Monazite REE spiderplots. ....	35
Figure 12: Apatite concordia plot and REE spiderplot. ....	37
Figure 13: Rutile concordia plot and cumulative probability distribution plot. ....	38
Figure 14: Zr-in-rutile temperature vs. $^{238}\text{U}/^{206}\text{Pb}$ age plot. ....	40
Figure 15: WGC2019J-25B $P$ – $T$ pseudosection r. ....	42
Figure 16: WGC2019J-31A $P$ – $T$ pseudosection. ....	44
Figure 17: WGC2019J-25B phase diagram coloured by computed garnet mode. ....	52
Figure 18: Annotated summary of Ulsteinvik and Fjortoft age data. ....	55
Table 1: Summary of the metamorphic deformation events experienced in the Western Gneiss Region. ....	9
Table 2: Geochronological summary of Caledonian ages from Nordøyane. ....	13
Table 3: Geochronological summary of Caledonian ages from Sørøyane. ....	16
Table 4: EPMA operating conditions. ....	18
Table 5: LA–ICP–MS operating conditions. ....	19
Table 6: Summary of mineral chemistry. ....	24
Table 7: Average Zr-in-rutile temperatures. ....	39

## INTRODUCTION

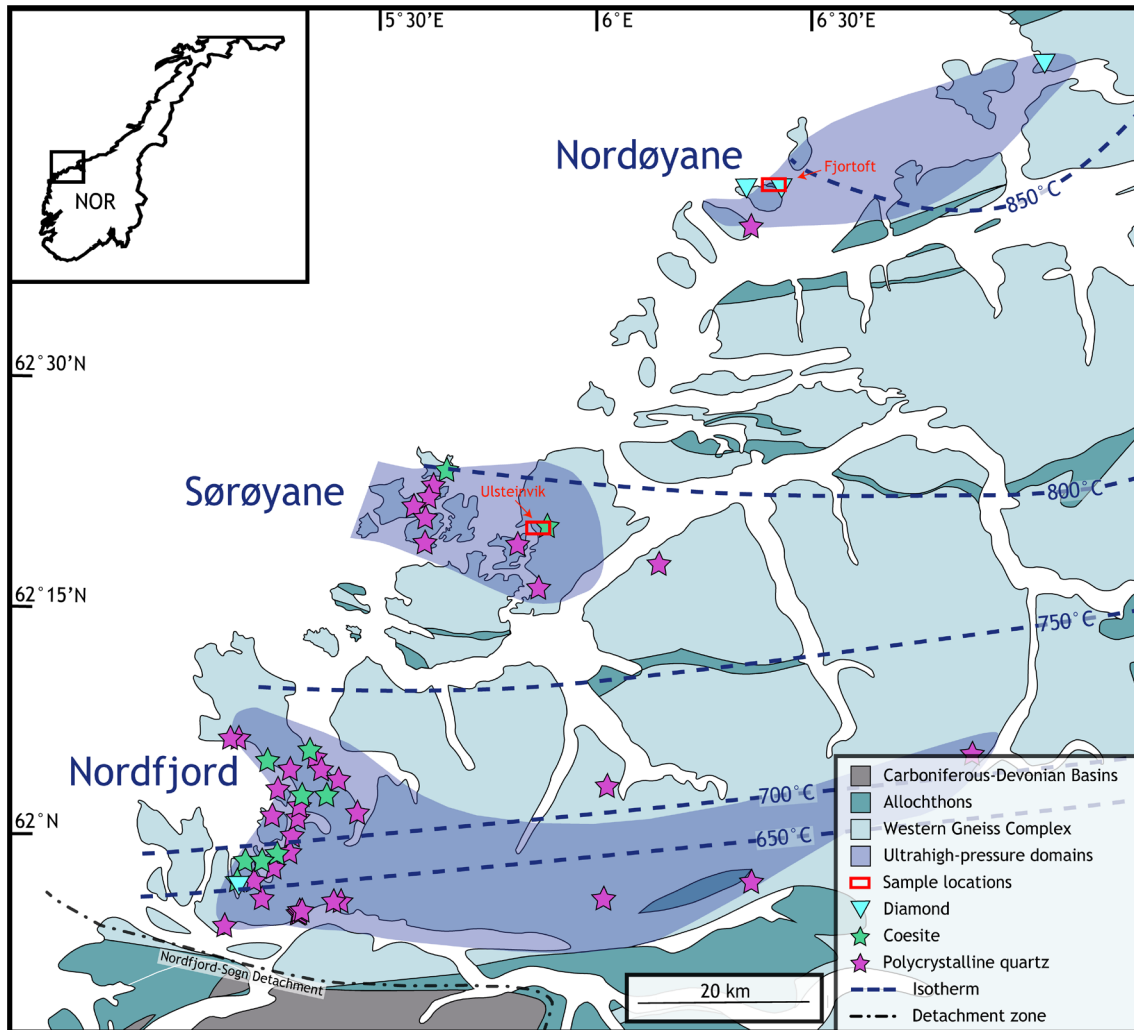
The sensitivity of metamorphic mineral assemblages to pressure-temperature ( $P$ - $T$ ) changes within the Earth make them an ideal proxy for inferring past conditions (e.g. Brown & Johnson, 2018). When coupled with robust geochronological constraints, metamorphic rocks form the foundation for decoding the evolution of underlying geodynamic processes (e.g. Kornprobst, 2002; Brown, 2014; Lanari et al., 2019). Continental collision is one of the most dramatic and visible manifestations of plate tectonics on Earth, comprising a fundamental role in the evolution of modern continents (e.g. Batt & Braun, 1999; Nance & Murphy, 2013). The relative buoyancy of continental crust compared to oceanic crust allows subducted continental ultrahigh-pressure (UHP) terranes to be more frequently exhumed than subducted oceanic slabs (e.g. Ernst et al., 1997; Hacker et al., 2011). Thus, exhumed continental crust can provide valuable insight into UHP geodynamic processes, where UHP metamorphism refers to crustal rocks that have been subject to pressures high enough ( $> 2.8$  GPa) to stabilise coesite (the UHP polymorph of quartz) and/or diamond (Chopin, 1984; Smith, 1984; Sobolev & Shatsky, 1990).

The Western Gneiss Region (WGR) preserves one of the best examples of continental subduction known, as it not only experienced the burial of continental lithosphere to mantle depths in excess of 120 km, but over 30,000 km<sup>2</sup> of the subducted continental crust was also subsequently exhumed (Walsh & Hacker, 2004; Hacker, 2007; Hacker et al., 2010; Walsh et al., 2013). Consequently, the WGR is among the largest, best-exposed, and most-studied UHP terranes in the world (Terry et al., 2000a; Root et al., 2005; Kylander-Clark et al., 2007; DesOrmeau et al., 2015). It provides the unique opportunity to investigate the timescales of deep continental burial and exhumation, as

well as the structural processes associated with UHP metamorphism (Roberts, 2002; Butler et al., 2018; Cutts et al., 2019).

The identification of coesite, microdiamond and polycrystalline quartz grains (after coesite) within mafic eclogites (Dobrzhinetskaya et al., 1995; Cuthbert et al., 2000; van Roermund et al., 2002) has aided in defining three distinct UHP domains within the WGR; Nordøyane, Sørøyane and Nordfjord (Fig. 1; Root et al., 2005).  $P$ - $T$  conditions increase north-westwards within these domains (Cuthbert et al., 2000), indicative of the past coherence of Nordøyane, Sørøyane and Nordfjord and their oblique subduction (E. J. Krogh, 1977; Griffin & Brueckner, 1985; Cuthbert et al., 2000; Carswell & Cuthbert, 2003; Carswell et al., 2006; Hacker et al., 2010). UHP domains are dominated by quartzofeldspathic host gneiss with minor amounts of quartzite, marble, calc-silicate, anorthosite, gabbro, peridotite and metapelitic gneiss (Gjelsvik, 1951; Bryhni, 1966; Dransfield, 1994; Robinson, 1995).

There has been a large amount of work focused on understanding the timing and subduction behaviour of continental crust within the WGR and its associated  $P$ - $T$  conditions, the vast bulk of which has concentrated on the mafic eclogites of the region (Griffin & Brueckner, 1985; Cuthbert et al., 2000; Carswell et al., 2003; Kylander-Clark et al., 2007; T. E. Krogh et al., 2011; Corfu et al., 2013; Beckman et al., 2014).  $P$ - $T$  analysis on the eclogite facies rocks have relied on techniques such as inverse thermobarometry, and the presence of diagnostic minerals such as coesite and diamond to constrain  $P$ - $T$  conditions (Wain, 1997; Terry et al., 2000b; Carswell et al., 2003; Vrijmoed et al., 2006; Vrijmoed et al., 2008; Smith & Godard, 2013; Walczak et al., 2019). Contrary to mafic eclogites, the volumetrically minor metapelites of the WGR have received little attention in past studies, with the minor research that has been



**Figure 1: Geologic map of the Western Gneiss Region, Norway, highlighting UHP terranes and sample locations, modified from Walsh et al. (2013). Coesite and polycrystalline quartz locations from Wain et al. (1997), Cuthbert et al. (2000), Carswell et al. (2003), Root et al. (2005) and Spengler et al. (2006), where polycrystalline quartz aggregates are interpreted to indicate the former presence of coesite. Diamond locations from Dobrzhinetskaya et al. (1995), van Roermund et al. (2002), Vrijmoed et al. (2008) and Smith and Godard (2013). Isotherms from Kylander-Clark et al. (2008).**

undertaken primarily being focused on geochronology (Terry et al., 2000b; Cuthbert & van Roermund, 2011; Hacker et al., 2015; Holder et al., 2015; Walczak et al., 2019).

Metapelitic rocks typically contain higher concentrations of U and Th and can therefore provide greater potential to correlate evolving mineral assemblages with geochronological data.

Improving the current understanding for the  $P$ - $T$ - $time$  history of the WGR facilitates comparison with previously calculated geodynamic numerical simulations of

continental subduction and exhumation (e.g. Sizova et al., 2019). Sizova et al. (2019), predicts that continental material will take ~10 million-years (Myr) to enter a subduction zone and reach peak UHP conditions. Metapelitic rocks are an ideal proxy to explore this modelled evolution, due to their progressive growth of useful geochronometers such as zircon and monazite that may track the prograde and retrograde history.

The aim of this study is to undertake  $P$ – $T$  forward modelling coupled with U–Pb multi-mineral geochronology in metapelitic rocks from the WGR. By using minerals from different textural locations, a thermal system can effectively be tracked. The results from this study will improve the current understanding for  $P$ – $T$  paths associated with continental subduction and subsequent exhumation. Samples are derived from two key localities: (a) a newly discovered set of metapelitic outcrops in close proximity to the renowned Hareidland eclogite in Ulsteinvik (Mysen & Heier, 1972; Carswell et al., 2003), and (b) a diamond-bearing outcrop on the island of Fjørtoft (Fig. 1; Dobrzhinetskaya et al., 1995; van Roermund et al., 2002; Cuthbert & van Roermund, 2011).

## **GEOLOGICAL BACKGROUND**

### **Overview of the Western Gneiss Region**

The Western Gneiss Region consists of an autochthonous polymetamorphic terrane, referred to as the Western Gneiss Complex (WGC), overlain by a series of oceanic and continental-derived allochthons. The WGC is dominated by granodioritic-tonalitic intrusive rocks that formed during the Gothian Orogeny, from ca. 1700–1500 Ga (Åhäll & Connelly, 2008). The Sveconorwegian Orogeny (ca. 1100–900 Ma) imparted a

granulite-facies overprint over the WGC, and was accompanied by migmatitisation, plutonism and mafic dyke emplacement (Brueckner, 1972; Tucker et al., 2004; Kylander-Clark et al., 2008; Corfu et al., 2013).

The Caledonian Orogeny spanned from ca. 480–380 Ma, with early deformation, metamorphism, and juxtaposition of continental and oceanic allochthons. The final phase of the Caledonian Orogeny is termed the Scandian Orogeny (~430–380 Ma).

During the terminal Scandian collision: (1) the Iapetus Ocean closed and allochthonous terranes were thrust over the autochthonous Baltican basement from ca. 430–415 Ma (Gee, 1975; Roberts, 2003; Hacker & Gans, 2005); (2) the Baltican basement and portions of overlying allochthons beneath Laurentia experienced westward subduction to UHP depths (Griffin & Brueckner, 1980; Andersen et al., 1998; Terry et al., 2000b; Root et al., 2005; Kylander-Clark et al., 2009; T. E. Krogh et al., 2011); and then (3), near-isothermal exhumation to shallow crustal levels from ca. 400–385 Ma (Andersen et al., 1998; Terry et al., 2000b; Tucker et al., 2004; Hacker, 2007; Walsh et al., 2007).

A two-stage exhumation is suggested for the UHP rocks of the WGR: (1) rapid buoyancy-driven exhumation from the mantle to crustal depths (e.g. Andersen et al., 1991); and (2) a slower period of crustal exhumation related to extension (Walsh et al., 2013).

The Scandian Laurentia-Baltica collision and exhumation resulted in the exposure of high-pressure (HP) and UHP terranes across the WGR. The spatial distribution of coesite-bearing eclogites and  $^{40}\text{Ar}/^{39}\text{Ar}$  ages have been used to conclude that these UHP terranes (Fig. 1) outcrop in three east-southeast plunging antiforms along the west coast; Nordfjord, Sørøyane and Nordøyane (Root et al., 2005). The WGR is structurally

imbricated by discontinuous remnants of Caledonian thrust nappes, for example, the Seve-Blåhø nappe (e.g. Terry et al., 2000b).

### Metamorphism of the Western Gneiss Region

Incomplete overprinting reactions have allowed the sequence of metamorphic events in the WGR to be relatively well constrained (Bryhni & Andréasson, 1985). The Sveconorwegian amphibolite- to granulite-facies metamorphism was associated with peak conditions of ~800–900 °C and 1.0 GPa. (Tucker et al., 1990; Corfu & Andersen, 2002; Root et al., 2005)

Relicts of this event within the WGC are rare but tend to be more prevalent within allochthons that were thrust over the Baltican basement during the early stages of the Caledonian Orogeny (Jolivet et al., 2005). Low H<sub>2</sub>O contents, coarse grain size and limited deformation have been attributed to the sporadic preservation of these granulite-facies assemblages during the subsequent Caledonian Orogeny (Austrheim, 1987; Krabbendam et al., 2000). Pre-Scandian Caledonian metamorphism potentially involved multiple episodes of amphibolite facies metamorphism, with peak conditions of ~725 °C and 1.2 GPa recorded in overlying allochthons of the WGR (Gee, 1975; Hacker &

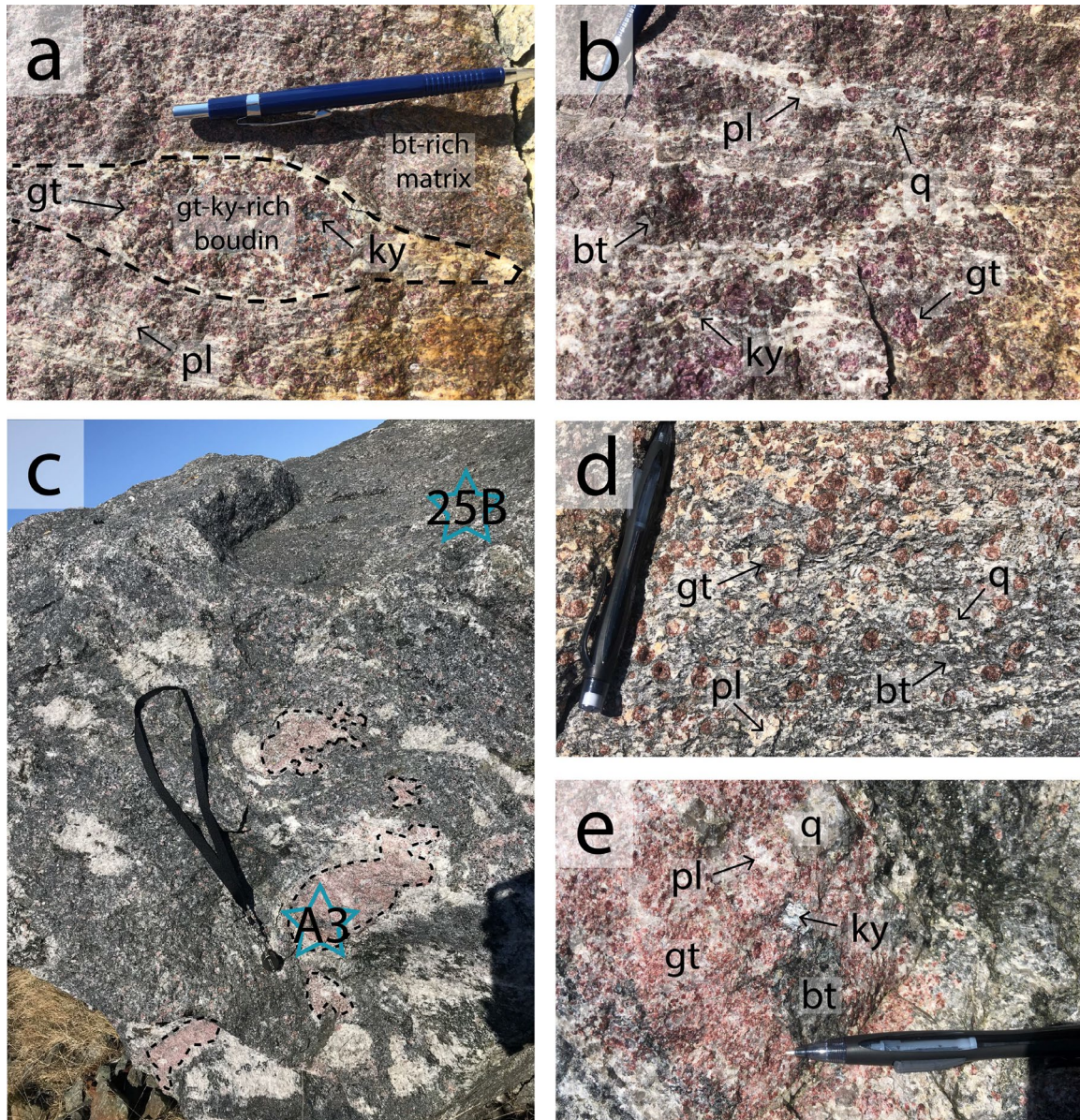
**Table 1: Summary of the metamorphic deformation events experienced in the Western Gneiss Region. Modified from Hacker et al. (2010).**

Event		Timing (Ma)	Pressure (Gpa)	Temperature (°C)	
Caledonian Orogeny	Scandian Orogeny	Amphibolite-facies overprint	400–380	0.5–1.5	650–800
		Baltica-Laurentia HP-UHP event	430–400	1.8–3.6	600–750
	Early Caledonian allochthonous events	480–430	1.2	725	
	Sveconorwegian granulite-facies event	~1100–900	1	900	
	Gothian Orogeny	~1700–1500			

Gans, 2005). This phase of the Caledonian Orogeny has not been recorded within the WGC basement. Scandian subduction of the Baltican margin beneath Laurentia resulted in widespread HP-UHP metamorphism, evidenced by the presence of mantle peridotites, eclogites and eclogite-facies metagabbros (Wain, 1997; van Roermund & Drury, 1998; Cuthbert et al., 2000). Eclogites from these regions record  $P$ - $T$  conditions of 1.5–3.9 GPa and 600–820 °C, with an overall northwestward increasing  $P$ - $T$  gradient (Wain, 1997; Cuthbert et al., 2000; Labrousse et al., 2004; Root et al., 2005; Carswell et al., 2006; Young et al., 2007; Hacker et al., 2010; Butler, 2013). Nordfjord records the transition between HP quartz eclogites (~600 °C and 2.4 GPa) and UHP coesite- and microdiamond-bearing eclogites (750 °C and >3.5 GPa; Cuthbert et al., 2000; Young et al., 2007; Smith & Godard, 2013). Sørøyane, the UHP domain where Ulsteinvik samples are sourced from, yields peak conditions of 795 °C and 3.2 GPa (Carswell et al., 2003; Root et al., 2004). Nordøyane records the maximum  $P$ - $T$  conditions across the WGR, with eclogites and microdiamond-bearing paragneiss recording peak conditions of 820–850 °C and 3.8–3.9 GPa (Terry et al., 2000b; Carswell et al., 2006). Fjørtoft exists in the northern region of this UHP terrane and records some of the highest peak  $P$ - $T$  conditions in the WGR. The late Scandian exhumation and decompression of the WGR imparted a pervasive amphibolite-facies overprint and local partial melting. Peak conditions during this event reached 650–800 °C and 0.5–1.5 GPa, almost completely destroying the past record of UHP metamorphism (e.g. Dransfield, 1994; Labrousse et al., 2004; Walsh & Hacker, 2004; Root et al., 2005). The WGR was exhumed almost isothermally to depths of ~15–20 km during this period, causing some regions to undergo partial melting (Tucker et al., 2004; Kylander-Clark et al., 2008). The second stage of exhumation and cooling was slow and parts of the WGR are



thought to have remained above the closure temperature of rutile (~600 °C) until as late as ca. 375 Ma (Butler et al., 2018).



**Figure 2: Field photos from sample locations. (a) Fjærtøft WGC2019J-30 garnet-kyanite-plagioclase rich boudin (dashed line) surrounded by a garnet-kyanite-biotite-plagioclase bearing matrix. (b) Fjærtøft WGC2019J-31C garnet-kyanite metapelite with felsic interlayers of plagioclase, suggesting partial melting. (c) Ulsteinvik WGC2019J-25B, WGC2019A-3 outcrop, showing garnet-rich patches (dashed line) with kyanite and quartz. Biotite-bearing gneiss encloses the garnet-bearing patches. (d) Ulsteinvik WGC2019A-25B: detailed view of garnet-plagioclase-biotite-bearing gneiss. (e) Ulsteinvik WGC2019A-3: detailed view of garnet-rich patches. Annotations: gt = garnet, ky = kyanite, pl = plagioclase, bt = biotite, q = quartz.**

### **Past geochronological work in Nordøyane and Sørøyane**

Over the past ~40 years, there have been numerous studies focused on constraining the evolution of the WGR. Past geochronological work for the Nordøyane and Sørøyane UHP terranes are summarised below and in Tables 2 and 3. A more extensive interpretation of age data can be found in DesOrmeau et al. (2015).

### **Samples**

Sample WGC2019J-31A was collected from an allochthonous terrane called the Seve-Blåhø nappe on the island of Fjørtoft (32V 368303 6956199, WGS 84 UTM). Samples WGC2019J-25B and WGC2019A-3 are collected from the same outcrop in Ulsteinvik (32V 335031 6916093, WGS 84 UTM), proximal to the UHP Hareidland eclogite, a sheet-like body with an area of ~4 km<sup>2</sup> (Mysen & Heier, 1972). Both samples are garnet-kyanite metapelitic gneisses (Fig. 2).

Age	Method	Location	Rock type	Notes
374 ± 1 Ma	Single-grain isotope dilution-thermal ionization mass spectrometry (ID-TIMS) rutile <sup>206</sup> Pb/ <sup>238</sup> U age	Flem Gabbro	Gabbro pegmatite	(Krogh et al., 2011)
374.6 ± 2.7 Ma	EPMA monazite mean-chemical <sup>206</sup> Pb/ <sup>238</sup> U age	Fjørtoft	Kyanite-garnet mylonite	(Terry et al., 2000b)
374.9 ± 3.7 Ma	Laser-ablation inductively-coupled-plasma mass-spectrometry (LA-ICP-MS) rutile <sup>206</sup> Pb/ <sup>238</sup> U weighted mean age	Otrøy	Eclogite	(Cutts et al., 2019)
376 ± 2 Ma	Chemical abrasion TIMS titanite single concordant <sup>206</sup> Pb/ <sup>238</sup> U age	Harøya	Migmatitic gneiss	(Butler et al., 2018)
377 ± 1 Ma	ID-TIMS rutile <sup>206</sup> Pb/ <sup>238</sup> U age	Flem Gabbro	Eclogite margin of Flem Gabbro	(Krogh et al., 2011)
377 ± 1.6 Ma	Chemical abrasion TIMS and laser ablation multi-collector inductively coupled mass spectrometry (LA-MC-ICP-MS) rutile <sup>206</sup> Pb/ <sup>238</sup> U ages	Harøya	Migmatite	(Butler et al., 2018)
378 ± 1.6 Ma	Chemical abrasion TIMS and LA-MC-ICP-MS rutile <sup>206</sup> Pb/ <sup>238</sup> U ages	Harøya	Eclogite	(Butler et al., 2018)
379.0 ± 3.8 Ma	LA-ICP-MS rutile <sup>206</sup> Pb/ <sup>238</sup> U weighted mean age	Otrøy	Eclogite	(Cutts et al., 2019)
380.0 ± 2.0 Ma	LA-MC-ICPMS <sup>238</sup> U/ <sup>206</sup> Pb- <sup>207</sup> Pb/ <sup>206</sup> Pb titanite isochron	Otrøy	Migmatitic hornblende-K-feldspar gneiss	(Spencer et al., 2013)
380 ± 14 Ma	Four- and three-point Lu-Hf isochron	Otrøy	UHP eclogite	(Kylander-Clark et al., 2007)
381.0 ± 6.2 Ma	LA-ICP-MS rutile <sup>206</sup> Pb/ <sup>238</sup> U weighted mean age	Fjørtoft	UHP eclogite	(Cutts et al., 2019)
381.3 ± 7.2 Ma	LA-MC-ICPMS <sup>238</sup> U/ <sup>206</sup> Pb- <sup>207</sup> Pb/ <sup>206</sup> Pb titanite isochron	Gossa	Biotite gneiss	(Spencer et al., 2013)
384 ± 11 Ma	Three- and two-point isochron	Remøya	UHP eclogite	(Kylander-Clark et al., 2007)
384.5 ± 7.3 Ma	LA-MC-ICPMS <sup>238</sup> U/ <sup>206</sup> Pb- <sup>207</sup> Pb/ <sup>206</sup> Pb titanite isochron	Otrøy	Hornblende-plagioclase pegmatite	(Spencer et al., 2013)

**Table 2: Geochronological summary of Caledonian ages from Nordøyane.**

<b>385 ± 1 Ma</b>	ID-TIMS titanite $^{206}\text{Pb}/^{238}\text{U}$ age	Flemsøya	Granitic pegmatite	(Krogh et al., 2011)
<b>386 ± 5 Ma</b>	LA-ICP-MS $^{206}\text{Pb}/^{238}\text{U}$ rutile age	Fjørtoft	UHP microdiamond gneiss	(Zack et al., 2011)
<b>388 ± 10 Ma</b>	Three- and two-point isochron	Otrøy	UHP eclogite	(Kylander-Clark et al., 2007)
<b>390 ± 2 Ma</b>	ID-TIMS zircon $^{206}\text{Pb}/^{238}\text{U}$ age	Flemsøya	Granitic pegmatite	(Krogh et al., 2011)
<b>390 ± 12 Ma</b>	LA-MC-ICPMS $^{238}\text{U}/^{206}\text{Pb}$ - $^{207}\text{Pb}/^{206}\text{Pb}$ titanite isochron	Otrøy	Retrogressed eclogite	(Spencer et al., 2013)
<b>392.5 ± 1.1 Ma</b>	Chemical abrasion TIMS titanite $^{206}\text{Pb}/^{238}\text{U}$ age	Otrøy	Leucosome	(Kylander-Clark et al., 2008)
<b>393.4 ± 3.4 Ma</b>	Two-point Sm-Nd isochron	Svartberget	Garnet peridotite body and garnet websterite vein	(Vrijmoed et al., 2008)
<b>ca. 395 Ma</b>	Zircon $^{206}\text{Pb}/^{238}\text{U}$ age	Averøya, Fjørtoft	Pegmatite	(Krogh et al., 2004)
<b>ca. 395–392 Ma</b>	Chemical abrasion TIMS and LA-MC-ICP-MS zircon $^{206}\text{Pb}/^{238}\text{U}$ ages	Harøya	Migmatite hosting eclogite bodies	(Butler et al., 2018)
<b>397.5 ± 4.4 Ma</b>	Electron probe micro analysis (EPMA) monazite mean-chemical $^{206}\text{Pb}/^{238}\text{U}$ age	Fjørtoft	Matrix of UHP microdiamond gneiss	(Terry et al., 2000b)
<b>399.4 ± 2.9 Ma</b>	LA-MC-ICPMS $^{238}\text{U}/^{206}\text{Pb}$ - $^{207}\text{Pb}/^{206}\text{Pb}$ titanite isochron	Gossa	Calc-silicate gneiss	(Spencer et al., 2013)
<b>400 ± 16 Ma</b>	Three-point Sm-Nd isochron	Flemsøya	Eclogite	(Mørk & Mearns, 1986)
<b>402.7 ± 4.6 Ma</b>	Three-point isochron and two-point isochron	Vigra (~20km SW of Nordøyane)	Eclogite	(Kylander-Clark et al., 2007)
<b>405.0 ± 0.9 Ma</b>	ID-TIMS zircon weighted mean $^{206}\text{Pb}/^{238}\text{U}$ age	Midsund Bruk	UHP eclogite	(Krogh et al., 2011)
<b>407 ± 24 Ma</b>	Two-point Sm-Nd isochron	Frei (~45km NE of Nordøyane)	Eclogite	(Mearns, 1986)
<b>407.0 ± 2.1 Ma</b>	EPMA monazite mean-chemical $^{206}\text{Pb}/^{238}\text{U}$ age	Fjørtoft	UHP microdiamond gneiss and mylonite	(Terry et al., 2000b)
<b>408.0 ± 5.6 Ma</b>	EPMA monazite mean-chemical $^{206}\text{Pb}/^{238}\text{U}$ age	Fjørtoft	UHP microdiamond gneiss	Monazite inclusions inside garnet (Terry et al., 2000b).
<b>409 ± 3 Ma</b>	Weighted mean $^{206}\text{Pb}/^{238}\text{U}$ age	Flemsøya	Eclogite margin of Flem Gabbro	(Krogh et al., 2011)
<b>409.6 ± 1.5 Ma</b>	ID-TIMS zircon $^{206}\text{Pb}/^{238}\text{U}$ ages	~20km NE of Nordøyane	Eclogite	(Krogh et al., 2011)

<b>410 ± 16 Ma</b>	Three-point Sm–Nd isochron	Flemsøya	Eclogite	Same sample as analysed by Mørk and Mearns (1986). Recalculated by Root et al. (2004).
<b>410.8 ± 1.4 Ma</b>	ID–TIMS zircon <sup>206</sup> Pb/ <sup>238</sup> U ages	~20km NE of Nordøyane	Eclogite	(Krogh et al., 2011)
<b>411 ± 2 Ma</b>	Weighted mean <sup>206</sup> Pb/ <sup>238</sup> U age	Flem gabbro	UHP eclogite	(Krogh et al., 2011)
<b>412 ± 1 Ma</b>	Weighted mean <sup>206</sup> Pb/ <sup>238</sup> U age	Lepsøya	Hornblende-eclogite	(Krogh et al., 2011)
<b>ca. 400–413 Ma</b>	Chemical abrasion TIMS and LA–MC–ICP–MS zircon <sup>206</sup> Pb/ <sup>238</sup> U ages	Harøya	Eclogite	Among these ages, an age of 413.1 ± 6.6 Ma was constrained from a UHP coesite-bearing eclogite (Butler et al., 2018)
<b>413.9 ± 3.7 Ma</b>	Four-point Sm–Nd isochron	Gossa	Eclogite	(Kylander-Clark et al., 2009)
<b>415.0 ± 6.8 Ma</b>	Secondary ion mass spectrometry (SIMS) monazite weighted-mean <sup>206</sup> Pb/ <sup>238</sup> U age	Fjørtoft	UHP microdiamond gneiss	Monazite inclusions inside garnet (Terry et al., 2000b).
<b>416.3 ± 3.7 Ma</b>	Four- and three-point Lu–Hf isochrons	Vigra (~20km SW of Nordøyane)	UHP eclogite	(Kylander-Clark et al., 2007)
<b>418 ± 11 Ma</b>	Sm–Nd garnet-clinopyroxene mineral-pair isochron	Tverrfjell (15km NE of Nordøyane)	Eclogite	(Griffin & Brueckner, 1980, 1985)
<b>ca. 421–400 Ma</b>	Split-stream LA–ICP–MS zircon separate ages	Midsund Bruk	UHP eclogite	Data from Krogh et al. (2011). REE abundances suggest three distinct groups; ca. 421 Ma, 409–404 Ma, 400 Ma (Kylander-Clark et al., 2013)
<b>429.5 ± 3.1 Ma</b>	Weighted mean age of two two-point isochrons and one three-point Sm–Nd isochron	Otrøy and Flemsøy	Garnet pyroxenite	(Spengler et al., 2009)



**Table 3: Geochronological summary of Caledonian ages from Sørøyane.**

Age	Method	Location	Rock type	Notes
369 ± 11 Ma	Four- and three-point Lu–Hf isochron	Remøya	UHP eclogite	(Kylander-Clark et al., 2007)
381.9 ± 1.9 Ma	LA–MC–ICPMS $^{238}\text{U}/^{206}\text{Pb}$ - $^{207}\text{Pb}/^{206}\text{Pb}$ titanite isochron	Nerlandsøya	Quartzofeldspathic ultramylonite	(Spencer et al., 2013)
386.1 ± 2.2 Ma	Chemical abrasion TIMS rutile $^{206}\text{Pb}/^{238}\text{U}$ age	Remøya	Unspecified	(Kylander-Clark et al., 2008)
387.0 ± 0.9 Ma	Chemical abrasion TIMS rutile $^{206}\text{Pb}/^{238}\text{U}$ age	Remøya	Unspecified	(Kylander-Clark et al., 2008)
388.8 ± 2.4 Ma	LA–MC–ICPMS $^{238}\text{U}/^{206}\text{Pb}$ - $^{207}\text{Pb}/^{206}\text{Pb}$ titanite isochron	Gurskøya	Sillimanite gneiss	(Spencer et al., 2013)
388.8 ± 3.1 Ma	LA–MC–ICPMS $^{238}\text{U}/^{206}\text{Pb}$ - $^{207}\text{Pb}/^{206}\text{Pb}$ titanite isochron	Ulsteinvik	Retrogressed eclogite (overprinted by garnet granulite)	(Spencer et al., 2013)
390.2 ± 0.8 Ma	Chemical abrasion TIMS titanite $^{206}\text{Pb}/^{238}\text{U}$ age	Hareidlandet	Leucosome	(Kylander-Clark et al., 2008)
390.3 ± 4.9 Ma	Split stream LA–ICP–MS monazite weighted mean $^{206}\text{Pb}/^{238}\text{U}$ age	Leinøya	Garnet-muscovite-kyanite gneiss	(Kylander-Clark et al., 2013)
390.5 ± 0.9 Ma	Chemical abrasion TIMS titanite $^{206}\text{Pb}/^{238}\text{U}$ age	Ulsteinvik	Leucosome	(Kylander-Clark et al., 2008)
390.6 ± 2.5 Ma	LA–MC–ICPMS $^{238}\text{U}/^{206}\text{Pb}$ - $^{207}\text{Pb}/^{206}\text{Pb}$ titanite isochron	Remøyholmen	Perthite-biotite mylonite with amphibolite facies fabric	(Spencer et al., 2013)
391 ± 13 Ma	Three-point Lu–Hf isochron	Sandvik	Eclogite	(Kylander-Clark et al., 2009)
392.7 ± 2.3 Ma	LA–MC–ICPMS $^{238}\text{U}/^{206}\text{Pb}$ - $^{207}\text{Pb}/^{206}\text{Pb}$ titanite isochron	Blankholmen	Single titanite rim on rutile in gneiss	(Spencer et al., 2013)
395.0 ± 3.9 Ma	Split stream LA–ICP–MS monazite weighted mean $^{206}\text{Pb}/^{238}\text{U}$ age	Leinøya	Garnet-muscovite-kyanite gneiss	(Kylander-Clark et al., 2013)
395.9 ± 1.4 Ma	LA–MC–ICPMS $^{238}\text{U}/^{206}\text{Pb}$ - $^{207}\text{Pb}/^{206}\text{Pb}$ titanite isochron	Hareidlandet	Biotite gneiss	(Spencer et al., 2013)
396.3 ± 4.6 Ma	LA–MC–ICPMS $^{238}\text{U}/^{206}\text{Pb}$ - $^{207}\text{Pb}/^{206}\text{Pb}$ titanite isochron	Dimnøya	Hornblende-plagioclase-titanite leucosome	Discordant. (Spencer et al., 2013)
397.1 ± 4.8 Ma	Four-point Sm–Nd isochron	Sandvik	Eclogite	(Kylander-Clark et al., 2009)

398.3 ± 5.5 Ma	Three-point isochron and two-point isochron	NW Gurskøy (~5km S of Sørøyane)	Eclogite	(Kylander-Clark et al., 2007)
401 ± 20 Ma	Zircon multi-grain ID–TIMS weighted-mean <sup>206</sup> Pb/ <sup>238</sup> U age	Ulsteinvik	Eclogite	(Krogh et al., 1974)
401 ± 20 Ma	Zircon multi-grain ID–TIMS weighted-mean <sup>206</sup> Pb/ <sup>238</sup> U age	Ulsteinvik	Eclogite	(Krogh et al., 1974)
401.6 ± 1.6 Ma	Zircon (air) multi-grain ID–TIMS weighted-mean <sup>206</sup> Pb/ <sup>238</sup> U age	Ulsteinvik	Eclogite	(Carswell et al., 2003)
ca. 402 Ma	ID–TIMS zircon <sup>206</sup> Pb/ <sup>238</sup> U age	Ulsteinvik	Coesite-bearing eclogite	(Tucker et al., 2004)
408.8 ± 6.3 Ma	Split stream LA–ICP–MS monazite weighted mean <sup>206</sup> Pb/ <sup>238</sup> U age	Leinøya	Garnet-muscovite-kyanite gneiss	(Kylander-Clark et al., 2013)
ca. 401–410 Ma	ID–TIMS zircon <sup>206</sup> Pb/ <sup>238</sup> U age	Ulsteinvik	Eclogite	(DesOrmeau et al., 2015)
411.5 ± 4.1 Ma	Four- and three-point Lu–Hf isochrons	NW Gurskøy (~5km S of Sørøyane)	Eclogite	(Kylander-Clark et al., 2007)
412.0 ± 4.7 Ma	Four- and three-point Lu–Hf isochrons	NW Gurskøy (~5km S of Sørøyane)	Eclogite	(Kylander-Clark et al., 2007)
412 ± 12 Ma	Two-point Sm–Nd isochron	Eiksunddal	Eclogite	(Jamtveit et al., 1991)
412 ± 25 Ma	SIMS and LA–ICP–MS zircon concordia ages	~20km E of Sørøyane	Eclogite	(Walsh et al., 2007)
412 ± 4 Ma	Two-point Sm–Nd isochron	Eiksunddal	Eclogite	Same sample as analysed by Jamtveit et al. (1991). Recalculated by Root et al. (2004).
401–413 Ma	Split stream LA–ICP–MS zircon <sup>206</sup> Pb/ <sup>238</sup> U age	Ulsteinvik	Eclogite	(DesOrmeau et al., 2015)
423 ± 30 Ma	Sm–Nd garnet-clinopyroxene mineral-pair isochron	Ulsteinvik	Eclogite	(Griffin & Brueckner, 1980, 1985)
426.5 ± 5.6 Ma	Split stream LA–ICP–MS monazite weighted mean <sup>206</sup> Pb/ <sup>238</sup> U age	Leinøya	Garnet-muscovite-kyanite gneiss	(Kylander-Clark et al., 2013)
ca. 475–430 Ma	LA–ICP–MS zircon <sup>206</sup> Pb/ <sup>238</sup> U ages	Ulsteinvik	Eclogite	Nearly continuous spread of concordant data (DesOrmeau et al., 2015).

## METHODS

### Whole-rock geochemistry

Whole-rock chemical compositional data was acquired at Bureau Veritas, Adelaide for seven samples: two from Ulsteinvik and five from Fjørtoft. The data from two of these samples was used in the calculation of metamorphic mineral equilibria forward modelling. Geochemical assays and extended methods are presented in Appendix 1.

### Electron Probe Micro Analyses (EPMA)

Mineral composition element analyses and element X-ray maps were acquired at Adelaide Microscopy, using a CAMECA SXFive Electron Microprobe under standard operating conditions (Table 4). Appendix 2 contains extended EPMA methods and results. Stoichiometric charges were effectively balanced with AX-62 software (Droop, 1987; Holland & Powell, 1990; Holland et al., 1998; Jennings & Holland, 2015; Holland et al., 2018) and then used to calculate the amount of Fe<sup>3+</sup> present in iron-bearing phases within the sample (see Appendix 4A).

**Table 4: EPMA operating conditions.**

Analysis Type	Beam Current (nA)	Accelerating Voltage (15kV)	Spot Size (µm)	Dwell time (µs)	Step Size (µm)
Garnet composition element analysis traverse	20	15	5	-	-
31A garnet element x-ray map	200	20	-	30	16
25B garnet element x-ray map	200	20	-	30	9
Crd-sp reaction texture element x-ray maps	200	20	-	30	4-8



### LA-ICP-MS: Geochronology

Zircon, monazite, rutile and apatite U–Pb isotopic data were acquired using a RESOLUTION LR 193nm Excimer laser system and coupled Agilent 7700s ICP-MS at Adelaide Microscopy, following the standard methods. Zircon was analysed in grain mount, while monazite, rutile and apatite data were collected in-situ. Operating conditions are detailed in Table 5. Data processing and reduction was done using Iolite 3.6 software (Hellstrom et al., 2008; Paton et al., 2011).

Mineral separate preparation, extended LA-ICP-MS methods, LA-ICP-MS standards, and data processing procedures are detailed in Appendix 3A.

**Table 5: LA-ICP-MS operating conditions.**

Mineral	Sample/Analysis type	Spot size (µm)	Fluence (J/cm <sup>2</sup> )	Energy (mJ)	Frequency (Hz)	Scan speed (µm/s)
Zircon	WGC2019J-25B spot data	19	2	28	5	-
	WGC2019J-31A spot data	19	2	30	5	-
Monazite	WGC2019A-3 spot data	19	2	33	5	-
	WGC2019J-25B spot data	19	2	33	5	-
	WGC2019J-31A spot data	19	2	33	5	-
Rutile	WGC2019A-3 spot data	29	5	45	5	-
	WGC2019J-25B spot data	29	5	45	5	-
Apatite	WGC2019A-3 spot data	29	3.5	45	5	-
	WGC2019J-25B spot data	29	3.5	45	5	-
Garnet	WGC2019J-25B (1) spot data	51	3.5	45	5	-
	WGC2019J-25B (2) spot data	51	3.5	45	5	-
	WGC2019J-31A spot data	51	3.5	45	5	-
	WGC2019J-25B (1) map	61	3.5	45	10	90
	WGC2019J-25B (2) map	61	3.5	45	10	90
	WGC2019J-31A map	91	3.5	45	10	135

### **LA-ICP-MS: Trace elements**

Trace element data for zircon, monazite and apatite were acquired using a RESOLUTION LR 193nm Excimer laser system and coupled Agilent 7700s ICP-MS at Adelaide Microscopy. In addition to spot analysis, 2D trace element mapping was undertaken on garnet. Iolite 3.6 software (Hellstrom et al., 2008; Paton et al., 2011) was used for data processing and reduction. Refer to Appendix 3A for extended LA-ICP-MS methods.

### **Mineral equilibria forward modelling**

Mineral equilibria models were calculated using THERMOCALC v.3.40 software in the model system MnNCKFMASHTO (MnO-Na<sub>2</sub>O-CaO-K<sub>2</sub>O-FeO-MgO-Al<sub>2</sub>O<sub>3</sub>-SiO<sub>2</sub>-H<sub>2</sub>O-TiO<sub>2</sub>-O), using the internally consistent thermodynamic dataset 'ds62'. (Holland & Powell, 2011; Green et al., 2016). The most recent activity-composition (a-x) models (White et al., 2000; Holland & Powell, 2003; Smye et al., 2010; Holland & Powell, 2011; Diener & Powell, 2012; White, Powell, Holland, et al., 2014; White, Powell, & Johnson, 2014; Green et al., 2016) were used to calculate *P-T* pseudosections for samples WGC2019J-25B and WGC2019J-31A. An additional *P-Mo* pseudosection was used to constrain oxidation state in sample WGC2019J-25B (Appendix 4B), as whole-rock geochemical analyses are not considered representative of FeO and Fe<sub>2</sub>O<sub>3</sub> content (e.g. Rapp & Watson, 1995; Rebay et al., 2010; Johnson & White, 2011; Kelsey & Hand, 2015; Palin et al., 2016a). In the initial *P-Mo* calculation, temperature was fixed at 790 °C while pressure and oxidation state were varied. The oxidation compositional axis varied from 90% Fe<sub>2</sub>O<sub>3</sub> to 10% Fe<sub>2</sub>O<sub>3</sub> (10-90% FeO). Oxidation state in WGC2019J-31A was estimated based on garnet and biotite abundance and respective average Fe<sup>3+</sup> and Fe<sup>2+</sup> cations calculated by EPMA. Water content in both samples was determined by multiplying total wt% biotite by EPMA-calculated wt%

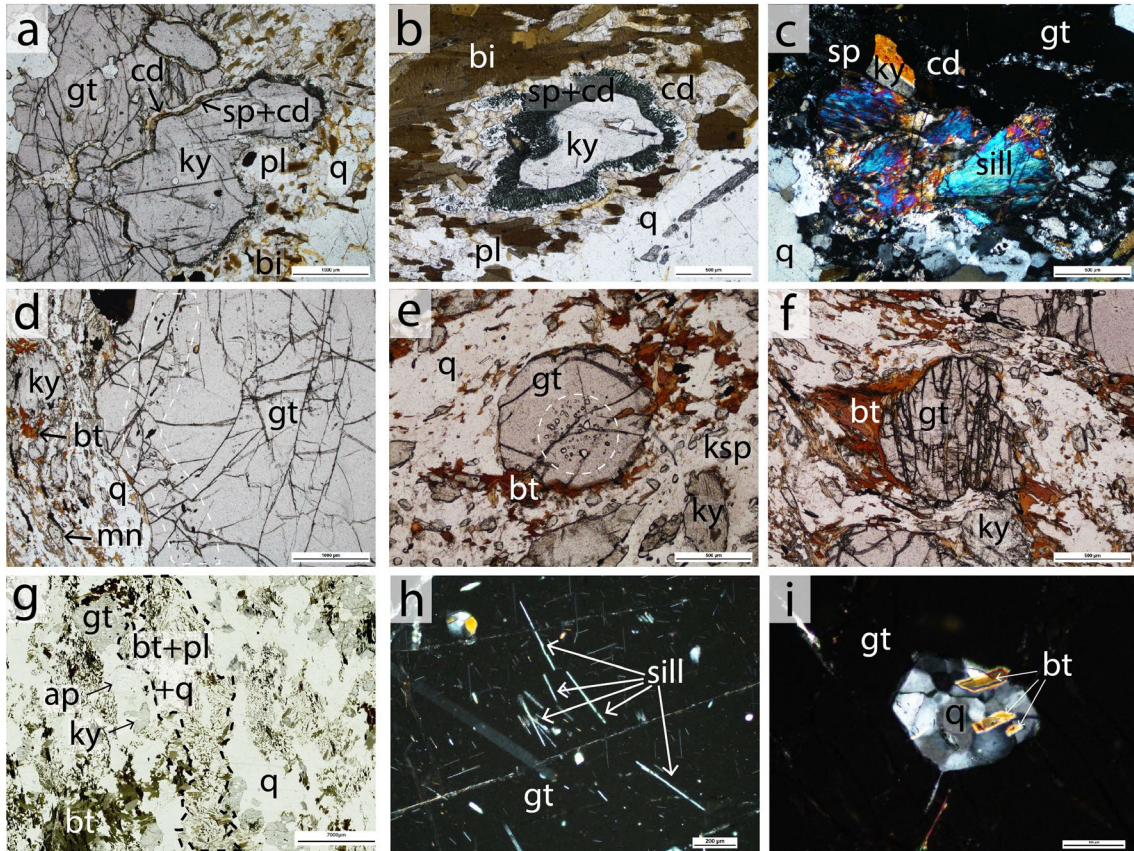
H<sub>2</sub>O in biotite. Water content was determined based on the abundance of biotite in the rock.

## RESULTS

### Petrography

#### WGC2019J-25B

Peak minerals consist of porphyroblastic garnet (~1 cm), variably pseudomorphed relict kyanite (up to 3000  $\mu$ m), rutile, quartz and apatite which occurs as a coarse-grained porphyroblast within the matrix (~2000  $\mu$ m) or as finer-grained inclusions (~250  $\mu$ m) inside garnet. Kyanite contains inclusions of rutile, apatite and quartz. The matrix is defined by coarse-grained domains of quartz interspersed with finer-grained polygonal quartz intergrown with plagioclase and unoriented laths of biotite (Fig. 3g), along with occasional clusters of coarse-grained biotite. These biotite-bearing intergrowths have sharply defined boundaries delineating elongate domains that parallel the gneissic layering. Garnet porphyroblasts contain inclusions of kyanite, ilmenite, rutile, zircon, apatite, muscovite, biotite and quartz. Quartz inclusions occasionally form mosaic structures reminiscent of polycrystalline quartz after coesite (Fig. 3i; Mosenfelder & Bohlen, 1997). Garnet is systematically separated from kyanite/sillimanite and biotite by either a monomineralic cordierite corona, or by a composite texture comprising symplectic cordierite, plagioclase and spinel associated with a simple corona of cordierite (Fig. 3a). Additionally, kyanite is locally partially replaced by sillimanite (Fig. 3c), and in rare instances, sillimanite has acted as a substrate for the cordierite-spinel bearing reaction textures.



**Figure 3: Photomicrographs from this study. (a) WGC2019J-25B: Porphyroblastic kyanite and garnet separated by symplectic cordierite and spinel, and a simple corona of cordierite. (b) WGC2019J-25B: Spinel-cordierite symplectite and cordierite corona isolating kyanite from biotite. (c) WGC2019J-25B. Sillimanite retrogression of kyanite. (d) WGC2019J-31A. A trail of inclusions (dotted line) concentrated in the rim of a coarse-grained garnet porphyroblast. (e) WGC2019J-31A. Inclusions (dotted line) concentrated in the core of a fine-grained garnet porphyroblast. (f) WGC2019J-31A. A retrograde biotite strain shadow adjacent to porphyroblastic garnet. (g) WGC2019J-25B. Fine-grained biotite-plagioclase-quartz domains that potentially formed after the breakdown of phengite and omphacite. (h) WGC2019J-31A: Sillimanite inclusions inside garnet. (i) WGC2019J-25B: Mosaic quartz inside garnet. Annotations: gt = garnet, ky = kyanite, pl = plagioclase, cd = cordierite, ksp = K-feldspar, bt = biotite, mn = monazite, q = quartz.**

### WGC2019J-31A

Porphyroblastic garnet within WGC2019J-31A is coarse-grained (up to 5 cm) and often intensely fractured. Garnet contains inclusions of kyanite, sillimanite, biotite, pyrite, pyrrhotite, chalcopyrite, zircon, monazite, apatite and quartz. With the exception of sillimanite, these inclusions are typically concentrated in a thin domain that occurs near the rim in coarser-grained garnets (Fig. 3d), and closer to the core in finer-grained garnets (Fig. 3e). The garnets are enclosed in a protomylonitic matrix consisting of plagioclase, K-feldspar, biotite, kyanite, quartz, rutile, pyrrhotite, chalcopyrite,

muscovite and graphite. Three generations of biotite are present: (1) fine-grained inclusions within garnet and kyanite, (2) matrix, foliation defining biotite, exhibiting partial replacement by chlorite, and (3) retrograde biotite localised in strain shadows adjacent to garnet (Fig. 3f).

## Mineral chemistry

Representative endmember compositions of garnet, plagioclase and K-feldspar are presented in Table 6. Appendix 2 contains an extended summary of elemental oxide and cation values for each analysed mineral, along with additional garnet EPMA maps.

Appendix 3B contains additional LA-ICP-MS garnet maps, trace element spiderplots and traverse plots.

### GARNET

Garnet composition from WGC2019J-25B is dominantly almandine (Fig. 4c; Table 6), with  $X_{\text{alm}} (\text{Fe}^{2+} / (\text{Fe}^{2+} + \text{Ca} + \text{Mg} + \text{Mn}))$  values of 0.48–0.54 in garnet cores, 0.49–0.64 in garnet rims and 0.64–0.71 in garnet partially consumed in retrograde reaction textures. Qualitative elemental maps (Fig. 4a, b) and quantitative traverse data (Fig. 4c) record prograde zoning. Almandine, grossular and spessartine are enriched in WGC2019J-25B garnet cores, and steadily decrease in concentration towards the rim. Pyrope is depleted within garnet cores and increases toward the rim. Resorption in the outermost rim of garnet records a steep increase in almandine and spessartine concentrations, and a decrease in pyrope and grossular (Fig. 4a, c).

WGC2019J-31A garnet is principally almandine ( $X_{\text{alm}} = 0.59\text{--}0.68$ ) and preserves a flat zoning profile (Fig. 4f), indicative of compositional resetting after retrograde diffusion.

**Table 6: Summary of mineral chemistry for WGC2019J-25B and WGC2019J-31A.**

Mineral	End-member proportions	WGC2019J-25B		WGC2019J-25B reaction textures	WGC2019J-31A	
		Garnet rim	Garnet core		Garnet rim	Garnet core
<b>Garnet</b>	$X_{gt}$	0.59–0.73	0.60–0.70	0.65–0.73	0.65–0.74	0.67–0.72
	$X_{alm}$	0.49–0.64	0.48–0.54	0.64–0.71	0.59–0.67	0.63–0.68
	$X_{py}$	0.21–0.30	0.16–0.32	0.26–0.34	0.20–0.29	0.24–0.28
	$X_{grs}$	0.08–0.17	0.17–0.23	0	0.06–0.10	0.03–0.04
	$X_{sps}$	0.01–0.04	0.01–0.02	0.03–0.04	0.01	0.01–0.02
<b>Plagioclase</b>	$X_{ab}$	0.06–0.76		0.01–0.05	0.74–0.75	
	$X_{an}$	0.23–0.94		0.95–0.99	0.24–0.25	
<b>K-Feldspar</b>	$X_{ab}$	–		–	0.11–0.15	
	$X_{or}$	–		–	0.85–0.89	
<b>Spinel</b>	$X_{sp}$	0.61–0.65		0.72–0.78	–	
	<b>ZnO (wt%)</b>	1.43–2.36		–	–	
	<b>Cr<sub>2</sub>O<sub>3</sub> (wt%)</b>	0.16–0.46		0.12–0.62	–	
	<b>MnO (wt%)</b>	0.08–0.21		0.13–0.22	–	
<b>Biotite</b>	$X_{bi}$	0.24–0.26		0.36–0.46	0.40–0.42	
	<b>TiO<sub>2</sub> (wt%)</b>	2.84–3.25		2.46–5.05	4.42–5.49	
	<b>Al<sub>2</sub>O<sub>3</sub> (wt%)</b>	16.62–17.55		16.56–18.05	16.87–18.48	
	<b>MnO (wt%)</b>	–0.03–0.8		0	–0.02–0.08	
<b>Cordierite</b>	$X_{crd}$	–		0.22–0.25	–	
<b>Ilmenite</b>	<b>MnO</b>	–		0–0.42	–	
	<b>TiO<sub>2</sub></b>	–		44.01–47.98	–	

Unless indicated otherwise by the units (wt%), proportions are atomic/molar.

$$X_{gt} = \text{Fe}^{2+} / (\text{Fe}^{2+} + \text{Mg})$$

$$X_{alm} = \text{Fe}^{2+} / (\text{Fe}^{2+} + \text{Mg} + \text{Ca} + \text{Mn})$$

$$X_{py} = \text{Mg} / (\text{Fe}^{2+} + \text{Mg} + \text{Ca} + \text{Mn})$$

$$X_{gr} = \text{Ca} / (\text{Fe}^{2+} + \text{Mg} + \text{Ca} + \text{Mn})$$

$$X_{sps} = \text{Mn} / (\text{Fe}^{2+} + \text{Mg} + \text{Ca} + \text{Mn})$$

$$X_{ab} = \text{Na} / (\text{Na} + \text{Ca})$$

$$X_{an} = \text{Ca} / (\text{Ca} + \text{Na} + \text{K})$$

$$X_{or} = \text{K} / (\text{Ca} + \text{Na} + \text{K})$$

$$X_{sp} = \text{Mg} / (\text{Fe}^{2+} + \text{Mg})$$

$$X_{bi} = \text{Fe}^{2+} / (\text{Fe}^{2+} + \text{Mg})$$

$$X_{crd} = \text{Fe}^{2+} / (\text{Fe}^{2+} + \text{Mg})$$

Almandine and spessartine exhibit subtle rim-ward depletion. Pyrope records limited variation throughout the zoning profile. Grossular occurs in low concentrations and records a primarily flat profile that abruptly rises toward the rim (Fig. 4d, g).

#### PLAGIOCLASE

Plagioclase is present in both samples. WGC2019J-25B yields  $X_{an}$  ( $Ca / (Ca + Na + K)$ ) values of 0.23–0.99 and  $X_{ab}$  ( $Na / (Na + Ca)$ ) values of 0.01–0.076 (Table 6). Plagioclase that occurs in WGC2019J-25B reaction textures is more anorthitic ( $X_{an} = 0.95–0.99$ ). Figure 5 shows rim-ward Ca-enrichment in plagioclase interacting with these reaction textures. WGC2019J-31A plagioclase calculates  $X_{an}$  values of 0.24–0.25, and  $X_{ab}$  values of 0.74–0.75.

#### K-FELDSPAR

K-feldspar occurs only in WGC2019J-31A. It records  $X_{ab}$  values of 0.11–0.15 and  $X_{or}$  ( $K / (Ca + Na + K)$ ) values of 0.85–0.89 (Table 6).

#### SPINEL

Spinel is present in WGC2019J-25B.  $X_{sp}$  ( $Mg / (Fe^{2+} + Mg)$ ) ranges from 0.61–0.78 and is higher in reaction texture spinel. It contains small amounts of ZnO (Fig. 5), Cr<sub>2</sub>O<sub>3</sub> and MnO.

#### BIOTITE

$X_{bi}$  ( $Fe^{2+} / (Fe^{2+} + Mg)$ ) values in WGC2019J-25B range from 0.24–0.46, with reaction texture biotite recording the higher proportion of these values ( $X_{bi} = 0.36–0.46$ ).

WGC2019J-31A records  $X_{bi}$  values between 0.40–0.42. TiO<sub>2</sub> in WGC2019J-25B biotite



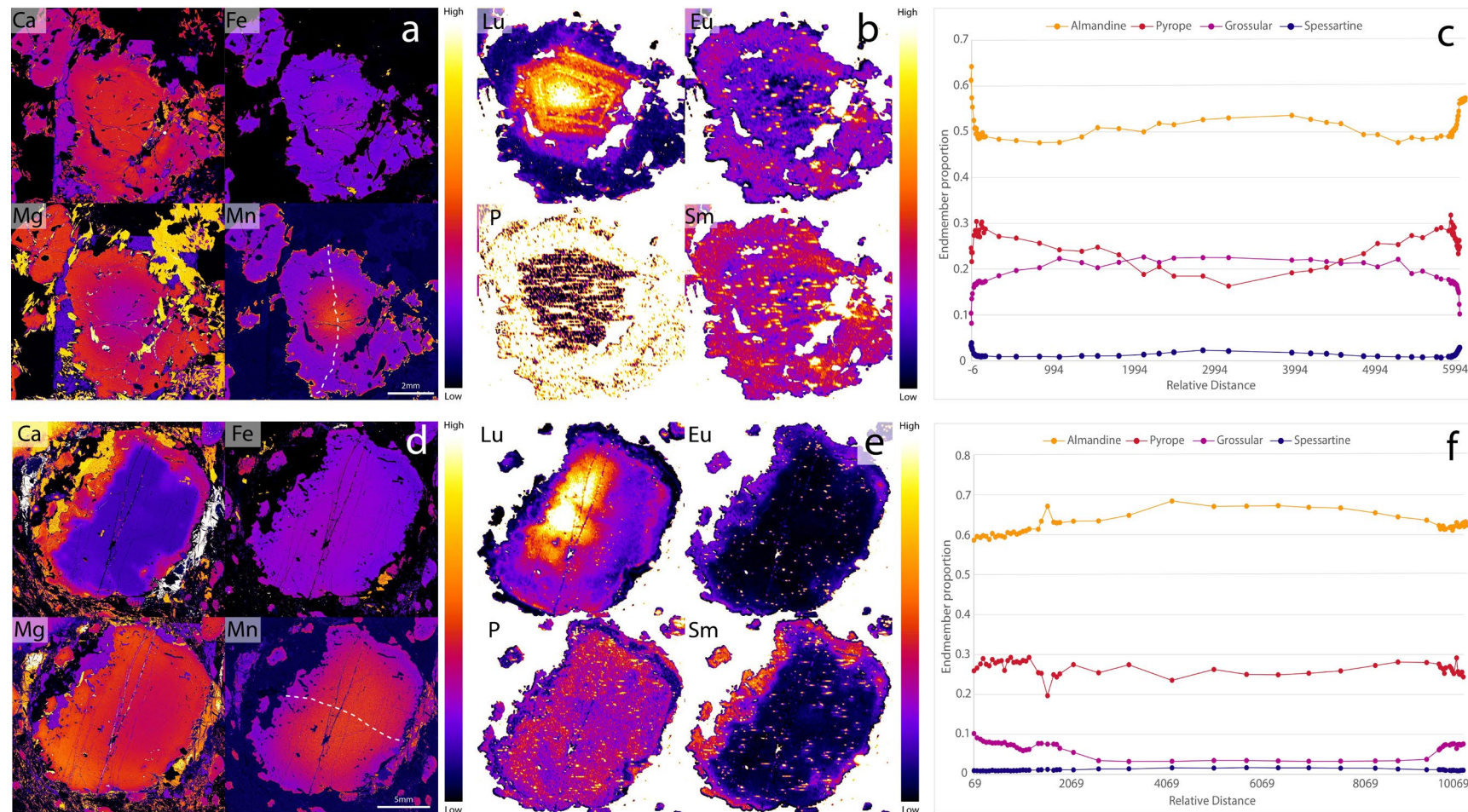
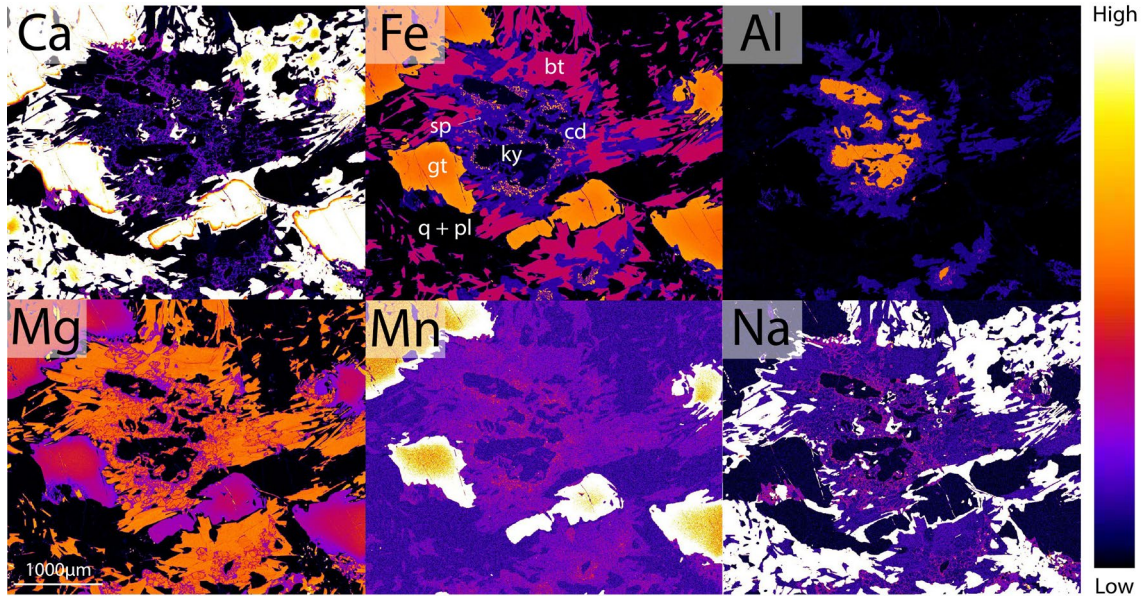


Figure 4: Garnet EPMA and LA-ICP-MS elemental maps and traverse data. *WGC2019J-25B*: (a) EPMA garnet major element maps for Ca, Fe, Mg and Mn. (b) LA-ICP-MS garnet trace element maps for Lu, Eu, Sm and P. (c) EPMA garnet major element rim to rim traverse, showing end-member proportions. Traverse path is traced in Fig. 4a with a dotted line. *WGC2019J-31A*: (d) EPMA garnet major element maps for Ca, Fe, Mg and Mn. (e) LA-ICP-MS garnet trace element maps for Lu, Eu, Sm and P. (f) EPMA garnet major element rim to rim traverse, showing end-member proportions. Traverse path is traced in Fig. 4d with a dotted line.





**Figure 5: EPMA elemental maps for Ca, Fe, Al, Mg, Mn and Na in WGC2019J-25B reaction textures. Relative concentration is modelled using the scale bar to the right of the figure; where black indicates a low elemental concentration and white indicates higher concentrations. Minerals are labelled in the Fe map, where bt = biotite, sp = spinel, cd = cordierite, ky = kyanite, gt = garnet, q = quartz and pl = plagioclase.**

ranges from 2.46–5.05 wt%, while WGC2019J-31A is comparatively enriched, with values between 4.42–5.49 wt%.

#### CORDIERITE

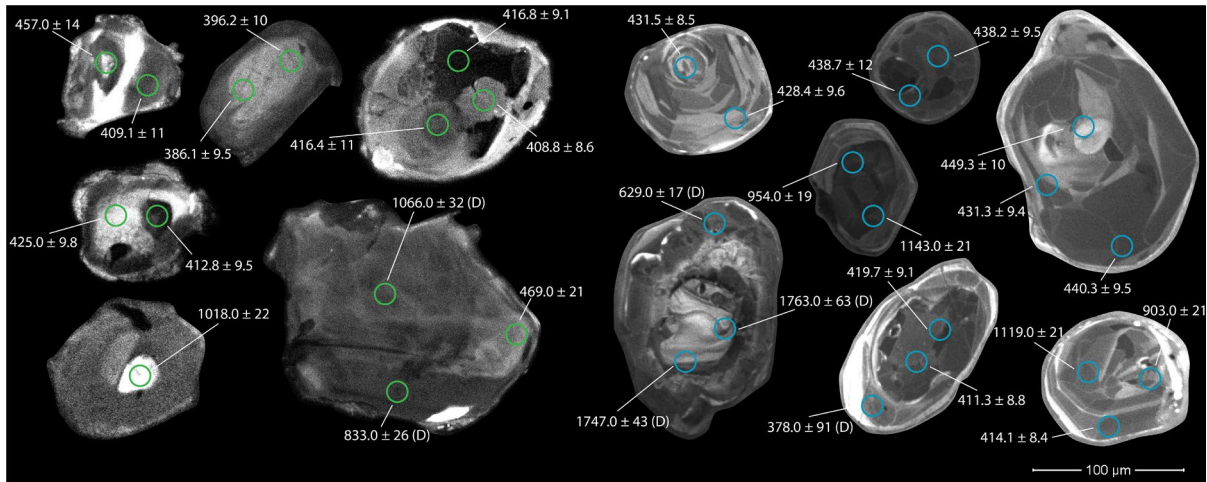
$X_{\text{crd}} (\text{Fe}^{2+} / (\text{Fe}^{2+} + \text{Mg}))$  in WGC2019J-25B reaction textures ranges between 0.22–0.25.

#### ILMENITE

Ilmenite in WGC2019J-25B has low MnO content, with values ranging between 0 and 0.42 wt%.

#### Zircon U–Pb geochronology and trace elements

U–Pb dating and trace element analysis was undertaken on mounted zircons from samples WGC2019J-25B and WGC2019J-31A. Calculated Tera Wasserburg concordia

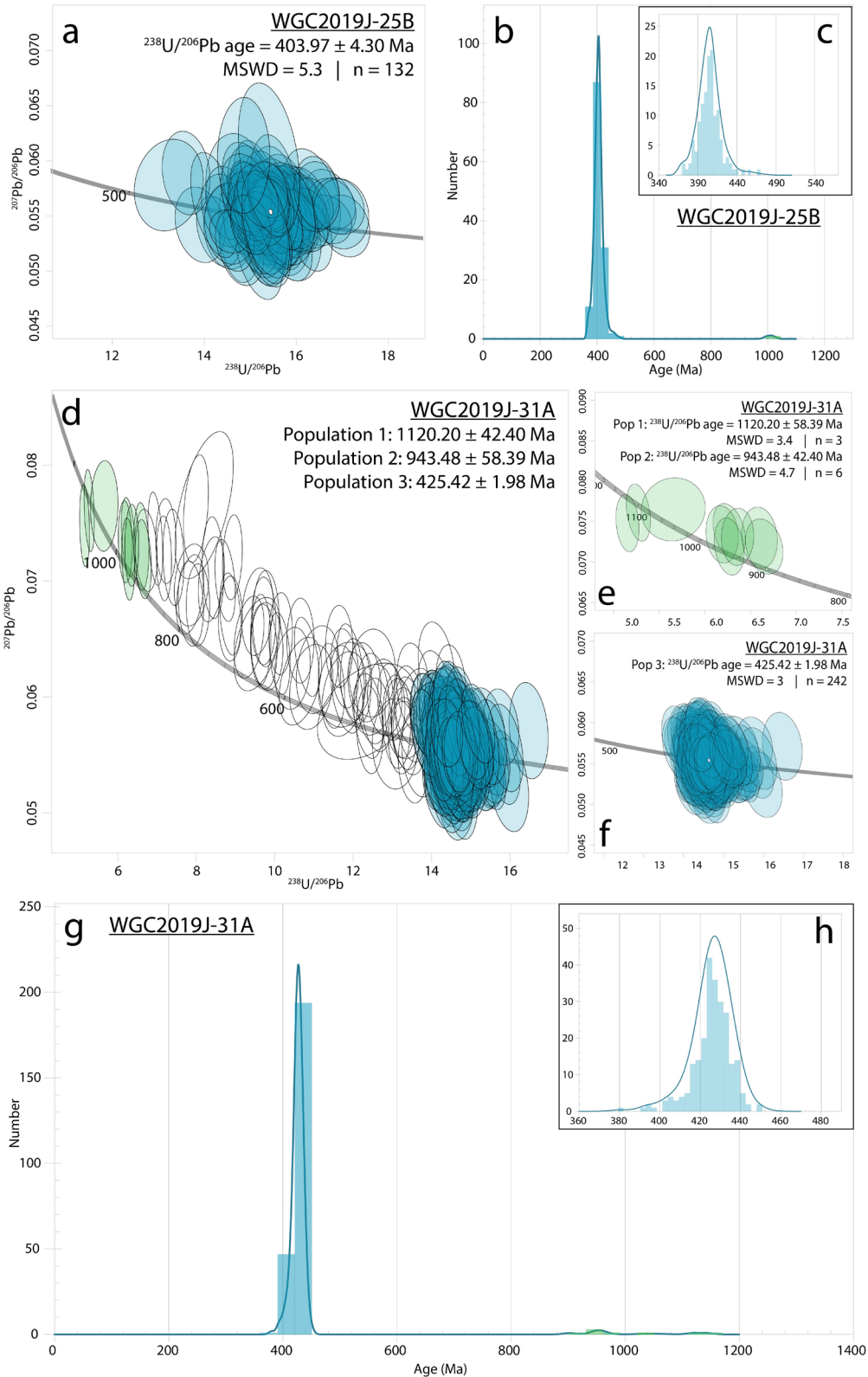


**Figure 6: Representative examples of zircon SEM-CL metamorphic zoning in Ulsteinvik (green) and Fjørtoft (blue). Ages are in Ma. Discordant analyses are indicated by (D).**

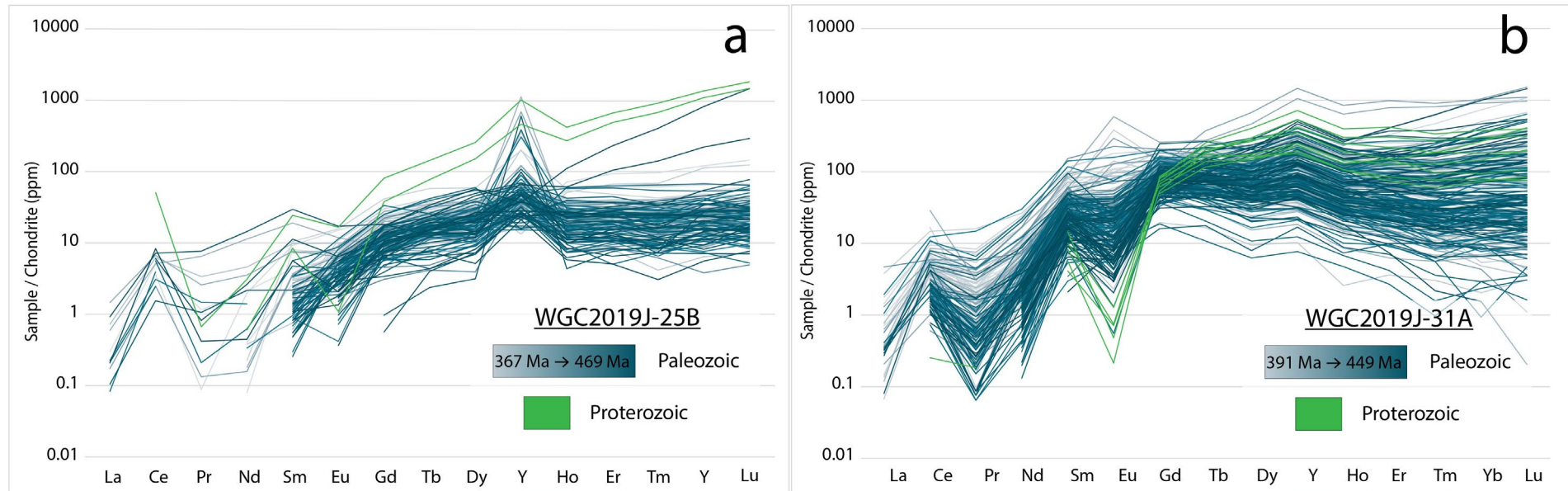
plots and probability density plots are in Figure 7. Extended morphological descriptions, U–Pb ratios and trace element concentrations for zircon are in Appendix 3C.

#### WGC2019J-25B

Zircons are ~50–200 µm, sub-rounded to rounded and commonly display spectacular metamorphic patchy to polygonal sector zoning in CL (Fig. 6). Analysis of eighty-five zircons reveal an almost continuous spread of ages from ~470–370 Ma (Fig. 7c), yielding a concordia age of  $404.0 \pm 4.3$  Ma, with an MSWD indicating significant dispersion (Fig. 7a). Two Proterozoic-aged analyses (~1009 Ma) were also recorded. Palaeozoic-aged zircons are enriched in Y, exhibit no significant Eu anomaly, and record a flat HREE slope (mean  $\text{Lu}_N/\text{Gd}_N = 2.6$ ,  $n = 131$ ), with the exception of the two oldest Palaeozoic-aged analyses ( $\text{Lu}_N/\text{Gd}_N = 25.5\text{--}86.8$ ,  $n = 2$ ). Late Mesoproterozoic-aged analyses have notably higher HREEs ( $\text{Lu}_N/\text{Gd}_N = 22.7\text{--}39.6$ ,  $n = 2$ ) and slightly negative Eu anomalies (Fig. 8a).



**Figure 7:** Zircon age data from Ulsteinvik and Fjortoft. *WGC2019J-25B*: (a) U–Pb Tera Wasserburg concordia for concordant Paleozoic-aged data, (b) Probability density plot for all concordant U–Pb ages, (c) Probability density plot for concordant Paleozoic U–Pb ages. *WGC2019J-31A*: (d) U–Pb Tera Wasserburg concordia, (e) U–Pb Tera Wasserburg concordia for concordant Sveconorwegian-aged data, (f) U–Pb Tera Wasserburg concordia for concordant Caledonian-aged data, (g) Probability density plot for all concordant U–Pb ages, (h) Probability density plot for concordant Caledonian U–Pb ages.



**Figure 8: Chondrite-normalised zircon trace element data presented in REE spiderplots. A) WGC2019J-25B. B) WGC2019J-31A. Spiderplots are coloured by age: Proterozoic = green, Paleozoic = blue gradient, where pale blue lines represent younger zircon U–Pb ages.**

### WGC2019J-31A

Zircons are ~50–150  $\mu\text{m}$ , are primarily equant and rounded, and display well-defined metamorphic internal morphology in CL similar to WGC2019J-25B but with the occasional atypical dark core (Fig. 6). One-hundred and seventy individual zircon grains generate a ~450–390 Ma range of Palaeozoic-aged data, yielding a concordia age of  $425.9 \pm 2.0$  Ma (Fig. 7d), and nine isolated older analyses comprising two populations ranging in age from ca. 1143–903 Ma (Fig. 7e). Proterozoic-aged analyses occur exclusively within the dark cores of grains, but dark cores are not exclusively Proterozoic. Palaeozoic-aged REE patterns are variably enriched in HREEs ( $\text{Lu}_\text{N}/\text{Gd}_\text{N} = 0.002\text{--}38.2$ ,  $n = 242$ ). Younger Palaeozoic-aged analyses record positive Eu anomalies and higher concentrations of Ce. Eu anomalies become increasingly negative and Ce concentrations progressively decrease with increasing age. Proterozoic-aged zircons have the most negative Eu anomalies and flat HREE slopes ( $\text{Lu}_\text{N}/\text{Gd}_\text{N} = 1.1\text{--}6.6$ ,  $n = 9$ ; Fig. 8b).

### **Monazite U–Pb geochronology and trace elements**

In-situ geochronology and trace element analysis were undertaken on monazite grains from various textural locations in samples WGC2019J-25B, WGC2019A-3 and WGC-2019J-31A. Samples WGC2019J-25B and WGC2019A-3 are from the same outcrop, with A3 from the edge of a garnet-rich domain, and 25B from the more biotite rich matrix (Figure 2c). Appendix 3D contains LA–ICP–MS U–Pb ratios, trace element concentrations and morphological descriptions.

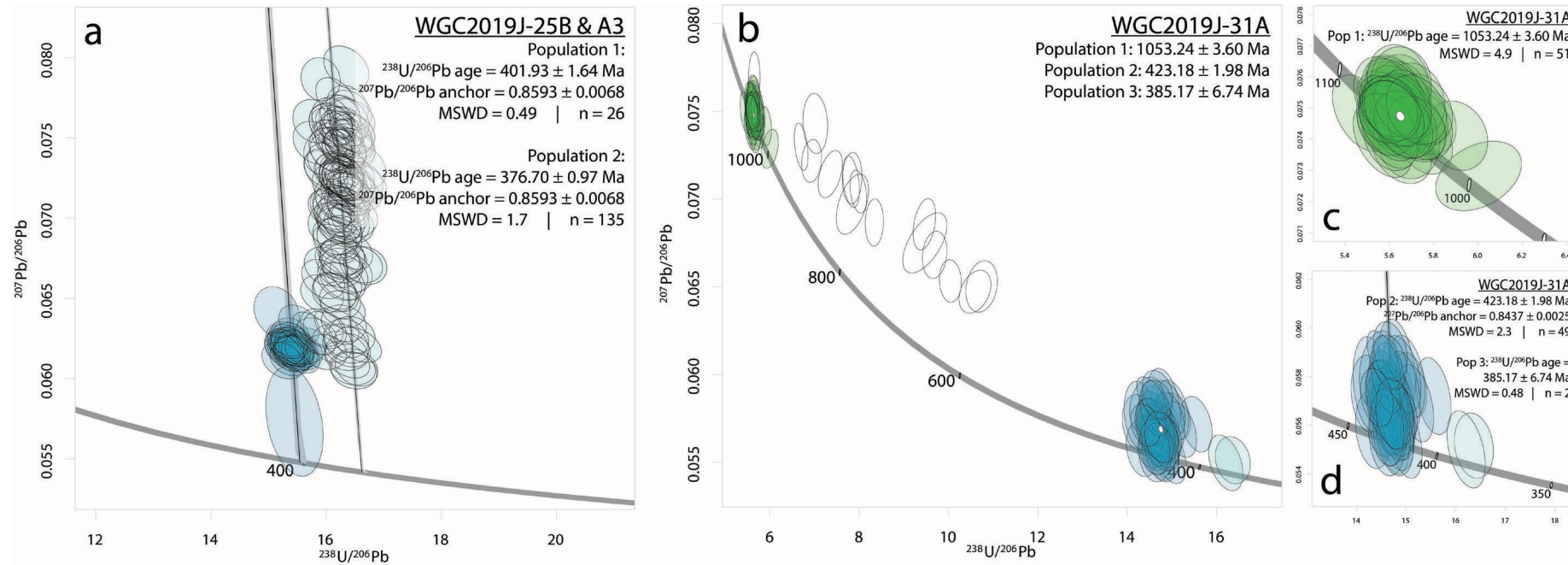


### WGC2019J-25B & WGC2019A-3

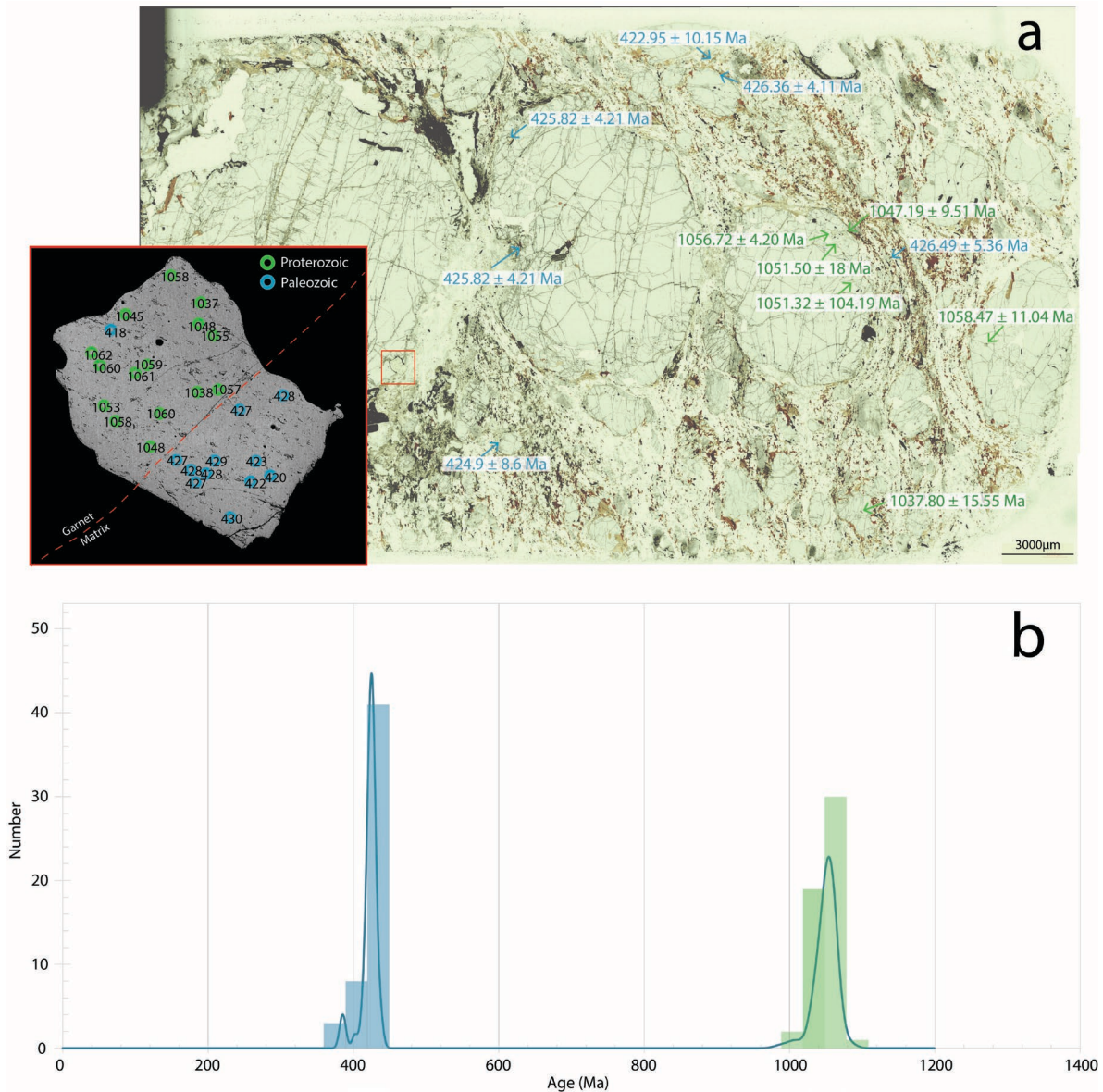
Monazite is not abundant, and ranges in size from ~75–1000  $\mu\text{m}$ . Crystal habit is primarily anhedral and BSE-defined zoning is either non-existent or weak. A total of eight monazite grains were analysed; four from WGC2019A-3 and four from WGC2019J-25B. Texturally, all grains are located within the matrix, with the exception of a single monazite inclusion within kyanite. LA–ICP–MS results from one hundred and sixty-four analyses yield two distinct discordant populations. These results are anchored to a common  $^{207}\text{Pb}/^{206}\text{Pb}$  ratio of  $0.8593 \pm 0.00068$  acquired from matrix biotite (Appendix 3F) and yield well-defined ages of  $401.9 \pm 1.6$  Ma and  $376.7 \pm 1.0$  Ma (Fig. 9a). Population one ( $401.9 \pm 1.6$  Ma) consists of analyses from the monazite inclusion in kyanite. It is comparatively enriched in LREEs, less enriched in HREEs and calculates a steep middle rare earth element (MREE) slope (average  $\text{Dy}_\text{N}/\text{Gd}_\text{N} = 0.03$ ,  $n = 26$ ) relative to population two (average  $\text{Dy}_\text{N}/\text{Gd}_\text{N} = 0.09$ ,  $n = 135$ ; Fig. 11a). An Eu anomaly is absent in population one. The majority of population two analyses have no Eu anomaly; however, four analyses have a negative Eu anomaly and are also enriched in HREEs relative to the remaining population.

### WGC2019J-31A

In-situ WGC2019J-31A monazite grains range in size from ~75–700  $\mu\text{m}$ , have variable crystal habit and exhibit weak to no zoning in BSE (Appendix 3C). One hundred and twenty-two spots within eighteen grains were analysed. Three populations are defined:  $1053.2 \pm 3.6$  Ma ( $n = 51$ ),  $423.2 \pm 2.0$  Ma ( $n = 49$ ) and  $385.2 \pm 6.7$  Ma ( $n = 2$ ; Fig. 9b, c, d). The ages of populations one and three are given by concordia ages, and an age for population two is constrained by an anchoring  $^{207}\text{Pb}/^{206}\text{Pb}$  value of  $0.8437 \pm 0.002$



**Figure 9: Tera Wasserburg concordia diagrams for monazite analyses from Ulsteinvik and Fjortoft. Lower intercept ages for discordant or a combination of discordant and concordant data are anchored by a calculated  $^{207}\text{Pb}/^{206}\text{Pb}$  ratio from biotite and K-feldspar (Appendix 3G). A) WGC2019J-25B & A3. B) WGC2019J-31A. C) WGC2019J-31A upper intercept, showing Proterozoic analyses. D) WGC2019J-31A lower intercept, showing Paleozoic analyses. Ellipses are coloured based on population.**



**Figure 10:** (a) WGC2019J-31A thin section scan annotated with monazite locations and weighted mean grain ages. Inset: monazite grain located at the edge of a garnet grain. A red dotted line marks the garnet grain boundary. (b) WGC2019J-31A cumulative probability distribution plot showing the spread of monazite data. In both plots: blue = Paleozoic, green = Proterozoic.

defined by biotite and K-feldspar (Fig. 9d). Texturally, older ages tend to be associated with monazites that occur as inclusions within garnet on the inner side of the inclusion trail rims (Fig. 3d). Figure 10a highlights the textural position of monazite ages, with the inset figure demonstrating the distribution and spatial organisation of individual Palaeozoic and Mesoproterozoic ages on the matrix versus garnet side of a monazite



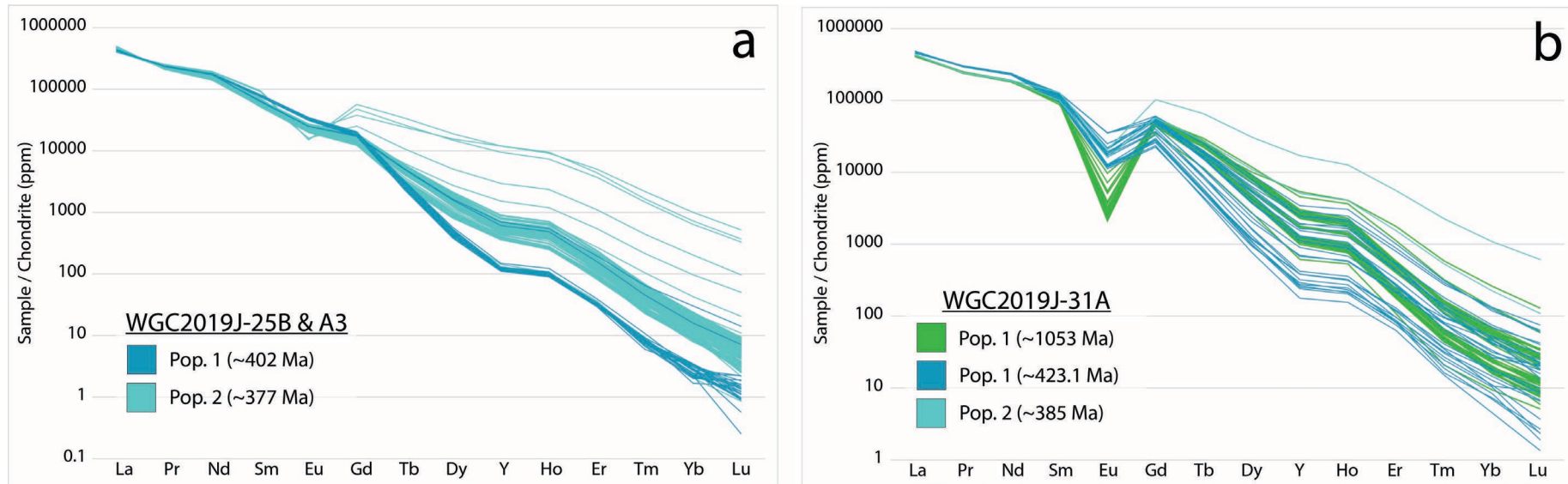


Figure 11: Chondrite-normalised monazite trace element data presented in REE spiderplots. (a) WGC2019J-25B & A3. (b) WGC2019J-31A. Plots are coloured by population. Green = Proterozoic, dark blue = old Paleozoic, light blue = young Paleozoic.

grain partially included within garnet. There is a distinct relationship between age and trace element concentration (Fig. 11b). Population two is the most enriched in LREEs. All populations exhibit a negative Eu anomaly, with the Paleozoic populations recording similar magnitudes ( $\sim 0.2$ ) and population one calculating the most negative anomaly ( $\sim 0.04$ ). HREEs are the most depleted in population two and the least depleted in population three. All populations record a similar MREE slope.

### **Apatite U-Pb geochronology and trace elements**

#### **WGC2019J-25B & WGC2019A-3**

Geochronology and trace element analysis was undertaken in-situ from Ulsteinvik samples WGC2019J-25B and WGC2019A-3. Analysed grains range from  $\sim 250$ – $2500 \mu\text{m}$  and occur within the matrix or within garnet. An extended summary of morphology, LA-ICP-MS geochronology and trace element data is presented in Appendix 3D. Nine apatite grains were analysed, totalling one hundred and eighty-three analyses which plot discordantly on a Tera-Wasserburg concordia. Anchoring of these analyses using the biotite  $^{207}\text{Pb}/^{206}\text{Pb}$  ratio yields an age of  $399.9 \pm 1.9 \text{ Ma}$  (Fig. 12a). HREE concentrations and Eu anomaly magnitude are directly related to textural location (Fig. 12b); apatite analyses texturally included within garnet lack Eu anomalies and exhibit depletion in HREEs ( $\text{Lu}_\text{N}/\text{Gd}_\text{N} = 0.0055$ ,  $n = 33$ ), while matrix apatite has a negative Eu anomaly and is comparatively enriched in HREEs ( $\text{Lu}_\text{N}/\text{Gd}_\text{N} = 0.087$ ,  $n = 111$ ). There is no obvious correlation between age and Eu anomaly magnitude (Fig. 11a).

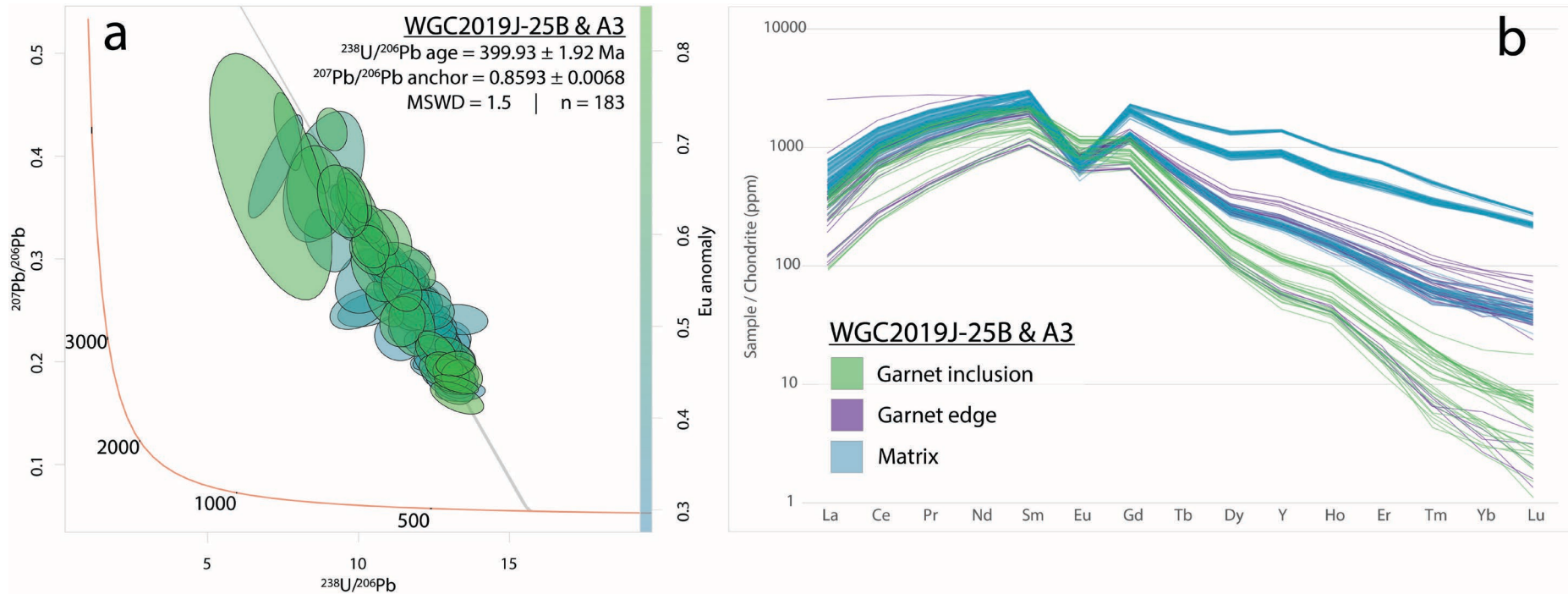
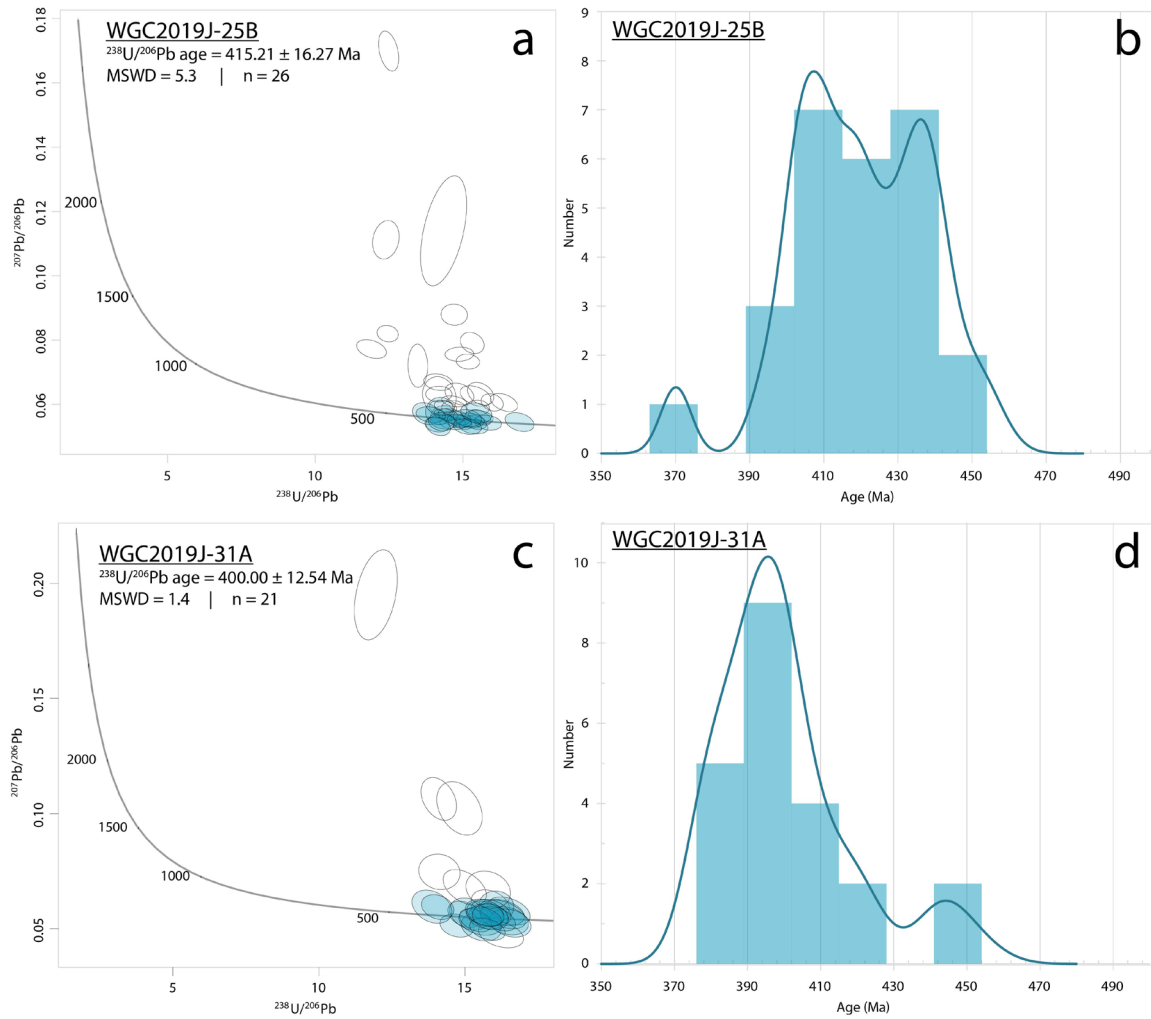


Figure 12: Ulsteinvik apatite geochronology and trace element data. (a) Tera Wasserburg concordia anchored by  $^{207}\text{Pb}/^{206}\text{Pb}$  from biotite and coloured by the magnitude of Eu anomaly. (b) REE spiderplot for chondrite-normalised apatite trace element data coloured by textural location.



**Figure 13: Rutile age data. (a) WGC2019J-25B Tera Wasserburg concordia, (b) WGC2019J-25B cumulative probability distribution plot, (c) WGC2019J-31A Tera Wasserburg concordia, (d) WGC2019J-31A cumulative probability distribution plot.**

### Rutile U–Pb geochronology

Geochronology and trace element analysis of in-situ rutile was undertaken for WGC2019J-25B and WGC2019J-31A. Extended morphology descriptions and results are presented in Appendix 3E.

#### WGC2019J-25B

Rutile grains vary in size between 50–400  $\mu\text{m}$  and, with the exception of one matrix grain, are texturally associated with garnet. Out of forty-nine total analyses, twenty-six are concordant and define a spread from ~453–370 Ma (Fig. 13b), giving a concordia

age of  $415.2 \pm 16.3$  Ma (Fig. 13a) with significant dispersion, suggesting the data do not represent a single age population.

#### WGC2019J-31A

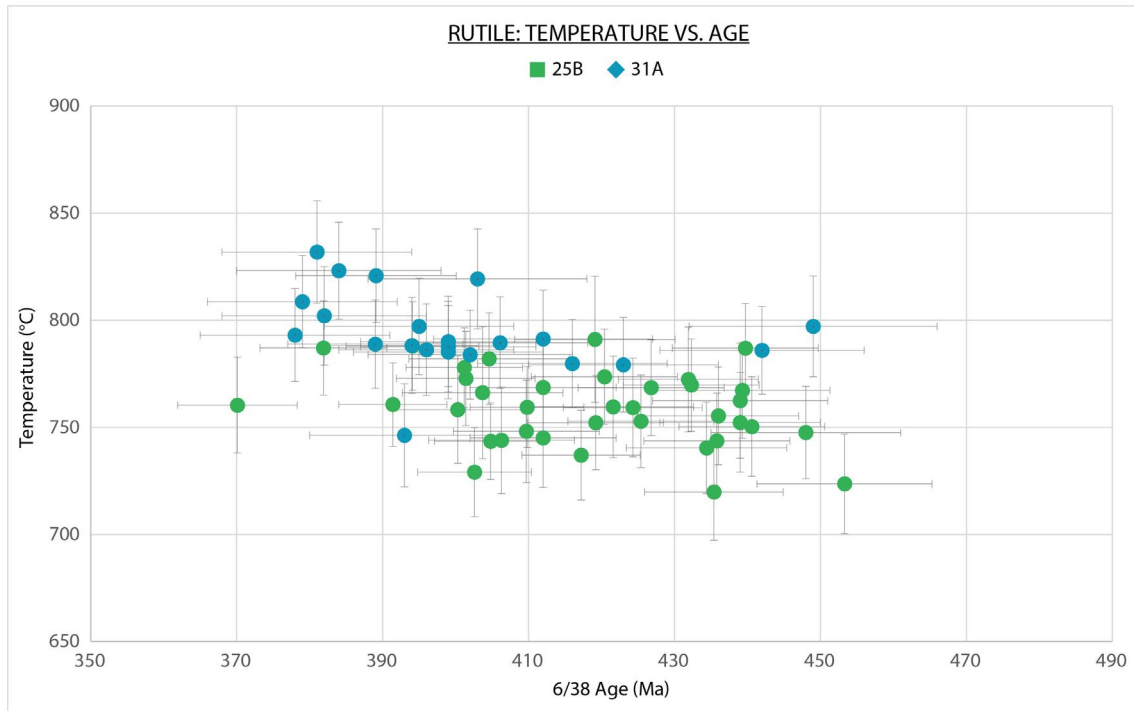
Seventeen rutile grains ranging in size between 50–650  $\mu\text{m}$  and from both matrix and inclusions in garnet were analysed, totalling thirty-one analyses. Twenty-one of these analyses plot concordantly, defining an almost continuous spread from  $\sim 449$ –379 Ma (Fig. 13d) and giving a concordia age of  $400.0 \pm 12.5$  Ma (Fig. 13c).

#### Zr-in-rutile thermometry

**Table 7: Average Zr-in-rutile temperatures for WGC2019J-25B and WGC2019J-31A data at 25 kbar.**

Sample	Zr-in-rutile temperature ( $^{\circ}\text{C}$ ) (Kohn, 2020)
WGC2019J-25B	$750.9 \pm 72.2$
WGC2019J-31A	$788.6 \pm 77.0$

Trace element compositions of rutile were used for Zr-in-rutile thermometry in samples WGC2019J-25B and WGC2019J-31A (Kohn, 2020). Weighted means calculated from the thermometry are summarised in Table 7. There is little to no correlation between temperature and age (Fig. 14). Extended thermometry data is in Appendices 3C and 3E.



**Figure 14: Zr-in-rutile temperature (Kohn, 2020) versus concordant  $^{238}\text{U}/^{206}\text{Pb}$  age. Green = WGC2019J-25B, blue = WGC2019J-31A.**

## Mineral equilibria forward modelling

### WGC2019J-25B

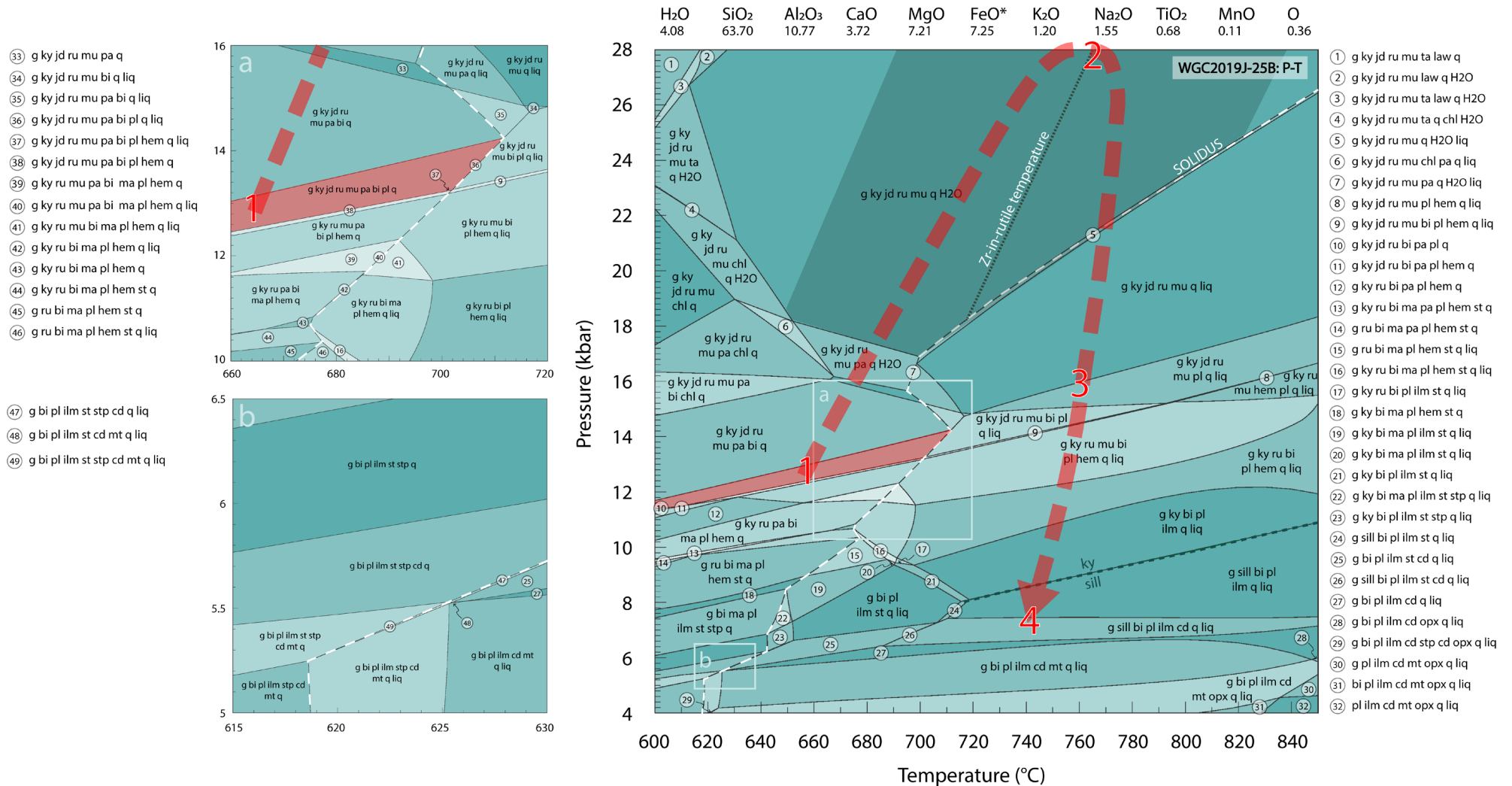
The inferred peak assemblage in WGC2019J-25B is located at  $M=0.150$  in the  $P$ – $M_o$  diagram calculated prior to  $P$ – $T$  modelling (Appendix 4B).

The prograde path for Ulsteinvik is a conservative estimate based on inclusions observed within garnet. Thus, the rock is speculated to pass through  $\sim 11$ – $13$  kbar and  $\sim 600$ – $700$  °C, in a field containing rutile, muscovite and plagioclase (Fig. 15; Point 1).

The peak assemblage (Fig. 15; Point 2) for the WGC2019J-25B metapelite is interpreted as garnet + kyanite + omphacite + coesite + muscovite + rutile + quartz +  $\text{H}_2\text{O}$ . Neither coesite nor omphacite are directly observed in the preserved assemblage but are inferred from secondary mineral textures (Fig. 3g, i). The transition from quartz to coesite occurs above the pressure window in Figure 15, ranging between 2.8 GPa at 600 °C and 2.9 GPa at 850 °C. A minimum  $P$ – $T$  point for the peak assemblage is

thereby given where Zr-in-rutile intersects the quartz-coesite reaction at  $\sim 2.9$  GPa and  $760$  °C.

Retrograde conditions have been inferred by computing independent thermobarometer reactions for the cordierite-spinel bearing symplectites (pers. comm. Hand, 2020). The intersection of these equilibria lines give a  $P$ - $T$  point at  $\sim 7$  kbar and  $\sim 740$  °C (Fig. 15; Point 4). The position of this  $P$ - $T$  point correlates with the known retrograde assemblage in the rock, plotting below the kyanite-sillimanite transformation within the sillimanite field, and almost directly on top of the cordierite-in line in Figure 5. The absence of spinel in Figure 15 reflects that it only forms in highly localised Al-rich areas of the rock, whereas Figure 15 is computed for the overall rock composition.



**Figure 15:** *P-T* pseudosection for metapelite WGC2019J-25B. The red arrow represents the inferred *P-T* path, defined by points 1-4. The red shaded area represents the prograde field (Point 1). Point 2 is a minimum peak constraint. Point 4 defines a *P-T* point calculated from a retrograde bulk composition. Variance increases with shading in the diagram. Complex regions are magnified in insets (a) and (b). Bulk composition used for the calculation of the phase diagram is listed in mol% at the top of the diagram. Oxidation ( $M_0$ ) was constrained at 0.15 (see additional  $PM_0$  pseudosection in Appendix 4B). Abbreviations: g = garnet, ky = kyanite, sill = sillimanite, jd = jadeite, ru = rutile, mu = muscovite, ta = talc, law = lawsonite, pa = paragonite, ma = margarite, bi = biotite, chl = chlorite, pl = plagioclase, hem = hematite, ilm = ilmenite, st = staurolite, stp = stipnomelane, q = quartz, mt = magnetite, opx = orthopyroxene, cd = cordierite, liq = liquid, H<sub>2</sub>O = water.



### WGC2019J-31A

Ambiguity surrounding the age of garnet cores within metapelitic WGC2019J-31A (pp. 33-37) prevents interpretation into the prograde history of Fjørtoft. Plagioclase inclusions do not occur within garnet rims, suggestive of peak conditions exceeding plagioclase stability. The peak field in WGC2019J-31A is therefore interpreted as garnet + kyanite + omphacite + muscovite + K-feldspar + rutile + quartz. By calculating the intersection between this field and the calculated Zr-in-rutile temperature, minimum peak conditions for Fjørtoft are constrained at ~17.8 kbar and ~750 °C (Fig. 16; Point 1). Limited constraints exist within the rock for retrograde  $P$ - $T$  conditions. The only retrograde reaction observed in thin section is biotite rimming muscovite. As a result, point 2 of Figure 16 is defined based on the location of the first biotite-bearing field down-pressure.

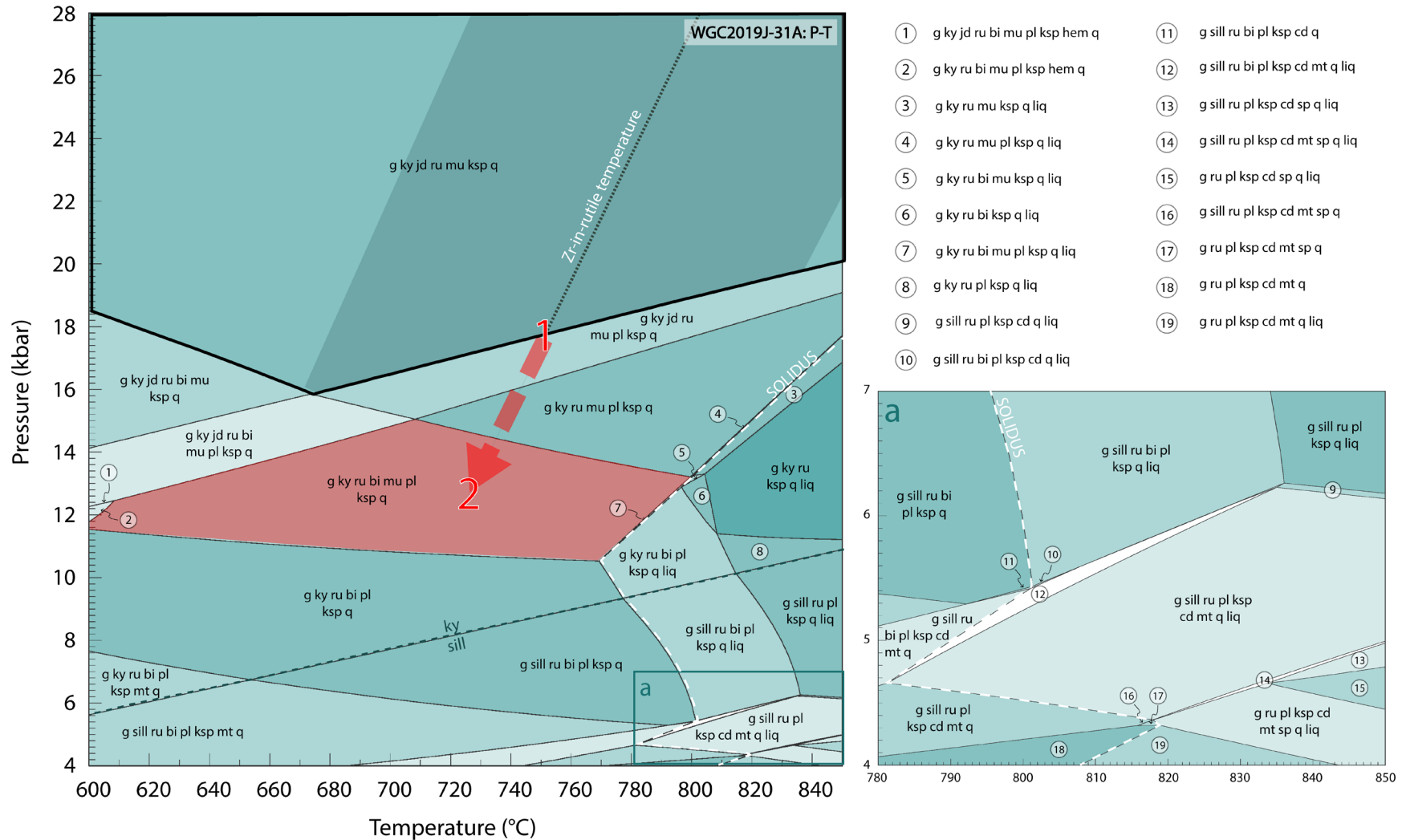


Figure 16:  $P$ - $T$  pseudosection for metapelite WGC2019J-31A. The red arrow represents the inferred  $P$ - $T$  path, where point 1 indicates the minimum constraint for peak conditions and the red shaded area indicates a retrograde field (Point 2). Inset (a) magnifies a complex region of the diagram. Bulk composition used for the calculation of the phase diagram is listed in mol% at the top of the diagram. Variance increases with shading in the diagram. Oxidation (MO) was constrained at 0.5 (see notes on calculation in Appendix 4B). Abbreviations: g = garnet, ky = kyanite, jd = jadeite, ru = rutile, mu = muscovite, ksp = k-feldspar, q = quartz, bi = biotite, pl = plagioclase, hem = hematite, cd = cordierite, mt = magnetite, sp = spinel.

## DISCUSSION

Past geochronological work on (U)HP eclogites and the discovery of diagnostic UHP minerals such as polycrystalline quartz, coesite and microdiamond (Dobrzhinetskaya et al., 1995; Spengler et al., 2006; Smith & Godard, 2013) in the WGR have provided evidence for the deep burial and exhumation of continental crust during the Caledonian Orogeny between ca. 430–370 Ma. In this study, multi-mineral geochronology and  $P$ – $T$  forward modelling offers further insight into the dynamics of continental subduction.

### Interpretation of U–Pb geochronology and trace elements

U–Pb geochronology of zircon, monazite, apatite and rutile from Ulsteinvik documents a predominantly Caledonian-aged history, with the exception of two Sveconorwegian-aged zircon analyses (Fig. 7b). Caledonian zircon ages span from ca. 469–367 Ma (Fig. 7a, c), suggestive of a protracted period of (re)crystallisation. Despite this extensive history, REE concentrations in zircon do not vary systematically with age, and the majority exhibit relatively flat HREE profiles without Eu anomalies. (Fig. 7a). Rutile analyses record a similar prolonged history, with ages ranging from ca. 453–370 Ma (Fig. 12a, b). Ordovician to Early Silurian zircon and rutile age components within these results are generally uncommon or absent within the WGR, but are of similar age to the Seve-Blåhø nappe in Sweden, supporting the conclusion made by Root et al. (2005) regarding the potentially allochthonous history of rocks in the Ulsteinvik region. Ulsteinvik and the Blåhø nappe were initially correlated based on the similarity of their host-rock lithologies (Root et al., 2005), and have been further linked by zircon age data from mafic eclogite at Ulsteinvik, which shows a near continuous spread of older concordant Caledonian zircon ages ranging from ca. 475–430 Ma (DesOrmeau et al.,

2015). A similar record of pre-Scandian U–Pb zircon and rutile ages from metapelites in this study (Fig. 7a, c; Fig. 13a, b) corroborates data from DesOrmeau et al. (2015) and further validates the hypothesis made by Root et al. (2005). The ability of rutile to record ca. 450–440 Ma data without significant diffusional loss of Pb and resultant age resetting is attributed to its textural location as an inclusion within garnet, where it was effectively ‘armoured’ and allowed to retain diffusional elements above its nominal closure temperature (<640 °C; Kooijman et al., 2010). Old rutile ages (ca. 450 Ma) are therefore interpreted to give the timing of garnet growth in Ulsteinvik, whilst younger ages record variable diffusional resetting.

In addition to the Early Caledonian ages, zircon and rutile preserve a pervasive record of concordant ages from ~430–370 Ma associated with Scandian subduction and exhumation of the WGR. Monazite occurs in two discordant Scandian-aged populations (~402 Ma and ~377 Ma; Fig. 8a) anchored by common  $^{207}\text{Pb}/^{206}\text{Pb}$  in biotite (Appendix 3G). Monazite populations occur either within the matrix or within kyanite and are generally devoid of an Eu anomaly (Fig. 10a). Europium anomalies are used to infer whether a mineral crystallised in the presence of plagioclase. Negative Eu anomalies suggest coeval plagioclase growth, where  $\text{Eu}^{2+}$  was preferentially incorporated into plagioclase and substituted with  $\text{Ca}^{2+}$  (Weill & Drake, 1973; McLennan, 1989). Apatite U–Pb data plots discordantly and is anchored by common  $^{207}\text{Pb}/^{206}\text{Pb}$  in biotite giving an age of  $399.9 \pm 1.9$  Ma (Fig. 11a). An obvious relationship exists between textural location and REE concentrations in apatite, where apatite within garnet lacks an Eu anomaly and is characterised by flat HREE signatures, whilst matrix apatite exhibits a strongly negative Eu anomaly and comparative enrichment in HREEs (Fig. 11b). The geochemical differences in apatite grains of the same age can be explained by relative differences in diffusion, where REEs such as Eu tend to be less mobile than Pb (e.g.

Bau, 1991; Cherniak, 2000). As a result, apatite often preserves prograde REE signatures, but only records ages representative of cooling through a nominal closure temperature (620 °C; Krogstad & Walker, 1994). Due to apatite giving discordant age data (Fig. 12a), differentiating age populations is complex. However, based on REE signatures and textural location, it appears that apatite inclusions in garnet likely formed on the prograde path during garnet growth and when plagioclase was absent from the rock, accounting for the lack of an Eu anomaly. Comparatively, matrix apatite appears to have grown in the presence of plagioclase (based on the presence of an Eu anomaly) and is thus more likely to have formed during exhumation. The absence of an Eu anomaly in effectively age-equivalent monazite suggests the rock traversed from plagioclase-absent to plagioclase-bearing parts of  $P$ – $T$  space at ~400 Ma (Fig. 15; Point 3). This provides a well-defined constraint for the end of UHP metamorphism and beginning of exhumation and retrograde plagioclase crystallisation. The retrograde  $P$ – $T$  path traverses melt-bearing fields, accounting for leucosome patches within the sample outcrop (Fig. 2c). The lack of Eu anomaly in 377 Ma monazite is interpreted as inheritance from the previous 402 Ma monazite generation. This population likely formed in response to apatite breakdown (e.g. Finger & Krenn, 2007).

U–Pb results from monazite and zircon in the Fjørtoft metapelite record evidence of the Sveconorwegian Orogeny (e.g. Bingen et al., 2008). Zircon yields a small number of concordant upper intercept ages (3.6% of total concordant analyses) ranging from ca. 1143–903 Ma (Fig. 7g), while monazite retains a more ubiquitous record with 51 concordant analyses (64% of total concordant), giving a well-constrained age of  $1053.2 \pm 3.6$  Ma (Fig. 9c, 10b). Sveconorwegian-aged zircon and monazite record strong negative Eu anomalies and enriched HREEs relative to Caledonian-aged populations, suggesting the Sveconorwegian assemblage contained plagioclase. Sveconorwegian-

aged monazite occurs predominantly in the interior of garnet (Fig. 10a), inside the internal boundary defined by fine-grained inclusion trails (Fig. 3d, e). Monazites in garnet rims and in the matrix define a bimodal distribution, comprised of the ~1053 Ma population and a second  $423.2 \pm 2.0$  Ma age peak. This suggests either resetting of monazite or a second period of growth. The incidence of one monazite grain at the edge of garnet (Fig. 10a) may indicate partial resetting of monazite; the garnet side of the monazite grain records Sveconorwegian ages, and the matrix side records Caledonian ages. As discussed by Cuthbert and van Roermund et al. (2011), who reported analogous monazite U–Pb ages in garnet-kyanite gneiss from Fjørtoft, the prevalence of Sveconorwegian-aged monazite within garnet could result from three different scenarios: (1) Sveconorwegian-aged detrital monazite from the sedimentary protolith was reset when it became entrapped by garnet during Scandian UHP metamorphism; (2) monazites record Sveconorwegian-aged garnet growth, and then later diffusional resetting of garnet rim and matrix monazite grains during Scandian metamorphism; or (3), Fjørtoft garnet records two phases of growth, where monazite constrains the age of garnet cores at ~1053 Ma, and new garnet rim growth at ~423 Ma. The prevalence of Sveconorwegian-aged analyses across different studies (Cuthbert & van Roermund, 2011; DesOrmeau et al., 2015; Walczak et al., 2019) that are all within a narrow age bracket and frequently occur as inclusions within garnet is unlikely to reflect a detrital population. If monazites were detrital, an extremely uniform and proximal source would be required. Therefore, it seems likely there are two phases of garnet growth recorded at Fjørtoft: ca. 1053 Ma and ca. 420 Ma. Supporting this, Sveconorwegian-aged Lu–Hf garnet ages occur in NE Yell, Shetland (Walker et al 2020), a terrane that was subsequently incorporated into the Baltica-Laurentia collision with the Norwegian Caledonides; and in a Fjørtoft metapelite study, a Lu–Hf garnet age of  $422.2 \pm 2$  Ma

was constrained (Tual et al., 2020). Tentatively, it is therefore suggested that Fjørtoft garnet cores are Sveconorwegian-aged, whilst rims formed at ca.  $422 \pm 2$  Ma. Similar to Ulsteinvik, Fjørtoft Caledonian zircon, rutile and monazite data are suggestive of an extensive period of (re)crystallisation. Concordant zircon ages range from ca. 449–380 Ma (Fig. 7h), with the oldest exhibiting overall lower REE concentrations and stronger negative Eu anomalies relative to the younger ages (Fig. 8b). Concordant rutile analyses span an identical age range from ca. 449–378 Ma (Fig. 13c, d), and monazite records dates between ca. 438–382 Ma. The Late Ordovician–Early Silurian components of this history are attributed to the imbrication of the Blåhø nappe, a sliver of which exists on the island of Fjørtoft (e.g. Terry et al., 2000a). Monazite Caledonian U–Pb results are split into two populations:  $423.2 \pm 2.0$  Ma and  $385.2 \pm 6.7$  Ma (Fig. 9b, d). The older and more abundant population occurs both as inclusions within garnet rims and the matrix, while the younger population occurs solely within the matrix. Despite the ca. 423 Ma monazites occurring frequently within garnet, each of these grains are connected to the matrix through fractures. This direct interaction with the matrix means that monazite grains may have crystallised in response to fracture-hosted fluid migration (Tartakovsky et al., 2007). As a result, their age may not relate to textural location (Fig. 10b). Both populations exhibit negative Eu anomalies, interpreted as coeval (re)crystallisation with plagioclase. The plagioclase-bearing matrix of the Fjørtoft metapelite is strongly foliated, and in some places protomylonitic. The prevalence of ~423 Ma monazites within this protomylonitic matrix provides convincing evidence for early exhumation of Fjørtoft, promoting the stability of plagioclase. Although the precise onset of Scandian Fjørtoft subduction is not constrained in this study, based on the assumption that Late Ordovician–Early Silurian ages are associated with the imbrication of the Blåhø nappe

and that exhumation had begun by at least  $\sim 423$  Ma, Scandian subduction and exhumation of the Fjørtoft metapelite must have been rapid. The assumed timing of subduction onset within the WGR is 430 Ma (Terry et al., 2000b; Tucker et al., 2004; Kylander-Clark et al., 2007; T. E. Krogh et al., 2011), and applying this to the Fjørtoft metapelite gives a  $\sim 7$  Myr window in which the terrane was subducted and exhumed.

### **Pressure–temperature conditions during metamorphism**

The  $P$ – $T$  conditions calculated from mineral equilibria forward modelling suggest cool thermal gradients were experienced by metapelites at Ulsteinvik (Fig. 15). Based on conservative estimations for the prograde path and minimum peak conditions, the thermal gradient ranges from 30–91 °C/GPa, consistent with conditions during subduction (Brown & Johnson, 2018, 2019).

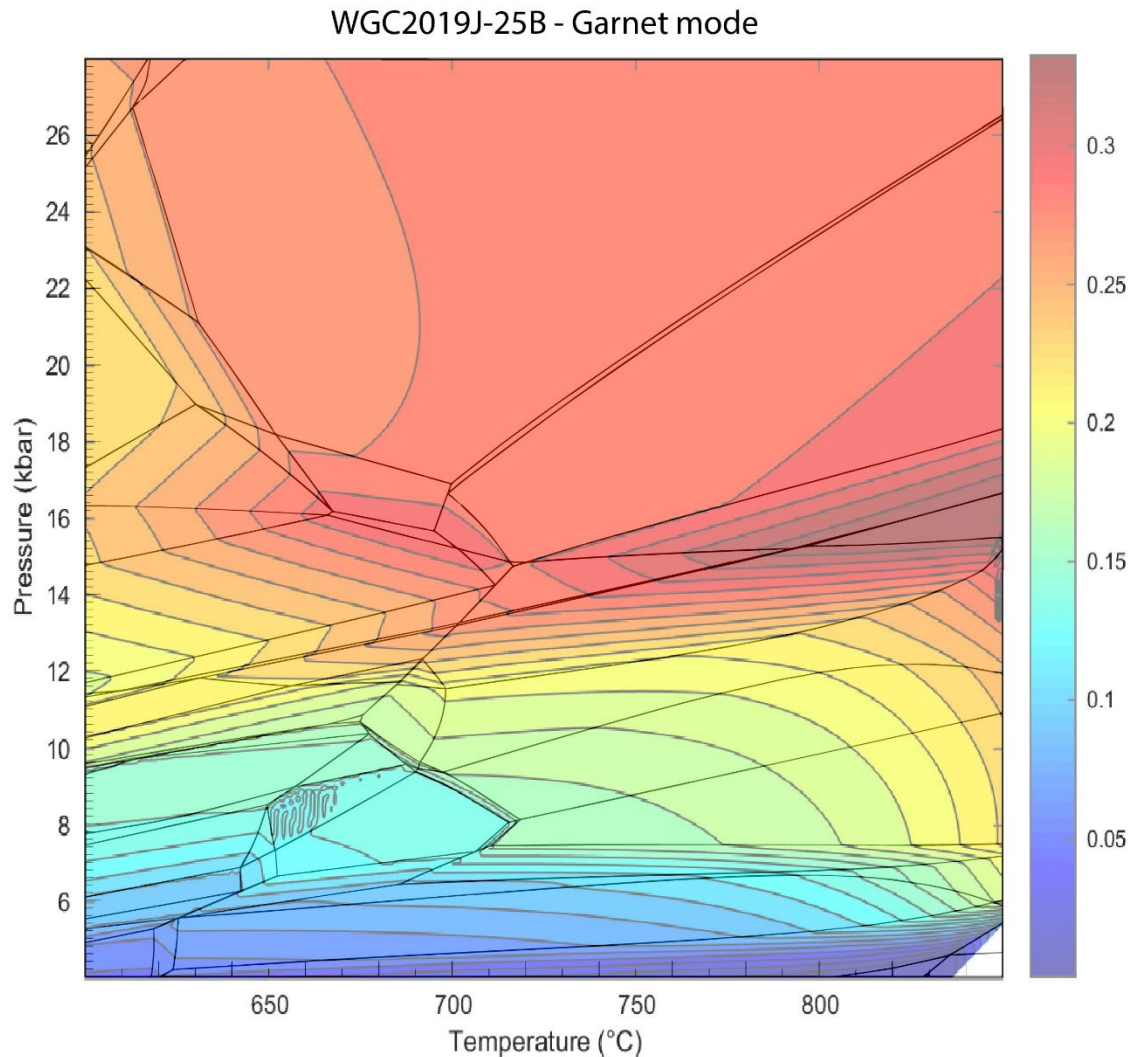
The presence of rutile, muscovite and plagioclase inclusions within garnet are useful to determine a prograde assemblage. The intersection of the base of this field with Zr-in-rutile further constrains the prograde evolution of the rock, inferring that it traversed through conditions of  $\sim 13$  kbar and 690 °C (Fig. 15; Point 1). Garnet is stable throughout the calculated  $P$ – $T$  window (Fig. 15) and should grow during the prograde history. As a result, it would be expected to entrap early prograde inclusions.

Contradictory to this, Zr-in-rutile thermometry conducted on inclusions in garnet would indicate that garnet only began nucleating at high temperatures ( $750.9 \pm 72.2$  °C; Fig. 14d), with the lowest Zr-in-rutile temperature calculated at  $678 \pm 43$  °C. This suggests garnet experienced a degree of ‘overstepping’, where minerals may not immediately grow despite being subject to stable equilibrium conditions (e.g. Castro & Spear, 2016; Spear, 2017). Garnet nucleation has been known to occur after overstepping of up to 80 °C or 4–5 kbar (Wilbur & Ague, 2006; Spear et al., 2014; Castro & Spear, 2016). Lack



of early porphyroblastic garnet growth inhibits constraints for Ulsteinvik's early prograde evolution.

Minimum peak conditions in WGC2019J-25B are interpreted to occur at ~2.9 GPa and 760 °C. Though not directly observed in the rock, the presence of omphacite as a peak mineral is interpreted based upon the crystallisation of fine-grained biotite + plagioclase + quartz textures (Fig. 3g), which likely formed via breakdown of omphacite + phengite + rutile. Quartz mosaics within garnet (Fig. 3i) were possibly formed after coesite decompression (e.g. Smyth, 1977; Enami & Qija, 1990; Mosenfelder & Bohlen, 1997). The potential presence of this UHP mineral is further validated by its record in the neighbouring Hareidland eclogite (e.g. Carswell et al., 2003a). The assigned peak  $P$ - $T$  is a minimum constraint, as it is impossible to constrain how far the sample progressed into the peak coesite-bearing field. Garnet growth primarily occurs during the prograde history and effectively stops after ~1.6 GPa (Fig. 17). Furthermore, the garnet rims are consumed during exhumation and retrogression. As a result, rutile captured inside of garnet can only be used to elucidate the prograde component of Ulsteinvik's history. The absence of an Eu anomaly in Ulsteinvik monazite (Fig. 11A) suggests it grew outside of plagioclase stability until at least 377 Ma (Fig. 9B, D; McLennan, 1989). This adds a time constraint to the Ulsteinvik  $P$ - $T$  path, as it appears the rock did not traverse through retrograde plagioclase-stable fields until after 377 Ma. Based upon this hypothesis, Ulsteinvik must have experienced either a long-lived prograde path and/or stalled in the mantle before its retrograde evolution and remained at  $P$ - $T$  conditions above 16 kbar (Fig. 15; Point 3) until at least 377 Ma. Three distinct retrograde mineral reaction textures were identified: (1) fine-grained intergrown biotite + plagioclase + quartz domains (Fig. 3g); (2) fine-grained cordierite + plagioclase + spinel symplectic coronas (Fig. 3a, b); and (3), partial replacement of kyanite by sillimanite (Fig. 3c). As



**Figure 17: WGC2019J-25B phase diagram coloured by computed garnet mode. Above 16 kbar, garnet mode and thereby garnet growth stalls.**

discussed above, biotite-plagioclase-quartz intergrowths are interpreted as the retrograde product of peak omphacite + phengite + rutile breakdown. Cordierite-plagioclase-spinel coronas are interpreted to form at the expense of garnet + kyanite + biotite reactants, some of which still exist in the current assemblage. Calculation of a single  $P$ - $T$  point was used to constrain retrograde conditions within the Ulsteinvik metapelite at  $\sim 7$  kbar and  $\sim 740$  °C (Fig. 15; Point 4), at which point the rock contains both cordierite and sillimanite. This supports the petrographic observation of cordierite-spinel-plagioclase coronas occasionally consuming retrograde sillimanite.

Decompression during exhumation would have caused minor melting within the rock (Fig. 2c). The lack of K-feldspar within cordierite-spinel reaction textures suggests some melt loss, however this is likely to be volumetrically minor due to the preservation of abundant biotite and the lack of migmatitic character observed in the rock.

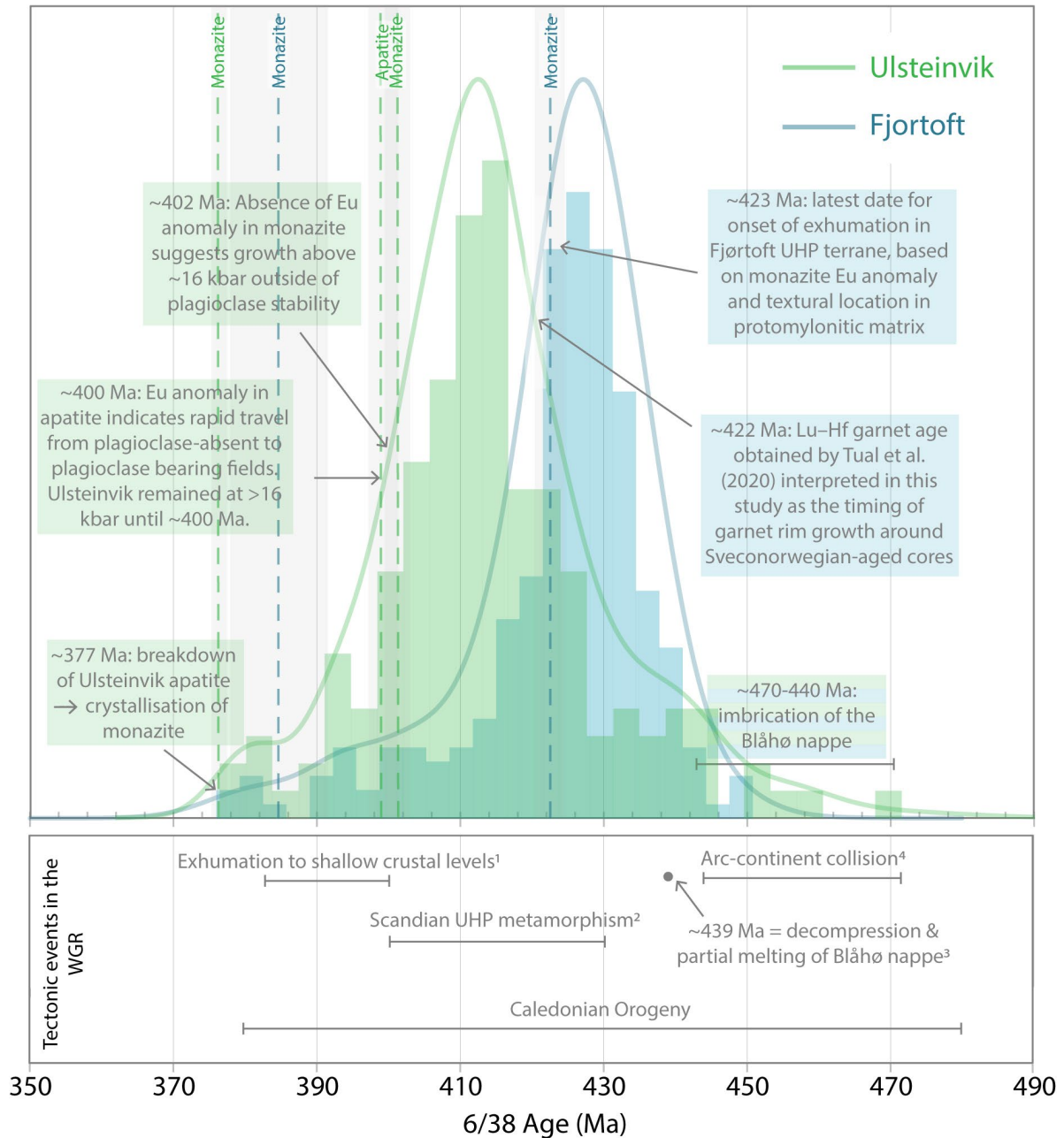
At Fjørtoft, Sveconorwegian-aged monazite occurs frequently inside of garnet inclusion trails (Fig. 3e, f). This means the age of Fjørtoft garnets is ambiguous and makes the estimation of a prograde Caledonian history difficult. Therefore, it is not discussed in this study. Based on the inferred peak assemblage and Zr-in-rutile temperatures, minimum peak conditions at Fjørtoft are interpreted as ~18 kbar and ~750 °C (Fig. 16; Point 1). Diamond has been reported from the Fjørtoft outcrop, implying pressures >3.6 GPa and suggesting extensive reworking of the sampled metapelite. Retrograde rims of biotite around muscovite suggest the Fjørtoft metapelite traversed through conditions of ~11 kbar and ~710 °C (Fig. 16; Point 2).

### **Tectonic implications for the Caledonian evolution of the Western Gneiss Region**

Ulsteinvik and Fjørtoft record protracted and potentially coupled metamorphic histories. Both samples contain U–Pb zircon and monazite ages that correlate with the Sveconorwegian Orogeny, although Fjørtoft preserves a more extensive record. Similarly, both Fjørtoft and Ulsteinvik record a Late Ordovician–Early Silurian peak in zircon and rutile ages (Fig. 18). Ca. 470–440 Ma ages pre-date the onset of Scandian subduction in the WGR (~430 Ma; e.g. Griffin & Brueckner, 1980; Tucker et al., 2004; T. E. Krogh et al., 2011). In Fjørtoft, these ages record its well-known history as a constituent of the Seve-Blåhø nappe, an allochthonous terrane that was imbricated onto the Baltican margin prior to Scandian subduction (ca. 430 Ma; Robinson, 1995; Terry et

al., 2000a; Carswell et al., 2006). The overlap of Ulsteinvik ages with the Fjørtoft age peak suggests the Ulsteinvik metapelite could have also been a constituent of the Blåhø nappe, and may share its pre-Scandian history with the Fjørtoft metapelite. This hypothesis is supported by observations made by Root et al. (2005) regarding similarities in host-rock lithologies between Ulsteinvik and the Blåhø nappe, as well as by age data similar to Ordovician-Silurian dates from this metapelitic study presented by DesOrmeau et al. (2015) in neighbouring eclogitic rocks from Hareidland, Ulsteinvik. The Ulsteinvik and Fjørtoft metapelites are therefore suggested to have both been partially subducted within the Blåhø nappe at ca. 450 Ma and accreted to the base of the upper plate (Majka et al. 2014). These terranes were then imbricated upon the Baltica continent during Scandian subduction at ca. 430 Ma. The fact that both Ulsteinvik and Fjørtoft record Sveconorwegian histories suggests a Baltic provenance for the allochthonous Blåhø nappe, where the sedimentary protolith for these metapelites must have been deposited either within the Baltica continent or proximally in the Iapetus Ocean (Stephens & Gee, 1985; Gee et al., 2013). At some stage during either pre-Scandian subduction, partial(?) exhumation, or imbrication on the Baltican margin, the Blåhø nappe possibly experienced slab tear, separating the Ulsteinvik and Fjørtoft domains. Monazite geochronology and geochemistry within Ulsteinvik and Fjørtoft record different histories during the Scandian phase of the WGR, possibly indicative of this decoupling (Fig. 9, 18). Figure 18 demonstrates the extent of the out of phase relationship between metapelites at Ulsteinvik and Fjørtoft.

At Fjørtoft, a relatively rapid Scandian subduction and exhumation history is proposed. Monazite occurs in two populations (~423 Ma and ~385 Ma; Figure 9B), which both



<sup>1</sup>Andersen et al. (1998), Terry et al. (2000b), Tucket et al. (2004), Hacker (2007), Walsh et al. (2007).  
<sup>2</sup>Griffin & Brueckner (1980), Terry et al. (2000), Tucket et al. (2004), Kylander-Clark et al. (2007), Krogh et al. (2011).  
<sup>3</sup>Majka et al. (2014)  
<sup>4</sup>Andersen & Andresen (1994), Bruckner & van Roermund (2004), Hacker & Gans (2005), Root et al. (2005), Janák et al. (2013a), Majka et al. (2014), Klonowska et al. (2014), DesOrmeau et al. (2015)

**Figure 18: Age distribution for Ulsteinvik (green) and Fjørtoft (blue). Rutile and zircon age data are combined in cumulative age distribution curves, monazite and apatite are indicated by dotted lines and associated error bars. Note that distribution curve heights have been normalised for visual comparison. The plot is annotated based on observations and interpretations made within this study. The bottom panel presents inferred tectonic events that occur within the WGR based on past studies.**

have negative Eu anomalies and therefore crystallised in the presence of plagioclase.

The growth of these monazites in association with a strongly foliated matrix (Fig. 10a)

suggests they crystallised during the retrograde evolution of Fjørtoft. This suggests that

the Fjørtoft metapelite had already experienced UHP metamorphism and begun exhumation by ca. 423 Ma, indicating an early and rapid burial and exhumation relative to the rest of the WGR, where UHP metamorphism is constrained as late as 397 Ma (Kylander-Clark et al., 2007; Kylander-Clark et al., 2009). Contrastingly, Fjørtoft metapelite garnet zoning profiles (Fig. 4f) exhibit compositional diffusion, interpreted as the result of prolonged exposure at (U)HT. This could be attributed to the pre-Scandian component of the Fjørtoft metapelite's history, during the early subduction of the Blåhø nappe. Speculatively, the Blåhø nappe could have experienced slab tear and consequent exhumation, leaving behind the Fjørtoft metapelite and allowing it to reside within the subduction channel for a prolonged period of time.

Based on geochronology, geochemistry and  $P$ - $T$  modelling, the Ulsteinvik metapelite appears to have experienced a comparatively long-lived prograde history and later exhumation relative to the Fjørtoft metapelite. The preservation of Ulsteinvik garnet zoning profiles (Fig. 4c) indicates that the terrane could not have remained in the mantle for longer than ~10 Myr (Caddick et al., 2010). The absence of an Eu anomaly in ~402 Ma monazite (Fig. 9a) and its strong presence in ~400 Ma apatite is interpreted as rapid travel from plagioclase-absent to plagioclase-bearing fields. This suggests that the Ulsteinvik metapelite remained above ~16 kbar until ~400 Ma (Fig. 15; Point 3).

## CONCLUSION

The Western Gneiss Region, Norway offers fascinating insight into the dynamics of continental subduction and emphasises that it is not always a smooth, 'conveyor belt' process. Geochronology, geochemistry and thermometry, along with  $P$ - $T$  forward modelling from the Ulsteinvik and Fjørtoft metapelites supports the following conclusions:

1. Sveconorwegian-ages of ca. 1064–903 Ma were recorded in Fjørtoft, and 1018–998 Ma in Ulsteinvik. The prevalence of this record across both localities, along with the occurrence Sveconorwegian-aged monazite entrapped within garnet is interpreted as supporting a period of Sveconorwegian-growth within the WGR.
2. The Ulsteinvik metapelite records a Late Ordovician-Early Silurian age peak that pre-dates the onset of Scandian UHP subduction. The similarity of this pre-Scandian age peak to ages recorded within the Blåhø nappe on the island of Fjørtoft supports the conclusion made by Root et al. (2005) regarding Ulsteinvik's affinity for the Seve-Blåhø nappe and shared Ordovician-Early Silurian history with Fjørtoft.
3. Negative Eu anomalies within ~423 Ma monazite from the Fjørtoft metapelite suggest crystallisation in the presence of retrograde plagioclase, constraining the beginning of exhumation within Fjørtoft. This indicates that subduction and exhumation were extremely rapid (potentially <7 Myr) within this part of the WGR.
4. Ulsteinvik experienced a long-lived prograde history and potentially rapid growth of retrograde plagioclase based on the lack of negative Eu anomaly in ~402 Ma monazite, and its presence in ~400 Ma apatite. This suggests that Ulsteinvik was at pressures (~16 kbar) that inhibited plagioclase growth until as late as ~402 Ma before rapid exhumation.

## **ACKNOWLEDGMENTS**

I would like to thank my supervisors, Martin Hand and Renée Tamblyn for their unending support, guidance, patience and adaptability throughout the 'unprecedented times' of 2020. I am extremely grateful to the AusIMM, OZ Minerals and Playford Trust organisations for their financial assistance that has allowed me to dedicate myself fully to this project. A huge thank you must be extended to the team at Adelaide

Microscopy: Sarah Gilbert, Aoife McFadden and Benjamin Wade, who have gone well and truly above and beyond this year and without whom this thesis would be very short. Derrick Hasterok is acknowledged for all the effort and time that he has put into coordinating Honours this year. Finally, thank you to my cohort for the endless (long-distance) support and chats, especially to Kelly MacDonald.

## REFERENCES

- ÅHÄLL, K., & CONNELLY, J. N. (2008). Long-term convergence along SW Fennoscandia: 330 m.y. of Proterozoic crustal growth. *Precambrian Research*, 161(3-4), 452-474. doi:10.1016/j.precamres.2007.09.007
- ANDERSEN, T. B., H.B., B., LUX, D. R., & ANDRESEN, A. (1998). The tectonic significance of pre-Scandian <sup>40</sup>Ar/<sup>39</sup>Ar phengite cooling ages in the Caledonides of western Norway. *Journal of the Geological Society, London*, 155, 297-309.
- ANDERSEN, T. B., JAMTVEIT, B., DEWEY, J. F., & SWENSSON, E. (1991). Subduction and exhumation of continental crust: major mechanisms during continent–continent collision and orogenic extensional collapse, a model based on the south Norwegian Caledonides. *Terra Nova*, 3, 303-310.
- AUSTRHEIM, H. (1987). Eclogitization of lower crustal granulites by fluid migration through shear zones. *Earth and Planetary Science Letters*, 81, 221-232.
- BATT, G. E., & BRAUN, J. (1999). The tectonic evolution of the Southern Alps, New Zealand: insights from fully thermally coupled dynamical modelling. *Geophysical Journal International*, 136(2), 403-420. doi:10.1046/j.1365-246X.1999.00730.x
- BAU, M. (1991). Rare-earth mobility during hydrothermal and metamorphic fluid-rock interaction and the significance of the oxidation state of europium. *Chemical Geology*, 93, 219-230. doi:10.1016/0009-2541(91)90115-8
- BECKMAN, V., MÖLLER, C., SÖDERLUND, U., CORFU, F., PALLON, J., & CHAMBERLAIN, K. R. (2014). Metamorphic zircon formation at the transition from gabbro to eclogite in Trollheimen–Surnadalen, Norwegian Caledonides. In: *Corfu, F., Gasser, D., Chew, D.M. (Eds), New Perspectives on the Caledonides of Scandinavia and Related Areas. Geological Society of London Special Publications*, 390, 403-424.
- BINGEN, B., NORDGULEN, Ø., & VIOLA, G. (2008). A four-phase model for the Sveconorwegian orogeny, SW Scandinavia. *Norwegian Journal of Geology*, 88, 43-72.
- BROWN, M. (2014). The contribution of metamorphic petrology to understanding lithosphere evolution and geodynamics. *Geoscience Frontiers*, 5(4), 553-569. doi:10.1016/j.gsf.2014.02.005
- BROWN, M., & JOHNSON, T. (2018). Secular change in metamorphism and the onset of global plate tectonics. *American Mineralogist*, 103(2), 181-196. doi:10.2138/am-2018-6166
- BROWN, M., & JOHNSON, T. (2019). Metamorphism and the evolution of subduction on Earth. *American Mineralogist*, 104(8), 1065-1082. doi:10.2138/am-2019-6956
- BRUECKNER, H. K. (1972). Interpretation of Rb-Sr Ages from the Precambrian and Paleozoic rocks of Southern Norway. *American Journal of Science*, 272, 334-358.



- BRYHNI, I. (1966). Reconnaissance studies of gneisses, ultrabasites, eclogites and anorthosites in outer Nordfjord, western Norway. *Norges Geologiske Undersøkelse*, 241, 68.
- BRYHNI, I., & ANDRÉASSON, P.-G. (1985). Metamorphism in the Scandinavian Caledonides. *D.G. Gee, B.A. Sturt (Eds), The Caledonide Orogen - Scandinavia and Related Areas*, John Wiley and Sons, Chichester, 763-781.
- BUTLER, J. P. (2013). Crustal subduction and the exhumation of (ultra)high-pressure terranes: Constrasting modes with examples from the Alps ad Caledonides. *Unpublished Ph.D. thesis. Dalhousie University, Halifax, N.S.*, 291 pp.
- BUTLER, J. P., JAMIESON, R. A., DUNNING, G. R., PECHA, M. E., ROBINSON, P., & STEENKAMP, H. M. (2018). Timing of metamorphism and exhumation in the Nordøyane ultra-high-pressure domain, Western Gneiss Region, Norway: New constraints from complementary CA-ID-TIMS and LA-ICP-MS geochronology. *Lithos*, 310-311, 153-170. doi:10.1016/j.lithos.2018.04.006
- CADDICK, M. J., KONOPÁSEK, J., & THOMPSON, J. (2010). Preservation of garnet growth zoning and the duration of prograde metamorphism. *Journal of Petrology*, 51(11), 2327–2347. doi:10.1093/petrology/egq059
- CARSON, C. J., POWELL, R., & CLARKE, G. L. (1999). Calculated mineral equilibria for eclogites in CaO-Na<sub>2</sub>O-FeO-MgO-Al<sub>2</sub>O<sub>3</sub>-SiO<sub>2</sub>-H<sub>2</sub>O: application to the Pouébo Terrane, Pam Peninsula, New Caledonia. *Journal of Metamorphic Geology*, 17(1), 9-24. doi:10.1046/j.1525-1314.1999.00177.x
- CARSWELL, D. A., & CUTHBERT, S. J. (2003). Ultrahigh pressure metamorphism in the Western Gneiss Region of Norway. *International Geology Review*, 11, 955-966.
- CARSWELL, D. A., TUCKER, R. D., O'BRIEN, P. J., & KROGH, T. E. (2003). Coesite micro-inclusions and the U/Pb age of zircons from the Hareidland Eclogite in the Western Gneiss Region of Norway. *Lithos*, 67(3-4), 181-190. doi:10.1016/S0024-4937(03)00014-8
- CARSWELL, D. A., TUCKER, R. D., O'BRIEN, P. J., & KROGH, T. E. (2003a). Coesite inclusions and the U–Pb age of zircons from the Hareidland Eclogite in the Western Gneiss Region of Norway. *Lithos*, 67, 181-190.
- CARSWELL, D. A., VAN ROERMUND, H. L. M., & WIGGERS DE VRIES, D. F. (2006). Scandian ultrahigh-pressure metamorphism of Proterozoic basement rocks on Fjørtoft and Otrøy, Western Gneiss Region, Norway. *International Geology Review*, 48(11), 957-977. doi:10.2747/0020-6814.48.11.957
- CASTRO, A., & SPEAR, F. S. (2016). Reaction overstepping and reevaluation of the peak P-T conditions of the Blueschist unit Sifnos, Greece: implications for the Cyclades subduction zone. *International Geology Review*, 59, 548-562. doi:10.1080/00206814.2016.1200499
- CHERNIAK, D. J. (2000). Rare earth element diffusion in apatite. *Geochimica et Cosmochimica Acta*, 64, 3871-3885. doi:10.1016/S0016-7037(00)00467-1
- CHOPIN. (1984). Coesite and pure pyrope in high-grade blueschists of the Western Alps: a first record and some consequences. *Contributions to Mineralogy and Petrology*, 86(2), 107-118. doi:10.1007/BF00381838
- CORFU, F., & ANDERSEN, T. B. (2002). U-Pb ages of the Dalsfjord Complex, SW Norway, and their bearing on the correlation of allochthonous crystalline segments of the Scandinavian Caledonides. *International Journal of Earth Science*, 91, 955-963.
- CORFU, F., AUSTRHEIM, H., & GANZHORN, A. C. (2013). Localized granulite and eclogite facies metamorphism at Flatraket and Kråkeneset, Western Gneiss

- Region: U–Pb data and tectonic implications. *Geological Society of London, Special Publication*, 390, 425-442.
- CUTHBERT, S. J., CARSWELL, D. A., KROGH-RAVNA, E. J., & WAIN, A. (2000). Eclogites and eclogites in the Western Gneiss Region, Norwegian Caledonides. *Lithos*, 52(1-4), 165-195. doi:10.1016/S0024-4937(99)00090-0
- CUTHBERT, S. J., & VAN ROERMUND, H. L. M. (2011). In-situ monazite dating of a microdiamond-bearing gneiss, Fjortoft, Norway: Age pattern in relation to garnet zoning and growth history. *9th International Eclogite Conference 2011*.
- CUTTS, J. A., SMIT, M. A., KOOIJMAN, E., & SCHMITT, M. (2019). Two stage cooling and exhumation of deeply subducted continents. *Tectonics*, 38, 863-877. doi:10.1029/2018TC005292
- DESORMEAU, J. W., GORDON, S. M., KYLANDER-CLARK, A. R. C., HACKER, B. R., BOWRING, S. A., SCHOENE, B., & SAMPERTON, K. M. (2015). Insights into (U)HP metamorphism of the Western Gneiss Region, Norway: A high-spatial resolution and high-precision zircon study. *Chemical Geology*, 414, 138-155.
- DIENER, J. F. A., & POWELL, R. (2012). Revised activity-composition models for clinopyroxene and amphibole. *Journal of Metamorphic Geology*, 30(2), 131-142. doi:10.1111/j.1525-1314.2011.00959.x
- DOBZHINETSAYA, L. F., EIDE, E. A., LARSEN, R. B., STURT, B. A., TRØNNES, R. G., SMITH, D. C., TAYLOR, W. R., & POSUKHOVA, T. V. (1995). Microdiamond in high-grade metamorphic rocks of the Western Gneiss region, Norway. *Geology*, 23(7), 597-600.
- DRANSFIELD, M. (1994). Extensional Exhumation of High-Grade Rocks in Western Norway and the Zaskar Himalaya. *University of Oxford*.
- DROOP, G. T. R. (1987). A general equation for estimating Fe<sup>3+</sup> concentrations in ferromagnesian silicates and oxides from microprobe analyses, using stoichiometric criteria. *Mineralogical Society*, 51(361), 431-435. doi:10.1180/minmag.1987.051.361.10
- ENAMI, M., & QIA, Z. (1990). Quartz pseudomorphs after coesite in eclogites from Shandong province, East China. *American Mineralogist*, 75(3-4), 381-386.
- ERNST, W. G., MARUYAMA, S., & WALLIS, S. (1997). Buoyancy-driven, rapid exhumation of ultrahigh-pressure metamorphosed continental crust. *The National Academy of Sciences*, 94(18), 9532-9537. doi:10.1073/pnas.94.18.9532
- FINGER, F., & KRENN, E. (2007). Three metamorphic monazite generations in a high-pressure rock from the Bohemian Massif and the potentially important role of apatite in stimulating polyphase monazite growth along a PT loop. *Lithos*, 95(1-2), 103-115. doi:10.1016/j.lithos.2006.06.003
- GEE, D. G. (1975). A tectonic model for the central part of the Scandinavian Caledonides. *American Journal of Science*, 275-A, 468-515.
- GJELSVIK, T. (1951). Oversikt over bergartene på Sunnmøre og tilgrensende deler av Nordfjord. *Med geologisk oversiktskart av T. Gjelsvik & Chr. C. Gleditsch. Norges Geologiske Undersøkelse*, 179, 1-45.
- GREEN, E. C. R., WHITE, R. W., DIENER, J. F. A., POWELL, R., HOLLAND, T. J., & PALIN, R. M. (2016). Activity-composition relations for the calculation of partial melting equilibria in metabasic rocks. *Journal of Metamorphic Geology*, 34(9), 845-869. doi:10.1111/jmg.12211
- GRIFFIN, W. L., & BRUECKNER, H. K. (1980). Caledonian Sm-Nd ages and crustal origin for Norwegian eclogites. *Nature*, 285, 319-321. doi:10.1038/285319a0.

- GRIFFIN, W. L., & BRUECKNER, H. K. (1985). REE, Rb-Sr and Sm-Nd studies of Norwegian eclogites. *Chemical Geology*, 52, 249-271.
- HACKER, B. R. (2007). Ascent of the ultrahigh-pressure Western Gneiss Region, Norway. *Convergent Margin Terranes and Associated Regions: A Tribute to W.G. Ernst, M. Cloos, W.D. Carlson, M.C. Gilbert, J.G. Liou, S.S. Soreson*, 171-184.
- HACKER, B. R., ANDERSEN, T. B., JOHNSTON, S., KYLANDER-CLARK, A. R. C., PETERMAN, E. M., WALSH, E. O., & YOUNG, D. J. (2010). High-temperature deformation during continental-margin subduction and exhumation: The ultrahigh-pressure Western Gneiss Region of Norway. *Tectonophysics*, 480, 149-171.
- HACKER, B. R., & GANS, P. B. (2005). Continental collisions and the creation of ultrahigh-pressure terranes: Petrology and thermochronology of nappes in the central Scandinavian Caledonides. *GSA Bulletin*, 117(1/2), 117-134. doi:10.1130/B25549.1
- HACKER, B. R., KELEMAN, P. B., & BEHN, M. D. (2011). Differentiation of the continental crust by relamination. *Earth and Planetary Science Letters*, 307(3-4), 501-516. doi:10.1016/j.epsl.2011.05.024
- HACKER, B. R., KYLANDER-CLARK, A. R. C., HOLDER, R., ANDERSEN, T. B., PETERMAN, E. M., WALSH, E. O., & MUNNIKHUIS, J. K. (2015). Monazite response to ultrahigh-pressure subduction from U-Pb dating by laser ablation split stream. *Chemical Geology*, 409, 28-41. doi:10.1016/j.chemgeo.2015.05.008
- HAND, M. (2020). [Calculation of a retrograde P-T point].
- HELLSTROM, J., PATON, C., WOODHEAD, J., & HERGT, J. (2008). Iolite: Software for spatially resolved LA-(quad and MC) ICPMS analysis. *Mineralogical Association of Canada short course series*, 40, 343-348.
- HOLDER, R. M., HACKER, B. R., KYLANDER-CLARK, A. R. C., & COTTLE, J. M. (2015). Monazite trace-element and isotopic signatures of (ultra)high-pressure metamorphism: Examples from the Western Gneiss Region, Norway. *Chemical Geology*, 409, 99-111. doi:10.1016/j.chemgeo.2015.04.021
- HOLLAND, T. J., BAKER, J., & POWELL, R. (1998). Mixing properties and activity-composition relationships of chlorites in the system MgO-FeO-Al<sub>2</sub>O<sub>3</sub>-SiO<sub>2</sub>-H<sub>2</sub>O. *European Journal of Mineralogy*, 10(3), 395-406. doi:10.1127/ejm/10/3/0395
- HOLLAND, T. J., GREEN, E. C. R., & POWELL, R. (2018). Melting of peridotites through to granites: A simple thermodynamic model in the system KNCFMASHTOCr. *Journal of Petrology*, 59(5), 881-900. doi:10.1093/petrology/egy048
- HOLLAND, T. J., & POWELL, R. (1990). An enlarged and updated internally consistent thermodynamic dataset with uncertainties and correlations: the system K<sub>2</sub>O-Na<sub>2</sub>O-CaO-MgO-MnO-FeO-Fe<sub>2</sub>O<sub>3</sub>-Al<sub>2</sub>O<sub>3</sub>-TiO<sub>2</sub>-SiO<sub>2</sub>-C-H<sub>2</sub>-O<sub>2</sub>. *Journal of Metamorphic Geology*, 8(1), 89-124. doi:10.1111/j.1525-1314.1990.tb00458.x
- HOLLAND, T. J., & POWELL, R. (2003). Activity-composition relations for phases in petrological calculations: an asymmetric multicomponent formulation. *Contributions to Mineralogy and Petrology*, 145, 492-501. doi:10.1007/s00410-003-0464-z
- HOLLAND, T. J., & POWELL, R. (2011). An improved and extended internally consistent thermodynamic dataset for phases of petrological interest, involving a new

- equation of state for solids. *Journal of Metamorphic Geology*, 29(3), 333-383.  
doi:10.1111/j.1525-1314.2010.00923.x
- JACKSON, S. E., PEARSON, N. J., GRIFFIN, W. L., & BELOUSOVA, E. A. (2004). The application of laser ablation-inductively coupled plasma-mass spectrometry to in situ U–Pb zircon geochronology. *Chemical Geology*, 211(1), 47-69.
- JENNINGS, E. S., & HOLLAND, T. J. (2015). A simple thermodynamic model for melting of peridotite in the system NCFMASOCr. *Journal of Petrology*, 56(5), 869-892.  
doi:10.1093/petrology/egv020
- JOHNSON, T. E., & WHITE, R. W. (2011). Phase equilibrium constrains on conditions of granulite-facies metamorphism at Scourie, NW Scotland. *Journal of the Geological Society*, 168(1), 147-158. doi:10.1144/0016-76492010-069
- JOLIVET, L., RAIMBOURG, H., LABROUSSE, L., AVIGAD, D., Y., L., AUSTRHEIM, H., & ANDERSEN, T. B. (2005). Softening triggered by eclogitisation, the first step toward exhumation during continental subduction. *Earth and Planetary Science Letters*, 237(3-4), 532-547.
- KELSEY, D. E., & HAND, M. (2015). On ultrahigh temperature crustal metamorphism: phase equilibria, trace element thermometry, bulk composition, heat sources, timescales and tectonic settings. *Geoscience Frontiers*, 6(3), 311-356.
- KOHN, M. J. (2020). A refined zirconium-in-rutile thermometer. *American Mineralogist*, 105(6), 963-971. doi:10.2138/am-2020-7091
- KOOIJMAN, E., MEZGER, K., & BERNDT, J. (2010). Constraints on the U-Pb systematics of metamorphic rutile from in situ LA-ICP-MS analysis. *Earth and Planetary Science Letters*, 293, 321-330. doi:10.1016/j.epsl.2010.02.047
- KORNPROBST, J. (2002). *Metamorphic Rocks and Their Geodynamic Significance* (Vol. 12): Springer Netherlands.
- KRABBENDAM, M., WAIN, A., & ANDERSEN, T. B. (2000). Pre-Caledonian granulite and gabbro enclaves in the Western Gneiss Region, Norway: indications of incomplete transition at high pressure. *Geological Magazine*, 137, 235-255.
- KROGH, E. J. (1977). Evidence for Precambrian continent-continent collision in western Norway. *Nature*, 267, 17-19.
- KROGH, T. E., KAMO, S. L., ROBINSON, P., TERRY, M. P., & KWOK, K. (2011). U–Pb zircon geochronology of eclogites from the Scandian Orogen, northern Western Gneiss Region, Norway: 14–20 million years between eclogite crystallization and return to amphibolite facies conditions. *Canadian Journal of Earth Sciences*, 48(2), 441-472.
- KROGSTAD, E., & WALKER, R. J. (1994). High closure temperatures of the U-Pb system in large apatites from the Tin Mountain pegmatite, Black Hills, South Dakota, USA. *Geochimica et Cosmochimica Acta*, 58(18), 3845-3853.  
doi:10.1016/0016-7037(94)90367-0
- KYLANDER-CLARK, A. R. C., HACKER, B. R., & JOHNSON, C. M. (2009). Slow subduction of a thick ultrahigh-pressure terrane. *Tectonics*, 28(2), TC2003.  
doi:10.1029/2007TC002251
- KYLANDER-CLARK, A. R. C., HACKER, B. R., JOHNSON, C. M., BEARD, B. L., MAHLEN, N. J., & LAPEN, T. J. (2007). Coupled Lu-Hf and Sm-Nd geochronology constrains prograde and exhumation histories of high- and ultrahigh-pressure eclogites from western Norway. *Chemical Geology*, 242, 137-154.  
doi:10.1016/j.chemgeo.2007.03.006
- KYLANDER-CLARK, A. R. C., HACKER, B. R., & MATTINSON, J. M. (2008). Slow exhumation of UHP terranes: Titanite and rutile ages of the Western Gneiss

- Region, Norway. *Earth and Planetary Science Letters*, 272, 531-540.  
doi:10.1016/j.epsl.2008.05.019
- LABROUSSE, L., JOLIVET, L., ANDERSEN, T. B., AGARD, P., HÉBERT, R., MALUSKI, H., & SCHÄRER, U. (2004). Pressure-temperature-time deformation history of the exhumation of ultra-high pressure rocks in the Western Gneiss Region, Norway. *Special Paper of the Geological Society of America*, 380. doi:10.1130/0-8137-2380-9.155
- LANARI, P., FERRERO, S., GONCALVES, P., & GROSCH, E. G. (2019). Metamorphic geology: progress and perspectives. *Metamorphic Geology: Microscale to Mountain Belts*, 478, 1-12. doi:10.1144/SP478-2018-186
- LUVIZOTTO, G. L., & ZACK, T. (2009). Nb and Zr behavior in rutile during high-grade metamorphism and retrogression: an example from the Ivrea–Verbano Zone. *Chemical Geology*, 261(3-4), 303-317. doi:10.1016/j.chemgeo.2008.07.023
- MAJKA, J., ROSÉN, Å., JANÁK, M., FROITZHEIM, N., KLONOWSKA, I., MANECKI, M., SASINKOVÁ, V., & YOSHIDA, K. (2014). Microdiamond discovered in the Seve Nappe (Scandinavian Caledonides) and its exhumation by the "vacuum-cleaner" mechanism. *Geology*, 42(12), 1107-1110. doi:10.1130/G36108.1
- MCLENNAN, S. M. (1989). Rare earth elements in sedimentary rocks: Influence of provenance and sedimentary processes. *Reviews in Mineralogy*, 21, 169-200. doi:10.1515/9781501509032-010
- MOSENFELDER, J. L., & BOHLEN, S. R. (1997). Kinetics of the coesite to quartz transformation. *Earth and Planetary Science Letters*, 153(1-2), 133-147. doi:10.1016/S0012-821X(97)00159-3
- MYSEN, B. O., & HEIER, K. S. (1972). Petrogenesis of eclogites in high-grade metamorphic gneisses exemplified by the Hareidland eclogite, west Norway. *Contributions to Mineralogy and Petrology*, 36, 73-94.
- NANCE, D. R., & MURPHY, B. J. (2013). Origins of the supercontinent cycle. *Geoscience Frontiers*, 4(4), 439-448. doi:10.1016/j.gsf.2012.12.007
- PALIN, R. M., WHITE, R. W., & GREEN, E. C. R. (2016a). Partial melting of metabasic rocks and the generation of tonalitic-trondhjemitic-granodiorite (TTG) crust in the Archaean: Constraints from phase equilibrium modelling. *Precambrian Research*, 287, 73-90. doi:10.1016/j.precamres.2016.11.001
- PATON, C., HELLSTROM, J., PAUL, B., WOODHEAD, J., & HERGT, J. (2011). Iolite: Freeware for the visualisation and processing of mass spectrometric data. *Journal of Analytical Atomic Spectrometry*, 26(12), 2508-2518.
- PAYNE, J. L., HAND, M., BAROVICH, K., & WADE, B. (2008). Temporal constraints on the timing of high-grade metamorphism in the northern Gawler Craton: implications for assembly of the Australian Proterozoic. *Australian Journal of Earth Sciences*, 55(5), 623-640.
- PEARCE, M. A., WHITE, A., & GAZLEY, M. (2016). TCIInvestigator. v3. CSIRO. Software Collection. doi:10.4225/08/56B82163D956B
- RAPP, R. P., & WATSON, E. B. (1995). Dehydration melting of metabasalt at 8-32 kbar: implications for continental growth and crust-mantle recycling. *Journal of Petrology*, 36(4), 891-931. doi:10.1093/petrology/36.4.891
- REBAY, G., POWELL, R., & DIENER, J. F. A. (2010). Calculated phase equilibria for a MORB composition in a P-T range, 450-650°C and 18-28 kbar: the stability of eclogite. *Journal of Metamorphic Geology*, 28(6), 635-645. doi:10.1111/j.1525-1314.2010.00882.x

- ROBERTS, D. (2002). The Scandinavian Caledonides: event chronology, palaeogeographic settings and likely modern analogues. *Tectonophysics*, 365, 283-299. doi:10.1016/S0040-1951(03)00026-X
- ROBERTS, D. (2003). The Scandinavian Caledonides: event chronology, palaeogeographic settings and likely modern analogues. *Tectonophysics*, 365, 283-299. doi:10.1016/S0040-1951(03)00026-X
- ROBINSON, P. (1995). Extension of Trollheimen tectono-stratigraphic sequence in deep synclines near Molde and Brattvåg, Western Gneiss Region, southern Norway. *Norsk Geologisk Tidsskrift*, 75, 181-198.
- ROOT, D. B., HACKER, B. R., GANS, P. B., DUCEA, M. N., EIDE, E. A., & MOSENFELDER, J. L. (2005). Discrete ultrahigh-pressure domains in the Western Gneiss Region, Norway: implications for formation and exhumation. *Journal of Metamorphic Geology*, 23, 45-61. doi:10.1111/j.1525-1314.2005.00561.x
- ROOT, D. B., HACKER, B. R., MATTINSON, J. M., & WOODEN, J. L. (2004). Zircon geochronology and ca. 400 Ma exhumation of Norwegian ultrahigh-pressure rocks: an ion microprobe and chemical abrasion study. *Earth and Planetary Science Letters*, 228, 325-341.
- SCHOENE, B., & BOWRING, S. A. (2006). U–Pb systematics of the McClure Mountain syenite: thermochronological constraints on the age of the  $^{40}\text{Ar}/^{39}\text{Ar}$  standard MMhb. *Contributions to Mineralogy and Petrology*, 151, 615-630. doi:10.1007/s00410-006-0077-4
- SIZOVA, E., HAUZENBERGER, C., FRITZ, H., FARYAD, S. W., & GERYA, T. (2019). Late orogenic heating of (ultra)high pressure rocks: Slab rollback vs. slab breakoff. *Geosciences*, 9(12), 499. doi:10.3390/geosciences9120499
- SLÁMA, J., KOŠLER, J., CONDON, D. J., CROWLEY, J. L., GERDES, A., HANCHAR, J. M., HORSTWOOD, M. S. A., MORRIS, G. A., NASDALA, L., NORBERG, N., SCHALTEGGER, U., SCHOENE, B., TUBRETT, M. N., & WHITEHOUSE, M. J. (2008). Plešovice zircon—a new natural reference material for U–Pb and Hf isotopic microanalysis. *Chemical Geology*, 249(1-2), 1-35. doi:10.1016/j.chemgeo.2007.11.005
- SMITH, D. C. (1984). Coesite in clinopyroxene in the Caledonides and its implications for geodynamics. *Nature*, 310, 641-644.
- SMITH, D. C., & GODARD, G. (2013). A Raman spectroscopic study of diamond and disordered  $\text{sp}^3$ -carbon in the coesite-bearing Straumen Eclogite Pod, Norway. *Journal of Metamorphic Geology*, 31(1), 19-33.
- SMYE, A. J., GREENWOOD, T. J., & HOLLAND, T. J. (2010). Garnet-chloritoid-kyanite assemblages: eclogite facies indicators of subduction constraints in orogenic belts. *Journal of Metamorphic Geology*, 28(7), 753-768. doi:10.1111/j.1525-1314.2010.00889.x
- SMYTH, J. R. (1977). Quartz pseudomorphs after coesite. *American Mineralogist*, 63(7-8), 828-830.
- SOBOLEV, N. V., & SHATSKY, V. S. (1990). Diamond inclusions in garnets from metamorphic rocks: a new environment of diamond formation. *Nature*, 343, 742-746.
- SPEAR, F. S. (2017). Garnet growth after overstepping. *Chemical Geology*, 466, 491-499. doi:10.1016/j.chemgeo.2017.06.038
- SPEAR, F. S., THOMAS, J. B., & HALLETT, B. W. (2014). Overstepping the garnet isograd: a comparison of QuiG barometry and thermodynamic modelling. *Contributions to Mineralogy and Petrology*, 168(3), 1-15. doi:10.1007/s00410-014-1059-6

- SPENGLER, D., VAN ROERMUND, H. L. M., DRURY, M. R., OTTOLINI, L., MASON, R. D., & DAVIES, G. R. (2006). Deep origin and hot melting of an Archaean orogenic peridotite massif in Norway. *Nature*, *440*(13), 913-917.
- TARTAKOVSKY, A. M., MEAKIN, P., SCHEIBE, T. D., & WOOD, B. D. (2007). A smoothed particle hydrodynamics model for reactive transport and mineral precipitation in porous and fractured porous media. *Water resources research*, *43*(5). doi:10.1029/2005WR004770
- TERRY, M. P., ROBINSON, P., HAMILTON, M. A., & JERCINOVIC, M. J. (2000b). Monazite geochronology of UHP and HP metamorphism, deformation, and exhumation, Nordøyane, Western Gneiss Region, Norway. *American Mineralogist*, *85*, 1651-1664.
- TERRY, M. P., ROBINSON, P., & KROGH RAVNA, E. J. (2000a). Kyanite eclogite thermobarometry and evidence for thrusting of UHP over HP metamorphic rocks, Nordøyane, Western Gneiss Region, Norway. *American Mineralogist*, *85*, 1637-1650.
- THOMPSON, J., MEFFRE, S., MAAS, R., KAMENETSKY, V., KAMENETSKY, M., GOEMANN, K., EHRIG, K., & DANYUSHEVSKY, L. (2016). Matrix effects in Pb/U measurements during LA-ICP-MS analysis of the mineral apatite. *Journal of Analytical Atomic Spectrometry*, *31*(6), 1206-1215.
- THOMSON, S. N., GEHRELS, G. E., RUIZ, J., & BUCHWALDT, R. (2012). Routine low-damage apatite U-Pb dating using laser ablation–multicollector–ICPMS. *Geochemistry, Geophysics, Geosystems*, *13*(2). doi:10.1029/2011GC003928
- TUAL, L., SMIT, M. A., KOOIJIMAN, E., & SCHMITT, M. (2020). Comparative chronology of garnet, zircon and monazite in (ultra)high-temperature and -pressure rocks. *Goldschmidt Conference, Abstract*. doi:10.46427/gold2020.2630
- TUCKER, R. D., KROGH, T. E., & RÅHEIM, A. (1990). Proterozoic evolution and age-province boundaries in the central part of the Western Gneiss Region, Norway. Results of U-Pb dating of accessory minerals from Trondheimsfjord to Geiranger. In: Gower, C.F., Ryan, A.B., Rivers, T. (Eds.), *Mid-Proterozoic Laurentia–Baltica. Geological Association of Canada, Special Paper 38*, 149-173.
- TUCKER, R. D., ROBINSON, P., SOLLI, A., GEE, D. G., THORSNES, T., KROGH, T. E., NORDGULEN, Ø., & BICKFORD, M. E. (2004). Thrusting and extension in the Scandian hinterland, Norway: new U–Pb ages and tectonostratigraphic evidence. *American Journal of Science*, *304*(6), 477-532.
- VAN ROERMUND, H. L. M., CARSWELL, D. A., DRURY, M. R., & HEIJBOER, T. C. (2002). Microdiamonds in a megacrystic garnet websterite pod from Bardane on the island of Fjørtoft, western Norway: Evidence for diamond formation in mantle rocks during deep continental subduction. *Geology*, *30*(11), 959-962.
- VAN ROERMUND, H. L. M., & DRURY, M. R. (1998). Ultra-high pressure (P>6 GPa) garnet peridotites in Western Norway: exhumation of mantle rocks from >185km depth. *Terra Nova*, *10*, 295-301.
- VRIJMOED, J. C., SMITH, D. C., & VAN ROERMUND, H. L. M. (2008). Raman confirmation of microdiamond in the Svartberget Fe-Ti type garnet peridotite, Western Gneiss Region, Western Norway. *Terra Nova*, *20*(4), 295-301.
- VRIJMOED, J. C., VAN ROERMUND, H. L. M., & DAVIS, G. R. (2006). Evidence for diamond-grade ultrahigh-pressure metamorphism and fluid interaction in the Svartberget Fe–Ti garnet peridotite–websterite body, Western Gneiss Region, Norway. *Mineralogy and Petrology*, *88*, 381-405.

- WAIN, A. (1997). New evidence for coesite in eclogite and gneisses: defining an ultrahigh-pressure province in the Western Gneiss Region of Norway. *Geology*, 25, 927-930.
- WALCZAK, K., CUTHBERT, S., KOOIJMAN, E., MAJKA, J., & SMIT, M. A. (2019). U-Pb zircon age dating of diamond-bearing gneiss from Fjortoft reveals repeated burial of the Baltoscandian margin during the Caledonian Orogeny. *Geological Magazine*, 156, 1949-1964. doi:10.1017/S0016756819000268
- WALSH, E. O., & HACKER, B. R. (2004). The fate of subducted continental margins: two-stage exhumation of the high-pressure to ultrahigh-pressure Western Gneiss complex, Norway. *Journal of Metamorphic Geology*, 22, 671-689.
- WALSH, E. O., HACKER, B. R., GANS, P. B., WONG, M. S., & ANDERSEN, T. B. (2013). Crustal exhumation of the Western Gneiss region UHP terrane, Norway:  $^{40}\text{Ar}/^{39}\text{Ar}$  thermochronology and fault-slip analysis. *Tectonophysics*, 608, 1159-1179. doi:10.1016/j.tecto.2013.06.030
- WALSH, E. O., HACKER, B. R., GROVE, M., GANS, P. B., & GEHRELS, G. (2007). Timing the exhumation of (ultra)high-pressure rocks across the Western Gneiss Region, Norway. *Geological Society of America Bulletin*, 119, 289-301.
- WEILL, D. F., & DRAKE, M. J. (1973). Europium anomaly in plagioclase feldspar: Experimental results and semiquantitative model. *Science*, 180(4090), 1059-1060. doi:10.1126/science.180.4090.1059
- WHITE, R. W., POWELL, R., HOLLAND, T. J., JOHNSON, T. E., & GREEN, E. C. R. (2014). New mineral activity-composition relations for thermodynamic calculations in metapelitic systems. *Journal of Metamorphic Geology*, 32(3), 261-286. doi:10.1111/jmg.12071
- WHITE, R. W., POWELL, R., HOLLAND, T. J., & WORLEY, B. A. (2000). The effect of  $\text{TiO}_2$  and  $\text{Fe}_2\text{O}_3$  on metapelitic assemblages at greenschist and amphibolite facies conditions: mineral equilibria calculations in the system  $\text{K}_2\text{O}-\text{FeO}-\text{MgO}-\text{Al}_2\text{O}_3-\text{SiO}_2-\text{H}_2\text{O}-\text{TiO}_2-\text{Fe}_2\text{O}_3$ . *Journal of Metamorphic Geology*, 18(5), 497-511. doi:10.1046/j.1525-1314.2000.00269.x
- WHITE, R. W., POWELL, R., & JOHNSON, T. E. (2014). The effect of Mn on mineral stability in metapelites revisited: new a-x relations for manganese-bearing minerals. *Journal of Metamorphic Geology*, 32(8), 809-828. doi:10.1111/jmg.12095
- WIEDENBECK, M., ALLE, P., CORFU, F., GRIFFIN, W. L., MEIER, M., OBERLI, F., VON QUADT, A., RODDICK, J. C., & SPIEGEL, W. (1995). Three natural zircon standards for U-Th-Pb, Lu-Hf, trace element and REE analyses. *Geostandards Newsletter*, 19(1), 1-23. doi:10.1111/j.1751-908X.1995.tb00147.x
- WILBUR, D. E., & AGUE, J. J. (2006). Chemical disequilibrium during garnet growth: Monte Carlo simulations of natural crystal morphologies. *Geology*, 34(8), 689-692. doi:10.1130/G22483.1
- YOUNG, D. J., HACKER, B. R., ANDERSEN, T. B., & CORFU, F. (2007). Prograde amphibolite facies to ultrahigh-pressure transition along Nordfjord, western Norway: implications for exhumation tectonics. *Tectonics*, 26(1).
- ZACK, T., STOCKLI, D. F., LUVIZOTTO, G. L., BARTH, M. G., BELOUSOVA, E. A., WOLFE, M. R., & HINTON, R. W. (2011). In situ U-Pb rutile dating by LA-ICP-MS: 208Pb correction and prospects for geological applications. *Contributions to Mineralogy and Petrology*, 162(3), 515-530. doi:10.1007/s00410-011-0609-4



## APPENDIX 1: WHOLE-ROCK GEOCHEMISTRY

Samples were crushed at the University of Adelaide using a tungsten carbide ring mill and then delivered to Bureau Veritas for analysis. Hydrofluoric, nitric, hydrochloric and perchloric acids were used to digest and reflux samples. Zn was determined through Inductively Coupled Plasma Mass Spectrometry (ICP–MS). Cu and Ni were calculated by Inductively Coupled Plasma Optical Emission Spectrometry (ICP–OES). Aliquots of each sample were then fused with lithium metaborate in a PT crucible at high temperature. The resultant fused glass was then digested in nitric acid, causing the complete dissolution of most minerals, with volatile elements being lost at high fusion temperatures. ICP–OES was used to determine Al<sub>2</sub>O<sub>3</sub>, CaO, Cr, Fe<sub>2</sub>O<sub>3</sub>, K<sub>2</sub>O, MgO, MnO, Na<sub>2</sub>O, P<sub>2</sub>O<sub>5</sub>, SiO<sub>2</sub>, TiO<sub>2</sub>, and V. Following digestion in hydrochloric and hydrofluoric acids, ICP-MS was used to determine Ba, Ce, Co, Ga, La, Nb, Rb, Sr, Th, U, Y and Zr.

IDENT	Ag	Al2O3	As	Ba	Be	Bi	CaO	Cd	Co	Cr	Cs	Cu	Fe2O3	Ga
<b>UNITS</b>	ppm	%	ppm	ppm	ppm	ppm	%	ppm	ppm	ppm	ppm	ppm	%	ppm
<b>SCHEME</b>	MA102	LB101	MA102	MA101	MA102	MA102	LB101	MA102	MA102	LB101	MA102	MA102	LB101	LB102
<b>DETECTION LIMIT</b>	0.2	0.01	1	2	0.5	0.1	0.01	0.5	1	20	0.1	1	0.01	1
<b>WGC 2019J_25B-1</b>	<0.2	15.3	<1	48	1	<0.1	2.77	<0.5	24	420	3.1	66	8.62	14
<b>WGC 2019J_25B-2</b>	<0.2	17.3	<1	136	1.5	<0.1	3.29	<0.5	24	360	3.5	88	9.12	23
<b>WGC 2019J_27</b>	<0.2	18.2	<1	566	<0.5	<0.1	1.76	<0.5	25	460	0.4	32	9.02	24
<b>WGC 2019J_29</b>	<0.2	19.3	<1	640	<0.5	<0.1	1.34	<0.5	25	300	0.7	33	10.1	26
<b>WGC 2019J_30</b>	<0.2	27.2	<1	204	<0.5	<0.1	2.41	<0.5	40	420	0.1	80	18.2	32
<b>WGC 2019J_31A</b>	<0.2	21.5	<1	538	<0.5	<0.1	1.05	<0.5	27	380	0.5	53	11.5	28
<b>WGC 2019J_31B</b>	<0.2	22.1	<1	560	<0.5	<0.1	0.99	<0.5	28	520	0.5	43	11.6	28

## APPENDIX 2: EXTENDED EPMA METHODS AND RESULTS

Wavelength Dispersive Spectrometers (WDS) at Adelaide Microscopy were used to analyse major oxides (SiO<sub>2</sub>, ZrO<sub>2</sub>, TiO<sub>2</sub>, Cr<sub>2</sub>O<sub>3</sub>, Al<sub>2</sub>O<sub>3</sub>, FeO, MnO, MgO, CaO, P<sub>2</sub>O<sub>5</sub>, Na<sub>2</sub>O, K<sub>2</sub>O, BaO, NiO, F and Cl). Energy Dispersive Spectrometers (EDS) were used to obtain qualitative x-ray compositional maps for major elements in garnet and cordierite-spinel reaction textures (Al, Ca, Fe, K, Mg, Mn, Na, P, Si and Ti).

<b>WGC2019J-25B</b>					
<b>Oxides</b>	<b>Garnet core</b>	<b>Garnet rim</b>	<b>Plagioclase</b>	<b>Spinel</b>	<b>Biotite</b>
<b>SiO<sub>2</sub></b>	38.59	38.61	52.73	0.00	36.15
<b>TiO<sub>2</sub></b>	0.03	0.01	0.00	0.03	3.01
<b>Al<sub>2</sub>O<sub>3</sub></b>	22.05	22.18	30.55	60.55	17.22
<b>Cr<sub>2</sub>O<sub>3</sub></b>	0.03	0.03	0.00	0.27	0.09
<b>FeO</b>	24.38	25.21	0.08	28.23	14.99
<b>MnO</b>	0.53	0.75	0.00	0.14	0.03
<b>MgO</b>	7.45	7.91	-0.01	8.79	13.06
<b>ZnO</b>	-	-	0.00	1.78	0.00
<b>CaO</b>	7.23	5.68	12.71	0.17	0.00
<b>Na<sub>2</sub>O</b>	0.01	0.01	4.40	0.00	0.23
<b>K<sub>2</sub>O</b>	-	-	0.05	0.00	9.00
<b>Cl</b>	0.00	0.00	0.00	0.00	0.00
<b>F</b>	0.01	0.01	0.00	0.00	0.00
<b>H<sub>2</sub>O</b>	0.00	0.00	0.00	0.00	3.96
<b>Total</b>	<b>100.31</b>	<b>100.40</b>	<b>100.51</b>	<b>99.96</b>	<b>97.75</b>

<b>WGC2019J-25B</b>					
<b>Cations</b>	<b>Garnet core</b>	<b>Garnet rim</b>	<b>Plagioclase</b>	<b>Spinel</b>	<b>Biotite</b>
<b>Si</b>	2.96	2.96	2.37	0.00	2.68
<b>Ti</b>	0.00	0.00	0.00	0.00	0.17
<b>Al</b>	1.99	2.00	1.63	1.95	1.50
<b>Cr</b>	0.00	0.00	0.00	0.01	0.01
<b>Fe<sup>3+</sup></b>	0.08	0.07	0.00	0.05	0.45
<b>Fe<sup>2+</sup></b>	1.48	1.54	0.00	0.60	0.47
<b>Mn<sup>2+</sup></b>	0.03	0.05	0.00	0.00	0.00
<b>Mg</b>	0.85	0.90	0.00	0.36	1.44
<b>Zn</b>	0.00	0.00	0.00	0.04	0.00
<b>Ca</b>	0.59	0.47	0.62	0.01	0.00
<b>Na</b>	0.00	0.00	0.38	0.00	0.03
<b>K</b>	0.00	0.00	0.00	0.00	0.85
<b>Cl</b>	0.00	0.00	0.00	0.00	0.00
<b>F</b>	0.00	0.00	0.00	0.00	0.00
<b>OH-</b>	0.00	0.00	0.00	0.00	2.00

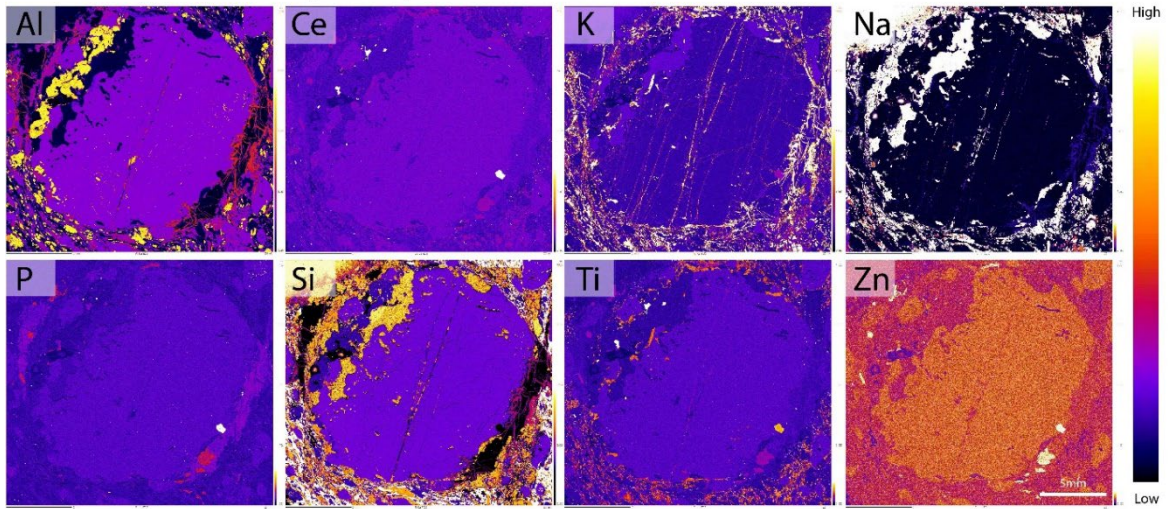
WGC2019J-25B reaction textures						
Oxides	Garnet	Spinel	Biotite	Plagioclase	Cordierite	Ilmenite
<b>SiO2</b>	38.39	0.07	36.41	62.07	49.27	0.09
<b>TiO2</b>	0.00	0.00	3.76	0.00	0.00	46.46
<b>Al2O3</b>	22.15	58.75	17.13	24.37	33.59	0.17
<b>Cr2O3</b>	0.00	0.27	0.14	0.00	0.00	0.09
<b>FeO</b>	28.79	32.36	15.88	0.06	5.42	51.90
<b>MnO</b>	1.35	0.16	0.00	0.00	0.00	0.27
<b>MgO</b>	6.54	5.74	12.67	0.00	9.90	0.47
<b>ZnO</b>	3.69	0.00	0.00	5.51	0.00	0.00
<b>CaO</b>	0.00	0.00	0.16	8.44	0.00	0.00
<b>Na2O</b>	0.00	0.00	9.37	0.12	0.00	0.00
<b>K2O</b>	0.00	0.00	0.00	0.00	0.00	0.00
<b>Cl</b>	0.00	0.00	0.00	0.00	0.00	0.00
<b>F</b>	0.00	0.00	0.00	0.00	0.00	0.00
<b>H2O</b>	0.00	0.00	4.10	0.00	0.00	0.00
<b>Total</b>	<b>100.89</b>	<b>97.35</b>	<b>99.62</b>	<b>100.56</b>	<b>98.18</b>	<b>99.44</b>

WGC2019J-25B reaction textures						
Cations	Garnet	Spinel	Biotite	Plagioclase	Cordierite	Ilmenite
<b>Si</b>	3.01	0.00	2.66	2.98	5.01	0.00
<b>Ti</b>	0.00	0.00	0.21	0.00	0.00	0.88
<b>Al</b>	2.04	1.97	1.47	1.38	4.03	0.00
<b>Cr</b>	0.00	0.01	0.01	0.00	0.00	0.00
<b>Fe3+</b>	0.00	0.02	0.05	0.00	0.00	0.23
<b>Fe2+</b>	1.89	0.75	0.92	0.00	0.46	0.86
<b>Mn2+</b>	0.09	0.00	0.00	0.00	0.00	0.01
<b>Mg</b>	0.76	0.24	1.38	0.00	1.50	0.02
<b>Zn</b>	0.21	0.00	0.00	0.20	0.00	0.00
<b>Ca</b>	0.00	0.00	0.01	0.43	0.00	0.00
<b>Na</b>	0.00	0.00	1.33	0.01	0.00	0.00
<b>K</b>	0.00	0.00	0.00	0.00	0.00	0.00
<b>Cl</b>	0.00	0.00	0.00	0.00	0.00	0.00
<b>F</b>	0.00	0.00	0.00	0.00	0.00	0.00
<b>OH-</b>	0.00	0.00	2.00	0.00	0.00	0.00

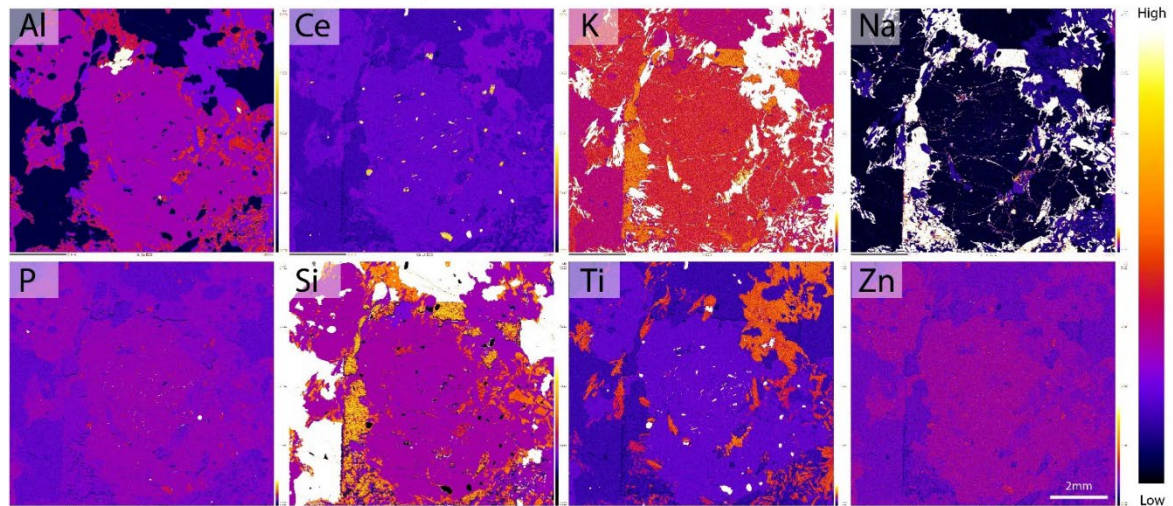
WGC2019J-31A					
Oxides	Garnet core	Garnet rim	K-feldspar	Plagioclase	Biotite
SiO <sub>2</sub>	38.19	38.39	64.38	62.16	36.63
TiO <sub>2</sub>	0.00	0.01	0.00	0.00	4.90
Al <sub>2</sub> O <sub>3</sub>	22.02	22.10	18.88	23.97	17.46
Cr <sub>2</sub> O <sub>3</sub>	0.00	0.01	0.00	0.00	0.05
FeO	31.02	29.23	0.04	0.04	15.30
MnO	0.68	0.46	0.00	0.00	0.02
MgO	7.47	7.80	-0.02	-0.02	11.74
ZnO	-	-	0.00	0.00	0.00
CaO	1.21	2.66	0.00	5.19	0.00
Na <sub>2</sub> O	0.02	0.01	1.30	8.60	0.14
K <sub>2</sub> O	-	-	14.12	0.13	9.61
Cl	0.00	0.00	0.00	0.00	0.00
F	0.01	0.01	0.00	0.00	0.00
H <sub>2</sub> O	0.00	0.00	0.00	0.00	0.00
<b>Total</b>	100.62	100.68	98.70	100.07	95.85

WGC2019J-31A					
Cations	Garnet core	Garnet rim	K-feldspar	Plagioclase	Biotite
Si	2.96	2.96	3.00	2.76	2.71
Ti	0.00	0.00	0.00	0.00	0.27
Al	2.01	2.01	1.04	1.25	1.52
Cr	0.00	0.00	0.00	0.00	0.00
Fe <sup>3+</sup>	0.06	0.07	0.00	0.00	0.05
Fe <sup>2+</sup>	1.95	1.81	0.00	0.00	0.90
Mn <sup>2+</sup>	0.04	0.03	0.00	0.00	0.00
Mg	0.86	0.90	0.00	0.00	1.30
Zn	0.00	0.00	0.00	0.00	0.00
Ca	0.10	0.22	0.00	0.25	0.00
Na	0.00	0.00	0.12	0.74	0.02
K	0.00	0.00	0.84	0.01	0.91
Cl	0.00	0.00	0.00	0.00	0.00
F	0.00	0.00	0.00	0.00	0.00
OH-	0.00	0.00	0.00	0.00	2.00

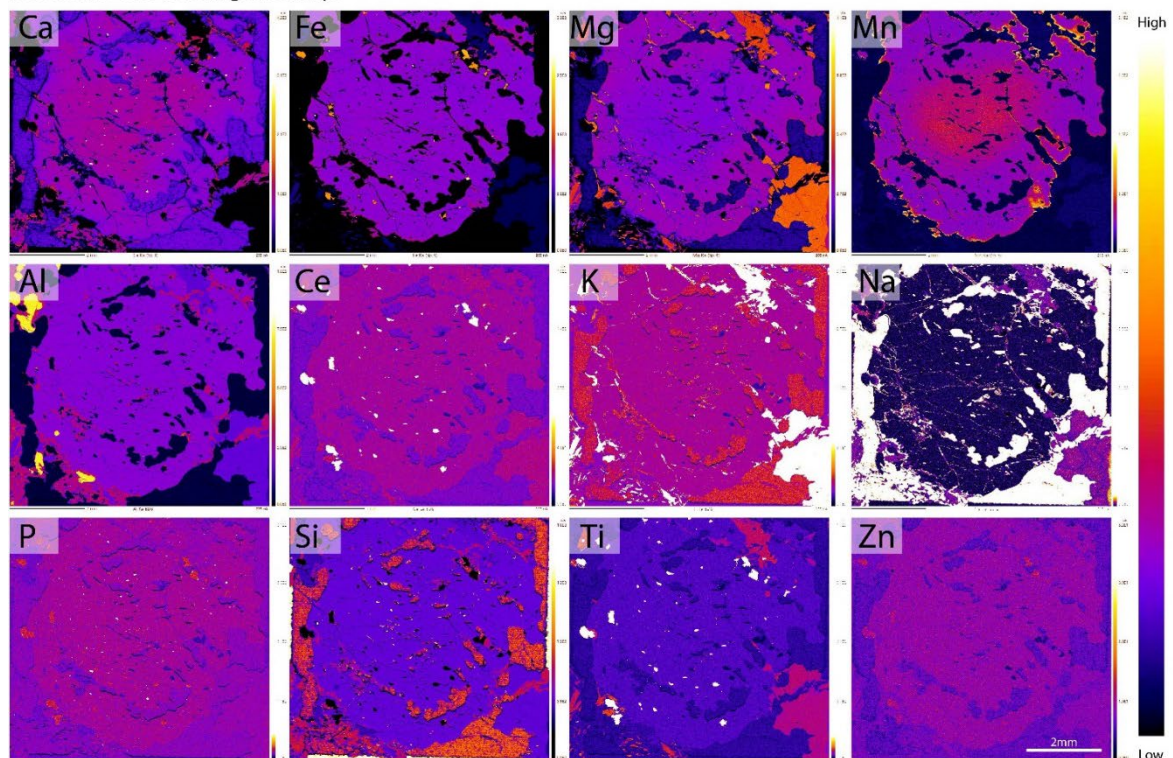
WGC2019J-31A: Additional EPMA garnet maps



WGC2019J-25B-1: Additional EPMA garnet maps

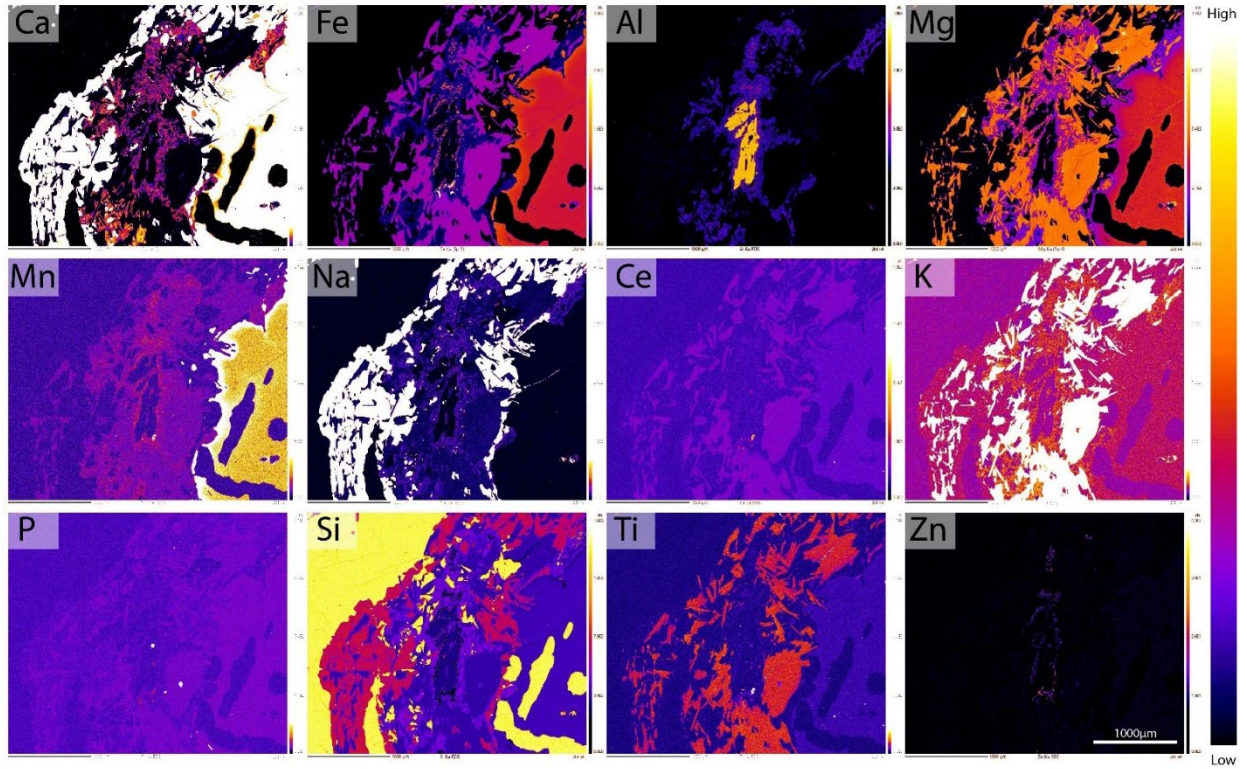


WGC2019J-25B-2: EPMA garnet maps

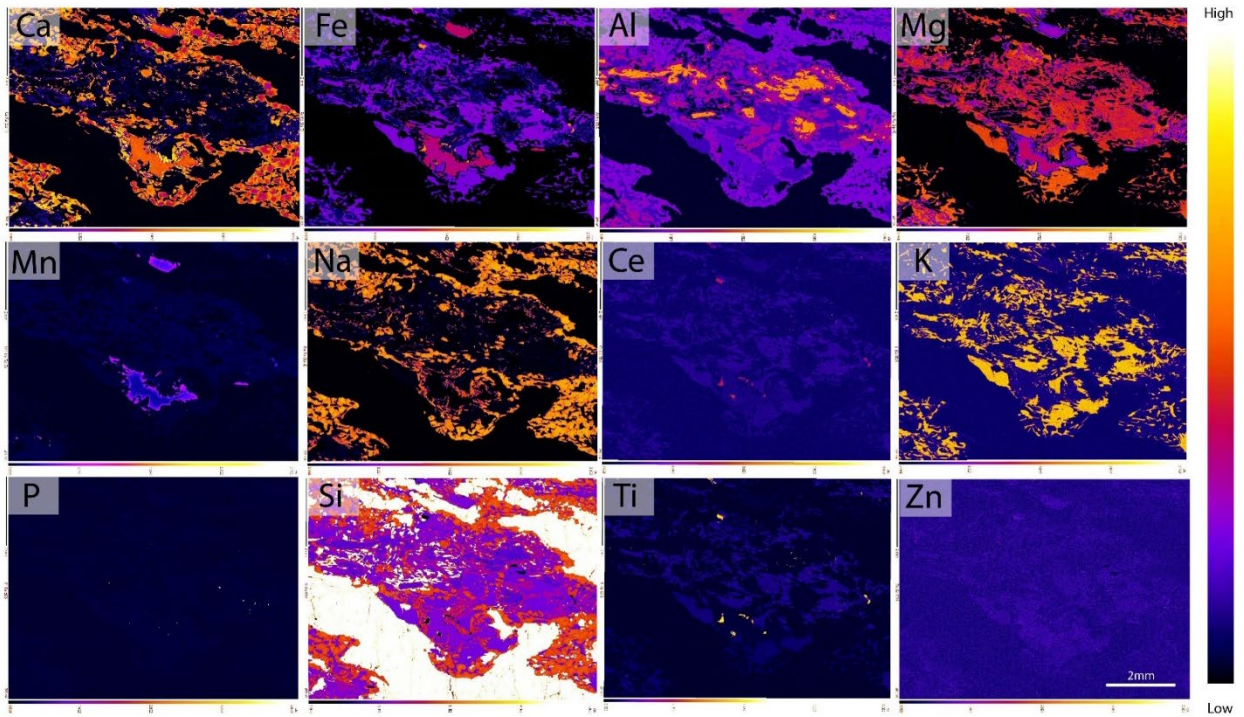




WGC2019J-25B-2: EPMA reaction texture maps

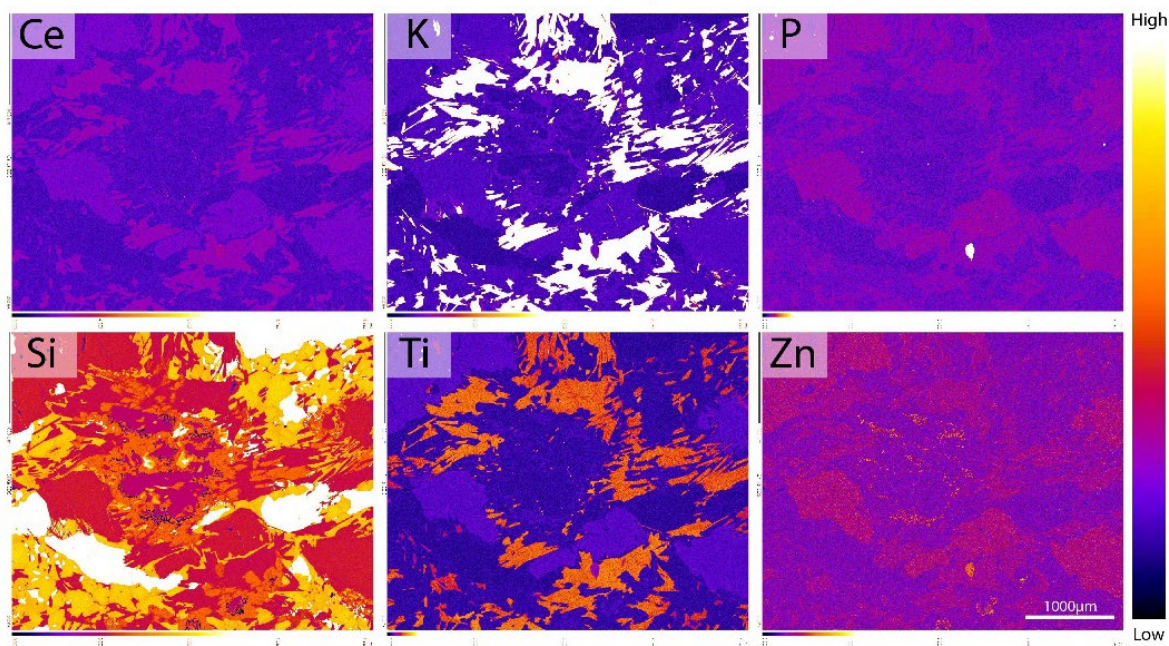


WGC2019J-25B-3: EPMA reaction texture maps





WGC2019J-25B-1: Additional EPMA reaction texture maps



## APPENDIX 3A: EXTENDED LA-ICP-MS METHODS

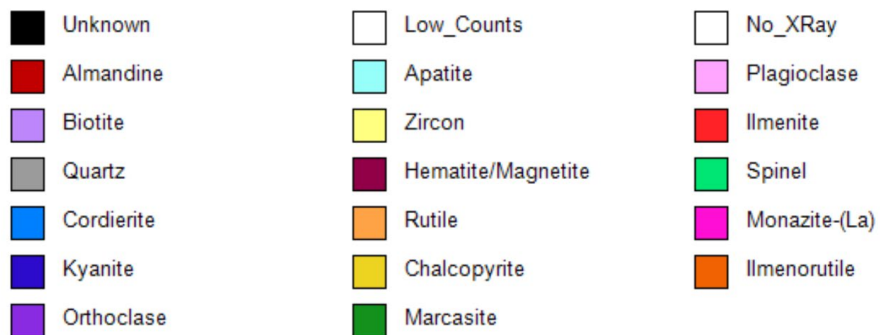
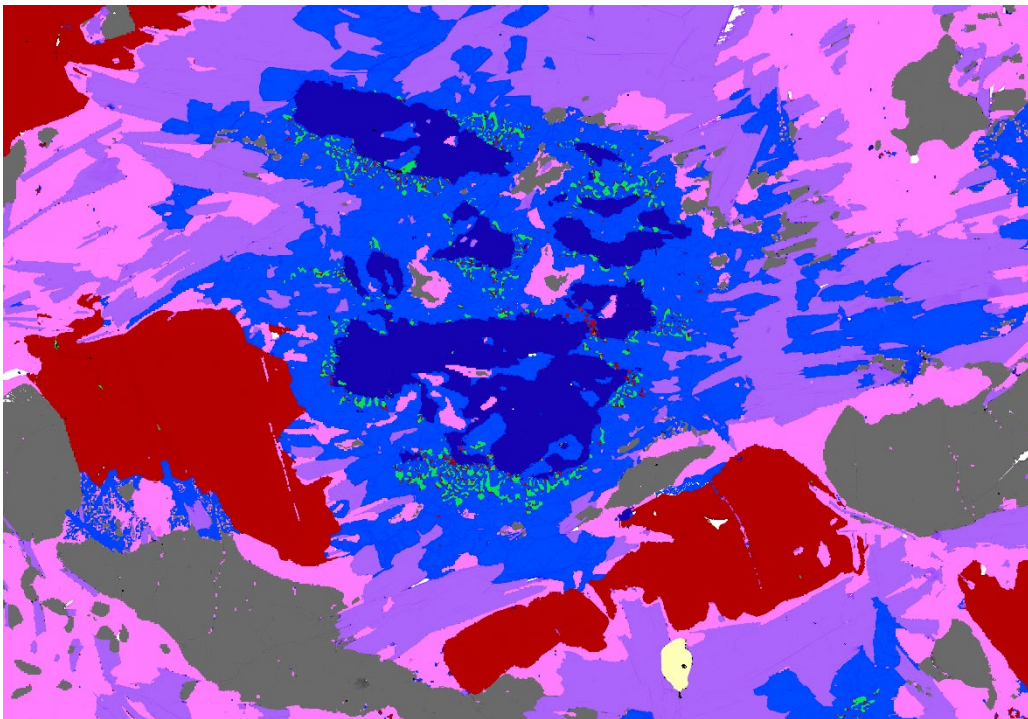
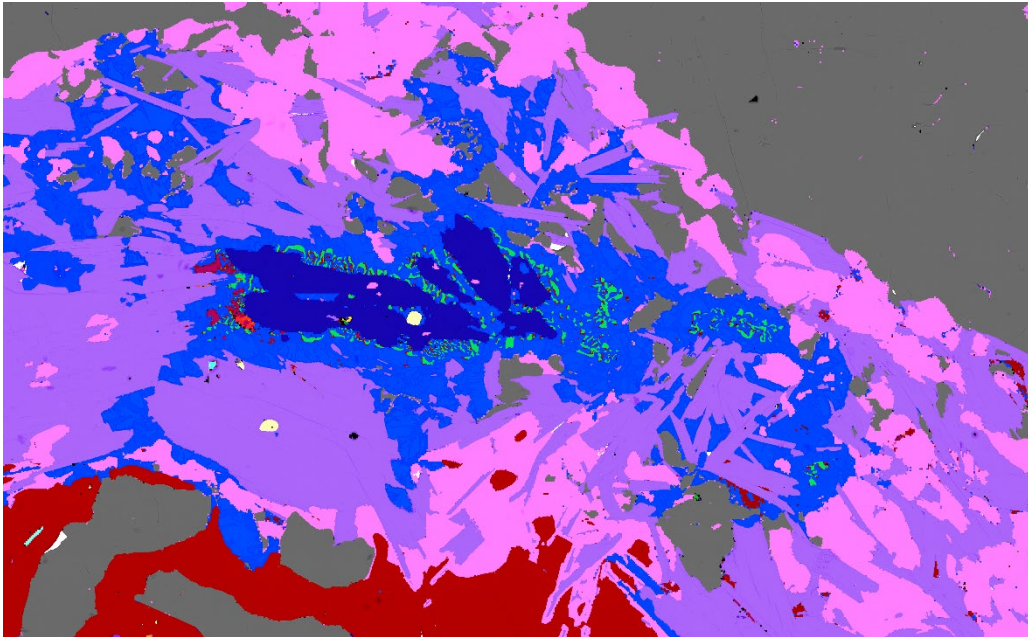
### Mineral separate preparation

Zircon grains were separated under standard crushing, sieving and panning procedures. Additionally, sample WGC2019J-31A was subject to heavy liquid separation. Approximately 100 grains were hand-picked and mounted from WGC2019J-25B, and approximately 300 hand-picked from WGC2019J-31A. 2.5 cm-diameter moulds for each sample were then filled with epoxy resin and hardener, allowed to set, and then polished to expose the centre of each grain.

### Scanning electron microscope analysis

Prior to LA-ICP-MS analysis, both zircon (mounted) and monazite (in-situ) were imaged with a back-scatter electron (BSE) detector on the FEI Quanta MLA-600 scanning electron microscope (SEM) equipped with a tungsten filament electron source at Adelaide Microscopy. Zircon grains were then imaged using the Gatan cathodoluminescence (CL) analyser, also attached to the FEI Quanta MLA-600 SEM. Zircon grains are dull in BSE images, but tend to exhibit zoning or other characteristic textures under the CL analyser. Comparatively, monazite has a higher atomic mass and is therefore more likely to demonstrate zoning in BSE images.

E-DAX software was used in conjunction with SEM-BSE and -CL images and the Genesis Spectrum program to distinguish between minerals and formulate mineral liberation analysis maps of key reaction textures in WGC2019J-25B.





### **LA-ICP-MS analysis**

LA-ICP-MS analyses were performed at Adelaide Microscopy using a RESolution LR 193nm Excimer laser system coupled with an Agilent 7700s ICP-MS under a He-ablation atmosphere. Zircon, monazite and apatite were analysed for U-Pb geochronology and trace elements, whilst rutile was analysed exclusively for U-Pb geochronology and garnet exclusively for trace elements.  $^{207}\text{Pb}/^{206}\text{Pb}$  ratios were calculated in biotite and K-feldspar so that anchoring ages could be used for the concordia plots of common-Pb bearing minerals. A total of 60 s of acquisition time for each zircon and monazite analysis was subdivided into 30 s of background acquisition and 30 s of sample ablation. For rutile, apatite, garnet, biotite and K-feldspar, total acquisition time spanned 70 s, distributed between 30 s of background acquisition and 40 s of sample ablation.

### **LA-ICP-MS standards**

Geochronological analyses were corrected for elemental fractionation and mass bias in zircon, monazite, apatite, rutile, biotite and K-feldspar through various primary standards. Data accuracy was monitored through the use of secondary standards. All trace element analyses were corrected using the external standard NIST610. Biotite and K-feldspar were standardised against GSD and NIST610 for Pb isotope calculations.

Mineral	Standard	Type	Known age (Ma)	Weighted mean 6/38 age (Ma)	Concordia age (Ma)
<b>25B Zircon</b>	GJ	Primary	608.5 ± 0.4 (Jackson et al., 2004)	601.81 ± 2.46	603.01 ± 2.31
	Pleisovice	Secondary	337.13 ± 0.37 (Sláma et al., 2008)	338.59 ± 1.82	339.22 ± 1.68
	91500	Secondary	1065.4 ± 0.3 (Wiedenbeck et al., 1995)	1054.36 ± 9.38	1058.46 ± 10.76
<b>31A Zircon</b>	GJ	Primary	608.5 ± 0.4 (Jackson et al., 2004)	601.80 ± 1.78	602.48 ± 1.73
	Pleisovice	Secondary	337.13 ± 0.37 (Sláma et al., 2008)	338.48 ± 1.91	338.17 ± 2.04
	91500	Secondary	1065.4 ± 0.3 (Wiedenbeck et al., 1995)	1059.32 ± 5.21	1057.51 ± 5.23
<b>Monazite</b>	MAdel	Primary	518.37 ± 0.99 (updated from Payne et al., 2008 with additional TIMS analysis)	518.06 ± 1.52	515.99 ± 1.47
	Ambat 222	Secondary	~525 (in-house)	520.24 ± 2.19	518.09 ± 2.21
		Secondary	450.2 ± 3.4 (in-house)	449.67 ± 1.46	450.57 ± 1.27
<b>Apatite</b>	MAD	Primary	486.58 ± 0.85 & 474.25 ± 0.41 (Thomson et al., 2012)	473.81 ± 3.22	474.44 ± 3.22
	McClure	Secondary	523.51 ± 1.47 (Schoene & Bowring, 2006)	Discordant.	540.8 ± 21
	401	Secondary	530.3 ± 1.5 (Thompson et al., 2016)	537.21 ± 6.78	541.26 ± 10.11
<b>Rutile</b>	R10	Primary	1090 ± 5 (Luvizotto & Zack, 2009)	1091.67 ± 4.70	1091.28 ± 3.27
	R19	Secondary	489.5 ± 0.9 (Zack et al., 2011)	498.51 ± 10.49	496.17 ± 10.69

## Data processing and reduction

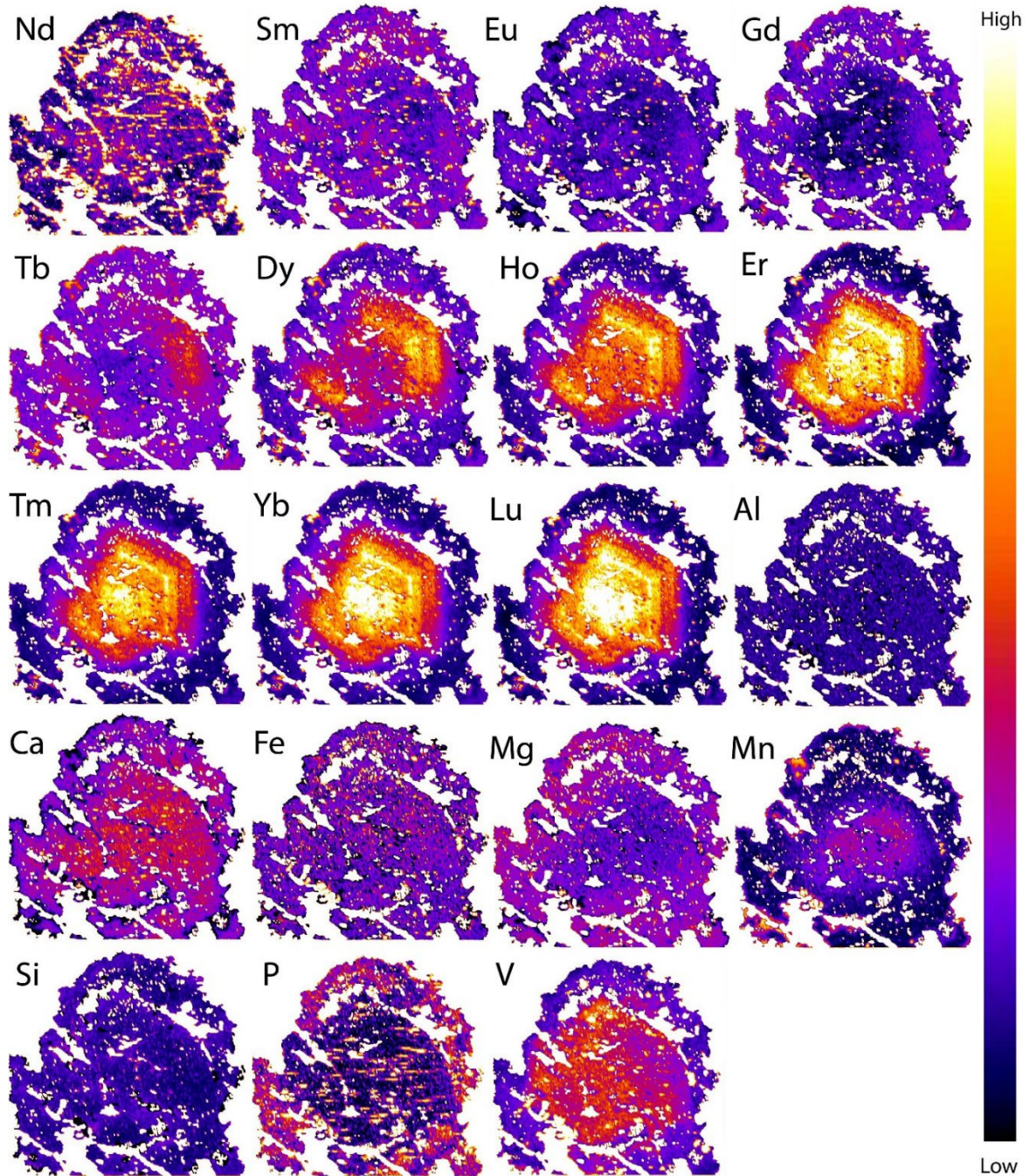
Iolite version 3.6 data processing software (Paton et al., 2011) was used to reduce U-Pb isotopic data. This software uses data from well-constrained standards to correct for down-hole fractionation and instrument drift during data acquisition. Background signal is typically collected by the laser during the first 30 s of data acquisition. This portion of signal should be flat, any spikes that are observed must be removed. Samples and standards are subsequently identified and cropped to remove background. A data reduction scheme (DRS) is then applied. A linear fit typically best represents the data, though it is important to check other schemes as well. The DRS application is used to correct for instrument drift and down-hole fractionation. Next, sample and standard signals are cropped to exclude anomalous data and improve the overall quality of analyses. Good analyses should have relatively steady U and Pb isotope values (i.e. reasonably flat slopes), no major signal spikes (usually indicative of ablating an inclusion), and no major decrease in signal towards the end of the analysis (typically suggestive of firing through the grain). In the case of a bi-modal signal, the earlier section of the signal should be retained as this is more representative of the original target. Both halves of the signal should not be included, as this would constitute a mixed and thereby meaningless age. It is important to not let the bracketing of signals be influenced by personal bias. The previous DRS is once again applied to the data prior to exportation from Iolite 3.6 and the creation of concordia plots.

The final step (where relevant) is to process trace element data. In order to maintain consistency between chemistry and age, it is important that the signals selected for trace elements are cropped identically to U-Pb geochronology analyses. An internal element standard must be assigned in order to process trace element data for minerals in Iolite 3.6. Index elements are selected based on their relative consistency within a mineral. Trace element data was processed using Zr = 43.14% for zircon, Ce = 20% for monazite, Ca = 39.36% for apatite and Si = 18.71% for garnet. Trace element data were reduced using the same method outlined previously for U-Pb geochronology.

APPENDIX 3B: LA-ICP-MS GARNET RESULTS

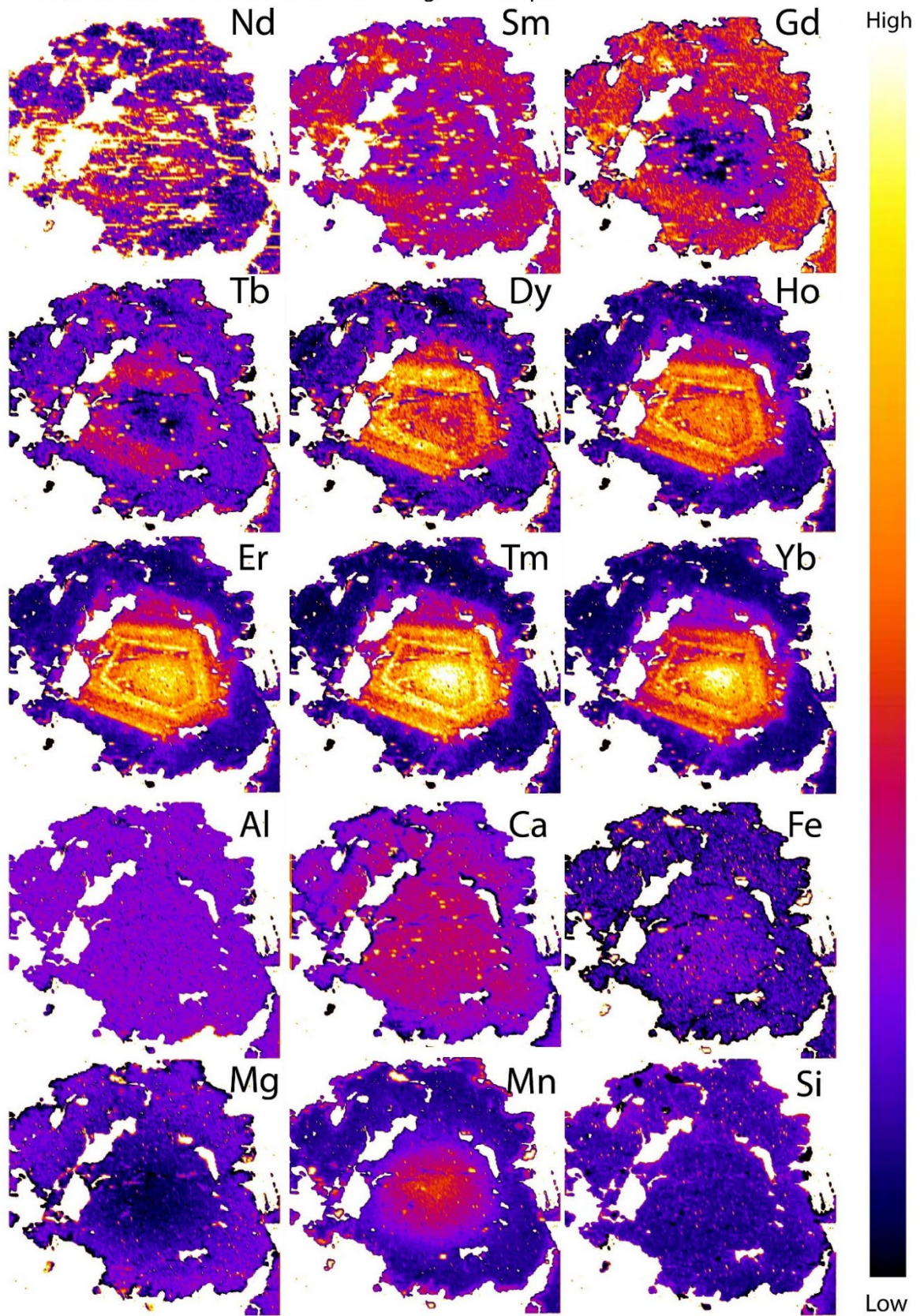
Garnet trace element maps

WGC2019J-25B-2: LA-ICP-MS garnet maps



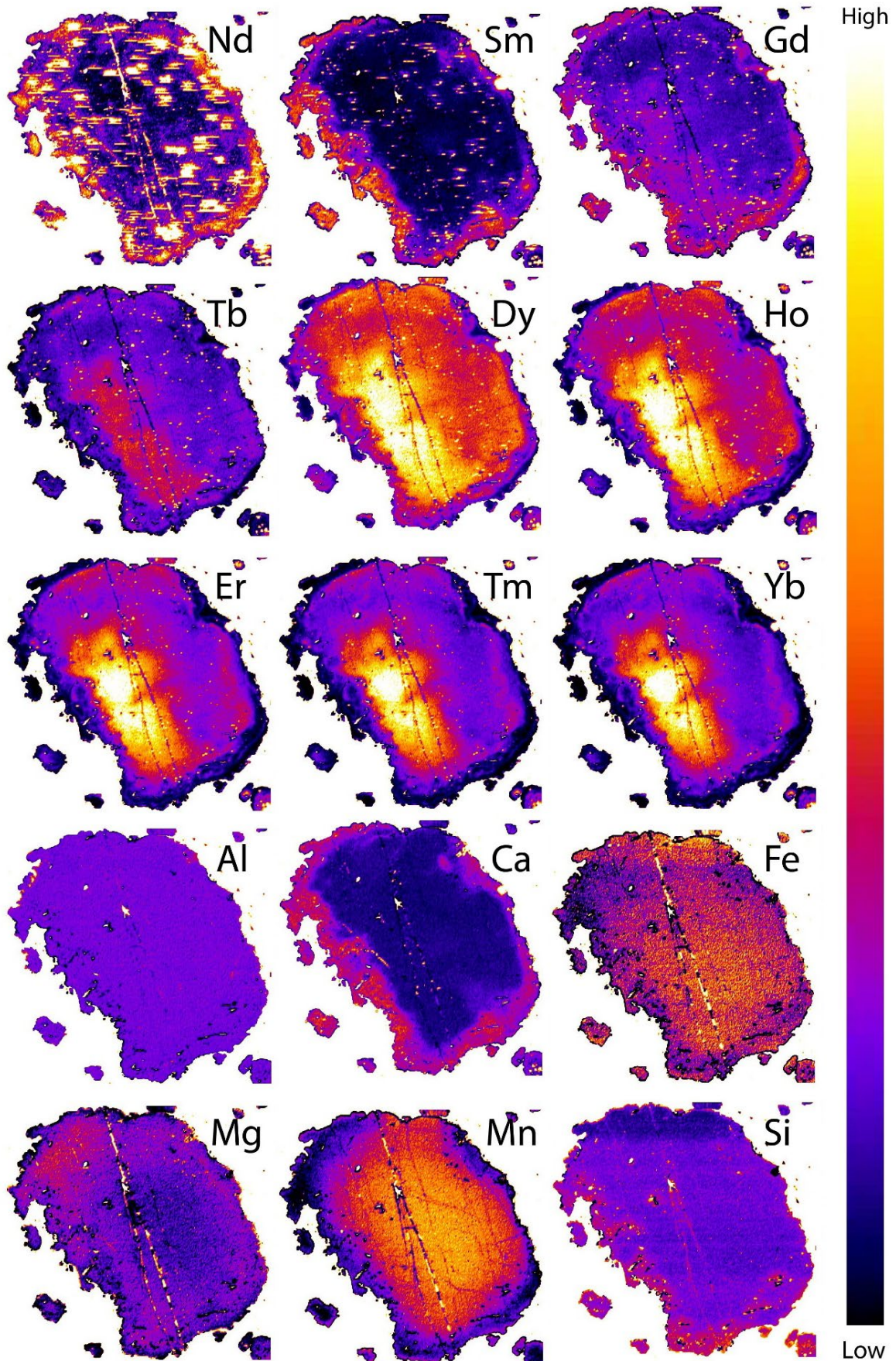


WGC2019J-25B-1: Additional LA-ICP-MS garnet maps





WGC2019J-31A: Additional LA-ICP-MS garnet maps



## Garnet trace elements

Sample	La	Ce	Pr	Nd	Sm	Eu	Gd	Tb	Dy	Y	Ho	Er	Tm	Yb	Lu	Total HRE Es	Eu anomal y	Mg	Ca	M n	Fe
<b>25B-3b- C9_gnt - 1.d</b>	0.021 097	0.011 9086	0.177 8017	1.218 8184	19.72 973	24.95 5595	40.45 2261	47.89 4737	46.74 7967	61. 48	38.79 1209	34.43 75	28.70 4453	30.37 2671	27.47 9675	315.9 0821	0.88335 64	433 40	390 00	34 95	173 900
<b>25B-3b- C9_gnt - 2.d</b>	0.018 0591	0.018 7602	0.175 6466	1.673 9606	20.20 2703	26.87 389	46.98 4925	56.53 7396	53.90 2439	68. 28	46.79 4872	39.56 25	32.59 1093	33.22 9814	29.43 0894	360.3 2901	0.87226 11	441 80	395 00	28 02	170 000
<b>25B-3b- C9_gnt - 3.d</b>	- 0.083 9662	0.020 3915	0.229 5259	1.183 8074	17.63 5135	24.19 1829	42.66 3317	50.41 5512	51.66 6667	64. 28	44.21 2454	44 25	39.71 6599	39.87 5776	42.64 2276	376.8 0929	0.88196 63	435 00	407 00	27 28	171 100
<b>25B-3b- C9_gnt - 4.d</b>	0.013 7848	0.028 5481	0.221 9828	1.466 0832	16.01 3514	24.45 8259	41.10 5528	50.41 5512	47.47 9675	61. 84	43.05 8608	39.87 5	35.14 17	35.65 2174	35.81 3008	349.2 7568	0.95330 55	432 20	416 00	26 93	170 000
<b>25B-3b- C9_gnt - 5.d</b>	- 0.003 4135	0.017 7814	0.212 2845	1.448 5777	17.83 7838	24.24 5115	43.61 809	51.85 5956	53.57 7236	67. 4	47.94 8718	48.31 25	47.61 1336	48.75 7764	51.09 7561	416.5 6107	0.86920 02	432 50	438 00	27 33	173 500
<b>25B-3b- C9_gnt - 6.d</b>	0.001 0072	0.021 3703	0.119 6121	1.334 7921	18.31 0811	24.01 421	42.31 1558	51.13 5734	50.48 7805	64. 1	43.86 4469	41.37 5	39.83 8057	42.17 3913	39.18 6992	372.1 6197	0.86275 01	425 30	457 00	27 00	170 700
<b>25B-3b- C9_gnt - 7.d</b>	- 0.000 2166	0.011 9086	0.137 931	1.072 2101	14.72 973	21.75 8437	40.85 4271	53.15 7895	57.39 8374	72 5	54.17 5824	53.87 5	55.90 5466	58.17 0621	58.17 0732	457.6 3391	0.88697 54	403 00	496 00	27 36	168 600
<b>25B-3b- C9_gnt - 8.d</b>	6.464 E-05	0.026 1011	0.161 6379	1.210 0656	16.28 3784	22.78 8632	42.11 0553	52.10 5263	58.65 8537	85. 2	59.15 7509	73.93 75	77.36 8421	92.73 2919	94.14 6341	593.3 0649	0.87025 22	400 10	467 00	29 44	170 800
<b>25B-3b- C9_gnt - 9.d</b>	- 1.728 E-05	0.015 3344	0.167 0259	0.936 5427	11.28 3784	17.67 3179	36.48 2412	59.58 4488	78.45 5285	12 2.9	94.50 5495	117.6 875	118.6 6397	126.1 4907	116.6 6667	834.6 1247	0.87105 49	382 70	499 00	31 54	172 000
<b>25B-3b- C9_gnt - 10.d</b>	5.055 E-06	0.055 4649	0.301 7241	1.757 1116	17.70 2703	21.66 9627	42.36 1809	68.42 1053	86.17 8862	13 9.3	99.45 0549	119.8 125	117.0 0405	126.7 0807	114.6 3415	871.5 0923	0.79130 59	383 00	499 00	39 90	185 400
<b>25B-3b- C9_gnt - 11.d</b>	- 1.162 E-06	0.060 3589	0.476 2931	2.407 0022	15.87 8378	20.81 7052	39.44 7236	63.07 4792	84.02 439	13 4.3	93.95 6044	110.8 75	112.9 1498	119.1 9255	110.9 3496	829.2 7271	0.83177 88	359 60	508 00	42 70	182 400
<b>25B-3b- C9_gnt - 12.d</b>	0.012 6582	0.101 1419	0.409 4828	2.085 3392	13.17 5676	16.92 7176	32.36 1809	65.98 338	105.0 4065	17 8.6	134.2 4908	175.5 0364	175.3 1739	185.2 6585	185.3 6585	1205. 26	0.81975 04	345 20	482 00	45 59	177 900
<b>25B-3b- C9_gnt - 13.d</b>	0.012 6582	0.089 7227	0.448 2759	2.188 1838	12.56 7568	15.52 3979	25.17 5879	53.07 4792	79.55 2846	13 9.2	94.32 2344	116.9 375	120.6 0729	130.8 6957	127.1 1382	861.6 7816	0.87274 04	329 00	482 00	48 12	180 900
<b>25B-3b- C9_gnt - 14.d</b>	0.028 692	0.117 4551	0.603 4483	2.472 6477	12.63 5135	14.60 0355	22.56 2814	48.83 6565	80.73 1707	15 2.5	108.2 4176	133.3 125	141.4 17	154.3 4783	152.2 3577	971.6 2313	0.86472 27	314 30	505 00	54 63	182 800
<b>25B-3b- C9_gnt - 15.d</b>	0.057 384	0.145 1876	0.538 7931	1.838 0744	6.621 6216	8.117 2291	16.43 2161	45.78 9474	91.46 3415	18 0.6	123.4 4322	146.5 5668	158.0 5528	165.1 6667	166.6 6747	1077. 6747	0.77817 68	312 20	526 00	60 20	185 800
<b>25B-3b- C9_gnt - 16.d</b>	6.54E -06	0.137 031	0.700 431	2.800 8753	15.74 3243	16.98 0462	23.46 7337	39.83 3795	73.33 3333	15 8.7	107.3 2601	148.2 5	160.7 2874	182.4 8447	194.3 0894	1064. 9653	0.88342 66	308 80	511 00	61 03	185 900
<b>25B-3b- C9_gnt - 17.d</b>	0.032 0675	0.159 8695	0.603 4483	1.816 1926	9.459 4595	10.58 6146	14.22 1106	29.52 9086	68.00 813	17 3.1	119.4 1392	171.8 75	191.4 9798	223.7 2671	246.3 4146	1223. 4923	0.91272 1	306 10	514 00	64 18	185 100
<b>25B-3b- C9_gnt - 18.d</b>	0.022 7848	0.184 3393	0.625	2.625 8206	15.20 2703	16.23 4458	25.07 5377	38.19 9446	69.55 2846	16 3.1	113.0 0366	166.6 25	185.0 2024	226.5 8385	245.1 2195	1207. 207	0.83148 36	304 90	530 00	66 20	185 000

Samantha Nicole March  
Ultrahigh-pressure metapelites in the WGR

25B-3b-	0.130	0.300	0.883	2.997	19.18	22.13	31.25	49.77	82.23	17	119.5	167.8	191.4	228.5	250.4	1264.	0.90367	304	531	67	183
C9_gnt - 19.d	8017	1631	6207	8118	9189	1439	6281	8393	5772	4.9	9707	125	9798	7143	065	7996	59	60	00	90	100
25B-3b-	0.043	0.156	0.477	2.210	11.08	12.48	20.80	46.81	84.02	16	109.8	133.3	141.4	152.7	150.5	983.4	0.82239	309	538	69	183
C9_gnt - 20.d	038	6069	3707	0656	1081	6679	402	4404	439	4.6	9011	75	5749	3292	2846	2277	84	50	00	13	000
25B-3b-	-	0.114	0.754	2.188	13.17	14.33	27.08	54.40	90.60	16	117.3	145.5	146.5	153.6	138.2	1013.	0.75877	317	509	65	181
C9_gnt - 21.d	0.005	1925	3103	1838	5676	3925	5427	4432	9756	6.9	9927	625	587	646	1138	3106	12	50	00	14	000
	5781																				
25B-3b-	0.046	0.088	0.506	2.582	16.62	19.41	32.66	58.55	88.04	14	103.1	113.5	112.5	117.9	101.3	843.2	0.83319	328	512	58	180
C9_gnt - 22.d	4135	0914	4655	0569	1622	3854	3317	9557	878	8.2	1355		5061	5031	0081	2362	17	70	00	96	400
25B-3b-	-	0.187	0.851	2.735	16.14	20.26	37.63	72.52	109.9	17	128.5	142.3	130.3	120.8	108.6	985.2	0.82204	328	533	53	179
C9_gnt - 23.d	0.027	602	2931	2298	8649	643	8191	0776	187	2.1	7143	125	6437	6957	1789	7523	35	60	00	12	700
	0042																				
25B-3b-	0.093	0.226	1.012	3.063	16.68	22.87	40.95	71.16	101.8	15	115.9	127.1	110.9	106.8	87.03	877.8	0.87505	334	510	47	175
C9_gnt - 24.d	2489	7537	931	4573	9189	7442	4774	3435	2927	6.9	3407	875	3117	323	252	1026	95	90	00	63	700
25B-3b-	0.105	0.176	0.515	2.275	14.86	20.40	39.14	63.49	79.43	12	83.69	87.31	76.55	75.52	65.20	653.1	0.84603	334	493	42	172
C9_gnt - 25.d	9072	1827	0862	7112	4865	8526	5729	0305	0894	1.9	9634	25	8704	795	3252	2324	62	60	00	74	700
25B-3b-	0.000	0.045	0.235	1.426	12.77	16.18	40.25	67.11	85.08	12	85.53	88.43	80.28	76.33	61.50	669.1	0.71370	367	482	38	183
C9_gnt - 26.d	8477	677	9914	6958	027	1172	1256	9114	1301	4.9	1136	75	3401	5404	4065	9192	74	40	00	86	500
25B-3b-	0.012	0.073	0.415	1.494	14.86	21.93	42.76	65.78	79.06	11	82.60	86.12	77.48	73.10	58.17	637.1	0.87004	368	499	35	176
C9_gnt - 27.d	2363	4095	9483	5295	4865	6057	3819	9474	5041	4.8	0733	5	9879	559	0732	4645	12	90	00	74	400
25B-3b-	6.764	0.027	0.266	1.485	16.75	22.80	43.41	53.73	59.14	88.	64.83	74.56	71.05	68.44	63.25	543.5	0.84553	382	508	30	170
C9_gnt - 28.d	E-05	5693	1638	7768	6757	6394	7085	9612	6341	5	5165	25	2632	7205	2033	3549	45	90	00	73	700
25B-3b-	-	0.055	0.357	1.750	21.89	31.13	52.01	58.89	59.91	83.	57.19	57.18	51.57	51.30	45	464.7	0.92275	390	504	29	169
C9_gnt - 29.d	1.938	4649	7586	547	1892	6767	005	1967	8699	7	7802	75	8947	4348		7926	89	30	00	77	800
	E-05																				
25B-3b-	4.236	0.016	0.240	1.498	18.24	25.27	44.72	53.24	49.39	61.	39.74	33.12	28.86	27.88	24.59	318.0	0.88486	394	505	27	167
C9_gnt - 30.d	E-06	9657	3017	9059	3243	5311	3618	0997	0244	2	359	5	6397	8199	3496	4792	5	60	00	48	800
25B-3b-	0.009	0.026	0.221	1.750	18.58	25.39	45.07	51.57	46.99	57.	36.73	32.56	25.58	23.66	19.06	293.4	0.87765	412	453	27	169
C9_gnt - 31.d	2827	9168	9828	547	1081	9645	5377	8947	187	3	9927	25	7045	4596	5041	8993	22	20	00	12	400
25B-3b-	3.671	0.033	0.257	1.925	19.39	25.50	42.61	49.77	46.26	56.	37.54	31.18	25.87	23.72	20.69	291.8	0.88728	413	465	26	168
C9_gnt - 32.d	E-07	6052	5431	6018	1892	6217	3065	8393	0163	8	5788	75	0445	6708	1057	6005	79	40	00	52	500
25B-3b-	-	0.022	0.197	1.794	19.25	27.76	45.57	50.77	45.44	55.	35.49	30.62	25.26	23.97	21.50	288.7	0.93709	431	452	26	170
C9_gnt - 33.d	2.426	5122	1983	3107	6757	1989	7889	5623	7154	65	4505	5	3158	5155	4065	3466	13	20	00	50	400
	E-07																				
25B-3b-	5.523	0.013	0.200	1.553	18.98	24.70	42.91	48.39	44.51	54.	35.07	30.87	25.91	22.91	20.28	282.0	0.86555	428	455	26	170
C9_gnt - 34.d	E-07	8662	431	6105	6486	6927	4573	3352	2195	11	326	5	0931	9255	4553	7855	37	40	00	50	200
25B-3b-	-	0.013	0.216	1.450	17.09	24.63	44.82	50.16	46.54	55.	35.80	31.43	24.93	24.09	20.16	288.8	0.88998	398	433	36	173
C9_gnt - 35.d	2.034	54	5948	7659	4595	5879	4121	6205	4715	69	5861	75	9271	9379	2602	4553	52	70	00	46	800
	E-06																				
25B-3b-	7.553	0.012	0.149	1.352	18.24	25.73	45.32	51.93	47.84	59.	38.22	34.37	27.81	25.21	22.80	307.4	0.89501	424	401	28	171
C9_gnt - 36.d	E-06	398	7845	2976	3243	7123	6633	9058	5528	19	3443	5	3765	7391	4878	0906	9	80	00	42	600
25B-3b-	-	0.027	0.293	1.367	18.31	22.82	42.66	55.45	59.43	82.	62.63	70.81	62.95	66.45	65.16	525.5	0.81660	440	394	29	173
C10_gnt - 1.d	3.013	8956	1034	6149	0811	4156	3317	7064	0894	6	7363	25	5466	9627	2602	1552	8	80	00	78	300
	E-05																				
25B-3b-	0.009	0.048	0.362	1.621	18.58	23.46	44.82	54.59	60.56	85.	64.46	67.31	63.48	69.75	64.55	530.3	0.81302	441	412	30	173
C10_gnt - 2.d	2827	2871	069	4442	1081	3588	4121	8338	9106	6	8864	25	1781	1553	2846	3499	34	40	00	05	200
25B-3b-	-	0.033	0.282	1.641	18.51	25.82	42.76	56.28	68.04	10	85.71	102.5	98.09	105.4	106.0	729.4	0.91785	430	426	30	172
C10_gnt - 3.d	0.000	279	3276	1379	3514	5933	3819	8089	878	7.3	4286		7166	0373	9756	4961	35	90	00	48	900
	3895																				



Samantha Nicole March  
Ultrahigh-pressure metapelites in the WGR

<b>25B-3b- C10_gnt - 4.d</b>	0.013 5021	0.048 4502	0.463 3621	1.757 1116	17.63 5135	25.43 5169	43.46 7337	55.78 9474	72.68 2927	12 0.9	97.43 5897	127.5 625	121.4 5749	134.3 4783	136.7 8862	866.9 6473	0.91867 88	430 60	435 00	31 63	176 100
<b>25B-3b- C10_gnt - 5.d</b>	- 0.005 6118	0.081 5661	0.417 0259	2.253 8293	18.85 1351	25.68 3837	40.60 3015	55.45 7064	77.76 4228	13 4.5	105.8 6081	134 6842	137.3 142.3	142.9 143.7	143.0 158.0	930.9 922.0	0.92834 52	433 10	434 00	32 90	172 700
<b>25B-3b- C10_gnt - 6.d</b>	0.019 1983	0.083 1974	0.398 7069	2.188 1838	20 20.54	23.71 2256	38.39 196	53.04 7091	84.51 2195	15 3.1	118.3 1502	141.8 75	138.8 664	147.4 5342	139.9 187	977.0 8782	0.85573 19	415 50	445 00	34 44	170 700
<b>25B-3b- C10_gnt - 7.d</b>	- 0.077 6371	0.065 0897	0.528 0172	2.603 9387	20.54 0541	26.26 9982	40.75 3769	54.29 3629	80.65 0407	15 5.3	110.9 8901	142.3 75	143.7 247	158.0 1242	146.7 4797	992.0 9313	0.90796 68	427 60	464 00	37 79	177 200
<b>25B-3b- C10_gnt - 8.d</b>	0.054 4304	0.143 5563	0.470 9052	2.177 2429	17.97 2973	23.69 4494	34.27 1357	50.94 1828	82.23 5772	17 2.8	124.5 4212	165.8 75	175.8 2996	196.2 7329	190.6 5041	1159. 1484	0.95471 08	396 40	463 00	39 45	173 700
<b>25B-3b- C10_gnt - 9.d</b>	0.034 1772	0.138 6623	0.765 0862	2.297 593	15.40 5405	20.12 4334	29.34 6734	44.40 4432	86.74 7967	21 4.3	153.8 4615	238.1 25	257.0 8502	274.5 3416	280.0 813	1549. 124	0.94646 61	394 10	494 00	41 52	170 400
<b>25B-3b- C10_gnt - 10.d</b>	0.035 865	0.192 4959	0.866 3793	3.763 6761	24.66 2162	26.14 5648	37.88 9447	49.94 4598	83.37 3984	18 7.7	132.4 1758	189.4 375	206.4 7773	230.4 3478	229.6 748	1309. 461	0.85531 23	392 30	472 00	41 46	169 200
<b>25B-3b- C10_gnt - 11.d</b>	0.028 692	0.150 0816	0.840 5172	3.413 5667	20.67 5676	26.85 6128	38.89 4472	50.16 6205	80.48 7805	18 8	132.0 5128	200.1 25	225.9 1093	266.4 5963	270.7 3171	1413. 9326	0.94704 28	395 30	493 00	43 21	170 400
<b>25B-3b- C10_gnt - 12.d</b>	0.014 346	0.102 7732	0.625 3479	2.713 8919	18.91 1012	22.61 4824	32.96 374	44.65 894	74.43 0894	18 9.5	130.4 0293	224.3 75	275.3 0364	346.5 8385	389.8 374	1675. 0875	0.90541 25	391 40	481 00	45 08	169 400
<b>25B-3b- C10_gnt - 13.d</b>	0.021 519	0.135 3997	0.700 431	2.997 8118	22.09 4595	26.02 1314	36.88 4422	47.67 313	76.05 6911	19 5.9	136.6 3004	233.0 625	291.4 9798	372.6 7081	419.1 0569	1772. 5971	0.91151 69	383 50	501 00	45 35	169 800
<b>25B-3b- C10_gnt - 14.d</b>	1.62E -06	0.081 5661	0.538 7931	2.100 6565	14.59 4595	17.65 5417	23.31 6583	35.20 7756	71.99 187	22 0.2	153.4 7985	283.8 125	355.4 6559	434.1 6149	469.1 0569	2023. 4247	0.95708 28	379 00	503 00	47 19	168 400
<b>25B-3b- C10_gnt - 15.d</b>	1.059 E-05	0.070 1468	0.391 1638	1.969 3654	16.95 9459	21.82 9485	34.57 2864	45.67 867	81.34 1463	21 9.3	157.1 4286	269.6 875	315.7 8947	378.8 8199	403.2 5203	1871. 074	0.90150 85	390 50	506 00	45 37	170 400
<b>25B-3b- C10_gnt - 16.d</b>	- 4.515 E-05	0.062 969	0.463 3621	2.194 7484	17.77 027	22.27 3535	40.90 4523	55.42 9363	90.89 4309	19 5.4	142.4 9084	203.7 5	221.4 5749	252.1 118	263.4 1463	1424. 9484	0.82614 53	391 80	465 00	42 14	175 100
<b>25B-3b- C10_gnt - 17.d</b>	0.021 9409	0.088 0914	0.424 569	1.947 4836	18.24 3243	22.84 1918	36.23 1156	52.16 0665	85.40 6504	18 2.1	131.8 6813	181.2 5	192.3 0769	216.5 8385	210.9 7561	1252. 6525	0.88846 53	395 80	465 00	39 48	175 300
<b>25B-3b- C10_gnt - 18.d</b>	- 0.000 6329	0.070 9625	0.360 9914	1.706 7834	16.08 1081	20.28 4192	31.80 9045	55.59 5568	107.0 7317	22 3.5	171.7 9487	229.1 25	233.1 9838	256.5 2174	242.6 8293	1519. 4917	0.89686 02	388 80	477 00	38 67	175 100
<b>25B-3b- C10_gnt - 19.d</b>	0.002 3165	0.060 3589	0.351 2931	1.369 8031	15.54 0541	18.34 8135	31.70 8543	63.13 0194	135.4 878	28 4.8	226.0 0733	311.0 625	307.6 9231	336.5 8385	325.2 0325	1989. 9672	0.82655 3	400 20	497 00	36 02	173 700
<b>25B-3b- C10_gnt - 20.d</b>	- 0.009 9156	0.053 0179	0.378 2328	2.140 0438	15.67 5676	21.91 8295	37.53 7688	58.78 1163	107.9 6748	20 7.3	166.3 0037	217.1 25	225.1 0121	248.8 1988	246.7 4797	1478. 1431	0.90356 6	409 10	473 00	31 99	170 100
<b>25B-3b- C10_gnt - 21.d</b>	0.061 6034	0.127 2431	0.775 8621	3.172 8665	20 7833	24.93 8744	39.74 8744	56.26 0388	87.23 5772	15 9	125.8 2418	167.0 625	178.7 0445	206.5 8385	206.5 0407	1187. 1752	0.88446 78	415 60	444 00	30 60	170 900

Samantha Nicole March  
Ultrahigh-pressure metapelites in the WGR

<b>25B-3b- C10_gnt - 22.d</b>	0.054 0084	0.210 4405	1.002 1552	3.873 0853	23.10 8108	27.30 0178	42.76 3819	57.89 4737	79.67 4797	13 3	100.9 1575	122.0 625	125.7 4899	139.5 6522	133.7 3984	892.6 0183	0.86845 04	426 40	441 00	29 37	174 100
<b>25B-3b- C10_gnt - 23.d</b>	- 0.000 8776	0.130 5057	0.754 3103	3.194 7484	20.67 5676	29.09 4139	46.48 2412	58.11 6343	74.06 5041	11 2.8	87.36 2637	102.5	98.29 9595	110.2 4845	112.0 3252	755.4 2458	0.93849 36	425 80	431 00	28 84	172 800
<b>25B-3b- C10_gnt - 24.d</b>	0.000 2464	0.053 8336	0.326 5086	2.122 5383	20.54 0541	26.51 865	47.08 5427	58.61 4958	68.45 5285	95. 5	75.91 5751	87.5	83.40 081	86.89 441	96.50 4065	652.7 8528	0.85271 17	436 60	422 00	28 96	172 500
<b>25B-3b- C10_gnt - 25.d</b>	0.143 4599	0.143 5563	0.415 9483	1.759 2998	25.40 5405	23.58 7922	54.42 2111	60.66 482	64.83 7398	89. 8	64.65 2015	68.81 25	63.23 8866	63.04 3478	65.08 1301	540.1 3038	0.63436 46	468 10	330 00	30 16	180 100
<b>25B-3b- C10_gnt - 26.d</b>	0.020 6751	0.040 6199	0.246 7672	1.822 7571	22.16 2162	24.65 3641	51.20 603	59.11 3573	59.51 2195	83	57.27 1062	58.12 5	56.07 2874	59.81 3665	57.03 252	489.9 4089	0.73183 72	456 00	367 00	29 40	175 600
<b>25B-3b- C10_gnt - 27.d</b>	0.000 1637	0.062 8059	0.395 4741	2.516 4114	24.93 2432	29.30 7282	51.80 9045	58.61 4958	59.34 9593	83. 2	57.96 7033	58.56 25	55.74 8988	56.70 8075	56.13 8211	486.2 8936	0.81543 7	445 50	392 00	28 85	172 800
<b>25B-3b- C10_gnt - 28.d</b>	- 0.000 6582	0.050 571	0.337 2845	1.838 0744	18.64 8649	26.02 1314	42.96 4824	51.99 446	51.30 0813	68. 8	45.25 641	42.25	38.70 4453	40.06 2112	35.20 3252	373.5 715	0.91928 26	442 20	419 00	28 44	170 500
<b>25B-3b- C10_gnt - 29.d</b>	0.002 4051	0.036 8679	0.223 0603	1.750 547	17.02 7027	25.50 6217	45.97 9899	52.10 5263	49.67 4797	64. 21	41.95 9707	39.06 25	34.33 1984	31.18 0124	28.61 7886	341.1 4226	0.91157 55	437 10	411 00	27 82	169 200
<b>25B-3b- C10_gnt - 30.d</b>	- 0.008 0591	0.027 5693	0.269 3966	1.794 3107	21.35 1351	28.59 6803	49.84 9246	57.89 4737	55.12 1951	70. 3	45.93 4066	41.31 25	33.56 2753	33.85 0932	29.26 8293	367.2 4523	0.87654 76	449 00	394 00	28 38	169 500
<b>25B-3b- C10_gnt - 31.d</b>	0.032 1519	0.028 385	0.216 5948	1.312 9103	18.58 1081	23.78 3304	49.54 7739	55.56 7867	51.38 2114	67. 1	43.90 1099	40.81 25	36.03 2389	33.22 9814	29.10 5691	357.1 3147	0.78383 52	450 40	408 00	30 66	175 100
<b>25B-3b- C10_gnt - 32.d</b>	- 0.154 4304	0.014 6819	0.153 0172	1.026 2582	18.17 5676	16.44 7602	58.94 4724	67.59 0028	61.86 9919	74. 3	50.01 8315	43.68 75	37.24 6964	36.77 0186	33.17 0732	404.6 5364	0.50249 86	398 20	319 00	58 04	195 100
<b>31A-3-gnt - 1.d</b>	0.006 8017	0.091 354	1.282 3276	4.573 3042	17.70 2703	9.573 7123	71.55 7789	96.39 8892	73.41 4634	60. 3	41.53 8462	25.62 5	16.88 2591	14.40 9938	12.60 1626	341.1 7114	0.26898 75	392 40	159 20	30 77	209 100
<b>31A-3-gnt - 2.d</b>	- 0.001 3654	0.051 7129	0.915 9483	4.310 7221	17.5 3393	12.43 8291	81.65 2493	131.0 2493	125.4 065	12 9	94.13 9194	69.81 25	54.25 1012	50.31 0559	46.91 0569	700.8 5527	0.32890 5	402 70	164 80	31 56	207 700
<b>31A-3-gnt - 3.d</b>	0.000 4017	0.026 1011	0.538 7931	3.501 0941	18.04 0541	12.07 8153	82.96 4824	131.8 5596	129.3 0894	13 1.3	83.51 6484	62.68 75	46.07 2874	46.95 6522	43.08 9431	674.7 8771	0.31219 7	396 30	170 20	34 76	203 700
<b>31A-3-gnt - 4.d</b>	- 0.000 102	0.012 7243	0.237 069	2.231 9475	11.41 8919	6.571 9361	62.06 0302	127.1 4681	153.5 3659	17 3.7	119.0 4762	90.93 75	73.48 1781	70.93 1677	73.29 2683	882.0 7466	0.24687 32	408 90	121 90	37 56	208 200
<b>31A-3-gnt - 5.d</b>	7.426 E-06	0.009 1354	0.282 3276	1.903 7199	8.445 9459	3.570 1599	55.12 5628	134.6 2604	168.7 3984	19 4.1	130.0 3663	98	73.07 6923	69.31 677	68.37 3984	936.2 7018	0.16545 76	416 20	895 0	38 61	207 700
<b>31A-3-gnt - 6.d</b>	7.679 E-05	0.008 9723	0.232 7586	1.553 6105	9.054 0541	2.753 1083	56.78 392	130.7 4792	176.5 0407	20 7.3	143.0 4029	102.8 125	78.74 4939	72.17 3913	68.53 6585	979.8 6022	0.12141 97	419 00	842 0	40 02	210 400
<b>31A-3-gnt - 8.d</b>	0.001 2152	- 8.173 E-06	0.084 0517	0.844 6389	8.851 3514	2.468 9165	48.04 0201	111.3 5734	158.7 3984	21 5	144.1 3919	132.5 625	110.2 834	107.9 5031	102.1 5447	1082. 1871	0.11972 9	409 30	764 0	41 92	210 100

Samantha Nicole March  
Ultrahigh-pressure metapelites in the WGR

<b>31A-3-gnt - 9.d</b>	- 0.004 7679	0.004 894	0.210 1293	1.216 6302	10.06 7568	2.824 1563	47.83 9196	111.9 1136	154.1 0569	21 5.9	144.6 8864	128.3 125	108.4 6154	104.6 5839	97.11 3821	1065. 1519	0.12868 7	406 40	798 0	42 65	211 500
<b>31A-3-gnt - 10.d</b>	0.016 6667	0.005 0571	0.098 0603	1.597 3742	10.33 7838	2.806 3943	46.08 0402	108.0 3324	151.5 0407	20 6.9	140.4 7619	125 6559	105.4 1056	100.3 1463	91.34 0311	1029. 07	0.12858 70	400 0	770 17	43 100	211
<b>31A-3-gnt - 11.d</b>	- 0.082 2785	- 1.917 E-05	0.209 0517	1.772 4289	10.47 2973	2.966 2522	49.49 7487	112.4 6537	157.7 2358	21 4.8	147.8 022	130.5 8381	111.9 2981	103.2 6016	101.2 7649	1079. 11	0.13028 80	411 0	817 18	45 100	219
<b>31A-3-gnt - 12.d</b>	0.015 2321	- 4.026 E-05	0.052 8017	0.737 4179	8.378 3784	3.410 302	49.19 598	109.4 1828	150.8 5366	20 0.3	136.0 8059	117 0121	92.51 7081	87.26 6098	79.75 8583	973.1 63	0.16797 70	393 0	771 18	45 200	216
<b>31A-3-gnt - 13.d</b>	- 0.003 0338	- 4.509 E-05	0.064 6552	0.919 0372	9.189 1892	2.735 3464	47.83 9196	110.2 4931	151.3 4146	20 0.6	128.9 3773	111.6 875	89.67 6113	83.72 6708	75.08 1301	951.3 0012	0.13046 13	396 20	769 0	45 94	217 400
<b>31A-3-gnt - 14.d</b>	0.000 8932	- 4.721 E-05	0.064 6552	0.954 0481	9.054 0541	2.309 0586	51.20 603	119.9 446	154.9 187	19 5.2	128.5 7143	105.1 25	82.38 8664	78.94 4099	67.88 6179	932.9 7867	0.10723 9	385 90	751 0	46 64	214 400
<b>31A-3-gnt - 15.d</b>	- 0.000 2409	0.001 3051	0.084 0517	0.691 4661	8.716 2162	2.628 7744	50.70 3518	113.8 5042	143.3 3333	18 7.7	117.5 8242	100.9 375	81.74 0891	81.30 4348	75.32 5203	901.7 7411	0.12504 61	373 90	746 0	48 11	215 100
<b>31A-3-gnt - 16.d</b>	0.117 2996	0.148 4502	0.385 7759	1.415 7549	11.35 1351	2.326 8206	52.96 4824	118.0 0554	144.1 0569	19 7	119.2 3077	106.6 25	88.98 7854	82.23 6025	80 9088	936.1 54	0.09489 20	368 0	704 83	48 500	215
<b>31A-3-gnt - 17.d</b>	- 1.512 E-05	0.002 7732	0.155 1724	1.185 9956	7.635 1351	2.273 5346	49.44 7236	113.0 1939	149.1 8699	20 2.8	121.7 9487	108.3 125	95.30 3644	90.68 323	87.92 6829	969.0 2746	0.11700 98	365 10	688 0	49 29	215 200
<b>31A-3-gnt - 18.d</b>	4.506 E-06	0.058 7276	0.528 0172	1.509 8468	7.702 7027	1.829 4849	52.36 1809	122.7 1468	154.3 4959	21 6.8	134.7 9853	120.8 75	101.0 1215	99.19 2547	94.10 5691	1043. 8482	0.09109 61	363 90	707 0	50 05	215 300
<b>31A-3-gnt - 19.d</b>	- 1.198 E-06	0.036 2153	0.395 4741	1.728 6652	10.20 2703	2.646 5364	57.78 8945	124.9 3075	161.9 1057	23 3.4	139.7 4359	124 7611	109.6 3106	105.0 9756	101.0 7896	1099. 7896	0.10899 28	373 70	663 0	51 25	218 600
<b>31A-3-gnt - 20.d</b>	3.92E -07	0.015 3344	0.186 4224	1.238 512	8.310 8108	2.770 8703	54.07 0352	131.5 7895	170.6 0976	25 2.2	149.2 674	136.0 625	120.2 834	114.1 6149	110.7 3171	1184. 8952	0.13071 18	372 30	712 0	50 80	218 000
<b>31A-3-gnt - 21.d</b>	- 2.148 E-07	- 7.201 E-05	- 0.000 7295	0.636 7615	6.756 7568	1.651 865	57.73 8693	134.6 2604	177.5 6098	27 1.2	160.2 5641	145.9 375	127.3 2794	128.0 7453	123.1 7073	1268. 1541	0.08363 19	374 90	688 0	51 22	217 700
<b>31A-3-gnt - 22.d</b>	5.688 E-07	0.008 1566	0.171 3362	1.039 3873	8.918 9189	2.166 9627	58.74 3719	140.4 4321	195.9 3496	30 6.5	187.7 2894	178.3 75	155.4 6559	155.9 6273	145.9 3496	1466. 3454	0.09467 05	366 20	752 0	50 46	215 600
<b>31A-3-gnt - 23.d</b>	- 2.101 E-06	- 8.189 E-05	0.066 8103	0.923 4136	8.783 7838	1.936 0568	56.83 4171	137.9 5014	200.8 1301	32 5.6	195.7 8755	191.0 625	168.8 2591	168.6 9565	156.5 0407	1545. 2388	0.08665 08	384 00	751 0	51 29	222 300
<b>31A-3-gnt - 24.d</b>	7.848 E-06	- 8.369 E-05	- 0.000 778	0.361 0503	7.432 4324	2.166 9627	57.68 8442	146.8 144	218.6 9919	36 8.7	220.5 1282	219.1 25	202.0 2429	200.1 2422	184.9 5935	1760. 9593	0.10465 06	382 30	691 0	49 81	220 700
<b>31A-3-gnt - 25.d</b>	- 2.869 E-05	- 8.858 E-05	- 0.000 7823	0.398 2495	7.364 8649	2.042 6288	62.91 4573	162.3 2687	249.5 935	42 7.7	262.6 3736	274.1 875	250.6 0729	257.7 6398	243.9 0244	2128. 7189	0.09489 24	381 70	742 0	48 41	214 500
<b>31A-3-gnt - 26.d</b>	0.000 1076	- 9.054 E-05	- 0.000 7716	0.358 8621	7.027 027	2.184 7247	62.71 3568	160.3 8781	250.8 1301	44 3.8	278.7 5458	301.1 875	281.7 8138	288.1 9876	285.7 7236	2290. 6954	0.10407 11	385 80	677 0	47 82	215 500

Samantha Nicole March  
Ultrahigh-pressure metapelites in the WGR

<b>31A-3-gnt - 27.d</b>	- 0.000 4105	- 9.657 E-05	0.042 0259	0.404 814	6.756 7568	1.989 3428	58.59 2965	160.1 108	245.1 2195	43 4.8	268.1 3187	284.3 75	263.5 6275	272.0 4969	254.0 6504	2182. 2171	0.09998 11	393 70	716 0	47 03	215 600
<b>31A-3-gnt - 28.d</b>	0.001 6329	- 0.000 102	- 0.000 8233	0.275 7112	5.743 2432	2.202 4867	61.15 5779	159.0 0277	253.6 5854	47 3.6	293.0 4029	320.6 25	313.7 6518	324.2 236	308.1 3008	2446. 0455	0.11752 11	394 60	750 0	46 30	217 000
<b>31A-3-gnt - 29.d</b>	- 0.005 6962	0.004 2414	- 0.000 8114	0.437 6368	6.891 8919	2.397 8686	69.74 8744	188.3 6565	308.1 3008	56 2.8	359.8 9011	402.1 875	386.2 3482	408.6 9565	397.1 5447	3013. 4583	0.10936 74	398 70	739 0	44 56	214 900
<b>31A-3-gnt - 30.d</b>	0.021 8987	- 0.000 1062	- 0.000 8244	0.494 5295	7.297 2973	2.042 6288	67.88 9447	180.8 8643	308.1 3008	57 1.8	365.0 1832	416.2 5	401.6 1943	416.7 7019	402.8 4553	3063. 32	0.09177 14	406 20	725 0	43 84	216 900
<b>31A-3-gnt - 31.d</b>	- 0.099 5781	- 0.000 1078	0.101 2931	1.262 5821	7.837 8378	2.557 7265	68.29 1457	183.6 5651	301.6 2602	54 8.1	358.7 9121	406.8 75	381.3 7652	391.9 2547	380.0 813	2952. 432	0.11055 36	402 40	729 0	42 23	212 600
<b>31A-3-gnt - 32.d</b>	0.013 9578	- 0.000 1308	0.022 6293	1.260 3939	13.85 1351	4.706 9272	73.26 6332	184.4 8753	303.2 5203	55 0.6	355.6 7766	387.5	365.9 919	370.1 8634	345.9 3496	2863. 6304	0.14775 4	410 30	790 0	41 73	216 400
<b>31A-3-gnt - 33.d</b>	- 0.003 8017	0.039 1517	- 0.000 9084	0.726 477	15.74 3243	9.076 3766	72.21 1055	183.1 0249	282.1 1382	48 3.5	302.9 304	304.3 75	272.8 7449	261.4 9068	232.5 2033	2322. 9072	0.26919 29	406 00	114 10	40 41	217 900
<b>31A-3-gnt - 34.d</b>	0.000 9797	0.007 9935	- 0.000 8718	0.555 7987	19.59 4595	10.07 1048	66.33 1658	159.8 338	232.1 1382	38 2.4	218.8 6447	193.2 5	164.3 7247	157.0 8075	122.6 0163	1630. 5169	0.27934 83	398 00	134 50	38 26	211 400
<b>31A-3-gnt - 35.d</b>	- 0.000 3447	0.014 1925	0.044 181	0.452 954	24.93 2432	13.65 897	73.61 809	152.6 3158	219.1 4634	35 4.7	204.2 1245	183.1 25	151.4 17	141.9 2547	115.6 5041	1522. 8083	0.31881 84	389 60	159 70	36 61	208 700
<b>31A-3-gnt - 36.d</b>	0.000 2844	0.022 8385	- 0.000 8696	0.816 1926	29.05 4054	15.55 9503	66.23 1156	130.4 7091	177.3 9837	28 2.5	169.7 8022	157.3 125	133.6 0324	130.1 2422	119.7 9675	1300. 9862	0.3547 40	385 60	176 60	35 38	207 100
<b>31A-3-gnt - 37.d</b>	- 0.000 7831	0.008 1566	0.026 9397	1.269 1466	31.08 1081	11.66 9627	55.67 8392	107.7 5623	123.1 7073	15 2.4	79.67 033	60.62 5	42.55 0607	42.85 7143	30.97 561	640.0 0565	0.28052 11	456 00	155 00	34 00	219 400
<b>31A-3-gnt - 38.d</b>	0.118 1435	0.154 9755	0.366 3793	2.078 7746	26.68 9189	13.32 1492	54.37 1859	93.35 1801	98.04 878	12 9.3	80.21 978	69.31 25	61.74 0891	62.54 6584	62.60 1626	657.1 2196	0.34970 2	416 00	152 80	30 83	203 300
<b>31A-3-gnt - 39.d</b>	0.084 3882	0.053 0179	0.214 4397	2.231 9475	29.45 9459	13.32 1492	65.72 8643	99.72 2992	110.9 7561	14 7.2	98.53 4799	89.12 5	81.33 6032	86.89 441	81.42 2764	795.2 1161	0.30273 54	416 30	177 80	28 13	199 600
<b>31A-3-gnt - 40.d</b>	0.053 5865	0.081 5661	0.560 3448	3.938 7309	34.66 2162	13.97 8686	71.65 8291	121.1 9114	131.6 6667	15 2.4	102.3 8095	76.68 75	59.59 5142	56.83 2298	47.84 5528	748.5 9922	0.28048 22	418 50	167 30	27 01	199 500
<b>31A-3-gnt - 41.d</b>	- 0.004 5992	0.064 2741	0.394 3966	4.157 5492	47.77 027	19.36 0568	66.53 2663	68.42 1053	44.67 4797	40. 31	24.15 7509	15	8.704 4534	6.832 2981	4.959 3496	213.0 5946	0.34341 7	423 40	181 00	27 28	203 200
<b>31A-3-gnt - 42.d</b>	0.008 4388	0.035 7259	0.261 8534	3.238 512	56.41 8919	26.99 8224	81.95 9799	52.85 3186	30.56 9106	25. 14	13.99 2674	8.293 75	4.696 3563	4.267 0807	1.910 5691	141.7 2272	0.39702 91	392 10	218 00	27 98	204 000
<b>31A-3-gnt - 43.d</b>	0.017 7215	0.066 8842	0.418 1034	5.579 8687	58.51 3514	29.25 3996	79.14 5729	55.78 9474	30.60 9756	26. 22	16.11 7216	9.562 5	5.425 1012	4.534 1615	3.414 6341	151.6 7284	0.42987 62	385 70	231 20	27 93	207 200
<b>31A-3-gnt - 44.d</b>	0.027 4262	0.058 7276	0.743 5345	5.623 6324	59.45 9459	22.71 7584	75.92 9648	50.30 4709	26.70 7317	20. 38	13.31 5018	7.468 75	4.615 3846	3.378 882	2.764 2276	128.9 3429	0.33810 06	378 10	197 70	30 07	211 100
<b>31A-3-gnt - 45.d</b>	8.11E -05	0.101 1419	1.314 6552	8.468 2713	52.97 2973	14.81 3499	72.21 1055	45.23 5457	22.56 0976	14. 79	8.553 1136	4.356 25	3.076 9231	2.335 4037	1.743 9024	102.6 5203	0.23951 27	393 40	176 20	26 52	207 800

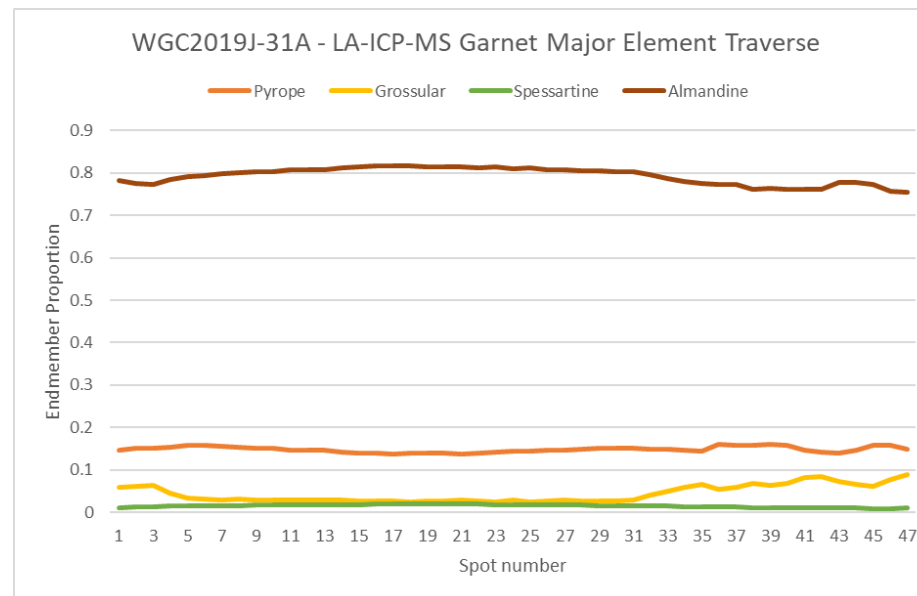
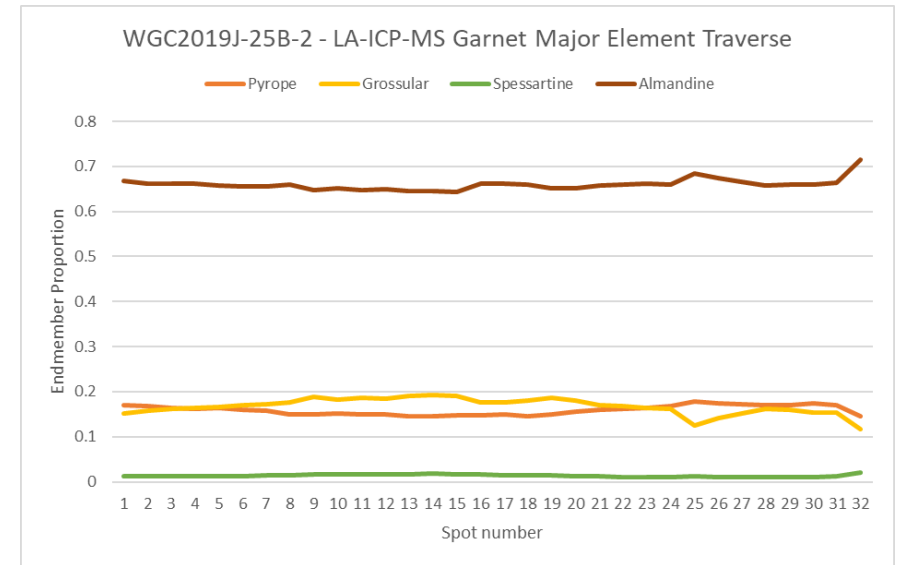
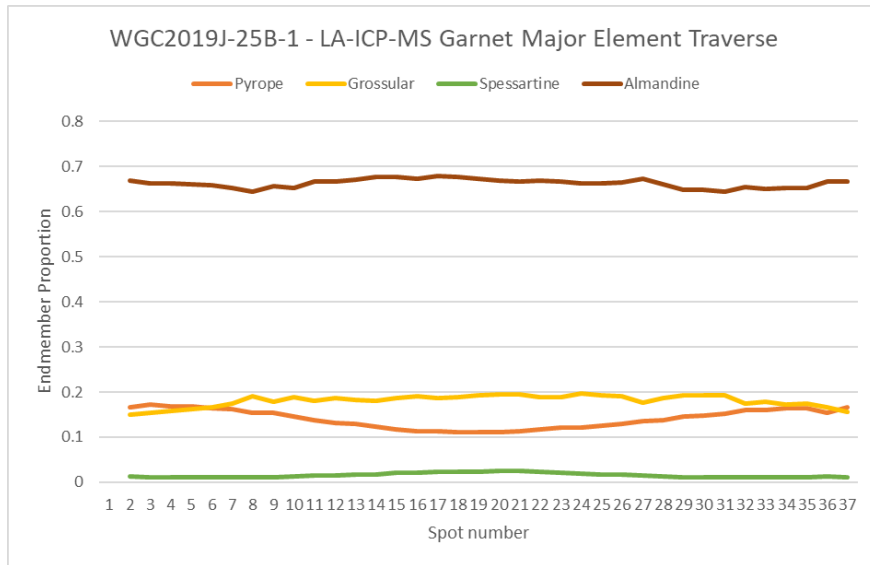
<b>31A-3-gnt - 46.d</b>	6.793 E-05	0.200 6525	2.058 1897	9.737 4179	45.74 3243	12.53 9964	64.62 3116	38.58 7258	17.47 9675	11. 25	6.703 2967	3.406 25	1.967 6113	1.534 1615	1.004 065	81.93 2317	0.23064 23	415 00	159 80	21 66	203 500
<b>31A-3-gnt - 47.d</b>	0.032	0.055	0.560	5.185	59.59	24.93	74.17	41.77	17.84	10.	6.959	2.643	1.412	1.031	1.130	83.27	0.37509	415	207	21	200
<b>31A-3-gnt - 48.d</b>	0.018 5654	0.049 7553	0.387 931	3.172 8665	61.21 6216	36.05 6838	113.6 1809	83.43 4903	44.22 7642	34. 45	22.72 8938	13.31 25	8.259 1093	7.869 5652	5.447 1545	219.7 2981	0.43234 52	392 00	234 20	25 81	199 900

### Garnet trace element standards

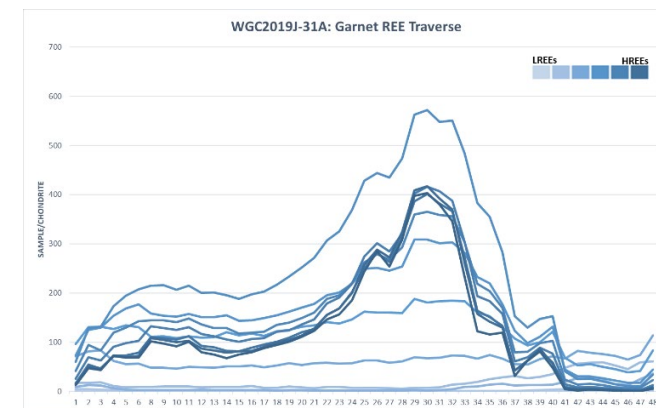
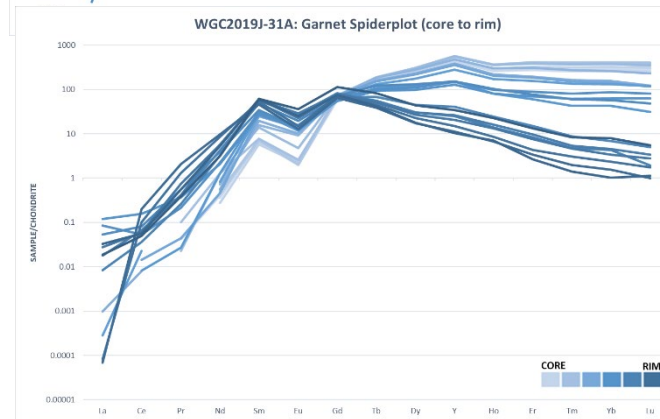
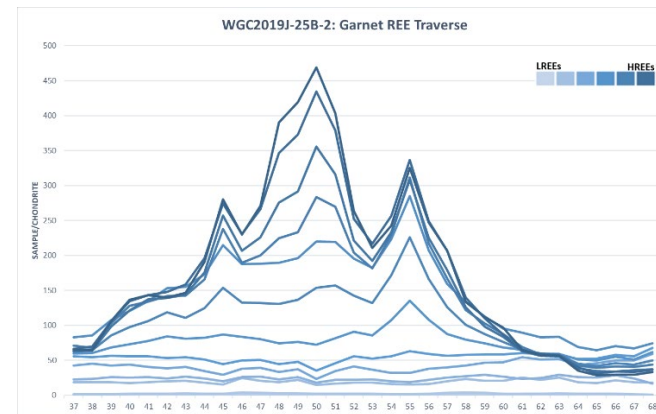
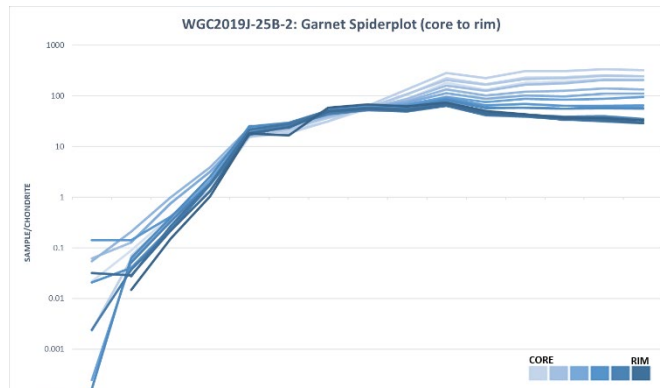
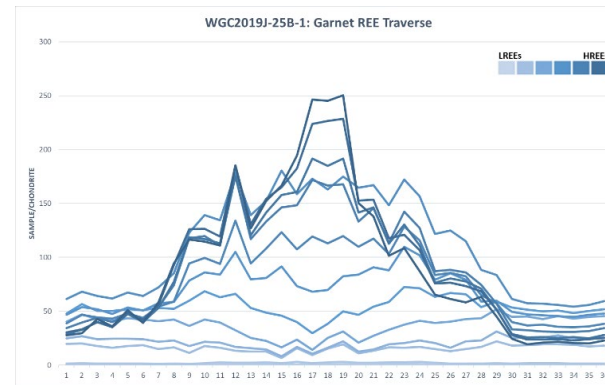
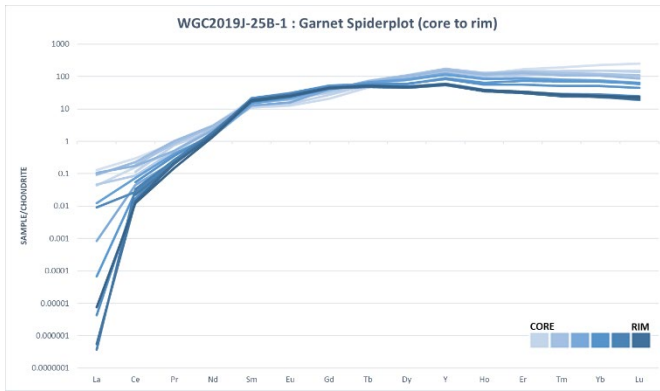
Standard	La	Ce	Pr	Nd	Sm	Eu	Gd	Tb	Dy	Ho	Er	Tm	Yb	Lu
<b>GSD_29 - 1.d</b>	23.37	27.2	29.74	28.65	31.68	26.55	31.98	30.74	32.69	32.11	25.58	31.91	32.25	32.51
<b>GSD_29 - 2.d</b>	24.32	27.31	30.27	29.38	32.96	26.86	33.2	31.15	33.82	33.13	25.91	32.72	33.32	33.04
<b>GSD_29 - 3.d</b>	21.57	27.5	29.4	28.31	30.9	26.02	32.2	30.54	32.75	32.14	26.19	31.72	31.77	32.3
<b>GSD_29 - 4.d</b>	23.78	27.77	30.15	28.92	32.29	26.72	32.61	31.17	32.97	32.91	25.19	32.21	34.03	33.48
<b>GSD_29 - 5.d</b>	18.88	27.82	30.35	29.41	32.23	26.94	32.4	31.36	33.99	32.97	25.78	32.8	32.75	33.99
<b>GSD_29 - 6.d</b>	22.84	27.41	29.3	28.56	31.32	26.94	32.71	30.47	34.28	32.66	25.77	32.79	32.03	33.18
<b>GSD_29 - 7.d</b>	22.21	27.77	29.94	28.73	32.5	26.71	31.8	30.5	33.82	32.38	25.33	32.75	33.77	33.32
<b>GSD_29 - 8.d</b>	26.24	27.74	30.5	29.77	32.8	27.29	31.9	31.32	33.61	32.61	25.43	32.36	33.49	34.28
<b>GSD_29 - 9.d</b>	26.63	28.72	31.43	30.31	32.43	27.86	33.3	31.6	34.46	33.06	26.19	33.78	34.44	34.21
<b>GSD_29 - 10.d</b>	26.42	28.08	30.61	29.67	31.99	26.84	32.82	31.33	33.99	32.74	26.04	32.98	33.06	34.18
<b>GSD_29 - 11.d</b>	26	27.81	29.97	29.25	31.35	26.96	33.3	31.15	33.22	32.58	25.48	32.97	33.15	34.21
<b>GSD_29 - 12.d</b>	25.96	27.57	30.42	29.3	31.8	27.23	32.5	31.25	33.79	32.93	25.81	32.81	32.81	34.17
<b>GSD_29 - 13.d</b>	24.37	27.49	30.6	29.22	31.83	27.1	33.4	31.02	33.91	32.81	25.9	32.75	33.09	34.31
<b>GSD - 1.d</b>	25.4	28.44	31.59	30.3	32.96	27.99	34.12	32.67	35.6	34.31	27.01	34.35	34.78	35.38
<b>GSD - 2.d</b>	26.15	28.77	31.3	30.82	33.56	28.48	34.43	32.89	35.46	34.55	27.09	34.52	35.23	35.72
<b>GSD - 3.d</b>	26.69	28.97	31.71	30.82	33.02	28.25	34.9	33.34	36.36	34.54	27.21	34.75	35.38	35.81
<b>GSD - 4.d</b>	26.84	29.03	31.92	31.33	33.37	28.69	35.19	33.34	36.17	34.69	27.48	34.92	35.42	35.96
<b>GSD - 5.d</b>	25.2	28.94	31.93	31.15	33.95	28.65	34.4	32.92	35.91	34.56	27.45	34.63	34.9	35.59
<b>GSD - 6.d</b>	25.52	28.86	31.5	30.47	33.63	28.3	34.03	32.87	35.66	34.2	27.21	34.39	35.06	35.7
<b>GSD - 7.d</b>	25.46	28.37	30.84	29.88	32.01	27.82	33.48	32.23	35.14	33.72	27.13	33.64	34.32	34.7
<b>GSD - 8.d</b>	25.88	28.89	31.41	30.89	32.47	28.2	33.44	32.59	35.49	33.89	27	34.21	34.37	35.06
<b>GSD - 9.d</b>	24.52	28.75	31.63	30.67	33.33	28.32	34.89	33.11	35.85	34.54	27.28	34.58	35.25	35.69

<b>GSD - 10.d</b>	25.27	29.33	32.14	31.39	33.96	28.49	35.53	33.42	36.24	34.9	27.54	35.32	35.76	36.22
<b>GSD - 11.d</b>	25.98	29.03	31.55	31.04	32.88	28	34.43	32.76	35.3	34.46	26.96	34.44	35.33	35.61
<b>GSD - 12.d</b>	26.24	28.74	31.2	30.35	33.52	28.23	34.2	32.65	35.2	34.21	26.66	34.24	34.42	35.41
<b>GSD - 13.d</b>	25.7	29.17	31.88	29.97	33.13	28.29	33.9	32.42	35.37	34.13	26.93	34.3	35.14	35.58
<b>GSD - 14.d</b>	25.95	29.22	31.75	30.52	32.93	27.85	33.95	32.32	35.15	34.15	27.13	34.16	34.65	35.27
<b>GSD - 15.d</b>	26.95	28.96	31.08	30.66	32.88	27.9	34.34	32.33	35.18	33.92	26.92	34.01	34.01	34.89
<b>GSD - 16.d</b>	27.54	29.51	32.07	30.82	33.28	28.5	34.99	32.95	35.57	34.45	27.35	34.7	35.17	36.16
<b>GSD - 17.d</b>	27.58	29.37	32.33	31.87	34.4	28.86	34.93	33.36	36.79	35.19	27.99	35.36	35.98	36.74
<b>GSD - 18.d</b>	28.25	30.25	32.8	32.3	33.97	29.33	35.84	34.21	37.63	35.7	28.32	36.11	36.77	37.41
<b>GSD - 19.d</b>	27.8	29.39	31.96	30.5	33.86	28.84	34.8	33.03	35.95	34.39	27.47	35.01	35.33	36.23
<b>GSD - 20.d</b>	27.58	29.53	32.26	31.49	33.64	28.64	34.56	33.29	35.91	34.61	27.87	35.11	35.6	36.23
<b>GSD - 21.d</b>	26.88	28.85	31.46	30.51	33.16	28.01	33.89	32.38	35.39	34	27.31	34.26	34.93	35.37
<b>GSD - 22.d</b>	26.92	28.51	31.21	30.14	32.32	27.97	33.73	32.01	35.17	33.44	27.06	34.1	34.41	35.2
<b>GSD - 23.d</b>	27.02	28.82	31.62	30.69	33.41	28.07	34.29	32.45	35.87	34.12	27.26	34.31	34.79	35.59
<b>GSD - 24.d</b>	27.1	29.2	31.56	30.74	32.91	28.23	34.75	32.94	35.12	34.34	27.47	34.35	34.69	35.42
<b>GSD - 25.d</b>	26.85	28.87	31.51	30.74	32.84	28.29	34.76	32.69	35.35	33.93	27.16	34.46	35.02	35.73
<b>GSD - 26.d</b>	26.81	28.58	31.44	30.42	32.72	28.4	34.72	32.92	35.79	34.3	27.25	34.78	35.15	36.12
<b>NIST610 - 1.d</b>	249.2	260.9	257.6	246.2	259.9	256	257.2	250.2	250.3	256.2	259.5	248.3	255.6	250.7
<b>NIST610 - 2.d</b>	253.2	259	257.3	246.8	259.4	255.5	255.9	249.6	249.4	256.6	259.5	247.7	257.6	249.6
<b>NIST610 - 3.d</b>	255.7	261.2	258.2	249.1	261.4	259.4	258.5	252.4	252.7	259.5	263.8	252	260.4	254.1
<b>NIST610 - 4.d</b>	256.8	262.8	260.3	250.4	262.8	260.2	262.2	254.3	253.6	260.8	263.9	252.5	261.2	255.4
<b>NIST610 - 5.d</b>	253.1	260.5	258.1	246.9	260	257.1	257.7	251.1	252.8	258.3	262.2	249.6	259.2	252.9
<b>NIST610 - 6.d</b>	254.5	261.1	258.2	247.8	261.8	258	258.5	250.6	251.2	258.7	263.4	250.5	258.7	253.1
<b>NIST610 - 7.d</b>	249.6	257.4	254.8	244	255.5	254.1	255.3	248.7	248.1	255.6	259	247.9	256.3	249.5
<b>NIST610 - 8.d</b>	251.8	258.5	255.4	246.9	258.7	254.7	256.9	249.7	250.5	256.1	261.1	248.8	257.2	252.3
<b>NIST610 - 9.d</b>	250.6	258.6	256.8	246.1	259.4	256.6	258.3	250.3	249.9	257.4	260.7	249.8	258.9	252.8
<b>NIST610 - 10.d</b>	251.8	259.5	257.5	246.9	261.7	257.5	257.8	251.2	250.4	258.7	261.9	250	258.5	252.8
<b>NIST610 - 11.d</b>	248	256.3	253.2	242.3	256.1	253.6	254	247.1	248.1	254.9	258.1	246.3	254	249.2
<b>NIST610 - 12.d</b>	250.7	258.7	256	246.1	258.8	255.8	256	249.7	250.5	257.7	261	248.6	258.1	251.8
<b>NIST610 - 13.d</b>	251.9	260.7	258.1	246.3	261.7	257.3	257.3	251.6	251.4	257.8	261	249.7	258.8	252.6
<b>NIST610 - 14.d</b>	252.4	260.7	258.2	247.1	260.3	258	256.7	251.4	250.4	259.1	261.9	250.5	259.3	252.9

<b>NIST610 - 15.d</b>	251.2	257.8	254.9	246.3	259.2	254.9	256.9	250.7	250.9	257.7	260.1	249.2	258.6	251.2
<b>NIST610 - 16.d</b>	251.9	259	256.3	246.7	258.3	256.8	257.9	251.5	249.2	256.1	260	249.6	257.2	252.4
<b>NIST610 - 17.d</b>	254.8	261	258.1	247.2	261.4	259.7	259	252.4	252.1	258.2	262	252.2	259.5	253.6
<b>NIST610 - 18.d</b>	259.9	267.2	263.4	252.9	265.9	262.2	264.4	255.6	256.5	262.6	266	255.2	264.6	256.3
<b>NIST610 - 19.d</b>	254.2	260.2	258.2	247.3	261.2	258.1	258	250.8	252	257.7	261.9	249.8	258.9	253.1
<b>NIST610 - 20.d</b>	256.6	262.9	261.5	248.9	262.2	260.2	260.9	253.2	254.1	260.9	263.7	252.5	261.2	256
<b>NIST610 - 21.d</b>	254.4	262.1	258.5	248.6	261.1	258.5	258.6	252.2	252.8	259.7	262.8	251.8	259.4	253.7
<b>NIST610 - 22.d</b>	252.4	260.2	256.9	247.2	261.3	257.1	256.8	250.9	250.6	258	261.9	248.9	258.9	251.4
<b>NIST610 - 23.d</b>	252.7	261	257.1	247.6	258.6	256.4	257.7	250.4	250.7	257.5	262	248.6	258	251.5
<b>NIST610 - 24.d</b>	252.3	260.1	257	247.1	259.7	257.4	257.6	251.7	250.2	257.4	262	250.1	258.7	251.7
<b>NIST610 - 25.d</b>	248.7	256.7	254.8	243.7	257.7	253.4	253.7	247.8	247.5	254.7	257.2	246	255	249.5
<b>NIST610 - 26.d</b>	251.2	259.7	256.1	245.4	257.8	255.5	257.9	249	249.4	256.8	260.2	248.3	256.2	250.5

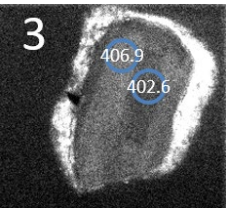
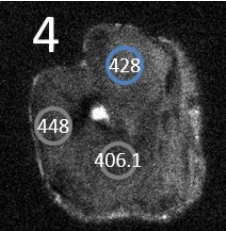
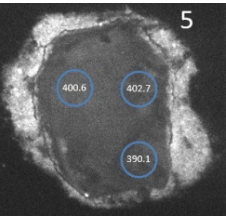
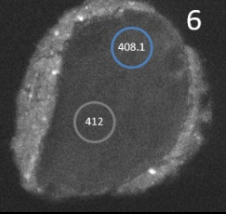


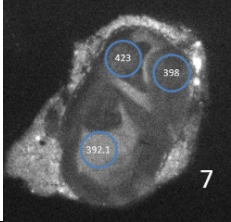
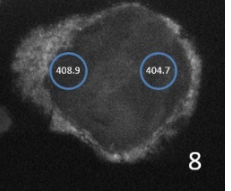
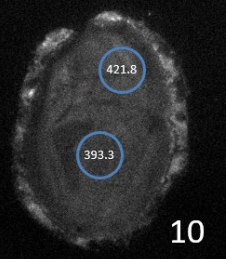
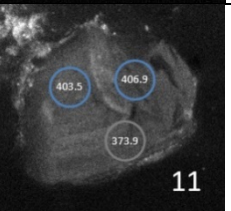
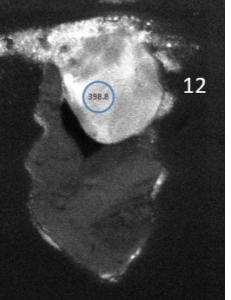




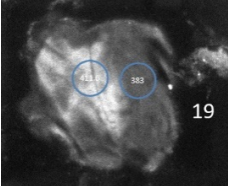
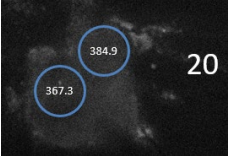
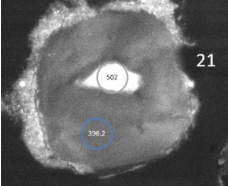
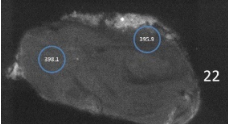
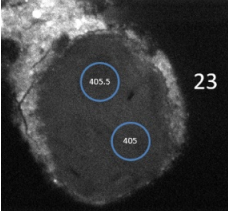
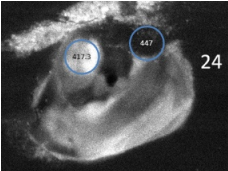
### APPENDIX 3C: LA-ICP-MS ZIRCON RESULTS

#### Zircon morphology

Sample	Textural location	Zoning	Size (long axis)	Crystal habit	Comments	SEM-CL image
WGC-25B-3 - 1.d	core					
WGC-25B-3 - 2.d	rim	Y	~200µm	Euhedral, tabular		
WGC-25B-4 - 1.d	rim					
WGC-25B-4 - 2.d	core	Y	~200µm	Euhedral, equant	Relatively flat zoning throughout grain, tiny detrital core not targeted	
WGC-25B-4 - 3.d	rim					
WGC-25B-5 - 1.d	core					
WGC-25B-5 - 2.d	rim	N	~100µm	Euhedral, tabular		
WGC-25B-5 - 3.d	rim					
WGC-25B-6 - 1.d	core					
WGC-25B-6 - 2.d	rim	N	~100µm	Euhedral, tabular		
WGC-25B-7 - 1.d	rim	Y	~100µm	Euhedral, tabular	Random, smeared looking zoning.	
WGC-25B-7 - 2.d	rim					

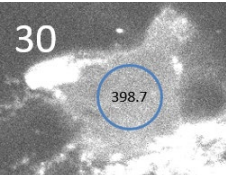
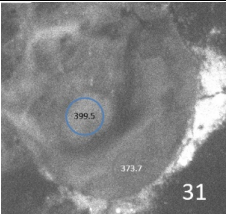
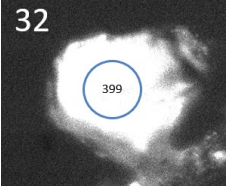
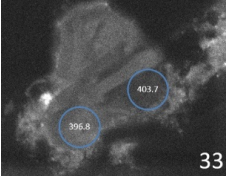
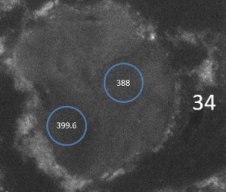
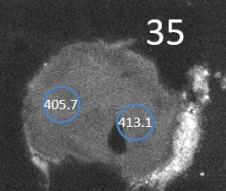
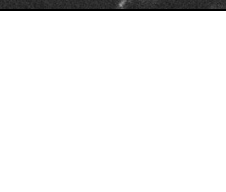

WGC-25B-7 - 3.d	core						
WGC-25B-8 - 1.d	rim						
WGC-25B-8 - 2.d	rim	N	~75µm	Euhedral, equant	Slight patchiness? But overall flat zoning		
WGC-25B-10 - 1.d	core						
WGC-25B-10 - 2.d	rim	Y	~100µm	Euhedral, prismatic			
WGC-25B-11 - 1.d	core						
WGC-25B-11 - 2.d	rim						
WGC-25B-11 - 3.d	rim	Y	~100µm	Subhedral, equant	Patchy zoning radiating outwards from 11-1		
WGC-25B-12 - 1.d	core						

WGC-25B-13 - 1.d	core						<p>13</p>
WGC-25B-13 - 2.d	rim	N	~75µm	Subhedral, equant	Slight patchiness? But overall flat zoning		
WGC-25B-14 - 1.d	core	Y	~75µm	Euhedral, tabular	Patchy	<p>14</p>	
WGC-25B-15 - 1.d	core					<p>15</p>	
WGC-25B-15 - 2.d	rim	Y	~100µm	Euhedral, prismatic	Complex zoning. Dark core, bright mantle, dark, light, dark rim.		
WGC-25B-16 - 1.d	core					<p>16</p>	
WGC-25B-16 - 2.d	rim	Y	~100µm	Euhedral, prismatic			
WGC-25B-17 - 1.d	core					<p>17</p>	
WGC-25B-17 - 2.d	rim	Y	~75µm	Euhedral, equant			
WGC-25B-18 - 1.d	core					<p>18</p>	
WGC-25B-18 - 2.d	core	N	~100µm	Subhedral, tabular			
WGC-25B-19 - 1.d	core	Y	~100µm				

WGC-25B-19 - 2.d	rim				Anhedral, tabular	
WGC-25B-20 - 1.d	core					
WGC-25B-20 - 2.d	core	N	~50µm		Subhedral, equant	
WGC-25B-21 - 1.d	core					
WGC-25B-21 - 2.d	rim	Y	~100µm		Euhedral, equant	
WGC-25B-22 - 1.d	rim					
WGC-25B-22 - 2.d	rim	N	~150µm		Euhedral, tabular	
WGC-25B-23 - 1.d	core					
WGC-25B-23 - 2.d	rim	N	~75µm		Euhedral, equant	
WGC-25B-24 - 1.d	mantle					
WGC-25B-24 - 2.d	core	Y	~75µm		Euhedral, equant	Complex zoning radiating out from 24-2
WGC-25B-25 - 1.d	rim	Y	~150µm			

Samantha Nicole March  
 Ultrahigh-pressure metapelites in the WGR

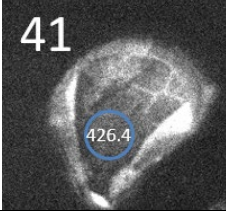
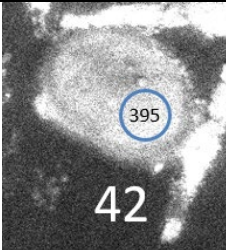
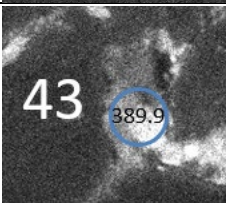
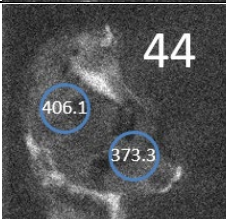
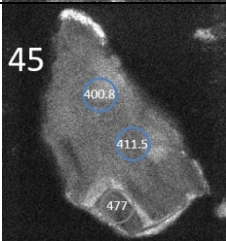
WGC-25B-25 - 2.d	rim				Euhedral, tabular	Weird fractured looking zoning? 25-1 on dark patch	
WGC-25B-26 - 1.d	core						
WGC-25B-26 - 2.d	rim	Y	~100µm		Euhedral, tabular		
WGC-25B-27 - 1.d	rim						
WGC-25B-27 - 2.d	rim	Y	~100µm		Anhedra	27-1 located on darker patch. Asymmetric crystal habit	
WGC-25B-28 - 1.d	rim						
WGC-25B-28 - 2.d	rim	Y	~75µm		Anhedra, tabular	Swirly zoning. 28-2 on darker patch	
WGC-25B-29 - 1.d	core	Y	~150µm		Euhedral, tabular		

WGC-25B-30 - 1.d	core	N	~50µm	Anhedral		
WGC-25B-31 - 1.d	core					
WGC-25B-31 - 2.d	rim	Y	~100µm	Euhedral, equant	Faint, patchy zoning	
WGC-25B-32 - 1.d	core	Y	~50µm	Euhedral, equant		
WGC-25B-33 - 1.d	core					
WGC-25B-33 - 2.d	rim	Y	~75µm	Subhedral, triangular	Faint, patchy zoning	
WGC-25B-34 - 1.d	core					
WGC-25B-34 - 2.d	rim	Y	~75µm	Euhedral, equant	Faint, patchy zoning	
WGC-25B-35 - 1.d	rim					
WGC-25B-35 - 2.d	core	Y	~100µm	Euhedral, equant	Flat zoning aside from a small, dark core	
WGC-25B-36 - 1.d	rim	Y	~100µm			

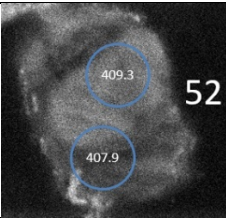
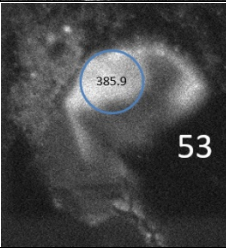
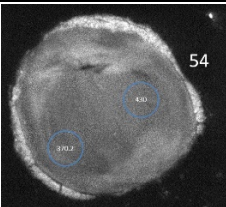
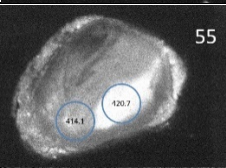
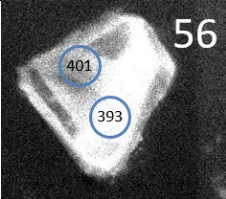
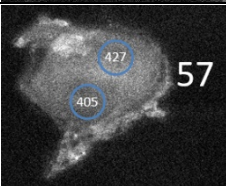


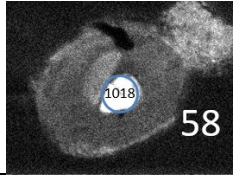
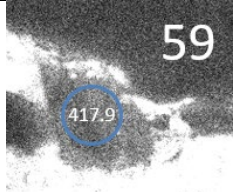
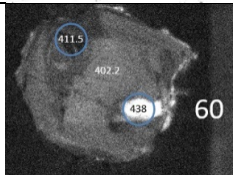
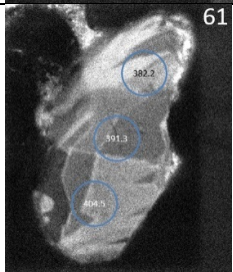
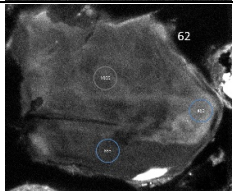


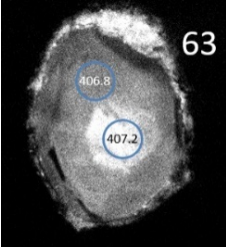
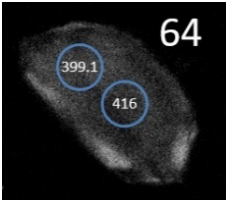
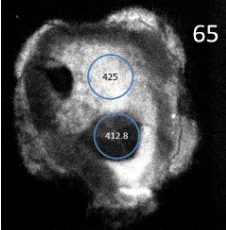
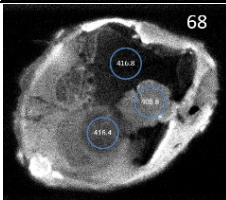
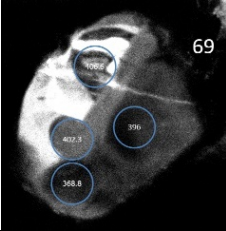


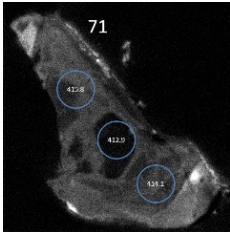
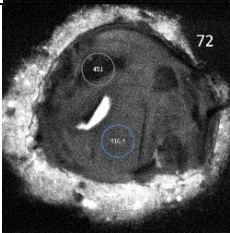
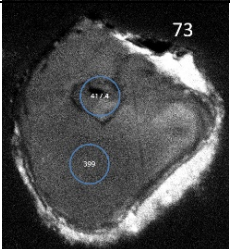
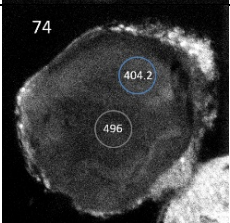
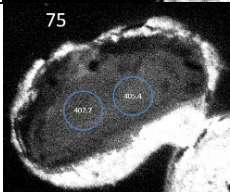
WGC-25B-41 - 1.d	core	Y	~75 $\mu$ m	Euhedral, tabular	41 
WGC-25B-42 - 1.d	core	N	~50 $\mu$ m	Euhedral, equant	42 
WGC-25B-43 - 1.d	core	N	~50 $\mu$ m	Subhedral, tabular	43 
WGC-25B-44 - 1.d	rim				44 
WGC-25B-44 - 2.d	core	Y	~75 $\mu$ m	Anhedral, tabular	
WGC-25B-45 - 1.d	core				45 
WGC-25B-45 - 2.d	rim				
WGC-25B-45 - 3.d	rim	Y	~100 $\mu$ m	Anhedral, tabular	
WGC-25B-46 - 1.d	core	Y	~100 $\mu$ m	Faint, patchy zoning	

WGC-25B-46 - 2.d	core				Euhedral, equant		46 
WGC-25B-47 - 1.d	rim						47 
WGC-25B-47 - 2.d	core	Y	~75µm		Subhedral, equant		
WGC-25B-48 - 1.d	core						48 
WGC-25B-48 - 2.d	core	Y	~100µm		Euhedral, tabular	Zoned but both targets located in core due to thin rim	
WGC-25B-49 - 1.d	core						49 
WGC-25B-49 - 2.d	rim	Y	~75µm		Euhedral, tabular	Faint, patchy zoning	
WGC-25B-50 - 1.d	rim						50 
WGC-25B-50 - 2.d	core	Y	~100µm		Anhedral, tabular	Faint, patchy zoning	
WGC-25B-51 - 1.d	core	Y	~50µm		Euhedral, prismatic		51 

WGC-25B-52 - 1.d	core						
WGC-25B-52 - 2.d	rim	Y	~75µm	Euhedral, tabular	Faint, patchy zoning		
WGC-25B-53 - 1.d	core						
WGC-25B-53 - 2.d	rim	Y	~75µm	Anhedral			
WGC-25B-54 - 1.d	core						
WGC-25B-54 - 2.d	rim	Y	~100µm	Euhedral, equant			
WGC-25B-55 - 1.d	core						
WGC-25B-55 - 2.d	rim	Y	~75µm	Euhedral, tabular			
WGC-25B-56 - 1.d	core						
WGC-25B-56 - 2.d	core	Y	~75µm	Anhedral			
WGC-25B-57 - 1.d	core						
WGC-25B-57 - 2.d	rim	Y	~75µm	Subhedral, tabular			

WGC-25B-58 - 1.d	core	Y	~75µm	Euhedral, equant	Bright, detrital core	
WGC-25B-59 - 1.d	core	N	~50µm	Anhedral		
WGC-25B-60 - 1.d	core	Y	~100µm	Subhedral, equant	Small, bright core and faint, irregular zoning surrounding	
WGC-25B-60 - 2.d	rim					
WGC-25B-60 - 3.d	rim					
WGC-25B-61 - 1.d	rim	Y	~100µm	Anhedral, tabular		
WGC-25B-61 - 2.d	core					
WGC-25B-61 - 3.d	rim					
WGC-25B-62 - 1.d	rim	Y	~200µm	Subhedral, equant	Patchy and irregular. Difficult to differentiate between zoning boundaries	
WGC-25B-62 - 2.d	rim					
WGC-25B-62 - 3.d	core					
WGC-25B-63 - 1.d	core	Y	~100µm			

WGC-25B-63 - 2.d	rim				Subhedral, prismatic		
WGC-25B-64 - 1.d	core						
WGC-25B-64 - 2.d	rim	Y	~75µm		Subhedral, prismatic	Relatively flat, slight patchy zoning around edges	
WGC-25B-65 - 1.d	core						
WGC-25B-65 - 2.d	rim	Y	~100µm		Subhedral, equant	Patchy zoning with distinct dark sectors	
WGC-25B-68 - 1.d	core						
WGC-25B-68 - 2.d	core						
WGC-25B-68 - 3.d	mantle	Y	~125µm		Euhedral, equant		
WGC-25B-69 - 1.d	rim						
WGC-25B-69 - 2.d	core						
WGC-25B-69 - 3.d	rim	Y	~100µm		Euhedral, equant	Very complex zoning. Grain looks like it has been halved	
WGC-25B-69 - 4.d	core						
WGC-25B-71 - 1.d	rim	Y	~125µm		Anhedral		
WGC-25B-71 - 2.d	core						

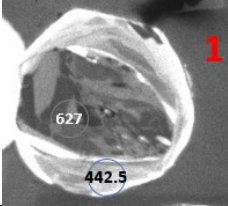
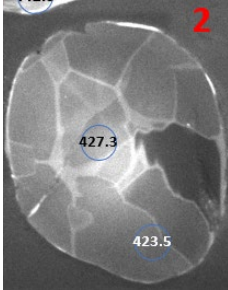
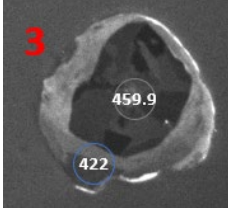
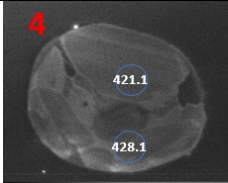
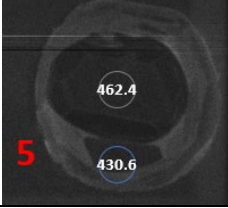
WGC-25B-71 - 3.d	rim						
WGC-25B-72 - 1.d WGC-25B-72 - 2.d	core						
WGC-25B-73 - 1.d	core						
WGC-25B-73 - 2.d	rim	Y	~100µm	Subhedral, equant			
WGC-25B-74 - 1.d	rim						
WGC-25B-74 - 2.d	core	Y	~100µm	Euhedral, equant	Faint, patchy zoning		
WGC-25B-75 - 1.d	core						
WGC-25B-75 - 2.d	core	N	~100µm	Euhedral, tabular	Relatively flat, slight patchy zoning around edges		
WGC-25B-76 - 1.d	core	Y	~150µm		Faint, patchy zoning		

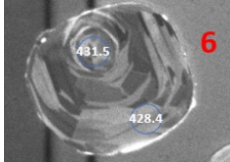
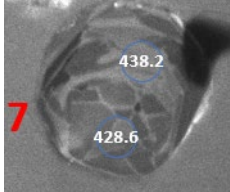
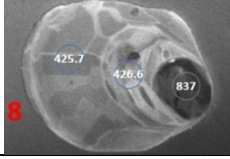
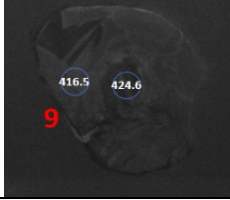
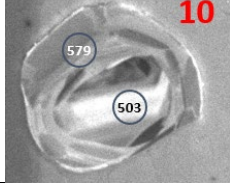
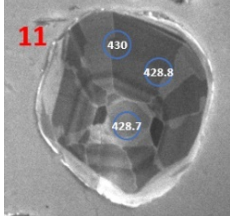

WGC-25B-76 - 2.d	core			Anhedral, tabular		
WGC-25B-77 - 1.d	core					
WGC-25B-77 - 2.d	core	Y	~75µm	Euhedral, equant	Relatively flat, slight patchy zoning around edges	
WGC-25B-78 - 1.d	core					
WGC-25B-78 - 2.d	mantle	Y	~200µm	Subhedral, hexagonal	78-1 is located on top of a complex zoned area around what looks like a detrital core. Slightly prismatic	
WGC-25B-78 - 3.d	rim					
WGC-25B-79 - 1.d	core					
WGC-25B-79 - 2.d	core	Y	~75µm	Euhedral, equant	Relatively flat, slight patchy zoning around edges	
WGC-25B-80 - 1.d	rim					
WGC-25B-80 - 2.d	core	Y	~100µm	Anhedral	Very patchy	
WGC-25B-81 - 1.d	core	N	~75µm			

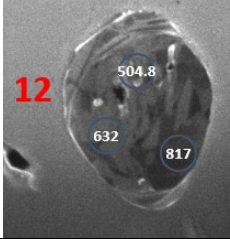
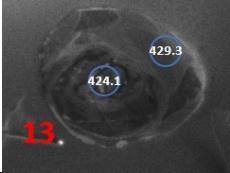
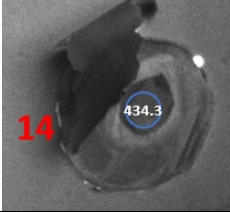
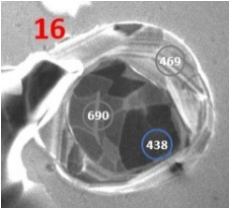
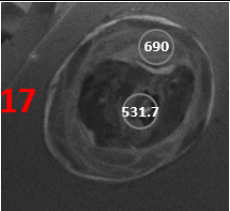
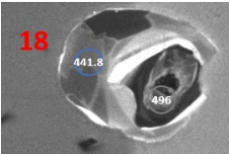


WGC-25B-81 - 2.d	core				Euhedral, equant	
WGC-25B-82 - 1.d	rim					
WGC-25B-82 - 2.d	core					
WGC-25B-82 - 3.d	core	Y	~100µm		Subhedral, prismatic	
WGC-25B-83 - 1.d	rim					
WGC-25B-83 - 2.d	core	Y	~100µm		Subhedral, prismatic	
WGC-25B-84 - 1.d	core	Y	~100µm		Euhedral, prismatic	
WGC-25B-85 - 1.d	rim					
WGC-25B-85 - 2.d	core	Y	~100µm		Subhedral, prismatic	
31A-1 - 1.d	core	Y	~100µm			detrital core?

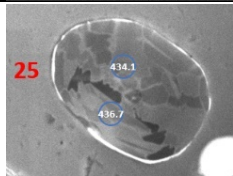
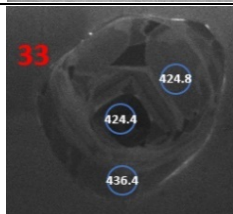
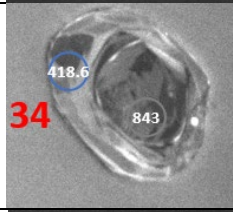
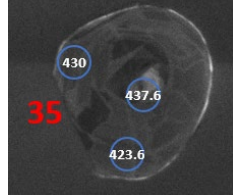
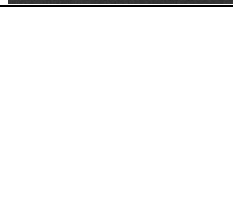


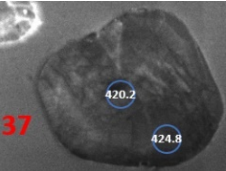
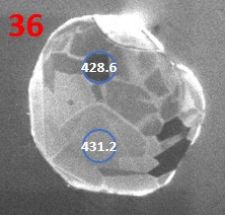
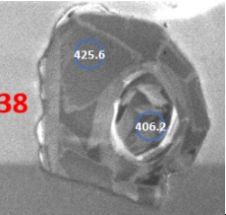
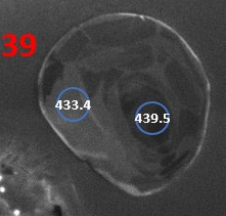
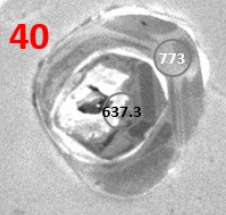
31A-1 - 2.d	rim				Euhedral, equant		
31A-2 - 1.d	core						
31A-2 - 2.d	rim	N	~125μm		Euhedral, tabular	Relatively flat zoning	
31A-3 - 1.d	core						
31A-3 - 2.d	rim	Y	~75μm		Euhedral, equant	detrital core?	
31A-4 - 1.d	core						
31A-4 - 2.d	rim	N	~100μm		Euhedral, tabular	Relatively flat zoning	
31A-5 - 1.d	core						
31A-5 - 2.d	rim	Y	~100μm		Euhedral, equant	Dark, detrital core	
31A-6 - 1.d	core	Y	~75μm			detrital core?	

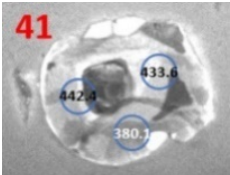
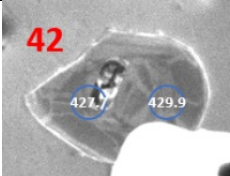
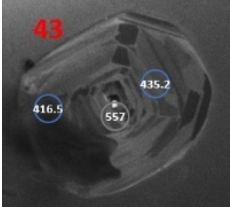
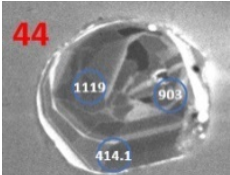
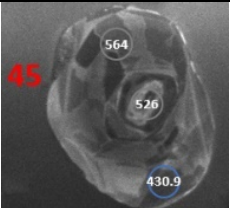
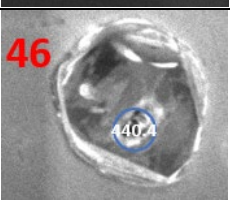
31A-6 - 2.d	rim				Euhedral, equant		
31A-7 - 1.d	core						
31A-7 - 2.d	rim	minor	~50µm		Euhedral, equant		
31A-8 - 1.d	core				Euhedral, tabular	detrital core?	
31A-8 - 2.d	mantle	Y	~100µm			second zoned sector	
31A-8 - 3.d	rim					third zoned sector	
31A-9 - 1.d	core						
31A-9 - 2.d	rim	N	~100µm		Subhedral, equant		
31A-10 - 1.d	core						
31A-10 - 2.d	rim	Y	~75µm		Euhedral, equant	quite a bright core - could just be reflective crystal plane? Dark around	
31A-11 - 1.d	core						
31A-11 - 2.d	rim						
31A-11 - 3.d	rim	Y	~125µm		Euhedral, equant	pale core compared to usual dark core in other zircons	
31A-12 - 1.d	core						
31A-12 - 2.d	rim	Y	~75µm		Euhedral, prismatic	overall messy looking grain in terms of zoning	

31A-12 - 3.d	rim						
31A-13 - 1.d	core						
31A-13 - 2.d	rim	Y	~75µm	Euhedral, equant	dark detrital core?		
31A-14 - 1.d	core	Y	~75µm	Euhedral, equant			
31A-16 - 1.d	mantle				second zone of dark, detrital core		
31A-16 - 2.d	rim	Y	~100µm	Euhedral, equant			
31A-16 - 3.d	core				Dark, detrital core		
31A-17 - 1.d	core						
31A-17 - 2.d	rim	Y	~75µm	Euhedral, equant	dark, detrital core		
31A-18 - 1.d	mantle						
31A-18 - 2.d	rim	Y	~100µm	Subhedral, equant	Second zone of dark, detrital core		

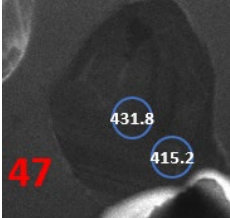
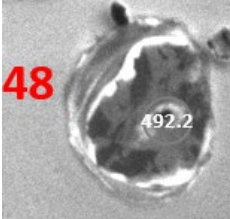
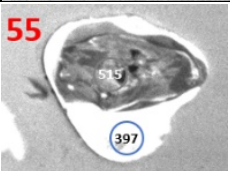
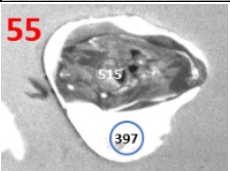
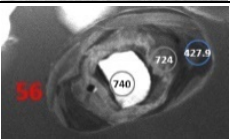
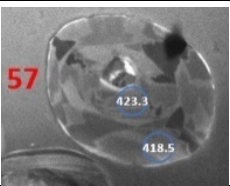
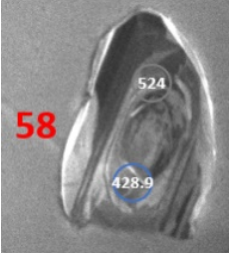
31A-19 - 1.d	mantle						
31A-19 - 2.d	mantle	Y	~75µm	Euhedral, tabular			
31A-20 - 1.d	core						
31A-20 - 2.d	rim	N	~125µm	Euhedral, equant			
31A-21 - 1.d	mantle						
31A-21 - 2.d	rim				Second zone of dark, detrital core. Could have potentially overlapped between two zones		
31A-21 - 3.d	rim	Y	~100µm	Euhedral, equant			
31A-22 - 1.d	mantle						
31A-22 - 2.d	rim	Y	~100µm	Anhedral	second zone of dark, detrital core		
31A-23 - 1.d	core						
31A-23 - 2.d	rim	Y	~125µm	Euhedral, equant			
31A-24 - 1.d	core	Y	~100µm				

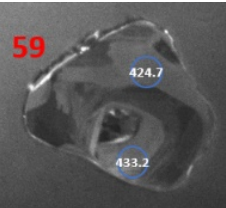
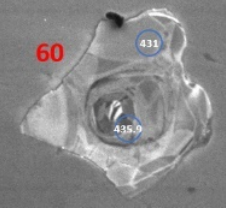
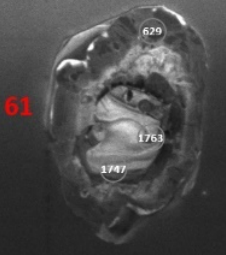
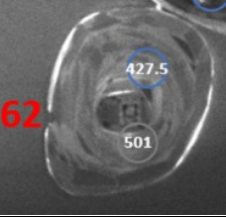
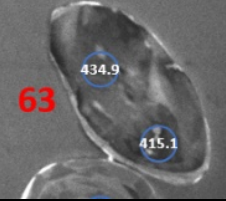
31A-24 - 2.d	rim				Subhedral, equant	
31A-25 - 1.d	core					
31A-25 - 2.d	rim	N	~125μm		Euhedral, tabular	
31A-32 - 1.d	core					
31A-32 - 2.d	rim	Y	~100μm		Euhedral, equant	potentially overlapping mantle and core
31A-33 - 1.d	core					
31A-33 - 2.d	mantle	Y	~100μm		Euhedral, tabular	
31A-33 - 3.d	rim					
31A-34 - 1.d	core					
31A-34 - 2.d	rim	Y	~75μm		Euhedral, tabular	
31A-35 - 1.d	core					
31A-35 - 2.d	rim					
31A-35 - 3.d	rim	Y	~100μm		Euhedral, equant	

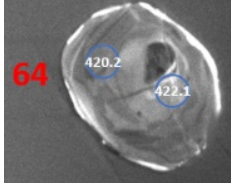
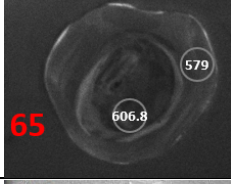
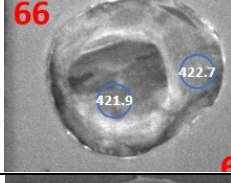
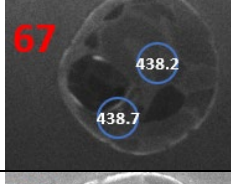
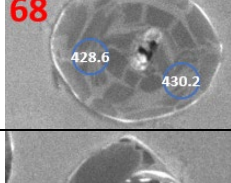
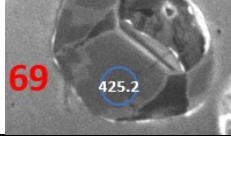
31A-37 - 1.d	core						
31A-37 - 2.d	rim	N	~125 $\mu$ m	Euhedral, equant	Very patchy looking		
31A-36 - 1.d	core						
31A-36 - 2.d	rim	minor	~75 $\mu$ m	Subhedral, equant			
31A-38 - 1.d	core						
31A-38 - 2.d	rim	Y	~100 $\mu$ m	Anhedral			
31A-39 - 1.d	core						
31A-39 - 2.d	rim	minor	~75 $\mu$ m	Euhedral, equant			
31A-40 - 1.d	mantle						
31A-40 - 2.d	rim	Y	~75 $\mu$ m	Euhedral, equant	potentially overlapping mantle and core		
31A-41 - 1.d	core	Y	~75 $\mu$ m	Subhedral, equant	potentially overlapping core and rim		
31A-41 - 2.d	rim						

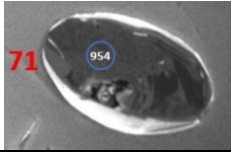
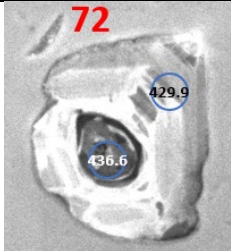
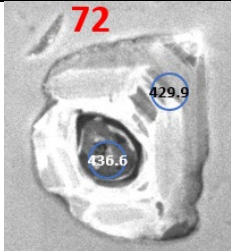
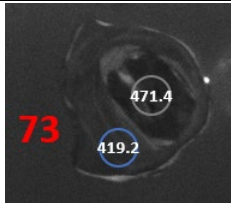
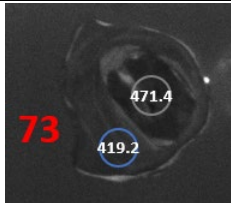
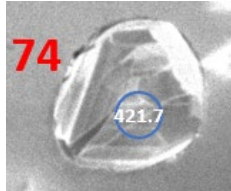
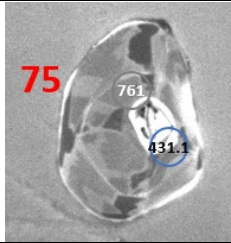
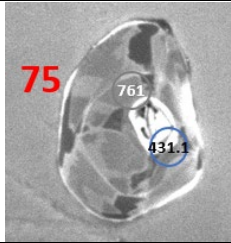
31A-41 - 3.d	rim					
31A-42 - 1.d	core					
31A-42 - 2.d	rim	Y	~75µm	Anhedral		
31A-43 - 1.d	core					
31A-43 - 2.d	rim					
31A-43 - 3.d	rim	Y	~125µm	Euhedral	detrital core but very small. Overlap with mantle	
31A-44 - 1.d	mantle					
31A-44 - 2.d	core					
31A-44 - 3.d	rim	Y	~75µm	Euhedral, equant	could be straddling zoning boundary between core and rim	
31A-45 - 1.d	core					
31A-45 - 2.d	rim					
31A-45 - 3.d	rim	Y	~125µm	Euhedral, tabular	detrital core?	
31A-46 - 1.d						
31A-47 - 1.d	core	minor	~100µm	Subhedral	detrital core?	


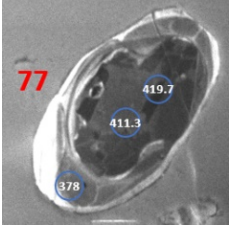
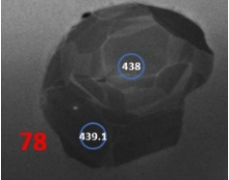
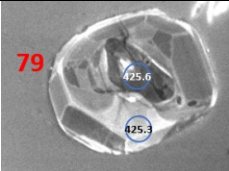
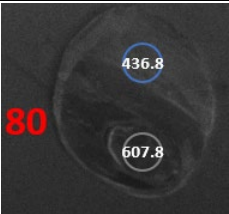
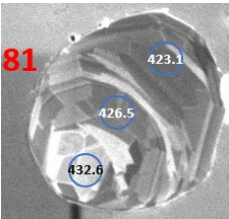


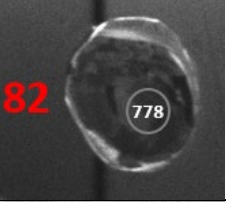
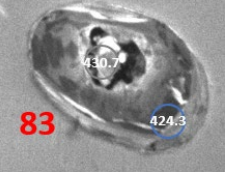
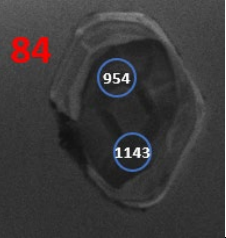
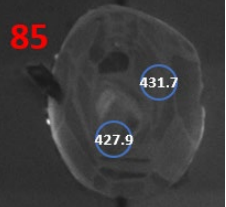
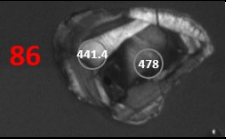
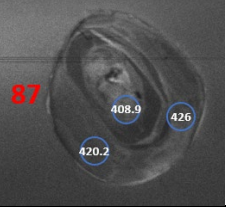
31A-47 - 2.d	rim						
31A-48 - 1.d	core	Y	~75µm	Euhedral, tabular	detrital core?		
31A-55 - 1.d	core					quite a messy core in terms of growth zones, could be overlapping multiple	
31A-55 - 2.d	rim	Y	~75µm	Anhedral		Very bright rim compared to previous zircons	
31A-56 - 1.d	core						
31A-56 - 2.d	mantle	Y	~125µm	Euhedral, tabular		potentially overlapping core and mantle	
31A-56 - 3.d	rim						
31A-57 - 1.d	mantle						
31A-57 - 2.d	rim	Y	~100µm	Euhedral, equant			
31A-58 - 1.d	mantle						
31A-58 - 2.d	mantle	Y	~100µm	Anhedral, prismatic		could be overlapping mantle and core	

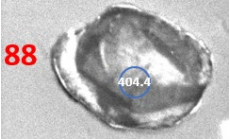
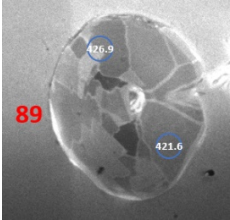
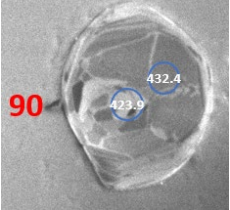
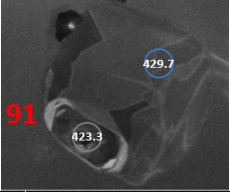
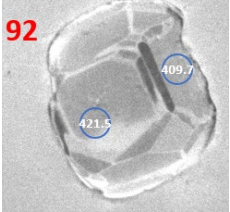
31A-59 - 1.d	mantle						
31A-59 - 2.d	rim	Y	~125µm	Anhedral			
31A-60 - 1.d	mantle						
31A-60 - 2.d	rim	Y	~125µm	Anhedral	potentially overlapping mantle and core		
31A-61 - 1.d	core						
31A-61 - 2.d	core						
31A-61 - 3.d	rim	Y	~150µm	Subhedral, prismatic	very patchy, cloudy complex zoning		
31A-62 - 1.d	core						
31A-62 - 2.d	rim	Y	~100µm	Subhedral, tabular	potentially overlapping core and rim		
31A-63 - 1.d	rim						
31A-63 - 2.d	rim	minor	~100µm	Euhedral, prismatic	patchy zoning		
31A-64 - 1.d	mantle	Y	~100µm				

31A-64 - 2.d	rim			Subhedral, tabular		
31A-65 - 1.d	core			Subhedral, equant	maybe overlapping core and mantle	
31A-65 - 2.d	rim	Y	~100µm	Subhedral, equant		
31A-66 - 1.d	core			Euhedral, equant	patchy zoning	
31A-66 - 2.d	rim	Y	~100µm	Euhedral, equant		
31A-67 - 1.d	rim			Euhedral, equant		
31A-67 - 2.d	rim	Y	~75µm	Euhedral, equant		
31A-68 - 1.d	rim			Euhedral, equant		
31A-68 - 2.d	rim	Y - tiny detrital core but flat zoning for majority of grain	~100µm	Euhedral, equant		
31A-69 - 1.d	rim	Y	~100µm	Subhedral		

31A-71 - 1.d	core	Y	~125µm	Euhedral, prismatic		
31A-70 - 1.d	?	?	?	?	no CL image	
31A-72 - 1.d	core					
31A-72 - 2.d	rim	Y	~100µm	Anhedral	Fragmented	
31A-73 - 1.d	core					
31A-73 - 2.d	rim	Y	~75µm	Anhedral		
31A-74 - 1.d	core	Y	~75µm	Subhedral, equant		
31A-75 - 1.d	mantle				potentially overlapping core and mantle	
31A-75 - 2.d	rim	Y	~75µm	Subhedral, tabular	potentially overlapping mantle and rim	
31A-76 - 1.d	core	Y	~75µm			

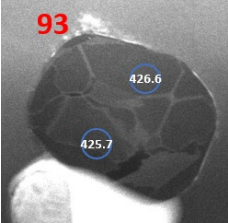
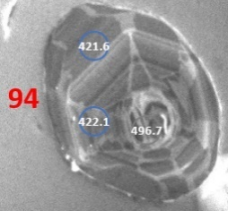
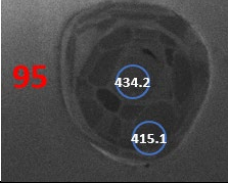
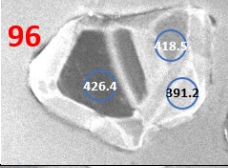
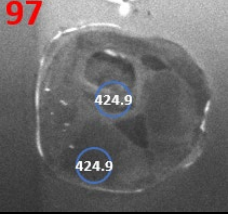
31A-76 - 2.d	rim				Euhedral, equant	potentially overlapping core and rim	
31A-77 - 1.d	core						
31A-77 - 2.d	core						
31A-77 - 3.d	rim	Y	~150µm		Euhedral, prismatic	Very bright rim compared to previous zircons	
31A-78 - 1.d	core						
31A-78 - 2.d	rim	minor	~125µm		Subhedral, equant		
31A-79 - 1.d	core						
31A-79 - 2.d	rim	Y	~125µm		Subhedral, equant		
31A-80 - 1.d	core						
31A-80 - 2.d	rim	Y	~75µm		Euhedral, equant		
31A-81 - 1.d	core						
31A-81 - 2.d	mantle						
31A-81 - 3.d	rim	Y	~125µm		Subhedral, equant		

31A-82 - 1.d	core	Y	~50µm	Equant	dark detrital core?	82 
31A-83 - 1.d	core					
31A-83 - 2.d	rim	Y	~100µm	Euhedral, tabular		83 
31A-84 - 1.d	core					
31A-84 - 2.d	core	Y	~100µm	Subhedral, prismatic		84 
31A-85 - 1.d	core					
31A-85 - 2.d	rim	minor	~100µm	Euhedral, tabular		85 
31A-86 - 1.d	core					
31A-86 - 2.d	mantle	Y	~100µm	Anhedral		86 
31A-87 - 1.d	core					
31A-87 - 2.d	rim					87 
31A-87 - 3.d	rim	Y	~125µm	Euhedral, equant		

31A-88 - 1.d	core	Y	~75µm	Subhedral	Very patchy	88 
31A-89 - 1.d	rim					89 
31A-89 - 2.d	rim	N - tiny detrital core but overall flat	~125µm	Euhedral, equant		
31A-90 - 1.d	core					90 
31A-90 - 2.d	rim	Y	~100µm	Subhedral		
31A-91 - 1.d	core					91 
31A-91 - 2.d	rim	Y	~100µm	Euhedral, equant		
31A-92 - 1.d	core					92 
31A-92 - 2.d	rim	Y	~125µm	Subhedral, tabular		
31A-93 - 1.d	core	N	~125µm			



Samantha Nicole March  
 Ultrahigh-pressure metapelites in the WGR

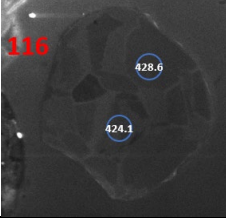
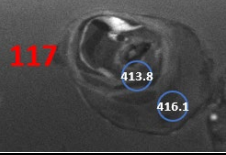
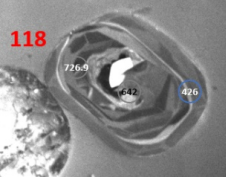
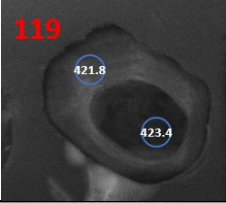
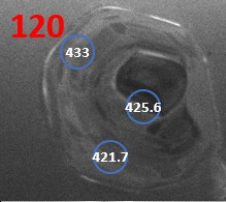
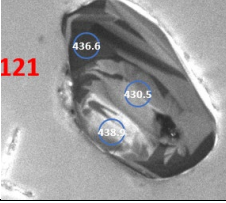
31A-93 - 2.d	rim				Euhedral, tabular	
31A-94 - 1.d	core					
31A-94 - 2.d	mantle	Y	~150µm	Euhedral, prismatic		
31A-94 - 3.d	rim					
31A-95 - 1.d	core					
31A-95 - 2.d	rim	Y	~100µm	Euhedral, equant		
31A-96 - 1.d	core					
31A-96 - 2.d	mantle	Y	~125µm	Anhedral	Pale rim	
31A-96 - 3.d	rim					
31A-97 - 1.d	core					
31A-97 - 2.d	rim	Y	~100µm	Euhedral, equant		
31A-98 - 1.d	core	Y	~100µm			

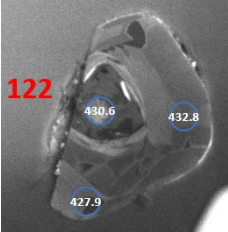
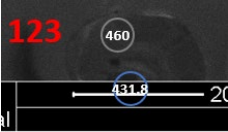
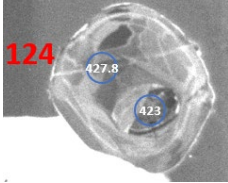
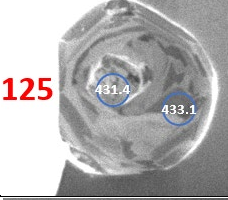
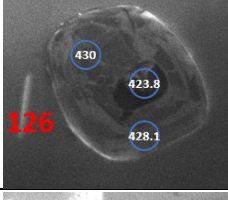
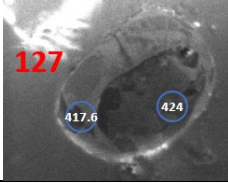
31A-98 - 2.d						
31A-99 - 1.d	core					
31A-99 - 2.d	rim	Y	~100µm	Subhedral		
31A-100 - 1.d	mantle					
31A-100 - 2.d	rim	Y	~100µm	Subhedral, tabular		
31A-101 - 1.d	core					
31A-101 - 2.d	rim	Y	~100µm	Euhedral, equant		
31A-102 - 1.d	core					
31A-102 - 2.d	rim	Y	~100µm	Subhedral, equant		
31A-103 - 1.d	core					
31A-103 - 2.d	rim	N	~125µm	Subhedral		
31A-104 - 1.d	core	Y	~100µm			

Samantha Nicole March  
 Ultrahigh-pressure metapelites in the WGR

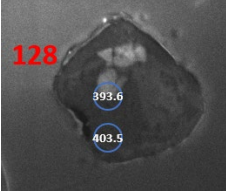
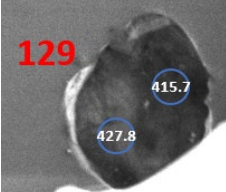
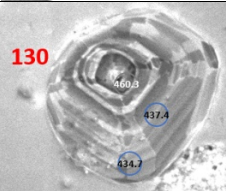
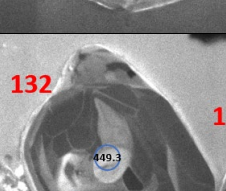
31A-104 - 2.d	rim				Euhedral, tabular		
31A-105 - 1.d	core						
31A-105 - 2.d	mantle						
31A-105 - 3.d	rim	Y	~125μm		Subhedral, tabular		
31A-106 - 1.d	core						
31A-107 - 1.d	rim						
31A-107 - 2.d	rim	Y	~100μm		Euhedral, tabular	looks like broken grain. Core broken off	
31A-108 - 1.d	core						
31A-108 - 2.d	core						
31A-109 - 1.d	core						
31A-109 - 2.d	rim	Y	~100μm		Subhedral		

31A-110 - 1.d	core	N	~100µm	Euhedral, equant	
31A-110 - 2.d	core				
31A-111 - 1.d	core				
31A-111 - 2.d	rim	Y	~100µm	Subhedral, prismatic	
31A-112 - 1.d	core				
31A-112 - 2.d	rim	Y	~125µm	Subhedral, tabular	
31A-113 - 1.d	core				
31A-113 - 2.d	rim	Y	~100µm	Subhedral, tabular	
31A-114 - 1.d	core				
31A-114 - 2.d	rim				
31A-114 - 3.d	rim	Y	~150µm	Euhedral, prismatic	
31A-115 - 1.d	core				
31A-115 - 2.d	mantle	Y	~150µm	Euhedral, equant	
31A-115 - 3.d	rim				

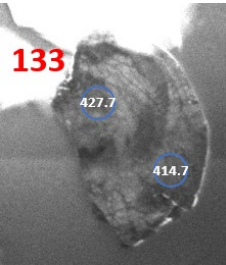
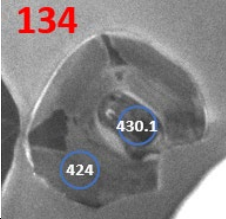
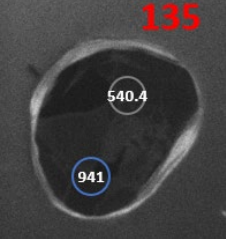
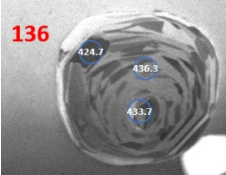
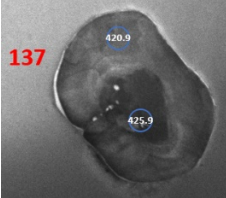
31A-116 - 1.d	core					
31A-116 - 2.d	rim	N	~125µm	Subhedral		
31A-117 - 1.d	core					
31A-117 - 2.d	rim	Y	~75µm	Euhedral		
31A-118 - 1.d	core				likely overlapping core and mantle	
31A-118 - 2.d	mantle	Y	~125µm	Euhedral, tabular		
31A-118 - 3.d	rim					
31A-119 - 1.d	core					
31A-119 - 2.d	rim	Y	~100µm	Euhedral, tabular		
31A-120 - 1.d	core				likely overlapping core and rim	
31A-120 - 2.d	rim	Y	~100µm	Euhedral, equant		
31A-120 - 3.d	rim					
31A-121 - 1.d	core					
31A-121 - 2.d	mantle	Y	~125µm	Subhedral, tabular		
31A-121 - 3.d	rim					
31A-122 - 1.d	core	Y	~125µm		Tabular grain split in half	

31A-122 - 2.d	mantle					
31A-122 - 3.d	rim			Fragmented subhedral		
31A-123 - 1.d	core					
31A-123 - 2.d	rim	N	~100μm	Euhedral, equant		
31A-124 - 1.d	core					
31A-124 - 2.d	rim	Y	~100μm	Euhedral, equant		
31A-125 - 1.d	core					
31A-125 - 2.d	rim	Y	~100μm	Euhedral, equant		
31A-126 - 1.d	core					
31A-126 - 2.d	rim					
31A-126 - 3.d	rim	Y	~100μm	Euhedral, equant		
31A-127 - 1.d	core					
31A-127 - 2.d	rim	Y	~100μm	Euhedral, tabular		
31A-128 - 1.d	rim	Y	~100μm			

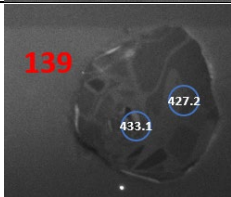
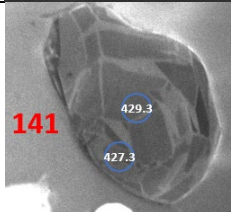

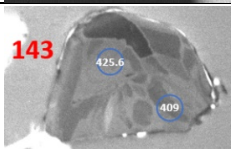
Samantha Nicole March  
 Ultrahigh-pressure metapelites in the WGR

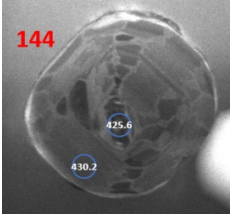
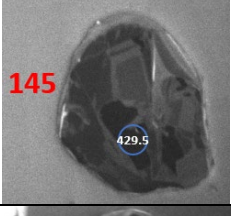
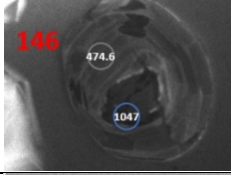
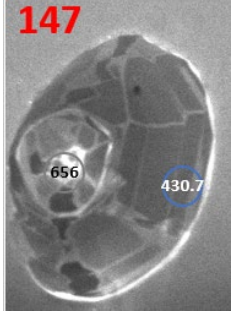
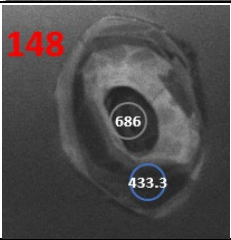
31A-128 - 2.d	rim			Subhedral, equant		
31A-129 - 1.d	core					
31A-129 - 2.d	core	Y	~75µm	Subhedral		
31A-130 - 1.d	core				likely overlapping growth zones	
31A-130 - 2.d	mantle					
31A-130 - 3.d	rim	Y	~125µm	Euhedral, equant		
31A-131 - 1.d	rim					
31A-131 - 2.d	rim	N	~100µm	Euhedral, tabular		
31A-132 - 1.d	core					
31A-132 - 2.d	rim					
31A-132 - 3.d	rim	Y	~150µm	Subhedral		
31A-133 - 1.d	core	Y	~100µm	Anhedral	very patchy zoning	



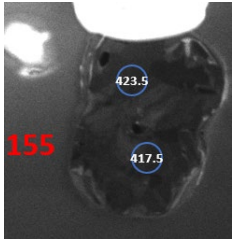
31A-133 - 2.d	rim					
31A-134 - 1.d	core					
31A-134 - 2.d	rim	Y	~75µm	Euhedral, equant, fragmented		
31A-135 - 1.d	core					
31A-135 - 2.d	core	Y	~75µm	Euhedral, equant	very dark core	
31A-136 - 1.d	core					
31A-136 - 2.d	mantle	Y	~125µm	Euhedral, equant		
31A-136 - 3.d	rim					
31A-137 - 1.d	core					
31A-137 - 2.d	rim	Y	~125µm	Euhedral, tabular	very patchy/dusty looking	
31A-138 - 1.d	core	Y	~100µm			

Samantha Nicole March  
 Ultrahigh-pressure metapelites in the WGR

31A-138 - 2.d	rim				likely overlapping core and rim Euhedral, tabular	<b>138</b> 
31A-139 - 1.d	core					<b>139</b> 
31A-139 - 2.d	rim	Y - tiny detrital core but flat zoning for majority of grain	~100µm		Subhedral, equant	
31A-140 - 1.d	core					<b>140</b> 
31A-140 - 2.d	rim	Y	~125µm		Anhedral	
31A-141 - 1.d	rim					<b>141</b> 
31A-141 - 2.d	core	N	~125µm		Subhedral, tabular	
31A-142 - 1.d	core					<b>142</b> 
31A-142 - 2.d	rim	Y	~125µm		Euhedral, equant	
31A-143 - 1.d	core					<b>143</b> 
31A-143 - 2.d	rim	N	~125µm		Subhedral, fragmented	
31A-144 - 1.d	core	Y	~150µm			

31A-144 - 2.d	rim				Euhedral, equant	
31A-145 - 1.d	core	Y	~100µm		Subhedral, tabular	
31A-146 - 1.d	core					
31A-146 - 2.d	rim	Y	~125µm		Euhedral, equant	
31A-147 - 1.d	core					
31A-147 - 2.d	rim	Y	~125µm		Euhedral, prismatic	
31A-148 - 1.d	core					
31A-148 - 2.d	rim	Y	~100µm		Euhedral, prismatic	
31A-149 - 1.d	core	Y	~100µm			

31A-149 - 2.d	rim			Euhedral, equant	
31A-150 - 1.d	rim				
31A-150 - 2.d	rim	Y	~100µm	Euhedral, equant	
31A-151 - 1.d	core				
31A-151 - 2.d	rim	Y	~100µm	Euhedral	
31A-152 - 1.d	core				
31A-152 - 2.d	mantle				
31A-152 - 3.d	rim	Y	~125µm	Euhedral, equant	
31A-153 - 1.d	core				
31A-153 - 2.d	rim	Y	~150µm	Subhedral, tabular	
31A-154 - 1.d	core				
31A-154 - 2.d	rim	Y	~100µm	Euhedral, equant	
31A-155 - 1.d	core	N	~100µm		

31A-155 - 2.d	core			Subhedral, tabular		
31A-156 - 1.d	core				detrital core?	
31A-156 - 2.d	mantle					
31A-156 - 3.d	rim	Y	~100µm	Subhedral, prismatic		
31A-158 - 1.d	core					
31A-158 - 2.d	rim	Y	~150µm	Euhedral, equant		
31A-159 - 1.d	rim					
31A-159 - 2.d	rim	N	~125µm	Euhedral, equant		
31A-160 - 1.d	core				likely overlap	
31A-160 - 2.d	rim	Y	~100µm	Euhedral, prismatic	likely overlap	

31A-161 - 1.d	core					
31A-161 - 2.d	rim	Y	~100µm	Subhedral, tabular		
31A-162 - 1.d	core	N	~100µm	Anhedral		
31A-163 - 1.d	rim	Y	~75µm	Tabular		
31A-164 - 1.d	core					
31A-164 - 2.d	rim	Y	~125µm	Euhedral, prismatic		
31A-164 - 3.d	rim					
31A-165 - 1.d	core					
31A-165 - 2.d	rim	Y	~100µm	Euhedral, equant		
31A-166 - 1.d	core	N	~125µm	Euhedral, tabular		





Samantha Nicole March  
Ultrahigh-pressure metapelites in the WGR

WGC-25B-4 - 1.d	0.493	0.033	0.0687	0.0022	0.0541	0.0032	0.5007	0.062073	412	24	428	13	C - Caledonian	-3.8835
WGC-25B-4 - 2.d	0.54	0.029	0.06503	0.0015	0.0612	0.003	0.39478	-0.09824	438	19	406.1	9.3	D	7.283105
WGC-25B-4 - 3.d	0.712	0.094	0.072	0.0036	0.0662	0.0057	0.76947	-0.60217	531	52	448	21	D	15.63089
WGC-25B-5 - 1.d	0.484	0.021	0.06411	0.0015	0.0536	0.002	0.25552	0.13106	401	15	400.6	9.2	C - Caledonian	0.099751
WGC-25B-5 - 2.d	0.481	0.017	0.06239	0.0014	0.0564	0.0022	-0.19993	0.52532	400	12	390.1	8.5	C - Caledonian	2.475
WGC-25B-5 - 3.d	0.489	0.019	0.06446	0.0015	0.0549	0.0021	-0.04657	0.42395	406	13	402.7	9.3	C - Caledonian	0.812808
WGC-25B-6 - 1.d	0.553	0.037	0.0661	0.0024	0.0591	0.0031	0.62936	-0.04736	444	23	412	14	D	7.207207
WGC-25B-6 - 2.d	0.496	0.023	0.0654	0.0016	0.0535	0.0024	-0.11289	0.39624	407	16	408.1	9.5	C - Caledonian	-0.27027
WGC-25B-7 - 1.d	0.533	0.044	0.0678	0.0027	0.0571	0.0044	0.19001	0.1639	427	30	423	16	C - Caledonian	0.936768
WGC-25B-7 - 2.d	0.474	0.04	0.0636	0.0021	0.0551	0.0045	0.17652	0.19802	396	27	398	13	C - Caledonian	-0.50505
WGC-25B-7 - 3.d	0.465	0.029	0.0627	0.0019	0.0529	0.0031	0.22789	0.16206	390	20	392.1	12	C - Caledonian	-0.53846
WGC-25B-8 - 1.d	0.481	0.023	0.0655	0.0015	0.0536	0.0025	0.059581	0.24905	399	16	408.9	9	C - Caledonian	-2.4812
WGC-25B-8 - 2.d	0.474	0.022	0.0648	0.0015	0.0531	0.0024	0.000908	0.29063	392	15	404.7	8.8	C - Caledonian	-3.2398
WGC-25B-10 - 1.d	0.501	0.023	0.0629	0.0015	0.0558	0.0025	-0.06694	0.42409	411	15	393.3	9.3	C - Caledonian	4.306569
WGC-25B-10 - 2.d	0.523	0.043	0.0676	0.0018	0.0541	0.0042	0.14327	0.1252	429	27	421.8	11	C - Caledonian	1.678322
WGC-25B-11 - 1.d	0.494	0.022	0.0646	0.0016	0.0556	0.0026	0.087463	0.3241	408	15	403.5	9.5	C - Caledonian	1.102941
WGC-25B-11 - 2.d	0.478	0.02	0.0597	0.0016	0.0563	0.0024	0.098093	0.37443	395	14	373.9	9.5	D	5.341772
WGC-25B-11 - 3.d	0.503	0.02	0.06517	0.0014	0.0552	0.0021	-0.09213	0.39363	416	13	406.9	8.6	C - Caledonian	2.1875
WGC-25B-12 - 1.d	0.489	0.029	0.0638	0.0017	0.0544	0.0032	0.078596	0.23456	404	19	398.8	10	C - Caledonian	1.287129
WGC-25B-13 - 1.d	0.475	0.021	0.0656	0.0016	0.0516	0.0024	0.2166	0.14053	393	15	409.7	9.9	RD	-4.24936
WGC-25B-13 - 2.d	0.47	0.018	0.06367	0.0014	0.0527	0.0021	-0.07198	0.37109	390	13	397.9	8.4	C - Caledonian	-2.02564
WGC-25B-14 - 1.d	0.468	0.027	0.0633	0.0018	0.0529	0.0031	0.14043	0.4094	395	18	395.8	11	C - Caledonian	-0.20253
WGC-25B-15 - 1.d	4.08	0.14	0.2715	0.0071	0.1072	0.0027	0.55232	0.10084	1646	27	1548	36	D	5.953827
WGC-25B-15 - 2.d	1.216	0.095	0.1048	0.0057	0.0824	0.0037	0.8278	-0.41692	804	43	641	33	D	20.27363
WGC-25B-16 - 1.d	0.515	0.019	0.06595	0.0014	0.0562	0.0019	0.091548	0.27538	421	13	411.7	8.7	C - Caledonian	2.209026
WGC-25B-16 - 2.d	0.528	0.027	0.0699	0.0019	0.0536	0.0026	0.020829	0.33945	435	18	436.7	12	C - Caledonian	-0.3908
WGC-25B-17 - 1.d	0.528	0.02	0.06756	0.0015	0.0567	0.0018	0.33783	0.005117	431	14	421.4	9.2	C - Caledonian	2.227378
WGC-25B-17 - 2.d	0.477	0.019	0.06287	0.0014	0.0544	0.0018	0.18398	0.1717	395	13	393	8.7	C - Caledonian	0.506329
WGC-25B-18 - 1.d	0.474	0.018	0.06257	0.0014	0.0541	0.002	-0.15506	0.44595	393	13	391.9	8.1	C - Caledonian	0.279898
WGC-25B-18 - 2.d	0.492	0.02	0.0623	0.0014	0.0568	0.0022	0.11726	0.27806	405	14	389.6	8.4	C - Caledonian	3.802469
WGC-25B-19 - 1.d	0.476	0.034	0.0659	0.0019	0.0522	0.0039	-0.13884	0.39735	394	24	411.6	11	C - Caledonian	-4.46701

Samantha Nicole March  
Ultrahigh-pressure metapelites in the WGR

WGC-25B-19 - 2.d	0.485	0.029	0.0612	0.0019	0.0567	0.0036	-0.00454	0.35756	399	20	383	12	C - Caledonian	4.010025
WGC-25B-20 - 1.d	0.437	0.021	0.0586	0.0015	0.0541	0.0023	0.26137	0.19683	367	15	367.3	9	C - Caledonian	-0.08174
WGC-25B-20 - 2.d	0.477	0.021	0.06153	0.0015	0.0565	0.0024	-0.13702	0.46086	395	15	384.9	8.9	C - Caledonian	2.556962
<del>WGC-25B-21 - 1.d</del>	<del>0.95</del>	<del>0.12</del>	<del>0.081</del>	<del>0.0038</del>	<del>0.082</del>	<del>0.0078</del>	<del>0.79842</del>	<del>-0.57845</del>	<del>655</del>	<del>61</del>	<del>502</del>	<del>23</del>	<del>D</del>	<del>23.35878</del>
WGC-25B-21 - 2.d	0.507	0.021	0.0634	0.0016	0.0566	0.0021	0.21046	0.20165	416	15	396.2	9.6	C - Caledonian	4.759615
WGC-25B-22 - 1.d	0.493	0.02	0.06335	0.0015	0.0566	0.0019	0.16018	0.1862	407	13	395.9	9.1	C - Caledonian	2.727273
WGC-25B-22 - 2.d	0.496	0.017	0.0637	0.0014	0.0563	0.0017	0.12591	0.30255	408.2	11	398.1	8.6	C - Caledonian	2.474277
WGC-25B-23 - 1.d	0.487	0.024	0.06493	0.0015	0.0544	0.0023	0.20395	0.12056	403	16	405.5	9	C - Caledonian	-0.62035
WGC-25B-23 - 2.d	0.481	0.02	0.0649	0.0016	0.0541	0.002	0.28011	0.15565	398	14	405	9.8	C - Caledonian	-1.75879
WGC-25B-24 - 1.d	0.523	0.024	0.06689	0.0016	0.0568	0.0025	0.050977	0.26064	426	16	417.3	9.5	C - Caledonian	2.042254
WGC-25B-24 - 2.d	0.544	0.031	0.0719	0.0023	0.0542	0.0028	0.27956	0.2064	443	20	447	14	C - Caledonian	-0.90293
WGC-25B-25 - 1.d	0.492	0.02	0.06309	0.0015	0.0555	0.002	0.056527	0.29276	405	14	394.3	8.9	C - Caledonian	2.641975
WGC-25B-25 - 2.d	0.489	0.017	0.06457	0.0015	0.0544	0.002	-0.14845	0.52547	403.8	11	403.3	9.2	C - Caledonian	0.123824
WGC-25B-26 - 1.d	0.475	0.023	0.06087	0.0015	0.057	0.0024	0.28966	0.040403	393	16	380.9	8.9	C - Caledonian	3.07888
WGC-25B-26 - 2.d	0.501	0.022	0.0639	0.0018	0.0569	0.0027	0.048552	0.3912	413	15	399.5	11	C - Caledonian	3.268765
WGC-25B-27 - 1.d	0.461	0.017	0.0599	0.0015	0.0547	0.0018	0.3284	0.21154	384	12	374.8	9.1	C - Caledonian	2.395833
WGC-25B-27 - 2.d	0.49	0.022	0.06338	0.0015	0.0565	0.0025	0.010602	0.31424	405	16	396.1	9.1	C - Caledonian	2.197531
WGC-25B-28 - 1.d	0.488	0.032	0.0651	0.0016	0.0529	0.0034	0.14579	0.085775	400	22	407.4	9.8	C - Caledonian	-1.85
WGC-25B-28 - 2.d	0.487	0.03	0.0629	0.0016	0.0558	0.0032	0.074786	0.20464	402	20	393.1	9.5	C - Caledonian	2.21393
WGC-25B-29 - 1.d	0.514	0.033	0.0645	0.0017	0.0573	0.0033	0.14305	0.19383	420	21	403	11	C - Caledonian	4.047619
WGC-25B-30 - 1.d	0.492	0.021	0.0638	0.0016	0.0549	0.0022	0.14409	0.26773	405	14	398.7	9.5	C - Caledonian	1.555556
WGC-25B-31 - 1.d	0.484	0.025	0.0638	0.0016	0.0549	0.0026	0.35583	-0.03298	401	17	399.5	9.6	C - Caledonian	0.374065
<del>WGC-25B-31 - 2.d</del>	<del>0.468</del>	<del>0.017</del>	<del>0.05968</del>	<del>0.0015</del>	<del>0.0566</del>	<del>0.0015</del>	<del>0.3453</del>	<del>0.2101</del>	<del>389</del>	<del>12</del>	<del>373.7</del>	<del>9</del>	<del>D</del>	<del>3.933162</del>
WGC-25B-32 - 1.d	0.503	0.024	0.0639	0.0016	0.0562	0.0023	0.2679	0.12143	412	16	399	9.5	C - Caledonian	3.15534
WGC-25B-33 - 1.d	0.488	0.02	0.06463	0.0015	0.0549	0.002	0.16184	0.19177	402	14	403.7	8.9	C - Caledonian	-0.42289
WGC-25B-33 - 2.d	0.487	0.025	0.06349	0.0015	0.0549	0.0028	-0.13561	0.41115	401	17	396.8	9.1	C - Caledonian	1.047382
WGC-25B-34 - 1.d	0.474	0.019	0.06204	0.0015	0.056	0.0023	0.021529	0.33366	395	14	388	9	C - Caledonian	1.772152
WGC-25B-34 - 2.d	0.484	0.022	0.064	0.0016	0.0539	0.0024	0.039257	0.32572	401	15	399.6	9.4	C - Caledonian	0.349127
<del>WGC-25B-35 - 1.d</del>	<del>0.482</del>	<del>0.021</del>	<del>0.06496</del>	<del>0.0015</del>	<del>0.0522</del>	<del>0.0021</del>	<del>0.030808</del>	<del>0.32848</del>	<del>400</del>	<del>14</del>	<del>405.7</del>	<del>9.2</del>	<del>RD</del>	<del>-1.425</del>
WGC-25B-35 - 2.d	0.521	0.022	0.06618	0.0015	0.0575	0.0024	-0.12153	0.40949	428	15	413.1	9	C - Caledonian	3.481308
WGC-25B-36 - 1.d	0.49	0.023	0.06485	0.0016	0.0544	0.0024	0.25395	0.094547	405	16	405.8	9.2	C - Caledonian	-0.19753

Samantha Nicole March  
Ultrahigh-pressure metapelites in the WGR

WGC-25B-36 - 2.d	0.525	0.026	0.0692	0.002	0.0555	0.0027	0.21578	0.24381	426	18	431.5	12	C - Caledonian	-1.29108
WGC-25B-36 - 3.d	0.503	0.02	0.06531	0.0015	0.0556	0.0021	0.069033	0.2668	414	14	408.6	8.9	C - Caledonian	1.304348
WGC-25B-37 - 1.d	0.511	0.019	0.06501	0.0015	0.0567	0.0016	0.40755	0.11916	418	12	406	9.3	C - Caledonian	2.870813
WGC-25B-37 - 2.d	0.502	0.018	0.06508	0.0015	0.0562	0.0018	0.09339	0.32611	412	12	406.4	9	C - Caledonian	1.359223
WGC-25B-38 - 1.d	0.597	0.063	0.0666	0.003	0.0637	0.0051	0.63171	-0.19051	470	39	416	18	D	11.48936
WGC-25B-39 - 1.d	0.493	0.018	0.06384	0.0015	0.0561	0.002	0.03629	0.32714	409	12	398.9	8.9	C - Caledonian	2.469438
WGC-25B-40 - 1.d	0.457	0.023	0.06124	0.0014	0.0533	0.0027	0.013619	0.29361	380	16	383.1	8.7	C - Caledonian	-0.81579
WGC-25B-41 - 1.d	0.499	0.021	0.06838	0.0016	0.0524	0.0021	-0.11953	0.42198	411	15	426.4	9.5	RD	-3.74696
WGC-25B-42 - 1.d	0.482	0.021	0.0632	0.0016	0.0545	0.0021	0.26875	0.2081	400	15	395	9.9	C - Caledonian	1.25
WGC-25B-43 - 1.d	0.477	0.022	0.06236	0.0015	0.0545	0.0024	0.027783	0.28505	394	15	389.9	9.1	C - Caledonian	1.040609
WGC-25B-44 - 1.d	0.462	0.016	0.05963	0.0015	0.0561	0.0019	0.24586	0.18046	384.9	11	373.3	8.9	C - Caledonian	3.01377
WGC-25B-44 - 2.d	0.488	0.021	0.06503	0.0015	0.0535	0.0021	0.15179	0.17299	402	14	406.1	8.8	C - Caledonian	-1.0199
WGC-25B-45 - 1.d	0.85	0.11	0.0768	0.0034	0.0726	0.0065	0.71516	-0.35304	598	54	477	20	D	20.23411
WGC-25B-45 - 2.d	0.523	0.041	0.0659	0.0019	0.0566	0.0043	0.018745	0.44206	426	28	411.5	12	C - Caledonian	3.403756
WGC-25B-45 - 3.d	0.495	0.023	0.06416	0.0015	0.0551	0.0025	0.17478	0.20091	410	15	400.8	8.9	C - Caledonian	2.243902
WGC-25B-46 - 1.d	0.467	0.025	0.0639	0.0017	0.0536	0.0028	0.22513	0.13314	389	17	399.2	11	C - Caledonian	-2.62211
WGC-25B-46 - 2.d	0.469	0.026	0.0655	0.0016	0.0527	0.0027	0.092459	0.17843	391	17	409	9.8	C - Caledonian	-4.60358
WGC-25B-47 - 1.d	0.478	0.032	0.0655	0.0018	0.0529	0.0035	-0.12361	0.37671	393	22	409.1	11	C - Caledonian	-4.09669
WGC-25B-47 - 2.d	0.595	0.033	0.0735	0.0023	0.0589	0.0031	0.28184	0.14567	477	21	457	14	C - Caledonian	4.192872
WGC-25B-48 - 1.d	0.487	0.027	0.0634	0.0017	0.0549	0.003	-0.06996	0.44502	405	18	396.2	10	C - Caledonian	2.17284
WGC-25B-48 - 2.d	0.469	0.024	0.0617	0.0016	0.0555	0.0028	-0.08356	0.41407	391	17	386.1	9.5	C - Caledonian	1.253197
WGC-25B-49 - 1.d	0.477	0.019	0.06287	0.0014	0.0551	0.002	0.023292	0.32158	395	13	393	8.8	C - Caledonian	0.506329
WGC-25B-49 - 2.d	0.495	0.019	0.0635	0.0015	0.0567	0.002	0.1408	0.32049	407	13	396.9	9.4	C - Caledonian	2.481572
WGC-25B-50 - 1.d	0.466	0.018	0.0616	0.0014	0.0541	0.0019	0.13694	0.22561	387	13	385.3	8.4	C - Caledonian	0.439276
WGC-25B-50 - 2.d	0.51	0.022	0.0673	0.0016	0.0543	0.0023	0.19673	0.14252	417	15	419.8	9.9	C - Caledonian	-0.67146
WGC-25B-51 - 1.d	0.497	0.03	0.0662	0.0018	0.0539	0.0034	-0.00352	0.35734	410	19	412.9	11	C - Caledonian	-0.70732
WGC-25B-52 - 1.d	0.487	0.019	0.06556	0.0015	0.0539	0.002	-0.08691	0.40482	403	13	409.3	8.9	C - Caledonian	-1.56328
WGC-25B-52 - 2.d	0.501	0.021	0.0653	0.0016	0.0554	0.0023	-0.06357	0.44787	411	14	407.9	9.6	C - Caledonian	0.754258
WGC-25B-53 - 1.d	0.48	0.017	0.0617	0.0014	0.0556	0.0016	0.17725	0.24476	399	12	385.9	8.3	C - Caledonian	3.283208
WGC-25B-54 - 1.d	0.532	0.026	0.069	0.0018	0.0562	0.0027	0.12991	0.22877	431	17	430	11	C - Caledonian	0.232019
WGC-25B-54 - 2.d	0.462	0.021	0.0591	0.0016	0.0559	0.0021	0.29484	0.16688	384	14	370.2	9.5	C - Caledonian	3.59375

Samantha Nicole March  
Ultrahigh-pressure metapelites in the WGR

WGC-25B-55 - 1.d	0.486	0.025	0.0675	0.0018	0.052	0.0027	0.12181	0.22534	405	16	420.7	11	C - Caledonian	-3.87654
WGC-25B-55 - 2.d	0.523	0.032	0.0664	0.002	0.0571	0.0035	0.027904	0.31289	424	21	414.1	12	C - Caledonian	2.334906
WGC-25B-56 - 1.d	0.489	0.026	0.0629	0.0017	0.0558	0.0031	0.044635	0.36718	402	18	393	10	C - Caledonian	2.238806
<del>WGC-25B-56 - 2.d</del>	<del>0.525</del>	<del>0.03</del>	<del>0.0642</del>	<del>0.0019</del>	<del>0.0596</del>	<del>0.0037</del>	<del>-0.00802</del>	<del>0.37022</del>	<del>428</del>	<del>21</del>	<del>401</del>	<del>11</del>	<del>D</del>	<del>6.308411</del>
WGC-25B-57 - 1.d	0.514	0.031	0.0686	0.0022	0.0543	0.003	0.40977	0.060827	418	20	427	13	C - Caledonian	-2.15311
WGC-25B-57 - 2.d	0.493	0.023	0.0649	0.0016	0.0556	0.0026	-0.0228	0.36356	406	16	405	10	C - Caledonian	0.246305
WGC-25B-58 - 1.d	1.788	0.067	0.171	0.004	0.0755	0.0024	0.34723	0.17154	1040	25	1018	22	C - Sveconorwegian	2.115385
WGC-25B-59 - 1.d	0.515	0.026	0.0668	0.0017	0.0557	0.0028	0.085252	0.21919	422	18	417.9	11	C - Caledonian	0.971564
WGC-25B-60 - 1.d	0.553	0.039	0.0703	0.0021	0.056	0.0039	-0.22738	0.47813	448	26	438	13	C - Caledonian	2.232143
<del>WGC-25B-60 - 2.d</del>	<del>0.504</del>	<del>0.017</del>	<del>0.06439</del>	<del>0.0015</del>	<del>0.0574</del>	<del>0.0018</del>	<del>0.21171</del>	<del>0.24218</del>	<del>415</del>	<del>12</del>	<del>402.2</del>	<del>9</del>	<del>D</del>	<del>3.084337</del>
WGC-25B-60 - 3.d	0.495	0.02	0.06591	0.0014	0.0537	0.0018	0.1456	0.16478	409	13	411.5	8.6	C - Caledonian	-0.61125
WGC-25B-61 - 1.d	0.473	0.019	0.06117	0.0014	0.056	0.002	0.24285	0.21967	394	14	382.7	8.5	C - Caledonian	2.86802
WGC-25B-61 - 2.d	0.479	0.02	0.0626	0.0016	0.0546	0.0023	0.12073	0.26628	396	14	391.3	9.7	C - Caledonian	1.186869
WGC-25B-61 - 3.d	0.473	0.021	0.0648	0.0017	0.0539	0.0027	-0.14315	0.49783	395	15	404.5	10	C - Caledonian	-2.40506
<del>WGC-25B-62 - 1.d</del>	<del>1.36</del>	<del>0.096</del>	<del>0.138</del>	<del>0.0045</del>	<del>0.0706</del>	<del>0.004</del>	<del>0.34948</del>	<del>0.063672</del>	<del>867</del>	<del>42</del>	<del>833</del>	<del>26</del>	<del>D - ellipse touching concordia</del>	<del>3.921569</del>
WGC-25B-62 - 2.d	0.608	0.052	0.0756	0.0035	0.0578	0.0034	0.66468	-0.13544	483	32	469	21	C - Caledonian	2.898551
<del>WGC-25B-62 - 3.d</del>	<del>2.05</del>	<del>0.13</del>	<del>0.1799</del>	<del>0.0059</del>	<del>0.0839</del>	<del>0.0062</del>	<del>0.16162</del>	<del>0.24322</del>	<del>1129</del>	<del>46</del>	<del>1066</del>	<del>32</del>	<del>D</del>	<del>5.580159</del>
WGC-25B-63 - 1.d	0.52	0.029	0.0652	0.0017	0.0571	0.0031	0.049351	0.27929	422	20	407.2	10	C - Caledonian	3.507109
WGC-25B-63 - 2.d	0.493	0.03	0.0651	0.0018	0.0526	0.0033	-0.07294	0.399	406	20	406.8	11	C - Caledonian	-0.19704
WGC-25B-64 - 1.d	0.523	0.03	0.0668	0.0021	0.0574	0.0035	0.024256	0.39997	424	20	416	13	C - Caledonian	1.886792
WGC-25B-64 - 2.d	0.489	0.036	0.0639	0.0016	0.055	0.0038	-0.02241	0.28016	410	24	399.1	9.9	C - Caledonian	2.658537
WGC-25B-65 - 1.d	0.519	0.02	0.06613	0.0016	0.0563	0.002	0.2087	0.18807	425	14	412.8	9.5	C - Caledonian	2.870588
WGC-25B-65 - 2.d	0.501	0.024	0.0682	0.0016	0.0528	0.0023	0.18852	0.16929	410	16	425	9.8	C - Caledonian	-3.65854
WGC-25B-68 - 1.d	0.521	0.029	0.0667	0.0017	0.0561	0.0031	0.058064	0.26959	423	19	416.4	11	C - Caledonian	1.560284
WGC-25B-68 - 2.d	0.51	0.018	0.06548	0.0014	0.0567	0.0017	0.24705	0.14167	421	13	408.8	8.6	C - Caledonian	2.897862
WGC-25B-68 - 3.d	0.518	0.019	0.0668	0.0015	0.0566	0.002	-0.06	0.39927	423	13	416.8	9.1	C - Caledonian	1.465721
WGC-25B-69 - 1.d	0.457	0.024	0.0589	0.0017	0.0552	0.0026	0.29541	0.090591	380	17	368.8	11	C - Caledonian	2.947368
WGC-25B-69 - 2.d	0.51	0.039	0.0644	0.0018	0.057	0.0044	0.001751	0.28339	413	26	402.3	11	C - Caledonian	2.590799
WGC-25B-69 - 3.d	0.475	0.025	0.0651	0.0016	0.053	0.0027	0.16845	0.14728	392	17	406.6	9.5	C - Caledonian	-3.72449
WGC-25B-69 - 4.d	0.473	0.033	0.0634	0.0021	0.0552	0.0038	0.1106	0.21873	393	23	396	13	C - Caledonian	-0.76336

Samantha Nicole March  
Ultrahigh-pressure metapelites in the WGR

WGC-25B-71 - 1.d	0.51	0.021	0.06635	0.0015	0.0564	0.0021	0.10799	0.23906	420	15	414.1	8.9	C - Caledonian	1.404762
WGC-25B-71 - 2.d	0.513	0.021	0.06615	0.0015	0.0556	0.002	0.091335	0.24677	419	14	412.9	8.8	C - Caledonian	1.455847
WGC-25B-71 - 3.d	0.528	0.021	0.0666	0.0016	0.0573	0.0022	-0.06632	0.49927	429	14	415.8	9.6	C - Caledonian	3.076923
WGC-25B-72 - 1.d	0.507	0.021	0.06673	0.0015	0.0544	0.0021	-0.05803	0.39693	415	14	416.4	8.8	C - Caledonian	-0.33735
WGC-25B-72 - 2.d	0.604	0.035	0.0725	0.0022	0.0601	0.0029	0.49237	-0.05658	476	22	451	13	D	5.252101
WGC-25B-73 - 1.d	0.512	0.021	0.0669	0.0016	0.0557	0.002	0.19344	0.15668	420	15	417.4	9.4	C - Caledonian	0.619048
WGC-25B-73 - 2.d	0.484	0.02	0.06372	0.0015	0.0545	0.0021	-0.19389	0.47392	401	13	399	9.5	C - Caledonian	0.498753
WGC-25B-74 - 1.d	0.496	0.021	0.06472	0.0015	0.0558	0.0022	0.17631	0.24309	408	14	404.2	9.4	C - Caledonian	0.931373
WGC-25B-74 - 2.d	0.852	0.087	0.08	0.0038	0.0743	0.005	0.85929	-0.69177	614	48	496	23	D	19.21824
WGC-25B-75 - 1.d	0.499	0.023	0.06447	0.0015	0.0563	0.0023	-0.07269	0.35864	411	15	402.7	9.1	C - Caledonian	2.019465
WGC-25B-75 - 2.d	0.515	0.022	0.0649	0.0016	0.0572	0.0022	0.17045	0.20565	420	15	405.4	9.6	C - Caledonian	3.47619
WGC-25B-76 - 1.d	0.501	0.021	0.06498	0.0015	0.0558	0.0023	-0.00129	0.30831	411	14	405.8	8.9	C - Caledonian	1.265207
WGC-25B-76 - 2.d	0.511	0.016	0.06356	0.0014	0.0587	0.0017	-0.00483	0.41132	418.8	11	397.2	8.4	C - Caledonian	5.157593
WGC-25B-77 - 1.d	0.506	0.025	0.0663	0.0016	0.0558	0.0025	0.14273	0.16353	418	16	413.8	9.8	C - Caledonian	1.004785
WGC-25B-77 - 2.d	0.536	0.029	0.0671	0.002	0.0571	0.0029	0.14769	0.25207	436	19	418.4	12	C - Caledonian	4.036697
WGC-25B-78 - 1.d	0.676	0.045	0.0695	0.0023	0.0717	0.0054	-0.10994	0.43234	522	26	433	14	D	17.04981
WGC-25B-78 - 2.d	0.509	0.019	0.0687	0.0017	0.0536	0.0016	0.24789	0.15332	417	13	428.2	10	C - Caledonian	-2.68585
WGC-25B-78 - 3.d	0.5	0.022	0.06536	0.0015	0.055	0.0022	0.051748	0.26691	410	15	408.1	8.9	C - Caledonian	0.463415
WGC-25B-79 - 1.d	0.499	0.021	0.06477	0.0014	0.0562	0.002	0.22953	0.089115	413	14	404.5	8.6	C - Caledonian	2.058111
WGC-25B-79 - 2.d	0.5	0.019	0.06487	0.0015	0.056	0.002	0.15757	0.21872	412	13	405.2	8.8	C - Caledonian	1.650485
WGC-25B-80 - 1.d	0.486	0.024	0.0608	0.0015	0.0571	0.0027	0.15113	0.1745	405	16	380.7	9.1	C - Caledonian	6
WGC-25B-80 - 2.d	0.479	0.027	0.0651	0.0019	0.0533	0.0032	0.068326	0.44671	397	20	406.2	12	C - Caledonian	-2.31738
WGC-25B-81 - 1.d	0.515	0.021	0.06501	0.0015	0.0574	0.0021	0.1576	0.21174	421	14	406	9	C - Caledonian	3.562945
WGC-25B-81 - 2.d	0.495	0.022	0.06662	0.0016	0.0542	0.0022	0.083955	0.26683	407	15	415.7	9.6	C - Caledonian	-2.13759
WGC-25B-82 - 1.d	0.51	0.022	0.06595	0.0016	0.0568	0.0023	0.087681	0.33485	417	15	411.7	9.5	C - Caledonian	1.270983
WGC-25B-82 - 2.d	0.52	0.046	0.0649	0.0023	0.0601	0.0057	-0.03013	0.32515	418	31	405	14	C - Caledonian	3.110048
WGC-25B-82 - 3.d	0.475	0.035	0.0652	0.0018	0.054	0.0042	-0.10929	0.42864	401	25	407	11	C - Caledonian	-1.49626
WGC-25B-83 - 1.d	0.841	0.085	0.0894	0.0058	0.0662	0.0047	0.75117	-0.16244	614	46	561	38	D	8.631922
WGC-25B-83 - 2.d	0.844	0.099	0.0874	0.0064	0.0677	0.0032	0.96146	-0.63755	603	49	539	37	D	10.6136
WGC-25B-84 - 1.d	0.564	0.043	0.0673	0.0021	0.0605	0.0043	0.39001	-0.00775	451	27	420	13	C - Caledonian	6.873614
WGC-25B-85 - 1.d	1.284	0.034	0.1303	0.0029	0.072	0.0012	0.40514	0.30765	839	15	789.6	17	D	5.887962

WGC-25B-85 - 2.d	1.658	0.056	0.1676	0.0042	0.0725	0.002	0.23885	0.28713	990	21	998	23	C - Sveconorwegian	-0.80808
------------------	-------	-------	--------	--------	--------	-------	---------	---------	-----	----	-----	----	-----------------------	----------

~~Crossed-out~~ = discordant, C = concordant, NC = near concordant, D = discordant, RD = reversely discordant.

### WGC2019J-25B zircon geochronology standards

Standard	Type	207/235	2 $\sigma$	206/238	2 $\sigma$	207/206	2 $\sigma$	ErrCorr 6/38vs7/35	ErrCorr 38/6vs7/6	207/235 age	2 $\sigma$	206/238 age	2 $\sigma$	Concordant?
GJ - 1.d	Primary	0.788	0.037	0.0977	0.0023	0.0579	0.0027	-0.04451	0.36194	587	21	601	14	C
GJ - 2.d	Primary	0.814	0.036	0.098	0.0022	0.0598	0.0027	0.023979	0.29155	605	21	602.7	13	C
GJ - 3.d	Primary	0.813	0.03	0.0986	0.0023	0.0599	0.0019	0.12723	0.31547	609	16	606.1	13	C
GJ - 4.d	Primary	0.792	0.029	0.0964	0.0023	0.0598	0.0022	0.092785	0.31467	595	17	593.1	13	C
GJ - 5.d	Primary	0.839	0.033	0.0976	0.0022	0.062	0.0024	-0.19716	0.51644	617	18	600.4	13	C
GJ - 6.d	Primary	0.84	0.032	0.0983	0.0023	0.062	0.0022	0.16401	0.26034	620	18	604.2	14	C
GJ - 7.d	Primary	0.801	0.038	0.0984	0.0023	0.0584	0.0027	-0.01351	0.31492	597	21	604.9	14	C
GJ - 8.d	Primary	0.816	0.032	0.0977	0.0022	0.0594	0.002	-0.06326	0.37228	606	18	601.1	13	C
GJ - 9.d	Primary	0.838	0.033	0.0984	0.0023	0.0616	0.0024	-0.13216	0.46058	618	18	604.7	13	C
GJ - 10.d	Primary	0.809	0.037	0.0976	0.0024	0.0595	0.0028	0.1752	0.21622	602	21	600.2	14	C
GJ - 11.d	Primary	0.802	0.032	0.0967	0.0023	0.0602	0.0021	0.25299	0.12381	598	18	595	14	C
GJ - 12.d	Primary	0.824	0.037	0.0981	0.0022	0.0597	0.0024	0.12398	0.24831	608	21	603.5	13	C
GJ - 13.d	Primary	0.792	0.035	0.0972	0.0023	0.0597	0.0028	-0.20313	0.50618	594	20	597.7	14	C
GJ - 14.d	Primary	0.817	0.037	0.0963	0.0024	0.0608	0.0024	0.12786	0.23342	603	21	592.7	14	C
GJ - 15.d	Primary	0.821	0.034	0.0982	0.0023	0.0613	0.0027	-0.19384	0.51198	606	19	603.7	13	C
GJ - 16.d	Primary	0.837	0.034	0.0993	0.0024	0.0608	0.0023	0.09212	0.26506	618	19	610.2	14	C
GJ - 17.d	Primary	0.826	0.037	0.0971	0.0023	0.0613	0.0027	0.037429	0.29329	608	21	597.2	14	C
GJ - 18.d	Primary	0.821	0.033	0.0993	0.0023	0.0599	0.002	0.34765	0.05318	611	19	610.5	13	C
GJ - 19.d	Primary	0.837	0.034	0.0991	0.0023	0.0608	0.0023	-0.0475	0.41023	615	19	608.9	14	C
GJ - 20.d	Primary	0.807	0.027	0.0994	0.0023	0.0594	0.0017	0.06055	0.31326	602	14	610.8	13	C
GJ - 21.d	Primary	0.818	0.032	0.0982	0.0024	0.0596	0.0025	-0.17964	0.55734	607	18	604	14	C
GJ - 22.d	Primary	0.821	0.038	0.0967	0.0024	0.0616	0.0029	-0.08009	0.43514	608	22	594.8	14	C
GJ - 23.d	Primary	0.801	0.033	0.0959	0.0021	0.0598	0.0024	0.05617	0.30637	600	18	590.4	13	C

Samantha Nicole March  
Ultrahigh-pressure metapelites in the WGR

<b>GJ - 24.d</b>	Primary	0.786	0.035	0.0986	0.0024	0.0588	0.0026	0.091591	0.28067	594	21	606.1	14	C
<b>Plesovice - 1.d</b>	Secondary	0.384	0.016	0.05412	0.0012	0.0508	0.0022	-0.0962	0.41931	330	11	339.7	7.5	C
<del><b>Plesovice - 2.d</b></del>	<del>Secondary</del>	<del>0.383</del>	<del>0.013</del>	<del>0.05431</del>	<del>0.0013</del>	<del>0.0502</del>	<del>0.0015</del>	<del>0.06266</del>	<del>0.36698</del>	<del>328.8</del>	<del>9.6</del>	<del>340.9</del>	<del>7.8</del>	<del>D</del>
<del><b>Plesovice - 3.d</b></del>	<del>Secondary</del>	<del>0.379</del>	<del>0.015</del>	<del>0.05449</del>	<del>0.0013</del>	<del>0.0497</del>	<del>0.0019</del>	<del>0.20127</del>	<del>0.23506</del>	<del>325</del>	<del>11</del>	<del>342</del>	<del>8</del>	<del>D</del>
<b>Plesovice - 4.d</b>	Secondary	0.396	0.016	0.0532	0.0012	0.0531	0.0021	0.11821	0.21873	338	12	334.1	7.3	C
<b>Plesovice - 5.d</b>	Secondary	0.406	0.014	0.05485	0.0012	0.0527	0.0017	0.004865	0.3547	345.5	10	344.2	7.4	C
<b>Plesovice - 6.d</b>	Secondary	0.386	0.015	0.0543	0.0012	0.0513	0.0021	-0.05118	0.3871	331.8	11	340.8	7.4	C
<b>Plesovice - 7.d</b>	Secondary	0.401	0.016	0.05459	0.0013	0.0521	0.0019	0.12279	0.2714	343	12	342.6	7.7	C
<b>Plesovice - 8.d</b>	Secondary	0.4	0.017	0.05432	0.0012	0.0527	0.002	-0.03639	0.34784	342	12	341	7.5	C
<b>Plesovice - 9.d</b>	Secondary	0.407	0.017	0.05477	0.0012	0.0528	0.002	0.11103	0.24681	346	12	343.7	7.5	C
<b>Plesovice - 10.d</b>	Secondary	0.417	0.014	0.05389	0.0012	0.0554	0.0016	-0.0421	0.37943	353.6	10	338.4	7.1	C
<del><b>Plesovice - 11.d</b></del>	<del>Secondary</del>	<del>0.397</del>	<del>0.017</del>	<del>0.05369</del>	<del>0.0012</del>	<del>0.0531</del>	<del>0.0021</del>	<del>-0.01193</del>	<del>0.307</del>	<del>338</del>	<del>12</del>	<del>337.1</del>	<del>7.1</del>	<del>D</del>
<b>Plesovice - 12.d</b>	Secondary	0.401	0.016	0.05312	0.0012	0.0541	0.002	0.1019	0.26766	342	11	333.7	7.6	C
<b>Plesovice - 13.d</b>	Secondary	0.403	0.015	0.05417	0.0012	0.0539	0.0019	0.091521	0.31248	343	11	340.1	7.5	C
<b>Plesovice - 14.d</b>	Secondary	0.39	0.016	0.05418	0.0012	0.0516	0.0019	0.040166	0.26424	333	12	340.1	7.5	C
<b>Plesovice - 15.d</b>	Secondary	0.394	0.014	0.05439	0.0012	0.0524	0.0018	-0.12974	0.46543	338.2	11	341.4	7.3	C
<b>Plesovice - 16.d</b>	Secondary	0.415	0.016	0.0543	0.0013	0.055	0.0019	0.16405	0.24466	353	12	340.9	7.7	C
<del><b>Plesovice - 17.d</b></del>	<del>Secondary</del>	<del>0.416</del>	<del>0.017</del>	<del>0.05307</del>	<del>0.0012</del>	<del>0.0563</del>	<del>0.002</del>	<del>0.11068</del>	<del>0.22872</del>	<del>354</del>	<del>12</del>	<del>333.3</del>	<del>7.1</del>	<del>D</del>
<b>Plesovice - 18.d</b>	Secondary	0.412	0.015	0.0536	0.0012	0.0549	0.0019	-0.05199	0.41352	349.6	11	336.6	7.1	C
<del><b>Plesovice - 19.d</b></del>	<del>Secondary</del>	<del>0.42</del>	<del>0.015</del>	<del>0.05321</del>	<del>0.0012</del>	<del>0.0567</del>	<del>0.002</del>	<del>-0.00962</del>	<del>0.38845</del>	<del>355.5</del>	<del>11</del>	<del>334.2</del>	<del>7.2</del>	<del>D</del>
<b>Plesovice - 20.d</b>	Secondary	0.405	0.017	0.05333	0.0012	0.0549	0.0024	-0.12529	0.38994	345	13	334.9	7.4	C
<b>Plesovice - 21.d</b>	Secondary	0.397	0.018	0.05356	0.0012	0.0536	0.0023	0.062391	0.28693	338	13	336.3	7.6	C
<b>Plesovice - 22.d</b>	Secondary	0.39	0.016	0.05432	0.0013	0.0526	0.0023	-0.16403	0.49866	333	12	340.9	8.2	C
<b>Plesovice - 23.d</b>	Secondary	0.41	0.016	0.05299	0.0012	0.0557	0.0023	-0.06974	0.38759	349	11	332.8	7.3	C
<b>Plesovice - 24.d</b>	Secondary	0.393	0.017	0.05284	0.0012	0.0538	0.002	0.097799	0.22436	335	12	331.9	7.4	C
<b>91500 - 1.d</b>	Secondary	1.79	0.11	0.1777	0.0053	0.0742	0.0045	0.080328	0.27531	1049	41	1054	29	C
<del><b>91500 - 2.d</b></del>	<del>Secondary</del>	<del>1.78</del>	<del>0.1</del>	<del>0.1792</del>	<del>0.0051</del>	<del>0.0696</del>	<del>0.0035</del>	<del>0.26868</del>	<del>0.11935</del>	<del>1035</del>	<del>39</del>	<del>1065</del>	<del>29</del>	<del>D</del>
<b>91500 - 3.d</b>	Secondary	1.96	0.11	0.1774	0.0047	0.078	0.0043	0.096842	0.28612	1094	38	1055	26	C
<b>91500 - 4.d</b>	Secondary	1.869	0.095	0.1808	0.0059	0.0752	0.0041	0.05796	0.43928	1066	34	1074	33	C
<del><b>91500 - 5.d</b></del>	<del>Secondary</del>	<del>1.963</del>	<del>0.089</del>	<del>0.1759</del>	<del>0.0046</del>	<del>0.0805</del>	<del>0.0037</del>	<del>-0.07537</del>	<del>0.41503</del>	<del>1101</del>	<del>30</del>	<del>1044</del>	<del>25</del>	<del>D</del>
<b>91500 - 6.d</b>	Secondary	1.885	0.1	0.1787	0.0053	0.0761	0.0043	0.17853	0.24168	1071	37	1059	29	C



Samantha Nicole March  
Ultrahigh-pressure metapelites in the WGR

<b>91500 - 7.d</b>	Secondary	1.83	0.11	0.1808	0.0048	0.0717	0.0043	-0.01321	0.35618	1053	<b>40</b>	1071	26	C
<b>91500 - 8.d</b>	Secondary	1.95	0.092	0.1798	0.005	0.0773	0.0035	0.009377	0.44881	1108	33	1065	27	C
<b>91500 - 9.d</b>	Secondary	1.736	0.099	0.174	0.0047	0.0742	0.0044	0.014138	0.3756	1042	38	1034	26	C
<b>91500 - 10.d</b>	Secondary	1.818	0.1	0.1742	0.0048	0.0773	0.0044	0.13791	0.29145	1051	38	1035	26	C
<b>91500 - 11.d</b>	Secondary	1.837	0.093	0.1772	0.005	0.0775	0.004	0.072065	0.37602	1060	35	1051	27	C
<b>91500 - 12.d</b>	Secondary	1.89	0.12	0.1778	0.0048	0.0778	0.0049	-0.11226	0.41905	1073	40	1054	26	C

~~Crossed out~~ = discordant, C = concordant, NC = near concordant, D = discordant, RD = reversely discordant.

### WGC2019J-31A zircon geochronology

Sample	207/235	2 $\sigma$	206/238	2 $\sigma$	207/206	2 $\sigma$	ErrCorr 6/38vs7/35	ErrCorr 38/6vs7/6	207/235 age	2 $\sigma$	206/238 age	2 $\sigma$	Concordant?	% discordance
<b>31A-1-1.d</b>	0.906	0.05	0.1022	0.0035	0.0644	0.0031	0.5617	0.076329	652	26	627	20	<del>D</del> —ellipse touching concordia	3.834356
<b>31A-1-2.d</b>	0.567	0.033	0.0711	0.0019	0.0583	0.0033	0.33115	0.10429	456	21	442.5	11	C - Caledonian	2.960526
<b>31A-2-1.d</b>	0.5	0.027	0.0685	0.0017	0.0536	0.003	0.085745	0.3712	416	20	427.3	10	C - Caledonian	-2.71635
<b>31A-2-2.d</b>	0.507	0.029	0.0679	0.0016	0.0533	0.0031	-0.00225	0.3527	417	20	423.5	9.4	C - Caledonian	-1.55875
<b>31A-3-1.d</b>	0.558	0.03	0.074	0.0017	0.0543	0.0028	0.20641	0.11583	451	19	459.9	10	<del>D</del> —ellipse touching concordia	-1.97339
<b>31A-3-2.d</b>	0.526	0.024	0.06766	0.0015	0.0565	0.0025	0.033139	0.45108	428.2	16	422	9	C - Caledonian	1.447922
<b>31A-4-1.d</b>	0.503	0.034	0.0675	0.0016	0.0541	0.0035	0.28395	0.10892	413	22	421.1	9.9	C - Caledonian	-1.96126
<b>31A-4-2.d</b>	0.538	0.033	0.0687	0.0018	0.0568	0.0033	0.20493	0.10251	438	23	428.1	11	C - Caledonian	2.260274
<b>31A-5-1.d</b>	0.593	0.03	0.0744	0.0018	0.0581	0.003	0.15696	0.32544	473	20	462.4	11	<del>D</del> —ellipse touching concordia	2.241015
<b>31A-5-2.d</b>	0.503	0.031	0.06908	0.0014	0.0526	0.0031	0.19704	0.10135	411	21	430.6	8.7	C - Caledonian	-4.76886
<b>31A-6-1.d</b>	0.534	0.027	0.06922	0.0014	0.0561	0.0028	0.10254	0.23575	433	18	431.5	8.5	C - Caledonian	0.34642
<b>31A-6-2.d</b>	0.507	0.027	0.0687	0.0016	0.054	0.0029	0.18287	0.19609	417	19	428.4	9.6	C - Caledonian	-2.73381
<b>31A-7-1.d</b>	0.516	0.026	0.06876	0.0015	0.0547	0.0027	-0.08225	0.37086	421	17	428.6	9.1	C - Caledonian	-1.80523
<b>31A-7-2.d</b>	0.538	0.027	0.07034	0.0015	0.0551	0.0026	0.13605	0.30689	437	18	438.2	9.3	C - Caledonian	-0.2746
<b>31A-8-1.d</b>	1.401	0.069	0.1387	0.0041	0.0735	0.003	0.70483	0.054193	889	30	837	23	<del>D</del>	5.849269
<b>31A-8-2.d</b>	0.497	0.033	0.0684	0.0018	0.0518	0.0034	0.29382	0.099368	407	23	426.6	11	C - Caledonian	-4.81572

Samantha Nicole March  
Ultrahigh-pressure metapelites in the WGR

<del>31A-8 - 3.d</del>	0.513	0.028	0.0683	0.0016	0.0552	0.0031	-0.06378	0.39575	423	19	425.7	9.5	C - Caledonian	-0.6383
<del>31A-9 - 1.d</del>	0.496	0.027	0.06809	0.0015	0.0527	0.0028	0.14242	0.2053	407	19	424.6	9.1	C - Caledonian	-4.32432
<del>31A-9 - 2.d</del>	0.511	0.028	0.0668	0.0015	0.0549	0.0029	0.15966	0.22664	417	19	416.5	9.3	C - Caledonian	0.119904
<del>31A-10 - 1.d</del>	0.661	0.091	0.0812	0.0067	0.0588	0.0034	0.89248	-0.38349	507	49	503	39	D—ellipse touching concordia	0.788955
<del>31A-10 - 2.d</del>	0.841	0.047	0.094	0.0025	0.0649	0.003	0.56964	-0.00611	617	25	579	15	D	6.158833
<del>31A-11 - 1.d</del>	0.537	0.025	0.0688	0.0016	0.0556	0.0027	0.04163	0.39742	436	17	428.7	9.8	C - Caledonian	1.674312
<del>31A-11 - 2.d</del>	0.516	0.027	0.06879	0.0014	0.0543	0.0026	0.26598	0.10804	421	18	428.8	8.6	C - Caledonian	-1.85273
<del>31A-11 - 3.d</del>	0.545	0.026	0.06898	0.0015	0.0583	0.0028	0.20358	0.21106	444	17	430	9	C - Caledonian	3.153153
<del>31A-12 - 1.d</del>	0.674	0.038	0.0815	0.0023	0.0613	0.0028	0.35241	0.14839	529	23	504.8	14	D—ellipse touching concordia	4.574669
<del>31A-12 - 2.d</del>	0.946	0.051	0.1031	0.0027	0.0666	0.0031	0.49142	-0.00166	673	26	632	16	D	6.092125
<del>31A-12 - 3.d</del>	1.348	0.076	0.1351	0.004	0.0721	0.0034	0.33008	0.1218	864	34	817	23	D	5.439815
<del>31A-13 - 1.d</del>	0.509	0.027	0.068	0.0017	0.0548	0.0029	0.065376	0.40072	417	18	424.1	10	C - Caledonian	-1.70264
<del>31A-13 - 2.d</del>	0.529	0.03	0.0689	0.0016	0.0562	0.003	0.037091	0.32429	431	19	429.3	9.8	C - Caledonian	0.394432
<del>31A-14 - 1.d</del>	0.516	0.027	0.0697	0.0015	0.0552	0.0027	0.34949	0.093629	426	18	434.3	9.2	C - Caledonian	-1.94836
<del>31A-16 - 1.d</del>	1.039	0.052	0.113	0.0032	0.0668	0.003	0.60968	-0.01583	726	26	690	18	D	4.958678
<del>31A-16 - 2.d</del>	0.589	0.029	0.0755	0.0017	0.0567	0.0027	0.41305	-0.07563	469	19	469	10	D—ellipse touching concordia	0
<del>31A-16 - 3.d</del>	0.564	0.028	0.0703	0.0017	0.0582	0.0028	0.15197	0.30636	456	19	438	9.9	C - Caledonian	3.947368
<del>31A-17 - 1.d</del>	0.755	0.038	0.086	0.0021	0.0644	0.0029	0.47242	0.013806	573	22	531.7	12	D	7.207679
<del>31A-17 - 2.d</del>	1.031	0.049	0.113	0.0028	0.0672	0.0029	0.38156	0.24542	722	24	690	16	D—ellipse touching concordia	4.432133
<del>31A-18 - 1.d</del>	0.653	0.035	0.0801	0.0027	0.0598	0.0025	0.76458	-0.14571	509	21	496	16	D—ellipse touching concordia	2.554028
<del>31A-18 - 2.d</del>	0.564	0.029	0.071	0.0016	0.0574	0.0029	0.059247	0.33968	453	19	441.8	9.7	C - Caledonian	2.472406
<del>31A-19 - 1.d</del>	0.483	0.024	0.0673	0.0016	0.0526	0.0025	0.26703	0.16127	399	16	419.9	9.6	C - Caledonian	-5.2381
<del>31A-19 - 2.d</del>	0.505	0.026	0.0701	0.0016	0.053	0.0025	0.34282	0.076884	417	17	437	9.5	C - Caledonian	-4.79616
<del>31A-20 - 1.d</del>	0.484	0.025	0.06824	0.0015	0.0515	0.0025	0.12318	0.28856	401	16	425.5	9.2	C - Caledonian	-6.10973
<del>31A-20 - 2.d</del>	0.514	0.028	0.0687	0.0016	0.0554	0.003	-0.07305	0.35899	422	19	428.1	9.4	C - Caledonian	-1.4455
<del>31A-21 - 1.d</del>	0.718	0.038	0.0846	0.0024	0.0607	0.0031	0.16595	0.34325	549	22	524	14	D—ellipse touching concordia	4.553734

Samantha Nicole March  
Ultrahigh-pressure metapelites in the WGR

<del>31A-21 - 2.d</del>	0.533	0.031	0.0691	0.0018	0.0555	0.0031	0.22168	0.23668	432	21	430.8	11	C - Caledonian	0.277778
<del>31A-21 - 3.d</del>	0.506	0.027	0.0682	0.0017	0.0545	0.003	0.091109	0.32229	414	18	426.1	10	C - Caledonian	-2.92271
<del>31A-22 - 1.d</del>	1.238	0.078	0.1272	0.0058	0.0697	0.0029	0.86694	-0.16779	814	36	770	33	D	5.405405
<del>31A-22 - 2.d</del>	1.538	0.069	0.1516	0.0037	0.073	0.0031	0.50174	0.10374	951	27	912	21	D	4.100946
<del>31A-23 - 1.d</del>	0.483	0.024	0.0653	0.0016	0.0535	0.0027	0.32943	0.15611	399	16	408	9.5	C - Caledonian	-2.25564
<del>31A-23 - 2.d</del>	0.461	0.023	0.06305	0.0013	0.0539	0.0026	0.055477	0.30824	384	16	394.1	8.1	C - Caledonian	-2.63021
<del>31A-24 - 1.d</del>	0.528	0.029	0.0667	0.0015	0.0568	0.0031	0.082625	0.26998	429	19	416	9.1	C - Caledonian	3.030303
<del>31A-24 - 2.d</del>	0.517	0.03	0.0672	0.0016	0.0555	0.0033	-0.07627	0.38546	421	20	419	9.7	C - Caledonian	0.475059
<del>31A-25 - 1.d</del>	0.538	0.031	0.0701	0.0016	0.0557	0.003	0.02587	0.40137	437	20	436.7	9.8	C - Caledonian	0.06865
<del>31A-25 - 2.d</del>	0.551	0.033	0.0697	0.0017	0.0574	0.0033	0.21256	0.12668	446	21	434.1	10	C - Caledonian	2.668161
<del>31A-32 - 1.d</del>	0.955	0.078	0.1049	0.0053	0.0646	0.0033	0.87709	-0.41018	674	40	642	31	D	4.747774
<del>31A-32 - 2.d</del>	0.53	0.029	0.06959	0.0015	0.056	0.003	0.28809	0.012666	432	19	433.6	9.3	C - Caledonian	-0.37037
<del>31A-33 - 1.d</del>	0.526	0.026	0.06805	0.0015	0.0566	0.0027	0.21874	0.098919	430	18	424.4	8.8	C - Caledonian	1.302326
<del>31A-33 - 2.d</del>	0.519	0.026	0.06812	0.0014	0.0551	0.0026	0.28915	0.067784	426	18	424.8	8.6	C - Caledonian	0.28169
<del>31A-33 - 3.d</del>	0.524	0.029	0.07	0.0016	0.0542	0.0031	-0.10601	0.48216	428	20	436.4	9.6	C - Caledonian	-1.96262
<del>31A-34 - 1.d</del>	1.39	0.064	0.1397	0.0031	0.072	0.003	0.45515	0.087248	884	28	843	18	D	4.638009
<del>31A-34 - 2.d</del>	0.513	0.027	0.0671	0.0015	0.0557	0.0028	0.025397	0.29026	419	18	418.6	8.8	C - Caledonian	0.095465
<del>31A-35 - 1.d</del>	0.553	0.03	0.0702	0.0016	0.0577	0.0031	0.08375	0.32906	445	20	437.6	9.8	C - Caledonian	1.662921
<del>31A-35 - 2.d</del>	0.538	0.029	0.0679	0.0016	0.0562	0.0029	0.34965	0.034947	436	19	423.6	9.7	C - Caledonian	2.844037
<del>31A-35 - 3.d</del>	0.525	0.031	0.069	0.0016	0.0548	0.003	0.070013	0.27855	428	21	430	9.8	C - Caledonian	-0.46729
<del>31A-37 - 1.d</del>	0.498	0.025	0.06735	0.0015	0.0535	0.0026	0.24847	0.19853	411	17	420.2	8.8	C - Caledonian	-2.23844
<del>31A-37 - 2.d</del>	0.501	0.024	0.06811	0.0014	0.0531	0.0024	0.091134	0.2467	411.6	16	424.8	8.2	C - Caledonian	-3.207
<del>31A-36 - 1.d</del>	0.517	0.028	0.06875	0.0015	0.0548	0.0028	0.19033	0.22044	423	19	428.6	9	C - Caledonian	-1.32388
<del>31A-36 - 2.d</del>	0.537	0.029	0.0692	0.0017	0.0559	0.0029	0.16791	0.25396	437	19	431.2	10	C - Caledonian	1.327231
<del>31A-38 - 1.d</del>	0.479	0.027	0.0651	0.0016	0.0538	0.0028	0.12543	0.36638	396	18	406.2	10	C - Caledonian	-2.57576
<del>31A-38 - 2.d</del>	0.512	0.025	0.06825	0.0015	0.0542	0.0025	0.02812	0.37691	422	18	425.6	9	C - Caledonian	-0.85308
<del>31A-39 - 1.d</del>	0.496	0.025	0.0706	0.0016	0.0521	0.0028	-0.08217	0.42268	408	17	439.5	9.6	C - Caledonian	-7.72059
<del>31A-39 - 2.d</del>	0.505	0.029	0.0695	0.0017	0.053	0.003	0.090772	0.25972	413	19	433.4	10	C - Caledonian	-4.93947
<del>31A-40 - 1.d</del>	0.932	0.05	0.1039	0.0023	0.065	0.0032	0.31833	-0.01007	672	25	637.3	14	D—ellipse touching eonecordia	5.16369

Samantha Nicole March  
Ultrahigh-pressure metapelites in the WGR

<del>31A-40 - 2.d</del>	1.186	0.062	0.1275	0.0043	0.0681	0.003	0.68906	0.1504	793	30	773	24	D-ellipse touching concordia	2.522068
31A-41 - 1.d	0.568	0.029	0.071	0.0017	0.0586	0.0028	0.26899	0.1966	459	18	442.4	10	C - Caledonian	3.616558
31A-41 - 2.d	0.541	0.032	0.0696	0.0017	0.0561	0.0031	0.049728	0.32136	439	21	433.6	10	C - Caledonian	1.230068
31A-41 - 3.d	0.483	0.03	0.0607	0.0015	0.0571	0.0034	0.17902	0.16731	401	20	380.1	9.3	C - caledonian	5.21197
31A-42 - 1.d	0.554	0.029	0.0686	0.0017	0.0589	0.0032	0.04537	0.34388	446	19	427.7	10	C - Caledonian	4.103139
31A-42 - 2.d	0.51	0.028	0.06897	0.0015	0.053	0.0027	0.15788	0.18997	419	19	429.9	9.1	C - Caledonian	-2.60143
<del>31A-43 - 1.d</del>	0.764	0.051	0.0903	0.0036	0.0624	0.0031	0.80332	-0.22425	574	29	557	21	D-ellipse touching concordia	2.961672
31A-43 - 2.d	0.528	0.032	0.0699	0.0017	0.0551	0.0033	0.18052	0.2859	430	22	435.2	10	C - Caledonian	-1.2093
31A-43 - 3.d	0.504	0.031	0.0668	0.0015	0.0542	0.0034	0.084757	0.17418	415	20	416.5	9.2	C - Caledonian	-0.36145
31A-44 - 1.d	1.982	0.083	0.1897	0.0039	0.0761	0.0029	0.33451	0.30288	1110	29	1119	21	C - Sveconorwegian	-0.81081
31A-44 - 2.d	1.492	0.067	0.1504	0.0038	0.0719	0.0028	0.60914	0.2308	929	27	903	21	C - Sveconorwegian	2.798708
31A-44 - 3.d	0.505	0.024	0.06635	0.0014	0.0551	0.0026	0.062461	0.3489	414	16	414.1	8.4	C - Caledonian	-0.02415
<del>31A-45 - 1.d</del>	0.711	0.045	0.0851	0.0033	0.0603	0.003	0.734	-0.2671	550	27	526	19	D-ellipse touching concordia	4.363636
<del>31A-45 - 2.d</del>	0.76	0.051	0.0916	0.0038	0.0609	0.003	0.77067	-0.19756	574	30	564	23	D-ellipse touching concordia	1.74216
31A-45 - 3.d	0.526	0.026	0.0691	0.0016	0.0558	0.0029	0.00131	0.36427	432	18	430.9	9.7	C - Caledonian	0.25463
31A-46 - 1.d	0.553	0.032	0.0707	0.0017	0.0569	0.003	-0.03537	0.2669	449	21	440.4	10	C - Caledonian	1.915367
31A-47 - 1.d	0.53	0.026	0.06929	0.0015	0.0558	0.0027	0.000815	0.3133	432	18	431.8	8.9	C - Caledonian	0.046296
31A-47 - 2.d	0.494	0.026	0.06653	0.0015	0.0539	0.0027	0.17654	0.1816	406	18	415.2	9.1	C - Caledonian	-2.26601
<del>31A-48 - 1.d</del>	0.641	0.031	0.0794	0.0019	0.0585	0.0026	0.37493	0.1993	502	19	492.2	11	D-ellipse touching concordia	1.952191
<del>31A-55 - 1.d</del>	0.711	0.039	0.083	0.0022	0.0614	0.003	0.39404	0.15659	543	23	515	14	D	5.156538
<del>31A-55 - 2.d</del>	0.5	0.037	0.0635	0.0019	0.0564	0.0039	-0.02576	0.32793	412	25	397	11	D	3.640777
<del>31A-56 - 1.d</del>	1.32	0.17	0.1222	0.0091	0.0766	0.0052	0.9049	-0.53576	849	72	740	52	D	12.83863
<del>31A-56 - 2.d</del>	1.193	0.065	0.1189	0.0032	0.0712	0.0036	0.35086	0.098198	798	29	724	19	D	9.273183
31A-56 - 3.d	0.539	0.026	0.06863	0.0015	0.0569	0.0027	0.017795	0.36894	437	17	427.9	8.9	C - Caledonian	2.08238
31A-57 - 1.d	0.525	0.029	0.0679	0.0016	0.0565	0.003	0.069566	0.30281	429	19	423.3	9.6	C - Caledonian	1.328671
31A-57 - 2.d	0.509	0.027	0.0671	0.0015	0.0546	0.003	0.039815	0.3441	416	18	418.5	9.2	C - Caledonian	-0.60096

Samantha Nicole March  
Ultrahigh-pressure metapelites in the WGR

<del>31A-58 - 1.d</del>	0.528	0.03	0.0688	0.0016	0.0541	0.0029	0.099759	0.2657	429	20	428.9	9.4	C - Caledonian	0.02331
<del>31A-58 - 2.d</del>	0.721	0.051	0.0849	0.004	0.0611	0.003	0.79079	-0.16417	546	30	524	24	D	4.029304
31A-59 - 1.d	0.547	0.031	0.0695	0.0016	0.0558	0.003	0.23227	0.19291	441	21	433.2	9.9	C - Caledonian	1.768707
31A-59 - 2.d	0.539	0.029	0.068	0.0017	0.0585	0.003	0.1982	0.25811	440	18	424.7	9.8	C - Caledonian	3.477273
31A-60 - 1.d	0.534	0.03	0.07	0.0016	0.0561	0.0032	-0.05684	0.37152	433	20	435.9	9.5	C - Caledonian	-0.66975
31A-60 - 2.d	0.535	0.03	0.06915	0.0015	0.0562	0.003	0.10773	0.28714	433	20	431	9.2	C - Caledonian	0.461894
<del>31A-61 - 1.d</del>	7.41	0.34	0.3115	0.0088	0.1716	0.0065	0.67931	0.045277	2157	41	1747	43	D	19.00788
<del>31A-61 - 2.d</del>	7.35	0.5	0.315	0.013	0.1657	0.0069	0.929	-0.55712	2135	61	1763	63	D	17.42389
<del>31A-61 - 3.d</del>	0.947	0.054	0.1025	0.0029	0.0668	0.0034	0.44786	0.001492	678	28	629	17	D	7.227139
<del>31A-62 - 1.d</del>	0.647	0.036	0.0808	0.002	0.0584	0.003	0.17359	0.23987	505	22	501	12	D—ellipse touching concordia	0.792079
31A-62 - 2.d	0.555	0.033	0.0686	0.0016	0.0588	0.0035	-0.03223	0.34996	448	21	427.5	9.6	C - Caledonian	4.575893
31A-63 - 1.d	0.52	0.029	0.0665	0.0015	0.0561	0.0029	0.29585	0.080005	427	19	415.1	9.2	C - Caledonian	2.786885
31A-63 - 2.d	0.513	0.026	0.06979	0.0014	0.0531	0.0026	0.11755	0.25844	419	17	434.9	8.7	C - Caledonian	-3.79475
31A-64 - 1.d	0.49	0.029	0.06768	0.0015	0.0515	0.0031	0.085861	0.18888	403	20	422.1	9	C - Caledonian	-4.73945
31A-64 - 2.d	0.508	0.03	0.0674	0.0015	0.0546	0.0032	0.057554	0.28677	417	19	420.2	9.2	C - Caledonian	-0.76739
<del>31A-65 - 1.d</del>	0.886	0.045	0.0987	0.0024	0.0655	0.0029	0.55692	-0.05734	642	24	606.8	14	D	5.482866
<del>31A-65 - 2.d</del>	0.809	0.058	0.094	0.0039	0.0614	0.0031	0.83141	-0.38497	599	32	579	23	D—ellipse touching concordia	3.338898
31A-66 - 1.d	0.522	0.031	0.0676	0.0015	0.0554	0.0032	0.16704	0.15152	429	21	421.9	9.3	C - Caledonian	1.655012
31A-66 - 2.d	0.517	0.03	0.06777	0.0014	0.0546	0.0032	-0.03846	0.33371	421	20	422.7	8.6	C - Caledonian	-0.4038
31A-67 - 1.d	0.562	0.038	0.0704	0.002	0.0567	0.0032	0.5402	-0.05522	449	24	438.7	12	C - Caledonian	2.293987
31A-67 - 2.d	0.518	0.027	0.0704	0.0016	0.053	0.0026	0.17189	0.21365	423	18	438.2	9.5	C - Caledonian	-3.59338
31A-68 - 1.d	0.53	0.029	0.069	0.0017	0.0557	0.003	0.12905	0.3455	430	19	430.2	10	C - Caledonian	-0.04651
31A-68 - 2.d	0.517	0.03	0.06875	0.0015	0.0543	0.003	0.24321	0.007033	421	20	428.6	9	C - Caledonian	-1.80523
31A-69 - 1.d	0.533	0.026	0.0682	0.0016	0.0565	0.0028	0.19518	0.24834	433	18	425.2	9.8	C - Caledonian	1.801386
31A-71 - 1.d	1.623	0.068	0.1596	0.0037	0.0738	0.0028	0.47133	0.3225	978	25	954	20	C - Sveconorwegian	2.453988
31A-70 - 1.d	0.532	0.029	0.06789	0.0015	0.0568	0.003	0.18229	0.208	432	19	423.4	9	C - Caledonian	1.990741
31A-72 - 1.d	0.532	0.028	0.0701	0.0016	0.0551	0.0028	-0.03013	0.42805	432	18	436.6	9.7	C - Caledonian	-1.06481
31A-72 - 2.d	0.525	0.032	0.069	0.0018	0.056	0.0034	0.035028	0.36397	426	21	429.9	11	C - Caledonian	-0.91549

Samantha Nicole March  
Ultrahigh-pressure metapelites in the WGR

<del>31A-73 - 1.d</del>	0.605	0.031	0.0759	0.0018	0.0582	0.0028	0.21225	0.16074	480	19	471.4	10	D - ellipse touching eoneordia	1.791667
31A-73 - 2.d	0.497	0.028	0.06719	0.0015	0.0538	0.003	-0.03775	0.373	408	19	419.2	8.9	C - Caledonian	-2.7451
31A-74 - 1.d	0.511	0.03	0.0676	0.0016	0.0533	0.0031	0.293	0.06638	417	20	421.7	9.5	C - Caledonian	-1.1271
31A-75 - 1.d	0.539	0.03	0.0692	0.0017	0.0575	0.0031	0.2229	0.094511	436	20	431.1	10	C - Caledonian	1.123853
<del>31A-75 - 2.d</del>	1.317	0.086	0.1254	0.0041	0.0763	0.0038	0.77787	-0.30284	849	37	761	24	D	10.36514
31A-76 - 1.d	1.617	0.073	0.1616	0.0038	0.0734	0.0029	0.60153	0.10859	982	26	966	21	C - Sveconorwegian	1.629328
<del>31A-76 - 2.d</del>	1.168	0.062	0.1195	0.0039	0.0702	0.003	0.80718	-0.293	782	30	727	22	D	7.033248
31A-77 - 1.d	0.509	0.025	0.0659	0.0015	0.0555	0.0029	-0.06572	0.43574	417	17	411.3	8.8	C - Caledonian	1.366906
31A-77 - 2.d	0.531	0.026	0.0673	0.0015	0.0574	0.0029	-0.11705	0.46773	432	18	419.7	9.1	C - Caledonian	2.847222
<del>31A-77 - 3.d</del>	0.531	0.55	0.0604	0.016	0.0596	0.032	0.44222	0.027465	428	77	378	91	D	11.68224
31A-78 - 1.d	0.523	0.03	0.0703	0.0016	0.054	0.003	-0.00456	0.39547	427	19	438	9.6	C - Caledonian	-2.57611
31A-78 - 2.d	0.517	0.027	0.0705	0.0015	0.0534	0.0026	0.4506	-0.13742	424	19	439.1	8.8	C - Caledonian	-3.56132
31A-79 - 1.d	0.521	0.027	0.0683	0.0016	0.0551	0.0026	0.27259	0.14411	424	18	425.6	9.7	C - Caledonian	-0.37736
31A-79 - 2.d	0.511	0.03	0.0682	0.0018	0.0554	0.0033	0.19041	0.30795	417	20	425.3	11	C - Caledonian	-1.99041
<del>31A-80 - 1.d</del>	0.878	0.041	0.0989	0.0021	0.0638	0.0029	0.193	0.26035	638	22	607.8	13	D	4.733542
31A-80 - 2.d	0.532	0.03	0.0701	0.0016	0.0546	0.003	0.067766	0.24761	430	21	436.8	9.4	C - Caledonian	-1.5814
31A-81 - 1.d	0.501	0.03	0.0694	0.0018	0.0522	0.0032	0.14729	0.26791	415	21	432.6	11	C - Caledonian	-4.24096
31A-81 - 2.d	0.504	0.027	0.0684	0.0015	0.0538	0.0026	0.34632	-0.02522	415	18	426.5	9	C - Caledonian	-2.77108
31A-81 - 3.d	0.523	0.028	0.0678	0.0016	0.0558	0.0029	0.1936	0.24526	428	18	423.1	9.5	C - Caledonian	1.14486
<del>31A-82 - 1.d</del>	1.215	0.075	0.1278	0.0047	0.0689	0.0028	0.87003	-0.34648	801	36	778	26	D	2.871411
<del>31A-83 - 1.d</del>	0.575	0.03	0.0691	0.0015	0.061	0.0029	0.30502	0.14689	460	19	430.7	9.2	D	6.369565
31A-83 - 2.d	0.526	0.029	0.06804	0.0015	0.0559	0.003	0.22636	0.14463	431	19	424.3	9.2	C - Caledonian	1.554524
31A-84 - 1.d	1.982	0.085	0.1941	0.0039	0.0748	0.0029	0.41422	0.18913	1108	29	1143	21	C - Sveconorwegian	-3.15884
31A-84 - 2.d	1.6	0.071	0.1596	0.0034	0.0719	0.0029	0.27257	0.20871	970	28	954	19	C - Sveconorwegian	1.649485
31A-85 - 1.d	0.508	0.027	0.0686	0.0016	0.0546	0.0028	0.13685	0.19924	419	18	427.9	9.8	C - Caledonian	-2.12411
31A-85 - 2.d	0.525	0.03	0.0693	0.0016	0.0543	0.003	0.12132	0.23033	426	20	431.7	9.5	C - Caledonian	-1.33803
<del>31A-86 - 1.d</del>	0.767	0.17	0.077	0.0069	0.0735	0.007	0.86075	-0.37744	571	77	478	42	D	16.28722
<del>31A-86 - 2.d</del>	0.629	0.036	0.0709	0.0019	0.0626	0.0032	0.15046	0.24727	496	22	441.4	11	D	11.00806
31A-87 - 1.d	0.489	0.028	0.0655	0.0015	0.0536	0.0028	0.11091	0.27074	406	19	408.9	9.2	C - Caledonian	-0.71429

Samantha Nicole March  
Ultrahigh-pressure metapelites in the WGR

31A-87 - 2.d	0.521	0.026	0.06736	0.0015	0.0558	0.0028	0.055912	0.31605	425	18	420.2	8.9	C - Caledonian	1.129412
31A-87 - 3.d	0.535	0.032	0.0683	0.0015	0.0571	0.0033	0.059005	0.23727	432	21	426	9.2	C - Caledonian	1.388889
31A-88 - 1.d	0.481	0.024	0.06474	0.0014	0.0536	0.0025	0.18965	0.22183	398	17	404.4	8.7	C - Caledonian	-1.60804
31A-89 - 1.d	0.536	0.031	0.06848	0.0014	0.0563	0.0034	-0.08618	0.36443	433	21	426.9	8.7	C - Caledonian	1.408776
31A-89 - 2.d	0.534	0.03	0.0676	0.0016	0.0576	0.0032	0.074836	0.29788	433	20	421.6	9.7	C - Caledonian	2.632794
31A-90 - 1.d	0.523	0.026	0.068	0.0016	0.0552	0.0028	0.0306	0.41312	426	17	423.9	9.8	C - Caledonian	0.492958
31A-90 - 2.d	0.527	0.03	0.0694	0.0016	0.0548	0.0031	-0.08996	0.38739	430	20	432.4	9.5	C - Caledonian	-0.55814
<del>31A-91 - 1.d</del>	<del>0.562</del>	<del>0.028</del>	<del>0.0679</del>	<del>0.0016</del>	<del>0.0588</del>	<del>0.0027</del>	<del>0.28617</del>	<del>0.22395</del>	<del>453</del>	<del>18</del>	<del>423.3</del>	<del>9.9</del>	<del>D</del>	<del>6.556291</del>
31A-91 - 2.d	0.514	0.031	0.0689	0.0016	0.0532	0.0032	-0.07601	0.33683	421	22	429.7	9.5	C - Caledonian	-2.06651
31A-92 - 1.d	0.512	0.031	0.0676	0.0017	0.0545	0.0033	-0.03009	0.346	420	20	421.5	10	C - Caledonian	-0.35714
31A-92 - 2.d	0.498	0.025	0.06562	0.0015	0.0552	0.0028	-0.11712	0.49972	409	17	409.7	8.8	C - Caledonian	-0.17115
31A-93 - 1.d	0.516	0.025	0.06827	0.0014	0.0547	0.0026	0.091156	0.25222	423	18	425.7	8.7	C - Caledonian	-0.6383
31A-93 - 2.d	0.505	0.027	0.06843	0.0015	0.0527	0.0029	-0.11348	0.46114	413	18	426.6	9.2	C - Caledonian	-3.29298
<del>31A-94 - 1.d</del>	<del>0.663</del>	<del>0.039</del>	<del>0.0801</del>	<del>0.0022</del>	<del>0.0599</del>	<del>0.0032</del>	<del>0.35379</del>	<del>0.1392</del>	<del>516</del>	<del>24</del>	<del>496.7</del>	<del>13</del>	<del>D - ellipse touching concordia</del>	<del>3.74031</del>
31A-94 - 2.d	0.501	0.03	0.0677	0.0016	0.0536	0.0031	0.15292	0.17955	411	20	422.1	9.5	C - Caledonian	-2.70073
31A-94 - 3.d	0.521	0.03	0.0676	0.0015	0.0554	0.0032	-0.11431	0.4032	424	20	421.6	9.1	C - Caledonian	0.566038
31A-95 - 1.d	0.539	0.029	0.0697	0.0016	0.0559	0.0031	-0.15899	0.47096	436	19	434.2	9.7	C - Caledonian	0.412844
31A-95 - 2.d	0.508	0.027	0.0665	0.0016	0.0554	0.0029	0.084261	0.33169	419	18	415.1	10	C - Caledonian	0.930788
31A-96 - 1.d	0.526	0.026	0.06838	0.0015	0.056	0.0026	0.20024	0.25494	431	18	426.4	9.1	C - Caledonian	1.067285
31A-96 - 2.d	0.511	0.029	0.0671	0.0016	0.0548	0.003	0.067925	0.32294	419	20	418.5	9.6	C - Caledonian	0.119332
31A-96 - 3.d	0.455	0.029	0.0626	0.0016	0.0524	0.0033	0.10807	0.25622	382	21	391.2	9.8	C - Caledonian	-2.40838
31A-97 - 1.d	0.53	0.027	0.0681	0.0015	0.0561	0.0029	0.045098	0.32596	431	18	424.9	9.3	C - Caledonian	1.415313
31A-97 - 2.d	0.508	0.025	0.06815	0.0015	0.0546	0.0026	0.16033	0.20539	418	18	424.9	8.8	C - Caledonian	-1.65072
31A-98 - 1.d	0.531	0.027	0.06966	0.0015	0.0552	0.0027	0.042176	0.32705	431	18	434.1	9.2	C - Caledonian	-0.71926
31A-98 - 2.d	0.524	0.029	0.0651	0.0018	0.057	0.0031	0.23128	0.22583	426	20	406.5	11	C - Caledonian	4.577465
31A-99 - 1.d	0.49	0.024	0.0643	0.0015	0.0548	0.0027	0.012337	0.31984	404	17	401.7	8.8	C - Caledonian	0.569307
31A-99 - 2.d	0.5	0.029	0.0669	0.0016	0.0549	0.0033	0.037655	0.23914	414	21	417.2	9.6	C - Caledonian	-0.77295
<del>31A-100 - 1.d</del>	<del>0.483</del>	<del>0.025</del>	<del>0.06277</del>	<del>0.0014</del>	<del>0.0555</del>	<del>0.0028</del>	<del>0.1182</del>	<del>0.31732</del>	<del>401</del>	<del>17</del>	<del>392.4</del>	<del>8.6</del>	<del>D</del>	<del>2.144638</del>



Samantha Nicole March  
Ultrahigh-pressure metapelites in the WGR

31A-100 - 2.d	0.486	0.029	0.0647	0.0015	0.0543	0.0033	-0.24848	0.49036	400	20	404.6	9.1	C - Caledonian	-1.15
31A-101 - 1.d	0.833	0.049	0.0958	0.0034	0.0625	0.0029	-0.73962	-0.12964	617	27	589	20	D	4.538088
31A-101 - 2.d	0.588	0.031	0.0751	0.0017	0.0573	0.0029	0.22673	0.18362	468	20	466.8	10	D - ellipse touching concordia	0.25641
31A-102 - 1.d	0.519	0.029	0.0679	0.0016	0.0544	0.0029	0.27612	0.17304	423	20	423.6	9.8	C - Caledonian	-0.14184
31A-102 - 2.d	0.51	0.026	0.06722	0.0015	0.0548	0.0028	0.044578	0.342	419	18	419.3	9	C - Caledonian	-0.0716
31A-103 - 1.d	0.52	0.028	0.0681	0.0015	0.0545	0.0029	-0.03301	0.40467	425	18	424.8	9.3	C - Caledonian	0.047059
31A-103 - 2.d	0.496	0.028	0.0679	0.0016	0.0529	0.003	0.14532	0.20243	409	20	423.7	9.7	C - Caledonian	-3.59413
31A-104 - 1.d	0.532	0.027	0.06795	0.0015	0.0564	0.0027	0.093609	0.27273	434	17	423.7	9	C - Caledonian	2.373272
31A-104 - 2.d	0.516	0.028	0.0694	0.0016	0.0541	0.0028	0.17072	0.22472	425	19	433.5	9.6	C - Caledonian	-2
31A-105 - 1.d	0.536	0.028	0.0693	0.0016	0.0558	0.0028	0.15053	0.28923	436	19	432	9.6	C - Caledonian	0.917431
31A-105 - 2.d	0.511	0.039	0.0665	0.0017	0.0558	0.004	0.074644	0.21007	418	27	415.2	10	C - Caledonian	0.669856
31A-105 - 3.d	0.503	0.028	0.0679	0.0016	0.0537	0.003	-0.02768	0.44246	412	19	423.5	9.4	C - Caledonian	-2.79126
31A-106 - 1.d	0.54	0.031	0.0695	0.0017	0.0559	0.0031	0.2585	0.10285	438	20	433.4	10	C - Caledonian	1.050228
31A-107 - 1.d	0.526	0.028	0.0679	0.0016	0.0555	0.0028	-0.01308	0.38254	428	19	423.2	9.6	C - Caledonian	1.121495
31A-107 - 2.d	0.516	0.026	0.06727	0.0014	0.0555	0.0026	0.15526	0.16388	423	17	419.7	8.1	C - Caledonian	0.780142
31A-108 - 1.d	0.484	0.024	0.06433	0.0014	0.0539	0.0025	0.14621	0.22009	400	17	401.9	8.5	C - Caledonian	-0.475
31A-108 - 2.d	0.492	0.025	0.0634	0.0015	0.0574	0.0027	0.29353	0.20557	407	17	396.3	9.2	C - Caledonian	2.628993
31A-109 - 1.d	0.513	0.031	0.0683	0.0019	0.0546	0.0034	-0.08413	0.46399	422	21	425.6	12	C - Caledonian	-0.85308
31A-109 - 2.d	0.543	0.032	0.0676	0.0018	0.0558	0.0032	0.31585	0.17985	440	21	421.8	11	C - Caledonian	4.136364
31A-110 - 1.d	0.553	0.031	0.0709	0.0018	0.0561	0.003	0.4269	0.040801	445	20	441.4	11	C - Caledonian	0.808989
31A-110 - 2.d	0.563	0.03	0.0714	0.002	0.058	0.0027	0.53028	0.030777	452	20	444.8	12	C - Caledonian	1.59292
31A-111 - 1.d	0.815	0.036	0.0926	0.0022	0.0635	0.0028	0.17588	0.46416	604	21	571	13	D - ellipse touching concordia	5.463576
31A-111 - 2.d	0.922	0.047	0.103	0.0029	0.0644	0.003	0.44526	0.12185	665	26	632	17	D	4.962406
31A-112 - 1.d	0.546	0.029	0.06858	0.0015	0.058	0.0031	0.054938	0.31207	443	20	427.5	9.1	C - Caledonian	3.498871
31A-112 - 2.d	0.546	0.026	0.06824	0.0014	0.0578	0.0029	-0.11463	0.44714	442	17	425.5	8.7	C - Caledonian	3.733032
31A-113 - 1.d	0.514	0.03	0.0704	0.0018	0.054	0.0029	0.2375	0.2019	419	20	438.6	11	C - Caledonian	-4.6778
31A-113 - 2.d	0.522	0.032	0.0689	0.0016	0.055	0.0034	-0.06834	0.36106	428	21	429.5	9.9	C - Caledonian	-0.35047
31A-114 - 1.d	10.02	0.42	0.4132	0.01	0.1756	0.0068	0.53087	0.41346	2437	40	2228	45	D	8.576118

Samantha Nicole March  
Ultrahigh-pressure metapelites in the WGR

31A-114 - 2.d	1.46	0.067	0.1441	0.0032	0.0737	0.0033	0.22483	0.33879	912	27	868	18	Đ	4.824561
31A-114 - 3.d	6.06	0.5	0.2984	0.017	0.145	0.0074	0.75558	-0.24861	1980	99	1689	90	Đ	14.69697
31A-115 - 1.d	0.563	0.037	0.0693	0.0016	0.0584	0.0035	0.17605	0.18949	450	24	432.1	9.9	C - Caledonian	3.977778
31A-115 - 2.d	0.528	0.031	0.0675	0.0016	0.0559	0.0035	0.071264	0.29489	428	21	421.1	9.7	C - Caledonian	1.61215
31A-115 - 3.d	0.532	0.029	0.0686	0.0017	0.0564	0.0032	-0.00402	0.36532	432	20	427.8	10	C - Caledonian	0.972222
31A-116 - 1.d	0.508	0.027	0.06801	0.0015	0.054	0.0028	0.084709	0.32262	417	18	424.1	9	C - Caledonian	-1.70264
31A-116 - 2.d	0.515	0.029	0.0688	0.0016	0.0547	0.0032	-0.04001	0.42234	422	20	428.6	9.5	C - Caledonian	-1.56398
31A-117 - 1.d	0.508	0.028	0.06618	0.0015	0.056	0.003	0.10895	0.22029	419	18	413.8	8.7	C - Caledonian	1.24105
31A-117 - 2.d	0.501	0.026	0.06669	0.0015	0.055	0.0027	0.2561	0.10727	413	18	416.1	9.1	C - Caledonian	-0.75061
31A-118 - 1.d	0.986	0.062	0.1048	0.0036	0.0674	0.0031	0.74614	-0.18392	701	31	642	21	Đ	8.416548
31A-118 - 2.d	1.34	0.058	0.1194	0.0026	0.0808	0.0032	0.2613	0.29534	863	25	726.9	15	Đ	15.77057
31A-118 - 3.d	0.519	0.028	0.06833	0.0015	0.0544	0.0027	0.14891	0.23917	425	19	426	9	C - Caledonian	-0.23529
31A-119 - 1.d	0.52	0.028	0.06789	0.0014	0.0563	0.0029	0.18049	0.081923	428	19	423.4	8.6	C - Caledonian	1.074766
31A-119 - 2.d	0.523	0.026	0.06762	0.0015	0.0558	0.0027	0.045542	0.33388	427	17	421.8	8.8	C - Caledonian	1.217799
31A-120 - 1.d	0.527	0.027	0.06814	0.0015	0.0557	0.0027	0.12425	0.2233	429	18	425.6	9.1	C - Caledonian	0.792541
31A-120 - 2.d	0.549	0.028	0.0676	0.0017	0.058	0.0029	0.020206	0.35265	443	19	421.7	10	C - Caledonian	4.808126
31A-120 - 3.d	0.543	0.027	0.06948	0.0015	0.0576	0.0028	0.16434	0.20567	441	17	433	9.3	C - Caledonian	1.814059
31A-121 - 1.d	0.545	0.032	0.0705	0.0017	0.0568	0.003	0.16126	0.1881	446	21	438.9	10	C - Caledonian	1.591928
31A-121 - 2.d	0.541	0.029	0.0691	0.0015	0.0566	0.0029	0.28215	0.055762	439	19	430.5	9.3	C - Caledonian	1.936219
31A-121 - 3.d	0.542	0.029	0.07008	0.0015	0.0564	0.0029	0.21459	0.15004	439	19	436.6	8.9	C - Caledonian	0.546697
31A-122 - 1.d	0.544	0.028	0.0691	0.0017	0.0565	0.0028	0.16326	0.28666	440	18	430.6	10	C - Caledonian	2.136364
31A-122 - 2.d	0.513	0.032	0.0694	0.0016	0.0532	0.0034	-0.1525	0.42354	418	22	432.8	9.5	C - Caledonian	-3.54067
31A-122 - 3.d	0.516	0.031	0.0686	0.0018	0.0539	0.0031	0.003533	0.36219	423	20	427.9	11	C - Caledonian	-1.15839
31A-123 - 1.d	0.531	0.029	0.0691	0.0017	0.0551	0.0032	-0.02505	0.4017	433	19	431.8	10	C - Caledonian	0.277136
31A-123 - 2.d	0.624	0.046	0.074	0.0023	0.0586	0.0032	0.81701	-0.37324	487	28	460	14	Đ	5.544148
31A-124 - 1.d	0.504	0.028	0.0677	0.0016	0.0538	0.003	0.048551	0.37341	416	18	423	10	C - Caledonian	-1.68269
31A-124 - 2.d	0.531	0.029	0.06863	0.0015	0.0561	0.003	0.1738	0.19202	433	19	427.8	9.2	C - Caledonian	1.200924
31A-125 - 1.d	0.527	0.029	0.06922	0.0015	0.0564	0.0032	-0.09965	0.40009	428	19	431.4	9.1	C - Caledonian	-0.79439
31A-125 - 2.d	0.521	0.03	0.0695	0.0016	0.0545	0.0031	0.1312	0.26524	423	20	433.1	9.9	C - Caledonian	-2.38771
31A-126 - 1.d	0.506	0.024	0.06795	0.0014	0.0544	0.0026	0.032869	0.35324	416	16	423.8	8.7	C - Caledonian	-1.875
31A-126 - 2.d	0.521	0.025	0.069	0.0016	0.054	0.0026	-0.00539	0.39083	425	17	430	9.6	C - Caledonian	-1.17647

Samantha Nicole March  
Ultrahigh-pressure metapelites in the WGR

31A-126 - 3.d	0.539	0.03	0.0687	0.0016	0.0568	0.0031	-0.00165	0.33243	438	19	428.1	9.6	C - Caledonian	2.260274
31A-127 - 1.d	0.525	0.029	0.068	0.0015	0.0563	0.0031	0.047038	0.31551	427	20	424	9.3	C - Caledonian	0.702576
31A-127 - 2.d	0.507	0.028	0.06693	0.0015	0.0555	0.003	0.16101	0.19896	417	18	417.6	9	C - Caledonian	-0.14388
31A-128 - 1.d	0.484	0.028	0.063	0.0015	0.0556	0.0031	-0.02624	0.35512	401	19	393.6	9.3	C - Caledonian	1.845387
31A-128 - 2.d	0.496	0.028	0.0646	0.0015	0.0561	0.003	0.17019	0.22569	409	19	403.5	9.3	C - Caledonian	1.344743
31A-129 - 1.d	0.537	0.026	0.06852	0.0014	0.0559	0.0026	0.2993	0.047012	437	17	427.8	8.5	C - Caledonian	2.105263
31A-129 - 2.d	0.507	0.025	0.0666	0.0016	0.055	0.0025	0.15033	0.38804	415	17	415.7	9.5	C - Caledonian	-0.16867
31A-130 - 1.d	0.609	0.033	0.074	0.0019	0.0609	0.0031	0.24716	0.18575	483	21	460.3	11	D - ellipse touching concordia	4.699793
31A-130 - 2.d	0.558	0.033	0.0702	0.0017	0.0579	0.0035	-0.06896	0.46175	448	21	437.4	11	C - Caledonian	2.366071
31A-130 - 3.d	0.561	0.031	0.0698	0.0016	0.0587	0.0031	0.14061	0.24785	450	20	434.7	9.9	C - Caledonian	3.4
31A-131 - 1.d	0.532	0.029	0.0691	0.0016	0.0563	0.0031	-0.13513	0.46261	433	19	430.6	9.8	C - Caledonian	0.554273
31A-131 - 2.d	0.536	0.031	0.0686	0.0018	0.0557	0.0034	0.082244	0.39184	434	21	427.8	11	C - Caledonian	1.428571
31A-132 - 1.d	0.592	0.03	0.0722	0.0017	0.0585	0.0029	0.1946	0.21906	471	19	449.3	10	C - Caledonian	4.607219
31A-132 - 2.d	0.525	0.027	0.0692	0.0016	0.0542	0.0026	0.21541	0.15547	427	18	431.3	9.4	C - Caledonian	-1.00703
31A-132 - 3.d	0.544	0.025	0.0707	0.0016	0.056	0.0024	0.2429	0.30943	440.2	16	440.3	9.5	C - Caledonian	-0.02272
31A-133 - 1.d	0.529	0.027	0.0686	0.0016	0.0553	0.0029	-0.16303	0.5463	432	18	427.7	9.6	C - Caledonian	0.99537
31A-133 - 2.d	0.491	0.025	0.0665	0.0016	0.0535	0.0026	0.22764	0.22511	404	17	414.7	9.9	C - Caledonian	-2.64851
31A-134 - 1.d	0.521	0.029	0.069	0.0016	0.0537	0.0028	0.19293	0.18074	426	20	430.1	9.5	C - Caledonian	-0.96244
31A-134 - 2.d	0.511	0.03	0.068	0.0016	0.0544	0.0031	0.36401	-0.00187	420	21	424	9.5	C - Caledonian	-0.95238
31A-135 - 1.d	1.587	0.074	0.1573	0.0036	0.0731	0.0029	0.63072	-0.03307	962	29	941	20	C - Sveconorwegian	2.182952
31A-135 - 2.d	0.733	0.039	0.0875	0.0021	0.061	0.003	0.18576	0.23319	557	22	540.4	12	D	2.980251
31A-136 - 1.d	0.521	0.029	0.0696	0.0016	0.0538	0.0029	0.11984	0.30507	424	20	433.7	9.7	C - Caledonian	-2.28774
31A-136 - 2.d	0.542	0.028	0.07	0.0016	0.0558	0.0029	-0.05384	0.422	442	19	436.3	9.6	C - Caledonian	1.289593
31A-136 - 3.d	0.527	0.029	0.06796	0.0015	0.0557	0.003	0.047811	0.26315	430	20	424.7	9.1	C - Caledonian	1.232558
31A-137 - 1.d	0.532	0.027	0.0683	0.0015	0.0557	0.0026	0.19934	0.24665	432	18	425.9	9	C - Caledonian	1.412037
31A-137 - 2.d	0.538	0.026	0.0675	0.0016	0.0576	0.0027	0.13141	0.44797	436	17	420.9	9.5	C - Caledonian	3.463303
31A-138 - 1.d	1.49	0.075	0.1492	0.0052	0.0727	0.0029	0.7776	0.18919	923	30	895	29	D	3.033586
31A-138 - 2.d	1.113	0.051	0.1147	0.0028	0.0701	0.0029	0.5054	0.32934	758	25	700	16	D	7.651715
31A-139 - 1.d	0.525	0.033	0.0695	0.0016	0.0555	0.0033	0.24939	0.048923	431	23	433.1	9.9	C - Caledonian	-0.48724
31A-139 - 2.d	0.518	0.029	0.0685	0.0016	0.0545	0.0032	0.070997	0.26709	426	19	427.2	9.5	C - Caledonian	-0.28169

Samantha Nicole March  
Ultrahigh-pressure metapelites in the WGR

31A-140 - 1.d	0.524	0.028	0.0684	0.0016	0.0553	0.0031	-0.03028	0.35727	430	17	426.2	9.8	C - Caledonian	0.883721
31A-140 - 2.d	0.53	0.029	0.0673	0.0015	0.0575	0.0034	-0.13178	0.56717	435	21	419.9	9.4	C - Caledonian	3.471264
31A-141 - 1.d	0.535	0.031	0.0689	0.0016	0.056	0.003	0.20026	0.16571	439	19	429.3	9.7	C - Caledonian	2.209567
31A-141 - 2.d	0.516	0.026	0.0685	0.0016	0.055	0.0027	0.044419	0.34219	423	18	427.3	9.7	C - Caledonian	-1.01655
31A-142 - 1.d	0.526	0.033	0.0703	0.0017	0.0536	0.0032	0.1157	0.26191	426	22	438	10	C - Caledonian	-2.8169
31A-142 - 2.d	0.515	0.026	0.0682	0.0016	0.0544	0.0028	-0.00987	0.40645	422	18	425	9.5	C - Caledonian	-0.7109
31A-143 - 1.d	0.516	0.028	0.0683	0.0016	0.0547	0.0031	-0.27351	0.56075	421	19	425.6	9.8	C - Caledonian	-1.09264
31A-143 - 2.d	0.516	0.031	0.0655	0.0016	0.0565	0.0035	-0.14549	0.47326	420	21	409	9.7	C - Caledonian	2.619048
31A-144 - 1.d	0.547	0.03	0.0699	0.0017	0.0569	0.0032	0.072424	0.31626	441	20	435.6	10	C - Caledonian	1.22449
31A-144 - 2.d	0.533	0.03	0.069	0.0016	0.0551	0.0031	0.08948	0.22347	432	20	430.2	9.7	C - Caledonian	0.416667
31A-145 - 1.d	0.525	0.024	0.0689	0.0014	0.0553	0.0025	-0.01361	0.37732	427.8	16	429.5	8.7	C - Caledonian	-0.39738
31A-146 - 1.d	1.86	0.13	0.1769	0.009	0.0765	0.0032	0.88626	-0.04866	1060	45	1047	50	C - Sveconorwegian	1.226415
31A-146 - 2.d	0.618	0.038	0.0764	0.0017	0.0579	0.0033	0.2065	0.10078	488	24	474.6	10	D - ellipse touching eonecordia	2.745902
31A-147 - 1.d	0.967	0.056	0.1072	0.0036	0.0652	0.0029	0.79377	-0.32024	683	29	656	21	D	3.953148
31A-147 - 2.d	0.528	0.027	0.0691	0.0015	0.0555	0.0029	0.068693	0.32955	431	18	430.7	9.3	C - Caledonian	0.069606
31A-148 - 1.d	1.129	0.054	0.1123	0.0026	0.0721	0.003	0.68541	-0.17386	767	27	686	15	D	10.56063
31A-148 - 2.d	0.563	0.028	0.0695	0.0017	0.0584	0.0028	0.11004	0.34729	452	19	433.3	10	C - Caledonian	4.137168
31A-149 - 1.d	5.67	0.26	0.2664	0.0064	0.1543	0.0063	0.53864	0.23534	1926	39	1522	33	D	20.97612
31A-149 - 2.d	3.83	0.18	0.2052	0.0055	0.1344	0.0051	0.73345	0.032505	1598	36	1206	30	D	24.53066
31A-150 - 1.d	0.53	0.028	0.0687	0.0016	0.0569	0.0031	0.093396	0.27483	431	19	428.3	9.5	C - Caledonian	0.62645
31A-150 - 2.d	0.525	0.029	0.0695	0.0017	0.055	0.0029	0.1853	0.1998	429	19	433	10	C - Caledonian	-0.9324
31A-151 - 1.d	0.651	0.034	0.0782	0.0022	0.06	0.0027	0.54001	0.069401	507	21	485	13	D	4.33925
31A-151 - 2.d	0.535	0.033	0.0692	0.0017	0.0554	0.0034	0.08635	0.23148	433	22	431	10	C - Caledonian	0.461894
31A-152 - 1.d	0.684	0.045	0.0802	0.0031	0.0621	0.0031	0.71512	-0.04855	525	27	497	19	D	5.333333
31A-152 - 2.d	0.551	0.032	0.0731	0.002	0.0552	0.0031	0.30469	0.17701	446	21	455	12	D - ellipse touching eonecordia	-2.01794
31A-152 - 3.d	0.529	0.031	0.0695	0.0017	0.0553	0.0032	0.066032	0.3081	431	20	432.9	10	C - Caledonian	-0.44084
31A-153 - 1.d	0.569	0.031	0.0691	0.0016	0.0593	0.0031	0.045928	0.33937	457	20	430.6	9.4	C - Caledonian	5.776805
31A-153 - 2.d	0.535	0.028	0.06791	0.0015	0.0569	0.003	-0.13313	0.47428	434	19	423.5	9.2	C - Caledonian	2.419355
31A-154 - 1.d	0.511	0.026	0.0661	0.0016	0.056	0.003	-0.05267	0.5002	418	17	412.3	9.9	C - Caledonian	1.363636

Samantha Nicole March  
Ultrahigh-pressure metapelites in the WGR

31A-154 - 2.d	0.502	0.027	0.06713	0.0014	0.0537	0.0026	0.062387	0.29441	413	18	418.8	8.6	C - Caledonian	-1.40436
31A-155 - 1.d	0.526	0.024	0.0669	0.0015	0.0555	0.0025	-0.13873	0.47031	428	16	417.5	9	C - Caledonian	2.453271
31A-155 - 2.d	0.532	0.024	0.06791	0.0015	0.0561	0.0026	-0.12928	0.53285	432.1	16	423.5	9.1	C - Caledonian	1.99028
<del>31A-156 - 1.d</del>	<del>1.356</del>	<del>0.071</del>	<del>0.1193</del>	<del>0.0035</del>	<del>0.0814</del>	<del>0.0035</del>	<del>0.74429</del>	<del>-0.23974</del>	<del>870</del>	<del>31</del>	<del>728</del>	<del>20</del>	<del>D</del>	<del>16.32184</del>
31A-156 - 2.d	0.64	0.031	0.0772	0.0017	0.0596	0.0027	0.28335	0.17845	501	19	479.2	10	D—ellipse touching eonecordia	4.351297
31A-156 - 3.d	0.611	0.031	0.0745	0.0018	0.0593	0.0028	0.24674	0.24239	483	19	463.1	11	D—ellipse touching eonecordia	4.120083
31A-158 - 1.d	0.579	0.031	0.0721	0.0017	0.0569	0.0031	-0.0208	0.35262	464	20	448.5	10	C - Caledonian	3.340517
31A-158 - 2.d	0.65	0.038	0.0806	0.0018	0.0572	0.0031	0.26089	0.12353	505	24	499.5	11	D—ellipse touching eonecordia	1.089109
31A-159 - 1.d	0.514	0.026	0.06929	0.0015	0.0547	0.0029	-0.04785	0.39675	420	17	431.9	9.2	C - Caledonian	-2.83333
31A-159 - 2.d	0.515	0.026	0.06985	0.0015	0.0532	0.0028	-0.11712	0.44026	422	17	435.2	8.9	C - Caledonian	-3.12796
31A-160 - 1.d	1.185	0.062	0.1246	0.0038	0.068	0.0029	0.65922	-0.00543	796	29	757	22	D	4.899497
31A-160 - 2.d	0.583	0.029	0.0747	0.0019	0.0565	0.0026	0.20516	0.30586	467	18	464.4	11	D—ellipse touching eonecordia	0.556745
31A-161 - 1.d	0.518	0.035	0.0687	0.0019	0.0541	0.0038	-0.054	0.4037	423	24	428.1	11	C - Caledonian	-1.20567
31A-161 - 2.d	0.521	0.036	0.0702	0.0016	0.0554	0.0036	0.050845	0.20603	428	25	437.4	9.8	C - Caledonian	-2.19626
31A-162 - 1.d	0.736	0.035	0.085	0.0021	0.0625	0.0028	0.32584	0.17566	559	21	526.1	12	D	5.88551
31A-163 - 1.d	0.531	0.032	0.0681	0.0016	0.056	0.0032	0.20831	0.15006	435	21	425.5	9.8	C - Caledonian	2.183908
31A-164 - 1.d	0.487	0.027	0.0669	0.0016	0.0531	0.0029	0.17892	0.21887	404	19	417.6	9.5	C - Caledonian	-3.36634
31A-164 - 2.d	0.533	0.032	0.0676	0.0016	0.0582	0.0036	0.005276	0.33656	436	22	421.6	9.4	C - Caledonian	3.302752
31A-164 - 3.d	0.551	0.031	0.0692	0.0017	0.0584	0.0034	0.079965	0.30978	444	20	431.2	10	C - Caledonian	2.882883
31A-165 - 1.d	0.717	0.041	0.0839	0.002	0.0622	0.0034	0.032583	0.38431	546	24	519.5	12	D	4.85348
31A-165 - 2.d	0.538	0.031	0.0686	0.0016	0.0571	0.0032	-0.08402	0.39134	435	20	427.7	9.8	C - Caledonian	1.678161
31A-166 - 1.d	0.517	0.028	0.0687	0.0016	0.0548	0.0028	0.21198	0.1848	425	18	428.2	9.5	C - Caledonian	-0.75294
31A-167 - 1.d	0.518	0.027	0.0682	0.0015	0.0551	0.0027	0.2765	0.13734	424	18	425.5	9.3	C - Caledonian	-0.35377
31A-167 - 2.d	0.51	0.027	0.066	0.0015	0.0556	0.0029	0.099234	0.25119	419	18	412.1	9.1	C - Caledonian	1.646778
31A-168 - 1.d	0.592	0.04	0.0766	0.0028	0.056	0.0032	0.66639	0.012106	468	25	475	17	D—ellipse touching eonecordia	-1.49573
31A-168 - 2.d	0.522	0.03	0.0678	0.0016	0.0551	0.003	0.29788	0.15292	424	20	422.8	9.9	C - Caledonian	0.283019
31A-169 - 1.d	0.517	0.026	0.06642	0.0015	0.0563	0.0028	0.091633	0.28095	422	18	414.5	8.9	C - Caledonian	1.777251

Samantha Nicole March  
Ultrahigh-pressure metapelites in the WGR

<b>31A-169 - 2.d</b>	0.518	0.025	0.06584	0.0015	0.0577	0.0028	-0.07507	0.43655	423	17	411.7	8.8	C - Caledonian	2.671395
<del><b>31A-170 - 1.d</b></del>	<del>0.592</del>	<del>0.033</del>	<del>0.071</del>	<del>0.0019</del>	<del>0.06</del>	<del>0.0033</del>	<del>0.16871</del>	<del>0.30759</del>	476	21	442.2	12	D	7.10084
<b>31A-170 - 2.d</b>	0.548	0.026	0.0695	0.0016	0.0569	0.0024	0.48318	0.15131	445	17	432.8	9.7	C - Caledonian	2.741573

~~Crossed out~~ = discordant, C = concordant, NC = near concordant, D = discordant, RD = reversely discordant.

### WGC2019J-31A zircon geochronology standards

Standard	Type	207/235	2 $\sigma$	206/238	2 $\sigma$	207/206	2 $\sigma$	ErrCorr 6/38vs7/35	ErrorCorr 8/6vs7/6	207/235 age	2 $\sigma$	206/238	2 $\sigma$	Concordant?
GJ - 1.d	Primary	0.87	0.047	0.0993	0.0024	0.0633	0.0035	-0.10222	0.46702	635	25	609.9	14	C
GJ - 2.d	Primary	0.836	0.044	0.099	0.0022	0.061	0.0031	0.069843	0.32519	615	25	608.3	13	C
GJ - 3.d	Primary	0.844	0.049	0.0978	0.0023	0.062	0.0033	0.21295	0.19355	620	26	601.5	13	C
GJ - 4.d	Primary	0.805	0.043	0.0994	0.0025	0.0578	0.0031	-0.0029025	0.39743	597	24	611	14	C
GJ - 5.d	Primary	0.812	0.047	0.0971	0.0022	0.0597	0.0035	0.20931	0.17202	602	27	597.1	13	C
GJ - 6.d	Primary	0.823	0.047	0.0983	0.0022	0.0601	0.0032	0.1279	0.21928	606	26	604.4	13	C
GJ - 7.d	Primary	0.833	0.045	0.0983	0.0023	0.0619	0.0032	0.24369	0.18632	615	24	604.1	13	C
GJ - 8.d	Primary	0.811	0.046	0.0984	0.0023	0.06	0.0034	0.037796	0.32182	603	25	604.7	14	C
GJ - 9.d	Primary	0.806	0.044	0.0985	0.0024	0.0595	0.003	0.19398	0.18295	602	25	605.6	14	C
GJ - 10.d	Primary	0.785	0.044	0.0975	0.0023	0.0579	0.0034	-0.073251	0.40869	586	25	599.4	14	C
GJ - 11.d	Primary	0.807	0.044	0.0972	0.0024	0.0598	0.0031	0.043577	0.37326	600	25	598	14	C
GJ - 12.d	Primary	0.853	0.048	0.0986	0.0023	0.0619	0.0033	0.17883	0.27398	623	26	606.3	14	C
GJ - 13.d	Primary	0.8	0.044	0.0974	0.0021	0.0588	0.0031	0.19722	0.18578	594	25	599.1	12	C
GJ - 14.d	Primary	0.76	0.045	0.0957	0.0023	0.0584	0.0033	0.11013	0.24448	579	26	589	13	C
GJ - 15.d	Primary	0.824	0.05	0.0972	0.0023	0.0612	0.0038	0.0097138	0.2991	612	27	597.6	13	C
GJ - 16.d	Primary	0.809	0.049	0.0978	0.0024	0.0601	0.0039	-0.17937	0.54839	597	28	601	14	C
GJ - 17.d	Primary	0.803	0.041	0.0971	0.0021	0.0593	0.003	0.11732	0.21835	596	23	597.1	12	C
GJ - 18.d	Primary	0.808	0.045	0.0974	0.0023	0.0604	0.0034	0.17717	0.19817	598	26	599.3	14	C
GJ - 19.d	Primary	0.817	0.044	0.0952	0.0022	0.0606	0.0034	0.009745	0.40589	604	25	586.2	13	C
GJ - 20.d	Primary	0.824	0.045	0.0985	0.0023	0.0606	0.0034	0.042158	0.39978	607	26	605.8	14	C
GJ - 21.d	Primary	0.824	0.046	0.098	0.0024	0.0605	0.0033	0.22052	0.14998	607	26	602	14	C
GJ - 22.d	Primary	0.785	0.045	0.0982	0.0025	0.0581	0.0034	-0.0018249	0.38081	588	26	604	15	C

Samantha Nicole March  
Ultrahigh-pressure metapelites in the WGR

<b>GJ - 23.d</b>	Primary	0.838	0.046	0.0987	0.0024	0.0618	0.0033	0.12666	0.22477	615	26	606.6	14	C
<b>GJ - 24.d</b>	Primary	0.779	0.043	0.0988	0.0024	0.058	0.0032	0.057941	0.39696	587	24	607.3	14	C
<b>GJ - 25.d</b>	Primary	0.819	0.042	0.0981	0.0024	0.0603	0.0032	-0.15759	0.5604	610	23	603	14	C
<b>GJ - 26.d</b>	Primary	0.802	0.045	0.0996	0.0024	0.0581	0.0033	-0.013642	0.35697	603	25	611.8	14	C
<b>GJ - 27.d</b>	Primary	0.794	0.048	0.0981	0.0024	0.0595	0.0036	0.1105	0.23372	596	27	603.2	14	C
<b>GJ - 28.d</b>	Primary	0.793	0.043	0.0973	0.0023	0.0585	0.0032	0.13285	0.21804	593	24	598.2	14	C
<b>GJ - 29.d</b>	Primary	0.812	0.045	0.0978	0.0025	0.0598	0.0034	0.039788	0.39313	606	27	601	14	C
<b>GJ - 30.d</b>	Primary	0.829	0.046	0.0975	0.0025	0.0612	0.0032	0.21971	0.26223	610	26	601	14	C
<b>GJ - 31.d</b>	Primary	0.825	0.044	0.0966	0.0023	0.063	0.0032	0.20137	0.19239	618	26	594.5	13	C
<b>GJ - 32.d</b>	Primary	0.826	0.049	0.0989	0.0023	0.0612	0.0034	0.067779	0.28007	611	26	608.1	14	C
<b>GJ - 33.d</b>	Primary	0.847	0.046	0.0986	0.0024	0.0617	0.0035	-0.096174	0.45218	622	26	606.1	14	C
<b>GJ - 34.d</b>	Primary	0.821	0.043	0.097	0.0023	0.0603	0.0031	0.083711	0.30996	608	24	596.9	14	C
<b>GJ - 35.d</b>	Primary	0.791	0.043	0.0957	0.0024	0.0593	0.0033	-0.16318	0.52746	589	24	589	14	C
<b>GJ - 36.d</b>	Primary	0.833	0.046	0.0983	0.0025	0.061	0.0033	0.2093	0.25564	612	26	604	15	C
<b>GJ - 37.d</b>	Primary	0.769	0.047	0.0973	0.0023	0.0566	0.0034	0.059232	0.21187	581	26	598.7	13	C
<b>GJ - 38.d</b>	Primary	0.814	0.039	0.0971	0.0025	0.0601	0.0028	0.163	0.32843	603	22	598	14	C
<b>GJ - 39.d</b>	Primary	0.799	0.047	0.0987	0.0022	0.0586	0.0034	-0.12628	0.40199	599	26	606.5	13	C
<b>GJ - 40.d</b>	Primary	0.841	0.047	0.0977	0.0025	0.0625	0.0036	-0.073296	0.48392	622	25	601	15	C
<b>GJ - 41.d</b>	Primary	0.801	0.047	0.0971	0.0023	0.0604	0.0033	0.26165	0.15643	597	27	597.1	14	C
<b>GJ - 42.d</b>	Primary	0.772	0.047	0.0985	0.0024	0.0573	0.0033	0.33101	0.083413	577	26	605	14	C
<b>GJ - 43.d</b>	Primary	0.825	0.045	0.0985	0.0023	0.0603	0.0032	0.24837	0.20201	608	25	605.6	14	C
<b>GJ - 44.d</b>	Primary	0.839	0.048	0.0985	0.0025	0.0612	0.0035	-0.053658	0.44439	615	26	606	15	C
<b>GJ - 45.d</b>	Primary	0.836	0.046	0.096	0.0023	0.0618	0.0034	-0.0483	0.41065	614	25	590.5	13	C
<b>GJ - 46.d</b>	Primary	0.852	0.051	0.0955	0.0024	0.0637	0.0037	0.17274	0.22451	627	29	589	14	C
<b>GJ - 47.d</b>	Primary	0.841	0.048	0.0999	0.0026	0.0619	0.0035	0.12941	0.27408	616	26	613	15	C
<b>GJ - 48.d</b>	Primary	0.815	0.048	0.0972	0.0023	0.06	0.0036	0.02387	0.36966	605	26	597.9	14	C
<b>GJ - 49.d</b>	Primary	0.814	0.043	0.097	0.0024	0.0607	0.0032	0.14431	0.24224	604	24	597	14	C
<b>GJ - 50.d</b>	Primary	0.781	0.045	0.0979	0.0022	0.0574	0.0032	0.16011	0.1724	586	26	601.7	13	C
<b>GJ - 51.d</b>	Primary	0.83	0.042	0.101	0.0023	0.0593	0.0029	-0.0066687	0.40132	618	23	620	14	C
<b>GJ - 52.d</b>	Primary	0.8	0.042	0.0995	0.0024	0.0583	0.003	-0.0078396	0.43912	595	23	611.3	14	C
<b>GJ - 53.d</b>	Primary	0.82	0.045	0.0968	0.0022	0.0618	0.0032	0.084614	0.28788	610	24	595.5	13	C

Samantha Nicole March  
Ultrahigh-pressure metapelites in the WGR

<b>GJ - 54.d</b>	Primary	0.856	0.047	0.0985	0.0022	0.0627	0.0034	0.16315	0.16281	627	26	605.6	13	C
<b>GJ - 55.d</b>	Primary	0.794	0.042	0.0986	0.0021	0.0582	0.003	0.031216	0.2965	593	23	606.1	12	C
<b>GJ - 56.d</b>	Primary	0.821	0.042	0.0965	0.0023	0.0615	0.0033	-0.0040528	0.36286	609	23	593.8	14	C
<b>Ples - 1.d</b>	Secondary	0.398	0.02	0.05504	0.0011	0.0517	0.0024	0.11346	0.26743	339.7	14	345.4	6.9	C
<b>Ples - 2.d</b>	Secondary	0.402	0.02	0.05447	0.0012	0.0537	0.0025	0.11756	0.33601	342.7	14	341.9	7.3	C
<b>Ples - 3.d</b>	Secondary	0.406	0.02	0.05393	0.0011	0.0544	0.0026	0.1394	0.20111	345.6	14	338.6	7	C
<b>Ples - 4.d</b>	Secondary	0.389	0.019	0.05324	0.0011	0.0534	0.0025	0.023048	0.30945	335.5	14	334.4	6.8	C
<b>Ples - 5.d</b>	Secondary	0.403	0.02	0.05398	0.0012	0.0548	0.0026	0.1161	0.31043	344.5	14	338.9	7.1	C
<b>Ples - 6.d</b>	Secondary	0.394	0.02	0.05333	0.0012	0.0529	0.0027	-0.0037622	0.35608	336.3	15	334.9	7.2	C
<b>Ples - 7.d</b>	Secondary	0.383	0.018	0.05406	0.0012	0.0511	0.0023	0.027716	0.37249	328.5	13	339.4	7.2	C
<b>Ples - 8.d</b>	Secondary	0.394	0.02	0.0538	0.0011	0.0532	0.0026	0.12746	0.27406	336.5	14	337.8	6.9	C
<b>Ples - 9.d</b>	Secondary	0.386	0.018	0.05269	0.0011	0.0524	0.0023	0.19845	0.17577	331.2	13	331	6.7	C
<b>Ples - 10.d</b>	Secondary	0.385	0.019	0.05376	0.0011	0.052	0.0024	0.26382	0.11429	330	14	337.5	7	C
<b>Ples - 11.d</b>	Secondary	0.386	0.02	0.05294	0.0011	0.0519	0.0024	0.24919	0.13767	330.5	14	332.5	7	C
<b>Ples - 12.d</b>	Secondary	0.372	0.021	0.05154	0.001	0.0508	0.0028	0.17819	0.11355	322	15	323.9	6.2	C
<b>Ples - 13.d</b>	Secondary	0.411	0.022	0.05486	0.0012	0.0537	0.0028	0.19137	0.25608	349	16	344.3	7.6	C
<b>Ples - 14.d</b>	Secondary	0.407	0.02	0.05415	0.0012	0.0544	0.0026	0.087338	0.3354	346.2	15	339.9	7.5	C
<b>Ples - 15.d</b>	Secondary	0.42	0.022	0.05526	0.0013	0.0556	0.0029	-0.078666	0.43044	355	15	346.7	8	C
<b>Ples - 16.d</b>	Secondary	0.389	0.019	0.05368	0.0011	0.0527	0.0024	0.1376	0.27502	334.3	14	337	7	C
<b>Ples - 17.d</b>	Secondary	0.399	0.019	0.05437	0.0012	0.0532	0.0025	0.09412	0.30232	341.7	14	341.3	7.4	C
<b>Ples - 18.d</b>	Secondary	0.396	0.019	0.05534	0.0011	0.0516	0.0024	0.19572	0.22728	337.8	14	347.2	7	C
<b>Ples - 19.d</b>	Secondary	0.387	0.019	0.05321	0.0011	0.0525	0.0024	0.13877	0.22121	333.1	13	334.2	6.5	C
<b>Ples - 20.d</b>	Secondary	0.4	0.022	0.05278	0.0013	0.0553	0.003	0.15185	0.32655	342	15	331.5	7.9	C
<b>Ples - 21.d</b>	Secondary	0.412	0.022	0.0537	0.0013	0.0554	0.0028	0.10715	0.32003	351	16	337.2	8	C
<b>Ples - 22.d</b>	Secondary	0.418	0.023	0.05427	0.0012	0.0557	0.0028	0.24799	0.17561	358	17	340.6	7.1	C
<b>Ples - 23.d</b>	Secondary	0.407	0.023	0.05448	0.0013	0.0533	0.003	0.037863	0.34776	345	17	342	7.8	C
<b>Ples - 24.d</b>	Secondary	0.403	0.022	0.05371	0.0013	0.0536	0.0029	-0.068238	0.44255	343	16	337.2	8	C
<b>Ples - 25.d</b>	Secondary	0.407	0.023	0.0546	0.0013	0.054	0.0031	0.020747	0.43593	348	16	342.7	8.1	C
<b>Ples - 26.d</b>	Secondary	0.393	0.022	0.0527	0.0013	0.0543	0.0031	-0.070016	0.41357	335	16	331.1	7.8	C
<b>Ples - 27.d</b>	Secondary	0.386	0.02	0.0533	0.0012	0.0523	0.0026	0.079296	0.34963	331.9	14	334.7	7.5	C
<b>Ples - 28.d</b>	Secondary	0.419	0.023	0.0542	0.0012	0.0545	0.003	0.11647	0.25066	354	17	340.2	7.5	C



Samantha Nicole March  
Ultrahigh-pressure metapelites in the WGR

<b>Ples - 29.d</b>	Secondary	0.409	0.018	0.05542	0.0012	0.0528	0.0023	0.29395	0.1785	347.7	13	347.7	7.4	C
<b>Ples - 30.d</b>	Secondary	0.583	0.032	0.055	0.0015	0.0761	0.0042	0.27295	0.40387	464	21	345.2	9	D
<b>Ples - 31.d</b>	Secondary	0.464	0.024	0.05519	0.0013	0.0608	0.0033	-0.042566	0.47251	386	17	346.3	7.7	D
<b>Ples - 32.d</b>	Secondary	0.426	0.021	0.05392	0.0011	0.0572	0.0028	0.032263	0.25631	362	15	338.5	6.8	D
<b>Ples - 33.d</b>	Secondary	0.405	0.018	0.05471	0.0012	0.053	0.0024	-0.16998	0.48852	344.8	13	343.3	7	C
<b>Ples - 34.d</b>	Secondary	0.396	0.021	0.05433	0.0012	0.0528	0.0027	-0.039162	0.35761	339	15	341	7.5	C
<b>Ples - 35.d</b>	Secondary	0.394	0.021	0.05495	0.0012	0.052	0.0027	-0.015028	0.41094	338	15	344.8	7.4	C
<b>Ples - 36.d</b>	Secondary	0.437	0.023	0.05472	0.0012	0.0568	0.0031	-0.039771	0.36439	367	16	343.4	7.6	C
<b>Ples - 37.d</b>	Secondary	0.418	0.018	0.05396	0.0011	0.0556	0.0023	0.097999	0.3578	355.2	14	338.7	6.7	C
<b>Ples - 38.d</b>	Secondary	0.408	0.019	0.05433	0.001	0.0541	0.0024	0.18156	0.14224	347.1	14	341	6.4	C
<b>Ples - 39.d</b>	Secondary	0.401	0.021	0.05187	0.0011	0.0564	0.0028	0.3273	0.065303	341	16	326	6.9	C
<b>Ples - 40.d</b>	Secondary	0.409	0.019	0.05435	0.0011	0.0539	0.0024	-0.014265	0.39516	348.8	14	341.1	6.7	C
<b>91500 - 1.d</b>	Secondary	1.859	0.12	0.1789	0.0054	0.076	0.0048	0.12423	0.38296	1066	41	1060	29	C
<b>91500 - 2.d</b>	Secondary	1.796	0.11	0.1762	0.0051	0.0722	0.0048	-0.017937	0.36592	1044	42	1052	29	C
<b>91500 - 3.d</b>	Secondary	1.76	0.12	0.1733	0.0046	0.0744	0.0054	0.00034892	0.34248	1024	47	1030	25	C
<b>91500 - 4.d</b>	Secondary	1.94	0.14	0.1825	0.0059	0.0783	0.0061	0.017782	0.44551	1082	53	1083	31	C
<b>91500 - 5.d</b>	Secondary	1.84	0.13	0.1778	0.0051	0.0747	0.0048	0.31799	0.1207	1057	46	1057	29	C
<b>91500 - 6.d</b>	Secondary	1.77	0.14	0.179	0.0056	0.0724	0.0059	-0.091747	0.49984	1030	51	1060	31	C
<b>91500 - 7.d</b>	Secondary	1.77	0.16	0.1764	0.0062	0.0752	0.0065	0.18727	0.25458	1024	60	1050	33	C
<b>91500 - 8.d</b>	Secondary	1.78	0.15	0.1773	0.006	0.0716	0.0059	0.032504	0.2765	1032	52	1051	33	C
<b>91500 - 9.d</b>	Secondary	1.68	0.15	0.1766	0.0056	0.069	0.0063	0.096621	0.28936	1023	56	1047	30	C
<b>91500 - 10.d</b>	Secondary	1.83	0.13	0.182	0.005	0.0729	0.0052	0.21309	0.2005	1053	48	1077	27	C
<b>91500 - 11.d</b>	Secondary	1.76	0.13	0.1829	0.0053	0.07	0.005	0.18386	0.18088	1037	48	1085	29	C
<b>91500 - 12.d</b>	Secondary	1.71	0.14	0.1734	0.0067	0.0723	0.006	0.04017	0.51848	1034	50	1029	37	C
<b>91500 - 13.d</b>	Secondary	1.85	0.14	0.1796	0.0059	0.0747	0.0063	-0.11178	0.47118	1061	50	1064	32	C
<b>91500 - 14.d</b>	Secondary	1.9	0.13	0.1789	0.0051	0.0774	0.0053	0.08669	0.3882	1075	46	1064	29	C
<b>91500 - 15.d</b>	Secondary	1.77	0.15	0.1763	0.0057	0.0726	0.0059	0.21803	0.15814	1034	50	1046	31	C
<b>91500 - 16.d</b>	Secondary	1.743	0.12	0.177	0.0059	0.0734	0.0053	0.018321	0.39511	1028	44	1049	32	C
<b>91500 - 17.d</b>	Secondary	1.77	0.14	0.1754	0.0053	0.0733	0.006	0.14684	0.24624	1035	52	1041	29	C
<b>91500 - 18.d</b>	Secondary	1.78	0.14	0.1807	0.0055	0.0722	0.006	0.021595	0.34478	1041	51	1073	30	C
<b>91500 - 19.d</b>	Secondary	1.87	0.13	0.1727	0.0054	0.0808	0.006	-0.10781	0.48947	1058	46	1030	30	D

Samantha Nicole March  
Ultrahigh-pressure metapelites in the WGR

91500 - 20.d	Secondary	1.84	0.14	0.1807	0.0057	0.0745	0.0063	-0.13426	0.50755	1062	50	1070	31	C
91500 - 21.d	Secondary	1.87	0.14	0.1816	0.0055	0.0741	0.0056	0.00057159	0.41764	1067	49	1075	30	C
91500 - 22.d	Secondary	1.844	0.12	0.1745	0.0052	0.0756	0.005	0.029253	0.43994	1056	40	1036	29	C
91500 - 23.d	Secondary	1.83	0.13	0.1797	0.0053	0.074	0.0052	0.080822	0.3795	1048	47	1065	29	C
91500 - 24.d	Secondary	1.68	0.13	0.1772	0.0058	0.0688	0.0053	0.054396	0.33539	997	49	1050	32	C
91500 - 25.d	Secondary	1.89	0.13	0.1766	0.0055	0.0756	0.0051	0.19798	0.26449	1065	48	1048	30	C
91500 - 26.d	Secondary	1.73	0.12	0.1763	0.0055	0.0716	0.005	0.064505	0.24721	1023	49	1046	30	C
91500 - 27.d	Secondary	1.86	0.13	0.1778	0.0053	0.0762	0.0058	-0.045769	0.34947	1059	47	1057	29	C
91500 - 28.d	Secondary	1.695	0.11	0.179	0.0053	0.0665	0.004	0.28503	0.14377	1006	42	1061	29	D
91500 - 29.d	Secondary	1.73	0.13	0.1784	0.0063	0.0708	0.0057	0.017395	0.4033	1027	50	1061	35	C
91500 - 30.d	Secondary	1.81	0.13	0.1833	0.0054	0.0723	0.0054	0.042876	0.38431	1062	49	1084	29	C
91500 - 31.d	Secondary	1.87	0.14	0.1812	0.0051	0.0731	0.0055	0.18279	0.33017	1062	50	1073	28	C
91500 - 32.d	Secondary	1.838	0.12	0.1786	0.0054	0.0742	0.0048	0.17436	0.33415	1058	41	1059	29	C
91500 - 33.d	Secondary	1.96	0.12	0.1768	0.0053	0.0796	0.0049	0.23508	0.25412	1096	43	1052	28	C
91500 - 34.d	Secondary	1.749	0.12	0.1745	0.0055	0.0723	0.0052	0.064847	0.34362	1015	44	1039	30	C
91500 - 35.d	Secondary	1.85	0.13	0.1769	0.0048	0.0742	0.0053	-0.027781	0.35429	1056	45	1050	26	C
91500 - 36.d	Secondary	1.91	0.14	0.1816	0.0057	0.0749	0.0056	0.057211	0.37311	1084	50	1075	31	C
91500 - 37.d	Secondary	1.93	0.13	0.1831	0.0056	0.0762	0.0052	0.11658	0.34719	1086	45	1086	31	C
91500 - 38.d	Secondary	1.8	0.14	0.1851	0.0062	0.0709	0.0055	0.18996	0.25411	1048	51	1093	34	C
91500 - 39.d	Secondary	1.94	0.13	0.1811	0.0051	0.0752	0.0049	0.13029	0.29129	1092	47	1072	28	C
91500 - 40.d	Secondary	1.95	0.13	0.1788	0.0056	0.0785	0.0056	-0.087073	0.49358	1104	46	1060	31	C

~~Crossed out~~ = discordant, C = concordant, NC = near concordant, D = discordant, RD = reversely discordant

### WGC2019J-25B zircon trace elements

Sample	Chondrite normalised REEs + Y																
	La	Ce	Pr	Nd	Sm	Eu	Gd	Tb	Dy	Y	Ho	Er	Tm	Yb	Lu	Total HREEs	Eu anomaly
WGC-25B-3 - 1.d	0	5.02447	0	0	3.378378	4.795737	18.19095	22.43767	27.56098	48.7	27.10623	29.1875	29.19028	30.24845	30.4878	244.9189	0.611749
WGC-25B-3 - 2.d	0	5.285481	0	0	0	4.795737	13.31658	22.16066	21.66667	39.6	22.34432	25.1875	25.50607	18.75776	26.01626	201.2393	#DIV/0!
WGC-25B-4 - 1.d	0	0.831974	0	0	0	2.895204	3.366834	4.32133	8.211382	23.6	9.89011	15.5	15.82996	34.16149	45.93496	157.4492	#DIV/0!

Samantha Nicole March  
Ultrahigh-pressure metapelites in the WGR

<b>WGC-25B-4-2.d</b>	0.080169	4.763458	0.991379	2.472648	1.891892	4.795737	8.040201	12.18837	14.02439	32.3	11.35531	15.4375	17.40891	16.89441	21.13821	140.7471	1.229628
<b>WGC-25B-4-3.d</b>	0	1.092985	0	0	0.945946	0.568384	4.572864	6.648199	9.186992	32.8	8.058608	10.3125	16.19433	22.98137	36.17886	142.3609	0.273284
<b>WGC-25B-5-1.d</b>	0	2.349103	0	0	0	0.79929	8.140704	7.617729	12.47967	24.1	13.91941	12.625	9.757085	11.0559	8.699187	100.254	#DIV/0!
<b>WGC-25B-5-2.d</b>	0	1.517129	0	0	0	1.829485	6.934673	11.96676	12.11382	16.2	14.46886	17.875	14.49393	22.73292	34.95935	144.8106	#DIV/0!
<b>WGC-25B-5-3.d</b>	0	2.218597	0	0	0	4.174067	9.698492	12.46537	13.53659	25.6	13.91941	11.4375	9.311741	13.6646	10.28455	110.2198	#DIV/0!
<b>WGC-25B-6-1.d</b>	0	3.099511	0	0	0.878378	5.683837	10.15075	15.51247	19.7561	36.7	20.51282	24.375	23.07692	27.51553	38.61789	206.0667	1.903494
<b>WGC-25B-6-2.d</b>	0	3.017945	0	0	0	0.71048	5.979899	7.423823	13.82114	26.7	11.72161	14.125	16.76113	17.20497	18.69919	126.4569	#DIV/0!
<b>WGC-25B-7-1.d</b>	0.902954	7.161501	7.650862	14.44201	29.7973	17.22913	18.24121	12.74238	14.39024	25.6	11.17216	10.6875	11.33603	8.136646	11.66667	105.7316	0.739006
<b>WGC-25B-7-2.d</b>	0.582278	5.106036	6.465517	11.33479	19.12162	11.90053	8.743719	8.199446	6.829268	38.4	7.289377	8.1875	8.299595	8.63354	13.41463	99.25336	0.920356
<b>WGC-25B-7-3.d</b>	0	2.69168	0	0	0.743243	2.344583	5.628141	6.952909	9.02439	23.8	8.260073	8.0625	4.129555	6.397516	7.195122	73.82206	1.146351
<b>WGC-25B-8-1.d</b>	0	4.013051	0	0	0.810811	5.150977	13.41709	13.10249	17.23577	22.7	17.21612	15.8125	15.82996	18.26087	14.10569	134.2634	1.561711
<b>WGC-25B-8-2.d</b>	0	3.60522	0	0	1.081081	4.973357	10.90452	15.23546	15.89431	17.3	16.11722	16.875	14.21053	17.70186	15.56911	128.9035	1.448496
<b>WGC-25B-10-1.d</b>	0.708861	6.182708	3.340517	4.573304	9.797297	9.946714	12.36181	14.95845	16.66667	17.76	13.91941	12.8125	16.07287	16.08696	14.43089	122.7078	0.903827
<b>WGC-25B-10-2.d</b>	0	1.239804	0	0	0	0.959147	4.924623	6.426593	7.235772	32.4	8.424908	6.5	7.449393	27.32919	35.77236	131.5382	#DIV/0!
<b>WGC-25B-11-1.d</b>	0	1.500816	0	0	0.540541	0	4.522613	4.875346	8.089431	31.7	7.545788	8.625	6.153846	3.78882	4.918699	75.69693	0
<b>WGC-25B-11-2.d</b>	0.637131	5.122349	3.103448	5.317287	8.716216	8.525755	14.77387	18.55956	26.01626	46.6	37.91209	54.375	45.74899	67.08075	85.77236	382.065	0.751314
<b>WGC-25B-11-3.d</b>	0	3.915171	0	0	1.148649	4.973357	7.487437	14.12742	12.88618	27.7	11.17216	11.5625	9.878543	11.24224	10.81301	109.3821	1.695858
<b>WGC-25B-12-1.d</b>	0	2.23491	0	0	0.540541	4.085258	11.65829	24.65374	28.61789	15.2	30.21978	27.6875	21.05263	27.63975	26.01626	201.0875	1.627376
<b>WGC-25B-13-1.d</b>	0	1.615008	0	0	0.243243	3.410302	10.45226	15.23546	21.78862	13.9	18.86447	19.8125	15.87045	19.62733	10.85366	135.9525	2.138786
<b>WGC-25B-13-2.d</b>	0	1.288744	0	0	3.243243	4.973357	20.40201	16.6205	13.69919	63.1	11.90476	16.0625	12.79352	13.6646	13.65854	161.5036	0.611397
<b>WGC-25B-14-1.d</b>	0	2.006525	0	0	2.22973	3.357016	15.17588	22.16066	25	22.4	29.67033	28.3125	24.69636	25.59006	20.3252	198.1551	0.577099
<b>WGC-25B-15-1.d</b>	0	1.712887	0	0.525164	7.635135	0	32.66332	60.66482	115.8537	41.1	209.707	391.25	716.5992	1270.807	1869.919	4675.901	0
<b>WGC-25B-15-2.d</b>	0.177215	1.598695	0	0	1.283784	2.326821	13.8191	26.5928	61.38211	227	116.3004	235	392.7126	757.764	1150.407	2967.158	0.55243
<b>WGC-25B-16-1.d</b>	0	1.82708	0	0	5.608108	8.703375	25.17588	39.61219	55.28455	50.4	58.79121	59.75	54.65587	53.72671	54.87805	427.0986	0.732465
<b>WGC-25B-16-2.d</b>	0	1.729201	0	0	1.081081	1.332149	10.60302	15.23546	20.97561	37.9	23.07692	23.75	18.21862	28.19876	27.64228	194.9976	0.393468
<b>WGC-25B-17-1.d</b>	0	1.141925	0	0	0	0	0.552764	3.98892	7.235772	27	10.07326	10.5625	11.09312	10.93168	12.27642	93.16167	#DIV/0!
<b>WGC-25B-17-2.d</b>	0	2.773246	0	0	0	1.580817	7.135678	9.695291	12.19512	47.8	10.07326	11.375	9.635628	11.0559	10.69106	122.5213	#DIV/0!
<b>WGC-25B-18-1.d</b>	0	2.920065	0	0	1.756757	4.440497	9.346734	9.66759	11.50407	370	11.17216	11.875	11.53846	9.31677	13.65854	448.7326	1.095837
<b>WGC-25B-18-2.d</b>	0	3.425775	0	0	3.108108	3.907638	12.51256	21.88366	21.09756	206	23.26007	22.8125	21.86235	22.79503	21.95122	361.6624	0.626604
<b>WGC-25B-19-1.d</b>	0	1.810767	0	0	2.027027	3.978686	7.085427	14.95845	24.02439	109.6	24.90842	27.1875	26.31579	24.96894	21.13821	273.1017	1.049849
<b>WGC-25B-19-2.d</b>	0	1.843393	0	0	0	3.161634	12.21106	17.72853	23.53659	41	26.37363	27.3125	27.53036	26.70807	32.92683	223.1165	#DIV/0!

Samantha Nicole March  
Ultrahigh-pressure metapelites in the WGR

<b>WGC-25B-20 - 1.d</b>	0.291139	5.057096	1.142241	2.100656	4.391892	6.039076	9.899497	14.40443	15.52846	19.73	17.39927	22.5	20.24291	27.76398	35.77236	173.3414	0.915879
<b>WGC-25B-20 - 2.d</b>	0	3.556281	0	0	0	1.918295	9.447236	11.08033	14.63415	19.8	12.08791	11.1875	9.271255	11.61491	13.13008	102.8061	#DIV/0!
<b>WGC-25B-21 - 1.d</b>	0	0.378467	0	0	0	0.550622	6.78392	13.85042	14.30894	22.8	14.28571	18.4375	15.54656	24.16149	30.0813	153.4719	#DIV/0!
<b>WGC-25B-21 - 2.d</b>	0	4.355628	0	0	2.972973	3.694494	13.51759	16.89751	19.39024	24.4	16.48352	17.0625	17.40891	15.96273	14.22764	141.833	0.582787
<b>WGC-25B-22 - 1.d</b>	0	4.159869	0	0	7.22973	7.282416	21.30653	26.31579	28.86179	39.7	26.92308	31.6875	29.95951	35.59006	36.58537	255.6231	0.586757
<b>WGC-25B-22 - 2.d</b>	0	5.742251	0	0.175055	3.648649	9.058615	27.78894	35.45706	37.72358	47.9	37.91209	40.375	40.89069	46.89441	42.27642	329.4292	0.899621
<b>WGC-25B-23 - 1.d</b>	0	2.577488	0	0	0	0.817052	6.532663	6.925208	10.56911	46	10.98901	11.5	9.473684	7.57764	9.715447	112.7501	#DIV/0!
<b>WGC-25B-23 - 2.d</b>	0	3.784666	0	0	0	0	5.577889	11.08033	13.37398	33.7	12.82051	11.25	13.19838	12.48447	12.31707	120.2248	#DIV/0!
<b>WGC-25B-24 - 1.d</b>	0	0.668842	0	0	0	3.907638	6.231156	12.18837	20.73171	24.7	19.23077	20.1875	17.69231	15.71429	15.36585	145.8108	#DIV/0!
<b>WGC-25B-24 - 2.d</b>	0	1.761827	0	0	0	2.042629	8.190955	15.23546	26.91057	28.1	26.92308	24.5625	25.10121	23.6646	21.13821	191.6356	#DIV/0!
<b>WGC-25B-25 - 1.d</b>	0	3.670473	0	0	1.148649	3.605684	11.70854	16.89751	18.82114	30.2	20.69597	17.0625	17.40891	20.55901	19.95935	161.6044	0.983202
<b>WGC-25B-25 - 2.d</b>	0	4.323002	0	0	2.5	3.907638	13.46734	14.95845	20.65041	55.9	20.51282	20.25	21.45749	23.04348	25.20325	201.9759	0.673447
<b>WGC-25B-26 - 1.d</b>	0	2.822186	0	0	1.689189	9.413854	18.24121	31.30194	37.39837	71.3	35.53114	36.4375	28.34008	33.91304	26.42276	300.6448	1.695905
<b>WGC-25B-26 - 2.d</b>	0.168776	2.479608	0.12931	0.153173	3.513514	6.571936	15.9799	25.76177	28.17073	21.2	28.57143	28.8125	24.2915	28.57143	31.30081	216.6802	0.877072
<b>WGC-25B-27 - 1.d</b>	0	5.986949	0	0.393873	2.635135	6.216696	16.88442	27.70083	30	23.6	30.03663	25.9375	22.46964	30.18634	34.55285	224.4838	0.931998
<b>WGC-25B-27 - 2.d</b>	0	4.159869	0	0	7.432432	7.815275	23.9196	27.14681	34.55285	42	34.79853	36.625	40.89069	46.08696	39.43089	301.5317	0.586141
<b>WGC-25B-28 - 1.d</b>	0	1.810767	0	0	0	2.85968	11.9598	18.55956	24.5122	51.8	21.97802	24.1875	26.72065	23.47826	21.13821	212.3744	#DIV/0!
<b>WGC-25B-28 - 2.d</b>	0	1.729201	0	0	1.283784	4.049734	7.889447	16.89751	22.64228	34.6	21.97802	22.3125	19.47368	17.57764	19.9187	175.4003	1.272498
<b>WGC-25B-29 - 1.d</b>	0	2.218597	0	0	1.148649	3.250444	14.42211	21.32964	28.73984	35.2	33.15018	32.75	29.1498	31.0559	32.11382	243.4892	0.79861
<b>WGC-25B-30 - 1.d</b>	1.434599	6.672104	2.553879	3.522976	7.635135	6.394316	15.32663	21.88366	20.2439	67.8	17.76557	16.375	13.84615	16.3354	14.63415	188.8838	0.591102
<b>WGC-25B-31 - 1.d</b>	0	3.817292	0	0	0	2.841918	7.788945	15.51247	13.57724	53.5	17.03297	14.8125	13.68421	13.91304	15.36585	157.3983	#DIV/0!
<b>WGC-25B-31 - 2.d</b>	0.329114	3.947798	0	0.4814	5.878378	6.039076	9.798995	15.42936	22.96748	19.15	20.69597	21.8125	25.34413	26.39752	25.60976	177.4067	0.795703
<b>WGC-25B-32 - 1.d</b>	0	0.815661	0	0	0	3.730018	10.65327	11.91136	9.634146	49.8	8.058608	11.0625	7.773279	8.881988	12.68293	119.8048	#DIV/0!
<b>WGC-25B-33 - 1.d</b>	0	2.202284	0	0	1.418919	6.927176	22.36181	32.13296	36.99187	66.8	32.60073	36.125	28.34008	26.70807	30.4878	290.1865	1.22977
<b>WGC-25B-33 - 2.d</b>	0	1.859706	0	0	2.22973	5.506217	19.84925	24.93075	31.78862	42.6	23.26007	26.125	23.07692	21.92547	20.73171	214.4385	0.827666
<b>WGC-25B-34 - 1.d</b>	0	3.066884	0	0	2.702703	5.506217	13.01508	17.17452	18.04878	42.1	19.23077	20.375	16.43725	19.68944	19.87805	172.9338	0.928391
<b>WGC-25B-34 - 2.d</b>	0	2.659054	0	0	1.486486	6.394316	10.25126	16.89751	19.8374	57.2	14.28571	18.8125	15.30364	20.99379	17.88618	181.2167	1.638042
<b>WGC-25B-35 - 1.d</b>	0	3.686786	0	0	0.743243	4.262877	12.31156	14.90305	15.65041	36.5	12.45421	13.375	14.12955	11.86335	10.97561	129.8512	1.409227
<b>WGC-25B-35 - 2.d</b>	0	3.278956	0	0	0.810811	3.357016	7.638191	11.82825	13.25203	26.7	12.82051	13.5625	8.54251	14.16149	10.36585	111.2332	1.348958
<b>WGC-25B-36 - 1.d</b>	0	1.761827	0	0.328228	0.945946	4.973357	10.20101	15.78947	23.25203	37.1	24.35897	27.875	21.86235	24.53416	18.69919	193.4712	1.601014
<b>WGC-25B-36 - 2.d</b>	0	0.489396	0	0	0.810811	1.793961	6.683417	7.479224	5.121951	21.2	5.769231	5.0625	3.036437	5.52795	7.642276	60.83957	0.770644

Samantha Nicole March  
Ultrahigh-pressure metapelites in the WGR

<b>WGC-25B-36 - 3.d</b>	0	0.50571	0	0	3.310811	11.36767	33.66834	25.76177	13.33333	60.1	9.52381	5	7.287449	9.31677	13.08943	143.4126	1.076697
<b>WGC-25B-37 - 1.d</b>	0.219409	3.066884	1.454741	1.378556	0	3.552398	7.085427	13.57341	17.92683	51	18.68132	20.6875	19.83806	26.77019	28.45528	196.9326	#DIV/0!
<b>WGC-25B-37 - 2.d</b>	0	1.060359	0	0	0	0	5.879397	5.844875	9.146341	38.1	12.27106	16.75	23.88664	39.06832	50.81301	195.8802	#DIV/0!
<b>WGC-25B-38 - 1.d</b>	0	0.766721	0	0	0	1.669627	3.61809	9.141274	15.52846	20.2	17.58242	24	27.12551	34.16149	40.65041	188.3896	#DIV/0!
<b>WGC-25B-39 - 1.d</b>	0	2.903752	0	0	2.702703	4.795737	13.36683	15.78947	20.20325	34.5	18.86447	21.3125	15.38462	17.76398	17.07317	160.8915	0.797888
<b>WGC-25B-40 - 1.d</b>	0	2.251223	0	0	3.716216	6.749556	22.21106	29.08587	31.70732	25.8	32.23443	37	33.19838	33.04348	34.55285	256.6223	0.742917
<b>WGC-25B-41 - 1.d</b>	0	1.32137	0	0	0	2.50444	9.19598	16.06648	26.05691	24.8	25.64103	25.8125	23.88664	22.48447	16.66667	181.4147	#DIV/0!
<b>WGC-25B-42 - 1.d</b>	0	3.14845	0	0	1.959459	3.74778	10.35176	17.72853	17.47967	45.7	19.96337	25.8125	29.95951	33.54037	44.30894	234.4929	0.832145
<b>WGC-25B-43 - 1.d</b>	0	1.957586	0	0	1.689189	5.861456	14.52261	29.9169	39.02439	13.3	51.64835	67.5	69.23077	114.2857	126.0163	510.9224	1.183434
<b>WGC-25B-44 - 1.d</b>	0	3.60522	0.086207	1.969365	9.256757	15.09769	23.66834	34.90305	50	17	72.71062	94.375	97.97571	122.3602	147.1545	636.4791	1.019993
<b>WGC-25B-44 - 2.d</b>	0	3.556281	0	0	1.351351	3.516874	9.045226	18.28255	16.70732	37.3	16.66667	12.625	9.149798	13.22981	12.03252	135.9937	1.005919
<b>WGC-25B-45 - 1.d</b>	0.687764	8.711256	3.87931	8.512035	59.45946	29.66252	192.9648	313.0194	495.935	23	732.6007	1075	1178.138	1515.528	1894.309	7227.53	0.276923
<b>WGC-25B-45 - 2.d</b>	0	1.468189	0	0	0	1.492007	5.728643	5.789474	9.512195	26.6	7.362637	10.1875	9.109312	14.40994	16.66667	99.63772	#DIV/0!
<b>WGC-25B-45 - 3.d</b>	0	3.311582	0	0.135667	0	1.030195	8.743719	11.24654	12.43902	32.7	15.38462	15.4375	19.83806	17.20497	23.17073	147.4214	#DIV/0!
<b>WGC-25B-46 - 1.d</b>	0	2.104405	0	0	1.756757	5.328597	14.82412	22.43767	31.78862	35.3	32.96703	32.25	33.60324	30.31056	28.45528	247.1124	1.044173
<b>WGC-25B-46 - 2.d</b>	0	2.969005	0	0	3.378378	4.795737	15.32663	19.11357	29.47154	59.5	31.68498	26	26.31579	28.19876	25.20325	245.4879	0.666466
<b>WGC-25B-47 - 1.d</b>	0	5.579119	0.204741	0.612691	4.72973	4.262877	16.73367	23.54571	30.44715	50.6	34.06593	30.25	28.34008	29.37888	29.26829	255.8961	0.479169
<b>WGC-25B-47 - 2.d</b>	0.202532	8.319739	0.409483	0.437637	5.608108	2.042629	17.33668	34.07202	57.72358	36.9	112.2711	234.375	412.9555	838.5093	1504.065	3230.871	0.207156
<b>WGC-25B-48 - 1.d</b>	0	1.924959	0	0	0	4.618117	13.06533	21.32964	30.3252	80	28.38828	30.9375	26.72065	27.26708	25.60976	270.5781	#DIV/0!
<b>WGC-25B-48 - 2.d</b>	0	2.071778	0	0	1.351351	5.150977	12.36181	24.65374	29.87805	120.5	28.38828	27.4375	25.50607	29.50311	23.17073	309.0375	1.260272
<b>WGC-25B-49 - 1.d</b>	0	2.446982	0	0	0	2.664298	7.286432	11.63435	11.95122	26.3	15.20147	13.0625	13.96761	17.8882	17.07317	127.0785	#DIV/0!
<b>WGC-25B-49 - 2.d</b>	0	3.800979	0	0	3.513514	4.262877	15.17588	19.66759	21.58537	1150	20.14652	20.75	15.62753	19.75155	13.33333	1280.862	0.583788
<b>WGC-25B-50 - 1.d</b>	0	3.278956	0	0	1.554054	10.83481	30.15075	42.10526	55.28455	21.5	54.7619	48.875	42.91498	49.13043	45.52846	360.1006	1.582848
<b>WGC-25B-50 - 2.d</b>	0	1.810767	0	0	1.013514	6.749556	17.53769	23.2687	38.61789	24.8	39.56044	37	34.0081	35.2795	30.0813	262.6159	1.600937
<b>WGC-25B-51 - 1.d</b>	0	1.288744	0	0	0.540541	2.806394	7.18593	12.18837	18.90244	53.2	17.21612	20	14.65587	18.9441	18.57724	173.6841	1.423945
<b>WGC-25B-52 - 1.d</b>	0	3.278956	0	0	1.418919	2.539964	10	13.2964	13.00813	52.1	15.20147	15.1875	19.02834	15.03106	15.85366	158.7065	0.674293
<b>WGC-25B-52 - 2.d</b>	0.080169	3.915171	0	0	1.283784	3.889876	10.1005	13.85042	16.05691	59.8	15.01832	15.9375	11.21457	16.08696	15.56911	163.5338	1.080235
<b>WGC-25B-53 - 1.d</b>	0	4.045677	0	0.218818	10.47297	15.80817	41.70854	58.72576	59.7561	202	57.32601	61.8125	61.94332	66.14907	67.88618	635.5989	0.75637
<b>WGC-25B-54 - 1.d</b>	0	1.729201	0	0	0	5.506217	12.91457	20.77562	23.57724	55.7	22.52747	28.4375	33.60324	55.2795	78.04878	317.9494	#DIV/0!
<b>WGC-25B-54 - 2.d</b>	0	2.430669	0	0.076586	7.972973	7.282416	22.66332	33.79501	37.80488	52.1	42.30769	37.3125	36.43725	41.18012	34.95935	315.8968	0.541756
<b>WGC-25B-55 - 1.d</b>	0	1.435563	0	0	0.472973	3.57016	8.190955	17.17452	25.2439	23.6	28.02198	23.0625	22.55061	24.47205	22.35772	186.4833	1.813854

Samantha Nicole March  
Ultrahigh-pressure metapelites in the WGR

WGC-25B-55 - 2.d	0	1.82708	0	0	0	2.166963	7.58794	16.06648	20.60976	38.2	20.14652	23.375	24.2915	19.62733	21.54472	183.8613	#DIV/0!
WGC-25B-56 - 1.d	0	2.169657	0	0	1.283784	1.705151	14.1206	24.65374	33.21138	92	32.78388	37.375	32.79352	33.91304	34.14634	320.8769	0.400489
WGC-25B-56 - 2.d	0	1.810767	0	0	0.945946	3.889876	14.22111	25.76177	32.68293	64.8	37.54579	38.25	29.1498	35.2795	35.77236	299.2421	1.060562
WGC-25B-57 - 1.d	0	1.941272	0	0	0.472973	3.019538	6.030151	17.17452	20.12195	39.6	20.32967	19.875	16.19433	20.74534	16.09756	170.1384	1.787962
WGC-25B-57 - 2.d	0	1.272431	0	0	0	1.669627	7.98995	14.68144	22.88618	29	25.64103	30.0625	21.21457	26.14907	24.39024	194.025	#DIV/0!
WGC-25B-58 - 1.d	0	51.63132	0.657328	3.063457	24.45946	16.69627	81.90955	145.4294	261.3821	1036	427.6557	678.125	938.8664	1397.516	1865.854	6750.828	0.373017
WGC-25B-59 - 1.d	0.101266	1.533442	1.045259	2.14442	2.162162	3.357016	6.331658	4.32133	6.910569	26.7	6.190476	8.0625	8.380567	11.98758	18.69919	91.25221	0.907299
WGC-25B-60 - 1.d	0	0.360522	0	0	0	0.35524	7.537688	10.19391	12.15447	100.1	12.08791	12.0625	8.137652	14.59627	15.85366	185.1864	#DIV/0!
WGC-25B-60 - 2.d	0	1.207178	0	0	0	0.17762	3.366834	4.709141	5.894309	40.7	7.637363	9.25	9.149798	7.142857	7.845528	92.329	#DIV/0!
WGC-25B-60 - 3.d	0	3.24633	0	0	0.743243	2.85968	7.487437	8.836565	10.77236	41.6	10.25641	10.875	8.461538	10.55901	8.861789	110.2227	1.212231
WGC-25B-61 - 1.d	0	3.132137	0	0	3.581081	7.104796	27.33668	37.67313	38.69919	67.8	39.01099	36.8125	32.38866	30.24845	34.14634	316.7793	0.718078
WGC-25B-61 - 2.d	0	2.430669	0	0.371991	0.743243	6.039076	21.25628	35.18006	39.8374	47.7	41.94139	35.9375	33.60324	34.09938	30.4878	298.7868	1.519362
WGC-25B-61 - 3.d	0	1.843393	0	0	2.432432	5.150977	12.31156	18.83657	23.17073	42.6	21.61172	25.1875	17.00405	18.01242	15.44715	181.8701	0.941267
WGC-25B-62 - 1.d	0	8.319739	0	0.109409	2.094595	0.26643	26.13065	59.55679	104.065	12.5	177.2894	298.75	432.7935	663.354	878.4553	2626.764	0.036013
WGC-25B-62 - 2.d	0	2.365416	0	0	0	0	13.9196	23.54571	46.34146	66.1	61.53846	105.625	142.915	224.8447	296.748	967.6583	#DIV/0!
WGC-25B-62 - 3.d	0	9.070147	0	0	4.256757	1.065719	30.65327	65.09695	130.0813	43.6	223.0769	400	542.1053	827.3292	1154.472	3385.761	0.093296
WGC-25B-63 - 1.d	0	2.69168	0	0	0.290541	5.150977	16.88442	26.31579	41.54472	62.2	36.44689	37.8125	36.43725	42.91925	31.70732	315.3837	2.325643
WGC-25B-63 - 2.d	0	1.908646	0	0	0.878378	4.049734	12.96482	18.83657	24.6748	37.4	27.65568	22.625	24.69636	23.22981	23.98374	203.1019	1.200058
WGC-25B-64 - 1.d	0	1.615008	0	0	0	5.506217	8.994975	15.78947	26.50407	47.9	22.89377	25	25.91093	24.03727	27.64228	215.6778	#DIV/0!
WGC-25B-64 - 2.d	0	1.712887	0	0	0.540541	4.440497	10.75377	20.22161	27.68293	705	24.54212	27.0625	21.45749	24.84472	29.26829	880.0797	1.841777
WGC-25B-65 - 1.d	0.206751	2.430669	0	0	1.351351	8.170515	25.27638	42.10526	60.56911	15.5	60.62271	63.875	65.58704	68.19876	65.04065	441.4985	1.398002
WGC-25B-65 - 2.d	0	6.003263	0.80819	2.603939	11.28378	6.394316	11.00503	19.39058	19.30894	23.7	25.82418	32.625	38.8664	46.02484	58.13008	263.87	0.573814
WGC-25B-68 - 1.d	0	1.239804	0	0	0	3.801066	12.46231	12.29917	22.35772	16.18	17.94872	18.4375	12.06478	16.45963	13.98374	129.7313	#DIV/0!
WGC-25B-68 - 2.d	0	1.566069	0	0	0.675676	3.339254	16.23116	20.49861	34.95935	21.3	39.92674	37	34.81781	35.90062	32.92683	257.33	1.008337
WGC-25B-68 - 3.d	0	0.91354	0	0	2.364865	5.506217	17.43719	31.57895	50	70.4	42.67399	44.875	34.41296	40.74534	30.89431	345.5805	0.857456
WGC-25B-69 - 1.d	0	1.924959	0	0	0	6.927176	15.07538	24.37673	26.91057	67.6	38.27839	36.5	39.27126	53.97516	61.78862	348.7007	#DIV/0!
WGC-25B-69 - 2.d	0	1.87602	0	0	2.027027	2.611012	9.698492	16.6205	26.86992	45.5	23.44322	22.4375	24.12955	22.6087	18.69919	200.3086	0.58888
WGC-25B-69 - 3.d	0	1.141925	0	0	0	3.9254	10.20101	16.89751	24.43089	312.8	30.21978	30.875	29.55466	40.93168	63.00813	548.7176	#DIV/0!
WGC-25B-69 - 4.d	0	1.549755	0	0	0.608108	5.506217	9.798995	20.22161	27.19512	124	24.72527	30.1875	27.53036	25.34161	30.4878	309.6893	2.255652
WGC-25B-71 - 1.d	0	3.556281	0	0	1.891892	2.930728	13.01508	16.6205	15.93496	394.6	14.28571	14.0625	12.18623	15.59006	11.95122	495.2312	0.590614
WGC-25B-71 - 2.d	0	3.14845	0	0	1.148649	6.394316	12.61307	17.17452	17.47967	70.8	14.65201	17.125	13.88664	15.21739	14.79675	181.132	1.679926

Samantha Nicole March  
Ultrahigh-pressure metapelites in the WGR

<del>WGC-25B-71 - 3.d</del>	0	2.512235	0	0	0.25	5.150977	9.949749	15.51247	15.0813	46.8	13.36996	13.75	7.165992	11.18012	14.5935	137.4533	3.26598
<del>WGC-25B-72 - 1.d</del>	0	3.115824	0	0	1.013514	2.646536	10.25126	14.18283	13.61789	46.4	15.56777	15.6875	16.68016	15.34161	18.29268	155.7704	0.821059
<del>WGC-25B-72 - 2.d</del>	0	0.619902	0	0	0	4.973357	14.07035	15.78947	11.78862	24	10.43956	13.8125	15.78947	24.2236	47.15447	162.9977	#DIV/0!
<del>WGC-25B-73 - 1.d</del>	0	2.69168	0	0	1.351351	3.623446	13.86935	17.45152	14.39024	51.5	13.18681	13.375	11.7004	12.48447	13.90244	147.9909	0.836969
<del>WGC-25B-73 - 2.d</del>	0	3.898858	0	0	1.824324	3.83659	10	16.34349	14.8374	123.4	20.69597	17	12.83401	16.89441	13.94309	235.9484	0.898244
<del>WGC-25B-74 - 1.d</del>	0	1.272431	0	0	0	1.722913	3.065327	4.127424	3.902439	49.9	7.582418	9.5	10.80972	11.24224	10.89431	107.9585	#DIV/0!
<del>WGC-25B-74 - 2.d</del>	0	3.099511	0.366379	0	0	1.136767	8.190955	12.74238	21.54472	19.21	41.75824	93.125	153.8462	223.6025	422.7642	988.5932	#DIV/0!
<del>WGC-25B-75 - 1.d</del>	0	3.376835	0	0	1.216216	6.039076	12.01005	16.06648	19.9187	36.2	23.26007	20.8125	20.64777	29.62733	26.82927	193.3621	1.58013
<del>WGC-25B-75 - 2.d</del>	0	2.707993	0	0	0	3.21492	9.447236	16.89751	19.79675	79.8	16.30037	19.25	20.89069	19.75155	15.85366	208.5405	#DIV/0!
<del>WGC-25B-76 - 1.d</del>	0	3.034258	0	0	0.540541	4.440497	11.60804	16.89751	16.70732	89.9	17.03297	18.0625	14.2915	15.2795	17.72358	205.8949	1.772711
<del>WGC-25B-76 - 2.d</del>	0	2.267537	0	0	0	1.847247	6.180905	12.74238	17.92683	62.3	18.13187	18.25	17.81377	24.53416	18.29268	189.9917	#DIV/0!
<del>WGC-25B-77 - 1.d</del>	0	2.022838	0	0	0.472973	4.440497	11.20603	21.88366	24.10569	45.6	26.00733	25.25	23.48178	34.78261	39.8374	240.9485	1.928802
<del>WGC-25B-77 - 2.d</del>	0	1.82708	0	0	0	1.687389	9.346734	17.72853	21.91057	49.1	23.62637	27.875	23.48178	27.51553	29.26829	220.5061	#DIV/0!
<del>WGC-25B-78 - 1.d</del>	25.7384	46.00326	66.81034	79.64989	108.7838	61.98934	66.83417	67.59003	86.58537	29	127.4725	305.625	599.1903	1279.503	2800.813	5295.779	0.727002
<del>WGC-25B-78 - 2.d</del>	0	0.619902	0	0	0	1.705151	9.849246	13.85042	13.61789	47.9	10.98901	12.625	10.32389	9.378882	17.11382	135.7989	#DIV/0!
<del>WGC-25B-78 - 3.d</del>	0	3.164763	0	0	1.081081	2.522202	5.628141	7.839335	8.943089	27.1	8.058608	11.0625	8.663968	7.267081	5.203252	84.13783	1.022512
<del>WGC-25B-79 - 1.d</del>	0	2.952692	0	0	0	2.362345	6.834171	13.2964	10.97561	31.2	9.89011	8.8125	9.554656	11.36646	8.292683	103.3884	#DIV/0!
<del>WGC-25B-79 - 2.d</del>	0	1.859706	0	0	0	3.39254	4.623116	12.18837	10.28455	25.7	11.53846	10.375	6.518219	11.92547	9.146341	97.67641	#DIV/0!
<del>WGC-25B-80 - 1.d</del>	0	1.892333	0	0	1.081081	4.031972	10.15075	15.51247	22.64228	28.9	24.35897	24.375	25.91093	20.93168	23.17073	185.8021	1.217136
<del>WGC-25B-80 - 2.d</del>	0	1.82708	0	0	1.959459	2.060391	9.698492	14.40443	21.82927	19.1	25.27473	26.5	20.24291	23.35404	25.20325	175.9086	0.472639
<del>WGC-25B-81 - 1.d</del>	0	3.556281	0	0	0	4.262877	7.738693	13.3518	11.99187	27	11.35531	11.75	9.838057	11.36646	11.30081	107.9543	#DIV/0!
<del>WGC-25B-81 - 2.d</del>	0	3.60522	0	0	1.689189	1.865009	3.869347	8.614958	11.78862	32.1	7.326007	8.375	7.165992	7.080745	6.99187	89.44319	0.729496
<del>WGC-25B-82 - 1.d</del>	0	0.799347	0	0	0	3.694494	12.36181	17.72853	15.2439	15.3	14.65201	19.875	22.67206	29.19255	38.21138	172.8754	#DIV/0!
<del>WGC-25B-82 - 2.d</del>	0	1.533442	0	0	0.878378	0.408526	8.844221	13.01939	20.77236	90	21.79487	20.9375	19.83806	19.25466	19.9187	225.5355	0.146571
<del>WGC-25B-82 - 3.d</del>	0	2.137031	0	0	1.351351	3.143872	11.65829	18.55956	31.34146	41.3	29.12088	28.0625	31.98381	27.95031	25.60976	233.9283	0.792069
<del>WGC-25B-83 - 1.d</del>	0	5.350734	2.155172	9.628009	25	10.83481	83.41709	161.7729	261.3821	38.1	386.4469	575	740.8907	968.9441	1182.927	4315.463	0.23726
<del>WGC-25B-83 - 2.d</del>	0	5.399674	1.163793	5.273523	21.62162	8.703375	78.89447	138.5042	215.4472	51.8	346.1538	525	595.1417	788.8199	1048.78	3709.647	0.210727
<del>WGC-25B-84 - 1.d</del>	0	0	0	0	0	0	0.954774	2.354571	3.130081	616	4.322344	7.5625	9.311741	20.31056	24.39024	687.382	#DIV/0!
<del>WGC-25B-85 - 1.d</del>	17.72152	53.83361	11.2069	12.25383	21.48649	7.104796	95.47739	189.1967	373.1707	530	624.5421	1056.25	1437.247	2126.708	2650.407	8987.521	0.156862
<del>WGC-25B-85 - 2.d</del>	0	22.69168	0	0.59081	8.445946	1.083481	38.19095	78.11634	153.6585	472	276.5568	498.125	692.3077	1118.012	1512.195	4800.972	0.060328

Crossed-out = discordant

**WGC2019J-25B zircon trace element standards**

Standard_spot size	La	Ce	Pr	Nd	Sm	Eu	Gd	Tb	Dy	Ho	Er	Tm	Yb	Lu
NIST610-51 - 1.d	427600	437200	435200	418500	439600	437000	436300	425100	423600	437200	441000	426100	440400	426100
NIST610-51 - 2.d	427800	441100	436100	421300	443600	435700	437200	428900	426800	440000	444800	428500	439900	431400
NIST610-51 - 3.d	423100	435300	429500	411100	433400	429000	432700	419900	419800	430700	436900	417300	433000	423400
NIST610-51 - 4.d	423900	434500	430000	415800	436200	431500	433200	420700	425800	433300	439700	420600	433200	425000
NIST610-51 - 5.d	427500	439400	434600	418900	440400	430900	434900	423900	422900	434900	441400	421800	434900	425900
NIST610-51 - 6.d	426500	438300	431500	415100	438400	429400	434400	420700	419400	434500	438700	418800	433700	424300
NIST610-51 - 7.d	428200	440500	435600	421500	438800	434600	435400	423900	418200	433800	437500	422500	435300	422900
NIST610-51 - 8.d	421900	436300	428900	411600	432400	428600	431200	420200	420600	432600	436000	417300	430300	419500
NIST610-51 - 9.d	422200	439200	432500	411800	434900	430500	429400	422100	421200	431700	440400	416300	433200	421200
NIST610-51 - 10.d	414400	427400	424800	404700	429700	422600	427000	413400	414400	424300	430100	411000	427500	416600
NIST610-51 - 11.d	417000	429400	424800	408800	431300	425500	426400	414100	414400	427000	434000	411400	428400	415300
NIST610-51 - 12.d	421100	435500	428800	408800	436500	426300	428700	416300	415200	428700	439000	415900	432500	421600
NIST610-51 - 13.d	426300	439600	432700	413900	434900	431900	429400	422100	420400	436700	439800	417800	437100	423600
NIST610-51 - 14.d	421300	434800	428200	411100	432800	428400	427400	417800	416700	430000	437300	417100	431200	419700
NIST610-51 - 15.d	422100	433800	428400	411900	434800	428100	428300	419800	420800	429600	435300	415300	429800	420200
NIST610-51 - 16.d	420400	435500	428300	410400	437600	427100	431500	420000	420100	430400	436000	416400	430400	420400
NIST610-51 - 17.d	422900	433500	433000	413800	435700	427200	433500	420300	420600	431600	437200	418300	433700	424300
NIST610-51 - 18.d	422100	433600	427700	412900	429200	428200	431800	418400	415400	428900	432500	413900	425300	417000
NIST610-51 - 19.d	424900	437900	432800	414800	434700	431600	431000	419900	423300	430500	437600	420200	432900	422900
NIST610-51 - 20.d	429000	440500	432900	416400	441300	433200	440000	421800	424700	435600	438700	420200	438700	424700
NIST610-51 - 21.d	421100	435400	432000	416700	434200	433500	429700	420900	418800	432100	440200	418700	437000	423400
NIST610-51 - 22.d	428600	439500	434200	414200	440500	433400	435400	424900	422600	432500	441900	424900	439200	424400
NIST610-51 - 23.d	426200	436000	434500	417500	438600	431100	435600	423300	425300	438800	444300	423800	437300	427200
NIST610-51 - 24.d	426000	440000	432600	419100	440000	434300	436900	424500	422800	436700	441000	423800	437200	426700
NIST610-19 - 1.d	425000	441000	436000	421000	439000	428000	428000	419000	418000	430000	441000	410000	432000	420000
NIST610-19 - 2.d	418000	440000	433000	410000	433000	426000	425000	416000	424000	433000	435000	415000	427000	424000
NIST610-19 - 3.d	401000	406000	405000	383000	400000	404000	393000	391000	386000	399000	408000	385000	396000	390000
NIST610-19 - 4.d	408000	414000	413000	386000	418000	407000	396000	398000	391000	408000	416000	395000	406000	397000



<b>NIST610-19 - 5.d</b>	412000	429000	413000	403000	422000	409000	406000	404000	404000	416000	419000	401000	419000	405000
<b>NIST610-19 - 6.d</b>	409000	416000	414000	398000	422000	412000	417000	403000	398000	414000	420000	396000	416000	401000
<b>NIST610-19 - 7.d</b>	425000	438000	429000	414000	424000	423000	423000	416000	408000	425000	437000	409000	422000	418000
<b>NIST610-19 - 8.d</b>	425000	436000	431000	411000	430000	425000	433000	409000	416000	424000	438000	410000	428000	410000
<b>NIST610-19 - 9.d</b>	426000	442000	433000	413000	440000	432000	426000	424000	420000	431000	432000	421000	433000	419000
<b>NIST610-19 - 10.d</b>	418000	437000	424000	408000	432000	419000	425000	412000	407000	419000	432000	406000	419000	413000
<b>NIST610-19 - 11.d</b>	426000	444000	429000	416000	431000	435000	444000	422000	427000	432000	444000	424000	441000	429000
<b>NIST610-19 - 12.d</b>	427000	442000	434000	426000	436000	435000	441000	418000	414000	433000	437000	419000	439000	429000

### WGC2019J-31A zircon trace elements

Sample	Chondrite normalised REEs + Y															Total HREEs	Eu anomaly
	La	Ce	Pr	Nd	Sm	Eu	Gd	Tb	Dy	Y	Ho	Er	Tm	Yb	Lu		
<b>31A-1 - 1.d</b>	0	0.39151 <sub>7</sub>	0	0	6.48648 <sub>6</sub>	0.67495 <sub>6</sub>	59.2964 <sub>8</sub>	145.706 <sub>4</sub>	230.487 <sub>8</sub>	408	243.223 <sub>4</sub>	243.75	319.838 <sub>4</sub>	472.049 <sub>7</sub>	658.536 <sub>6</sub>	2721.592	0.034416
<b>31A-1 - 2.d</b>	0	1.22349 <sub>1</sub>	0	0.74398 <sub>2</sub>	10.7432 <sub>4</sub>	11.3676 <sub>7</sub>	74.8743 <sub>7</sub>	66.2049 <sub>9</sub>	62.6016 <sub>3</sub>	90.9	51.4652	51.25	58.2996	98.1366 <sub>5</sub>	146.341 <sub>5</sub>	625.1995	0.400809
<b>31A-2 - 1.d</b>	0	1.32137	0	2.56017 <sub>5</sub>	15.6081 <sub>1</sub>	18.2948 <sub>5</sub>	54.2713 <sub>6</sub>	55.1246 <sub>5</sub>	51.2195 <sub>1</sub>	69.3	38.6446 <sub>9</sub>	41.375	35.6275 <sub>3</sub>	36.4596 <sub>3</sub>	41.4634 <sub>1</sub>	369.2144	0.628591
<b>31A-2 - 2.d</b>	0	1.20717 <sub>8</sub>	0	0.50328 <sub>2</sub>	15.2702 <sub>7</sub>	21.4920 <sub>1</sub>	52.7638 <sub>2</sub>	51.8005 <sub>5</sub>	47.9674 <sub>8</sub>	72.6	38.6446 <sub>9</sub>	43.9375	35.2226 <sub>7</sub>	45.9627 <sub>3</sub>	39.4308 <sub>9</sub>	375.5665	0.757156
<b>31A-3 - 1.d</b>	0.17721 <sub>5</sub>	1.30505 <sub>7</sub>	0	0.87527 <sub>4</sub>	10.7432 <sub>4</sub>	2.71758 <sub>4</sub>	74.3718 <sub>6</sub>	160.387 <sub>8</sub>	186.585 <sub>4</sub>	302 <sub>5</sub>	158.608 <sub>4</sub>	188.125	207.287 <sub>4</sub>	281.987 <sub>6</sub>	430.894 <sub>3</sub>	1916.376	0.096142
<b>31A-3 - 2.d</b>	0.63713 <sub>1</sub>	3.83360 <sub>5</sub>	4.41810 <sub>3</sub>	9.05908 <sub>1</sub>	32.6351 <sub>4</sub>	30.1953 <sub>8</sub>	90.9547 <sub>7</sub>	135.457 <sub>1</sub>	154.065 <sub>9</sub>	216.	123.443 <sub>2</sub>	106.25	106.882 <sub>6</sub>	110.559 <sub>1</sub>	113.008 <sub>1</sub>	1066.565	0.554224
<b>31A-4 - 1.d</b>	0	2.51223 <sub>5</sub>	0.71120 <sub>7</sub>	4.22319 <sub>5</sub>	45.9459 <sub>5</sub>	10.4795 <sub>7</sub>	120.603 <sub>7</sub>	76.4542 <sub>9</sub>	47.5609 <sub>8</sub>	54	29.3040 <sub>3</sub>	27.1875	19.4332	24.0993 <sub>8</sub>	22.7642 <sub>3</sub>	300.8036	0.14078
<b>31A-4 - 2.d</b>	0	1.99021 <sub>2</sub>	0	0.91903 <sub>7</sub>	18.1756 <sub>8</sub>	4.26287 <sub>7</sub>	39.6984 <sub>9</sub>	29.3628 <sub>8</sub>	16.5853 <sub>7</sub>	21.2	10.0732 <sub>6</sub>	9.4375	5.58704 <sub>5</sub>	8.69565 <sub>2</sub>	6.91056 <sub>9</sub>	107.8523	0.158698
<b>31A-5 - 1.d</b>	0	0.12724 <sub>3</sub>	0	0	10.4054 <sub>4</sub>	1.27886 <sub>3</sub>	67.8392 <sub>3</sub>	159.279 <sub>8</sub>	245.122 <sub>8</sub>	426	231.868 <sub>4</sub>	206.25	172.064 <sub>8</sub>	164.596 <sub>3</sub>	184.959 <sub>3</sub>	1790.14	0.048134
<b>31A-5 - 2.d</b>	0	2.64274 <sub>1</sub>	0	3.76367 <sub>6</sub>	39.1891 <sub>9</sub>	10.3019 <sub>5</sub>	115.075 <sub>4</sub>	84.7645 <sub>4</sub>	59.3495 <sub>9</sub>	74.3	45.9707	37.875	29.5546 <sub>6</sub>	29.3788 <sub>8</sub>	26.8292 <sub>7</sub>	388.0226	0.153407
<b>31A-6 - 1.d</b>	0	2.12071 <sub>8</sub>	0	2.84463 <sub>9</sub>	20.2027	27.7087	64.3216 <sub>1</sub>	56.7867	42.6829 <sub>3</sub>	62.7	36.2637 <sub>4</sub>	36.625	32.3886 <sub>6</sub>	40.1242 <sub>2</sub>	48.3739 <sub>8</sub>	355.9452	0.768658
<b>31A-6 - 2.d</b>	0	1.40293 <sub>6</sub>	0	1.70678 <sub>3</sub>	12.5675 <sub>7</sub>	16.6962 <sub>7</sub>	47.7386 <sub>9</sub>	41.8282 <sub>5</sub>	32.9268 <sub>3</sub>	49.7	28.2051 <sub>3</sub>	27.25	23.8866 <sub>4</sub>	29.4409 <sub>9</sub>	35.3658 <sub>5</sub>	268.6037	0.681646

Samantha Nicole March  
Ultrahigh-pressure metapelites in the WGR

31A-7 - 1.d	0	2.25122	0	2.23194	22.6351	6.39431	55.7788	55.6786	39.4308	42.2	21.7948	17.8125	10.0809	11.8012	14.4308	213.23	0.179957
		3		7	4	6	9	7	9		7		7	4	9		
31A-7 - 2.d	0	1.92495	0	2.03501	27.1621	12.2557	97.4874	72.0221	60.5691	62.1	37.3626	32.25	29.1498	34.1614	37.8048	365.4201	0.238168
		9		1	6	7	4	6	1		4			9	8		
31A-8 - 1.d	0.03797	0.65252	0.17241	1.35667	10.6081	2.30905	75.8794	146.814	148.374	188	105.860	89.375	73.6842	80.1242	101.219	933.4521	0.081387
		5		4	4	1	9	4			8		1	2	5		
31A-8 - 2.d	0	2.54486	0.36637	4.13566	30.2702	14.7424	63.3165	55.4016	47.5609	52.5	25.2747	23.3125	19.0283	17.5776	15.8536	256.5095	0.336746
		1		9	7	7	8	6	8		3		4	4	6		
31A-8 - 3.d	0	2.87112	0.07543	2.45076	27.9729	23.9786	64.8241	55.6786	46.3414	66	37.9120	29.9375	25.5060	28.6956	18.2926	308.3641	0.563103
		6		1	6	7	9	2	7		6		7	5	8		
31A-9 - 1.d	1.30801	5.88907	3.87931	7.39606	60.8108	291.651	145.226	142.936	115.447	161	85.3479	100.625	106.072	147.826	182.926	1042.182	3.103502
		7		1	1	9	1	3	2		9		9	1	8		
31A-9 - 2.d	0.13502	4.60032	2.71551	9.21225	45.2702	140.497	100.502	94.4598	73.9837	86.9	45.2381	38.9375	26.7206	32.6708	34.1463	433.057	2.082922
		1		6	7	4	3	5	3		4		5	1	4		
31A-10 - 1.d	0	0.32626	0	1.13785	5.13513	4.61811	79.8995	136.288	158.943	325	184.981	237.5	287.449	347.826	520.325	2198.314	0.227991
		4		6	5	7		1	1		7		4	1	2		
31A-10 - 2.d	0	0.63621	0	0.07658	10.7432	4.79573	52.7638	115.512	144.308	242	132.600	140	125.910	159.627	193.902	1253.863	0.201428
		5		6	4	7	2	5	9		7		9	3	4		
31A-11 - 1.d	0	0.76672	0	0.4814	23.5135	6.03907	96.4824	120.775	130.894	220.	131.685	130.625	120.242	135.403	132.113	1122.44	0.126791
		1			1	6	1	6	3		7		9	7	8		
31A-11 - 2.d	0	1.12561	0.07543	0.76586	21.8918	5.86145	79.3969	117.174	122.764	181.	106.410	111.25	98.3805	98.1366	91.8699	927.2861	0.140592
		2		1	4	9	6	8	5		3		7	5	2		
31A-11 - 3.d	0	1.15823	0.06465	0.41575	10.7432	5.68383	67.8392	83.6565	82.5203	137.	77.6556	82.875	75.7085	78.2608	65.8536	684.0305	0.210539
		8		5	5	4	7	1	3		5		8	7	6		
31A-12 - 1.d	0	0.48939	0	0.10284	11.8243	9.23623	89.9497	169.252	195.935	268.	145.054	128.75	119.028	111.180	121.544	1259.645	0.283209
		6		5	2	4	5	1	1		9		3	1	7		
31A-12 - 2.d	0	0.15986	0	0	5.27027	4.79573	53.2663	121.883	138.617	204.	123.260	105.625	78.9473	91.9254	100.813	965.6725	0.286228
		9			7	3	7	9	6		1		7	7			
31A-12 - 3.d	0.46413	0.52202	0	1.05032	17.3648	6.03907	93.4673	216.066	258.130	358.	201.098	167.5	148.583	154.658	165.040	1669.377	0.149901
		5		8	6	6	4	5	1		3		9	4	7		
31A-13 - 1.d	0.20675	1.01141	0	2.16630	15.6756	12.9662	58.2914	96.6759	171.544	414	231.501	408.125	618.623	1043.47	1516.26	4500.209	0.428942
		1		9	2	8	5	6	7		8		5	8			
31A-13 - 2.d	0	1.66394	0.43103	5.86433	36.4864	30.9058	106.532	83.3795	57.3170	65.5	35.1648	28.375	17.8137	26.5838	25.2032	339.3373	0.495717
		8		4	3	9	6	7	7		4		7	5	5		
31A-14 - 1.d	0.29535	2.78956	0.36637	4.92341	50.6756	73.5346	81.4070	82.5484	60.9756	73.9	45.4212	35	17.4089	31.6770	47.5609	394.4922	1.144883
		9		9	4	8	4	8	1		5		1	2	8		
31A-16 - 1.d	0	0.26264	0	0	3.98648	0	67.3366	181.163	223.170	328.	176.739	128.75	100	88.1987	72.7642	1299.587	0
		3			6		8	4	7		8			6	3		
31A-16 - 2.d	0	0.42414	0	0.2407	8.78378	2.11367	95.9799	193.351	268.292	407.	215.384	205.625	168.016	175.776	163.821	1797.568	0.072796
		4			4	7		8	7		3		2	4	1		
31A-16 - 3.d	0	0.78303	0.29094	0.87527	9.12162	3.37477	79.8995	191.689	236.585	354.	199.267	147.5	119.028	101.863	86.9918	1437.126	0.125008
		4		8	4	2	8	8	4		2		3	4	7		
31A-17 - 1.d	0	1.37031	0.07543	1.20350	7.63513	1.74067	41.2060	117.174	232.926	674	360.073	615.625	955.465	1515.52	2247.96	6718.761	0.098136
		1		1	5	5	3	5	8		3		6	8	7		
31A-17 - 2.d	0	0.08319	0	0	2.02702	0	40.2010	126.315	194.308	447	244.505	350	479.352	663.354	1028.45	3533.292	0
		7			7		1	8	9		5		2	5			
31A-18 - 1.d	0.03375	0.66884	0.54956	0.19693	4.25675	3.73001	25.4773	73.6842	120.731	267	137.179	186.25	230.769	329.192	414.634	1759.441	0.358174
		5		2	9	7	8	9	1		7		2	5	1		
31A-18 - 2.d	0.32067	4.15986	1.69181	3.80744	12.0945	7.81527	31.1557	32.6869	31.0569	43.1	25.2747	20.6875	15.7489	15.0931	15.3658	199.0141	0.402605
		5		9	9	5	8	8	1		3		9	7	5		

Samantha Nicole March  
Ultrahigh-pressure metapelites in the WGR

31A-19 - 1.d	0	0.23164 8	0	0	7.02702 7	2.06039 1	55.7788 9	140.997 2	208.536 6	435	241.758 2	255.625	251.012 1	238.509 3	265.447 2	2036.886	0.104071
31A-19 - 2.d	0	0.30995 1	0	0.35010 9	9.05405 4	5.86145 6	94.9748 7	185.041 6	279.268 3	529	283.882 8	317.5	295.546 6	296.894 4	329.268 3	2516.402	0.199885
31A-20 - 1.d	0	3.11582 4	1.15301 7	6.19256 6	62.1621 5	12.0781 3	152.261 3	108.587 5	64.6341 3	60.7	32.9670 3	21.6875	12.3886 6	14.3478 3	11.5040 7	326.8165	0.124149
31A-20 - 2.d	0	3.18107 7	0	4.09190 4	49.3243 2	8.17051 5	100	78.1163 4	45.1219 5	40.6	22.5274 7	14.6875	8.58299 6	9.87577 6	3.61788 6	223.1299	0.116337
31A-21 - 1.d	0	0.53833 6	0	0.15317 3	9.66216 2	7.28241 6	81.4070 4	156.786 7	175.609 8	236.	128.754 3	105.625	72.0647 8	77.6397 5	82.9268 3	1035.707	0.259661
31A-21 - 2.d	0	1.74551 4	0	2.05689 3	28.3783 8	32.5044 4	85.9296 5	87.5346 3	62.1951 2	81.4	49.4505 5	48.375	37.2469 6	44.0993 8	45.1219 5	455.4236	0.65823
31A-21 - 3.d	0	2.57748 8	1.20689 7	4.35448 6	43.9189 2	44.9378 3	123.618 1	115.235 5	80.0813 7	122.	70.5128 2	68.125	55.8704 5	72.6708 1	69.9187 1	655.1145	0.609881
31A-22 - 1.d	0	0.15823 8	0	0	6.28378 4	0.21314 4	59.2964 8	136.011 1	183.739 8	338	183.699 6	191.875	222.672 1	268.944 1	373.983 7	1898.925	0.011042
31A-22 - 2.d	0	0.21370 3	0	0.10065 6	5	2.66429 8	48.7437 2	152.077 6	219.105 7	416	246.520 1	285	357.085 7	482.608 7	613.821 1	2772.218	0.170663
31A-23 - 1.d	0.59071 7	6.78629 7	3.23275 9	6.78337	31.7567 6	19.0053 3	77.8894 5	186.703 6	215.447 2	303.	179.120 7	131.25	113.765 2	115.528 2	120.325 2	1365.84	0.382136
31A-23 - 2.d	0	2.30016 3	0.16163 8	1.99124 7	9.93243 2	4.26287 7	97.9899 5	224.930 7	269.105 7	357	209.340 7	166.875	116.194 3	144.720 5	152.032 5	1640.199	0.136642
31A-24 - 1.d	0	1.09298 5	0	0.74398 2	14.9324 3	22.0248 7	68.3417 1	99.1689 8	117.479 7	202	108.424 9	120	131.174 1	179.503 1	226.016 3	1183.767	0.689454
31A-24 - 2.d	0	1.61500 8	0	1.35667 4	15.8783 8	16.5186 5	54.2713 6	55.9556 8	32.5203 3	37.2	25.0915 8	16.1875	14.3724 7	9.13043 5	10.6910 6	201.149	0.562712
31A-25 - 1.d	0	0.94616 6	0	3.06345 7	21.4864 9	29.1296 6	98.9949 7	114.127 4	102.439 6	136.	69.5970 7	82.5	67.2064 8	70.1863 4	83.7398 4	726.3962	0.631606
31A-25 - 2.d	0	1.23980 4	0	0.72210 1	12.2297 3	8.70337 5	58.2914 6	55.1246 5	63.0081 3	85.3	48.3516 5	48.25	50.2024 3	45.9627 3	48.3739 8	444.5736	0.325969
31A-32 - 1.d	0	0.08319 7	0	0	5.60810 8	0.88809 9	53.2663 3	121.606 6	208.536 6	389	208.791 2	259.375	294.736 8	409.937 9	593.495 9	2485.48	0.051384
31A-32 - 2.d	0	1.32137	0	0.78774 6	10.4729 7	15.0976 9	45.2261 3	44.8753 5	28.9024 4	44.5	24.3589 7	23.4375	19.4332	22.4844 7	15.8536 6	223.8456	0.693715
31A-33 - 1.d	0	0.47308 3	0	0	9.79729 7	11.3676 7	115.577 9	372.022 2	671.544 7	145	842.490 8	983.125	902.429 1	1024.22 4	1096.74 8	7349.583	0.337817
31A-33 - 2.d	0	0.60358 9	0.24784 5	0.70021 9	23.1756 8	10.1243 3	122.110 6	170.914 1	177.642 3	294	166.483 5	175.625	176.113 4	185.714 3	193.902 4	1540.395	0.190315
31A-33 - 3.d	0	1.07667 2	0.39870 7	1.00656 5	21.3513 5	20.4262 9	71.3567 8	72.2991 7	76.0162 6	125.	70.1465 5	85	88.6639 7	119.254 7	132.520 3	769.4009	0.52331
31A-34 - 1.d	0	0.05546 5	0	0	4.12162 2	0	39.6984 9	103.047 1	136.991 9	244.	140.842 5	141.25	131.174 1	173.291 9	201.626	1272.423	0
31A-34 - 2.d	0	0.73409 5	0	1.66302 2	11.8243 2	2.29129 7	63.3165 8	137.396 1	166.666 7	252.	149.633 2	133.125	132.793 5	164.596 3	215.447 2	1351.858	0.08374
31A-35 - 1.d	0	1.79445 4	0	1.09409 2	16.9594 6	5.15097 7	59.2964 8	76.7313 9	59.3495 9	67.8	40.6593 4	34.375	30.3643 7	31.6770 2	26.4227 6	367.3794	0.162431
31A-35 - 2.d	0	1.35399 7	0.18319	1.90372	23.5135 1	22.9129 7	83.9196 5	98.3379 1	71.1382 1	82.8	45.6044 4	27.0625	25.1012 1	21.1801 2	20.7317 1	391.9561	0.515811
31A-35 - 3.d	0	2.07177 8	0.67887 9	2.60393 9	26.3513 5	19.5381 9	110.050 3	115.235 5	82.5203 3	84.7	47.2527 5	35.6875	25.5060 7	27.2670 8	20.3252	438.4944	0.362817

Samantha Nicole March  
Ultrahigh-pressure metapelites in the WGR

31A-37 - 1.d	0.78059 1	5.28548 1	3.67456 9	10.5251 6	85.8108 1	128.952	140.703 5	140.997 2	110.162 6	130. 6	75.4578 8	59.3125	57.0850 2	60.8695 7	68.6991 9	703.184	1.173559
31A-37 - 2.d	0.56540 1	5.07340 9	3.08189 7	11.0940 9	92.5675 7	127.353 5	183.417 1	177.008 3	139.430 9	182. 7	109.523 8	96.25	93.9271 3	101.242 2	123.170 7	1023.253	0.977375
31A-36 - 1.d	0	1.79445 4	0.50646 6	3.08533 9	37.1621 6	42.9840 1	151.758 8	141.551 2	113.008 1	133. 2	70.3296 7	62.3125	52.2267 2	52.7950 3	53.2520 3	678.6753	0.572374
31A-36 - 2.d	0	1.46818 9	0	2.34135 7	25	24.1563 1	74.8743 7	77.2853 2	60.9756 1	68.4	38.4615 4	30.5625	30.7692 3	24.7205 3	23.1707 3	354.3454	0.558334
31A-38 - 1.d	0.71308	2.78956	0.57112 1	5.20787 7	49.3243 2	76.0213 1	118.593	139.058 2	141.869 9	193	119.597 1	122.5	124.291 5	153.416 1	191.869 9	1185.603	0.993975
31A-38 - 2.d	0.36286 9	2.31647 6	0.85129 3	3.32603 9	35.8108 1	40.8525 8	97.4874 4	100.277 8	97.9674 9	123. 9	73.8095 2	72.5	65.1821 9	70.8074 5	87.3983 7	691.842	0.691414
31A-39 - 1.d	0	1.43556 3	0.48491 4	2.21006 6	26.4864 9	5.15097 7	85.4271 4	71.7451 5	52.4390 2	60.6	34.0659 3	29.9375	23.8866 4	18.8198 8	22.3577 2	313.8518	0.108288
31A-39 - 2.d	0	1.51712 9	0	2.23194 7	20.2027	21.4920 1	64.3216 1	56.5097 1	44.3089 4	52.4	32.9670 3	21.75	15.7894 7	18.0124 2	18.2926 8	260.0303	0.596202
31A-40 - 1.d	0	0.76672 1	0.16163 8	1.31291 4	3.51351 4	0.47957 4	73.3668 3	162.049 9	248.780 5	433. 2	208.241 8	220	190.688 3	178.882 7	165.040 7	1806.883	0.02987
31A-40 - 2.d	0.04219 4	0.32626 4	0	0.56892 8	5.06756 8	0	41.7085 4	127.700 8	232.520 3	510. 9	283.882 8	368.75	359.919 1	405.590 4	454.471 5	2743.735	0
31A-41 - 1.d	0	0.53833 6	0	0	2.09459 5	8.34813 5	37.6884 4	94.4598 3	173.577 2	466	260.622 7	408.75	627.530 4	993.788 8	1439.02 4	4463.753	0.939583
31A-41 - 2.d	0	2.16965 7	0.94827 6	2.40700 2	16.6891 9	21.4920 1	61.8090 5	48.4764 5	34.1463 4	40.9	20.3296 7	17.0625	12.7125 5	17.2049 7	16.0569 1	206.8894	0.669165
31A-41 - 3.d	1.68776 4	6.49265 9	3.77155 2	11.5973 7	60.1351 4	149.378 3	130.150 8	136.565 1	85.3658 5	98.4	59.5238 1	43.125	31.9838 1	34.7826 1	45.9349 6	535.6811	1.688496
31A-42 - 1.d	0	2.08809 1	0.56034 5	2.53829 3	28.7837 8	12.7886 3	83.9196	76.1772 9	58.5365 9	63.5	31.8681 3	36.875	39.2712 6	72.6708 1	111.788 6	490.6877	0.260207
31A-42 - 2.d	0	1.76182 7	0.33405 2	3.15098 5	28.0405 4	22.0248 7	90.4522 6	82.2714 7	60.1626 6	68.9	39.9267 4	32.3125	24.2915 5	21.8633 5	18.6991 9	348.4273	0.437331
31A-43 - 1.d	0	0.50571 3	0	0.39387 1	11.0135 1	3.37477 8	58.2914 6	126.315 8	166.260 2	288. 9	163.553 1	218.125	336.437 2	513.043 5	756.097 6	2568.732	0.133193
31A-43 - 2.d	0	1.45187 6	0.23706 9	2.58205 7	31.7567 6	4.44049 7	121.608	104.432 1	56.0975 6	56.4	30.0366 3	20.625	17.6518 2	12.4223 6	9.51219 5	307.1777	0.071455
31A-43 - 3.d	0	1.25611 7	0.77586 2	1.68490 2	31.7567 6	6.21669 6	143.718 6	131.301 9	98.3739 8	72.7	41.7582 4	25.25	16.6396 8	5.40372 7	6.09756 1	397.5251	0.092021
31A-44 - 1.d	0	0.01305 1	0	0	4.12162 2	0.71048	53.7688 4	187.257 6	297.967 5	534	301.465 2	305	272.874 5	303.726 7	314.634 1	2516.926	0.047726
31A-44 - 2.d	0	0.10277 3	0	0	8.44594 6	0	72.8643 2	201.385 2	265.447 2	416	250.915 8	217.5	188.259 1	180.124 2	194.308 9	1913.94	0
31A-44 - 3.d	0	0.53833 6	0	0.13129 1	12.6351 4	22.2024 9	113.567 8	237.673 1	280.894 3	407.	240.293 1	220.625	198.785 4	217.391 3	271.138 2	2073.9	0.586117
31A-45 - 1.d	0	0.63621 5	0	1.26914 7	18.8513 5	3.55239 8	73.3668 3	116.066 5	142.276 4	280	151.465 2	200	223.481 8	261.490 7	310.162 6	1684.943	0.095521
31A-45 - 2.d	0	0.8646 7	0.08620 4	1.11597 4	15.7432 4	6.21669 6	87.4371 9	127.700 8	139.430 9	228	123.260 1	135.625	152.226 7	172.049 7	193.495 9	1271.789	0.167558
31A-45 - 3.d	0	2.47960 8	0.33405 2	1.61925 6	28.7162 2	4.97335 7	93.4673 4	91.4127 4	64.6341 5	79.4	46.7033	35.5	24.6963 6	32.1118 4	33.7398 4	408.1982	0.095997
31A-46 - 1.d	0	1.28874 4	0	1.79431 1	6.41891 9	5.86145 6	68.8442 2	141.828 3	217.073 2	361	207.326	183.75	218.623 5	271.428 6	337.398 4	1938.428	0.278831

Samantha Nicole March  
Ultrahigh-pressure metapelites in the WGR

31A-47 - 1.d	0	2.83849 9	0.60344 8	4.81400 4	41.8918 9	41.7406 7	130.150 8	124.099 7	98.7804 9	133. 7	75.6410 3	65.375	55.0607 3	67.0807 5	63.4146 3	683.1523	0.56529
31A-47 - 2.d	0	2.72430 7	0.26939 7	4.98905 9	47.2973 9	53.6412 1	141.708 5	132.964 5	103.252 8	137. 8	79.6703 3	76.875	51.8218 6	57.7639 8	64.2276 4	704.3748	0.655213
31A-48 - 1.d	0.06329	0.61990 2	0	0.10065 6	8.37837 8	10.8348 1	64.8241 2	134.903 2	184.552 8	324	185.348	191.875	218.218 6	256.521 7	319.105 7	1814.525	0.464915
31A-55 - 1.d	0.37552	1.07667 2	1.71336 2	1.48796 5	6.82432 4	3.73001 8	50.2512 6	129.916 9	184.959 3	308	182.600 7	187.5	181.376 5	222.360 2	254.065	1650.779	0.201422
31A-55 - 2.d	0	3.55628 1	1.28232 8	5.25164 1	20.9459 5	17.4067 5	65.3266 3	57.6177 3	40.6504 1	46.9	26.0073 3	26.625	16.5991 9	25.4658 4	25.2032 5	265.0687	0.470568
31A-56 - 1.d	0	3.83360 5	0	0.65645 5	5.27027 5	6.74955 6	51.2562 8	124.930 7	250.813 7	763	423.076 9	653.75	910.121 5	1310.55 9	1682.92 7	6119.178	0.410663
31A-56 - 2.d	0	0	0	0	0	0	39.1959 8	129.362 9	214.634 1	506	235.348	248.125	235.627 5	257.142 9	243.902 4	2070.143	#DIV/0!
31A-56 - 3.d	0	0.66884 2	0	0.39387 3	2.97297 3	6.39431 6	32.6633 2	78.3933 5	117.886 2	201.	111.538 5	94.375	66.8016 2	75.1552 8	74.3902 4	820.3401	0.648886
31A-57 - 1.d	0	1.33768 4	0	3.10722 1	34.7297 3	30.7282 4	122.110 6	144.044 3	136.178 9	218.	125.457 9	136.25	139.271 3	159.006 2	191.056 9	1250.065	0.471857
31A-57 - 2.d	0	1.45187 6	0	2.45076 6	22.9729 7	35.7016 7	94.9748 7	119.113 6	97.1544 7	133.	70.8791 1	74.375	63.1578 9	67.0807 5	74.7967 5	699.6576	0.764319
31A-58 - 1.d	0	0.57096 2	0	0.19693 7	5.94594 6	5.32859 7	58.7939 7	154.570 6	221.951 2	402	245.421 2	268.125	266.396 8	288.819 9	361.788 6	2209.073	0.284994
31A-58 - 2.d	0	0.20391 5	0	0	4.18918 9	4.61811 7	58.7939 7	137.950 1	171.138 2	330	183.150 2	217.5	263.157 9	285.714 3	365.853 7	1954.464	0.294262
31A-59 - 1.d	0	0.32626 4	0	0.13129 1	7.63513 5	9.59147 4	45.2261 3	78.1163 4	97.9674 8	107.	58.9743 6	28.5	21.4574 9	20.8074 5	17.4796 7	431.0028	0.516158
31A-59 - 2.d	0	2.78956 2	0.33405 6	1.85995 8	26.0810 1	19.7158 6	70.3517 5	55.1246 9	39.0243 7	31.9	16.6666 7	11.375	6.19433 2	4.34782 6	1.09756 1	165.7304	0.460272
31A-60 - 1.d	0	2.69168 8	0.65732 2	4.31072 1	30.4054 9	21.3143 9	90.9547 7	111.080 3	117.073 2	180.	98.9011 2	109.375	97.5708 5	103.726 7	132.926 8	950.854	0.405308
31A-60 - 2.d	0	3.09951 1	0.94827 6	5.20787 7	33.7837 8	36.5897 6	105.527 1	93.6288 1	69.9187 9	90	49.6337	42.875	31.9838 1	39.3167 7	40.6504 1	458.0072	0.612804
31A-61 - 1.d	0	33.2789 6	0	0.50328 2	6.48648 6	1.49200 7	31.1557 8	64.2659 3	128.861 8	389	221.245 4	401.875	549.392 7	850.310 6	1142.27 6	3747.228	0.104953
31A-61 - 2.d	0	27.7324 6	0	1.53172 9	3.71621 6	3.19715 8	48.2412 1	74.7922 4	143.902 4	432	256.227 1	434.375	596.356 3	854.658 4	1227.64 2	4019.954	0.238784
31A-61 - 3.d	0	0.01305 1	0	0	1.14864 9	3.0373 2	24.6231 2	74.7922 4	171.951 2	594	331.318 7	684.375	1210.52 6	2234.16 1	3369.91 9	8671.044	0.571114
31A-62 - 1.d	0	0.73409 5	0	1.02844 6	7.02702 7	11.9005 3	57.7889 4	79.7783 9	126.016 3	271	155.860 8	229.375	284.615 4	438.509 3	587.804 9	2172.96	0.590552
31A-62 - 2.d	0	0.68515 5	0	0.21881 8	17.8378 4	12.7886 3	82.9145 7	112.742 4	113.414 6	147	93.2234 4	71.25	68.8259 1	57.7639 8	64.6341 5	728.8545	0.332535
31A-63 - 1.d	0.32489	4.53507 3	1.73491 4	6.80525 2	43.9189 2	19.3605 7	124.623 1	152.354 6	133.333 3	179	115.750 9	110	122.267 2	191.304 3	267.073 2	1271.084	0.261694
31A-63 - 2.d	0.27004	7.84665 6	5.92672 4	20.1312 9	95.9459 5	24.1563 1	196.482 4	217.728 5	204.878 5	311.	173.076 1	177.5	174.898 8	221.739 1	294.308 9	1775.23	0.175936
31A-64 - 1.d	0	2.20228 4	0	2.45076 6	35.1351 4	27.3534 6	88.4422 1	85.5955 7	64.6341 5	62.4	36.4468 9	25.4375	18.2186 2	15.5900 6	12.1138 2	320.4366	0.490695

Samantha Nicole March  
Ultrahigh-pressure metapelites in the WGR

31A-64 - 2.d	0	1.81076 7	0.25862 1	3.41356 7	37.1621 6	38.1882 8	123.618 1	97.7839 3	73.1707 3	80.6	45.2381	34.125	28.3400 8	16.8944 1	19.1056 9	395.2579	0.563428
31A-65 - 1.d	0	0.21696 6	0	0.07002 2	8.44594 6	2.27353 5	74.3718 6	162.603 9	213.821 4	307.	163.736 3	168.75	173.279 4	197.515 5	252.439	1639.245	0.090714
31A-65 - 2.d	0	0.53833 6	0	0.30634 6	11.4864 9	6.57193 6	58.7939 7	112.465 4	125.203 3	196	115.567 8	108.125	104.858 3	115.528 3	128.455 3	1006.203	0.252891
31A-66 - 1.d	0.38396	8.53181 6	7.54310 3	21.6630 2	82.4324 3	87.0337 5	94.4723 6	79.7783 9	74.7967 5	117	67.3992 7	75.0625	67.6113 4	59.0062 1	82.5203 3	623.1748	0.986248
31A-66 - 2.d	0.11814	8.05872 3	4.20258 6	16.6302 2	71.6216 2	68.3836 6	115.075 4	77.8393 4	48.3739 8	44.6	27.4725 3	14.75	9.71659 9	6.52173 9	6.95122	236.2254	0.75325
31A-67 - 1.d	0	1.54975 5	0.38793 1	1.92560 2	17.4324 3	25.2220 2	70.3517 6	88.3656 5	78.8617 9	126	71.0622 7	71.875	70.8502	73.9130 4	80.4878	661.4158	0.720217
31A-67 - 2.d	0	1.71288 7	0.56034 5	2.97593 4	35.1351 8	39.0763 5	100.502 5	91.6897 5	78.0487 8	82.7	54.5787 5	40	27.9352 2	33.4782 6	33.3333 3	441.7641	0.65759
31A-68 - 1.d	0	1.54975 5	0	1.85995 6	22.0945 9	22.0248 7	81.9095 5	72.0221 6	61.3821 1	62.7	34.6153 8	29.4375	27.9352 2	29.3167 7	39.4308 9	356.84	0.51773
31A-68 - 2.d	0	1.46818 9	0	1.20350 1	16.6216 2	10.1243 3	55.2763 8	52.6315 8	38.2113 8	47.8	27.2893 8	24.875	18.2186 2	22.7950 3	28.8617 9	260.6828	0.33401
31A-69 - 1.d	0	2.07177 8	1.70258 6	6.93654 3	52.7027 1	55.4174 1	144.221 4	113.019 5	85.3658 5	96.7	62.0879 1	41.125	35.6275 3	35.8385 1	37.3983 7	507.1626	0.635646
31A-71 - 1.d	0	0.34257 7	0	0	4.12162 2	0	61.3065 3	138.781 2	152.032 5	230.	129.487 7	150.625	184.210 5	263.975 2	406.504 1	1656.316	0
31A-70 - 1.d	0	4.17618 3	1.74569	5.99562 4	27.1621 6	20.0710 5	48.7437 2	30.4709 1	15.3658 5	18.4	8.60805 9	6.25	5.58704 5	6.52173 9	4.67479 7	95.87841	0.551605
31A-72 - 1.d	0	1.40293 6	0	1.22538 3	17.7027 7	6.39431 6	56.7839 2	72.2991 7	98.7804 9	208.	112.087 3	163.125	222.672 1	339.130 4	495.935	1712.33	0.201679
31A-72 - 2.d	0	2.13703 1	0.75431	4.13566 7	30.9459 5	11.3676 7	88.4422 1	59.5567 9	42.2764 2	47	26.9230 8	20.375	19.8380 6	18.3229 8	15.0813	249.3736	0.21729
31A-73 - 1.d	0	0.63621 5	0	0	15.2027 9	21.3143 6	90.4522 5	184.764 7	221.544 7	329.	184.981 7	191.875	192.307 7	229.192 5	276.016 3	1810.382	0.574781
31A-73 - 2.d	0	2.62642 7	0.68965 5	4.59518 6	38.5135 1	95.3818 8	106.532 7	86.4265 9	60.1626 9	68.7	41.3919 4	36.4375	27.1255 1	29.5652 2	33.7398 4	383.5492	1.48908
31A-74 - 1.d	0	1.12561 2	0	2.14442 8	28.3783 6	6.21669 6	145.728 6	187.811 6	142.276 4	127.	84.7985 3	41.875	9.71659 9	8.69565 2	4.34959 3	607.3234	0.09667
31A-75 - 1.d	0	1.06035 9	0	2.18818 4	21.2162 2	22.7353 5	76.3819 1	93.9058 2	95.9349 6	177	102.381 7	143.125	206.477 7	354.658 4	517.479 7	1690.963	0.564771
31A-75 - 2.d	0	1.25611 7	0	0	2.90540 5	4.79573 7	32.1608 7	89.4736 8	196.748 8	629	352.014 7	659.375	1098.78 5	1883.23 5	2752.03 3	7660.659	0.496122
31A-76 - 1.d	0	0.26753 7	0	0	8.17567 6	0.74600 4	80.9045 2	252.908 6	404.065 6	715	395.604 4	418.75	336.437 2	377.018 6	397.154 5	3296.938	0.029006
31A-76 - 2.d	0	0.27079 9	0	0.17505 5	11.8243 2	1.61634 4	71.3567 8	231.301 9	344.715 4	618	352.014 7	351.25	306.072 9	320.496 9	302.032 5	2825.884	0.055645
31A-77 - 1.d	0	3.42577 5	2.29525 9	5.77680 5	20.0675 7	26.9982 2	122.613 1	191.966 8	226.016 3	293.	160.439 7	150	131.174 1	145.962 7	173.983 7	1473.243	0.544276
31A-77 - 2.d	0	4.04567 7	1.93965 5	7.22100 7	32.4324 3	31.6163 4	109.045 2	214.127 4	223.983 7	306	195.421 2	157.5	142.915 9	152.173 9	194.308 9	1586.43	0.531641
31A-77 - 3.d	0	3.86623 2	1.07758 6	1.96936 5	14.8648 6	21.4920 4	56.7839 2	60.9418 3	44.7154 5	60.7	41.2087 9	21.875	17.4089 4	22.3602 5	15.8536 6	285.0639	0.739748

Samantha Nicole March  
Ultrahigh-pressure metapelites in the WGR

31A-78 - 1.d	0	0.50571	0	0.70021	12.7027	5.68383	104.020	149.584	118.292	147.	80.2197	65.8125	44.9392	35.2795	33.7398	675.1681	0.156363
31A-78 - 2.d	0	0.63621	0	1.90372	21.8243	8.88099	113.065	134.903	100.406	133.	70.3296	56.0625	44.9392	53.1677	39.4308	632.3396	0.178783
31A-79 - 1.d	4.68354	5.90538	5.81896	7.30853	25.6756	25.3996	81.9095	128.254	121.951	172.	101.098	90.625	86.6396	108.074	131.300	940.345	0.553859
31A-79 - 2.d	0	1.06035	0	1.90372	30.4054	45.8259	94.4723	111.634	86.9918	93.6	55.6776	43.9375	27.1255	25.1552	24.7967	468.9189	0.855034
31A-80 - 1.d	0	0.16476	0	0.37199	3.78378	0	74.8743	201.662	258.130	413.	217.216	180.625	144.129	131.677	170.731	1717.272	0
31A-80 - 2.d	0	1.32137	0	0	25.6756	9.94671	104.020	94.7368	89.0243	87.2	57.6923	31.875	18.2186	13.3540	10.9756	403.0768	0.192469
31A-81 - 1.d	0	0.66884	0	0	16.1486	3.19715	111.557	120.498	97.1544	104.	66.4835	61.5	58.7044	84.4720	105.691	699.2042	0.075326
31A-81 - 2.d	0	1.33768	0.25862	2.34135	41.8918	8.88099	204.522	210.803	130.081	137.	84.7985	79.375	76.9230	90.0621	106.097	915.9409	0.095946
31A-81 - 3.d	0	1.85970	0.17241	3.06345	38.5135	7.46003	144.723	136.842	86.1788	104.	59.7069	68.375	70.4453	95.0310	113.821	734.5005	0.099923
31A-82 - 1.d	0	0.03099	0	0	8.98648	0.51509	71.3567	178.670	243.495	356	199.633	189.375	178.137	167.080	207.317	1719.71	0.020341
31A-83 - 1.d	27.8481	49.4290	68.9655	81.4004	88.5135	117.229	114.070	180.055	285.772	805	487.179	824.375	1364.37	2249.06	3304.87	9500.701	1.16666
31A-83 - 2.d	0	1.64763	0.39870	2.56017	10.9459	26.2877	63.3165	102.493	110.569	173	100	93.125	108.097	122.981	143.089	953.3551	0.998546
31A-84 - 1.d	0	0	0	0	4.72973	0	49.7487	116.620	150.813	196.	106.227	84.375	76.9230	79.5031	76.0162	887.0781	0
31A-84 - 2.d	0	0.15660	0	0	5.67567	0.21314	85.4271	225.207	276.016	354	192.857	150.625	96.7611	94.4099	108.130	1498.007	0.00968
31A-85 - 1.d	0	1.84339	0.52801	1.26914	23.9864	24.6891	77.3869	63.9889	42.6829	49.7	31.3186	22.9375	17.0850	22.1739	23.5772	273.4642	0.573046
31A-85 - 2.d	0	1.56606	0	1.85995	23.4459	21.6696	65.8291	58.4487	48.3739	48	29.4871	21.25	19.4332	22.6708	25.6097	273.2737	0.55158
31A-86 - 1.d	0	9.44535	1.65948	2.66958	20.2702	11.9005	54.7738	90.8587	163.008	489	256.959	498.75	797.570	1329.19	1882.11	5507.454	0.357149
31A-86 - 2.d	12.6582	45.8401	8.62069	13.1291	42.5675	25.5772	93.9698	141.551	206.910	589	336.996	559.375	789.473	1173.91	1695.12	5492.342	0.404409
31A-87 - 1.d	0	2.96900	2.89870	5.01094	21.4864	24.8667	47.7386	100.554	126.829	191.	104.212	80.625	59.1093	63.9751	60.5691	787.5743	0.776429
31A-87 - 2.d	0.37130	3.55628	1.22844	4.68271	39.8648	36.9449	104.522	87.2576	64.2276	71.9	39.0109	30	36.0323	30.4968	27.2357	386.1613	0.572341
31A-87 - 3.d	0	4.64926	3.125	7.87746	37.1621	45.6483	98.9949	76.4542	65.0406	66	37.3626	31.25	22.6720	30.4347	17.4796	346.6941	0.752606
31A-88 - 1.d	0.96624	5.64437	2.42456	6.82713	50	107.637	94.4723	110.526	125.609	212.	114.468	112.5	107.692	136.646	145.528	1065.572	1.566127
31A-89 - 1.d	0	1.54975	0.26939	2.10065	33.7837	31.4387	107.035	89.1966	67.4796	78	42.8571	33.75	24.2915	35.6521	47.9674	419.1946	0.522814
31A-89 - 2.d	0	1.37031	0	0.70021	12.7027	13.4991	50.2512	56.7867	30.6910	37.8	18.1318	14.75	13.0364	12.1739	16.3821	199.7521	0.534298
31A-90 - 1.d	0	3.11582	0.625	3.30415	30.8108	35.3463	104.020	89.1966	66.2601	66.2	39.9267	31.25	16.2753	20.6211	23.9837	353.7137	0.624359

Samantha Nicole March  
Ultrahigh-pressure metapelites in the WGR

31A-90 - 2.d	0	2.36541 6	1.76724 1	4.39824 9	41.2162 2	40.8525 8	136.683 4	111.634 3	76.4227 6	80.8	47.2527 5	37.375	26.3157 9	27.0186 3	26.0162 6	432.8355	0.544286
31A-91 - 1.d	0	0.71778 1	0.26939 7	0.70021 9	10.7432 4	8.70337 5	57.7889 4	86.9806 1	97.1544 7	137. 4	76.3736 3	76.875	65.5870 4	84.4720 5	100.813	725.6558	0.349299
31A-91 - 2.d	0	4.32300 2	1.09913 8	9.40919 9	41.8918 1	17.0515 5	65.8291 4	37.9501 6	20.6910 6	22	12.0879 1	9	6.27530 4	10.9316 8	12.5609 8	131.4971	0.324705
31A-92 - 1.d	0	2.03915 2	0.84051 7	2.53829 3	29.7973	28.9520 4	91.4572 9	93.0747 9	75.6097 6	108	62.6373 6	63.125	62.7530 4	74.5341 6	86.1788 6	625.913	0.554602
31A-92 - 2.d	0	4.82871 1	2.38146 6	9.89059 1	50.6756 8	41.5630 6	127.638 2	99.1689 8	89.4308 9	127.	78.7545 1	80.25	72.4696 4	88.1987 6	95.1219 5	730.4948	0.516794
31A-93 - 1.d	0	1.41925 9	0.86206 9	4.20131 3	43.9189 2	41.0302	136.683 4	146.260 4	118.292 7	175.	107.692 3	98.125	96.3562 8	105.590 1	110.569 1	958.5858	0.529566
31A-93 - 2.d	0	1.45187 6	0	1.55361 1	15.2027	20.9591 5	57.2864 3	62.0498 6	51.6260 2	77.8	44.1391 9	35.75	37.6518 2	47.2049 7	44.3089 4	400.5308	0.710211
31A-94 - 1.d	0	0.20554 6	0	0	9.18918 9	3.73001 8	41.7085 4	108.033 2	146.748 7	286	163.736 3	191.25	174.493 9	224.844 7	247.967 5	1543.074	0.190528
31A-94 - 2.d	0	1.20717 8	0.39870 7	1.85995 6	33.1081 1	11.9005 3	128.140 7	117.728 5	76.8292 7	59.2	36.0805 9	22.75	12.7935 2	8.19875 8	8.13008 1	341.7107	0.182707
31A-94 - 3.d	0	1.69657 4	0	1.64113 8	15.4054 1	10.8348 1	51.2562 8	41.2742 4	24.3495 9	28	15.0183 2	9	6.84210 5	6.95652 2	8.33333 3	139.7741	0.385577
31A-95 - 1.d	0	2.08809 1	0	4.31072 2	35.8108 1	27.5310 8	98.9949 7	86.7036 5	64.6341 5	82.5	43.2234 4	39.5625	40.0809 7	31.4906 8	36.9918 7	425.1872	0.462391
31A-95 - 2.d	0	2.18597 1	0	2.16630 2	13.9864 9	10.4795 7	34.1708 5	32.1329 6	27.1544 7	34.6	15.5677 7	19.6875	10.6882 6	20.1242 2	10.9756 1	170.9308	0.47936
31A-96 - 1.d	0	5.25285 5	0.35560 3	6.17067 8	40.2702 7	28.0639 4	75.3768 8	55.6786 7	31.3821 1	29.4	15.9340 7	12.5	8.17813 8	9.44099 4	8.13008 1	170.6441	0.509375
31A-96 - 2.d	0	2.82218 6	0.09698 3	1.55361 1	14.9324 3	8.34813 5	19.4974 9	16.6205 5	9.47154 3	10.3	2.58241 8	3.625	3.03643 7	2.04968 9	3.08943 1	50.80502	0.489255
31A-96 - 3.d	0.24050	3.37683 6	0.95905 2	1.99124 7	8.37837 8	11.1900 5	29.1457 3	11.3573 4	10.8130 1	10.3	5.12820 5	2.25	1.37651 8	1.42857 1	1.42276 4	44.07641	0.716085
31A-97 - 1.d	0	2.56117 5	1.89655 2	2.93216 6	18.7162 2	20.9591 5	69.3467 3	126.592 8	175.203 3	348.	189.560 4	215	221.457 5	285.093 2	332.520 3	1894.227	0.58177
31A-97 - 2.d	0	2.65905 4	1.08836 2	3.98249 5	46.6216 2	53.4635 9	124.120 6	143.490 3	119.105 7	171	105.311 4	91.25	85.8299 6	98.1366 5	83.3333 3	897.4573	0.702817
31A-98 - 1.d	0	0.55464 9	0	0	9.59459 5	3.28596 8	35.6783 9	46.2603 9	38.6178 9	54	30.5860 8	28.125	19.4332 5	29.1925 5	37.3983 7	283.6135	0.177602
31A-98 - 2.d	0	2.23491 6	0.63577 9	2.01312 4	12.8378 9	22.2024 3	57.2864 9	57.6177 3	46.3414 6	51.1	29.1208 8	26.25	19.8380 6	26.0869 6	26.8292 7	283.1844	0.818709
31A-99 - 1.d	0.35443	7.03099 5	2.04741 4	6.52078 8	26.3513 5	16.5186 5	60.8040 2	91.9667 6	121.138 2	204.	113.186 8	120	114.574 9	129.813 7	160.975 6	1056.256	0.412674
31A-99 - 2.d	0	7.34094 6	3.57758 6	7.13347 9	37.6351 4	20.6039 1	100.502 5	91.1357 3	51.6260 2	67	40.4761 9	34.25	21.0526 3	33.9751 6	26.0162 6	365.532	0.335015
31A-100 - 1.d	0	2.85481 2	0.07543 1	3.76367 6	37.7027 1	9.23623 4	111.557 8	106.648 2	97.9674 8	141	78.3882 8	82.5	72.8744 9	73.9130 4	76.0162 6	729.3078	0.142416
31A-100 - 2.d	0	2.52854 8	1.92887 9	3.69803 1	24.3918 9	23.8010 7	64.3216 1	62.6038 8	41.4634 1	55.9	32.9670 3	28.875	25.5060 7	32.4223 6	32.9268 3	312.6646	0.60089
31A-101 - 1.d	0	0.07993 5	0	0.08752 7	6.35135 1	2.14920 1	54.2713 6	129.916 9	206.504 1	396	225.274 7	300.625	392.712 6	602.484 5	865.853 7	3119.371	0.11576



Samantha Nicole March  
Ultrahigh-pressure metapelites in the WGR

31A-101 - 2.d	0	0.53833	0	0.21881	8.10810	4.61811	75.3768	129.639	168.292	295	167.582	191.25	220.242	281.987	406.504	1860.5	0.186804
31A-102 - 1.d	0	2.00652	0.08620	3.30415	32.5	23.0905	80.4020	74.2382	57.7235	60.7	31.8681	29	20.2429	21.2422	14.6341	309.6492	0.45171
31A-102 - 2.d	0	2.80587	1.27155	5.97374	53.3783	54.3516	135.678	139.058	97.5609	112.	67.2161	54.4375	46.9635	52.8571	42.6829	613.3764	0.638668
31A-103 - 1.d	0	1.43556	0	0.78774	17.0270	17.0515	67.8392	71.7451	80.4878	168.	100.366	133.125	156.680	204.347	238.211	1153.564	0.50171
31A-103 - 2.d	0	1.33768	0	1.55361	13.4459	16.3410	45.7286	47.3684	52.4390	90	49.2674	58.75	61.5384	96.2732	104.065	559.7016	0.659006
31A-104 - 1.d	0	0.81566	0	1.42231	18.1756	5.15097	100.502	110.803	75.2032	65.9	37.9120	21.8125	7.93522	6.52173	8.65853	334.7467	0.120519
31A-104 - 2.d	0	1.19086	0.07543	3.01969	48.6486	17.0515	246.231	265.097	202.845	166.	105.311	54.1875	29.5546	18.8819	14.1869	856.365	0.155796
31A-105 - 1.d	0	2.31647	0	2.82275	14.1216	8.52575	37.1859	20.4986	10.7723	12.4	6.77655	4.1875	1.57894	2.36024	3.08943	61.66366	0.37205
31A-105 - 2.d	0	16.6557	1.04525	6.23632	52.0270	383.659	145.728	173.407	156.910	233.	147.619	170.625	217.813	298.757	376.829	1775.863	4.406141
31A-105 - 3.d	0	28.8743	3.06034	11.2691	91.2162	587.921	257.286	274.792	223.170	319.	191.758	220	251.417	305.590	373.983	2160.612	3.837736
31A-106 - 1.d	0	2.34910	0.25862	2.10065	43.2432	8.34813	116.080	88.6426	56.9105	62.1	34.0659	26.25	23.4817	22.5465	15.8536	329.8512	0.117829
31A-107 - 1.d	0	2.78956	1.64870	5.92997	41.8918	41.7406	122.613	115.512	68.2926	64.4	37.1794	23.3125	17.8137	15.9627	9.87804	352.3517	0.582406
31A-107 - 2.d	0	2.90375	0	1.64113	39.8648	38.1882	93.9698	85.3185	54.0650	50.8	26.7399	18.9375	16.5991	10	6.34146	268.8017	0.623937
31A-108 - 1.d	0	3.36052	0.64655	3.80744	21.1486	19.3605	86.9346	180.886	214.227	283.	157.875	126.75	104.453	100.621	113.008	1281.522	0.451523
31A-108 - 2.d	0.35021	3.89885	3.34051	4.81400	24.9324	30.5506	111.557	160.941	190.243	260.	154.029	123.75	121.052	149.068	183.739	1342.926	0.579279
31A-109 - 1.d	0	2.59380	0.75431	2.82275	35.1351	8.17051	84.4221	74.5152	40.2439	39.9	23.4432	15.375	9.67611	15.7764	12.4390	231.3689	0.15002
31A-109 - 2.d	0	2.61011	0.56034	2.25382	21.9594	11.7229	76.8844	63.1578	38.2113	36.4	18.6813	13.875	8.94736	9.31677	12.2357	200.8255	0.285302
31A-110 - 1.d	0	2.18597	0	1.26914	19.1891	6.92717	44.2211	42.6592	45.9349	89	42.3076	65	76.9230	124.844	174.796	661.4665	0.237801
31A-110 - 2.d	0	1.77814	0	2.40700	24.5270	4.44049	73.3668	73.4072	79.2682	130	69.5970	85	78.9473	105.590	132.113	753.9238	0.104679
31A-111 - 1.d	0	0.26101	0	0	7.63513	3.01953	67.3366	168.975	180.894	249.	150.183	116.25	117.004	112.422	136.991	1231.821	0.13317
31A-111 - 2.d	0	0.14355	0	0.17505	11.3513	2.04262	76.3819	165.097	197.154	260.	154.578	130	114.574	119.254	152.845	1293.705	0.06937
31A-112 - 1.d	0	1.30505	0	1.53172	17.5	16.6962	70.8542	80.0554	70.3252	107.	63.9194	63.6875	69.6356	92.5465	108.943	656.2128	0.474152
31A-112 - 2.d	0	1.72920	0	2.25382	31.6891	36.0568	104.020	127.146	121.544	199.	117.582	146.25	171.255	195.652	223.577	1302.308	0.62802
31A-113 - 1.d	0	1.64763	0.08620	1.94748	22.0270	19.0053	59.7989	70.6371	61.7886	123	61.7216	89.375	114.17	165.217	256.097	942.0073	0.523661
31A-113 - 2.d	0	1.99021	0.21551	2.45076	31.3513	36.7673	103.015	91.6897	69.5122	85.8	57.5091	46.8125	34.4129	39.3167	36.5853	461.6387	0.646969

Samantha Nicole March  
Ultrahigh-pressure metapelites in the WGR

31A-114-1.d	0.51898	69.1680	1.01293	1.37855	25.6081	5.15097	108.542	200.554	375.609	105	626.373	1018.12	1299.59	1821.11	2292.68	8692.058	0.097701
31A-114-2.d	0	0.02936	0	0	8.85135	3.05506	54.7738	199.723	373.577	828	458.791	541.25	565.991	632.298	663.821	4263.453	0.138749
31A-114-3.d	1.51898	52.5285	1.30387	1.53172	14.2567	3.55239	68.3417	156.232	282.113	747	426.739	625	732.793	1021.73	1280.48	5272.107	0.113807
31A-115-1.d	0	1.17455	0.15086	0.70021	16.0135	20.4262	70.8542	80.3324	77.2357	125	69.9633	61.875	68.8259	82.6087	95.1219	660.9631	0.606405
31A-115-2.d	0	1.43556	0	1.09409	12.9054	21.6696	49.7487	52.6315	44.7154	56.2	31.8681	29.375	26.3157	27.7018	26.8292	295.6371	0.855214
31A-115-3.d	0	1.15823	0	0.30634	20.0675	17.5843	49.7487	59.2797	48.3739	69.3	39.5604	41.8125	39.6761	36.6459	42.6829	377.3317	0.55653
31A-116-1.d	0	1.35399	0	3.74179	25.1351	23.2682	92.4623	85.3185	77.2357	119	68.3150	78.125	67.2064	81.9875	90.2439	667.4323	0.482658
31A-116-2.d	0	1.77814	0	1.44420	17.4324	16.3410	52.7638	56.7867	47.5609	77.1	39.3772	46.25	38.0566	57.7639	60.9756	423.8712	0.538806
31A-117-1.d	0.14346	3.80097	2.02586	5.25164	23.5135	19.1829	89.4472	112.188	117.073	164	89.3772	86.25	82.9959	87.5776	108.130	847.5925	0.418286
31A-117-2.d	0.08016	4.53507	2.82327	10.6126	47.9729	38.1882	96.4824	88.0886	59.3495	50	30.7692	18.5625	9.47368	8.44720	4.39024	269.0811	0.561316
31A-118-1.d	0	0.73409	0	0	1.68918	0.63943	40.7035	118.836	226.016	659	320.879	483.125	659.919	1024.84	1361.78	4854.409	0.077115
31A-118-2.d	0	3.7031	0.08620	0.35010	8.78378	3.23268	38.6934	95.5678	173.170	517.	281.318	555	889.473	1518.63	2252.03	6282.797	0.175349
31A-118-3.d	0	0.30832	0	0	3.44594	14.7424	42.2110	118.836	165.040	290.	147.619	124.375	136.842	137.888	145.935	1267.237	1.222369
31A-119-1.d	0	3.80097	2.04741	4.70459	20.6081	10.3019	67.8392	103.047	111.788	174.	103.113	75.75	64.7773	76.3975	75.6097	784.8839	0.275524
31A-119-2.d	0	3.86623	2.40301	5.31728	14.1891	9.94671	56.2814	102.216	122.357	185.	109.157	83.75	78.1376	90.6832	103.252	874.6542	0.35198
31A-120-1.d	0	1.20717	0	1.42231	18.2432	9.23623	75.3768	92.7977	106.097	201	116.117	140	136.842	159.627	175.203	1127.685	0.249072
31A-120-2.d	0	1.02773	0	1.31291	21.2837	22.9129	71.3567	85.5955	82.9268	149.	84.0659	96.875	113.765	141.614	156.097	910.141	0.587948
31A-120-3.d	0	1.35399	0.08620	0.43763	22.7027	12.0781	68.8442	91.6897	100	199	121.245	149.375	144.534	170.186	179.268	1155.299	0.305512
31A-121-1.d	0	0.31484	0	0	7.36486	3.01953	52.7638	121.883	206.097	500	274.725	368.75	376.518	465.838	540.650	2854.464	0.153176
31A-121-2.d	0	0.66884	0	0.19693	8.24324	0.55062	51.2562	67.5900	65.0406	118.	67.2161	74.3125	86.6396	101.242	101.626	681.7672	0.026787
31A-121-3.d	0	0.61990	0	0	9.05405	2.04262	51.2562	72.8531	82.5203	159.	93.7728	114.375	119.838	140.372	146.341	929.1736	0.094819
31A-122-1.d	0	0.73409	0.06465	0.59081	5.33783	6.39431	57.7889	128.808	186.585	327	181.868	209.375	218.218	282.608	370.731	1905.196	0.364073
31A-122-2.d	0	1.51712	0	2.66958	22.5675	37.6554	72.3618	85.5955	63.0081	97.2	58.0586	54.875	51.0121	51.5528	43.9024	505.2047	0.931816
31A-122-3.d	0	1.20717	0	0.39387	19.7973	30.373	63.3165	62.8808	57.3170	79.8	42.6739	40.4375	34.4129	39.8136	34.5528	391.8889	0.857879
31A-123-1.d	0	0.88091	0	0	12.0270	9.23623	38.1909	50.1385	72.7642	150.	83.6996	94.375	112.145	132.298	170.731	866.853	0.430959

Samantha Nicole March  
Ultrahigh-pressure metapelites in the WGR

31A-123 - 2.d	0	0.44371 9	0	0.39387 3	6.28378 4	6.39431 6	33.6683 4	69.2520 8	106.504 1	235	130.586 1	150.625	202.429 1	267.080 7	378.048 8	1539.526	0.439615
31A-124 - 1.d	0	1.97389 9	0.19396 6	1.68490 2	13.3108 1	31.0834 8	55.2763 8	93.9058 2	110.975 6	200. 5	106.959 7	145	172.469 6	270.807 5	414.634 1	1515.252	1.145929
31A-124 - 2.d	0	2.56117 5	0.63577 6	2.58205 7	24.0540 5	15.6305 5	53.2663 3	40.1662 8	27.6422 8	31.3	17.9487 2	14.3125	8.58299 6	11.8633 5	12.6016 3	164.4177	0.43667
31A-125 - 1.d	0	1.61500 8	0	2.58205 7	16.9594 6	6.39431 6	84.9246 2	71.4681 4	50.4065	66.1	39.3772 9	30.75	22.2672 1	27.5155 3	28.4552 8	336.34	0.168489
31A-125 - 2.d	0	1.28874 4	0.39870 7	2.10065 6	27.7027 3	16.3410 3	93.9698 5	82.2714 7	58.9430 9	73	36.9963 4	31.375	31.5789 5	29.5031 1	29.6748	373.3427	0.320276
31A-126 - 1.d	0	0.99510 6	0	1.29102 8	23.7837 8	17.2291 3	111.557 8	272.576 2	465.447 2	105	635.531 1	783.125	805.668 9	904.968 9	963.414 6	5881.731	0.334482
31A-126 - 2.d	0	1.61500 8	0	2.60393 9	34.4594 6	28.5968	118.593	131.856	142.682 9	233	125.457 9	143.75	129.959 5	165.217 4	161.382 1	1233.306	0.447336
31A-126 - 3.d	0	1.30505 7	0	2.53829 3	32.9729 7	25.9325	97.9899 5	122.714 7	93.0894 3	143.	88.0952 9	86.875	82.5910 9	102.484 5	114.227 6	833.9776	0.45622
31A-127 - 1.d	0	3.23001 6	1.42241 4	4.35448 6	58.1081 1	24.1563 1	167.336 7	140.166 2	100.406 5	113.	62.8205 7	57.6875	44.5344 1	40.3726 7	33.7398 4	593.4276	0.244972
31A-127 - 2.d	0	4.22512 2	1.01293 1	8.14004 4	80.4054 1	41.9182 9	183.919 6	161.772 9	108.536 6	120	68.8644 7	54.375	39.2712 6	42.6708 1	42.6829 3	638.1739	0.344705
31A-128 - 1.d	0.08016 9	3.47471 5	1.98275 9	6.01750 5	40.5405 4	47.2468 9	137.185 9	104.155 1	83.7398 4	99	60.0732 6	51.1875	38.0566 8	46.7080 7	58.1300 8	541.0506	0.633539
31A-128 - 2.d	0.14767 9	4.40456 8	2.01508 6	6.21444 2	42.5675 7	49.0230 9	91.9598 3	84.4875 2	61.7886 5	76.5	45.4212 5	38.8125	38.0566 8	34.0993 8	34.1463 4	413.3123	0.783542
31A-129 - 1.d	1.05485 2	10.8156 6	6.57327 6	22.3194 7	117.567 6	75.4884 5	162.814 1	114.681 4	91.8699 2	171.	108.058 6	151.25	240.890 7	422.981 4	638.211 4	1939.843	0.545621
31A-129 - 2.d	3.79746 8	14.6818 9	16.0560 3	26.4770 2	101.351 4	97.6909 4	190.452 3	122.714 7	113.414 6	244	142.490 8	185	293.117 4	500	670.731 7	2271.469	0.703148
31A-130 - 1.d	0	1.19086 5	0	1.11597 4	18.0405 4	2.82415 6	68.8442 2	84.4875 3	55.6910 6	75.9	42.1245 4	36.1875	29.1498 9	30.9937 9	31.7073 2	386.2415	0.080136
31A-130 - 2.d	0	1.33768 4	0	1.09409 2	12.0945 9	1.29662 5	61.8090 5	57.0637 1	47.1544 7	54.2	29.6703 3	21.25	15.8704 5	22.3602 5	16.6666 7	264.2359	0.047423
31A-130 - 3.d	0	1.12561 2	0	1.15973 7	15.8783 8	3.73001 8	49.2462 3	50.9695 3	41.4227 6	48.9	28.3882 8	22.25	15.0607 3	13.4782 6	15.8130 1	236.2826	0.133389
31A-131 - 1.d	0	0.94616 6	0	0.41575 5	24.5270 3	20.2486 7	55.2763 8	57.6177 3	46.3414 6	55	29.6703 3	27.8125	21.0526 3	19.3167 7	22.3577 2	279.1691	0.549926
31A-131 - 2.d	0	1.07667 2	0	1.00656 5	13.5810 8	21.4920 1	51.2562 8	49.0304 7	47.9674 8	55.3	28.2051 3	26.0625	20.6477 7	21.1801 2	19.5122	267.9057	0.814585
31A-132 - 1.d	0	1.02773 2	0.26939 7	2.73523 8	16.0810 8	7.99289 5	77.8894 5	119.944 6	150.406 5	266	153.846 2	173.75	179.757 1	217.391 3	263.414 6	1524.51	0.225843
31A-132 - 2.d	0	0.97879 3	0	0.78774 6	19.7297 3	3.19715 8	90.9547 7	99.4459 8	59.3495 9	49.6	26.9230 8	12.4375	5.58704 5	0.93167 7	4.67479 7	258.9497	0.075473
31A-132 - 3.d	0	1.23980 4	0	0.61269 1	17.5	2.87744 2	75.3768 8	75.3462 6	41.0569 1	31.8	18.4981 7	7.375	2.18623 5	1.55279 5	0.20325 2	178.0186	0.079226
31A-133 - 1.d	1.94092 8	12.3164 8	14.7629 3	30.1969 4	141.216 2	158.969 8	198.995	126.869 8	72.7642 3	78.7	48.7179 5	32.375	19.8380 6	23.2298 1	21.5447 2	424.0396	0.948312
31A-133 - 2.d	1.77215 2	9.52691 7	8.29741 4	24.0700 2	114.864 9	179.396 1	200	153.185 6	85.7723 6	87.6	52.9304 5	38	20.6477 7	24.4099 4	23.1707 3	485.7168	1.183598
31A-134 - 1.d	0.35021 1	1.82708	1.63793 1	2.10065 6	14.2567 6	29.1296 6	50.2512 6	99.4459 8	134.146 3	261	143.406 6	170	170.040 5	200.621 1	228.861 8	1407.522	1.088307

Samantha Nicole March  
Ultrahigh-pressure metapelites in the WGR

31A-134 - 2.d	0	3.7031	1.40086	3.67614	29.5945	130.195	145.728	173.961	143.089	178.	102.381	95	74.8987	80.7453	65.8536	914.7294	1.982517
31A-135 - 1.d	0	0	0	0	14.4594	0.47957	80.4020	177.562	163.414	179.	106.959	74.3125	59.5141	73.9130	84.5528	919.7292	0.014065
31A-135 - 2.d	0.16033	0.40783	0	0	7.97297	2.30905	58.2914	113.019	108.130	130.	73.8095	62.5	52.2267	63.3540	86.5853	690.1251	0.107108
31A-136 - 1.d	0	1.19086	0	0.21881	10	11.1900	36.6834	49.3074	55.6910	97	52.5641	53.125	47.7732	45.9627	54.0650	455.4887	0.584248
31A-136 - 2.d	0	1.69657	0.08620	1.37855	21.7567	22.3801	51.7587	50.1385	38.3739	45.7	25.0915	21.875	15.5465	19.0683	18.2926	234.0866	0.666919
31A-136 - 3.d	0	2.16965	0.71120	3.21663	30.9459	27.1758	81.9095	70.9141	50.4065	57.1	32.9670	23.8125	23.8866	16.9565	23.5772	299.6206	0.539776
31A-137 - 1.d	0.29113	7.22675	4.31034	12.3632	58.7837	80.9946	121.105	127.146	125.203	187.	114.652	108.75	119.433	155.279	196.341	1134.706	0.959944
31A-137 - 2.d	0	6.24796	4.20258	12.6914	49.3243	98.7566	108.040	110.249	124.796	197.	105.860	146.25	189.068	272.670	411.382	1557.479	1.35283
31A-138 - 1.d	0	0.61990	0.45258	0.85339	10.3378	3.42806	83.9196	176.177	198.780	280.	161.538	145.625	126.315	134.161	154.065	1377.264	0.116386
31A-138 - 2.d	0	0.35073	0	0.08533	7.63513	2.75310	93.9698	195.567	204.878	280.	170.146	148.75	118.218	136.024	143.495	1397.882	0.102783
31A-139 - 1.d	0	1.56606	0	2.42888	23.9864	20.2486	71.8593	59.2797	40.2439	45.4	24.9084	21.0625	21.8623	19.0062	19.9187	251.6819	0.487721
31A-139 - 2.d	0	1.95758	0.53879	2.97593	28.3783	23.6234	66.3316	52.6315	48.7804	47.4	30.7692	21.875	15.8299	20.1863	18.6991	256.1718	0.544489
31A-140 - 1.d	0	2.31647	0.17241	3.67614	45.2702	25.5772	100	80.3324	52.8455	53.9	31.3186	21.1875	16.5991	12.3602	9.18699	277.7306	0.380143
31A-140 - 2.d	0	2.16965	0	1.96936	15.4729	16.1634	49.7487	40.1662	28.0487	31.5	13.0036	12.875	9.43319	4.84472	3.57723	143.4488	0.582579
31A-141 - 1.d	0	1.81076	0.17241	3.71991	39.1891	30.0177	105.025	104.432	109.756	182.	106.410	123.75	131.174	166.459	170.731	1095.214	0.467895
31A-141 - 2.d	0	1.45187	0	3.45733	22.2297	27.7087	64.3216	85.8725	70.3252	122.	72.1611	77.5	79.7570	104.968	116.260	728.9451	0.732775
31A-142 - 1.d	0	1.63132	0	1.85995	27.7027	5.86145	92.4623	78.6703	46.3414	44.1	21.4285	13	10.3238	8.26087	8.94308	231.0682	0.115814
31A-142 - 2.d	0	3.19739	1.08836	5.57986	57.4324	11.1900	150.251	118.559	95.9349	130	77.1062	64.1875	70.4453	67.7018	58.5365	682.472	0.12046
31A-143 - 1.d	0	2.46329	1.70258	3.91684	36.6891	23.8010	102.010	79.7783	58.5365	68.5	39.1941	32.125	22.6720	25.2173	24.7967	350.8203	0.38905
31A-143 - 2.d	0	2.15334	0	2.29759	12.1621	11.9005	36.6834	30.1939	29.2682	28.7	17.5824	12	8.09716	16.8944	20.3252	163.0614	0.563412
31A-144 - 1.d	0	1.20717	0	0.4814	13.5810	6.03907	42.7135	76.1772	126.829	255.	147.252	194.375	254.251	393.788	544.715	1992.79	0.250738
31A-144 - 2.d	0	1.64763	0.59267	4.72647	47.2973	49.0230	128.140	118.282	89.0243	93.6	51.8315	47	36.8421	37.0186	34.5528	508.152	0.629708
31A-145 - 1.d	0	0.52202	0	0.94091	15.4729	6.57193	100.502	227.146	294.715	363	212.637	171.25	124.696	122.360	137.804	1653.611	0.166655
31A-146 - 1.d	0	0.25285	0.18319	0	10	1.27886	67.8392	157.063	176.016	250.	145.054	128.125	129.554	144.099	202.845	1333.259	0.0491
31A-146 - 2.d	0	0.78303	0	0.61269	27.6351	11.3676	98.9949	118.836	108.536	147.	82.7838	86.25	101.619	134.161	190.243	969.9319	0.217337

Samantha Nicole March  
Ultrahigh-pressure metapelites in the WGR

31A-147-1.d	0.36708	1.30505	0.17241	1.13785	11.4864	4.61811	70.8542	136.842	173.170	254	141.758	127.5	116.194	138.509	142.682	1230.658	0.161878
31A-147-2.d	0	2.87112	0	2.01312	19.9324	8.88099	69.3467	54.5706	52.8455	70.1	37.7289	33	38.0566	37.2670	41.4634	365.0323	0.238874
31A-148-1.d	0	0.39151	0	0	1.75675	0	39.1959	111.911	200	549	304.029	543.75	846.153	1546.58	2357.72	6459.152	0
31A-148-2.d	0	4.22512	0.18319	1.77242	16.1486	5.50621	16.0301	17.7285	7.92682	16.8	7.32600	9.9375	10	9.68944	11.0975	90.58587	0.342229
31A-149-1.d	1.51898	23.1647	2.69396	5.18599	27.7027	16.5186	93.9698	152.631	271.544	721	415.750	687.5	927.125	1354.03	1825.20	6354.793	0.323757
31A-149-2.d	1.22362	7.34094	1.77801	2.42888	5.20270	6.21669	34.6733	67.0360	104.878	324	169.230	305.625	486.639	814.285	1235.77	3508.368	0.462857
31A-150-1.d	0	1.85970	0.32327	2.27571	32.0270	7.46003	97.9899	90.0277	50.8130	50.6	28.5714	18.3125	12.2267	7.70186	9.02439	267.2776	0.133166
31A-150-2.d	0	1.54975	0	0.67833	11.2162	3.25044	43.7185	42.6592	19.9593	23.3	8.79120	7	3.60323	2.91925	3.53658	111.7689	0.146787
31A-151-1.d	0	1.50081	0	1.15973	11.6891	1.97158	38.6934	40.7202	30.6910	32.5	16.3003	13.375	11.5789	11.8012	10.4878	167.4546	0.092705
31A-151-2.d	0	3.42577	0	1.83807	10.2702	9.41385	18.6934	10.8033	6.26016	7.68	4.74359	2.6875	0.97166	2.91925	1.62601	37.69151	0.679409
31A-152-1.d	0	0.29037	0	0.28446	9.66216	1.97158	50.2512	94.4598	132.113	278	159.707	226.25	272.469	398.757	536.585	2098.343	0.089475
31A-152-2.d	0	2.39804	0.87284	5.47046	29.7297	15.2753	95.4773	77.8393	56.5040	71.8	35.7142	43.75	48.1781	75.7764	111.788	521.3508	0.286711
31A-152-3.d	0	2.62642	0.78663	2.23194	19.2567	11.9005	56.2814	45.1523	29.9187	30.8	15.7509	11.8125	9.31174	8.81987	6.09756	157.6636	0.361487
31A-153-1.d	0.41350	2.23491	1.28232	2.82275	12.8378	14.5648	60.3015	78.9473	87.8048	145	83.6996	95	74.4939	93.1677	104.065	762.1785	0.523474
31A-153-2.d	0	1.30505	0.18319	3.96061	39.1891	33.0373	128.643	139.335	104.878	122	72.8937	54.4375	42.9149	42.4223	43.9024	623.6843	0.465295
31A-154-1.d	0.57384	4.04567	2.27370	5.12035	20.6081	18.6500	77.3869	120.775	143.495	213	120.512	115.625	133.603	152.795	181.300	1181.608	0.467012
31A-154-2.d	0.06751	3.81729	1.46551	7.08971	26.6891	25.9325	85.9296	131.301	132.113	184	106.593	89.375	72.8744	95.6521	114.227	926.2385	0.541508
31A-155-1.d	0	1.50081	0	1.77242	47.9729	19.5381	110.050	208.310	211.382	271	164.835	135	140.890	146.583	197.154	1475.157	0.2689
31A-155-2.d	0	1.33768	0.15086	4.09190	19.3918	10.3019	97.4874	165.097	164.227	235	140.659	114.375	88.6639	101.863	123.577	1134.363	0.236938
31A-156-1.d	1814.34	1288.74	991.379	722.100	472.973	168.738	266.331	263.157	346.341	732	415.934	600.625	858.299	1389.44	1922.76	6528.563	0.475429
31A-156-2.d	0	0.29037	0	0	5.33783	2.27353	58.7939	154.847	228.861	423	220.696	246.875	279.757	384.472	528.455	2467.565	0.128337
31A-156-3.d	0	0.53833	0	0	7.70270	5.32859	58.7939	139.058	254.878	481	264.468	278.75	308.097	391.304	519.918	2638.275	0.250395
31A-158-1.d	0	0.38988	0	0.65645	11.5540	3.55239	65.8291	153.185	181.300	270	149.084	163.125	165.587	234.161	334.552	1651.897	0.128809
31A-158-2.d	0	0.61990	0	0.67833	11.8243	6.03907	58.7939	98.0609	115.853	209	120.512	146.25	206.477	281.987	426.829	1605.472	0.229042
31A-159-1.d	0	1.48450	0	1.92560	10.6081	15.4529	55.7788	41.5512	36.9918	42.4	26.5567	17	15.0607	11.9254	15.2845	206.7706	0.635268

Samantha Nicole March  
Ultrahigh-pressure metapelites in the WGR

31A-159 - 2.d	0	1.61500	0	1.00656	14.5945	12.6110	53.7688	47.6454	40.6504	44.5	26.0073	17.1875	17.4089	16.2111	23.5772	233.188	0.450182
		8		5	9	1	4	3	1		3		1	8	4		
31A-160 - 1.d	0	0.34257	0	0.10722	4.45945	0.19538	49.2462	98.0609	89.0243	100.	57.1428	44.375	37.2469	34.2857	37.8048	498.4407	0.013184
		7		4	9	2	3	4	9	5	6		6	4	8		
31A-160 - 2.d	0	0.32137	0	0.26258	11.9594	0.19538	58.2914	108.310	112.195	120.	70.6959	45.875	38.4615	43.4782	46.7479	586.2641	0.0074
				2	6	2	6	2	4	5	7		4	6	7		
31A-161 - 1.d	0.33333	5.48124	4.52586	12.0350	42.5675	24.5115	43.2160	30.1939	23.0894	32.1	23.4432	19.625	13.3603	16.5217	18.6991	177.0328	0.57149
		3	2	1	7	5	8	1	3		2		2	4	9		
31A-161 - 2.d	0.08016	5.07340	3.52370	8.68709	50	31.0834	56.2814	35.1800	22.6016	21.7	13.9194	9.75	6.47773	6.64596	7.07317	123.348	0.585952
		9	7			8	1	6	3		1		3	3	1		
31A-162 - 1.d	0	0.19739	0	0.26258	6.28378	0.44405	65.8291	152.908	147.967	186.	105.677	83.125	61.9433	65.2173	76.0162	879.4557	0.021833
				2	4		5	6	5	6	7		2	9	6		
31A-163 - 1.d	0	1.54975	0.51724	2.38512	33.0405	34.2806	105.025	111.911	91.8699	118.	60.9890	60.25	46.9635	53.4161	53.6585	597.8585	0.581941
		5	1		4	4	1	4	2	8	1		6	5	4		
31A-164 - 1.d	0	3.50734	1.48706	5.40481	11.5540	9.41385	75.8794	125.484	141.056	224.	130.219	132.5	117.004	184.472	225.609	1280.747	0.317935
		1	9	4	5	4		8	9	4	8				8		
31A-164 - 2.d	0	4.61663	2.09051	4.83588	33.7837	19.1829	52.7638	39.3351	21.9512	27.7	14.6520	14.5625	9.55465	11.1180	8.78048	147.6541	0.454353
		9	7	6	8	5	2	8	2		1		6	1	8		
31A-164 - 3.d	0	2.88743	0.44181	2.45076	20.7432	13.1438	90.4522	83.9335	63.8211	66.8	39.5604	30.875	33.1983	39.7515	43.0894	401.0295	0.303442
		9		6	4	7	6	2	4		4		8	5	3		
31A-165 - 1.d	0	0.44045	0	0.520270	2.78863	52.2613	127.977	184.552	367.	202.930	261.25	310.526	358.385	454.065	2266.888	0.169117	
		7		3	2	1	8	8	2	4		3	4	1			
31A-165 - 2.d	0	1.85970	0.35560	5.64551	51.3513	26.2877	140.703	119.113	75.2032	73.2	43.4065	24.3125	9.95951	11.5528	9.91869	366.6669	0.309261
		6	3	4	5	4	5	6	5	9		4	4	9	9		
31A-166 - 1.d	0	1.84339	0.08620	2.77899	34.4594	43.1616	157.286	160.110	121.138	137.	87.5457	56.25	30.7692	23.2298	26.4227	642.8666	0.58627
		3	7	3	6	3	4	8	2	4	9		3	1	6		
31A-167 - 1.d	0	11.0766	4.41810	16.8490	152.702	225.399	206.030	177.008	162.195	210.	130.219	125	128.340	192.546	313.008	1438.518	1.270763
		7	3	2	7	6	2	3	1	2	8		1	6	1		
31A-167 - 2.d	0.76793	5.70962	2.44612	11.3785	33.2432	59.5026	85.4271	63.4349	42.6829	43.2	23.9926	20.625	10.9716	10.7453	13.4146	229.0671	1.116572
		2	5	1	6	4	6	4	3		7		6	4	3		
31A-168 - 1.d	0	1.64763	0	1.96936	21.0810	4.97335	68.8442	74.2382	86.1788	208	114.468	157.5	222.672	287.577	402.439	1553.075	0.130548
		5		5	8	7	2	3	6		9		4	6			
31A-168 - 2.d	0	1.89233	1.48706	4.79212	48.6486	37.1225	129.145	111.357	94.7154	121.	71.7948	58.125	52.6315	40.4968	41.0569	591.678	0.468341
		3	9	3	5	6	7	3	5	5	7		8	9	1		
31A-169 - 1.d	0.75527	8.18923	5.38793	17.0678	60.1351	98.4014	89.4472	134.626	160.569	279	164.652	176.875	198.785	268.323	325.203	1708.034	1.341695
		4	3	1	3	4	2	4	1		4		4	3	3		
31A-169 - 2.d	1.43459	10.5872	7.00431	16.4113	66.8918	110.302	126.130	170.083	208.536	412	243.772	329.375	469.635	732.919	1077.23	3643.558	1.200843
		9	8		8	9	7	1	6		9		6	3	6		
31A-170 - 1.d	0	1.32137	0	1.75054	29.7297	2.73534	82.4120	91.4127	93.0894	143.	81.5018	80	97.5708	127.950	174.390	889.7154	0.055261
				7	3	6	6	4	3	8	3		5	3	2		
31A-170 - 2.d	0	1.10929	0.20474	2.07877	20.5405	28.0639	84.9246	78.3933	67.0731	81.3	44.5054	39	33.6032	37.3291	29.6748	410.8792	0.671933
		9	1	5	4	4	2	5	7		9		4	9			

Crossed-out = discordant

**WGC2019J-31A zircon trace elements standards**

Standard	La	Ce	Pr	Nd	Sm	Eu	Gd	Tb	Dy	Ho	Er	Tm	Yb	Lu
NIST610_51 - 1.d	421100	434100	427900	413400	434000	428200	427500	418600	423800	428400	433100	419200	432300	420400
NIST610_51 - 2.d	425500	436500	432400	411400	437500	432100	436900	422900	420000	434700	444600	421900	435900	427000
NIST610_51 - 3.d	421900	435200	433500	414300	435000	432200	428700	422700	419200	432400	436200	419800	434300	422000
NIST610_51 - 4.d	422400	434700	430500	411300	432900	425600	426700	417400	417200	426800	435500	415000	430000	419800
NIST610_51 - 5.d	422800	434900	427900	414100	433000	428500	430900	418400	421400	430000	436600	416300	430900	419600
NIST610_51 - 6.d	425100	436700	428900	414600	438100	432100	432300	420100	420800	432500	439600	418600	432300	421800
NIST610_51 - 7.d	425100	438500	433300	412700	436600	431100	437300	421600	422100	434800	435800	420600	432700	423000
NIST610_51 - 8.d	419900	431500	426800	412700	432100	425500	424500	413900	415200	425600	431300	415100	429700	416200
NIST610_51 - 9.d	420700	431400	431500	413100	434400	428000	428800	417200	417500	428200	437700	418500	430600	421600
NIST610_51 - 10.d	422600	436700	431800	413200	433800	430600	432800	421700	420000	431800	434900	417500	432700	422000
NIST610_51 - 11.d	421300	436300	431000	411800	437200	429600	429800	419300	417000	431800	433600	415000	433900	419300
NIST610_51 - 12.d	425500	439000	433200	418500	435400	433100	436700	423500	423000	431500	438000	418300	434800	425300
NIST610_51 - 13.d	421300	432000	429300	409200	433900	427500	431200	420100	419100	430900	438200	416900	433800	425100
NIST610_51 - 14.d	420800	430600	427400	411300	437900	425500	433400	419000	420500	431600	440100	416200	427200	419800
NIST610_51 - 15.d	426800	441200	432700	417200	439300	433100	436000	423200	426300	433400	440900	419100	435400	425000
NIST610_51 - 16.d	424900	439600	433200	414900	437500	433100	439500	419400	422500	435000	440600	421700	434100	425500
NIST610_51 - 17.d	425400	437300	436600	416800	437900	436600	438600	423900	421200	435300	441700	421100	438600	425900
NIST610_51 - 18.d	429100	439900	434600	418500	440400	435900	431900	423600	424100	439500	440600	424200	435200	423800
NIST610_51 - 19.d	428000	441700	434500	416900	437000	435800	435200	427900	426700	436900	442600	421500	435500	426100
NIST610_51 - 21.d	425600	441800	434500	414300	445100	436900	437200	426400	425100	437600	441000	422500	435000	423100
NIST610_51 - 22.d	429700	440300	436200	419500	442900	434000	434800	425700	425000	439200	442100	423600	439300	426400
NIST610_51 - 23.d	424600	440800	432400	419000	439000	429100	431000	423100	420800	434400	437600	421200	434200	422600
NIST610_51 - 24.d	429400	439800	436000	414700	436400	433000	437200	423900	421700	435200	442400	422300	431500	426300
NIST610_51 - 25.d	425800	439600	434400	416300	437000	433900	431700	422100	423300	431400	442400	422200	431800	424500
NIST610_51 - 26.d	422600	434400	432000	414500	433400	427700	430500	417200	420000	433100	435000	417300	431100	424200
NIST610_51 - 27.d	424400	436400	432700	412800	437700	430200	432000	419000	419700	431000	438800	414800	431300	419900
NIST610_51 - 28.d	419400	432300	427000	409900	430300	425300	429000	415800	417500	429400	433500	412800	431500	418800
NIST610_51 - 29.d	419300	432000	423800	410200	428500	425100	425200	416900	415800	428600	434300	412800	431400	417500

<b>NIST610_51 - 30.d</b>	425400	437300	437200	417600	439800	431300	436000	425200	422900	436800	441300	422300	439900	427700
<b>NIST610_51 - 31.d</b>	419900	435300	427100	412000	436300	429000	430500	418800	418200	432700	436200	416800	429800	421100
<b>NIST610_51 - 32.d</b>	423500	436400	429700	415600	437700	430500	436500	420800	418700	431900	442900	421000	433500	424000
<b>NIST610_51 - 33.d</b>	424600	436900	431700	415000	436700	430000	431800	422100	418300	432100	436500	416800	435400	421600
<b>NIST610_51 - 34.d</b>	426800	439700	435200	418300	434300	433900	433800	422200	421600	434500	440500	420700	440800	424800
<b>NIST610_51 - 35.d</b>	424200	435200	433200	413800	436300	432100	434600	419300	420700	432900	438300	422000	435800	423800
<b>NIST610_51 - 36.d</b>	423300	438800	431100	412100	435400	430800	437900	421800	421800	434300	436400	422500	434200	424800
<b>NIST610_51 - 37.d</b>	426600	439200	433100	418300	442700	433600	434600	425600	427800	437000	443000	423600	437900	428500
<b>NIST610_51 - 38.d</b>	421500	434500	429400	412700	437400	431200	432900	423700	423700	435200	438200	419200	435900	425600
<b>NIST610_51 - 39.d</b>	430700	442100	437400	421800	442400	436800	437400	427500	427400	437300	446400	424600	439600	426600
<b>NIST610_51 - 40.d</b>	420200	435000	428400	411900	430600	428000	431900	419800	418600	430500	437800	419300	435600	420000
<b>NIST610_51 - 41.d</b>	426100	438300	434400	415300	441100	435400	435000	423300	425000	432100	441400	422700	436900	424400
<b>NIST610_51 - 42.d</b>	424500	438300	433800	419900	438900	432400	435800	422800	426300	436300	440500	424900	436700	426600
<b>NIST610_51 - 43.d</b>	423700	433800	427600	409600	432300	428100	427900	417600	415400	429600	435600	415200	430900	416700
<b>NIST610_51 - 44.d</b>	419900	430600	428300	412600	431900	426700	423800	414900	415400	423200	431100	411600	425300	415200
<b>NIST610_51 - 45.d</b>	427400	438200	435000	417800	437500	433200	434400	425600	421100	433900	440900	421000	435000	424700
<b>NIST610_51 - 46.d</b>	421500	432200	427500	411400	433100	427700	426400	418900	420700	430400	436400	416700	431400	420500
<b>NIST610_51 - 47.d</b>	421400	434500	428200	409700	433900	424900	429900	418900	416400	427700	432300	415300	428400	419100
<b>NIST610_51 - 48.d</b>	423600	435400	429800	412600	432200	430200	430000	420300	421600	430900	437500	418800	432400	422400
<b>NIST610_51 - 49.d</b>	422300	434300	430100	411900	433500	428200	431000	419600	421500	431600	438600	414900	430800	421600
<b>NIST610_51 - 50.d</b>	424000	438400	431000	415800	438000	433900	432500	420100	421200	436300	439100	422700	435900	422400
<b>NIST610_51 - 51.d</b>	423000	436600	429400	410900	438800	428600	429700	417800	420300	431400	435300	415800	431600	419100
<b>NIST610_51 - 52.d</b>	419500	430400	428800	408600	427800	425900	424500	414700	417800	430600	433700	414000	427300	416000
<b>NIST610_51 - 53.d</b>	423700	438800	433300	414000	438700	428300	435900	419700	417800	430900	437000	417800	430300	422800
<b>NIST610_51 - 54.d</b>	422000	435100	431100	411200	435500	428800	432600	418900	420700	430100	438700	416200	433200	425500
<b>NIST610_51 - 55.d</b>	423500	435500	430100	415400	435800	430700	434900	419600	419000	432500	436800	418200	431100	422900
<b>NIST610_51 - 56.d</b>	425800	434000	433500	415500	439700	432800	437100	423100	421600	433100	439400	421200	438400	425400
<b>NIST610_19 - 1.d</b>	425000	443000	434000	420000	426000	421000	430000	413000	419000	428000	433000	409000	416000	416000
<b>NIST610_19 - 2.d</b>	433000	447000	436000	417000	439000	434000	432000	421000	422000	429000	442000	419000	439000	422000
<b>NIST610_19 - 3.d</b>	425000	438000	435000	414000	439000	433000	434000	421000	422000	432000	437000	419000	428000	420000
<b>NIST610_19 - 4.d</b>	422000	432000	420000	399000	416000	424000	424000	411000	412000	421000	425000	401000	428000	403000



<b>NIST610_19 - 5.d</b>	418000	433000	421000	406000	421000	423000	418000	406000	401000	420000	431000	400000	412000	407000
<b>NIST610_19 - 6.d</b>	416000	431000	416000	406000	431000	425000	419000	412000	416000	422000	430000	405000	417000	416000
<b>NIST610_19 - 7.d</b>	411000	428000	418000	417000	422000	417000	411000	414000	408000	422000	423000	412000	410000	405000
<b>NIST610_19 - 8.d</b>	417000	430000	426000	413000	426000	424000	423000	411000	412000	418000	417000	407000	417000	407000
<b>NIST610_19 - 9.d</b>	419000	434000	433000	417000	434000	430000	425000	414000	415000	423000	438000	407000	428000	412000
<b>NIST610_19 - 10.d</b>	429000	435000	431000	416000	438000	429000	420000	417000	420000	426000	434000	412000	428000	422000
<b>NIST610_19 - 11.d</b>	420000	435000	427000	412000	428000	426000	419000	408000	409000	422000	425000	409000	422000	415000
<b>NIST610_19 - 12.d</b>	425000	443000	434000	410000	425000	437000	431000	420000	418000	432000	440000	418000	429000	420000
<b>NIST610_19 - 13.d</b>	422000	431000	431000	406000	440000	425000	436000	409000	406000	425000	432000	412000	421000	410000
<b>NIST610_19 - 14.d</b>	417000	436000	431000	410000	440000	424000	429000	409000	422000	427000	433000	419000	436000	418000
<b>NIST610_19 - 15.d</b>	414000	429000	428000	406000	429000	417000	424000	410000	411000	419000	422000	403000	415000	411000
<b>NIST610_19 - 16.d</b>	423000	443000	433000	417000	442000	426000	434000	419000	423000	432000	441000	417000	432000	414000
<b>NIST610_19 - 17.d</b>	435000	441000	437000	416000	425000	432000	442000	424000	415000	435000	442000	418000	436000	421000
<b>NIST610_19 - 18.d</b>	441000	461000	442000	419000	452000	437000	443000	426000	434000	444000	454000	429000	451000	427000
<b>NIST610_19 - 19.d</b>	419000	435000	423000	411000	434000	424000	431000	412000	407000	424000	424000	402000	424000	413000
<b>NIST610_19 - 20.d</b>	422000	436000	430000	412000	429000	422000	420000	416000	415000	424000	424000	409000	427000	418000
<b>NIST610_19 - 21.d</b>	422000	441000	431000	427000	436000	429000	435000	420000	430000	428000	436000	425000	424000	422000
<b>NIST610_19 - 22.d</b>	427000	426000	430000	411000	446000	435000	428000	417000	421000	428000	440000	414000	429000	413000
<b>NIST610_19 - 23.d</b>	430000	443000	432000	431000	438000	432000	435000	420000	418000	423000	441000	412000	431000	414000
<b>NIST610_19 - 24.d</b>	423000	434000	425000	395000	425000	424000	415000	410000	415000	418000	419000	411000	425000	408000
<b>NIST610_19 - 25.d</b>	424000	431000	437000	423000	434000	434000	425000	411000	419000	423000	434000	414000	423000	412000
<b>NIST610_19 - 26.d</b>	423000	445000	433000	414000	445000	430000	426000	412000	409000	421000	425000	409000	430000	413000
<b>NIST610_19 - 27.d</b>	438000	456000	446000	422000	443000	445000	450000	431000	436000	446000	444000	425000	445000	428000
<b>NIST610_19 - 28.d</b>	424000	441000	431000	414000	444000	423000	434000	416000	425000	433000	436000	416000	433000	418000

**Ti-in-zircon thermometry**

Sample	No.	Ti (ppm)	±	T (Ferry & Watson, 2007)	±	Comments
WGC-25B-3 - 1.d	2	3	2.2	644.1018729	66.2875412	
WGC-25B-3 - 2.d	3	5.5	2.5	692.6709392	56.37272502	
WGC-25B-4 - 1.d	4	-0.000296	0.000013	#NUM!	#NUM!	<1 ppm Ti
WGC-25B-5 - 1.d	7	2.7	1.8	636.153545	65.50323946	
WGC-25B-5 - 2.d	8	-0.000332	0.00002	#NUM!	#NUM!	<1 ppm Ti
WGC-25B-5 - 3.d	9	1.2	1.2	579.3001555	100.9316229	
WGC-25B-6 - 2.d	11	3.7	1.9	660.3440167	59.08201147	
WGC-25B-7 - 1.d	12	4.3	2.3	672.3412466	59.18665898	
WGC-25B-7 - 2.d	13	2	1.5	614.2507604	71.92217594	
WGC-25B-7 - 3.d	14	3.9	2.2	664.51183	60.33546818	
WGC-25B-8 - 1.d	15	7	2.7	713.4563732	54.18140317	
WGC-25B-8 - 2.d	16	7.5	3.1	719.5684053	55.27340561	
WGC-25B-10 - 1.d	17	6	2.8	700.068554	56.78569314	
WGC-25B-10 - 2.d	18	3.2	2.4	649.0396247	66.28197714	
WGC-25B-11 - 1.d	19	2	1.6	614.2507604	73.07636112	
WGC-25B-11 - 3.d	21	3.7	2	660.3440167	59.86831794	
WGC-25B-12 - 1.d	22	2.4	1.6	627.429602	66.87698731	
WGC-25B-13 - 2.d	24	2.9	1.7	641.52924	62.71785767	
WGC-25B-14 - 1.d	25	0.9	1	560.8027106	#NUM!	<1 ppm Ti
WGC-25B-16 - 1.d	28	8.6	3.3	731.9195946	54.53436029	
WGC-25B-16 - 2.d	29	3.4	2.1	653.7266072	62.45393703	
WGC-25B-17 - 1.d	30	0.52	0.72	527.6676692	#NUM!	<1 ppm Ti
WGC-25B-17 - 2.d	31	3.7	2.1	660.3440167	60.64336389	
WGC-25B-18 - 1.d	32	1.4	1.2	589.5535378	86.31334198	
WGC-25B-18 - 2.d	33	1.1	1.1	573.6194806	113.7548977	
WGC-25B-19 - 1.d	34	5.2	2.6	687.9616042	57.84606729	
WGC-25B-19 - 2.d	35	4.7	2.4	679.5884537	58.27848302	
WGC-25B-20 - 1.d	36	3.7	2.5	660.3440167	63.6377924	

Samantha Nicole March  
Ultrahigh-pressure metapelites in the WGR

WGC-25B-20 - 2.d	37	6.9	2.9	712.1911588	55.37051228	
WGC-25B-21 - 2.d	39	8	3	725.3547918	54.03511511	
WGC-25B-22 - 1.d	40	2.4	1.7	627.429602	67.91181224	
WGC-25B-22 - 2.d	41	4.2	2.3	670.4424511	59.62387935	
WGC-25B-23 - 1.d	42	4.7	2.4	679.5884537	58.27848302	
WGC-25B-23 - 2.d	43	3.2	2.2	649.0396247	64.6740707	
WGC-25B-24 - 1.d	44	-0.000463	0.000025	#NUM!	#NUM!	<1 ppm Ti
WGC-25B-24 - 2.d	45	7.4	3	718.3733418	54.96729128	
WGC-25B-25 - 1.d	46	3.5	1.9	655.9845582	60.20772223	
WGC-25B-25 - 2.d	47	6.5	2.8	706.9744981	55.65428182	
WGC-25B-26 - 1.d	48	4.7	2.5	679.5884537	58.92666766	
WGC-25B-26 - 2.d	49	2.8	1.8	638.8814791	64.53686082	
WGC-25B-27 - 1.d	50	6.1	2.6	701.4866869	55.45050014	
WGC-25B-27 - 2.d	51	7.6	3	720.7504673	54.63988188	
WGC-25B-28 - 1.d	52	1.3	1.3	584.5936072	93.86872609	
WGC-25B-28 - 2.d	53	3.4	1.9	653.7266072	60.82156466	
WGC-25B-29 - 1.d	54	5	2.5	684.6957848	57.87421248	
WGC-25B-30 - 1.d	55	5.4	2.5	691.1252528	56.65090481	
WGC-25B-31 - 1.d	56	0.27	0.55	491.3754861	#NUM!	<1 ppm Ti
WGC-25B-32 - 1.d	58	0.27	0.54	491.3754861	#NUM!	<1 ppm Ti
WGC-25B-33 - 1.d	59	4.1	2.2	668.5057866	59.36787366	
WGC-25B-33 - 2.d	60	2.4	1.7	627.429602	67.91181224	
WGC-25B-34 - 1.d	61	3.8	2.2	662.4507046	60.85740141	
WGC-25B-34 - 2.d	62	4	2	666.529529	58.36287656	
WGC-25B-35 - 2.d	64	4.9	2.4	683.0221981	57.5772024	
WGC-25B-36 - 1.d	65	8	3	725.3547918	54.03511511	
WGC-25B-36 - 2.d	66	0.9	1.1	560.8027106	#NUM!	<1 ppm Ti
WGC-25B-36 - 3.d	67	6.1	2.5	701.4866869	54.89570453	
WGC-25B-37 - 1.d	68	3.3	2	651.4126887	62.30894618	
WGC-25B-37 - 2.d	69	3.8	2.1	662.4507046	60.10382871	
WGC-25B-39 - 1.d	71	4.1	2.2	668.5057866	59.36787366	

WGC-25B-40 - 1.d	72	3.8	2	662.4507046	59.33968835	
WGC-25B-42 - 1.d	74	7.8	3	723.0768275	54.32955696	
WGC-25B-43 - 1.d	75	4.7	2.4	679.5884537	58.27848302	
WGC-25B-44 - 1.d	76	5.6	2.6	694.1936044	56.68687889	
WGC-25B-44 - 2.d	77	4.8	2.3	681.3201228	57.27241125	
WGC-25B-45 - 2.d	79	3.6	1.9	658.1894637	59.62884231	
WGC-25B-45 - 3.d	80	4.4	2.2	674.2037839	58.08133334	
WGC-25B-46 - 1.d	81	1.6	1.3	598.6369314	79.41506975	
WGC-25B-46 - 2.d	82	6.3	2.8	704.266451	56.08540446	
WGC-25B-47 - 1.d	83	7.1	2.9	714.7068257	55.00235759	
WGC-25B-47 - 2.d	84	11.9	5.1	762.4974929	57.47694865	
WGC-25B-48 - 1.d	85	2.4	1.6	627.429602	66.87698731	
WGC-25B-48 - 2.d	86	1.8	1.4	606.8093388	75.00471897	
WGC-25B-49 - 1.d	87	-0.000562	0.000034	#NUM!	#NUM!	<1 ppm Ti
WGC-25B-49 - 2.d	88	1.9	1.3	610.6123488	71.48684748	
WGC-25B-50 - 1.d	89	2.7	1.7	636.153545	64.54593694	
WGC-25B-50 - 2.d	90	6.2	2.6	702.8857988	55.2272152	
WGC-25B-51 - 1.d	91	6.5	2.5	706.9744981	54.06429043	
WGC-25B-52 - 1.d	92	7.5	2.8	719.5684053	53.84624496	
WGC-25B-52 - 2.d	93	4.6	2.4	677.8260182	58.65177678	
WGC-25B-53 - 1.d	94	2.9	1.7	641.52924	62.71785767	
WGC-25B-54 - 1.d	95	2.3	1.7	624.3183366	69.2508733	
WGC-25B-54 - 2.d	96	3.9	2.3	664.51183	61.0688566	
WGC-25B-55 - 1.d	97	5.9	2.4	698.6308117	54.78342366	
WGC-25B-55 - 2.d	98	4.1	2.2	668.5057866	59.36787366	
WGC-25B-56 - 1.d	99	5.8	2.8	697.1728431	57.2923301	
WGC-25B-57 - 1.d	101	1.9	1.5	610.6123488	73.93988096	
WGC-25B-57 - 2.d	102	7.4	2.7	718.3733418	53.51755256	
WGC-25B-59 - 1.d	104	6.7	2.9	709.6148418	55.76075824	
WGC-25B-60 - 1.d	105	0.51	0.72	526.5429514	#NUM!	<1 ppm Ti
WGC-25B-60 - 3.d	107	5	2.5	684.6957848	57.87421248	

WGC-25B-61 - 1.d	108	2.8	1.7	638.8814791	63.59696743	
WGC-25B-61 - 2.d	109	2.1	1.4	617.7395314	68.98387345	
WGC-25B-61 - 3.d	110	1.9	1.5	610.6123488	73.93988096	
WGC-25B-62 - 2.d	112	3.5	2	655.9845582	61.01768856	
WGC-25B-63 - 1.d	114	6.8	2.7	710.910786	54.54342613	
WGC-25B-63 - 2.d	115	6.6	2.8	708.3028957	55.44852305	
WGC-25B-64 - 1.d	116	1.2	1.2	579.3001555	100.9316229	
WGC-25B-64 - 2.d	117	3.5	1.9	655.9845582	60.20772223	
WGC-25B-65 - 1.d	118	4.6	2.5	677.8260182	59.30747815	
WGC-25B-65 - 2.d	119	7	3	713.4563732	55.67881407	
WGC-25B-68 - 1.d	120	-0.000692	0.000041	#NUM!	#NUM!	<1 ppm Ti
WGC-25B-68 - 2.d	121	0.76	0.86	550.3012916	#NUM!	<1 ppm Ti
WGC-25B-68 - 3.d	122	3.7	2.1	660.3440167	60.64336389	
WGC-25B-69 - 1.d	123	-0.000692	0.000027	#NUM!	#NUM!	<1 ppm Ti
WGC-25B-69 - 2.d	124	5.8	2.6	697.1728431	56.16676843	
WGC-25B-69 - 3.d	125	4.5	2.5	676.0315702	59.70488775	
WGC-25B-69 - 4.d	126	1.7	1.4	602.8243343	77.64501988	
WGC-25B-71 - 1.d	127	3.8	2.1	662.4507046	60.10382871	
WGC-25B-71 - 2.d	128	8.3	2.9	728.685773	53.17281133	
WGC-25B-71 - 3.d	129	8.3	2.8	728.685773	52.72149265	
WGC-25B-72 - 1.d	130	4	2.2	666.529529	59.839592	
WGC-25B-73 - 1.d	132	2.5	1.8	630.4341806	67.68581495	
WGC-25B-73 - 2.d	133	1.9	1.5	610.6123488	73.93988096	
WGC-25B-74 - 1.d	134	2.8	1.8	638.8814791	64.53686082	
WGC-25B-75 - 1.d	136	5.4	2.6	691.1252528	57.2452501	
WGC-25B-75 - 2.d	137	2.4	1.6	627.429602	66.87698731	
WGC-25B-76 - 1.d	138	3.7	2.1	660.3440167	60.64336389	
WGC-25B-76 - 2.d	139	7.7	2.9	721.9198409	54.01422837	
WGC-25B-77 - 1.d	140	1.5	1.3	594.2229705	83.13822035	
WGC-25B-77 - 2.d	141	3	1.8	644.1018729	62.80805901	
WGC-25B-78 - 2.d	143	22.5	9.2	828.2161027	60.79418996	

WGC-25B-78 - 3.d	144	6.4	2.6	705.62918	54.80178416	
WGC-25B-79 - 1.d	145	0.85	0.97	557.222726	#NUM!	<1 ppm Ti
WGC-25B-79 - 2.d	146	7	2.8	713.4563732	54.68467307	
WGC-25B-80 - 1.d	147	2.7	1.8	636.153545	65.50323946	
WGC-25B-80 - 2.d	148	3	2.1	644.1018729	65.43892407	
WGC-25B-81 - 1.d	149	6.7	2.8	709.6148418	55.24893197	
WGC-25B-81 - 2.d	150	3.5	2.1	655.9845582	61.81562866	
WGC-25B-82 - 1.d	151	2.4	1.9	627.429602	69.92034633	
WGC-25B-82 - 2.d	152	3.8	2.1	662.4507046	60.10382871	
WGC-25B-82 - 3.d	153	5.7	2.5	695.6940007	39.12333737	
<b>Weighted mean = 676.35 ± 7.14*</b>						

Sample	No.	Ti (ppm)	±	T (Ferry & Watson, 2007)	±	Comments
31A-1 - 1.d	1	6.6	3.6	708.3029	59.459607	
31A-1 - 2.d	2	2.6	2.2	633.33985	70.276751	
31A-2 - 1.d	3	9.6	4	742.07196	56.101275	
31A-2 - 2.d	4	0.46	0.92	520.61902	#NUM!	<1 ppm Ti
31A-3 - 1.d	5	3.1	2.3	646.60395	66.276888	
31A-3 - 2.d	6	9	4.2	736.09075	57.674287	
31A-4 - 1.d	7	3.8	2.8	662.4507	65.173953	
31A-4 - 2.d	8	5.4	3.2	691.12525	60.689171	
31A-5 - 1.d	9	5.3	3.4	689.55575	62.133129	
31A-5 - 2.d	10	4.2	2.9	670.44245	63.67809	
31A-6 - 1.d	11	3.2	2.5	649.03962	67.068284	
31A-6 - 2.d	12	3.9	2.6	664.51183	63.212256	
31A-7 - 1.d	13	0	1	#NUM!	#NUM!	<1 ppm Ti
31A-7 - 2.d	14	3.7	2.7	660.34402	65.075913	

Samantha Nicole March  
Ultrahigh-pressure metapelites in the WGR

31A-8 - 1.d	15	0	1	#NUM!	#NUM!	<1 ppm Ti
31A-8 - 2.d	16	1	1.4	567.48328	#NUM!	
31A-8 - 3.d	17	0	1	#NUM!	#NUM!	<1 ppm Ti
31A-9 - 1.d	18	22.8	7.2	829.6713	56.681336	
31A-9 - 2.d	19	12.9	4.9	770.3852	55.976708	
31A-10 - 1.d	20	3.7	3.6	660.34402	71.124446	
31A-10 - 2.d	21	4.7	3	679.58845	62.061269	
31A-11 - 1.d	22	3.4	2.5	653.72661	65.57737	
31A-11 - 2.d	23	1.3	1.5	584.59361	96.76771	
31A-11 - 3.d	24	0	1	#NUM!	#NUM!	<1 ppm Ti
31A-12 - 1.d	25	1.5	1.7	594.22297	88.453505	
31A-12 - 2.d	26	0	1	#NUM!	#NUM!	<1 ppm Ti
31A-12 - 3.d	27	7.6	4.6	720.75047	61.740975	
31A-13 - 1.d	28	17	6.1	798.29679	56.655426	
31A-13 - 2.d	29	7.1	3.8	714.70683	59.285593	
31A-14 - 1.d	30	12.4	9.1	766.50592	68.553523	
31A-16 - 1.d	31	3.9	2.6	664.51183	63.212256	
31A-16 - 2.d	32	0.4	0.81	512.73369	#NUM!	<1 ppm Ti
31A-16 - 3.d	33	3.7	2.7	660.34402	65.075913	
31A-17 - 1.d	34	2.7	2.1	636.15354	68.273417	
31A-17 - 2.d	35	0	1	#NUM!	#NUM!	<1 ppm Ti
31A-18 - 1.d	36	4.9	2.9	683.0222	60.677791	
31A-18 - 2.d	37	3.3	2.4	651.41269	65.525565	
31A-19 - 1.d	38	0	1	#NUM!	#NUM!	<1 ppm Ti
31A-19 - 2.d	39	2.2	1.9	621.09162	72.819596	
31A-20 - 1.d	40	9.5	4.3	741.09671	57.374149	
31A-20 - 2.d	41	1.8	1.8	606.80934	79.79381	
31A-21 - 1.d	42	5.2	3.5	687.9616	63.039651	

Samantha Nicole March  
Ultrahigh-pressure metapelites in the WGR

31A-21 - 2.d	43	4.5	3	676.03157	62.910099	
31A-21 - 3.d	44	8.8	4.6	734.02456	59.54275	
31A-22 - 1.d	45	2.8	2.4	638.88148	69.846627	
31A-22 - 2.d	46	3.1	2.7	646.60395	69.446147	
31A-23 - 1.d	47	27	11	848.59065	62.237361	
31A-23 - 2.d	48	13.5	4.5	774.8825	54.310326	
31A-24 - 1.d	49	4.1	2.8	668.50579	63.522622	
31A-24 - 2.d	50	8	3.8	725.35479	57.582409	
31A-25 - 1.d	51	12.7	5.1	768.84838	56.758428	
31A-25 - 2.d	52	1.3	1.4	584.59361	95.340589	
31A-32 - 1.d	53	3.1	2.5	646.60395	67.884794	
31A-32 - 2.d	54	2.4	2.4	627.4296	74.623275	
31A-33 - 1.d	55	2.5	2.2	630.43418	71.481635	
31A-33 - 2.d	56	1.6	1.8	598.63693	85.798096	
31A-33 - 3.d	57	4.3	2.7	672.34125	61.888731	
31A-34 - 1.d	58	2.9	2.3	641.52924	68.027624	
31A-34 - 2.d	59	3.3	2.6	651.41269	67.064751	
31A-35 - 1.d	60	0	1	#NUM!	#NUM!	<1 ppm Ti
31A-35 - 2.d	61	3.9	2.8	664.51183	64.596532	
31A-35 - 3.d	62	1	1.3	567.48328	#NUM!	<1 ppm Ti
31A-37 - 1.d	63	12.4	4.9	766.50592	56.386542	
31A-37 - 2.d	64	16.8	5.2	797.06932	54.450824	
31A-36 - 1.d	65	14	5	778.50813	55.476543	
31A-36 - 2.d	66	0.9	1.3	560.80271	#NUM!	<1 ppm Ti
31A-38 - 1.d	67	31.2	7.1	865.29167	54.588811	
31A-38 - 2.d	68	13.1	5	771.9028	56.127872	
31A-39 - 1.d	69	2	2.2	614.25076	79.49175	
31A-39 - 2.d	70	1.5	1.7	594.22297	88.453505	



Samantha Nicole March  
Ultrahigh-pressure metapelites in the WGR

31A-40 - 1.d	71	0	1	#NUM!	#NUM!	<1 ppm Ti
31A-40 - 2.d	72	2.9	2.3	641.52924	68.027624	
31A-41 - 1.d	73	2.6	2.3	633.33985	71.168404	
31A-41 - 2.d	74	12.9	4.7	770.3852	55.354929	
31A-41 - 3.d	75	33	10	871.90542	58.928861	
31A-42 - 1.d	76	3.6	2.6	658.18946	64.982563	
31A-42 - 2.d	77	6.5	3.3	706.9745	58.213832	
31A-43 - 1.d	78	2.7	2.3	636.15354	70.041844	
31A-43 - 2.d	79	4.9	3.2	683.0222	62.460968	
31A-43 - 3.d	80	0	1	#NUM!	#NUM!	<1 ppm Ti
31A-44 - 1.d	81	0.41	0.82	514.11543	#NUM!	<1 ppm Ti
31A-44 - 2.d	82	3.9	2.6	664.51183	63.212256	
31A-44 - 3.d	83	0	1	#NUM!	#NUM!	<1 ppm Ti
31A-45 - 1.d	84	6.1	3.5	701.48669	60.223033	
31A-45 - 2.d	85	9.8	4.5	743.99786	57.734183	
31A-45 - 3.d	86	5.4	3.2	691.12525	60.689171	
31A-46 - 1.d	87	0	1	#NUM!	#NUM!	<1 ppm Ti
31A-47 - 1.d	88	10.5	4.5	750.49547	56.898359	
31A-47 - 2.d	89	10.4	4.8	749.58928	58.073492	
31A-48 - 1.d	90	5	3.2	684.69578	62.07992	
31A-55 - 1.d	91	5.7	3.4	695.694	60.842135	
31A-55 - 2.d	92	8	6.9	725.35479	69.71653	
31A-56 - 1.d	93	1.9	1.8	610.61235	77.403841	
31A-56 - 2.d	94	0	1	#NUM!	#NUM!	<1 ppm Ti
31A-56 - 3.d	95	0	1	#NUM!	#NUM!	<1 ppm Ti
31A-57 - 1.d	96	7.1	3.9	714.70683	59.743585	
31A-57 - 2.d	97	4.2	3.3	670.44245	66.2276	

Samantha Nicole March  
 Ultrahigh-pressure metapelites in the WGR

31A-58 - 1.d	98	0	1	#NUM!	#NUM!	<1 ppm Ti
31A-58 - 2.d	99	1.4	1.6	589.55354	91.94371	
31A-59 - 1.d	100	0	1	#NUM!	#NUM!	<1 ppm Ti
31A-59 - 2.d	101	15	5.4	785.4557	55.968539	
31A-60 - 1.d	102	12	4.7	763.30998	56.09124	
31A-60 - 2.d	103	13.6	4.9	775.61623	55.455443	
31A-61 - 1.d	104	1.7	1.6	602.82433	80.161596	
31A-61 - 2.d	105	12	6.3	763.30998	61.113553	
31A-61 - 3.d	106	1.4	1.6	589.55354	91.94371	
31A-62 - 1.d	107	4	2.9	666.52953	64.718084	
31A-62 - 2.d	108	4.2	2.9	670.44245	63.67809	
31A-63 - 1.d	109	6.7	4.3	709.61484	62.506904	
31A-63 - 2.d	110	15.1	5.6	786.12965	56.457038	
31A-64 - 1.d	111	5	3.4	684.69578	63.227561	
31A-64 - 2.d	112	10.4	4.8	749.58928	58.073492	
31A-65 - 1.d	113	3.5	2.8	655.98456	67.095152	
31A-65 - 2.d	114	0.46	0.92	520.61902	#NUM!	<1 ppm Ti
31A-66 - 1.d	115	11.1	4.8	755.7896	57.289866	
31A-66 - 2.d	116	12.3	4.7	765.71488	55.83339	
31A-67 - 1.d	117	1.9	1.9	610.61235	78.506757	
31A-67 - 2.d	118	14.7	5.9	783.4118	57.550538	
31A-68 - 1.d	119	8.7	4.1	732.97702	57.717252	
31A-68 - 2.d	120	1.7	1.6	602.82433	80.161596	
31A-69 - 1.d	121	14.4	5.5	781.33389	56.644253	
31A-71 - 1.d	122	9.8	5.7	743.99786	62.020405	
31A-70 - 1.d	123	4.1	2.6	668.50579	62.171807	
31A-72 - 1.d	124	0.9	1.3	560.80271	#NUM!	<1 ppm Ti
31A-72 - 2.d	125	2.5	2.2	630.43418	71.481635	
31A-73 - 1.d	126	6.3	3.8	704.26645	61.18538	
31A-73 - 2.d	127	9.7	4.4	743.03897	57.491046	

Samantha Nicole March  
 Ultrahigh-pressure metapelites in the WGR

31A-74 - 1.d	128	10.8	8.3	753.17248	68.697897	
31A-75 - 1.d	129	2.3	2	624.31834	72.294232	
31A-75 - 2.d	130	2.2	2.1	621.09162	74.82813	
31A-76 - 1.d	131	1.5	1.7	594.22297	88.453505	
31A-76 - 2.d	132	0.9	1.3	560.80271	#NUM!	<1 ppm Ti
31A-77 - 1.d	133	8.9	4.2	735.0624	57.819481	
31A-77 - 2.d	134	12	5.9	763.30998	59.892057	
31A-77 - 3.d	135	5.5	7.5	692.67094	80.409519	
31A-78 - 1.d	136	1.4	1.6	589.55354	91.94371	
31A-78 - 2.d	137	1.4	1.6	589.55354	91.94371	
31A-79 - 1.d	138	3	2.4	644.10187	67.945229	
31A-79 - 2.d	139	13.2	5.1	772.65457	56.354264	
31A-80 - 1.d	140	2.9	2.3	641.52924	68.027624	
31A-80 - 2.d	141	0	1	#NUM!	#NUM!	<1 ppm Ti
31A-81 - 1.d	142	5.2	3.1	687.9616	60.788294	
31A-81 - 2.d	143	0.38	0.76	509.87891	#NUM!	<1 ppm Ti
31A-81 - 3.d	144	6.4	3.6	705.62918	59.945467	
31A-82 - 1.d	145	2.1	2	617.73953	75.539295	
31A-83 - 1.d	146	39.5	8.9	893.63344	56.31171	
31A-83 - 2.d	147	16.8	5.7	797.06932	55.745343	
31A-84 - 1.d	148	0	1	#NUM!	#NUM!	<1 ppm Ti
31A-84 - 2.d	149	0.8	1.1	553.45909	#NUM!	
31A-85 - 1.d	150	3.6	2.6	658.18946	64.982563	
31A-85 - 2.d	151	4.1	2.8	668.50579	63.522622	
31A-86 - 1.d	152	6	4.3	700.06855	64.474856	
31A-86 - 2.d	153	21.9	9.2	825.25847	61.071182	
31A-87 - 1.d	154	2.5	2.2	630.43418	71.481635	
31A-87 - 2.d	155	2.5	2.2	630.43418	71.481635	
31A-87 - 3.d	156	4	5.6	666.52953	80.39295	
31A-88 - 1.d	157	31.5	8.1	866.41463	56.202449	

Samantha Nicole March  
 Ultrahigh-pressure metapelites in the WGR

31A-89 - 1.d	158	7.9	3.8	724.22172	57.753157	
31A-89 - 2.d	159	1.9	1.8	610.61235	77.403841	
31A-90 - 1.d	160	10.2	4.3	747.7554	56.516799	
31A-90 - 2.d	161	11.4	4.8	758.34978	56.983236	
31A-91 - 1.d	162	1	1.4	567.48328	#NUM!	<1 ppm Ti
31A-91 - 2.d	163	7.5	4	719.56841	59.366719	
31A-92 - 1.d	164	14.5	5.9	782.03039	57.694107	
31A-92 - 2.d	165	8.9	4.2	735.0624	57.819481	
31A-93 - 1.d	166	12.3	5.3	765.71488	57.733379	
31A-93 - 2.d	167	9.4	4.1	740.11303	56.73827	
31A-94 - 1.d	168	2	2	614.25076	77.442772	
31A-94 - 2.d	169	1.2	1.4	579.30016	104.0229	
31A-94 - 3.d	170	3.5	2.6	655.98456	65.638021	
31A-95 - 1.d	171	8.1	3.9	726.47632	57.842442	
31A-95 - 2.d	172	5.1	3	686.34193	60.553899	
31A-96 - 1.d	173	13	4.9	771.14637	55.898648	
31A-96 - 2.d	174	2.5	2.2	630.43418	71.481635	
31A-96 - 3.d	175	0.9	1.8	560.80271	#NUM!	<1 ppm Ti
31A-97 - 1.d	176	3.8	2.7	662.4507	64.477516	
31A-97 - 2.d	177	5.7	3.1	695.694	59.223258	
31A-98 - 1.d	178	3.6	2.8	658.18946	66.420683	
31A-98 - 2.d	179	11	6.9	754.92369	64.193927	
31A-99 - 1.d	180	14.5	5.4	782.03039	56.292921	
31A-99 - 2.d	181	15.2	5.1	786.80001	55.014294	
31A-100 - 1.d	182	15.7	5.7	790.0993	56.35698	
31A-100 - 2.d	183	2.1	2.1	617.73953	76.553448	
31A-101 - 1.d	184	0	1	#NUM!	#NUM!	<1 ppm Ti
31A-101 - 2.d	185	1.5	1.8	594.22297	89.695455	
31A-102 - 1.d	186	7.9	4.1	724.22172	59.041978	
31A-102 - 2.d	187	19.7	7	813.82515	57.459995	

Samantha Nicole March  
 Ultrahigh-pressure metapelites in the WGR

31A-103 - 1.d	188	3	2.3	644.10187	67.122823	
31A-103 - 2.d	189	4	3	666.52953	65.3815	
31A-104 - 1.d	190	0	1	#NUM!	#NUM!	<1 ppm Ti
31A-104 - 2.d	191	0	1	#NUM!	#NUM!	<1 ppm Ti
31A-105 - 1.d	192	2.2	1.9	621.09162	72.819596	
31A-105 - 2.d	193	10.7	4.6	752.28695	57.029918	
31A-105 - 3.d	194	18.8	6.5	808.85052	56.726848	
31A-106 - 1.d	195	1.6	1.8	598.63693	85.798096	
31A-107 - 1.d	196	6.6	3.3	708.3029	57.986467	
31A-107 - 2.d	197	2.8	2.4	638.88148	69.846627	
31A-108 - 1.d	198	19.6	6.1	813.28155	55.456161	
31A-108 - 2.d	199	23.3	7.8	832.06292	57.717716	
31A-109 - 1.d	200	4.6	2.9	677.82602	61.856988	
31A-109 - 2.d	201	0	1	#NUM!	#NUM!	<1 ppm Ti
31A-110 - 1.d	202	5.7	3.2	695.694	59.767813	
31A-110 - 2.d	203	1.9	1.9	610.61235	78.506757	
31A-111 - 1.d	204	41	15	898.2413	64.140683	
31A-111 - 2.d	205	7.7	4.5	721.91984	61.115322	
31A-112 - 1.d	206	8.4	4.2	729.77419	58.595622	
31A-112 - 2.d	207	6	3.6	700.06855	61.008604	
31A-113 - 1.d	208	1.5	1.7	594.22297	88.453505	
31A-113 - 2.d	209	6.6	3.6	708.3029	59.459607	
31A-114 - 1.d	210	1	1.3	567.48328	#NUM!	<1 ppm Ti
31A-114 - 2.d	211	2.7	2.4	636.15354	70.904282	
31A-114 - 3.d	212	10.1	5.8	746.82744	61.919583	
31A-115 - 1.d	213	8.8	4.1	734.02456	57.568057	
31A-115 - 2.d	214	2.1	2.1	617.73953	76.553448	
31A-115 - 3.d	215	2.9	2.6	641.52924	70.495278	
31A-116 - 1.d	216	9.1	4.3	737.10981	57.922325	
31A-116 - 2.d	217	2.5	2.2	630.43418	71.481635	

31A-117 - 1.d	218	16.3	6.4	793.94825	57.818246	
31A-117 - 2.d	219	8.3	4.1	728.68577	58.348886	
31A-118 - 1.d	220	1.4	1.6	589.55354	91.94371	
31A-118 - 2.d	221	3.4	2.5	653.72661	65.57737	
31A-118 - 3.d	222	0	1	#NUM!	#NUM!	<1 ppm Ti
31A-119 - 1.d	223	3.8	2.8	662.4507	65.173953	
31A-119 - 2.d	224	10.5	4.6	750.49547	57.252534	
31A-120 - 1.d	225	5.2	3.3	687.9616	61.924775	
31A-120 - 2.d	226	10.8	4.5	753.17248	56.573096	
31A-120 - 3.d	227	9	4	736.09075	56.882034	
31A-121 - 1.d	228	0	1	#NUM!	#NUM!	<1 ppm Ti
31A-121 - 2.d	229	1.1	1.5	573.61948	120.16056	
31A-121 - 3.d	230	0.46	0.91	520.61902	#NUM!	<1 ppm Ti
31A-122 - 1.d	231	2	2	614.25076	77.442772	
31A-122 - 2.d	232	3.6	2.6	658.18946	64.982563	
31A-122 - 3.d	233	10.2	4.5	747.7554	57.242692	
31A-123 - 1.d	234	4	2.9	666.52953	64.718084	
31A-123 - 2.d	235	1.5	1.7	594.22297	88.453505	
31A-124 - 1.d	236	5.5	3.4	692.67094	61.465617	
31A-124 - 2.d	237	0	1	#NUM!	#NUM!	<1 ppm Ti
31A-125 - 1.d	238	0.43	0.87	516.79434	#NUM!	<1 ppm Ti
31A-125 - 2.d	239	5.1	3.3	686.34193	62.283948	
31A-126 - 1.d	240	3.7	2.9	660.34402	66.477629	
31A-126 - 2.d	241	5.8	3.4	697.17284	60.545589	
31A-126 - 3.d	242	11	4.3	754.92369	55.670784	
31A-127 - 1.d	243	6.5	3.7	706.9745	60.186083	
31A-127 - 2.d	244	0.5	1.1	525.39921	#NUM!	<1 ppm Ti
31A-128 - 1.d	245	21	6.7	820.69785	56.264164	
31A-128 - 2.d	246	16.2	5.6	793.31479	55.805208	
31A-129 - 1.d	247	13.9	5.1	777.7915	55.838874	

Samantha Nicole March  
Ultrahigh-pressure metapelites in the WGR

31A-129 - 2.d	248	15.3	6.1	787.46681	57.679084	
31A-130 - 1.d	249	0.42	0.84	515.46855	#NUM!	
31A-130 - 2.d	250	4.9	3.1	683.0222	61.872658	
31A-130 - 3.d	251	5	3.2	684.69578	62.07992	
31A-131 - 1.d	252	10.5	5	750.49547	58.65062	
31A-131 - 2.d	253	1	1.4	567.48328	#NUM!	<1 ppm Ti
31A-132 - 1.d	254	0.6	1.1	536.05484	#NUM!	<1 ppm Ti
31A-132 - 2.d	255	0	1	#NUM!	#NUM!	<1 ppm Ti
31A-132 - 3.d	256	2.6	2.3	633.33985	71.168404	
31A-133 - 1.d	257	14.4	5.2	781.33389	55.78997	
31A-133 - 2.d	258	34.6	9.5	877.54831	57.861107	
31A-134 - 1.d	259	3.8	2.8	662.4507	65.173953	
31A-134 - 2.d	260	15.8	5.7	790.74894	56.297597	
31A-135 - 1.d	261	2	1.9	614.25076	76.386312	
31A-135 - 2.d	262	2.4	2.7	627.4296	77.25414	
31A-136 - 1.d	263	0	1	#NUM!	#NUM!	<1 ppm Ti
31A-136 - 2.d	264	5.6	3.3	694.1936	60.609053	
31A-136 - 3.d	265	6.1	3.6	701.48669	60.73054	
31A-137 - 1.d	266	13.3	5.1	773.40173	56.277182	
31A-137 - 2.d	267	6.6	3.7	708.3029	59.94283	
31A-138 - 1.d	268	4.1	2.8	668.50579	63.522622	
31A-138 - 2.d	269	1.5	1.7	594.22297	88.453505	
31A-139 - 1.d	270	2.5	2.1	630.43418	70.558459	
31A-139 - 2.d	271	7.3	4	717.16495	59.771716	
31A-140 - 1.d	272	4.3	2.9	672.34125	63.192617	
31A-140 - 2.d	273	3.9	2.8	664.51183	64.596532	
31A-141 - 1.d	274	12.8	5.1	769.61923	56.675007	
31A-141 - 2.d	275	8	4.1	725.35479	58.86249	
31A-142 - 1.d	276	6.3	3.6	704.26645	60.199328	
31A-142 - 2.d	277	5	3.2	684.69578	62.07992	

Samantha Nicole March  
 Ultrahigh-pressure metapelites in the WGR

31A-143 - 1.d	278	9.3	4	739.12077	56.47912	
31A-143 - 2.d	279	0	1	#NUM!	#NUM!	<1 ppm Ti
31A-144 - 1.d	280	2.1	2.1	617.73953	76.553448	
31A-144 - 2.d	281	15	5.6	785.4557	56.521333	
31A-145 - 1.d	282	2.1	2	617.73953	75.539295	
31A-146 - 1.d	283	2.5	2.2	630.43418	71.481635	
31A-146 - 2.d	284	4.8	3	681.32012	61.662043	
31A-147 - 1.d	285	1.9	1.9	610.61235	78.506757	
31A-147 - 2.d	286	3.5	2.8	655.98456	67.095152	
31A-148 - 1.d	287	8.2	4.2	727.58656	58.93154	
31A-148 - 2.d	288	5	3.2	684.69578	62.07992	
31A-149 - 1.d	289	10.2	5.5	747.7554	60.757194	
31A-149 - 2.d	290	6.3	3.6	704.26645	60.199328	
31A-150 - 1.d	291	2.1	2	617.73953	75.539295	
31A-150 - 2.d	292	3.5	2.8	655.98456	67.095152	
31A-151 - 1.d	293	2.6	2.3	633.33985	71.168404	
31A-151 - 2.d	294	7	3.8	713.45637	59.500635	
31A-152 - 1.d	295	3.1	2.7	646.60395	69.446147	
31A-152 - 2.d	296	3.9	2.9	664.51183	65.276009	
31A-152 - 3.d	297	2.4	2.1	627.4296	71.853097	
31A-153 - 1.d	298	3.8	2.8	662.4507	65.173953	
31A-153 - 2.d	299	11.1	4.9	755.7896	57.627867	
31A-154 - 1.d	300	12.3	4.8	765.71488	56.153754	
31A-154 - 2.d	301	8.2	4	727.58656	58.097879	
31A-155 - 1.d	302	40	15	895.18449	64.359089	
31A-155 - 2.d	303	18.4	5.8	806.5779	55.240253	
31A-156 - 1.d	304	10.7	4.5	752.28695	56.679488	
31A-156 - 2.d	305	31	10	864.53826	59.382018	
31A-156 - 3.d	306	0.8	1.1	553.45909	#NUM!	<1 ppm Ti
31A-158 - 1.d	307	3	2.4	644.10187	67.945229	



<b>31A-158 - 2.d</b>	308	0	1	#NUM!	#NUM!	
<b>31A-159 - 1.d</b>	309	4.4	3	674.20378	63.361867	
<b>31A-159 - 2.d</b>	310	5.2	3.3	687.9616	61.924775	
<b>31A-160 - 1.d</b>	311	2.4	2.1	627.4296	71.853097	
<b>31A-160 - 2.d</b>	312	5.8	3.4	697.17284	60.545589	
<b>31A-161 - 1.d</b>	313	11.2	4.7	756.64918	56.847833	
<b>31A-161 - 2.d</b>	314	7.6	3.9	720.75047	58.733195	
<b>31A-162 - 1.d</b>	315	0	1	#NUM!	#NUM!	<1 ppm Ti
<b>31A-163 - 1.d</b>	316	9.6	4.3	742.07196	57.244099	
<b>31A-164 - 1.d</b>	317	9.2	4.3	738.11975	57.78092	
<b>31A-164 - 2.d</b>	318	5.8	3.7	697.17284	62.107832	
<b>31A-164 - 3.d</b>	319	2.5	2.2	630.43418	71.481635	
<b>31A-165 - 1.d</b>	320	0	1	#NUM!	#NUM!	<1 ppm Ti
<b>31A-165 - 2.d</b>	321	5.8	3.4	697.17284	60.545589	
<b>31A-166 - 1.d</b>	322	6.5	3.9	706.9745	61.148734	
<b>31A-167 - 1.d</b>	323	21.6	7.5	823.75523	57.739318	
<b>31A-167 - 2.d</b>	324	10.7	5.4	752.28695	59.768936	
<b>31A-168 - 1.d</b>	325	0	1	#NUM!	#NUM!	<1 ppm Ti
<b>31A-168 - 2.d</b>	326	10.4	5	749.58928	58.772513	
<b>31A-169 - 1.d</b>	327	10	4.7	745.89195	58.209496	
<b>31A-169 - 2.d</b>	328	16.9	6.2	797.68452	56.961346	
<b>31A-170 - 1.d</b>	329	1	1.4	567.48328	#NUM!	<1 ppm Ti
<b>31A-170 - 2.d</b>	330	1.7	1.9	602.82433	83.708736	

### APPENDIX 3C: LA-ICP-MS MONAZITE RESULTS

#### Monazite morphology

Sample	Textural location	Location	Zoning	Size (long axis)	Crystal habit	Comments	
WGC2019J-25B-C5_mon_G1 - 1.d	Matrix	rim	Y	~150µm (broken off fragment = ~75µm)	Asymmetric	Broken off fragment of Grain 1. Fragment has paler zoning than the relatively homogenous dark zoning in the main fraction of the grain.	
WGC2019J-25B-C5_mon_G1 - 2.d	Matrix	rim					Second broken off fragment of Grain 1. Very minor and patchy zoning present.
WGC2019J-25B-C5_mon_G1 - 3.d	Matrix	rim	N				
WGC2019J-25B-C5_mon_G1 - 4.d	Matrix	rim					Potentially landed on very small region of patchy, pale zoning
WGC2019J-25B-C5_mon_G1 - 5.d	Matrix	core					
WGC2019J-25B-C5_mon_G1 - 6.d	Matrix	rim					
WGC2019J-25B-C5_mon_G1 - 7.d	Matrix	rim					
WGC2019J-25B-C5_mon_G1 - 8.d	Matrix	rim					
WGC2019J-25B-C6_mon_G2 - 1.d	Matrix	core	N	~75µm	Asymmetric	Small amount of patchy zoning but very minor	
WGC2019J-25B-C6_mon_G2 - 2.d	Matrix	core				Small amount of patchy zoning but very minor	
WGC2019J-25B-C7_mon_G3 - 1.d	Matrix	rim	N	~600µm	Oval		
WGC2019J-25B-C7_mon_G3 - 2.d	Matrix	rim					
WGC2019J-25B-C7_mon_G3 - 3.d	Matrix	rim					
WGC2019J-25B-C7_mon_G3 - 4.d	Matrix	rim					
WGC2019J-25B-C7_mon_G3 - 5.d	Matrix	rim					
WGC2019J-25B-C7_mon_G3 - 6.d	Matrix	rim					
WGC2019J-25B-C7_mon_G3 - 7.d	Matrix	rim					
WGC2019J-25B-C7_mon_G3 - 8.d	Matrix	rim					
WGC2019J-25B-C7_mon_G3 - 9.d	Matrix	rim					
WGC2019J-25B-C7_mon_G3 - 10.d	Matrix	core					
WGC2019J-25B-C7_mon_G3 - 11.d	Matrix	mid					
WGC2019J-25B-C7_mon_G3 - 12.d	Matrix	mid					
WGC2019J-25B-C7_mon_G3 - 13.d	Matrix	core					
WGC2019J-25B-C7_mon_G3 - 14.d	Matrix	rim					
WGC2019J-25B-C7_mon_G3 - 15.d	Matrix	mid					

WGC2019J-25B-C7_mon_G3 - 16.d	Matrix	core			
WGC2019J-25B-C7_mon_G3 - 17.d	Matrix	core			
WGC2019J-25B-C7_mon_G3 - 18.d	Matrix	core			
WGC2019J-25B-C7_mon_G3 - 19.d	Matrix	core			
WGC2019J-25B-C7_mon_G3 - 20.d	Matrix	core			
WGC2019J-25B-C7_mon_G3 - 21.d	Matrix	core			
WGC2019J-25B-C7_mon_G3 - 22.d	Matrix	mid			
WGC2019J-25B-C7_mon_G3 - 23.d	Matrix	rim			
WGC2019J-25B-C7_mon_G3 - 24.d	Matrix	mid			
WGC2019J-25B-C7_mon_G3 - 25.d	Matrix	core			
WGC2019J-25B-C7_mon_G3 - 26.d	Matrix	core			
WGC2019J-25B-C7_mon_G3 - 27.d	Matrix	mid			
WGC2019J-25B-C7_mon_G3 - 28.d	Matrix	mid			
WGC2019J-25B-C7_mon_G3 - 29.d	Matrix	mid			
WGC2019J-25B-C7_mon_G3 - 30.d	Matrix	rim			
WGC2019J-25B-C7_mon_G3 - 31.d	Matrix	rim			
WGC2019J-25B-C7_mon_G3 - 32.d	Matrix	rim			
WGC2019J-25B-C7_mon_G3 - 33.d	Matrix	rim			
WGC2019J-25B-C7_mon_G3 - 34.d	Matrix	rim			
WGC2019J-25B-C7_mon_G3 - 35.d	Matrix	mid			
WGC2019J-25B-C7_mon_G3 - 36.d	Matrix	rim			
WGC2019J-25B-C7_mon_G3 - 37.d	Matrix	mid			
WGC2019J-25B-C7_mon_G3 - 38.d	Matrix	core			
WGC2019J-25B-C7_mon_G3 - 39.d	Matrix	mid			
WGC2019J-25B-C7_mon_G3 - 40.d	Matrix	core			
WGC2019J-25B-C15_mon_G4 - 1.d	Matrix	rim	N	~1000µm	Asymmetric
WGC2019J-25B-C15_mon_G4 - 2.d	Matrix	rim			
WGC2019J-25B-C15_mon_G4 - 3.d	Matrix	rim			
WGC2019J-25B-C15_mon_G4 - 4.d	Matrix	mid			
WGC2019J-25B-C15_mon_G4 - 5.d	Matrix	rim			
WGC2019J-25B-C15_mon_G4 - 6.d	Matrix	rim			Near eaten away region of monazite

---

WGC2019J-25B-C15_mon_G4 - 7.d	Matrix	mid	
WGC2019J-25B-C15_mon_G4 - 8.d	Matrix	rim	
WGC2019J-25B-C15_mon_G4 - 9.d	Matrix	rim	
WGC2019J-25B-C15_mon_G4 - 10.d	Matrix	mid	
WGC2019J-25B-C15_mon_G4 - 11.d	Matrix	mid	
WGC2019J-25B-C15_mon_G4 - 12.d	Matrix	mid	
WGC2019J-25B-C15_mon_G4 - 13.d	Matrix	rim	
WGC2019J-25B-C15_mon_G4 - 14.d	Matrix	rim	
WGC2019J-25B-C15_mon_G4 - 15.d	Matrix	mid	
WGC2019J-25B-C15_mon_G4 - 16.d	Matrix	rim	
WGC2019J-25B-C15_mon_G4 - 17.d	Matrix	rim	Near eaten away region of monazite
WGC2019J-25B-C15_mon_G4 - 18.d	Matrix	mid	
WGC2019J-25B-C15_mon_G4 - 19.d	Matrix	rim	
WGC2019J-25B-C15_mon_G4 - 20.d	Matrix	core	
WGC2019J-25B-C15_mon_G4 - 21.d	Matrix	core	
WGC2019J-25B-C15_mon_G4 - 22.d	Matrix	mid	
WGC2019J-25B-C15_mon_G4 - 23.d	Matrix	mid	
WGC2019J-25B-C15_mon_G4 - 24.d	Matrix	core	
WGC2019J-25B-C15_mon_G4 - 25.d	Matrix	mid	Near eaten away region of monazite
WGC2019J-25B-C15_mon_G4 - 26.d	Matrix	rim	
WGC2019J-25B-C15_mon_G4 - 27.d	Matrix	rim	
WGC2019J-25B-C15_mon_G4 - 28.d	Matrix	rim	
WGC2019J-25B-C15_mon_G4 - 29.d	Matrix	rim	
WGC2019J-25B-C15_mon_G4 - 30.d	Matrix	core	
WGC2019J-25B-C15_mon_G4 - 31.d	Matrix	core	
WGC2019J-25B-C15_mon_G4 - 32.d	Matrix	rim	
WGC2019J-25B-C15_mon_G4 - 33.d	Matrix	rim	
WGC2019J-25B-C15_mon_G4 - 34.d	Matrix	rim	Near second eaten away region of monazite
WGC2019J-25B-C15_mon_G4 - 35.d	Matrix	mid	Near second eaten away region of monazite
WGC2019J-25B-C15_mon_G4 - 36.d	Matrix	rim	
WGC2019J-25B-C15_mon_G4 - 37.d	Matrix	rim	

---

WGC2019J-25B-C15_mon_G4 - 38.d	Matrix	mid			
WGC2019J-25B-C15_mon_G4 - 39.d	Matrix	mid			
WGC2019J-25B-C15_mon_G4 - 40.d	Matrix	rim			
WGC2019J-25B-C15_mon_G4 - 41.d	Matrix	rim			
WGC2019A3-C1_mon_G1 - 1.d	Matrix	rim	N	~125µm	Equant
WGC2019A3-C1_mon_G1 - 2.d	Matrix	rim			
WGC2019A3-C1_mon_G1 - 3.d	Matrix	rim			
WGC2019A3-C1_mon_G1 - 4.d	Matrix	core			
WGC2019A3-C1_mon_G1 - 5.d	Matrix	core			
WGC2019A3-C1_mon_G1 - 6.d	Matrix	rim			
WGC2019A3-C1_mon_G1 - 7.d	Matrix	rim			
WGC2019A3-C1_mon_G1 - 8.d	Matrix	core			
WGC2019A3-C1_mon_G1 - 9.d	Matrix	core			
WGC2019A3-C1_mon_G1 - 10.d	Matrix	rim			
WGC2019A3-C1_mon_G2 - 1.d	Matrix	rim	N	~225µm	Asymmetric
WGC2019A3-C1_mon_G2 - 2.d	Matrix	rim			
WGC2019A3-C1_mon_G2 - 3.d	Matrix	mid			
WGC2019A3-C1_mon_G2 - 4.d	Matrix	core			Potentially along minor fracture
WGC2019A3-C1_mon_G2 - 5.d	Matrix	rim			
WGC2019A3-C1_mon_G2 - 6.d	Matrix	rim			
WGC2019A3-C1_mon_G2 - 7.d	Matrix	rim			
WGC2019A3-C1_mon_G2 - 8.d	Matrix	core			
WGC2019A3-C1_mon_G2 - 9.d	Matrix	core			
WGC2019A3-C1_mon_G2 - 10.d	Matrix	mid			
WGC2019A3-C1_mon_G2 - 11.d	Matrix	mid			
WGC2019A3-C1_mon_G2 - 12.d	Matrix	mid			
WGC2019A3-C1_mon_G2 - 13.d	Matrix	core			
WGC2019A3-C1_mon_G2 - 14.d	Matrix	rim			
WGC2019A3-C1_mon_G2 - 15.d	Matrix	rim			
WGC2019A3-C1_mon_G2 - 16.d	Matrix	core			
WGC2019A3-C2_mon_G3 - 1.d	Kyanite inclusion	rim	N	~375µm	Tabular

WGC2019A3-C2_mon_G3 - 2.d	Kyanite inclusion	rim				
WGC2019A3-C2_mon_G3 - 3.d	Kyanite inclusion	mid				
WGC2019A3-C2_mon_G3 - 4.d	Kyanite inclusion	mid				
WGC2019A3-C2_mon_G3 - 5.d	Kyanite inclusion	rim				
WGC2019A3-C2_mon_G3 - 6.d	Kyanite inclusion	core				
WGC2019A3-C2_mon_G3 - 7.d	Kyanite inclusion	core				
WGC2019A3-C2_mon_G3 - 8.d	Kyanite inclusion	rim				
WGC2019A3-C2_mon_G3 - 9.d	Kyanite inclusion	core				
WGC2019A3-C2_mon_G3 - 10.d	Kyanite inclusion	core				
WGC2019A3-C2_mon_G3 - 11.d	Kyanite inclusion	rim				
WGC2019A3-C2_mon_G3 - 12.d	Kyanite inclusion	core				
WGC2019A3-C2_mon_G3 - 13.d	Kyanite inclusion	rim				
WGC2019A3-C2_mon_G3 - 14.d	Kyanite inclusion	core				
WGC2019A3-C2_mon_G3 - 15.d	Kyanite inclusion	core				
WGC2019A3-C2_mon_G3 - 16.d	Kyanite inclusion	rim				
WGC2019A3-C2_mon_G3 - 17.d	Kyanite inclusion	rim				
WGC2019A3-C2_mon_G3 - 18.d	Kyanite inclusion	rim				
WGC2019A3-C2_mon_G3 - 19.d	Kyanite inclusion	core				
WGC2019A3-C2_mon_G3 - 20.d	Kyanite inclusion	core				
WGC2019A3-C2_mon_G3 - 21.d	Kyanite inclusion	core				
WGC2019A3-C2_mon_G3 - 22.d	Kyanite inclusion	rim				
WGC2019A3-C2_mon_G3 - 23.d	Kyanite inclusion	rim				
WGC2019A3-C2_mon_G3 - 24.d	Kyanite inclusion	mid				
WGC2019A3-C2_mon_G3 - 25.d	Kyanite inclusion	rim				
WGC2019A3-C2_mon_G3 - 26.d	Kyanite inclusion	rim				
WGC2019A3-C3_mon_G4 - 1.d	Quartz edge	rim	N	~300µm	Asymmetric	Inclusion at edge of garnet. One side facing out into matrix.
WGC2019A3-C3_mon_G4 - 2.d	Quartz edge	rim				
WGC2019A3-C3_mon_G4 - 3.d	Quartz edge	rim				
WGC2019A3-C3_mon_G4 - 4.d	Quartz edge	rim				
WGC2019A3-C3_mon_G4 - 5.d	Quartz edge	mid				
WGC2019A3-C3_mon_G4 - 6.d	Quartz edge	rim				

WGC2019A3-C3_mon_G4 - 7.d	Quartz edge	rim			
WGC2019A3-C3_mon_G4 - 8.d	Quartz edge	core			
WGC2019A3-C3_mon_G4 - 9.d	Quartz edge	core			
WGC2019A3-C3_mon_G4 - 10.d	Quartz edge	core			
WGC2019A3-C3_mon_G4 - 11.d	Quartz edge	rim			
WGC2019A3-C3_mon_G4 - 12.d	Quartz edge	core			
WGC2019A3-C3_mon_G4 - 13.d	Quartz edge	rim			
WGC2019A3-C3_mon_G4 - 14.d	Quartz edge	mid			
WGC2019A3-C3_mon_G4 - 15.d	Quartz edge	rim			
WGC2019A3-C3_mon_G4 - 16.d	Quartz edge	rim			
WGC2019A3-C3_mon_G4 - 17.d	Quartz edge	rim			
WGC2019A3-C3_mon_G4 - 18.d	Quartz edge	rim			
WGC2019A3-C3_mon_G4 - 19.d	Quartz edge	mid			
WGC2019A3-C3_mon_G4 - 20.d	Quartz edge	rim			
WGC2019A3-C3_mon_G4 - 21.d	Quartz edge	rim			
WGC2019J-31A-2-C1_mon_G1 - 1.d	Matrix	rim	N	~100µm	Equant
WGC2019J-31A-2-C1_mon_G1 - 2.d	Matrix	rim			
WGC2019J-31A-2-C1_mon_G1 - 3.d	Matrix	core			
WGC2019J-31A-2-C1_mon_G1 - 4.d	Matrix	core			
WGC2019J-31A-2-C1_mon_G1 - 5.d	Matrix	rim			
WGC2019J-31A-2-C5_mon_G4 - 1.d	Matrix	core	N	~75µm	Elongate
WGC2019J-31A-2-C5_mon_G4 - 2.d	Matrix	rim			
WGC2019J-31A-2-C5_mon_G4 - 3.d	Matrix	rim			
WGC2019J-31A-2-C6_mon_G2 - 1.d	Matrix	core	N	~125µm	Prismatic
WGC2019J-31A-2-C6_mon_G2 - 2.d	Matrix	core			
WGC2019J-31A-2-C6_mon_G2 - 3.d	Matrix	core			
WGC2019J-31A-2-C6_mon_G2 - 4.d	Matrix	rim			
WGC2019J-31A-2-C6_mon_G2 - 5.d	Matrix	rim			
WGC2019J-31A-2-C9_mon_G7 - 1.d	Garnet inclusion	rim	N	~125µm	Aysmmetric
WGC2019J-31A-2-C9_mon_G7 - 2.d	Garnet inclusion	core			
WGC2019J-31A-2-C9_mon_G7 - 3.d	Garnet inclusion	core			

WGC2019J-31A-2-C9_mon_G7 - 4.d	Garnet inclusion	rim				
WGC2019J-31A-2-C9_mon_G7 - 5.d	Garnet inclusion	rim				
WGC2019J-31A-3-C1_mon_G1 - 1.d	Garnet inclusion	core	Y - patchy	~100µm	Asymmetric	Inclusion in core of garnet. Cross cuts garnet fracture. Zoning seems to radiate from lower right.
WGC2019J-31A-3-C1_mon_G1 - 2.d	Garnet inclusion	rim				
WGC2019J-31A-3-C1_mon_G1 - 3.d	Garnet inclusion	rim				
WGC2019J-31A-3-C1_mon_G1 - 4.d	Garnet inclusion	rim				
WGC2019J-31A-3-C2_mon_G2 - 1.d	Garnet inclusion	core	N	~125µm	Equant	Inclusion in core of garnet. Gt fracture continues and cuts through monazite
WGC2019J-31A-3-C2_mon_G2 - 2.d	Garnet inclusion	rim				
WGC2019J-31A-3-C2_mon_G2 - 3.d	Garnet inclusion	rim				
WGC2019J-31A-3-C7_mon_G3 - 1.d	Matrix	rim	N	~300µm	Elongate	Lots of pits
WGC2019J-31A-3-C7_mon_G3 - 2.d	Matrix	mid				
WGC2019J-31A-3-C7_mon_G3 - 3.d	Matrix	rim				
WGC2019J-31A-3-C7_mon_G3 - 4.d	Matrix	core				
WGC2019J-31A-3-C7_mon_G3 - 5.d	Matrix	mid				
WGC2019J-31A-3-C7_mon_G3 - 6.d	Matrix	mid				
WGC2019J-31A-3-C7_mon_G3 - 7.d	Matrix	rim				
WGC2019J-31A-3-C7_mon_G3 - 8.d	Matrix	mid				
WGC2019J-31A-3-C7_mon_G3 - 9.d	Matrix	rim				
WGC2019J-31A-3-C7_mon_G3 - 10.d	Matrix	rim				
WGC2019J-31A-3-C8_mon_G4 - 1.d	Garnet inclusion	rim	N	~125µm	Elongate	Inclusion in core of garnet. Cross cuts gt fracture
WGC2019J-31A-3-C8_mon_G4 - 2.d	Garnet inclusion	rim				
WGC2019J-31A-3-C8_mon_G4 - 3.d	Garnet inclusion	core				
WGC2019J-31A-3-C8_mon_G4 - 4.d	Garnet inclusion	core				
WGC2019J-31A-3-C9_mon_G7 - 1.d	Garnet inclusion	rim	N	~400µm	Elongate	Closer to edge of garnet than Grain 8 (same garnet). Very pitted.
WGC2019J-31A-3-C9_mon_G7 - 2.d	Garnet inclusion	rim				
WGC2019J-31A-3-C9_mon_G7 - 3.d	Garnet inclusion	rim				
WGC2019J-31A-3-C9_mon_G7 - 4.d	Garnet inclusion	rim				
WGC2019J-31A-3-C9_mon_G7 - 5.d	Garnet inclusion	rim				
WGC2019J-31A-3-C9_mon_G7 - 6.d	Garnet inclusion	mid				
WGC2019J-31A-3-C9_mon_G7 - 7.d	Garnet inclusion	rim				
WGC2019J-31A-3-C9_mon_G7 - 8.d	Garnet inclusion	core				



WGC2019J-31A-3-C9_mon_G7 - 9.d	Garnet inclusion	rim				
WGC2019J-31A-3-C9_mon_G7 - 10.d	Garnet inclusion	mid				
WGC2019J-31A-3-C9_mon_G7 - 11.d	Garnet inclusion	rim				
WGC2019J-31A-3-C9_mon_G7 - 12.d	Garnet inclusion	core				
WGC2019J-31A-3-C9_mon_G7 - 13.d	Garnet inclusion	mid				
WGC2019J-31A-3-C9_mon_G7 - 14.d	Garnet inclusion	core				
WGC2019J-31A-3-C9_mon_G7 - 15.d	Garnet inclusion	rim				
WGC2019J-31A-3-C9_mon_G7 - 16.d	Garnet inclusion	mid				
WGC2019J-31A-3-C9_mon_G8 - 1.d	Garnet inclusion	rim	N	~225µm	Equant	Inclusion in core of garnet
WGC2019J-31A-3-C9_mon_G8 - 2.d	Garnet inclusion	mid				
WGC2019J-31A-3-C9_mon_G8 - 3.d	Garnet inclusion	core				
WGC2019J-31A-3-C9_mon_G8 - 4.d	Garnet inclusion	mid				
WGC2019J-31A-3-C9_mon_G8 - 5.d	Garnet inclusion	rim				
WGC2019J-31A-3-C9_mon_G8 - 6.d	Garnet inclusion	rim				
WGC2019J-31A-3-C9_mon_G8 - 7.d	Garnet inclusion	core				
WGC2019J-31A-3-C9_mon_G8 - 8.d	Garnet inclusion	core				
WGC2019J-31A-3-C9_mon_G8 - 9.d	Garnet inclusion	rim				
WGC2019J-31A-3-C9_mon_G8 - 10.d	Garnet inclusion	core				
WGC2019J-31A-3-C9_mon_G8 - 11.d	Garnet inclusion	mid				
WGC2019J-31A-3-C9_mon_G8 - 12.d	Garnet inclusion	rim				
WGC2019J-31A-3-C9_mon_G8 - 13.d	Garnet inclusion	mid				
WGC2019J-31A-3-C9_mon_G5 - 1.d	Garnet inclusion	core	N	~30µm	Equant	Inclusion in core of garnet
WGC2019J-31A-3-C10_mon_G10 - 1.d	Matrix	rim	N	~100µm	Equant	
WGC2019J-31A-3-C10_mon_G10 - 2.d	Matrix	core				
WGC2019J-31A-3-C10_mon_G10 - 3.d	Matrix	rim				
WGC2019J-31A-3-C10_mon_G10 - 4.d	Matrix	core				
WGC2019J-31A-3-C10_mon_G10 - 5.d	Matrix	core				
WGC2019J-31A-3-C10_mon_G11 - 1.d	Garnet edge	rim	N	~225µm	Asymmetric	Inclusion at edge of garnet. One side facing out into matrix.
WGC2019J-31A-3-C10_mon_G11 - 2.d	Garnet edge	rim				
WGC2019J-31A-3-C10_mon_G11 - 3.d	Garnet edge	rim				
WGC2019J-31A-3-C10_mon_G11 - 4.d	Garnet edge	core				

WGC2019J-31A-3-C10_mon_G11 - 5.d	Garnet edge	core				
WGC2019J-31A-3-C10_mon_G11 - 6.d	Garnet edge	rim				
WGC2019J-31A-3-C10_mon_G11 - 7.d	Garnet edge	rim				
WGC2019J-31A-3-C15_mon_G21 - 1.d	Garnet edge	core	N	~75µm	Asymmetric	At edge of garnet, not quite touching. Alongside broken off fragments of garnet.
WGC2019J-31A-3-C16_mon_G20 - 1.d	Garnet edge	rim	N	~700µm	Tabular	
WGC2019J-31A-3-C16_mon_G20 - 2.d	Garnet edge	mid				
WGC2019J-31A-3-C16_mon_G20 - 3.d	Garnet edge	mid				
WGC2019J-31A-3-C16_mon_G20 - 4.d	Garnet edge	rim				
WGC2019J-31A-3-C16_mon_G20 - 5.d	Garnet edge	mid				
WGC2019J-31A-3-C16_mon_G20 - 6.d	Garnet edge	mid				
WGC2019J-31A-3-C16_mon_G20 - 7.d	Garnet edge	core				
WGC2019J-31A-3-C16_mon_G20 - 8.d	Garnet edge	core				
WGC2019J-31A-3-C16_mon_G20 - 9.d	Garnet edge	rim				
WGC2019J-31A-3-C16_mon_G20 - 10.d	Garnet edge	rim				
WGC2019J-31A-3-C16_mon_G20 - 11.d	Garnet edge	rim				
WGC2019J-31A-3-C16_mon_G20 - 12.d	Garnet edge	rim				
WGC2019J-31A-3-C16_mon_G20 - 13.d	Garnet edge	mid				
WGC2019J-31A-3-C16_mon_G20 - 14.d	Garnet edge	mid				
WGC2019J-31A-3-C16_mon_G20 - 15.d	Garnet edge	core				
WGC2019J-31A-3-C16_mon_G20 - 16.d	Garnet edge	core				
WGC2019J-31A-3-C16_mon_G20 - 17.d	Garnet edge	mid				
WGC2019J-31A-3-C16_mon_G20 - 18.d	Garnet edge	mid				
WGC2019J-31A-3-C16_mon_G20 - 19.d	Garnet edge	mid				
WGC2019J-31A-3-C16_mon_G20 - 20.d	Garnet edge	rim				
WGC2019J-31A-3-C16_mon_G20 - 21.d	Garnet edge	rim				
WGC2019J-31A-3-C16_mon_G20 - 22.d	Garnet edge	rim				
WGC2019J-31A-3-C16_mon_G20 - 23.d	Garnet edge	rim				
WGC2019J-31A-3-C16_mon_G20 - 24.d	Garnet edge	rim				
WGC2019J-31A-3-C16_mon_G20 - 25.d	Garnet edge	mid				
WGC2019J-31A-3-C16_mon_G20 - 26.d	Garnet edge	mid				
WGC2019J-31A-3-C16_mon_G20 - 27.d	Garnet edge	mid				

WGC2019J-31A-3-C16_mon_G20 - 28.d	Garnet edge	mid												
WGC2019J-31A-3-C16_mon_G20 - 29.d	Garnet edge	rim												
WGC2019J-31A-3-C16_mon_G20 - 30.d	Garnet edge	core												
WGC2019J-31A-3-C17_mon_G17 - 1.d	Garnet edge	rim	N	~100µm	Asymmetric									
WGC2019J-31A-3-C17_mon_G17 - 2.d	Garnet edge	rim												
WGC2019J-31A-3-C17_mon_G17 - 3.d	Garnet edge	rim												
WGC2019J-31A-3-C17_mon_G17 - 4.d	Garnet edge	core												
WGC2019J-31A-3-C17_mon_G17 - 5.d	Garnet edge	rim												
WGC2019J-31A-3-C18_mon_G15 - 1.d	Garnet inclusion	rim	N	~125µm	Tabular									
WGC2019J-31A-3-C18_mon_G15 - 2.d	Garnet inclusion	rim												
WGC2019J-31A-3-C18_mon_G15 - 3.d	Garnet inclusion	rim												
WGC2019J-31A-3-C18_mon_G15 - 4.d	Garnet inclusion	core												
WGC2019J-31A-3-C22_mon_Gx - 1.d	Matrix	core	-	~100µm	Tabular	No SEM image								

### Monazite geochronology

Sample	207/235	2σ	206/238	2σ	207/235	2σ	ErrCorr 6/38vs7/35	ErrCorr 38/6vs7/6	207/235 age	2σ	206/238 age	2σ	Concordant?	% discordance
WGC2019J-25B-C5_mon_G1 - 1.d	0.504	0.023	0.0647	0.0017	0.0573	0.0028	0.123	0.27173	414	15	404.1	10	C - Pop 1	2.391304348
WGC2019J-25B-C5_mon_G1 - 2.d	0.5459	0.013	0.06332	0.0012	0.06282	0.0011	0.17593	0.54847	442.2	8.2	395.8	7.4	D - pop 2	10.4929896
WGC2019J-25B-C5_mon_G1 - 3.d	0.582	0.016	0.06603	0.0014	0.0641	0.0013	0.42556	0.18753	465.3	10	412.2	8.7	D - pop 1	11.41199226
WGC2019J-25B-C5_mon_G1 - 4.d	0.6225	0.014	0.06064	0.0011	0.07468	0.001	0.58088	0.4151	491.3	8.5	379.9	6.8	D - pop 2	22.67453694
WGC2019J-25B-C5_mon_G1 - 5.d	0.6298	0.014	0.06067	0.0011	0.07531	0.001	0.48643	0.24963	496.3	8.8	379.7	6.6	D - pop 2	23.49385452
WGC2019J-25B-C5_mon_G1 - 6.d	0.6175	0.015	0.06179	0.0012	0.07283	0.001	0.7271	0.22778	488.1	9.1	386.5	7.3	D - pop 2	20.81540668
WGC2019J-25B-C5_mon_G1 - 7.d	0.5547	0.013	0.06182	0.0012	0.06542	0.001	0.55293	0.36258	447.9	8.4	386.7	7.3	D - pop 2	13.66376423
WGC2019J-25B-C5_mon_G1 - 8.d	0.6283	0.014	0.06081	0.0011	0.07497	0.001	0.56349	0.36503	494.9	8.6	380.5	6.9	D - pop 2	23.11578097
WGC2019J-25B-C6_mon_G2 - 1.d	0.6515	0.015	0.06318	0.0013	0.07471	0.0011	0.70765	0.25826	509.3	9.1	394.9	7.6	D - pop 2	22.46220302
WGC2019J-25B-C6_mon_G2 - 2.d	0.6316	0.014	0.06253	0.0012	0.07312	0.001	0.70357	0.26144	497	8.8	391	7.2	D - pop 2	21.32796781
WGC2019J-25B-C7_mon_G3 - 1.d	0.5759	0.013	0.06172	0.0012	0.06748	0.00097	0.68365	0.15822	461.6	8.7	386.1	7.3	D - pop 2	16.35615251
WGC2019J-25B-C7_mon_G3 - 2.d	0.6108	0.014	0.06068	0.0011	0.07285	0.001	0.65132	0.32569	483.9	8.6	379.7	6.9	D - pop 2	21.53337466
WGC2019J-25B-C7_mon_G3 - 3.d	0.6392	0.014	0.06152	0.0011	0.07524	0.0011	0.40984	0.34671	501.7	8.7	384.8	6.6	D - pop 2	23.30077736

Samantha Nicole March  
Ultrahigh-pressure metapelites in the WGR

WGC2019J-25B-C7_mon_G3 - 4.d	0.6396	0.014	0.06192	0.0011	0.07491	0.001	0.52771	0.41838	501.9	8.7	387.3	6.9	D - pop 2	22.83323371
WGC2019J-25B-C7_mon_G3 - 5.d	0.6346	0.014	0.06207	0.0012	0.0741	0.001	0.5515	0.27076	498.8	8.7	388.2	7	D - pop 2	22.17321572
WGC2019J-25B-C7_mon_G3 - 6.d	0.5441	0.012	0.06257	0.0012	0.06306	0.00096	0.54268	0.23858	441	8.1	391.3	7.2	D - pop 2	11.26984127
WGC2019J-25B-C7_mon_G3 - 7.d	0.6401	0.014	0.06208	0.0011	0.07496	0.00099	0.62916	0.34535	502.3	8.5	388.6	6.7	D - pop 2	22.63587498
WGC2019J-25B-C7_mon_G3 - 8.d	0.6459	0.014	0.06181	0.0011	0.07583	0.001	0.58883	0.29626	505.8	8.6	386.6	6.9	D - pop 2	23.56662713
WGC2019J-25B-C7_mon_G3 - 9.d	0.6815	0.015	0.06285	0.0011	0.07869	0.0011	0.71084	0.092926	527.6	8.9	392.9	6.9	D - pop 2	25.53070508
WGC2019J-25B-C7_mon_G3 - 10.d	0.6371	0.014	0.06185	0.0011	0.07471	0.001	0.58283	0.35464	500.4	8.6	386.9	6.8	D - pop 2	22.68185452
WGC2019J-25B-C7_mon_G3 - 11.d	0.6478	0.014	0.06106	0.0011	0.07695	0.0011	0.51321	0.20941	507.1	8.8	382.1	6.7	D - pop 2	24.64997042
WGC2019J-25B-C7_mon_G3 - 12.d	0.6446	0.014	0.06151	0.0011	0.07637	0.0011	0.59334	0.25074	505	8.9	384.8	7	D - pop 2	23.8019802
WGC2019J-25B-C7_mon_G3 - 13.d	0.6162	0.014	0.0613	0.0011	0.07272	0.001	0.49189	0.37091	487.4	8.5	383.5	6.8	D - pop 2	21.31719327
WGC2019J-25B-C7_mon_G3 - 14.d	0.5456	0.013	0.06278	0.0012	0.0632	0.00096	0.53965	0.30619	442	8.2	392.5	7.3	D - pop 2	11.19909502
WGC2019J-25B-C7_mon_G3 - 15.d	0.6161	0.014	0.06142	0.0012	0.07273	0.0011	0.57273	0.26046	487.3	8.7	384.3	7	D - pop 2	21.13687667
WGC2019J-25B-C7_mon_G3 - 16.d	0.6111	0.013	0.06117	0.0011	0.07235	0.001	0.564	0.2894	484.1	8.5	382.7	6.9	D - pop 2	20.94608552
WGC2019J-25B-C7_mon_G3 - 17.d	0.6499	0.015	0.06215	0.0012	0.07586	0.0011	0.71121	0.20063	508.3	9	388.7	7.1	D - pop 2	23.52941176
WGC2019J-25B-C7_mon_G3 - 18.d	0.6297	0.014	0.06226	0.0012	0.0735	0.001	0.73495	0.2354	495.8	8.9	389.3	7	D - pop 2	21.48043566
WGC2019J-25B-C7_mon_G3 - 19.d	0.614	0.013	0.06137	0.0011	0.07246	0.00097	0.56848	0.2941	486	8.3	383.9	6.8	D - pop 2	21.00823045
WGC2019J-25B-C7_mon_G3 - 20.d	0.6292	0.014	0.06122	0.0011	0.07445	0.001	0.5667	0.34133	495.5	8.6	383	6.9	D - pop 2	22.70433905
WGC2019J-25B-C7_mon_G3 - 21.d	0.6293	0.013	0.0612	0.0011	0.07436	0.00099	0.5073	0.41552	495.6	8.4	382.9	6.7	D - pop 2	22.74011299
WGC2019J-25B-C7_mon_G3 - 22.d	0.6275	0.013	0.06136	0.0011	0.074	0.001	0.57598	0.39278	494.4	8.4	383.9	6.8	D - pop 2	22.35032362
WGC2019J-25B-C7_mon_G3 - 23.d	0.6628	0.014	0.06181	0.0011	0.07744	0.0011	0.46771	0.40911	516.7	8.4	386.6	6.9	D - pop 2	25.17902071
WGC2019J-25B-C7_mon_G3 - 24.d	0.6356	0.014	0.06162	0.0011	0.0745	0.00099	0.60135	0.36924	499.5	8.5	385.5	6.9	D - pop 2	22.82282282
WGC2019J-25B-C7_mon_G3 - 25.d	0.6198	0.014	0.06124	0.0011	0.07313	0.00098	0.67828	0.036792	489.7	8.6	383.2	6.8	D - pop 2	21.74800899
WGC2019J-25B-C7_mon_G3 - 26.d	0.6135	0.013	0.06139	0.0011	0.07233	0.00096	0.61936	0.38531	486.1	8.3	384.1	7	D - pop 2	20.98333676
WGC2019J-25B-C7_mon_G3 - 27.d	0.6036	0.013	0.06084	0.0011	0.07164	0.001	0.47034	0.35398	479.4	8.4	380.7	6.7	D - pop 2	20.58823529
WGC2019J-25B-C7_mon_G3 - 28.d	0.6176	0.014	0.06147	0.0012	0.07266	0.001	0.68859	0.095517	488.2	9.1	384.6	7.1	D - pop 2	21.22081114
WGC2019J-25B-C7_mon_G3 - 29.d	0.6399	0.014	0.06077	0.0012	0.07623	0.001	0.69217	0.26969	502.1	8.9	380.3	7	D - pop 2	24.25811591
WGC2019J-25B-C7_mon_G3 - 30.d	0.6106	0.013	0.06131	0.0011	0.07191	0.00096	0.60667	0.36975	483.9	8.3	383.6	6.9	D - pop 2	20.72742302
WGC2019J-25B-C7_mon_G3 - 31.d	0.6237	0.014	0.06076	0.0012	0.07439	0.001	0.7683	0.27496	492.1	8.8	380.2	7	D - pop 2	22.73928063
WGC2019J-25B-C7_mon_G3 - 32.d	0.5886	0.014	0.06189	0.0012	0.06875	0.001	0.57572	0.31251	469.8	8.8	387.1	7.4	D - pop 2	17.60323542
WGC2019J-25B-C7_mon_G3 - 33.d	0.5846	0.014	0.06187	0.0012	0.06842	0.001	0.58936	0.3542	467.2	8.8	387	7.5	D - pop 2	17.16609589
WGC2019J-25B-C7_mon_G3 - 34.d	0.5701	0.013	0.06268	0.0012	0.06622	0.001	0.52624	0.32025	458.5	8.4	391.9	7.4	D - pop 2	14.52562704

Samantha Nicole March  
Ultrahigh-pressure metapelites in the WGR

WGC2019J-25B-C7_mon_G3 - 35.d	0.5968	0.013	0.05994	0.0011	0.0722	0.00097	0.47833	0.36871	475.1	8.2	375.2	6.6	D - pop 2	21.02715218
WGC2019J-25B-C7_mon_G3 - 36.d	0.5835	0.013	0.0616	0.0012	0.06874	0.0011	0.62094	0.19533	466.6	8.7	385.3	7.2	D - pop 2	17.4239177
WGC2019J-25B-C7_mon_G3 - 37.d	0.6145	0.014	0.06153	0.0011	0.07239	0.0011	0.46853	0.3088	486.3	8.5	384.9	6.8	D - pop 2	20.85132634
WGC2019J-25B-C7_mon_G3 - 38.d	0.6179	0.014	0.06136	0.0011	0.07263	0.001	0.6048	0.12999	488.4	8.6	383.9	6.8	D - pop 2	21.3963964
WGC2019J-25B-C7_mon_G3 - 39.d	0.5654	0.013	0.06275	0.0012	0.0653	0.00097	0.54699	0.22119	455.5	8.1	392.3	7.2	D - pop 2	13.87486279
WGC2019J-25B-C7_mon_G3 - 40.d	0.6122	0.013	0.0614	0.0011	0.07228	0.00096	0.52042	0.45082	485.3	8.6	384.1	6.9	D - pop 2	20.85308057
WGC2019J-25B-C15_mon_G4 - 1.d	0.5186	0.012	0.06037	0.0012	0.06213	0.0009	0.59503	0.39915	424.6	8	377.9	7.1	D - pop 2	10.99858691
WGC2019J-25B-C15_mon_G4 - 2.d	0.5564	0.012	0.06019	0.0011	0.06713	0.00093	0.62315	0.19039	449.1	8.1	376.8	6.7	D - pop 2	16.0988644
WGC2019J-25B-C15_mon_G4 - 3.d	0.5273	0.013	0.06114	0.0012	0.0622	0.001	0.5492	0.29307	430.4	8.5	382.5	7.3	D - pop 2	11.12918216
WGC2019J-25B-C15_mon_G4 - 4.d	0.6009	0.014	0.0606	0.0011	0.07195	0.001	0.60393	0.26453	477.7	8.6	379.3	6.9	D - pop 2	20.59870211
WGC2019J-25B-C15_mon_G4 - 5.d	0.6204	0.014	0.06182	0.0011	0.07294	0.001	0.63392	0.17001	490	8.5	386.7	6.9	D - pop 2	21.08163265
WGC2019J-25B-C15_mon_G4 - 6.d	0.5844	0.014	0.06085	0.0012	0.06972	0.001	0.65396	0.23995	467.2	8.7	380.8	7.3	D - pop 2	18.49315068
WGC2019J-25B-C15_mon_G4 - 7.d	0.5944	0.014	0.06161	0.0012	0.06967	0.001	0.67005	0.1631	473.5	9.1	385.4	7.4	D - pop 2	18.6061246
WGC2019J-25B-C15_mon_G4 - 8.d	0.5613	0.013	0.06194	0.0012	0.06536	0.00097	0.60025	0.16063	452.2	8.4	387.4	7.2	D - pop 2	14.3299425
WGC2019J-25B-C15_mon_G4 - 9.d	0.5635	0.013	0.0612	0.0012	0.06654	0.001	0.56638	0.27817	453.7	8.4	382.9	7.1	D - pop 2	15.60502535
WGC2019J-25B-C15_mon_G4 - 10.d	0.5872	0.014	0.06061	0.0012	0.07005	0.001	0.73945	0.10151	468.9	9	379.3	7.3	D - pop 2	19.10855193
WGC2019J-25B-C15_mon_G4 - 11.d	0.5906	0.014	0.06139	0.0012	0.06991	0.001	0.61047	0.22306	472.1	8.4	384.1	7.1	D - pop 2	18.64011862
WGC2019J-25B-C15_mon_G4 - 12.d	0.6018	0.014	0.06189	0.0012	0.07075	0.001	0.67943	0.23414	478.2	8.8	387.1	7.2	D - pop 2	19.05060644
WGC2019J-25B-C15_mon_G4 - 13.d	0.5944	0.013	0.06178	0.0012	0.07013	0.001	0.69631	0.16585	474.1	8.8	386.5	7.2	D - pop 2	18.47711453
WGC2019J-25B-C15_mon_G4 - 14.d	0.5909	0.013	0.06166	0.0012	0.06976	0.001	0.60772	0.33684	471.3	8.4	385.7	7.1	D - pop 2	18.16252917
WGC2019J-25B-C15_mon_G4 - 15.d	0.6014	0.014	0.06083	0.0012	0.0714	0.00099	0.77354	0.25696	478	8.7	380.7	7.2	D - pop 2	20.35564854
WGC2019J-25B-C15_mon_G4 - 16.d	0.6025	0.014	0.06222	0.0012	0.07054	0.001	0.6433	0.31405	478.7	8.8	389.1	7.3	D - pop 2	18.71735952
WGC2019J-25B-C15_mon_G4 - 17.d	0.6365	0.015	0.06215	0.0012	0.07431	0.0011	0.63111	0.22738	500.6	8.9	388.7	7.3	D - pop 2	22.35317619
WGC2019J-25B-C15_mon_G4 - 18.d	0.5974	0.014	0.06188	0.0012	0.07022	0.0011	0.58599	0.4346	475.4	8.7	387	7.4	D - pop 2	18.59486748
WGC2019J-25B-C15_mon_G4 - 19.d	0.6036	0.014	0.06169	0.0012	0.07092	0.001	0.62617	0.34498	479.4	8.7	385.9	7.4	D - pop 2	19.5035461
WGC2019J-25B-C15_mon_G4 - 20.d	0.6453	0.014	0.06085	0.0011	0.07677	0.001	0.72492	0.31646	505.5	8.7	380.8	7	D - pop 2	24.66864491
WGC2019J-25B-C15_mon_G4 - 21.d	0.6382	0.014	0.06139	0.0011	0.07533	0.0011	0.49423	0.26064	501.5	9	384.4	6.6	D - pop 2	23.34995015
WGC2019J-25B-C15_mon_G4 - 22.d	0.6048	0.013	0.05998	0.0011	0.07323	0.0011	0.64489	0.28226	480.2	8.5	375.5	6.8	D - pop 2	21.80341524
WGC2019J-25B-C15_mon_G4 - 23.d	0.6707	0.015	0.06114	0.0012	0.07941	0.0011	0.59584	0.32874	521	9	382.6	7	D - pop 2	26.56429942
WGC2019J-25B-C15_mon_G4 - 24.d	0.631	0.014	0.06076	0.0012	0.07542	0.001	0.63236	0.28535	497.1	8.5	380.2	7	D - pop 2	23.51639509
WGC2019J-25B-C15_mon_G4 - 25.d	0.6436	0.014	0.06197	0.0012	0.07553	0.0011	0.5431	0.49566	504.4	8.7	387.6	7.2	D - pop 2	23.15622522

Samantha Nicole March  
Ultrahigh-pressure metapelites in the WGR

WGC2019J-25B-C15_mon_G4 - 26.d	0.6477	0.015	0.06159	0.0011	0.07633	0.0011	0.74405	-0.024593	506.9	9.1	385.3	6.9	D - pop 2	23.98895246
WGC2019J-25B-C15_mon_G4 - 27.d	0.6412	0.014	0.06102	0.0011	0.07619	0.0011	0.60467	0.27514	503.5	9.2	381.8	6.9	D - pop 2	24.17080437
WGC2019J-25B-C15_mon_G4 - 28.d	0.6243	0.014	0.06071	0.0011	0.0749	0.0011	0.55072	0.27666	492.9	8.3	379.9	6.8	D - pop 2	22.92554271
WGC2019J-25B-C15_mon_G4 - 29.d	0.6397	0.014	0.06124	0.0011	0.07575	0.001	0.64298	0.39788	502	8.7	383.1	7	D - pop 2	23.68525896
WGC2019J-25B-C15_mon_G4 - 30.d	0.638	0.014	0.06146	0.0011	0.07554	0.001	0.61557	0.40364	501	8.7	384.5	7	D - pop 2	23.25349301
WGC2019J-25B-C15_mon_G4 - 31.d	0.6482	0.014	0.06214	0.0012	0.07579	0.0011	0.6322	0.25713	507.3	8.8	388.6	7	D - pop 2	23.3983836
WGC2019J-25B-C15_mon_G4 - 32.d	0.6291	0.014	0.06126	0.0012	0.07433	0.001	0.7076	0.21752	495.4	9	383.3	7	D - pop 2	22.62817925
WGC2019J-25B-C15_mon_G4 - 33.d	0.5988	0.013	0.06017	0.0011	0.07231	0.001	0.58726	0.20203	476.4	8.4	376.7	6.6	D - pop 2	20.92779177
WGC2019J-25B-C15_mon_G4 - 34.d	0.6367	0.014	0.06135	0.0011	0.07501	0.001	0.56813	0.29704	500.1	8.7	383.8	6.9	D - pop 2	23.25534893
WGC2019J-25B-C15_mon_G4 - 35.d	0.6498	0.014	0.06208	0.0011	0.07618	0.0011	0.61984	0.22633	508.2	8.7	388.2	6.9	D - pop 2	23.61275089
WGC2019J-25B-C15_mon_G4 - 36.d	0.5748	0.013	0.06249	0.0012	0.06701	0.00099	0.52408	0.21892	461	8.6	390.7	7.3	D - pop 2	15.2494577
WGC2019J-25B-C15_mon_G4 - 37.d	0.5975	0.013	0.0603	0.0011	0.07174	0.00099	0.53169	0.41942	475.6	8.3	377.4	6.8	D - pop 2	20.64760303
WGC2019J-25B-C15_mon_G4 - 38.d	0.6047	0.014	0.06108	0.0011	0.07201	0.001	0.67494	0.14314	480.6	8.9	382.2	6.9	D - pop 2	20.47440699
WGC2019J-25B-C15_mon_G4 - 39.d	0.6326	0.014	0.06084	0.0011	0.0755	0.0012	0.3411	0.46167	497.6	8.9	380.7	6.9	D - pop 2	23.49276527
WGC2019J-25B-C15_mon_G4 - 40.d	0.5989	0.015	0.06222	0.0012	0.06966	0.0011	0.69433	0.036176	476.3	9.4	389.1	7.5	D - pop 2	18.30778921
WGC2019J-25B-C15_mon_G4 - 41.d	0.5905	0.014	0.0616	0.0012	0.06896	0.001	0.67821	-0.021473	470.9	9.1	385.3	7.1	D - pop 2	18.1779571
WGC2019A3-C1_mon_G1 - 1.d	0.5314	0.012	0.06207	0.0011	0.0622	0.00096	0.54747	0.15274	432.6	8.2	388.2	6.9	D - pop 2	10.26352288
WGC2019A3-C1_mon_G1 - 2.d	0.5951	0.013	0.06101	0.0011	0.07072	0.00099	0.58707	0.32022	474.1	8.4	381.8	6.9	D - pop 2	19.46846657
WGC2019A3-C1_mon_G1 - 3.d	0.5077	0.012	0.06074	0.0012	0.06066	0.00085	0.68094	0.14925	416.8	7.8	380.1	7	D - pop 2	8.805182342
WGC2019A3-C1_mon_G1 - 4.d	0.597	0.014	0.0617	0.0011	0.07032	0.001	0.55879	0.1386	475.2	8.6	385.9	6.9	D - pop 2	18.79208754
WGC2019A3-C1_mon_G1 - 5.d	0.6176	0.014	0.0615	0.0012	0.07245	0.001	0.62419	0.23133	488.2	8.6	384.7	7	D - pop 2	21.20032773
WGC2019A3-C1_mon_G1 - 6.d	0.6264	0.014	0.06248	0.0012	0.07289	0.0011	0.65092	0.36978	493.7	8.8	390.6	7.5	D - pop 2	20.88312741
WGC2019A3-C1_mon_G1 - 7.d	0.5218	0.012	0.0612	0.0012	0.06185	0.00091	0.56673	0.36697	426.3	7.8	382.9	7.1	D - pop 2	10.18062397
WGC2019A3-C1_mon_G1 - 8.d	0.6009	0.014	0.06133	0.0012	0.07081	0.001	0.59707	0.25887	477.7	8.6	383.7	7	D - pop 2	19.67762194
WGC2019A3-C1_mon_G1 - 9.d	0.5604	0.013	0.06082	0.0011	0.06663	0.00099	0.53052	0.21229	452.2	8.2	380.6	6.9	D - pop 2	15.8337019
WGC2019A3-C1_mon_G1 - 10.d	0.5085	0.012	0.06048	0.0011	0.06071	0.00095	0.51282	0.2314	417.3	7.9	378.5	6.9	D - pop 2	9.297867242
WGC2019A3-C1_mon_G2 - 1.d	0.4987	0.011	0.06269	0.0012	0.0579	0.00085	0.52356	0.27182	410.7	7.7	391.9	7.2	D - between pops	4.577550523
WGC2019A3-C1_mon_G2 - 2.d	0.6035	0.014	0.06218	0.0011	0.07053	0.0011	0.43686	0.3548	479.3	8.6	388.9	7	D - pop 2	18.86083872
WGC2019A3-C1_mon_G2 - 3.d	0.566	0.013	0.06138	0.0012	0.06609	0.00095	0.55916	0.34878	455.3	8.2	384	7	D - pop 2	15.66000439
WGC2019A3-C1_mon_G2 - 4.d	0.5969	0.013	0.06102	0.0011	0.0705	0.001	0.42821	0.35889	475.2	8.5	381.8	6.8	D - pop 2	19.65488215
WGC2019A3-C1_mon_G2 - 5.d	0.5716	0.013	0.06079	0.0011	0.06801	0.00097	0.57502	0.30125	458.9	8.2	380.4	7	D - pop 2	17.10612334

Samantha Nicole March  
Ultrahigh-pressure metapelites in the WGR

WGC2019A3-C1_mon_G2 - 6.d	0.6184	0.014	0.06205	0.0011	0.07234	0.001	0.7075	-	488.8	8.5	388	6.9	D - pop 2	20.62193126
WGC2019A3-C1_mon_G2 - 7.d	0.6032	0.013	0.06112	0.0011	0.07161	0.001	0.56948	0.0061649	479.1	8.5	382.4	6.7	D - pop 2	20.18367773
WGC2019A3-C1_mon_G2 - 8.d	0.6082	0.013	0.0619	0.0011	0.07125	0.00099	0.55618	0.27761	482.3	8.3	387.1	6.9	D - pop 2	19.73875181
WGC2019A3-C1_mon_G2 - 9.d	0.6022	0.013	0.06067	0.0011	0.07213	0.001	0.50372	0.18369	478.5	8.4	379.7	6.7	D - pop 2	20.64785789
WGC2019A3-C1_mon_G2 - 10.d	0.6618	0.015	0.06332	0.0012	0.07607	0.0011	0.67518	0.166	515.6	9.3	395.8	7.3	D - pop 2	23.23506594
WGC2019A3-C1_mon_G2 - 11.d	0.5694	0.013	0.06151	0.0012	0.06743	0.00095	0.67336	0.34937	457.5	8.1	384.8	7.2	D - pop 2	15.89071038
WGC2019A3-C1_mon_G2 - 12.d	0.5918	0.013	0.06154	0.0012	0.06944	0.001	0.59386	0.36021	471.9	8.5	385	7	D - pop 2	18.41491841
WGC2019A3-C1_mon_G2 - 13.d	0.5974	0.013	0.06099	0.0011	0.07153	0.0011	0.42089	0.41418	475.5	8.5	381.6	6.9	D - pop 2	19.74763407
WGC2019A3-C1_mon_G2 - 14.d	0.572	0.013	0.06153	0.0012	0.06692	0.001	0.64813	0.084879	459.1	8.7	384.9	7.2	D - pop 2	16.1620562
WGC2019A3-C1_mon_G2 - 15.d	0.5604	0.013	0.06159	0.0012	0.06607	0.00097	0.5678	0.35586	451.7	8.2	385.3	7.1	D - pop 2	14.70002214
WGC2019A3-C1_mon_G2 - 16.d	0.6088	0.013	0.06089	0.0011	0.07236	0.001	0.50091	0.27388	482.7	8.4	381	6.7	D - pop 2	21.06898695
WGC2019A3-C2_mon_G3 - 1.d	0.5509	0.013	0.06473	0.0012	0.06185	0.00093	0.56794	0.22804	445.5	8.3	404.3	7.4	D - pop 1	9.248035915
WGC2019A3-C2_mon_G3 - 2.d	0.5467	0.013	0.06388	0.0012	0.06199	0.00092	0.63793	-8.535E-06	442.7	8.6	399.2	7.4	D - pop 1	9.826067314
WGC2019A3-C2_mon_G3 - 3.d	0.5563	0.013	0.06523	0.0012	0.06199	0.00093	0.62954	0.08336	449.5	8.3	407.3	7.5	D - pop 1	9.388209121
WGC2019A3-C2_mon_G3 - 4.d	0.5504	0.013	0.06466	0.0012	0.06204	0.00097	0.57497	0.22388	445.7	8.5	403.9	7.4	D - pop 1	9.378505721
WGC2019A3-C2_mon_G3 - 5.d	0.5498	0.012	0.06463	0.0013	0.06161	0.0009	0.68027	0.21353	444.7	8.1	403.7	7.7	D - pop 1	9.219698673
WGC2019A3-C2_mon_G3 - 6.d	0.5457	0.013	0.06417	0.0012	0.06162	0.00093	0.63326	0.15266	442.5	8.4	400.9	7.5	D - pop 1	9.401129944
WGC2019A3-C2_mon_G3 - 7.d	0.5507	0.013	0.06554	0.0013	0.06109	0.00094	0.48919	0.29768	445.3	8.3	409.2	7.6	D - pop 1	8.106894229
WGC2019A3-C2_mon_G3 - 8.d	0.562	0.013	0.06495	0.0012	0.06233	0.00091	0.5856	0.22238	452.7	8.5	405.6	7.3	D - pop 1	10.40424122
WGC2019A3-C2_mon_G3 - 9.d	0.5519	0.013	0.06504	0.0012	0.06122	0.00088	0.64726	0.19684	446.6	8.4	406.2	7.5	D - pop 1	9.046126288
WGC2019A3-C2_mon_G3 - 10.d	0.5341	0.012	0.06254	0.0012	0.06167	0.00089	0.67691	0.11936	434.4	8.3	391	7.3	D - pop 2	9.990791897
WGC2019A3-C2_mon_G3 - 11.d	0.5534	0.012	0.0648	0.0012	0.06153	0.00091	0.44118	0.34002	447.2	8	404.7	7.2	D - pop 1	9.503577818
WGC2019A3-C2_mon_G3 - 12.d	0.5474	0.012	0.06441	0.0012	0.06185	0.00096	0.49686	0.36643	443.2	8.1	402.4	7.5	D - pop 1	9.205776173
WGC2019A3-C2_mon_G3 - 13.d	0.5421	0.012	0.06447	0.0013	0.06146	0.00095	0.59962	0.38032	439.7	8.2	402.7	7.8	D - pop 1	8.414828292
WGC2019A3-C2_mon_G3 - 14.d	0.5549	0.012	0.06498	0.0012	0.06183	0.00086	0.54802	0.3192	448.1	8.1	405.8	7.5	D - pop 1	9.439857175
WGC2019A3-C2_mon_G3 - 15.d	0.5505	0.013	0.06475	0.0012	0.06152	0.00092	0.48495	0.099139	445.2	8.3	404.4	7.1	D - pop 2	9.164420485
WGC2019A3-C2_mon_G3 - 16.d	0.5476	0.013	0.06316	0.0012	0.06266	0.00093	0.61467	0.26367	443.3	8.3	394.8	7.5	D - pop 1	10.94067223
WGC2019A3-C2_mon_G3 - 17.d	0.5569	0.013	0.06497	0.0012	0.06204	0.00093	0.52437	0.27838	449.9	8.5	405.8	7.3	D - pop 1	9.802178262
WGC2019A3-C2_mon_G3 - 18.d	0.5566	0.012	0.06512	0.0012	0.06174	0.0009	0.46994	0.3696	449.2	8.1	406.7	7.5	D - pop 1	9.46126447
WGC2019A3-C2_mon_G3 - 19.d	0.5635	0.013	0.06523	0.0013	0.06236	0.00094	0.59227	0.17661	454.2	8.3	407.3	7.6	D - pop 1	10.32584764
WGC2019A3-C2_mon_G3 - 20.d	0.5523	0.013	0.06491	0.0013	0.06185	0.00094	0.56524	0.34825	446.4	8.2	405.4	7.6	D - pop 1	9.184587814

Samantha Nicole March  
Ultrahigh-pressure metapelites in the WGR

WGC2019A3-C2_mon_G3 - 21.d	0.5594	0.013	0.06542	0.0012	0.06165	0.001	0.17028	0.47644	451	8.3	408.5	7.3	D - pop 1	9.423503326
WGC2019A3-C2_mon_G3 - 22.d	0.5575	0.013	0.06502	0.0012	0.06255	0.00097	0.59182	0.12014	449.7	8.7	406	7.5	D - pop 1	9.717589504
WGC2019A3-C2_mon_G3 - 23.d	0.5615	0.013	0.06437	0.0012	0.06333	0.001	0.51755	0.3255	452.4	8.5	402.1	7.6	D - pop 1	11.11847922
WGC2019A3-C2_mon_G3 - 24.d	0.5581	0.013	0.06546	0.0012	0.06188	0.00093	0.46952	0.24226	450.2	8.5	408.7	7.5	D - pop 1	9.218125278
WGC2019A3-C2_mon_G3 - 25.d	0.5567	0.013	0.06519	0.0012	0.0622	0.00094	0.49417	0.31552	449.3	8.3	407.1	7.5	D - pop 1	9.392388159
WGC2019A3-C2_mon_G3 - 26.d	0.5543	0.012	0.06524	0.0012	0.06191	0.00096	0.32743	0.43778	448.1	8.3	407.4	7.4	D - pop 1	9.082794019
WGC2019A3-C3_mon_G4 - 1.d	0.5017	0.012	0.06207	0.0012	0.05838	0.00092	0.51668	0.25005	412.7	7.8	388.2	7.2	D - between pops	5.936515629
WGC2019A3-C3_mon_G4 - 2.d	0.5361	0.012	0.0613	0.0012	0.06347	0.00093	0.61055	0.17846	436.2	8	383.5	7	D - pop 2	12.08161394
WGC2019A3-C3_mon_G4 - 3.d	0.5379	0.012	0.06176	0.0012	0.06329	0.00094	0.47347	0.39811	437	8	386.3	7	D - pop 2	11.60183066
WGC2019A3-C3_mon_G4 - 4.d	0.5282	0.013	0.06116	0.0012	0.06252	0.001	0.59171	0.14998	431.6	8.8	382.7	7.3	D - pop 2	11.32993513
WGC2019A3-C3_mon_G4 - 5.d	0.5418	0.012	0.06137	0.0012	0.06435	0.00093	0.67272	0.21064	439.5	8.1	383.9	7.1	D - pop 2	12.65073948
WGC2019A3-C3_mon_G4 - 6.d	0.5604	0.013	0.06188	0.0012	0.06548	0.00093	0.69851	0.22942	451.7	8.3	387	7.2	D - pop 2	14.32366615
WGC2019A3-C3_mon_G4 - 7.d	0.5238	0.013	0.06076	0.0012	0.06273	0.00094	0.69663	0.15101	427.5	8.4	380.2	7.3	D - pop 2	11.06432749
WGC2019A3-C3_mon_G4 - 8.d	0.5577	0.013	0.05993	0.0011	0.06706	0.00097	0.60932	0.13551	449.8	8.5	375.2	6.9	D - pop 2	16.58514896
WGC2019A3-C3_mon_G4 - 9.d	0.5763	0.014	0.06142	0.0012	0.06765	0.001	0.58701	0.071458	461.9	8.8	384.3	7.1	D - pop 2	16.8001732
WGC2019A3-C3_mon_G4 - 10.d	0.5709	0.013	0.06153	0.0011	0.06722	0.001	0.54985	0.19766	458.4	8.6	384.9	7	D - pop 2	16.03403141
WGC2019A3-C3_mon_G4 - 11.d	0.5198	0.013	0.06105	0.0012	0.06167	0.00094	0.71637	0.039098	426.1	8.4	382	7.4	D - pop 2	10.34968317
WGC2019A3-C3_mon_G4 - 12.d	0.567	0.013	0.06128	0.0012	0.06731	0.00092	0.78272	-9.945E-05	456.6	8.6	383.4	7.1	D - pop 2	16.03153745
WGC2019A3-C3_mon_G4 - 13.d	0.5059	0.012	0.06064	0.0012	0.06051	0.00094	0.63122	0.13632	415.5	8.2	379.5	7.1	D - pop 2	8.664259928
WGC2019A3-C3_mon_G4 - 14.d	0.5726	0.013	0.06137	0.0012	0.06769	0.00095	0.70762	0.22084	459.6	8.6	383.9	7.2	D - pop 2	16.47084421
WGC2019A3-C3_mon_G4 - 15.d	0.5151	0.012	0.06109	0.0012	0.06119	0.00093	0.52882	0.38109	422.2	7.6	382.3	7.2	D - pop 2	9.450497395
WGC2019A3-C3_mon_G4 - 16.d	0.549	0.013	0.06155	0.0011	0.0649	0.00094	0.61027	0.1432	444.2	8.3	385	7	D - pop 2	13.32733003
WGC2019A3-C3_mon_G4 - 17.d	0.5865	0.014	0.0611	0.0012	0.06968	0.001	0.71278	0.12057	468.5	8.7	382.3	7.1	D - pop 2	18.39914621
WGC2019A3-C3_mon_G4 - 18.d	0.5965	0.014	0.06107	0.0012	0.07099	0.001	0.67335	0.25509	474.8	8.8	382.1	7.2	D - pop 2	19.52401011
WGC2019A3-C3_mon_G4 - 19.d	0.6059	0.014	0.06132	0.0012	0.07178	0.001	0.71646	0.12369	480.8	8.9	383.6	7.2	D - pop 2	20.21630616
WGC2019A3-C3_mon_G4 - 20.d	0.4844	0.012	0.06199	0.0012	0.0566	0.001	0.49883	0.075781	400.9	8.2	387.7	7.3	D - between pops	3.292591669
WGC2019A3-C3_mon_G4 - 21.d	0.6365	0.016	0.06253	0.0012	0.07421	0.0012	0.68072	-0.11585	499.8	10	391	7.2	D - pop 2	21.76870748
WGC2019J-31A-2-C1_mon_G1 - 1.d	0.4624	0.012	0.06111	0.0012	0.05515	0.0011	0.40969	0.1667	385.7	8.6	382.3	7.3	C - pop 3	0.88151413
WGC2019J-31A-2-C1_mon_G1 - 2.d	1.874	0.043	0.1769	0.0033	0.07692	0.0012	0.66201	0.0082006	1071.7	15	1049.7	18	NC - pop 1	2.052813287
WGC2019J-31A-2-C1_mon_G1 - 3.d	1.858	0.041	0.1778	0.0033	0.07571	0.0011	0.61249	0.32604	1066	15	1055.1	18	C - pop 1	1.022514071



Samantha Nicole March  
Ultrahigh-pressure metapelites in the WGR

WGC2019J-31A-2-C1_mon_G1 - 4.d	1.831	0.04	0.1771	0.0032	0.07476	0.0011	0.35829	0.39058	1057.1	14	1051.3	18	C - pop 1	0.548670892
WGC2019J-31A-2-C1_mon_G1 - 5.d	1.852	0.041	0.1786	0.0034	0.07501	0.001	0.70839	0.20882	1063.9	15	1059	19	C - pop 1	0.460569602
WGC2019J-31A-2-C5_mon_G4 - 1.d	0.541	0.016	0.06752	0.0013	0.0573	0.0013	0.16095	0.26778	438.4	10	421.2	7.8	NC - pop 2	3.923357664
WGC2019J-31A-2-C5_mon_G4 - 2.d	0.5257	0.013	0.06663	0.0012	0.05765	0.0011	0.21251	0.29912	428.7	8.7	413.8	7.4	NC - pop 2	3.475623979
WGC2019J-31A-2-C5_mon_G4 - 3.d	0.5062	0.014	0.06431	0.0012	0.0572	0.0013	0.1143	0.32661	415.5	9.5	401.8	7.4	NC - pop 2	3.29723225
WGC2019J-31A-2-C6_mon_G2 - 1.d	0.929	0.024	0.07031	0.0014	0.0958	0.0019	0.348	0.25762	667.4	13	438	8.2	D	34.37219059
WGC2019J-31A-2-C6_mon_G2 - 2.d	0.729	0.019	0.06821	0.0013	0.0779	0.0016	0.40943	0.15485	556.3	12	425.3	8.1	D	23.54844508
WGC2019J-31A-2-C6_mon_G2 - 3.d	0.614	0.016	0.06839	0.0014	0.0648	0.0014	0.34375	0.2269	485.5	10	426.4	8.3	D	12.17301751
WGC2019J-31A-2-C6_mon_G2 - 4.d	0.557	0.017	0.07022	0.0014	0.0573	0.0013	0.36948	0.1374	449.1	11	437.5	8.5	C - pop 2	2.582943665
WGC2019J-31A-2-C6_mon_G2 - 5.d	0.5273	0.014	0.06658	0.0013	0.058	0.0014	0.12334	0.3571	429.7	9.5	415.5	7.8	NC - pop 2	3.304631138
WGC2019J-31A-2-C9_mon_G7 - 1.d	0.84	0.027	0.0931	0.0025	0.06502	0.0012	0.84754	-0.19014	618	15	574	15	D	7.1197411
WGC2019J-31A-2-C9_mon_G7 - 2.d	1.253	0.031	0.1279	0.0025	0.07099	0.0012	0.55291	0.32512	824	14	775.9	15	D	5.837378641
WGC2019J-31A-2-C9_mon_G7 - 3.d	1.25	0.034	0.1275	0.0029	0.07119	0.0012	0.76261	-0.059901	822	15	774	17	D	5.839416058
WGC2019J-31A-2-C9_mon_G7 - 4.d	1.211	0.028	0.1253	0.0024	0.07042	0.001	0.51488	0.30622	805.2	13	761.2	14	D	5.464480874
WGC2019J-31A-2-C9_mon_G7 - 5.d	1.005	0.029	0.1057	0.0023	0.06856	0.0012	0.80723	-0.34187	705	15	647.5	13	D	8.156028369
WGC2019J-31A-3-C1_mon_G1 - 1.d	1.437	0.052	0.1425	0.0046	0.0743	0.0014	0.85602	0.093743	903	22	858	26	D	4.983388704
WGC2019J-31A-3-C1_mon_G1 - 2.d	1.782	0.04	0.1739	0.0032	0.07417	0.0011	0.41112	0.33165	1039.4	14	1033.4	18	C - pop 1	0.577256109
WGC2019J-31A-3-C1_mon_G1 - 3.d	1.789	0.04	0.1733	0.0032	0.07471	0.001	0.6463	0.22923	1041.1	15	1030.4	18	C - pop 1	1.027759101
WGC2019J-31A-3-C1_mon_G1 - 4.d	1.233	0.06	0.1274	0.0048	0.0697	0.0014	0.95323	-0.47051	813	27	773	27	D	4.9200492
WGC2019J-31A-3-C2_mon_G2 - 1.d	1.827	0.04	0.1768	0.0033	0.07502	0.001	0.66203	0.37951	1055.5	14	1049.4	18	C - pop 1	0.577925154
WGC2019J-31A-3-C2_mon_G2 - 2.d	1.858	0.044	0.1773	0.0035	0.07594	0.0011	0.66333	0.13304	1065.8	16	1052	19	C - pop 1	1.294802027
WGC2019J-31A-3-C2_mon_G2 - 3.d	1.836	0.042	0.1787	0.0034	0.07504	0.0012	0.49848	0.20834	1059	15	1059.6	18	C - pop 1	-0.05665722
WGC2019J-31A-3-C7_mon_G3 - 1.d	0.5384	0.014	0.06786	0.0013	0.05722	0.0011	0.37837	0.19151	437.1	9.1	423.2	7.7	NC - pop 2	3.180050332
WGC2019J-31A-3-C7_mon_G3 - 2.d	0.522	0.015	0.06795	0.0013	0.0557	0.0014	0.006926	0.39682	425.8	10	423.8	7.9	C - pop 2	0.469704086
WGC2019J-31A-3-C7_mon_G3 - 3.d	0.537	0.018	0.06752	0.0014	0.0583	0.0017	0.105	0.29652	437.3	12	421.2	8.3	NC - pop 2	3.681683055
WGC2019J-31A-3-C7_mon_G3 - 4.d	0.541	0.017	0.06977	0.0014	0.0558	0.0013	0.28462	0.20792	441.5	10	434.7	8.4	C - pop 2	1.540203851
WGC2019J-31A-3-C7_mon_G3 - 5.d	0.5213	0.014	0.06821	0.0013	0.0562	0.0012	0.18079	0.26778	426.6	8.9	425.8	7.9	C - pop 2	0.187529301
WGC2019J-31A-3-C7_mon_G3 - 6.d	0.5284	0.014	0.06771	0.0013	0.0571	0.0012	0.098319	0.3458	430.4	9.3	422.3	7.8	NC - pop 2	1.88197026
WGC2019J-31A-3-C7_mon_G3 - 7.d	0.538	0.017	0.06833	0.0013	0.0564	0.0015	0.27634	0.13835	436.5	11	426.1	7.9	C - pop 2	2.382588774
WGC2019J-31A-3-C7_mon_G3 - 8.d	0.519	0.014	0.06682	0.0013	0.0554	0.0013	0.12512	0.40229	424.1	9.4	417	7.9	C - pop 2	1.674133459
WGC2019J-31A-3-C7_mon_G3 - 9.d	0.542	0.017	0.06842	0.0014	0.0572	0.0016	-0.09975	0.5324	440	11	426.6	8.4	C - pop 2	3.045454545

Samantha Nicole March  
Ultrahigh-pressure metapelites in the WGR

WGC2019J-31A-3-C7_mon_G3 - 10.d	0.5177	0.013	0.06736	0.0013	0.0561	0.0011	0.28484	0.20091	423.3	8.9	420.2	7.8	C - pop 2	0.732341129
WGC2019J-31A-3-C8_mon_G4 - 1.d	1.879	0.043	0.1827	0.0035	0.07495	0.0012	0.49583	0.43387	1074.3	15	1081.7	19	C - pop 1	-0.68882063
WGC2019J-31A-3-C8_mon_G4 - 2.d	1.679	0.051	0.1665	0.0043	0.07294	0.0011	0.93377	-0.34759	999	20	993	24	C - pop 1	0.600600601
WGC2019J-31A-3-C8_mon_G4 - 3.d	1.847	0.043	0.1767	0.0033	0.07567	0.0011	0.58425	0.097866	1062.7	15	1049.1	18	C - pop 1	1.279759104
WGC2019J-31A-3-C8_mon_G4 - 4.d	0.892	0.022	0.0996	0.002	0.06533	0.00099	0.75254	0.068595	647.2	12	611.7	12	D	5.485166873
WGC2019J-31A-3-C9_mon_G7 - 1.d	1.339	0.05	0.136	0.0041	0.07142	0.0011	0.95028	-0.43739	860	22	821	23	D	4.534883721
WGC2019J-31A-3-C9_mon_G7 - 2.d	1.837	0.042	0.1774	0.0034	0.07497	0.0011	0.58791	0.20958	1058.5	15	1052.8	19	C - pop 1	0.538497874
WGC2019J-31A-3-C9_mon_G7 - 3.d	0.841	0.029	0.0944	0.0026	0.06472	0.001	0.92468	-0.34162	618	16	581	15	D	5.987055016
WGC2019J-31A-3-C9_mon_G7 - 4.d	0.5412	0.012	0.06856	0.0012	0.05691	0.00085	0.53198	0.050724	439.1	8.2	427.5	7.5	NC - pop 2	2.641767251
WGC2019J-31A-3-C9_mon_G7 - 5.d	1.843	0.042	0.1785	0.0033	0.07484	0.0011	0.54832	0.19309	1060.4	15	1058.9	18	C - pop 1	0.141456054
WGC2019J-31A-3-C9_mon_G7 - 6.d	1.796	0.04	0.1768	0.0033	0.07371	0.00099	0.63172	0.29183	1044.5	14	1049.3	18	C - pop 1	-0.45955002
WGC2019J-31A-3-C9_mon_G7 - 7.d	1.136	0.031	0.1199	0.0024	0.06866	0.0011	0.7402	-0.047412	769.6	15	729.8	14	D	5.171517672
WGC2019J-31A-3-C9_mon_G7 - 8.d	1.795	0.042	0.1758	0.0033	0.074	0.0011	0.63294	0.063317	1043.1	15	1043.7	18	C - pop 1	-0.05752085
WGC2019J-31A-3-C9_mon_G7 - 9.d	1.49	0.034	0.1492	0.0028	0.07298	0.0011	0.38588	0.38306	928.4	15	896.6	16	D	3.425247738
WGC2019J-31A-3-C9_mon_G7 - 10.d	1.723	0.039	0.1694	0.0031	0.07424	0.0011	0.57867	0.17359	1016.7	15	1008.7	17	C - pop 1	0.786859447
WGC2019J-31A-3-C9_mon_G7 - 11.d	1.794	0.04	0.1739	0.0032	0.07456	0.0011	0.48499	0.22895	1043	15	1033.4	17	C - pop 1	0.92042186
WGC2019J-31A-3-C9_mon_G7 - 12.d	1.829	0.041	0.177	0.0033	0.07507	0.0011	0.52048	0.29953	1055.4	15	1050.2	18	C - pop 1	0.492704188
WGC2019J-31A-3-C9_mon_G7 - 13.d	1.795	0.041	0.1751	0.0033	0.07459	0.0011	0.43611	0.33246	1044	14	1040	18	C - pop 1	0.383141762
WGC2019J-31A-3-C9_mon_G7 - 14.d	1.838	0.042	0.1781	0.0033	0.0754	0.0012	0.47225	0.30959	1058.7	15	1056.2	18	C - pop 1	0.236138661
WGC2019J-31A-3-C9_mon_G7 - 15.d	1.808	0.04	0.1746	0.0033	0.07498	0.001	0.57661	0.34657	1048	14	1037.3	18	C - pop 1	1.020992366
WGC2019J-31A-3-C9_mon_G7 - 16.d	1.846	0.042	0.1789	0.0034	0.07514	0.0011	0.52475	0.37766	1062.4	14	1060.6	19	C - pop 1	0.169427711
WGC2019J-31A-3-C9_mon_G8 - 1.d	1.844	0.043	0.1771	0.0034	0.07546	0.0011	0.65508	0.088775	1060.7	15	1051.2	18	C - pop 1	0.895634958
WGC2019J-31A-3-C9_mon_G8 - 2.d	1.864	0.042	0.1782	0.0034	0.07567	0.0011	0.55486	0.21443	1068	15	1058.1	18	C - pop 1	0.926966292
WGC2019J-31A-3-C9_mon_G8 - 3.d	1.84	0.041	0.178	0.0032	0.07536	0.0011	0.53366	0.1857	1060.2	15	1055.8	18	C - pop 1	0.415016035
WGC2019J-31A-3-C9_mon_G8 - 4.d	1.819	0.042	0.175	0.0033	0.0754	0.0011	0.62254	0.16675	1052.8	15	1039.3	18	C - pop 1	1.282294833
WGC2019J-31A-3-C9_mon_G8 - 5.d	1.84	0.043	0.1781	0.0033	0.07492	0.0011	0.58048	0.15431	1061.2	15	1056.8	18	C - pop 1	0.414624953
WGC2019J-31A-3-C9_mon_G8 - 6.d	1.868	0.043	0.1795	0.0034	0.07555	0.0012	0.50149	0.2279	1069.6	15	1064	19	C - pop 1	0.523560209
WGC2019J-31A-3-C9_mon_G8 - 7.d	1.829	0.041	0.1796	0.0034	0.07408	0.0011	0.30489	0.44607	1057.2	15	1064.4	18	C - pop 1	-0.68104427
WGC2019J-31A-3-C9_mon_G8 - 8.d	1.833	0.043	0.1783	0.0033	0.07434	0.0011	0.51931	0.16727	1056.7	15	1057.6	18	C - pop 1	-0.08517081
WGC2019J-31A-3-C9_mon_G8 - 9.d	1.828	0.042	0.177	0.0034	0.07467	0.0011	0.59365	0.20442	1056.1	15	1051.8	19	C - pop 1	0.407158413
WGC2019J-31A-3-C9_mon_G8 - 10.d	1.799	0.041	0.174	0.0032	0.0751	0.0011	0.50209	0.24206	1045.7	15	1033.9	18	C - pop 1	1.128430716

Samantha Nicole March  
Ultrahigh-pressure metapelites in the WGR

WGC2019J-31A-3-C9_mon_G8 - 11.d	1.838	0.043	0.1769	0.0033	0.07593	0.0011	0.62007	0.064401	1059.7	16	1049.8	18	C - pop 1	0.934226668
WGC2019J-31A-3-C9_mon_G8 - 12.d	1.828	0.042	0.1786	0.0034	0.07454	0.0012	0.35676	0.41173	1055.1	15	1059.4	18	C - pop 1	-0.40754431
WGC2019J-31A-3-C9_mon_G8 - 13.d	1.829	0.042	0.1768	0.0033	0.07515	0.0011	0.59211	0.045507	1055.3	15	1049.4	18	C - pop 1	0.559082725
WGC2019J-31A-3-C9_mon_G5 - 1.d	1.827	0.041	0.1772	0.0032	0.07501	0.0011	0.56227	0.21423	1054.8	15	1051.5	18	C - pop 1	0.312855518
WGC2019J-31A-3-C10_mon_G10 - 1.d	0.5147	0.014	0.06584	0.0013	0.0569	0.0013	0.13334	0.39147	422.1	9.4	411	7.8	NC - pop 2	2.6297086
WGC2019J-31A-3-C10_mon_G10 - 2.d	0.5147	0.014	0.06752	0.0013	0.0556	0.0012	0.19682	0.28365	421.2	9.4	421.2	7.8	C - pop 2	0
WGC2019J-31A-3-C10_mon_G10 - 3.d	0.514	0.015	0.06196	0.0013	0.0602	0.0014	0.28583	0.33882	421.7	10	387.5	7.8	NC - pop 3	8.110030828
WGC2019J-31A-3-C10_mon_G10 - 4.d	0.5288	0.015	0.0676	0.0014	0.0568	0.0012	0.38984	0.2148	431.4	9.9	421.6	8.3	C - pop 2	2.271673621
WGC2019J-31A-3-C10_mon_G10 - 5.d	0.536	0.015	0.06703	0.0014	0.0581	0.0013	0.14801	0.40035	435.2	9.8	418.2	8.3	NC - pop 2	3.90625
WGC2019J-31A-3-C10_mon_G11 - 1.d	0.522	0.015	0.0684	0.0014	0.0555	0.0013	0.33222	0.15131	426.2	10	426.5	8.2	C - pop 2	-0.07038949
WGC2019J-31A-3-C10_mon_G11 - 2.d	0.523	0.015	0.0675	0.0013	0.0564	0.0015	0.034236	0.40395	427	10	421	8	C - pop 2	1.405152225
WGC2019J-31A-3-C10_mon_G11 - 3.d	0.561	0.018	0.07002	0.0014	0.0577	0.0016	0.21772	0.20798	451.6	12	436.3	8.5	NC - pop 2	3.387953942
WGC2019J-31A-3-C10_mon_G11 - 4.d	0.539	0.019	0.06814	0.0014	0.0572	0.0018	0.13917	0.28303	437.8	12	424.9	8.6	C - pop 2	2.946550937
WGC2019J-31A-3-C10_mon_G11 - 5.d	0.529	0.016	0.06698	0.0013	0.0572	0.0015	0.16469	0.22528	430.7	11	418.5	8.2	NC - pop 2	2.832598096
WGC2019J-31A-3-C10_mon_G11 - 6.d	0.531	0.016	0.06826	0.0013	0.0565	0.0014	0.13533	0.28278	432.2	11	426.1	8	C - pop 2	1.411383619
WGC2019J-31A-3-C10_mon_G11 - 7.d	0.987	0.054	0.1056	0.0045	0.0675	0.0014	0.96832	-0.59224	691	28	646	26	D	6.512301013
WGC2019J-31A-3-C15_mon_G21 - 1.d	0.532	0.017	0.06814	0.0014	0.057	0.0017	-0.12171	0.48077	432.6	11	424.9	8.2	C - pop 2	1.779935275
WGC2019J-31A-3-C16_mon_G20 - 1.d	1.429	0.042	0.1442	0.0038	0.07217	0.001	0.91583	-0.14567	902	18	868	21	D	3.76940133
WGC2019J-31A-3-C16_mon_G20 - 2.d	1.857	0.041	0.1792	0.0033	0.07476	0.0011	0.46451	0.25279	1065.8	15	1062.6	18	C - pop 1	0.300243948
WGC2019J-31A-3-C16_mon_G20 - 3.d	1.848	0.04	0.1788	0.0033	0.0751	0.0011	0.44656	0.4515	1062.4	14	1060.3	18	C - pop 1	0.197665663
WGC2019J-31A-3-C16_mon_G20 - 4.d	0.546	0.016	0.06926	0.0015	0.0583	0.0013	0.74775	-0.23158	442	11	431.7	9.1	NC - pop 2	2.330316742
WGC2019J-31A-3-C16_mon_G20 - 5.d	1.849	0.04	0.1776	0.0033	0.07569	0.001	0.63287	0.45877	1063	14	1053.7	18	C - pop 1	0.874882408
WGC2019J-31A-3-C16_mon_G20 - 6.d	1.841	0.041	0.1784	0.0033	0.07495	0.001	0.62543	0.22855	1060.7	14	1058.4	18	C - pop 1	0.216837937
WGC2019J-31A-3-C16_mon_G20 - 7.d	1.843	0.04	0.1791	0.0033	0.0746	0.001	0.59362	0.24248	1061.3	14	1061.9	18	C - pop 1	-0.05653444
WGC2019J-31A-3-C16_mon_G20 - 8.d	1.83	0.04	0.1787	0.0033	0.07453	0.0011	0.48223	0.43271	1056	14	1059.9	18	C - pop 1	-0.36931818

Samantha Nicole March  
Ultrahigh-pressure metapelites in the WGR

WGC2019J-31A-3-C16_mon_G20 - 9.d	0.5171	0.012	0.06713	0.0012	0.05638	0.00096	0.38378	0.18749	423.6	8.5	418.8	7.4	C - pop 1	1.133144476
WGC2019J-31A-3-C16_mon_G20 - 10.d	1.809	0.04	0.1762	0.0034	0.07461	0.0011	0.66297	0.25206	1048.2	15	1045.9	18	C - pop 1	0.219423774
WGC2019J-31A-3-C16_mon_G20 - 11.d	1.852	0.04	0.1785	0.0033	0.07518	0.00098	0.68755	0.20894	1064	14	1058.9	18	C - pop 1	0.479323308
WGC2019J-31A-3-C16_mon_G20 - 12.d	1.783	0.038	0.1747	0.0032	0.07449	0.001	0.67282	0.26218	1039.2	14	1037.6	18	C - pop 1	0.153964588
WGC2019J-31A-3-C16_mon_G20 - 13.d	1.819	0.04	0.1766	0.0033	0.0746	0.0011	0.51383	0.28586	1052	14	1048.2	18	C - pop 1	0.36121673
WGC2019J-31A-3-C16_mon_G20 - 14.d	1.833	0.04	0.1767	0.0032	0.0752	0.001	0.53398	0.28534	1057.2	14	1048.8	18	C - pop 1	0.794551646
WGC2019J-31A-3-C16_mon_G20 - 15.d	1.841	0.041	0.1788	0.0034	0.07501	0.001	0.77212	0.072733	1060.8	15	1060.4	18	C - pop 1	0.037707391
WGC2019J-31A-3-C16_mon_G20 - 16.d	1.806	0.04	0.1748	0.0032	0.07508	0.0011	0.59003	0.23824	1047.5	14	1038.5	18	C - pop 1	0.859188544
WGC2019J-31A-3-C16_mon_G20 - 17.d	1.85	0.04	0.1782	0.0032	0.07512	0.001	0.63648	0.23007	1063.2	14	1057.2	18	C - pop 1	0.564334086
WGC2019J-31A-3-C16_mon_G20 - 18.d	0.5373	0.013	0.06854	0.0013	0.05686	0.0011	0.17694	0.37174	436.5	8.6	427.3	7.8	NC - pop 2	2.107674685
WGC2019J-31A-3-C16_mon_G20 - 19.d	1.834	0.04	0.1778	0.0033	0.07496	0.001	0.6477	0.36442	1057.4	14	1055.1	18	C - pop 1	0.217514659
WGC2019J-31A-3-C16_mon_G20 - 20.d	0.5354	0.013	0.06842	0.0013	0.05654	0.00097	0.31281	0.24892	435.2	8.3	427	7.4	C - pop 2	1.884191176
WGC2019J-31A-3-C16_mon_G20 - 21.d	0.5314	0.013	0.06867	0.0013	0.05647	0.001	0.08719	0.43478	432.5	8.4	428.1	7.7	C - pop 2	1.01734104
WGC2019J-31A-3-C16_mon_G20 - 22.d	0.5399	0.013	0.06871	0.0013	0.05732	0.0011	0.22446	0.34612	438.2	8.5	428.4	7.7	NC - pop 2	2.236421725
WGC2019J-31A-3-C16_mon_G20 - 23.d	0.5266	0.013	0.06862	0.0013	0.05585	0.00093	0.50817	0.039458	430	8.3	427.8	7.7	C - pop 2	0.511627907
WGC2019J-31A-3-C16_mon_G20 - 24.d	0.541	0.015	0.06892	0.0013	0.0571	0.0013	0.17828	0.23823	439.3	10	430.1	8.1	C - pop 2	2.094240838
WGC2019J-31A-3-C16_mon_G20 - 25.d	0.5438	0.013	0.06883	0.0013	0.05748	0.001	0.35673	0.10958	441.4	8.5	429.1	7.6	NC - pop 2	2.786588129
WGC2019J-31A-3-C16_mon_G20 - 26.d	0.524	0.015	0.06748	0.0013	0.0563	0.0013	0.037263	0.28006	427.3	9.9	420.9	7.7	C - pop 2	1.497776738
WGC2019J-31A-3-C16_mon_G20 - 27.d	0.517	0.015	0.06768	0.0014	0.0555	0.0013	0.22914	0.24529	423	10	422.2	8.2	C - pop 2	0.189125296
WGC2019J-31A-3-C16_mon_G20 - 28.d	0.5243	0.013	0.06782	0.0013	0.05588	0.0011	0.086142	0.42491	427.8	8.6	423	7.7	C - pop 2	1.122019635
WGC2019J-31A-3-C16_mon_G20 - 29.d	0.5427	0.013	0.06877	0.0013	0.05718	0.00095	0.51038	0.080378	440	8.6	428.7	7.7	NC - pop 2	2.568181818
WGC2019J-31A-3-C16_mon_G20 - 30.d	0.947	0.028	0.1032	0.0024	0.06682	0.0011	0.86326	-0.14607	675	15	632.9	14	D	6.237037037
WGC2019J-31A-3-C17_mon_G17 - 1.d	0.5186	0.014	0.06814	0.0013	0.0558	0.0012	0.36717	0.064636	423.8	9.6	424.9	7.7	C - pop 2	-0.25955639
WGC2019J-31A-3-C17_mon_G17 - 2.d	0.527	0.015	0.06785	0.0013	0.0565	0.0012	0.27211	0.21231	430.9	9.9	423.2	8	C - pop 2	1.786957531
WGC2019J-31A-3-C17_mon_G17 - 3.d	0.547	0.015	0.06838	0.0013	0.0581	0.0013	0.11104	0.31006	443.5	10	426.4	7.8	NC - pop 2	3.855693348

WGC2019J-31A-3-C17_mon_G17 - 4.d	0.5277	0.014	0.06775	0.0014	0.05646	0.0012	0.38524	0.1838	429.9	9.4	422.6	8.2	C - pop 2	1.698069318
WGC2019J-31A-3-C17_mon_G17 - 5.d	0.526	0.016	0.06843	0.0013	0.0559	0.0013	0.27414	0.16202	430.6	10	426.6	8	C - pop 2	0.928936368
WGC2019J-31A-3-C18_mon_G15 - 1.d	0.5563	0.013	0.06873	0.0013	0.05871	0.00097	0.079118	0.58	449.5	8.3	428.5	7.8	NC - pop 2	4.67185762
WGC2019J-31A-3-C18_mon_G15 - 2.d	0.556	0.013	0.06811	0.0013	0.05904	0.001	0.41325	0.27104	448.7	8.6	424.7	7.8	NC - pop 2	5.34878538
WGC2019J-31A-3-C18_mon_G15 - 3.d	0.553	0.013	0.06817	0.0013	0.05858	0.00093	0.45716	0.25137	446.8	8.6	425.1	8	NC - pop 2	4.856759176
WGC2019J-31A-3-C18_mon_G15 - 4.d	0.5469	0.013	0.0694	0.0013	0.05714	0.00098	0.4063	0.26814	442.8	8.6	432.5	8	NC - pop 2	2.326106594
WGC2019J-31A-3-C22_mon_Gx - 1.d	0.4641	0.012	0.0617	0.0012	0.055	0.0013	0.020753	0.39351	386.8	8.6	385.9	7.1	C - pop 3	0.232678387

C = concordant, NC = near concordant, D = discordant, RD = reversely discordant.

### Monazite geochronology standards:

Standard	Type	207/235	2σ	206/238	2σ	207/206	2σ	ErrorCorr 6/38vs7/35	ErrorCorr 38/6vs7/6	207/235 age	2σ	206/238	2σ	Concordant ?	% discordance
Ambat - 1.d	Secondary	0.6628	0.016	0.085	0	0.057	1E-03	0.31744	0.25305	516.7	9.8	524.9	9.5	C	-1.58699
Ambat - 2.d	Secondary	0.6777	0.017	0.085	0	0.058	0.001	0.26665	0.30793	525.1	10	525.9	9.6	C	-0.15235
Ambat - 3.d	Secondary	0.98	0.05	0.087	0	0.082	0.004	0.625	-0.51539	688	26	536.1	9.7	D	22.07849
Ambat - 4.d	Secondary	0.6717	0.016	0.085	0	0.057	0.001	0.30654	0.25835	522.2	9.7	525	9.4	C	-0.53619
Ambat - 5.d	Secondary	0.6601	0.015	0.084	0	0.057	1E-03	0.24276	0.40134	514.5	9.5	519.5	9.2	C	-0.97182
Ambat - 6.d	Secondary	0.6632	0.017	0.084	0	0.057	0.001	0.13407	0.42978	516.9	9.9	521	9.5	C	-0.79319
Ambat - 7.d	Secondary	0.659	0.016	0.083	0	0.057	0.001	0.36077	0.18029	513.7	10	516.7	9.3	C	-0.584
Ambat - 8.d	Secondary	0.6588	0.016	0.084	0	0.057	0.001	0.12992	0.42816	513.6	9.6	519.3	9.4	C	-1.10981
Ambat - 9.d	Secondary	0.654	0.017	0.083	0	0.057	0.001	0.32867	0.21233	510.7	10	516.1	9.5	C	-1.05737
Ambat - 10.d	Secondary	0.711	0.02	0.084	0	0.061	0.001	0.23745	0.1852	544.9	12	520.3	9.3	D	4.51459
Ambat - 11.d	Secondary	0.6586	0.016	0.085	0	0.057	0.001	0.18426	0.34587	514.2	9.8	523.6	9.2	C	-1.82808
Ambat - 12.d	Secondary	1.141	0.083	0.088	0	0.093	0.006	0.73626	-0.64908	759	41	546.5	11	D	27.99736

Samantha Nicole March  
Ultrahigh-pressure metapelites in the WGR

<b>Ambat - 13.d</b>	Secondary	0.6657	0.015	0.084	0	0.058	0.001	0.12973	0.55027	517.9	9.4	519.6	9.6	C	-0.32825
<b>Ambat - 14.d</b>	Secondary	0.656	0.016	0.084	0	0.057	0.001	0.24169	0.31098	511.9	9.8	517.3	9.3	C	-1.05489
<b>Ambat - 15.d</b>	Secondary	0.663	0.017	0.084	0	0.058	0.001	0.25146	0.29344	515.9	10	518.5	9.5	C	-0.50397
<b>Ambat - 16.d</b>	Secondary	0.6513	0.016	0.083	0	0.057	1E-03	0.35997	0.23489	509.1	9.6	515	9.4	C	-1.15891
<b>MAdel - 1.d</b>	Primary	0.6688	0.016	0.085	0	0.057	0.001	0.37765	0.21296	520.4	9.8	527	9.5	C	-1.26826
<b>MAdel - 2.d</b>	Primary	0.6552	0.015	0.084	0	0.057	9E-04	0.28418	0.36144	512.7	9.7	518.2	9.3	C	-1.07275
<b>MAdel - 3.d</b>	Primary	0.648	0.018	0.083	0	0.056	0.001	0.59354	0.099371	506.6	11	515.6	10	C	-1.77655
<b>MAdel - 4.d</b>	Primary	0.6612	0.016	0.084	0	0.057	9E-04	0.47313	0.10121	515.1	9.8	518.9	9.4	C	-0.73772
<b>MAdel - 5.d</b>	Primary	0.6515	0.015	0.084	0	0.057	1E-03	0.28355	0.31882	509.2	9.3	516.9	9.1	C	-1.51218
<b>MAdel - 6.d</b>	Primary	0.6551	0.016	0.084	0	0.056	9E-04	0.47146	0.12107	511.4	9.7	520.1	9.3	RD	-1.70121
<b>MAdel - 7.d</b>	Primary	0.649	0.017	0.083	0	0.057	0.001	0.20371	0.32182	507.7	10	514.5	9.4	C	-1.33937
<b>MAdel - 8.d</b>	Primary	0.658	0.016	0.084	0	0.057	1E-03	0.35308	0.32994	513.2	9.5	518.9	9.5	C	-1.11068
<b>MAdel - 9.d</b>	Primary	0.6621	0.016	0.083	0	0.058	1E-03	0.48531	0.085939	515.7	9.7	514.8	9.3	C	0.17452
<b>MAdel - 11.d</b>	Primary	0.6631	0.016	0.084	0	0.057	0.001	0.20623	0.36395	516.3	9.5	518.2	9.1	C	-0.368
<b>MAdel - 12.d</b>	Primary	0.6422	0.016	0.081	0	0.058	1E-03	0.57871	0.3391	503.4	10	502.6	9.9	C	0.158919
<b>MAdel - 13.d</b>	Primary	0.6585	0.015	0.083	0	0.057	1E-03	0.37792	0.34855	513.5	9.4	516.8	9.6	C	-0.64265
<b>MAdel - 14.d</b>	Primary	0.6496	0.016	0.084	0	0.056	1E-03	0.68105	0.063796	507.9	10	519.5	10	C	-2.28391
<b>MAdel - 15.d</b>	Primary	0.653	0.015	0.084	0	0.056	1E-03	0.37488	0.24186	510.1	9.5	519.9	9.3	RD	-1.92119
<b>MAdel - 16.d</b>	Primary	0.6587	0.015	0.084	0	0.057	1E-03	0.19502	0.36519	514.3	9.4	519.2	9	C	-0.95275
<b>MAdel - 17.d</b>	Primary	0.6553	0.015	0.083	0	0.057	9E-04	0.38336	0.3123	511.5	9.3	513.9	9.2	C	-0.46921
<b>MAdel - 18.d</b>	Primary	0.684	0.016	0.087	0	0.058	0.001	0.20472	0.33941	528.9	10	535.6	9.4	C	-1.26678
<b>MAdel - 19.d</b>	Primary	0.6519	0.015	0.083	0	0.057	1E-03	0.24512	0.31182	509.5	9.2	513	9.2	C	-0.68695
<b>MAdel - 22.d</b>	Primary	0.676	0.018	0.085	0	0.057	1E-03	0.69915	0.028346	524.8	11	527.8	10	C	-0.57165
<b>MAdel - 23.d</b>	Primary	0.6611	0.015	0.084	0	0.057	9E-04	0.45048	0.13614	515.7	9.7	518.9	9.2	C	-0.62052
<b>MAdel - 24.d</b>	Primary	0.6491	0.015	0.082	0	0.057	9E-04	0.30899	0.25189	508.3	9.5	510.8	9	C	-0.49184

Samantha Nicole March  
Ultrahigh-pressure metapelites in the WGR

<b>MAdel - 25.d</b>	Primary	0.6487	0.016	0.083	0	0.057	0.001	0.34747	0.24864	508.1	9.8	515.8	9.1	C	-1.51545
<b>MAdel - 26.d</b>	Primary	0.6614	0.016	0.084	0	0.057	0.001	0.32173	0.20573	515.2	9.9	521.2	9.3	C	-1.1646
<b>MAdel - 27.d</b>	Primary	0.6596	0.015	0.083	0	0.057	9E-04	0.41587	0.28455	514.2	9.3	516.4	9.3	C	-0.42785
<b>MAdel - 28.d</b>	Primary	0.6662	0.016	0.084	0	0.058	0.001	0.074816	0.50145	518.2	9.5	517.2	9.4	C	0.192976
<b>MAdel - 29.d</b>	Primary	0.6684	0.016	0.084	0	0.058	1E-03	0.32069	0.29492	520.1	9.9	518.9	9.3	C	0.230725
<b>MAdel - 30.d</b>	Primary	0.6524	0.016	0.084	0	0.057	1E-03	0.29823	0.26359	509.7	9.6	519.6	9.1	C	-1.94232
<b>MAdel - 31.d</b>	Primary	0.658	0.016	0.084	0	0.057	1E-03	0.39232	0.20009	513.1	9.9	521	9.4	C	-1.53966
<b>MAdel - 32.d</b>	Primary	0.6561	0.015	0.083	0	0.057	9E-04	0.45765	0.22957	512.1	9.3	515.4	9.5	C	-0.64441
<b>MAdel - 33.d</b>	Primary	0.6609	0.016	0.083	0	0.057	1E-03	0.37179	0.14343	515	9.5	516.6	9	C	-0.31068
<b>MAdel - 34.d</b>	Primary	0.6579	0.016	0.084	0	0.057	0.001	0.4217	0.19892	513	9.9	518.1	9.3	C	-0.99415
<b>MAdel - 35.d</b>	Primary	0.67	0.018	0.085	0	0.058	0.001	0.332	0.18631	521.3	11	523.4	9.3	C	-0.40284
<b>MAdel - 36.d</b>	Primary	0.6559	0.015	0.083	0	0.057	9E-04	0.25651	0.31893	511.9	9.3	516.8	9.1	C	-0.95722
<b>MAdel - 37.d</b>	Primary	0.6616	0.016	0.084	0	0.057	9E-04	0.43845	0.16344	515.3	9.6	519.8	9.1	C	-0.87328
<b>MAdel - 38.d</b>	Primary	0.6677	0.016	0.084	0	0.058	0.001	0.20735	0.3534	519	10	517.1	9.4	C	0.366089
<b>MAdel - 39.d</b>	Primary	0.6546	0.016	0.084	0	0.056	0.001	0.22686	0.35086	511.1	9.7	518.1	9.5	C	-1.36959
<b>MAdel - 40.d</b>	Primary	0.6462	0.016	0.083	0	0.056	9E-04	0.41301	0.15328	506.6	9.4	515.6	9.3	RD	-1.77655
<b>MAdel - 41.d</b>	Primary	0.6512	0.015	0.084	0	0.057	9E-04	0.48059	0.20647	509.1	9.1	517	9.4	C	-1.55176
<b>MAdel - 43.d</b>	Primary	0.6538	0.016	0.083	0	0.057	1E-03	0.38794	0.22247	510.5	9.7	516.5	9.2	C	-1.17532
<b>MAdel - 44.d</b>	Primary	0.6555	0.016	0.084	0	0.057	1E-03	0.26637	0.32939	512.2	9.6	517.2	9.3	C	-0.97618
<b>MAdel - 45.d</b>	Primary	0.6568	0.015	0.084	0	0.057	9E-04	0.28867	0.27569	512.5	9.2	517.8	9.1	C	-1.03415
<b>MAdel - 46.d</b>	Primary	0.661	0.016	0.084	0	0.057	1E-03	0.32127	0.28674	515	9.8	520.2	9.2	C	-1.00971
<b>MAdel - 47.d</b>	Primary	0.6546	0.015	0.084	0	0.056	1E-03	0.20653	0.41319	511.1	9.3	521.6	9.3	RD	-2.05439
<b>MAdel - 48.d</b>	Primary	0.6616	0.016	0.084	0	0.057	9E-04	0.50041	0.077282	515.3	9.7	519.6	9.1	C	-0.83447
<b>222 - 4.d</b>	Secondary	0.5716	0.014	0.074	0	0.056	0.001	0.27588	0.36726	458.8	9.1	457.3	8.4	C	0.32694
<b>222 - 5.d</b>	Secondary	0.5655	0.014	0.073	0	0.056	1E-03	0.29958	0.30264	454.8	9.2	453.4	8.5	C	0.307828

Samantha Nicole March  
Ultrahigh-pressure metapelites in the WGR

222 - 6.d	Secondary	0.5486	0.014	0.071	0	0.056	1E-03	0.49272	-0.02341	443.9	9	442.6	7.8	C	0.292859
222 - 7.d	Secondary	0.5604	0.013	0.073	0	0.056	1E-03	0.3477	0.31509	451.6	8.6	454	8.3	C	-0.53144
222 - 8.d	Secondary	0.5672	0.013	0.073	0	0.056	9E-04	0.32914	0.2961	456	8.4	452.8	8.1	C	0.701754
222 - 9.d	Secondary	0.5589	0.013	0.073	0	0.056	1E-03	0.16849	0.34645	450.7	8.6	452.8	8	C	-0.46594
222 - 10.d	Secondary	0.5661	0.014	0.073	0	0.057	1E-03	0.28916	0.20651	455.3	8.8	452.1	7.9	C	0.702833
222 - 11.d	Secondary	0.5517	0.013	0.072	0	0.056	9E-04	0.47426	0.1607	445.9	8.5	447.8	8	C	-0.4261
222 - 12.d	Secondary	0.5622	0.013	0.072	0	0.056	1E-03	0.25705	0.36579	452.8	8.5	451.1	8.1	C	0.375442
222 - 13.d	Secondary	0.5707	0.014	0.073	0	0.057	0.001	0.1077	0.38779	458.2	9.2	451.3	8.1	C	1.505893
222 - 14.d	Secondary	0.5633	0.013	0.072	0	0.057	9E-04	0.38662	0.28402	453.6	8.3	446.8	8	C	1.499118
222 - 15.d	Secondary	0.5604	0.013	0.072	0	0.057	9E-04	0.50628	0.10683	451.6	8.5	446.5	8	C	1.129318
222 - 16.d	Secondary	0.5572	0.014	0.071	0	0.057	1E-03	0.25983	0.25299	449.5	8.8	444	7.9	C	1.223582
222 - 17.d	Secondary	0.5559	0.013	0.072	0	0.056	1E-03	0.34878	0.2894	448.7	8.6	447	8.2	C	0.378872
222 - 18.d	Secondary	0.5541	0.013	0.072	0	0.056	0.001	0.27967	0.2607	447.5	8.8	449.2	8	C	-0.37989
222 - 19.d	Secondary	0.5592	0.014	0.072	0	0.056	9E-04	0.4467	0.077217	450.8	8.9	449.7	8	C	0.244011
222 - 20.d	Secondary	0.5652	0.014	0.072	0	0.057	9E-04	0.54918	0.082237	454.7	8.9	450.7	8.3	C	0.879701
222 - 21.d	Secondary	0.5585	0.014	0.072	0	0.056	0.001	0.36772	0.13822	450.3	9	448.8	8	C	0.333111
222 - 22.d	Secondary	0.5597	0.014	0.072	0	0.056	1E-03	0.44894	0.13144	451.1	9	450.9	8.3	C	0.044336
222 - 23.d	Secondary	0.5638	0.014	0.073	0	0.056	0.001	0.42684	0.10877	454.4	8.9	452.6	8.1	C	0.396127
222 - 24.d	Secondary	0.5518	0.013	0.072	0	0.056	9E-04	0.59768	0.092871	446.6	8.3	446	8.1	C	0.134348
222 - 25.d	Secondary	0.5519	0.013	0.072	0	0.055	9E-04	0.33377	0.3198	446.1	8.5	450.4	8.1	C	-0.96391
222 - 26.d	Secondary	0.5661	0.013	0.073	0	0.056	0.001	0.2616	0.30645	456	8.5	451.8	8.1	C	0.921053
222 - 27.d	Secondary	0.5604	0.015	0.073	0	0.056	0.001	0.40103	0.089494	451.4	9.6	452.2	8.3	C	-0.17723
222 - 28.d	Secondary	0.5614	0.014	0.072	0	0.056	0.001	0.30294	0.23822	452.2	9	450.9	8.1	C	0.287483
222 - 29.d	Secondary	0.5579	0.013	0.072	0	0.056	9E-04	0.27933	0.3282	450	8.3	445.7	7.9	C	0.955556
222 - 30.d	Secondary	0.5652	0.015	0.074	0	0.055	0.001	0.21163	0.29139	455.4	9.9	461.3	8.4	C	-1.29556



222 - 31.d	Secondar y	0.5695	0.01 4	0.072	0	0.057	0.001	0.23454	0.32168	457.5	9. 1	449.2	8. 4	C	1.814208
222 - 32.d	Secondar y	0.5554	0.01 4	0.071	0	0.057	0.001	0.36543	0.21185	449	8. 7	444.7	8. 1	C	0.957684
223 - 32.d	Secondar y	0.5597	0.01 3	0.072	0	0.056	9E- 04	0.40874	0.16749	451.1	8. 7	449.3	7. 9	C	0.399025
224 - 32.d	Secondar y	0.5591	0.01 3	0.072	0	0.056	1E- 03	0.17143	0.42977	450.8	8. 4	449.6	8	C	0.266193
225 - 32.d	Secondar y	0.5479	0.01 3	0.071	0	0.056	9E- 04	0.2431	0.36287	443.4	8. 4	441.3	7. 8	C	0.473613

~~Crossed-out~~ = discordant, C = concordant, NC = near concordant, D = discordant, RD = reversely discordant.

### Monazite trace elements:

Sample	Chondrite normalised REEs + Y															
	La	Pr	Nd	Sm	Eu	Gd	Tb	Dy	Y	Ho	Er	Tm	Yb	Lu	Total HREEs	Eu anomaly
WGC2019J-25B-C5_mon_G1	412236.	23868	173282.	64527.	25044.	17819.	5094.18	1643.49	699.	544.	196.9	64.77	30.37267	14.10569	8287.8942	0.738579
- 1.d	287	5.3	276	03	405	1	283	593	7	32	38	73	081	106	95	182
WGC2019J-25B-C5_mon_G1	413080.	23782	169693.	62918.	24920.	17060.	4936.28	1560.16	600.	472.	155.1	45.18	16.21118	7.682926	7792.9756	0.760615
- 2.d	169	3.3	654	92	071	3	809	26	1	16	88	22	012	829	56	724
WGC2019J-25B-C5_mon_G1	413924.	23717	170590.	62837.	24849.	17120.	4977.83	1591.05	611.	485.	158.9	45.34	15.96273	7.154471	7893.6262	0.757598
- 3.d	051	6.7	81	84	023	6	934	691	8	53	38	41	292	545	15	619
WGC2019J-25B-C5_mon_G1	413628.	23739	168774.	62945.	24902.	17135.	4997.22	1601.21	614	494.	162.0	46.84	17.51552	6.097560	7939.8389	0.758237
- 4.d	692	2.2	617	95	309	68	992	951	87	63	21	795	976	795	18	196
WGC2019J-25B-C5_mon_G1	411729.	23502	166892.	61932.	24600.	17075.	4894.73	1537.39	586.	471.	155.3	39.14	16.58385	6.544715	7707.9378	0.756479
- 5.d	958	1.6	779	43	355	38	684	837	6	61	13	98	093	447	02	495
WGC2019J-25B-C5_mon_G1	417721.	23836	169168.	62297.	25115.	17236.	4963.98	1584.14	605.	480.	158.3	42.79	15.83850	5.569105	7856.6686	0.766453
- 6.d	519	2.1	49	3	453	18	892	634	8	22	13	35	932	691	79	638
WGC2019J-25B-C5_mon_G1	411097.	23426	168555.	61216.	24476.	16814.	5008.31	1630.48	628.	497.	164.9	45.74	18.69565	6.544715	8000.3776	0.762906
- 7.d	046	7.2	799	22	021	07	025	78	4	25	38	9	217	447	57	213
WGC2019J-25B-C5_mon_G1	409831.	23340	167111.	61141.	24387.	16874.	4922.43	1601.62	617.	496.	161.2	44.41	16.77018	8.170731	7868.6708	0.759239
- 8.d	224	5.2	597	89	211	37	767	602	3	7	5	3	634	707	6	681
WGC2019J-25B-C6_mon_G2	420421.	22855	158905.	57567.	23072.	15467.	4385.04	1434.95	610	453.	151.2	42.71	15.34161	5.121951	7097.9068	0.773221
- 1.d	941	6	908	57	824	34	155	935	48	5	26	491	22	71	724	
WGC2019J-25B-C6_mon_G2	412489.	23394	166652.	61689.	24760.	16994.	5049.86	1647.96	638.	523.	167.4	47.44	19.31677	6.138211	8100.0803	0.764697
- 2.d	451	4	079	19	213	97	15	748	1	81	38	94	019	382	74	349
WGC2019J-25B-C7_mon_G3	409620.	23329	166608.	62094.	24523.	16658.	4941.82	1609.34	626.	486.	158.6	43.88	17.63975	8.495934	7892.3514	0.762515
- 1.d	253	7.4	315	59	979	29	825	959	2	26	88	66	155	959	11	724
WGC2019J-25B-C7_mon_G3	425696.	22963	162538.	58743.	21989.	15010.	3670.36	1152.84	506.	376.	136.1	46.11	18.26086	9.593495	5915.7681	0.740529
- 2.d	203	3.6	293	24	343	05	011	553	4	01	88	34	957	935	91	249
WGC2019J-25B-C7_mon_G3	435021.	22273	152625.	53966.	20959.	13040.	2878.11	878.455	402.	276.	100.3	26.27	10.93167	4.837398	4577.3814	0.790078
- 3.d	097	7.1	821	22	147	2	634	285	2	19	75	53	702	374	83	939
WGC2019J-25B-C7_mon_G3	432869.	22122	151334.	52932.	20746.	12979.	2822.71	880.487	386.	270.	91.31	28.25	10.06211	2.886178	4492.2520	0.791476
- 4.d	198	8.4	792	43	004	9	468	805	2	33	25	91	18	862	57	195

Samantha Nicole March  
Ultrahigh-pressure metapelites in the WGR

WGC2019J-25B-C7_mon_G3 - 5.d	419409. 283	23232 7.6	162407. 002	59459. 46	23818. 828	16386. 93	4864.26 593	1641.46 341	669. 7	518. 86	174.2 5	50.08 1	18.50931 677	5.934959 35	7943.0690 59	0.763064 138
WGC2019J-25B-C7_mon_G3 - 6.d	418143. 46	22834 0.5	159540. 481	57006. 76	22824. 156	15025. 13	4216.06 648	1510.56 911	694. 9	516. 85	178 1	54.25 1	21.11801 242	8.333333 333	7200.0877 62	0.779870 531
WGC2019J-25B-C7_mon_G3 - 7.d	430801. 688	22219 8.3	153304. 158	54121. 62	20863. 233	12944. 72	2858.72 576	873.577 236	392. 6	271. 61	96.43 75	26.03 24	9.627329 193	3.089430 894	4531.7013 68	0.788224 283
WGC2019J-25B-C7_mon_G3 - 8.d	431518. 987	22446 1.2	152188. 184	53074. 32	20799. 29	12804. 02	2847.64 543	855.691 057	385. 3	266. 3	93.81 25	26.80 16	9.937888 199	4.715447 154	4490.2043 07	0.797871 752
WGC2019J-25B-C7_mon_G3 - 9.d	432911. 392	22133 6.2	151334. 792	52533. 78	20337. 478	12668. 34	2781.16 343	862.195 122	389. 2	267. 4	92.12 5	31.41 7	10.74534 161	3.699186 992	4437.9443 57	0.788347 811
WGC2019J-25B-C7_mon_G3 - 10.d	424894. 515	23114 2.2	162275. 711	58155. 41	23108. 348	15834. 17	4753.46 26	1597.15 447	646. 9	496. 7	168.9 38	47.77 33	16.39751 553	6.951219 512	7734.2798 87	0.761511 024
WGC2019J-25B-C7_mon_G3 - 11.d	420337. 553	23049 5.7	161750. 547	57750. 872	23143. 97	15793. 219	4739.61 683	1582.92 219	633. 8	498. 72	166.3 75	50.89 07	15.65217 391	5.447154 472	7693.4219 83	0.766327 436
WGC2019J-25B-C7_mon_G3 - 12.d	427848. 101	22877 1.6	157789. 934	56439. 19	22024. 867	14763. 82	4033.24 114	1313.82 114	553. 89	409. 89	135 40	40 15.46583	4.674796 851	6505.0928 748	0.762998 81	
WGC2019J-25B-C7_mon_G3 - 13.d	402531. 646	23868 5.3	172603. 939	63783. 78	24422. 735	16492. 46	4379.50 139	1281.30 081	474. 2	385. 53	127.6 25	36.55 87	14.09937 888	6.544715 447	6705.3611 32	0.753002 492
WGC2019J-25B-C7_mon_G3 - 14.d	433755. 274	22424 5.7	151816. 193	52817. 57	20692. 718	12949. 75	2833.79 501	863.008 13	385. 8	273. 44	92.56 25	26.03 24	10.24844 72	3.821138 211	4488.7108 41	0.791220 737
WGC2019J-25B-C7_mon_G3 - 15.d	432489. 451	21961 2.1	150568. 928	52763. 51	20621. 67	12698. 49	2831.02 493	848.373 984	376. 8	264. 65	91.06 25	25.99 19	9.503105 59	3.414634 146	4450.8230 72	0.796674 449
WGC2019J-25B-C7_mon_G3 - 16.d	422362. 869	22079 7.4	152647. 702	53209. 46	20373. 002	12829. 15	2825.48 476	843.902 439	380. 5	257. 14	88.37 5	26.76 11	9.627329 193	3.861788 618	4435.6553 12	0.779761 396
WGC2019J-25B-C7_mon_G3 - 17.d	415189. 873	22931 0.3	158118. 162	55445. 95	22131. 439	13778. 89	3321.32 964	1029.67 48	437. 2	315. 57	107.2 5	31.01 21	11.30434 783	4.756097 561	5258.0947 93	0.800695 821
WGC2019J-25B-C7_mon_G3 - 18.d	431223. 629	22586 2.1	152472. 648	54128. 38	20905. 861	12844. 22	2847.64 543	892.276 423	395. 5	277. 84	93.18 75	29.35 22	8.695652 174	3.739837 398	4548.2358 96	0.792869 43
WGC2019J-25B-C7_mon_G3 - 19.d	430801. 688	22144 4	151094. 092	53263. 51	20738. 899	12829. 15	2883.65 651	868.699 187	389 6	269. 6	92.75 86	28.21 86	11.36645 963	3.292682 927	4546.5805 32	0.793362 953
WGC2019J-25B-C7_mon_G3 - 20.d	399029. 536	23933 1.9	171706. 783	64594. 59	25097. 691	17346. 73	4756.23 269	1443.49 593	526. 6	423. 63	138.1 25	38.05 67	15.03105 59	6.747967 48	7347.9156 99	0.749767 866
WGC2019J-25B-C7_mon_G3 - 21.d	404641. 35	22995 6.9	163019. 694	58445. 95	22735. 346	14055. 28	3052.63 158	915.040 65	396. 1	275. 46	93.43 75	22.51 01	9.503105 59	3.048780 488	4767.7296 12	0.793240 142
WGC2019J-25B-C7_mon_G3 - 22.d	405485. 232	23038 7.9	161072. 21	56466. 22	21953. 819	13542. 71	2958.44 875	889.430 894	390. 3	265. 38	90.68 75	25.54 66	8.819875 776	3.252032 52	4631.8702 3	0.793894 67
WGC2019J-25B-C7_mon_G3 - 23.d	419746. 835	23243 5.3	162231. 947	57837. 84	23001. 776	15130. 65	4476.45 429	1600 690	690 538.	538. 64	183.7 5	59.10 93	19.13043 478	8.902439 024	7575.9911 68	0.777546 748
WGC2019J-25B-C7_mon_G3 - 24.d	434725. 738	22801 7.2	157417. 943	56128. 38	21793. 961	13798. 99	3193.90 582	967.073 171	426. 1	306. 59	104.6 88	30.89 07	12.42236 025	4.146341 463	5045.8192 84	0.783107 155
WGC2019J-25B-C7_mon_G3 - 25.d	405822. 785	23706 9	168030. 635	61418. 92	24351. 687	16869. 35	4855.95 568	1529.26 829	584. 2	470. 7	152.1 88	43.36 03	13.47826 087	7.154471 545	7656.3004 98	0.756534 684
WGC2019J-25B-C7_mon_G3 - 26.d	407594. 937	23760 7.8	170853. 392	62385. 14	24973. 357	17005. 03	4869.80 609	1539.02 439	574 42	458. 42	150.5 63	43.52 23	16.58385 093	6.341463 415	7658.2654 74	0.766739 305
WGC2019J-25B-C7_mon_G3 - 27.d	429113. 924	22683 1.9	155667. 396	55635. 14	21705. 151	13809. 05	3235.45 706	984.552 846	439. 3	311. 17	110.6 25	31.37 65	12.67080 745	6.422764 228	5131.5771 6	0.783080 504
WGC2019J-25B-C7_mon_G3 - 28.d	416455. 696	23566 8.1	169299. 781	62567. 57	24884. 547	17145. 73	4947.36 842	1572.35 772	600. 8	475. 27	153.1 25	45.87 04	15.52795 031	8.008130 081	7818.3323 96	0.759761 236
WGC2019J-25B-C7_mon_G3 - 29.d	410970. 464	23663 7.9	168971. 554	62567. 57	24831. 261	16964. 82	4922.43 767	1578.45 528	597. 3	464. 47	155.2 5	43.23 89	18.44720 497	5.934959 35	7785.5328 53	0.762165 805

Samantha Nicole March  
Ultrahigh-pressure metapelites in the WGR

WGC2019J-25B-C7_mon_G3	401687.	24105	171050.	63581.	24920.	16778.	4678.67	1409.34	514.	413.	137.1	36.55	13.41614	5.731707	7209.3671	0.762963
- 30.d	764	6	328	08	071	89	036	959	9	55	88	87	907	317	28	305
WGC2019J-25B-C7_mon_G3	410126.	24019	172757.	63783.	25328.	17361.	5000	1572.76	599.	477.	159.8	46.55	16.27329	7.398373	7879.9627	0.761129
- 31.d	582	4	112	78	597	81		423	5	66	13	87	193	984	76	41
WGC2019J-25B-C7_mon_G3	396202.	24644	186652.	91081.	15133.	47638.	26177.2	14837.3	947	7326	3706.	1469.	636.6459	328.8617	63952.084	0.229741
- 32.d	532	4	079	08	215	19	853	984	0		25	64	627	886	4	515
WGC2019J-25B-C7_mon_G3	414852.	24288	183304.	69797.	16053.	25226.	10692.5	5056.91	295	2349	1101.	440.4	202.4844	96.34146	22890.434	0.382577
- 33.d	321	7.9	158	3	286	13	208	057	0	.8	88	86	72	341	96	406
WGC2019J-25B-C7_mon_G3	402953.	25377	193435.	94527.	14991.	56633.	33933.5	18902.4	119	9487	4387.	1655.	725.4658	369.1056	81451.078	0.204889
- 34.d	586	1.6	449	03	119	17	18	39	90	.2	5	87	385	911	49	939
WGC2019J-25B-C7_mon_G3	422447.	23265	162669.	59459.	23570.	16402.	4903.04	1625.60	670.	515.	170.7	49.59	18.07453	5.894308	7958.4891	0.754750
- 35.d	257	0.9	584	46	16	01	709	976	5	02	5	51	416	943	47	68
WGC2019J-25B-C7_mon_G3	425738.	23028	162013.	59054.	23712.	16497.	5000	1708.94	683.	527.	179.6	55.10	19.50310	8.577235	8182.8015	0.759694
- 36.d	397	0.2	129	05	256	49		309	7	29	88	12	559	772	23	722
WGC2019J-25B-C7_mon_G3	424894.	23502	164792.	60500	24103.	16638.	4886.42	1602.03	627.	502.	166.8	48.90	18.57142	7.235772	7859.7003	0.759697
- 37.d	515	1.6	123	02	19	659		252	7	01	13	69	857	358	49	528
WGC2019J-25B-C7_mon_G3	407172.	23750	171531.	64527.	24973.	17065.	4742.38	1431.30	538.	430.	141.6	43.72	15.03105	6.016260	7349.6493	0.752573
- 38.d	996	0	729	03	357	33	227	081	8	77	25	47	59	163	28	281
WGC2019J-25B-C7_mon_G3	422784.	22920	161378.	58804.	23943.	16211.	4941.82	1659.34	690.	521.	174.8	52.14	19.62732	8.252032	8068.1271	0.775482
- 39.d	81	2.6	556	05	162	06	825	959	5	61	13	57	919	52	81	89
WGC2019J-25B-C7_mon_G3	435738.	22974	164835.	65540.	25399.	15160.	2418.28	426.016	129.	104.	31	9.230	2.043478	0.853658	3121.5223	0.805770
- 40.d	397	1.4	886	54	645	8	255	26	7	4		77	261	537	19	784
WGC2019J-25B-	433755.	23071	165798.	65270.	25186.	15256.	2529.08	466.666	143.	105.	36.37	7.773	3.291925	1.422764	3293.6763	0.798152
C15_mon_G4 - 1.d	274	1.2	687	27	501	28	587	667	2	86	5	28	466	228	14	329
WGC2019J-25B-	404219.	23825	171553.	64054.	24831.	17311.	4806.09	1477.64	549.	447.	149.1	42.79	16.08695	5.447154	7494.5081	0.745688
C15_mon_G4 - 2.d	409	4.3	611	05	261	56	418	228	7	62	25	35	652	472	4	406
WGC2019J-25B-	426582.	22661	156389.	55020.	21385.	13537.	3002.77	897.967	398.	273.	98.5	27.40	11.42857	3.739837	4713.3918	0.783582
C15_mon_G4 - 3.d	278	6.4	497	27	435	69	008	48	5	08		89	143	398	02	043
WGC2019J-25B-	425316.	21864	150743.	52601.	20426.	12638.	2767.31	839.837	364.	254.	85.37	26.76	9.813664	2.154471	4350.3502	0.792224
C15_mon_G4 - 4.d	456	2.2	982	35	288	19	302	398	7	4	5	11	596	545	92	991
WGC2019J-25B-	431645.	22209	149978.	51729.	20017.	12351.	2689.75	808.943	358.	251.	88.81	22.63	8.385093	2.682926	4231.3373	0.791919
C15_mon_G4 - 5.d	57	0.5	118	73	762	76	069	089	3	83	25	16	168	829	83	461
WGC2019J-25B-	411392.	22370	153588.	53621.	20746.	12603.	2781.16	841.463	366.	249.	84.43	24.41	8.571428	4.756097	4360.6890	0.798044
C15_mon_G4 - 6.d	405	6.9	621	62	004	02	343	415	8	08	75	3	571	561	8	756
WGC2019J-25B-	403375.	23965	172319.	62702.	24191.	16241.	4277.00	1242.68	454.	358.	119.3	33.31	11.49068	4.756097	6502.1072	0.758082
C15_mon_G4 - 7.d	527	5.2	475	7	829	21	831	293	5	97	75	98	323	561	15	453
WGC2019J-25B-	407763.	23081	162166.	57628.	22611.	14356.	3418.28	1089.43	463.	337.	115.7	35.58	12.29813	3.821138	5476.2155	0.786091
C15_mon_G4 - 8.d	713	9	302	38	012	78	255	089	5	55	5	7	665	211	5	73
WGC2019J-25B-	415569.	22532	156892.	54135.	20905.	12748.	2844.87	838.211	374.	264.	81.62	24.04	9.130434	2.682926	4440.1088	0.795783
C15_mon_G4 - 9.d	62	3.3	779	14	861	74	535	382	7	84	5	86	783	829	38	188
WGC2019J-25B-	426160.	22133	149934.	51716.	20035.	12351.	2681.44	804.878	360.	248.	87.31	22.95	10.31055	2.642276	4218.8403	0.792725
C15_mon_G4 - 10.d	338	6.2	354	22	524	76	044	049	4	9	25	55	901	423	92	69
WGC2019J-25B-	414767.	22446	152910.	53986.	20728.	13005.	2844.87	850	371.	259.	84.31	23.92	9.503105	2.642276	4446.2841	0.782283
C15_mon_G4 - 11.d	932	1.2	284	49	242	03	535		5	52	25	71	59	423	63	791
WGC2019J-25B-	411054.	22920	158949.	55810.	21811.	13537.	2950.13	879.674	387.	261.	88.43	25.50	8.881987	3.170731	4604.0817	0.793521
C15_mon_G4 - 12.d	852	2.6	672	81	723	69	85	797	1	17	75	61	578	707	54	226
WGC2019J-25B-	417721.	23146	163019.	58520.	23392.	15286.	4157.89	1380.48	559.	425.	141.3	43.52	15.83850	7.073170	6730.6868	0.782115
C15_mon_G4 - 13.d	519	5.5	694	27	54	43	474	78	1	46	13	23	932	732	64	966
WGC2019J-25B-	418987.	22262	153544.	53621.	21012.	12989.	2878.11	873.983	386.	271.	91.18	27.08	10.06211	3.780487	4542.5932	0.796164
C15_mon_G4 - 14.d	342	9.3	858	62	433	95	634	74	4	98	75	5	18	805	25	195

Samantha Nicole March  
Ultrahigh-pressure metapelites in the WGR

WGC2019J-25B-	424894.	22198	154201.	54533.	21190.	13180.	2908.58	883.739	389.	266.	91.68	26.43	8.322981	3.739837	4578.4150	0.790363
C15_mon_G4 - 15.d	515	2.8	313	78	053	9	726	837	6	3	75	72	366	398	27	045
WGC2019J-25B-	425105.	22316	152866.	54479.	21207.	13155.	2905.81	881.707	393	275.	91.56	26.35	8.447204	3.577235	4585.5592	0.792173
C15_mon_G4 - 16.d	485	8.1	521	73	815	78	717	317	09	09	25	63	969	772	83	257
WGC2019J-25B-	442194.	21767	147855.	51027.	19721.	12301.	2711.91	828.455	379.	260.	89.5	29.23	10	4.308943	4314.0122	0.787141
C15_mon_G4 - 17.d	093	2.4	58	03	137	51	136	285	8	81	08	08	089	15	198	
WGC2019J-25B-	426582.	22456	155908.	54817.	21349.	13457.	2980.60	906.504	402	279.	97.87	30.16	12.79503	4.756097	4714.5550	0.786063
C15_mon_G4 - 18.d	278	9	096	57	911	29	942	065	85	5	19	106	561	35	163	
WGC2019J-25B-	417299.	22467	153960.	54837.	21332.	13437.	2933.51	882.520	391.	273.	89.37	26.27	9.875776	4.227642	4610.9015	0.785851
C15_mon_G4 - 19.d	578	6.7	613	84	149	19	801	325	3	81	5	53	398	276	77	141
WGC2019J-25B-	412953.	22575	155929.	54851.	21580.	13170.	2969.52	889.837	387.	270.	90.43	27.81	8.633540	4.512195	4648.6931	0.802910
C15_mon_G4 - 20.d	586	4.3	978	35	817	85	909	398	6	33	75	38	373	122	55	699
WGC2019J-25B-	404219.	23017	164923.	58209.	22806.	14070.	3138.50	935.772	407.	284.	93.06	25.02	10.18633	4.105691	4898.5498	0.796906
C15_mon_G4 - 21.d	409	2.4	414	46	394	35	416	358	1	8	25	02	54	057	17	498
WGC2019J-25B-	414767.	23609	166017.	61418.	24511.	16517.	4891.96	1605.28	634.	499.	163	46.19	15.90062	6.544715	7862.3583	0.769566
C15_mon_G4 - 22.d	932	9.1	505	92	545	59	676	455	2	27	43	43	112	447	8	747
WGC2019J-25B-	422784.	23125	160875.	57662.	23232.	15969.	4753.46	1655.69	699.	538.	188.2	51.17	22.42236	7.479674	7915.8581	0.765602
C15_mon_G4 - 23.d	81	0	274	16	682	85	26	106	1	28	5	41	025	797	73	74
WGC2019J-25B-	427848.	22165	153085.	53358.	20746.	12753.	2806.09	843.495	377	254.	87.68	26.23	9.254658	2.804878	4407.5170	0.795270
C15_mon_G4 - 24.d	101	9.5	339	11	004	77	418	935	95	75	48	385	049	27	67	
WGC2019J-25B-	405021.	23200	161728.	57837.	22717.	14005.	3044.32	908.130	398	277.	91.37	27.77	8.198757	3.414634	4758.3193	0.798204
C15_mon_G4 - 25.d	097	4.3	665	84	584	03	133	081	11	5	33	764	146	09	513	
WGC2019J-25B-	421012.	23071	162166.	58587.	23321.	15839.	4728.53	1581.70	641.	505.	162	48.74	16.95652	8.170731	7693.1890	0.765571
C15_mon_G4 - 26.d	658	1.2	302	84	492	2	186	732	4	68	49	174	707	21	98	
WGC2019J-25B-	405063.	23620	167155.	62614.	24600.	17085.	4781.16	1471.13	550.	435.	145.3	37.44	14.72049	4.593495	7440.5711	0.752124
C15_mon_G4 - 27.d	291	6.9	361	86	355	43	343	821	6	53	75	94	689	935	67	498
WGC2019J-25B-	413628.	23750	170503.	63283.	24795.	16909.	4770.08	1468.69	547.	438.	138.2	40.24	14.78260	5.487804	7422.9408	0.757992
C15_mon_G4 - 28.d	692	0	282	78	737	55	31	919	3	1	5	29	87	878	56	325
WGC2019J-25B-	403291.	24084	171159.	63925.	24902.	17050.	4761.77	1437.39	521.	425.	137.1	39.59	15.83850	5.406504	7344.2736	0.754286
C15_mon_G4 - 29.d	139	0.5	737	68	309	25	285	837	8	27	88	51	932	065	08	897
WGC2019J-25B-	406329.	22952	158752.	56554.	21989.	13723.	3055.40	912.195	395.	275.	88.62	24.21	9.627329	2.560975	4763.4953	0.789307
C15_mon_G4 - 30.d	114	5.9	735	05	343	62	166	122	6	27	5	05	193	61	4	204
WGC2019J-25B-	405907.	23793	168730.	63175.	25026.	17256.	4947.36	1558.94	582.	480.	155.9	44.85	15.90062	5.528455	7791.0730	0.757973
C15_mon_G4 - 31.d	173	1	853	68	643	28	842	309	5	04	38	83	112	285	17	537
WGC2019J-25B-	410970.	22898	162713.	57864.	22841.	13834.	3094.18	916.666	402.	281.	92.75	26.51	9.378881	3.414634	4826.7962	0.807325
C15_mon_G4 - 32.d	464	7.1	348	86	918	17	283	667	2	68	82	988	146	09	248	
WGC2019J-25B-	412236.	22640	158402.	55655.	21438.	13221.	2897.50	876.016	377.	269.	88.12	25.42	8.571428	2.682926	4545.6078	0.790335
C15_mon_G4 - 33.d	287	0.9	626	41	721	11	693	26	5	78	5	51	571	829	62	18
WGC2019J-25B-	403206.	24062	171597.	64121.	25150.	17391.	4831.02	1471.54	540.	441.	139.9	42.87	14.47204	5.650406	7486.7297	0.753144
C15_mon_G4 - 34.d	751	5	374	62	977	96	493	472	2	03	38	45	969	504	37	569
WGC2019J-25B-	419831.	22230	151247.	54168.	20710.	12989.	2844.87	856.097	375.	265.	87.87	22.95	9.006211	3.130081	4464.3411	0.780748
C15_mon_G4 - 35.d	224	6	265	92	48	95	535	561	2	2	5	55	18	301	31	819
WGC2019J-25B-	411814.	22963	157527.	55283.	21563.	13216.	2897.50	880.487	386.	264.	82.93	24.29	7.826086	3.455284	4547.6908	0.797737
C15_mon_G4 - 36.d	346	3.6	352	78	055	08	693	805	9	29	75	15	957	553	14	625
WGC2019J-25B-	424050.	22413	154595.	55574.	21385.	13296.	2944.59	878.048	386.	270.	88.93	25.66	9.006211	3.170731	4607.2086	0.786706
C15_mon_G4 - 37.d	633	7.9	186	32	435	48	834	78	9	88	75	8	18	707	98	276
WGC2019J-25B-	399578.	23965	169387.	62500	24031.	16110.	4301.93	1245.93	451.	365.	117.9	31.37	12.73291	4.146341	6530.9856	0.757345
C15_mon_G4 - 38.d	059	5.2	309	972	55	906	496	9	02	38	65	925	463	11	715	
WGC2019J-25B-	429535.	22683	155798.	54554.	21101.	13221.	2897.50	856.910	383	264.	94.18	24.33	9.689440	2.520325	4532.4324	0.785707
C15_mon_G4 - 39.d	865	1.9	687	05	243	11	693	569	29	75	2	994	203	59	041	

Samantha Nicole March  
Ultrahigh-pressure metapelites in the WGR

WGC2019J-25B-C15_mon_G4 - 40.d	432067.	22295	152319.	53885.	20799.	13125.	2897.50	878.048	391.	273.	90.31	27.69	10.68322	4.146341	4573.7996	0.782085
	511	2.6	475	14	29	63	693	78	6	81	25	23	981	463	08	014
WGC2019J-25B-C15_mon_G4 - 41.d	442194.	22004	149212.	51966.	19715.	12216.	2675.90	812.195	362.	251.	83.5	26.96	10.43478	2.479674	4224.9723	0.782506
	093	3.1	254	22	808	08	028	122	4	1		36	261	797	2	754
WGC2019A3-C1_mon_G1 - 1.d	447679.	22941	160612.	63581.	25452.	17567.	4736.84	1389.83	492.	397.	124.8	34.17	13.35403	4.715447	7193.2674	0.761578
	325	8.1	691	08	931	84	211	74	1	44	13		727	154	26	487
WGC2019A3-C1_mon_G1 - 2.d	446413.	22413	157855.	61277.	24529.	16809.	4335.18	1232.52	447.	365.	113.3	32.38	9.751552	4.552845	6540.2074	0.764301
	502	7.9	58	03	307	05	006	033	3	2	13	87	795	528	08	862
WGC2019A3-C1_mon_G1 - 3.d	464135.	21734	151531.	58716.	24458.	17678.	5559.55	1793.90	693.	552.	176.7	45.99	17.20496	6.178861	8845.3490	0.759145
	021	9.1	729	22	259	39	679	244	2	56	5	19	894	789	62	698
WGC2019A3-C1_mon_G1 - 4.d	447679.	22607	158949.	61486.	24440.	17020.	4434.90	1254.87	456.	369.	117.3	31.78	11.61490	4.593495	6680.7766	0.755508
	325	7.6	672	49	497	1	305	805	4	23	75	14	683	935	44	127
WGC2019A3-C1_mon_G1 - 5.d	463291.	22112	153851.	59391.	24973.	18015.	5551.24	1808.13	679	541.	176.1	49.31	16.89440	7.398373	8830.1100	0.763475
	139	0.7	204	89	357	08	654	008		94	88	17	994	984	35	85
WGC2019A3-C1_mon_G1 - 6.d	481012.	21530	145448.	55405.	23214.	16743.	5542.93	1945.93	772.	620.	202.6	60.85	19.93788	7.967479	9172.7439	0.762193
	658	1.7	578	41	92	72	629	496	1	33	88	02	82	675	88	369
WGC2019A3-C1_mon_G1 - 7.d	479324.	21422	143807.	54587.	22753.	16391.	5371.19	1923.98	796.	626.	210.6	63.36	20.80745	9.227642	9022.0482	0.760636
	895	4.1	44	84	108	96	114	374	6	19	88	03	342	276	71	827
WGC2019A3-C1_mon_G1 - 8.d	448523.	22446	158030.	61216.	24245.	16748.	4470.91	1295.12	470.	384.	119.5	32.75	12.42236	4.715447	6790.1553	0.757181
	207	1.2	635	22	115	74	413	195	6	07	63	3	025	154	57	33
WGC2019A3-C1_mon_G1 - 9.d	464556.	22176	151006.	58952.	24937.	18175.	5703.60	1858.94	720.	578.	184.6	54.37	18.63354	7.886178	9127.0458	0.761831
	962	7.2	565	7	833	88	111	309	9	02	88	25	037	862	64	87
WGC2019A3-C1_mon_G1 - 10.d	451476.	22349	157833.	61871.	25150.	18331.	5376.73	1663.00	608.	508.	157.3	47.36	15.09316	4.471544	8381.4387	0.746806
	793	1.4	698	62	977	66	13	813	6	79	75	84	77	715	74	746
WGC2019A3-C1_mon_G2 - 1.d	454008.	22241	154201.	56608.	21509.	14698.	3559.55	996.341	359.	289.	98.31	26.80	9.254658	3.170731	5342.2150	0.745692
	439	3.8	313	11	769	49	679	463	4	38	25	16	385	707	49	939
WGC2019A3-C1_mon_G2 - 2.d	490295.	21056	140984.	53175.	21793.	15738.	5182.82	1878.45	799.	617.	203.5	60.97	20.37267	9.227642	8772.5639	0.753347
	359	0.3	683	68	961	69	548	528	2	95	63	17	081	276	6	447
WGC2019A3-C1_mon_G2 - 3.d	454008.	22381	157592.	61824.	25683.	18798.	5689.75	1796.34	672.	545.	175.5	47.65	17.63975	7.398373	8953.2152	0.753377
	439	4.7	998	32	837	99	069	146	9	97	63	18	155	984	99	929
WGC2019A3-C1_mon_G2 - 4.d	464008.	22284	153129.	59270.	24813.	17929.	5518.00	1824.39	678.	549.	177.1	51.90	18.13664	8.211382	8826.0509	0.761173
	439	4.8	103	27	499	65	554	024	4	82	88	28	596	114	96	522
WGC2019A3-C1_mon_G2 - 5.d	468776.	21799	150831.	57297.	24156.	17457.	5487.53	1854.06	710	577.	183.6	51.98	17.63975	7.520325	8889.7204	0.763791
	371	5.7	51	3	306	29	463	504		29	88	38	155	203	26	949
WGC2019A3-C1_mon_G2 - 6.d	453586.	22575	157417.	61966.	25772.	18226.	5506.92	1694.71	612.	503.	158.3	44.61	16.83229	5.447154	8543.1734	0.766892
	498	4.3	943	22	647	13	521	545	6	66	75	54	814	472	96	144
WGC2019A3-C1_mon_G2 - 7.d	447257.	22629	159102.	63243.	26216.	18648.	5393.35	1621.13	582.	475.	148.2	40.76	13.78881	6.260162	8281.6329	0.763399
	384	3.1	845	24	696	24	18	821	8	27	5	92	988	602	5	651
WGC2019A3-C1_mon_G2 - 8.d	441350.	23275	163457.	64459.	26465.	18477.	5795.01	2141.86	906	713.	242.5	66.80	24.09937	8.170731	9897.6423	0.766856
	211	8.6	33	46	364	39	385	992		19		16	888	707	12	79
WGC2019A3-C1_mon_G2 - 9.d	468354.	22209	151225.	58668.	24706.	17839.	5423.82	1793.90	687	546.	179.4	51.21	18.19875	7.032520	8707.4949	0.763707
	43	0.5	383	92	927	2	271	244		89	38	46	776	325	54	497
WGC2019A3-C1_mon_G2 - 10.d	456118.	22349	157549.	62702.	26234.	18798.	5531.85	1689.43	611.	503.	159.4	42.59	15.65217	7.195121	8560.4762	0.764120
	143	1.4	234	7	458	99	596	089	2	11	38	11	391	951	92	153
WGC2019A3-C1_mon_G2 - 11.d	435021.	22974	166083.	66959.	27069.	18728.	5900.27	2144.30	892	711.	231.8	64.77	24.09937	9.227642	9977.9206	0.764394
	097	1.4	151	46	272	64	701	894		36	75	73	888	276	12	308
WGC2019A3-C1_mon_G2 - 12.d	453164.	22586	155623.	61418.	25985.	18567.	5650.96	1757.31	655.	531.	170.3	50.76	16.89440	5.609756	8838.3080	0.769492
	557	2.1	632	92	79	84	953	707	3	14	13	92	994	098	3	098
WGC2019A3-C1_mon_G2 - 13.d	467932.	22112	153238.	57702.	24458.	17427.	5565.09	2036.99	822	654.	218.7	63.56	21.80124	9.471544	9392.2531	0.771284
	489	0.7	512	7	259	14	695	187		58	5	28	224	715	17	248

Samantha Nicole March  
Ultrahigh-pressure metapelites in the WGR

WGC2019A3-C1_mon_G2 - 14.d	475527.426	21853.45	149015.317	57297.3	23783.304	17537.69	5681.44044	1963.82114	771.37	613.25	206.625	61.2551	18.88198758	8.292682927	9324.686276	0.750272345
WGC2019A3-C1_mon_G2 - 15.d	439662.447	23254.3.1	164989.059	67027.03	27406.75	19216.08	5916.89751	2113.82114	875.63	699.25	235.625	63.4413	22.98136646	8.37398374	9935.773991	0.763660187
WGC2019A3-C1_mon_G2 - 16.d	431054.852	23060.3.4	166477.024	66040.54	26838.366	18753.77	5814.40443	2133.33333	896.28	701.38	232.438	68.8259	22.91925466	8.170731707	9877.373214	0.762616997
WGC2019A3-C2_mon_G3 - 1.d	428016.878	23965.5.2	178533.917	81351.35	34724.689	20165.83	3240.99723	573.98374	148.9	123.08	39.5625	10.7692	2.795031056	2.235772358	4142.320427	0.857329839
WGC2019A3-C2_mon_G3 - 2.d	436286.92	23793.1	175995.624	77094.59	32291.297	18366.83	2526.31579	433.739837	122.3	99.084	34.3125	9.23077	3.47826087	1.382113821	3229.84352	0.858136485
WGC2019A3-C2_mon_G3 - 3.d	427426.16	23814.6.6	177308.534	81283.78	34564.831	20100.5	3130.19391	519.918699	130.3	104.76	32.5625	8.0568	3.416149068	1.219512195	3930.429351	0.855123866
WGC2019A3-C2_mon_G3 - 4.d	438818.565	23663.7.9	175864.333	77567.57	32113.677	18170.85	2379.50139	403.658537	118.2	91.392	32.8125	6.96356	2.118012422	1.62601626	3036.271954	0.855386265
WGC2019A3-C2_mon_G3 - 5.d	432489.451	23609.9.1	176783.37	77364.86	31829.485	18105.53	2556.7867	428.455285	122.9	93.73	33.8125	8.13765	3.105590062	1.341463415	3248.312087	0.850456553
WGC2019A3-C2_mon_G3 - 6.d	443459.916	23480.6	173982.495	76756.76	31047.957	17522.61	2318.55956	386.585366	113.3	89.744	29.5625	7.93522	2.422360248	2.235772358	2950.344368	0.846594202
WGC2019A3-C2_mon_G3 - 7.d	441350.211	23308.1.9	171728.665	75135.14	31101.243	17195.98	2349.03047	382.926829	110.5	89.56	31.375	7.40891	3.354037267	0.975609756	2975.131294	0.865252277
WGC2019A3-C2_mon_G3 - 8.d	425738.397	23642.2.4	175908.096	79527.03	33516.874	19592.96	2897.50693	482.926829	123.99	99.634	30.9375	7.97571	2.236024845	1.138211382	3645.354899	0.849094548
WGC2019A3-C2_mon_G3 - 9.d	424894.515	23588.3.6	176608.315	80000.542	33765.89	19778.917	2972.29917	491.463415	123.2	96.154	30.875	8.13765	2.236024845	0.25203252	3724.617139	0.848843685
WGC2019A3-C2_mon_G3 - 10.d	430801.688	24073.2.8	180962.801	81283.78	34458.259	20462.31	3116.34349	517.073171	128.106	106.59	33.3125	9.23077	2.173913043	1.869918699	3914.597169	0.844916969
WGC2019A3-C2_mon_G3 - 11.d	437552.743	23448.2.8	172603.939	76351.35	31829.485	18402.01	2601.10803	426.01626	116.1	90.125	31.8197	8.66397	1.677018634	1.504065041	3276.891735	0.849158213
WGC2019A3-C2_mon_G3 - 12.d	427848.101	23868.5.3	176542.67	80878.38	34689.165	20346.73	3207.75623	535.365854	130.103	103.66	31.625	7.89474	2.173913043	1.260162602	4019.738902	0.855126334
WGC2019A3-C2_mon_G3 - 13.d	435864.979	23825.4.3	176170.678	77770.27	32646.536	18482.41	2578.94737	424.796748	113.6	90.11	30.8125	8.2996	2.422360248	0.93495935	3249.923421	0.861094834
WGC2019A3-C2_mon_G3 - 14.d	435864.979	23696.1.2	174573.304	78108.11	32859.68	18773.87	2739.61219	450.813008	120.3	96.886	29.375	5.95142	3.105590062	1.341463415	3447.38514	0.858100942
WGC2019A3-C2_mon_G3 - 15.d	429957.806	24030.1.7	178118.162	81486.49	33801.066	19517.59	2933.51801	475.609756	122.2	99.084	30.7596	7.24605	2.484472854	1.585365854	3672.478812	0.847567948
WGC2019A3-C2_mon_G3 - 16.d	429957.806	23394.4	173588.621	78108.11	32877.442	19301.51	2911.35734	474.796748	120.1	95.421	31.375	7.81377	2.484472854	0.975609756	3644.324181	0.846748331
WGC2019A3-C2_mon_G3 - 17.d	429957.806	23631.4.7	178227.571	80810.81	33978.686	20045.23	3094.18283	511.788618	123.6	101.65	31.0625	7.40891	2.298136646	1.138211382	3873.12755	0.844240851
WGC2019A3-C2_mon_G3 - 18.d	429535.865	23976.2.9	177571.116	81351.35	34564.831	20015.08	3102.49307	508.130081	127.7	100.92	34.625	8.38057	2.857142857	0.93495935	3886.036576	0.856590868
WGC2019A3-C2_mon_G3 - 19.d	434599.156	23965.5.2	178008.753	80743.24	34316.163	20180.9	3224.37673	529.674797	125.6	104.21	31.2565	8.13765	3.229813665	1.829268293	4028.310716	0.850110379
WGC2019A3-C2_mon_G3 - 20.d	422784.81	23566.8.1	177768.053	79391.89	33960.924	19683.42	2925.20776	489.837398	125.7	102.01	34.3125	8.46154	2.732919255	0.894308943	3689.161073	0.859094957
WGC2019A3-C2_mon_G3 - 21.d	435021.097	23674.5.7	175317.287	79797.3	33925.4	19592.96	2991.68975	498.373984	124.6	100.92	32.125	8.58357	2.919254658	1.097560976	3760.304297	0.857987186
WGC2019A3-C2_mon_G3 - 22.d	435443.038	23685.3.4	177921.225	80608.11	34209.591	20371.86	3163.4349	524.390244	129.9	108.61	31.625	8.05668	3.354037267	1.585365854	3970.954289	0.844195805

Samantha Nicole March  
Ultrahigh-pressure metapelites in the WGR

WGC2019A3-C2_mon_G3 - 23.d	437130.802	23534.48	174682.713	78331.08	32611.012	18798.99	2653.73961	441.056911	122.4	96.154	32.875	8.21862	3.291925466	1.138211382	3358.874129	0.849825788
WGC2019A3-C2_mon_G3 - 24.d	437130.802	23793.1	178293.217	79729.73	33605.684	19527.64	2825.48476	471.95122	122.7	96.703	32.625	6.63968	2.00621118	1.910569106	3560.020737	0.851682515
WGC2019A3-C2_mon_G3 - 25.d	432489.451	23556.03	176761.488	78918.92	33250.444	19261.31	2855.95568	477.235772	123.3	97.07	31.3125	8.82591	2.670807453	1.504065041	3597.874332	0.852833035
WGC2019A3-C2_mon_G3 - 26.d	436708.861	23631.47	175514.223	77702.7	32575.488	18497.49	2512.46537	417.479675	117.1	90.476	31.0625	7.65182	2.857142857	0.569105691	3179.66181	0.859243991
WGC2019A3-C3_mon_G4 - 1.d	458227.848	22532.33	157768.053	59094.59	22646.536	15517.59	3886.42659	1105.69106	395.1	323.44	100.875	29.6356	10.49689441	3.617886179	5855.286281	0.747852248
WGC2019A3-C3_mon_G4 - 2.d	451476.793	22209.05	156214.442	60945.95	25399.645	18346.73	5415.51247	1678.45528	608.96	506.75	161.309	47.57	14.7826087	7.235772358	8439.891688	0.759584079
WGC2019A3-C3_mon_G4 - 3.d	457383.966	22801.72	158905.908	62027.03	24973.357	17638.19	4628.80886	1362.60163	495.8	393.41	128.625	38.3806	11.05590062	5.284552846	7063.963104	0.755021681
WGC2019A3-C3_mon_G4 - 4.d	453164.557	22381.47	154004.376	59993.24	25186.501	18160.8	5457.06371	1684.55285	619.2	498.35	157.813	41.0526	15.96273292	5.650406504	8479.646477	0.763043206
WGC2019A3-C3_mon_G4 - 5.d	452742.616	22295.26	158730.853	60405.41	24209.591	16914.57	4429.36288	1285.36585	461.6	374.91	118.313	31.9433	11.55279503	5.406504065	6718.452278	0.757389084
WGC2019A3-C3_mon_G4 - 6.d	456540.084	22155.17	155798.687	60337.84	25364.121	18467.34	5540.1662	1743.90244	641.1	517.22	165.313	44.7368	17.45341615	7.56097561	8677.448495	0.759841146
WGC2019A3-C3_mon_G4 - 7.d	452573.84	22672.41	158862.144	62432.43	24955.595	17356.78	4595.56787	1326.01626	479.6	391.03	128.25	31.9433	11.80124224	5.975609756	6970.17994	0.758102926
WGC2019A3-C3_mon_G4 - 8.d	447679.325	22403.02	158687.09	62500.883	25381.08	18015.116	5038.78116	1504.87805	551.6	448.17	137.125	38.7449	12.91925466	4.918699187	7737.135604	0.756424842
WGC2019A3-C3_mon_G4 - 9.d	465822.785	22219.83	152866.521	58716.22	24706.927	17874.37	5493.07479	1788.61789	670.7	540.48	172.438	45.2227	18.63354037	7.113821138	8736.276402	0.762648307
WGC2019A3-C3_mon_G4 - 10.d	470464.135	21691.81	146849.015	56432.43	23321.492	17246.23	5653.73961	1965.04065	797.86	642.75	214.336	61.13106	22.79503106	10.93495935	9367.875999	0.747557916
WGC2019A3-C3_mon_G4 - 11.d	475105.485	21336.21	146433.26	54722.97	22948.49	16723.62	5468.14404	1929.26829	776.2	628.21	202.688	57.613	19.25465839	8.902439024	9090.273399	0.758584835
WGC2019A3-C3_mon_G4 - 12.d	445147.679	22532.33	158315.098	62905.41	25808.171	18412.06	5080.33241	1486.58537	531.8	440.11	138.563	36.9231	13.78881988	6.62601626	7734.728079	0.758336644
WGC2019A3-C3_mon_G4 - 13.d	465822.785	22446.12	159168.49	71148.65	21207.815	37688.44	24072.0222	15601.626	119.60	9139.2	5012.5	2178.14	999.378882	517.0731707	69479.93202	0.40955149
WGC2019A3-C3_mon_G4 - 14.d	499578.059	20959.05	139562.363	52162.16	20923.623	16613.07	6204.98615	2739.8374	152.0	1188.6	543.75	214.575	96.89440994	50.40650407	12559.09405	0.710778392
WGC2019A3-C3_mon_G4 - 15.d	448101.266	22629.31	161312.91	63716.22	25577.265	18899.5	5556.7867	1865.85366	822.84	664.75	271.849	104.075	42.67080745	20.40650407	9348.476421	0.73706193
WGC2019A3-C3_mon_G4 - 16.d	449367.089	22629.31	160043.764	63378.38	25843.694	18145.73	4955.67867	1443.90244	517.82	425.75	128.854	34.61863	11.67701863	5.487804878	7523.060493	0.762073449
WGC2019A3-C3_mon_G4 - 17.d	446835.443	22790.95	158862.144	63608.11	25861.456	18597.99	5213.2964	1553.25203	555.6	455.68	145.063	39.9595	12.79503106	4.674796748	7980.317929	0.751906322
WGC2019A3-C3_mon_G4 - 18.d	448523.207	22435.34	158205.689	61743.24	25612.789	18472.36	5329.63989	1611.38211	584.1	476.37	146.813	40.081	14.72049689	4.308943089	8207.418541	0.758404556
WGC2019A3-C3_mon_G4 - 19.d	445569.62	22467.67	157855.58	62168.92	25595.027	17949.75	4847.64543	1424.39024	512.8	414.84	134.375	36.8421	10.80745342	5.325203252	7387.020625	0.766195755
WGC2019A3-C3_mon_G4 - 20.d	453375.527	22446.12	156520.788	61351.35	25452.931	18326.63	5379.50139	1673.98374	603.7	493.22	153.063	43.3603	13.72670807	5.243902439	8365.802003	0.759074471
WGC2019A3-C3_mon_G4 - 21.d	455696.203	22327.59	156083.151	60736.49	25506.217	18226.13	5445.98338	1678.45528	616.4	496.89	154.313	44.9798	14.53416149	5.772357724	8457.323887	0.766609105

Samantha Nicole March  
Ultrahigh-pressure metapelites in the WGR

WGC2019J-31A-2-C1_mon_G1 - 1.d	428607.	24482	190065.	12891	20657.	10281	65401.6	30894.3	170	1263	5581.	2255.	1086.956	609.7560	135526.35	0.179426
	595	7.6	646	8.9	194	4.1	62	089	60	7	25	06	522	976	7	554
WGC2019J-31A-2-C1_mon_G1 - 2.d	419831.	24504	184288.	95067.	9378.3	46834.	23157.8	9796.74	464	3864	1637.	631.5	293.1677	148.7804	44170.138	0.140549
	224	3.1	84	57	304	17	947	797	0	.5	5	79	019	878	71	051
WGC2019J-31A-2-C1_mon_G1 - 3.d	413544.	24676	185754.	10297	2218.4	50060.	19958.4	5731.70	179	1424	423.7	126.3	61.30434	33.86178	29555.296	0.030899
	304	7.2	923	3	725	3	488	732	5	.9	5	16	783	862	42	09
WGC2019J-31A-2-C1_mon_G1 - 4.d	408860.	24471	185776.	10216	2222.0	50351.	20052.6	5646.34	178	1435	446.2	136.0	59.06832	35.24390	29594.465	0.030981
	759	9.8	805	2.2	249	76	316	146	3	.9	5	32	298	244	09	08
WGC2019J-31A-2-C1_mon_G1 - 5.d	410548.	24547	188577.	10162	2113.6	49497.	19271.4	5467.47	172	1393	418.1	131.9	57.88819	35.32520	28505.042	0.029802
	523	4.1	681	1.6	767	49	681	967	9	.8	25	84	876	325	92	585
WGC2019J-31A-2-C5_mon_G4 - 1.d	437974.	23426	169452.	68040.	10223.	25075.	9335.18	3252.03	127	1012	331.8	99.59	34.78260	15.97560	15352.261	0.247516
	684	7.2	954	54	801	38	006	252	0	.8	75	51	87	976	45	855
WGC2019J-31A-2-C5_mon_G4 - 2.d	432067.	23092	162078.	49864.	10134.	8904.5	1526.31	285.772	65.7	57.6	16.31	5.263	1.509316	0.813008	1959.3784	0.480973
	511	6.7	775	86	991	23	579	358		92	25	16	77	13	38	035
WGC2019J-31A-2-C5_mon_G4 - 3.d	436708.	23383	166345.	60202.	14884.	13718.	2966.75	614.227	164	121.	33.62	7.570	3.416149	1.829268	3913.2227	0.517932
	861	6.2	733	7	547	59	9	642	79	5	85	068	293	84	84	119
WGC2019J-31A-2-C6_mon_G2 - 1.d	413080.	24278	181400.	75337.	6717.5	14909.	2163.43	281.707	46.9	44.1	11.12	2.631	0.614906	0.260162	2550.8130	0.200435
	169	0.2	438	84	844	55	49	317		39	5	58	832	602	63	35
WGC2019J-31A-2-C6_mon_G2 - 2.d	431223.	24385	183938.	87094.	9225.5	25683.	4883.65	742.682	131.	115.	21.93	4.777	2.670807	1.178861	5903.2222	0.195061
	629	7.8	731	59	773	42	651	927	3	02	75	33	453	789	49	494
WGC2019J-31A-2-C6_mon_G2 - 3.d	431223.	24375	184857.	85270.	8502.6	25427.	4695.29	717.073	122.	106.	20.56	4.210	1.813664	1.300813	5668.8954	0.182602
	629	0	768	27	643	14	086	171	6	04	25	53	596	008	89	825
WGC2019J-31A-2-C6_mon_G2 - 4.d	424894.	24558	185886.	87972.	9383.6	26693.	5146.81	871.544	201	171.	54.37	20.24	10.06211	5.406504	6480.8742	0.193640
	515	1.9	214	97	59	47	44	715		43	5	29	18	065	22	006
WGC2019J-31A-2-C6_mon_G2 - 5.d	428945.	24094	180612.	82635.	15097.	24010.	4551.24	706.504	126.	108.	27.06	5.627	2.173913	1.707317	5530.1962	0.338946
	148	8.3	691	14	691	05	654	065	9	97	25	53	043	073	22	868
WGC2019J-31A-2-C9_mon_G7 - 1.d	438396.	23911	181838.	90878.	8365.8	40552.	14570.6	3813.00	111	868.	246.8	72.46	29.81366	13.25203	20732.370	0.137807
	624	6.4	074	38	97	76	371	813	8	32	75	96	46	252	6	229
WGC2019J-31A-2-C9_mon_G7 - 2.d	428016.	24170	180853.	94054.	3676.7	44120.	15997.2	3943.08	107	819.	209.3	56.72	24.09937	11.95121	22132.696	0.057075
	878	2.6	392	05	318	6	299	943	1	23	75	06	888	951	36	861
WGC2019J-31A-2-C9_mon_G7 - 3.d	433333.	24558	183085.	94729.	3667.8	44874.	16415.5	4049.59	113	869.	223.8	61.53	27.20496	12.27642	22794.597	0.056256
	333	1.9	339	73	508	37	125	35	5	6	75	85	894	276	88	061
WGC2019J-31A-2-C9_mon_G7 - 4.d	429535.	24116	182363.	95810.	4033.7	45984.	17000	4402.43	127	979.	275	77.73	30.68322	16.58536	24061.293	0.060770
	865	3.8	239	81	478	92		902	9	85		28	981	585	89	63
WGC2019J-31A-2-C9_mon_G7 - 5.d	431645.	24051	182078.	92229.	7868.5	40854.	14626.0	3747.96	109	820.	219.3	64.37	25.21739	13.45528	20611.939	0.128186
	57	7.2	775	73	613	27	388	748	5	51	75	25	13	455	23	157
WGC2019J-31A-3-C1_mon_G1 - 1.d	417721.	24536	187089.	98513.	21598.	53216.	31218.8	16300.8	841	6904	2818.	1004.	466.4596	189.4308	67313.100	0.298301
	519	6.4	716	51	579	08	366	13	0	.8	75	05	273	943	58	773
WGC2019J-31A-3-C1_mon_G1 - 2.d	433755.	24073	183807.	93918.	5097.6	48341.	23296.3	10121.9	540	4084	1775	587.0	260.8695	129.2682	45654.781	0.075654
	274	2.8	44	92	909	71	989	512	0	.2		45	652	927	59	708
WGC2019J-31A-3-C1_mon_G1 - 3.d	432911.	23879	181794.	95945.	5527.5	54170.	29731.3	11922.7	457	3655	1124.	321.4	132.2360	60.60975	51524.422	0.076671
	392	3.1	311	95	311	85	019	642	6	.7	38	57	248	61	09	69
WGC2019J-31A-3-C1_mon_G1 - 4.d	437130.	23954	180306.	93648.	16110.	48793.	25844.8	11434.9	524	4056	1396.	420.6	164.5962	67.47967	48625.584	0.238322
	802	7.4	346	65	124	97	753	593	0	.8	25	48	733	48	97	507
WGC2019J-31A-3-C2_mon_G2 - 1.d	421940.	24428	184551.	97297.	2602.1	51557.	23551.2	7747.96	235	1835	443.1	111.7	47.39130	21.34146	36107.977	0.036739
	928	8.8	422	3	314	79	465	748	0	.2	25	41	435	341	51	37
WGC2019J-31A-3-C2_mon_G2 - 2.d	431223.	24536	186805.	97229.	2678.5	51356.	23952.9	7943.08	245	1862	446.2	108.0	39.93788	18.00813	36823.928	0.037904
	629	6.4	252	73	08	78	086	943	3	.6	5	97	82	008	57	825
WGC2019J-31A-3-C2_mon_G2 - 3.d	429535.	24213	182713.	96081.	2923.6	50854.	24681.4	8451.21	279	2108	490.6	125.1	46.08695	20.08130	38712.613	0.041825
	865	3.6	348	08	234	27	404	951	0	.1	25	01	652	081	04	272



Samantha Nicole March  
Ultrahigh-pressure metapelites in the WGR

WGC2019J-31A-3-C7_mon_G3 - 1.d	437130.	23911	179059.	90000	15714.	42567.	18493.0	6768.29	273	2217	756.8	237.6	102.4844	49.59349	31359.920	0.253878
	802	6.4	081		032	84	748	268	4	.9	75	52	72	593	98	296
WGC2019J-31A-3-C7_mon_G3 - 2.d	415443.	24816	185667.	76756.	5671.4	15251.	2346.26	347.154	70.4	61.9	18.43	4.696	1.658385	0.459349	2850.9712	0.165759
	038	8.1	396	76	032	26	039	472		05	75	36	093	593	12	873
WGC2019J-31A-3-C7_mon_G3 - 3.d	418987.	24321	182035.	68986.	7371.2	12829.	1817.17	243.495	42.9	38.8	11.93	3.238	1.124223	0.154471	2158.8533	0.247775
	342	1.2	011	49	256	15	452	935		28	75	87	602	545	51	761
WGC2019J-31A-3-C7_mon_G3 - 4.d	433333.	24245	183501.	81824.	13646.	31175.	9376.73	2330.48	691	565.	152.5	43.44	15.52795	7.398373	13182.288	0.270191
	333	6.9	094	32	536	88	13	78		2		13	031	984	19	616
WGC2019J-31A-3-C7_mon_G3 - 5.d	416877.	24579	183982.	83581.	8861.4	21638.	3753.46	572.764	116	95.7	25.81	6.315	1.590062	1.300813	4573.0335	0.208372
	637	7.4	495	08	565	19	26	228		88	25	79	112	008	42	615
WGC2019J-31A-3-C7_mon_G3 - 6.d	412362.	24773	185973.	81283.	7298.4	18989.	3055.40	450.406	84.2	68.4	18.87	2.995	1.490683	0.853658	3682.7216	0.185764
	869	7.1	742	78	014	95	166	504		98	5	95	23	537	28	996
WGC2019J-31A-3-C7_mon_G3 - 7.d	405907.	24719	187374.	78716.	5758.4	16608.	2506.92	355.691	63.6	53.6	17.12	2.591	1.018633	0.317073	3000.9310	0.159262
	173	8.3	179	22	369	04	521	057		63	5	09	54	171	68	422
WGC2019J-31A-3-C7_mon_G3 - 8.d	400000	25096	189759.	84527.	6222.0	18889.	2977.83	439.430	84.1	69.7	16.93	4.210	1.527950	0.268292	3594.0947	0.155712
		9.8	3	03	249	45	934	894		8	75	53	311	683	19	802
WGC2019J-31A-3-C7_mon_G3 - 9.d	419578.	24525	183807.	69121.	5642.9	12658.	1750.41	234.959	42.3	36.2	12.68	2.388	0.583850	0.142276	2079.7408	0.190771
	059	8.6	44	62	84	29	551	35		64	75	66	932	423	9	861
WGC2019J-31A-3-C7_mon_G3 - 10.d	432911.	23954	178271.	86621.	13571.	30839.	7612.18	1467.47	363.	277.	71.87	16.47	5.590062	3.292682	9817.4928	0.262589
	392	7.4	335	62	936	2	837	967		3	29	5	77	112	927	96
WGC2019J-31A-3-C8_mon_G4 - 1.d	425316.	24579	186433.	99189.	2497.3	48894.	18603.8	4756.09	128	1017	240.6	62.67	25.77639	12.43902	26001.521	0.035860
	456	7.4	26	19	357	47	781	756		3	25	21	752	439	13	379
WGC2019J-31A-3-C8_mon_G4 - 2.d	424472.	24299	183829.	96216.	7175.8	45427.	17110.8	4536.58	130	1016	264.3	66.39	28.81987	13.73983	24345.203	0.108540
	574	5.7	322	22	437	14	033	537		8	.5	75	68	578	74	335
WGC2019J-31A-3-C8_mon_G4 - 3.d	416877.	24784	189671.	10412	2710.4	49698.	18565.0	4707.31	129	993.	240.6	63.15	24.96894	13.33333	25904.539	0.037679
	637	4.8	772	1.6	796	49	97	707		7	04	25	79	41	333	49
WGC2019J-31A-3-C8_mon_G4 - 4.d	432911.	24073	180853.	89324.	17246.	39145.	14523.5	4333.33	145	1122	305	74.89	27.70186	11.91056	21854.100	0.291664
	392	2.8	392	32	892	73	457	333		5	.7		88	335	911	88
WGC2019J-31A-3-C9_mon_G7 - 1.d	427004.	24471	185120.	95270.	12113.	43216.	15429.3	3788.61	103	771.	188.7	51.90	18.94409	7.276422	21293.916	0.188788
	219	9.8	35	27	677	08	629	789		8	06	5	28	938	764	39
WGC2019J-31A-3-C9_mon_G7 - 2.d	420337.	24536	187899.	10013	2529.3	47437.	17360.1	4166.66	107	810.	190.1	51.65	18.07453	8.170731	23684.126	0.036698
	553	6.4	344	5.1	073	19	108	667		9	26	88	99	416	707	57
WGC2019J-31A-3-C9_mon_G7 - 3.d	440928.	24116	177461.	87432.	15808.	38844.	15595.5	5365.85	217	1749	637.5	214.9	89.44099	46.34146	25868.767	0.271257
	27	3.8	707	43	171	22	679	366		0	.1	8	379	341	99	73
WGC2019J-31A-3-C9_mon_G7 - 4.d	450632.	23200	168468.	73581.	24209.	22608.	5171.74	835.365	168.	118.	26.81	5.627	2.857142	1.219512	6330.9921	0.593571
	911	4.3	271	08	591	04	515	854		5	86	25	53	857	195	6
WGC2019J-31A-3-C9_mon_G7 - 5.d	429831.	24321	182757.	95540.	2360.5	44959.	16265.9	3905.69	994	754.	176.6	49.39	16.27329	7.804878	22170.110	0.036017
	224	1.2	112	54	684	8	28	106		4	25	27	193	049	52	251
WGC2019J-31A-3-C9_mon_G7 - 6.d	420632.	24903	187089.	10135	2614.5	49246.	17803.3	4195.93	108	815.	193.9	44.41	16.64596	9.796747	24168.803	0.037008
	911	0.2	716	1.4	648	23	241	496		9	75	38	3	273	967	14
WGC2019J-31A-3-C9_mon_G7 - 7.d	436708.	23900	179431.	75540.	9733.5	25025.	8088.64	2138.21	627	489.	132.5	35.42	13.97515	6.260162	11531.025	0.223869
	861	8.6	072	54	702	13	266	138		01		51	528	602	45	014
WGC2019J-31A-3-C9_mon_G7 - 8.d	420506.	25021	187527.	10081	2628.7	48653.	17279.7	4117.88	105	811.	194.0	49.91	20.31055	8.252032	23534.380	0.037535
	329	5.5	352	0.8	744	27	784	618		3	17	63	9	901	52	85
WGC2019J-31A-3-C9_mon_G7 - 9.d	425316.	24482	185842.	98378.	5062.1	48241.	19252.0	6036.58	224	1760	582.5	195.9	83.35403	41.05691	30191.598	0.073481
	456	7.6	451	38	67	21	776	537		0	.1		51	727	057	55
WGC2019J-31A-3-C9_mon_G7 - 10.d	424472.	24709	185689.	99054.	2856.1	47130.	17157.8	4117.88	106	808.	194.8	47.89	17.26708	9.268292	23419.510	0.041801
	574	0.5	278	05	279	65	947	618		6	42	75	47	075	683	93
WGC2019J-31A-3-C9_mon_G7 - 11.d	420506.	24622	187855.	99527.	2625.2	47336.	17185.5	4093.49	105	806.	177.1	43.92	19.56521	9.918699	23393.283	0.038246
	329	8.4	58	03	22	68	956	593		7	59	88	71	739	187	45

Samantha Nicole March  
Ultrahigh-pressure metapelites in the WGR

WGC2019J-31A-3-C9_mon_G7 - 12.d	424472.	24859	186870.	10013	2509.7	47839.	17409.9	4227.64	110	845.	186.8	49.39	19.75155	8.780487	23848.018	0.036261
	574	9.1	897	5.1	691	2	723	228	0	6	75	27	28	805	72	736
WGC2019J-31A-3-C9_mon_G7 - 13.d	421645.	24493	186564.	99324.	2552.3	47587.	17127.4	4117.88	107	820.	190.6	51.82	15.77639	7.439024	23406.547	0.037125
	57	5.3	551	32	979	94	238	618	5	51	88	19	752	39	61	483
WGC2019J-31A-3-C9_mon_G7 - 14.d	427004.	24989	188993.	10087	2477.7	47537.	17069.2	4142.27	107	820.	188.3	48.86	18.07453	8.536585	23371.710	0.035780
	219	2.2	435	8.4	975	69	521	642	6	33	75	64	416	366	69	61
WGC2019J-31A-3-C9_mon_G7 - 15.d	421561.	25053	188621.	10040	2547.0	47738.	17415.5	4227.64	107	816.	192.7	52.10	18.38509	9.186991	23806.882	0.036789
	181	8.8	444	5.4	693	69	125	228	5	3	5	53	317	87	46	759
WGC2019J-31A-3-C9_mon_G7 - 16.d	418143.	24946	189956.	10358	2626.9	50854.	18401.6	4369.91	110	853.	200.6	50.40	19.06832	8.983739	25006.325	0.036195
	46	1.2	236	1.1	982	27	62	87	2	66	25	49	298	837	67	605
WGC2019J-31A-3-C9_mon_G8 - 1.d	417721.	24762	187746.	10000	2506.2	47537.	16880.8	4142.27	108	835.	195.8	48.98	17.82608	5.894308	23211.094	0.036349
	519	9.3	171	0	167	69	864	642	4	35	75	79	696	943	08	596
WGC2019J-31A-3-C9_mon_G8 - 2.d	423206.	24299	185076.	98243.	2547.0	46934.	17238.2	4313.00	115	875.	207.9	55.46	22.60869	12.03252	23879.920	0.037509
	751	5.7	586	24	693	67	271	813	5	64	38	56	565	033	61	607
WGC2019J-31A-3-C9_mon_G8 - 3.d	417637.	24903	189934.	10263	2680.2	49497.	18349.0	4609.75	124	964.	222.2	64.77	22.73291	12.35772	25487.007	0.037604
	131	0.2	354	5.1	842	49	305	61	2	1	5	73	925	358	1	623
WGC2019J-31A-3-C9_mon_G8 - 4.d	419451.	24461	186433.	10033	2555.9	47683.	17822.7	4475.60	120	911.	215.3	58.70	19.50310	10.81300	24720.075	0.036951
	477	2.1	26	7.8	503	42	147	976	6	36	75	45	559	813	32	863
WGC2019J-31A-3-C9_mon_G8 - 5.d	426582.	24881	185733.	98986.	2490.2	47286.	17132.9	4170.73	108	827.	190.2	45.10	18.81987	9.186991	23479.709	0.036398
	278	4.7	042	49	309	43	64	171	5	66	5	12	578	87	46	492
WGC2019J-31A-3-C9_mon_G8 - 6.d	424472.	24191	181794.	95878.	2428.0	44251.	16063.7	3930.89	104	784.	184.0	48.98	18.63354	8.333333	22088.055	0.037276
	574	8.1	311	38	639	26	119	431	9	43	63	79	037	333	68	659
WGC2019J-31A-3-C9_mon_G8 - 7.d	426877.	24191	181378.	93581.	2404.9	44381.	16210.5	4077.23	113	846.	208.5	56.55	22.85714	11.38211	22564.213	0.037317
	637	8.1	556	08	734	91	263	577	1	15		87	286	382	9	561
WGC2019J-31A-3-C9_mon_G8 - 8.d	426582.	24547	185164.	97972.	2605.6	49447.	19844.8	5508.13	173	1335	401.2	123.8	54.65838	26.42276	29024.388	0.037436
	278	4.1	114	97	838	24	753	008	0	.2	5	87	509	423	05	7
WGC2019J-31A-3-C9_mon_G8 - 9.d	424177.	24622	184551.	95810.	2484.9	46180.	16584.4	4077.23	107	827.	190.8	50.68	18.32298	9.308943	22836.024	0.037356
	215	8.4	422	81	023	9	875	577	8	11	75	83	137	089	72	901
WGC2019J-31A-3-C9_mon_G8 - 10.d	415189.	24547	187658.	98581.	2468.9	47608.	17878.1	4544.71	125	965.	240.6	64.45	23.91304	11.66666	24980.057	0.036038
	873	4.1	643	08	165	04	163	545	1	57	25	34	348	667	71	729
WGC2019J-31A-3-C9_mon_G8 - 11.d	428270.	24515	183982.	95337.	2431.6	44969.	16243.7	4040.65	107	814.	193.0	47.77	18.63354	8.658536	22441.380	0.037136
	042	0.9	495	84	163	85	673	041	4	84	63	33	037	585	74	561
WGC2019J-31A-3-C9_mon_G8 - 12.d	418565.	24730	186673.	10020	2527.5	47462.	17326.8	4272.35	112	846.	190.2	43.52	20.31055	8.252032	23828.716	0.036650
	401	6	961	2.7	311	31	698	772	1	15	5	23	901	52	23	706
WGC2019J-31A-3-C9_mon_G8 - 13.d	410126.	24612	188905.	10222	2618.1	48944.	18246.5	4678.86	127	982.	233.1	61.13	22.98136	12.88617	25508.942	0.037012
	582	0.7	908	9.7	172	72	374	179	1	42	25	36	646	886	92	425
WGC2019J-31A-3-C9_mon_G5 - 1.d	425738.	24547	186367.	98986.	2579.0	47035.	17407.2	4487.80	123	941.	230	58.78	24.09937	10.69105	24395.158	0.037797
	397	4.1	615	49	409	18	022	488	5	58		54	888	691	05	135
WGC2019J-31A-3-C10_mon_G10 - 1.d	418143.	24633	182275.	74189.	8916.5	15190.	2512.46	439.430	114.	91.0	31.43	10.52	3.788819	1.747967	3205.2225	0.265602
	46	6.2	711	19	187	95	537	894	8	26	75	63	876	48	12	693
WGC2019J-31A-3-C10_mon_G10 - 2.d	412194.	24245	179824.	71081.	6296.6	14281.	2291.96	399.186	104.	84.0	27.12	7.611	2.981366	1.219512	2918.7569	0.197626
	093	6.9	945	08	252	41	676	992	6	66	5	34	46	195		57
WGC2019J-31A-3-C10_mon_G10 - 3.d	435443.	23900	178074.	80945.	22007.	27788.	7700.83	1918.69	604	478.	151.8	44.93	18.63354	9.674796	10926.674	0.464012
	038	8.6	398	95	105	94	102	919		02	75	93	037	748	8	129
WGC2019J-31A-3-C10_mon_G10 - 4.d	412236.	24375	179102.	70743.	6090.5	14241.	2307.47	381.300	103.	82.0	29.31	6.558	2.857142	1.463414	2914.3230	0.191885
	287	0	845	24	861	21	922	813	3	51	25	7	857	634	81	97
WGC2019J-31A-3-C10_mon_G10 - 5.d	421814.	24299	177877.	66648.	6621.6	12864.	2102.49	362.601	104.	78.0	28.68	7.327	3.416149	1.666666	2688.3149	0.226140
	346	5.7	462	65	696	32	307	626	1	22	75	94	068	667	3	522
WGC2019J-31A-3-C10_mon_G11 - 1.d	408860.	24094	177964.	64932.	5310.8	11969.	1855.95	297.154	75.8	57.6	20.75	5.425	1.962732	0.894308	2315.6346	0.190496
	759	8.3	989	43	348	85	568	472		92		1	919	943	01	77

Samantha Nicole March  
Ultrahigh-pressure metapelites in the WGR

WGC2019J-31A-3-C10_mon_G11 - 2.d	412658.	24310	181838.	72972.	5781.5	14346.	2160.66	314.634	67.6	52.0	18.12	3.076	0.968944	0.272357	2617.3568	0.178683
	228	3.4	074	97	275	73	482	146	15	5	92	099	724	43	751	
WGC2019J-31A-3-C10_mon_G11 - 3.d	426582.	24267	181531.	74662.	6051.5	15788.	2351.80	326.829	66.8	54.3	17.93	3.603	1.291925	1.260162	2823.9182	0.176253
	278	2.4	729	16	098	94	055	268	96	75	24	466	602	54	157	
WGC2019J-31A-3-C10_mon_G11 - 4.d	422784.	24008	181619.	73986.	5912.9	15778.	2315.78	319.918	60.1	49.4	15.56	3.522	1.198757	0.211382	2765.7536	0.173057
	81	6.2	256	49	663	89	947	699	51	25	27	764	114	29	694	
WGC2019J-31A-3-C10_mon_G11 - 5.d	417299.	24299	182713.	76013.	6188.2	15924.	2315.78	318.699	58.3	48.1	12.56	2.307	0.621118	0.126016	2756.5744	0.177864
	578	5.7	348	51	771	62	947	187	68	25	69	012	26	85	701	
WGC2019J-31A-3-C10_mon_G11 - 6.d	424894.	24040	183873.	88581.	11527.	32964.	10387.8	3130.08	109	908.	275.6	75.70	28.26086	11.58536	15907.497	0.213324
	515	9.5	085	08	531	82	116	13	0	42	25	85	957	585	58	351
WGC2019J-31A-3-C10_mon_G11 - 7.d	439240.	24062	180809.	93310.	16376.	48341.	23656.5	9707.31	466	3199	1098.	331.1	132.9192	60.16260	42845.841	0.243834
	506	5	628	81	554	71	097	707	0	.6	13	74	547	163	41	721
WGC2019J-31A-3-C15_mon_G21 - 1.d	425105.	24267	182056.	81148.	10138.	23613.	4074.79	550.406	104	85.3	20.68	5.708	2.285714	0.934959	4844.1634	0.231610
	485	2.4	893	65	544	07	224	504	48	75	5	286	35	09	764	
WGC2019J-31A-3-C16_mon_G20 - 1.d	427426.	24741	187811.	96824.	7300.1	48944.	21326.8	6959.34	221	1648	408.1	95.54	35.34161	16.13821	32703.722	0.106044
	16	3.8	816	32	776	72	698	959	4	.4	25	66	491	138	43	525
WGC2019J-31A-3-C16_mon_G20 - 2.d	428691.	24515	186214.	97432.	2671.4	50050.	23196.6	7849.59	251	1884	458.1	113.7	41.80124	21.74796	36078.324	0.038254
	983	0.9	442	43	032	25	759	35	2	.6	25	65	224	748	17	677
WGC2019J-31A-3-C16_mon_G20 - 3.d	427004.	24978	191378.	10128	2742.4	52045.	24260.3	8296.74	268	2005	503.7	128.7	50.55900	24.95934	37951.643	0.037772
	219	4.5	556	3.8	512	23	878	797	1	.5	5	45	621	959	58	74
WGC2019J-31A-3-C16_mon_G20 - 4.d	444303.	23846	181838.	93851.	19680.	41758.	13961.2	3682.92	107	835.	208.7	53.44	17.45341	6.788617	19835.743	0.314367
	797	9.8	074	35	284	79	188	683	0	16	5	13	615	886	83	127
WGC2019J-31A-3-C16_mon_G20 - 5.d	424894.	24536	186323.	10250	3266.4	54824.	25318.5	8349.59	265	2027	536.2	150.2	54.03726	28.61788	39118.733	0.043573
	515	6.4	851	0	298	12	596	35	4	.5	5	02	708	618	16	813
WGC2019J-31A-3-C16_mon_G20 - 6.d	423206.	24730	188096.	10371	3191.8	54824.	25462.6	8528.45	274	2075	546.8	148.5	58.50931	26.05691	39586.174	0.042328
	751	6	28	6.2	295	12	039	528	0	.1	75	83	677	057	96	269
WGC2019J-31A-3-C16_mon_G20 - 7.d	428270.	24795	189343.	10135	2964.4	53065.	24961.2	8239.83	263	2001	503.1	133.6	50.99378	22.80487	38550.414	0.040422
	042	2.6	545	1.4	76	33	188	74	7	.8	25	03	882	805	64	926
WGC2019J-31A-3-C16_mon_G20 - 8.d	424894.	24709	187680.	10081	2936.0	51457.	23783.9	7930.89	254	1913	482.5	133.6	50.12422	25.77235	36866.747	0.040765
	515	0.5	525	0.8	568	29	335	431	6	.9	03	36	772	06	002	
WGC2019J-31A-3-C16_mon_G20 - 9.d	433544.	24590	186039.	87837.	9751.3	35100.	11440.4	2756.91	616.	532.	108.3	20.85	9.440993	5.121951	15490.808	0.175616
	304	5.2	387	84	321	5	432	057	7	97	75	02	789	22	96	964
WGC2019J-31A-3-C16_mon_G20 - 10.d	435021.	24105	180306.	94391.	2923.6	48442.	22304.7	7247.96	228	1727	440	122.2	46.52173	20.60975	34194.181	0.043235
	097	6	346	89	234	21	091	748	5	.1	67	913	61	55	662	
WGC2019J-31A-3-C16_mon_G20 - 11.d	427004.	24838	188030.	10675	3639.4	58190.	27814.4	9138.21	287	2181	583.7	165.5	70	34.51219	42865.783	0.046175
	219	3.6	635	6.8	316	95	044	138	8	.3	5	87	512	74	131	
WGC2019J-31A-3-C16_mon_G20 - 12.d	421940.	24687	186652.	10445	3905.8	56582.	26969.5	8800.81	278	2117	548.7	162.3	64.78260	33.82113	41482.260	0.050804
	928	5	079	9.5	615	91	291	301	5	.2	5	48	87	821	14	279
WGC2019J-31A-3-C16_mon_G20 - 13.d	424472.	24612	187855.	10101	3115.4	53266.	25166.2	8414.63	276	2098	540.6	145.7	56.95652	28.94308	39219.013	0.042472
	574	0.7	58	3.5	529	33	05	415	7	.9	25	49	174	943	83	23
WGC2019J-31A-3-C16_mon_G20 - 14.d	431645.	24375	181816.	99527.	3142.0	53065.	25983.3	8882.11	284	2157	553.7	146.9	61.67701	27.19512	40656.588	0.043235
	57	0	193	03	959	33	795	382	4	.5	5	64	863	195	18	8
WGC2019J-31A-3-C16_mon_G20 - 15.d	431223.	24579	185820.	97567.	2932.5	50100.	23385.0	7772.35	252	1912	494.3	132.7	54.72049	24.67479	36299.051	0.041943
	629	7.4	569	57	044	5	416	772	3	.1	75	94	689	675	522	
WGC2019J-31A-3-C16_mon_G20 - 16.d	425316.	24622	185995.	10027	3238.0	52512.	24360.1	8268.29	266	2029	533.1	146.5	57.76397	26.01626	38088.171	0.044623
	456	8.4	624	0.3	107	56	108	268	7	.3	25	59	516	016	46	186
WGC2019J-31A-3-C16_mon_G20 - 17.d	422236.	24515	185842.	10243	3172.2	56130.	27296.3	9329.26	302	2302	580	154.2	64.84472	33.29268	42786.253	0.041836
	287	0.9	451	2.4	913	65	989	829	6	.2	51	05	293	4	396	
WGC2019J-31A-3-C16_mon_G20 - 18.d	437763.	24040	183260.	90675.	19639.	38155.	12700.8	3230.08	835	663.	149.8	32.95	12.29813	6.788617	17631.565	0.333889
	713	9.5	394	68	432	78	31	13	74	75	55	665	886	81	954	

Samantha Nicole March  
Ultrahigh-pressure metapelites in the WGR

WGC2019J-31A-3- C16_mon_G20 - 19.d	429535. 865	24784 4.8	187045. 952	10304 0.5	3264.6 536	55829. 15	27199.4 46	9325.20 325	303 7	2307 .7	581.8 75	153.4 41	66.95652 174	29.34959 35	42700.963 95	0.043043 002
WGC2019J-31A-3- C16_mon_G20 - 20.d	427004. 219	24181 0.3	181444. 201	91283. 78	20195. 382	38145. 73	13512.4 654	3552.84 553	895 74	726. 74	146 38	27.81 38	7.639751 553	4.227642 276	18872.731 99	0.342241 204
WGC2019J-31A-3- C16_mon_G20 - 21.d	425147. 679	24321 1.2	180525. 164	89459. 46	20532. 86	33618. 09	9667.59 003	2044.71 545	437 29	340. 29	68.37 5	13.07 69	4.968944 099	2.886178 862	12578.905 56	0.374412 021
WGC2019J-31A-3- C16_mon_G20 - 22.d	431223. 629	24536 6.4	184004. 376	90472. 97	20266. 43	30447. 24	7506.92 521	1726.42 276	517. 8	410. 26	122.6 88	36.63 97	14.22360 248	6.585365 854	10341.540 53	0.386139 19
WGC2019J-31A-3- C16_mon_G20 - 23.d	430801. 688	24461 2.1	183019. 694	90743. 24	20230. 906	30321. 61	7562.32 687	1728.86 179	529. 4	419. 41	118.1 25	32.83 4	14.09937 888	7.926829 268	10412.987 79	0.385684 394
WGC2019J-31A-3- C16_mon_G20 - 24.d	432489. 451	24105 6	184879. 65	90067. 57	11010. 657	35175. 88	10277.0 083	2747.96 748	915 55	787. 25	243.1 53	70.44 36	30.12422 36	15.52845 528	15086.744 6	0.195616 977
WGC2019J-31A-3- C16_mon_G20 - 25.d	439662. 447	23965 5.2	179934. 354	89864. 86	19911. 19	38693. 47	13797.7 839	3959.34 959	112 4	916. 85	214.3 75	43.56 28	13.72670 807	6.260162 602	20075.907 97	0.337662 966
WGC2019J-31A-3- C16_mon_G20 - 26.d	424556. 962	24504 3.1	184463. 895	83851. 35	8687.3 89	28869. 35	8565.09 695	2215.44 715	569. 6	517. 4	122 98	23.31 98	8.136645 963	3.048780 488	12024.048 64	0.176569 528
WGC2019J-31A-3- C16_mon_G20 - 27.d	422784. 81	24579 7.4	186695. 842	87500 027	9559.5 31	32261. 734	9911.35 106	2605.69 734	669 7	633. 5	146.2 95	29.95 95	9.316770 186	2.113821 138	14007.388 14	0.179924 497
WGC2019J-31A-3- C16_mon_G20 - 28.d	424894. 515	24892 2.4	186192. 56	89256. 76	11634. 103	37587. 94	13628.8 089	4260.16 26	134 4	1170 .3	321.8 75	81.78 14	26.27329 193	12.76422 764	20845.995 03	0.200857 519
WGC2019J-31A-3- C16_mon_G20 - 29.d	430801. 688	24353 4.5	181947. 484	90472. 97	20266. 43	35331. 66	11157.8 947	2423.17 073	515. 8	399. 63	68.37 5	11.86 23	5.341614 907	2.398373 984	14584.476 51	0.358455 962
WGC2019J-31A-3- C16_mon_G20 - 30.d	440928. 27	24127 1.6	184682. 713	95337. 84	15719. 361	44447. 24	16645.4 294	4760.16 26	142 3	1115 .4	283.7 5	74.49 39	26.33540 373	12.27642 276	24340.832 33	0.241479 266
WGC2019J-31A-3- C17_mon_G17 - 1.d	428059. 072	24525 8.6	185908. 096	82628. 38	8218.4 725	20944. 72	3991.68 975	739.430 894	211. 1	166. 85	52.12 5	15.95 14	6.024844 72	2.520325 203	5185.6920 49	0.197555 522
WGC2019J-31A-3- C17_mon_G17 - 2.d	428270. 042	24816 8.1	187308. 534	86621. 62	9378.3 304	26010. 05	5351.80 055	1012.19 512	282 11	203. 25	62.56 65	17.20 373	8.633540 373	3.861788 618	6941.3735 36	0.197579 452
WGC2019J-31A-3- C17_mon_G17 - 3.d	437130. 802	24364 2.2	182013. 129	87229. 73	11229. 13	34035. 18	9157.89 474	1792.68 293	426 21	304. 25	71.06 65	17.20 137	6.832298 137	3.902439 024	11779.793 83	0.206086 638
WGC2019J-31A-3- C17_mon_G17 - 4.d	432911. 392	24202 5.9	183085. 339	88716. 22	11559. 503	31859. 3	7742.38 227	1503.65 854	416 66	303. 25	86.81 12	20.93 54	10.18633 54	3.658536 585	10087.292 36	0.217430 044
WGC2019J-31A-3- C17_mon_G17 - 5.d	429535. 865	24224 1.4	181115. 974	87500 607	11566. 607	32467. 34	8155.12 465	1515.04 065	360. 2	269. 23	68.37 5	16.15 38	4.596273 292	3.455284 553	10392.176 48	0.217009 446
WGC2019J-31A-3- C18_mon_G15 - 1.d	431645. 57	24202 5.9	181925. 602	89256. 76	29076. 377	33487. 44	9659.27 978	2354.47 154	718. 8	543. 04	150.2 5	42.34 82	13.47826 087	6.951219 512	13488.619 27	0.531837 281
WGC2019J-31A-3- C18_mon_G15 - 2.d	447552. 743	24331 9	180415. 755	83310. 81	29769. 094	26994. 97	5803.32 41	997.560 976	239. 8	166. 85	42.5 06	9.838 075	3.726708 075	2.113821 138	7265.7134 78	0.627730 853
WGC2019J-31A-3- C18_mon_G15 - 3.d	442194. 093	24321 1.2	181509. 847	89054. 05	28898. 757	33015. 08	9335.18 006	2288.61 789	682 98	521. 98	146.8 75	36.43 72	13.41614 907	5.487804 878	13029.992 16	0.532961 901
WGC2019J-31A-3- C18_mon_G15 - 4.d	439662. 447	24213 3.6	181903. 72	88783. 78	30621. 67	37206. 03	12950.1 385	3357.31 707	931 55	687. 88	160.1 4	37.00 925	12.73291 925	4.918699 187	18140.844 53	0.532789 153
WGC2019J-31A-3- C22_mon_Gx - 1.d	437130. 802	24181 0.3	184704. 595	99864. 86	15968. 028	57185. 93	27202.2 161	10987.8 049	510 0	4022 75	1538. 79	531.5 025	224.2236 025	108.5365 854	49715.088 1	0.211300 412

### Monazite trace elements standards

Standard	La	Pr	Nd	Sm	Eu	Gd	Tb	Dy	Ho	Er	Tm	Yb	Lu
NIST610_51 - 1.d	194100	198400	189600	202300	197300	197100	193500	192400	198200	200400	191800	198300	193400
NIST610_51 - 2.d	193800	197000	190600	198800	196100	197400	191600	192000	196400	200900	190900	197700	192200
NIST610_51 - 3.d	194700	197700	191500	199000	197200	197600	193200	194100	198100	201000	192600	199100	193800
NIST610_51 - 4.d	195600	198500	191300	202000	198400	197100	194000	193000	198600	201300	193200	199800	194000
NIST610_51 - 5.d	193400	198400	188800	200300	197900	199300	192900	192800	198200	200300	192400	198500	193900
NIST610_51 - 6.d	193200	196500	190000	197900	197300	197900	192000	192100	197200	200000	190900	197200	193300
NIST610_51 - 7.d	194500	198000	188600	198000	196000	199500	191800	192200	197900	200200	191400	197900	193600
NIST610_51 - 8.d	193700	198200	189800	201000	196500	198500	192140	192300	198800	200000	191400	197800	192900
NIST610_51 - 9.d	194200	196400	189300	200400	196800	196400	192400	191700	197500	200000	191100	198700	193100
NIST610_51 - 10.d	194400	198400	191000	200000	198400	199800	194000	193200	199000	202100	193200	200000	195000
NIST610_51 - 11.d	193000	198300	188300	199700	197300	199000	193100	193400	197800	200500	192300	197400	193800
NIST610_51 - 12.d	194600	197900	190200	201600	197300	199700	193800	194500	199400	202300	192700	198800	195000
NIST610_51 - 13.d	194300	198300	189800	201500	198200	198600	193300	194100	199300	202100	192500	199200	194690
NIST610_51 - 14.d	195400	197300	189600	198300	197300	197300	193000	193100	198100	200200	191900	199500	193400
NIST610_51 - 15.d	194200	197800	187600	200100	197000	198500	191600	194000	197000	200500	192300	198500	193600
NIST610_51 - 16.d	195200	197400	188700	200100	198300	198600	193600	193100	199000	201800	192100	199400	194800
NIST610_51 - 17.d	194700	197000	191900	199000	197300	198500	194200	193400	198900	201600	192300	199500	194400
NIST610_51 - 18.d	195200	198500	190200	200100	197500	199200	194200	193200	198800	202300	192600	199100	194200
NIST610_51 - 19.d	194400	197100	190200	199800	198200	198700	193000	192200	198800	200800	192300	199800	194200
NIST610_51 - 20.d	193600	197400	189900	198700	197400	199900	193000	193700	198500	201900	192000	198200	194500
NIST610_51 - 21.d	194500	198500	193100	198600	198400	197700	193900	194300	199100	202000	193000	200200	194900
NIST610_51 - 22.d	193500	197600	188000	199000	197900	197400	192300	192500	198600	201700	192100	199200	193800
NIST610_51 - 23.d	194200	198000	189200	199800	197100	197300	192800	192800	198000	202100	192400	199100	193600
NIST610_51 - 24.d	194400	196400	189000	199700	197200	197100	192500	192200	197600	200300	190900	198200	193200
NIST610_51 - 25.d	194700	199400	189000	201500	196900	199300	193100	193400	198800	200000	192700	200000	194200
NIST610_51 - 26.d	193600	198100	190700	199900	197400	196000	193000	193600	199000	200200	191900	197800	194100
NIST610_51 - 27.d	193600	198800	190200	199200	197300	200900	192600	194000	197900	201500	191900	198700	194100
NIST610_51 - 28.d	193900	197100	191000	201200	196400	198800	192600	192400	197700	201200	192100	197700	193200

<b>NIST610_51 - 29.d</b>	194000	197000	189500	201100	197400	197000	193200	192300	197500	201600	192100	197600	193100
<b>NIST610_51 - 30.d</b>	194800	196600	188900	196900	196600	195400	191200	191300	196800	198400	190200	196500	191100
<b>NIST610_51 - 31.d</b>	194600	198600	191200	201100	197700	199200	193200	193100	198400	201400	192200	199300	194300
<b>NIST610_51 - 32.d</b>	194300	197700	189300	201900	196400	198200	192700	192100	197100	199300	191400	197800	192500
<b>NIST610_19 - 1.d</b>	192200	197000	185100	198700	195500	195600	190800	189100	195300	197700	189100	194700	187400
<b>NIST610_19 - 2.d</b>	190800	198400	189500	202600	197000	197800	192100	191600	196400	199800	187200	193600	189500
<b>NIST610_19 - 3.d</b>	197300	200500	187300	200900	199600	198700	194300	194800	199800	197800	192200	194800	192100
<b>NIST610_19 - 4.d</b>	190600	197500	190500	204900	196300	196300	190200	188700	194800	195500	188700	194600	188800
<b>NIST610_19 - 5.d</b>	187100	192700	187500	196400	193000	192400	185700	183100	191600	192700	181400	192000	185100
<b>NIST610_19 - 6.d</b>	192400	196700	185900	198300	192500	192700	187000	191100	193100	193100	186800	189600	188000
<b>NIST610_19 - 7.d</b>	193200	198300	188800	196600	196200	195000	190300	187900	193500	195400	188200	194100	190400
<b>NIST610_19 - 8.d</b>	193200	198100	196000	200500	195800	192300	191900	190100	193400	196500	189200	194300	188000
<b>NIST610_19 - 9.d</b>	193600	198900	190800	197200	196500	198800	190500	190000	194100	197700	189200	196300	190500
<b>NIST610_19 - 10.d</b>	191400	195500	186200	192700	192400	193600	184400	188600	193100	193000	185700	192300	187500
<b>NIST610_19 - 11.d</b>	190200	195800	186200	193100	197800	194500	188100	190800	195500	199400	186400	195000	188900
<b>NIST610_19 - 12.d</b>	194800	196300	185800	196400	195700	190800	188500	193500	194400	195100	189600	196300	187600
<b>NIST610_19 - 13.d</b>	194700	202100	192900	200000	196800	201000	191400	190000	194300	198600	191700	195200	191800
<b>NIST610_19 - 14.d</b>	192400	196600	186000	192600	196500	197800	189000	189200	191300	196000	189100	190400	186100
<b>NIST610_19 - 15.d</b>	194100	195100	184800	199900	196700	187900	188800	190500	194900	199100	188000	190600	190900
<b>NIST610_19 - 16.d</b>	190000	195900	185800	198200	192600	194700	185100	187800	189500	196100	186500	191600	187700

### APPENDIX 3D: LA-ICP-MS APATITE RESULTS

#### Apatite morphology

Sample	Textural location	Size (long axis)	Crystal Habit	Spot location	Comments
3-C2_ap - 1.d	Matrix	~700µm	Equant	rim	
3-C2_ap - 2.d	Matrix			mid	
3-C2_ap - 3.d	Matrix			rim	
3-C2_ap - 4.d	Matrix			rim	
3-C2_ap - 5.d	Matrix			mid	
3-C2_ap - 6.d	Matrix			rim	
3-C2_ap - 7.d	Matrix			core	
3-C2_ap - 8.d	Matrix			core	
3-C2_ap - 9.d	Matrix			mid	
3-C2_ap - 10.d	Matrix			rim	
3-C2_ap - 11.d	Matrix			core	
3-C2_ap - 12.d	Matrix			core	
3-C2_ap - 13.d	Matrix			mid	
3-C2_ap - 14.d	Matrix			rim	
3-C2_ap - 15.d	Matrix			rim	
3-C2_ap - 16.d	Matrix			rim	
3-C2_ap - 17.d	Matrix			rim	
3-C2_ap - 18.d	Matrix			mid	
3-C2_ap - 19.d	Matrix			rim	
3-C2_ap - 20.d	Matrix			rim	
3-C3_ap - 1.d	Matrix	~2500µm	Tabular	rim	
3-C3_ap - 2.d	Matrix			rim	
3-C3_ap - 3.d	Matrix			rim	
3-C3_ap - 4.d	Matrix			mid	
3-C3_ap - 5.d	Matrix			core	
3-C3_ap - 6.d	Matrix			core	

---

3-C3_ap - 7.d	Matrix	mid
3-C3_ap - 8.d	Matrix	rim
3-C3_ap - 9.d	Matrix	core
3-C3_ap - 10.d	Matrix	core
3-C3_ap - 11.d	Matrix	core
3-C3_ap - 12.d	Matrix	mid
3-C3_ap - 13.d	Matrix	mid
3-C3_ap - 14.d	Matrix	core
3-C3_ap - 15.d	Matrix	core
3-C3_ap - 16.d	Matrix	core
3-C3_ap - 17.d	Matrix	core
3-C3_ap - 18.d	Matrix	core
3-C3_ap - 19.d	Matrix	mid
3-C3_ap - 20.d	Matrix	mid
3-C3_ap - 21.d	Matrix	mid
3-C3_ap - 22.d	Matrix	rim
3-C3_ap - 23.d	Matrix	core
3-C3_ap - 24.d	Matrix	rim
3-C3_ap - 25.d	Matrix	rim
3-C3_ap - 26.d	Matrix	mid
3-C3_ap - 27.d	Matrix	rim
3-C3_ap - 28.d	Matrix	rim
3-C3_ap - 29.d	Matrix	rim
3-C3_ap - 30.d	Matrix	rim
3-C3_ap - 31.d	Matrix	core
3-C3_ap - 32.d	Matrix	mid
3-C3_ap - 33.d	Matrix	rim
3-C3_ap - 34.d	Matrix	mid
3-C3_ap - 35.d	Matrix	core
3-C3_ap - 36.d	Matrix	core
3-C3_ap - 37.d	Matrix	rim

---



---

3-C3_ap - 38.d	Matrix			rim
3-C3_ap - 39.d	Matrix			rim
3-C3_ap - 40.d	Matrix			rim
3-C3_ap - 41.d	Matrix			core
3-C3_ap - 42.d	Matrix			rim
3-C3_ap - 43.d	Matrix			mid
3-C3_ap - 44.d	Matrix			core
3-C3_ap - 45.d	Matrix			mid
3-C3_ap - 46.d	Matrix			rim
3-C3_ap - 47.d	Matrix			rim
3-C3_ap - 48.d	Matrix			mid
3-C3_ap - 49.d	Matrix			rim
3-C3_ap - 50.d	Matrix			mid
25B-3a-C1_ap - 1.d	Garnet inclusion	~600µm	Equant	mid
25B-3a-C1_ap - 2.d	Garnet inclusion			core
25B-3a-C1_ap - 3.d	Garnet inclusion			core
25B-3a-C1_ap - 4.d	Garnet inclusion			core
25B-3a-C1_ap - 5.d	Garnet inclusion			core
25B-3a-C1_ap - 6.d	Garnet inclusion			mid
25B-3a-C1_ap - 7.d	Garnet inclusion			rim
25B-3a-C1_ap - 8.d	Garnet inclusion			rim
25B-3a-C1_ap - 9.d	Garnet inclusion			mid
25B-3a-C1_ap - 10.d	Garnet inclusion			rim
25B-3a-C1_ap - 11.d	Garnet inclusion			mid
25B-3a-C1_ap - 12.d	Garnet inclusion			mid
25B-3a-C1_ap - 14.d	Garnet inclusion			rim
25B-3a-C2_ap1 - 1.d	Garnet inclusion	~300µm	Equant	rim
25B-3a-C2_ap1 - 2.d	Garnet inclusion			mid
25B-3a-C2_ap1 - 3.d	Garnet inclusion			rim
25B-3a-C2_ap1 - 4.d	Garnet inclusion			mid
25B-3a-C2_ap1 - 5.d	Garnet inclusion			rim

---

25B-3a-C2_ap1 - 6.d	Garnet inclusion			rim	
25B-3a-C2_ap1 - 7.d	Garnet inclusion			core	
25B-3a-C2_ap1 - 8.d	Garnet inclusion			rim	
25B-3a-C2_ap2 - 1.d	Garnet inclusion	~250µm	Equant	rim	
25B-3a-C2_ap2 - 2.d	Garnet inclusion			core	
25B-3a-C2_ap2 - 3.d	Garnet inclusion			rim	
25B-3a-C2_ap2 - 4.d	Garnet inclusion			rim	
25B-3a-C2_ap2 - 5.d	Garnet inclusion			rim	
25B-3a-C2_ap2 - 6.d	Garnet inclusion			rim	
25B-3a-C3_ap1 - 1.d	Garnet edge	~250µm	Equant	mid	matrix-facing edge
25B-3a-C3_ap1 - 3.d	Garnet edge			mid	matrix-facing edge
25B-3a-C3_ap1 - 4.d	Garnet edge			core	
25B-3a-C3_ap1 - 6.d	Garnet edge			rim	garnet-facing edge
25B-3a-C3_ap1 - 7.d	Garnet edge			rim	garnet-facing edge
25B-3a-C3_ap2 - 1.d	Garnet inclusion	~250µm	Equant	rim	
25B-3a-C3_ap2 - 2.d	Garnet inclusion			mid	
25B-3a-C3_ap2 - 3.d	Garnet inclusion			rim	
25B-3a-C3_ap2 - 4.d	Garnet inclusion			rim	
25B-3a-C3_ap2 - 5.d	Garnet inclusion			core	
25B-3a-C3_ap2 - 6.d	Garnet inclusion			rim	
25B-3a-C4_ap - 1.d	Matrix	~2500µm	Asymmetric/triangular	rim	
25B-3a-C4_ap - 2.d	Matrix			rim	
25B-3a-C4_ap - 3.d	Matrix			mid	
25B-3a-C4_ap - 4.d	Matrix			mid	
25B-3a-C4_ap - 5.d	Matrix			mid	
25B-3a-C4_ap - 6.d	Matrix			mid	
25B-3a-C4_ap - 7.d	Matrix			mid	
25B-3a-C4_ap - 8.d	Matrix			mid	
25B-3a-C4_ap - 9.d	Matrix			mid	
25B-3a-C4_ap - 10.d	Matrix			mid	
25B-3a-C4_ap - 11.d	Matrix			mid	

25B-3a-C4_ap - 12.d	Matrix			mid	
25B-3a-C4_ap - 13.d	Matrix			mid	
25B-3a-C4_ap - 14.d	Matrix			rim	
25B-3a-C4_ap - 15.d	Matrix			rim	
25B-3a-C4_ap - 17.d	Matrix			rim	
25B-3a-C4_ap - 19.d	Matrix			core	
25B-3a-C4_ap - 20.d	Matrix			core	
25B-3a-C4_ap - 21.d	Matrix			core	
25B-3a-C4_ap - 22.d	Matrix			mid	
25B-3a-C4_ap - 23.d	Matrix			mid	
25B-3a-C4_ap - 25.d	Matrix			core	
25B-3a-C4_ap - 26.d	Matrix			core	
25B-3a-C4_ap - 27.d	Matrix			rim	
25B-3a-C4_ap - 28.d	Matrix			rim	
25B-3a-C4_ap - 29.d	Matrix			mid	
25B-3a-C4_ap - 30.d	Matrix			core	
25B-3a-C4_ap - 31.d	Matrix			mid	
25B-3a-C4_ap - 32.d	Matrix			rim	
25B-3a-C4_ap - 33.d	Matrix			mid	
25B-3a-C4_ap - 34.d	Matrix			rim	
25B-3a-C4_ap - 35.d	Matrix			mid	
25B-3b-C7_ap - 1.d	Garnet edge	~2000µm	Asymmetric	rim	garnet-facing edge
25B-3b-C7_ap - 2.d	Garnet edge			rim	garnet-facing edge
25B-3b-C7_ap - 3.d	Garnet edge			rim	
25B-3b-C7_ap - 4.d	Garnet edge			rim	
25B-3b-C7_ap - 5.d	Garnet edge			rim	
25B-3b-C7_ap - 6.d	Garnet edge			rim	
25B-3b-C7_ap - 7.d	Garnet edge			rim	
25B-3b-C7_ap - 9.d	Garnet edge			core	
25B-3b-C7_ap - 10.d	Garnet edge			core	
25B-3b-C7_ap - 11.d	Garnet edge			core	garnet-facing edge

---

25B-3b-C7_ap - 12.d	Garnet edge	rim	garnet-facing edge
25B-3b-C7_ap - 13.d	Garnet edge	rim	garnet-facing edge
25B-3b-C7_ap - 14.d	Garnet edge	rim	garnet-facing edge
25B-3b-C7_ap - 15.d	Garnet edge	core	garnet-facing edge
25B-3b-C7_ap - 16.d	Garnet edge	core	
25B-3b-C7_ap - 17.d	Garnet edge	core	
25B-3b-C7_ap - 18.d	Garnet edge	core	
25B-3b-C7_ap - 19.d	Garnet edge	core	
25B-3b-C7_ap - 20.d	Garnet edge	rim	
25B-3b-C7_ap - 21.d	Garnet edge	mid	garnet-facing edge
25B-3b-C7_ap - 22.d	Garnet edge	rim	garnet-facing edge
25B-3b-C7_ap - 23.d	Garnet edge	mid	garnet-facing edge
25B-3b-C7_ap - 24.d	Garnet edge	rim	garnet-facing edge
25B-3b-C7_ap - 25.d	Garnet edge	mid	garnet-facing edge
25B-3b-C7_ap - 26.d	Garnet edge	rim	garnet-facing edge
25B-3b-C7_ap - 27.d	Garnet edge	mid	
25B-3b-C7_ap - 28.d	Garnet edge	core	
25B-3b-C7_ap - 29.d	Garnet edge	rim	
25B-3b-C7_ap - 30.d	Garnet edge	rim	
25B-3b-C7_ap - 32.d	Garnet edge	rim	
25B-3b-C7_ap - 33.d	Garnet edge	rim	garnet-facing edge
25B-3b-C7_ap - 34.d	Garnet edge	mid	garnet-facing edge
25B-3b-C7_ap - 35.d	Garnet edge	mid	garnet-facing edge
25B-3b-C7_ap - 36.d	Garnet edge	rim	garnet-facing edge
25B-3b-C7_ap - 37.d	Garnet edge	rim	garnet-facing edge
25B-3b-C7_ap - 38.d	Garnet edge	rim	garnet-facing edge
25B-3b-C7_ap - 39.d	Garnet edge	rim	garnet-facing edge
25B-3b-C7_ap - 40.d	Garnet edge	rim	garnet-facing edge
25B-3b-C7_ap - 41.d	Garnet edge	rim	
25B-3b-C7_ap - 42.d	Garnet edge	rim	
25B-3b-C7_ap - 43.d	Garnet edge	rim	

---

25B-3b-C7_ap - 44.d	Garnet edge	rim	garnet-facing edge
25B-3b-C7_ap - 45.d	Garnet edge	rim	garnet-facing edge

### Apatite geochronology

Sample	207/235	2 $\sigma$	206/238	2 $\sigma$	207/206	2 $\sigma$	ErrCorr 6/38vs7/35	ErrCorr 38/6vs7/6	207/235 age	2 $\sigma$	206/238 age	2 $\sigma$	Concordant?	% discordance
3-C2_ap - 1.d	3.365	0.081	0.0891	0.003	0.2756	0.0071	0.24341	0.38902	1496	18	550.3	18	D	63.21524064
3-C2_ap - 2.d	3.414	0.067	0.0898	0.0029	0.2749	0.0057	0.11765	0.52705	1506	15	554.5	17	D	63.18061089
3-C2_ap - 3.d	3.043	0.081	0.0886	0.0028	0.2494	0.0076	-0.042264	0.50354	1415	20	547.2	17	D	61.32862191
3-C2_ap - 4.d	3.127	0.07	0.0883	0.0027	0.2546	0.0057	0.24641	0.32086	1437	17	545.2	16	D	62.0598469
3-C2_ap - 5.d	3.162	0.07	0.0867	0.0028	0.2651	0.0053	0.20182	0.32176	1449	17	536.2	16	D	62.99516908
3-C2_ap - 6.d	2.864	0.061	0.084	0.0027	0.2455	0.006	0.075491	0.5022	1371	16	519.8	16	D	62.08606856
3-C2_ap - 7.d	3.325	0.083	0.0899	0.0028	0.2678	0.0066	0.39748	0.06943	1487	20	554.9	17	D	62.68325488
3-C2_ap - 8.d	3.216	0.071	0.08736	0.0027	0.2669	0.006	0.12262	0.37166	1464	16	539.9	16	D	63.1215847
3-C2_ap - 9.d	3.344	0.078	0.091	0.0031	0.2649	0.0049	0.54637	0.14767	1489	18	561.2	18	D	62.31027535
3-C2_ap - 10.d	3.153	0.075	0.08776	0.0027	0.2602	0.0066	0.00417	0.41389	1446	19	542.2	16	D	62.50345781
3-C2_ap - 11.d	3.377	0.071	0.088	0.0028	0.2775	0.0062	0.21932	0.36789	1497	16	543.9	17	D	63.66733467
3-C2_ap - 12.d	3.068	0.062	0.08633	0.0026	0.2593	0.0055	0.14123	0.35691	1430	15	533.7	16	D	62.67832168
3-C2_ap - 13.d	2.902	0.068	0.0878	0.0027	0.2396	0.0057	0.24509	0.33362	1380	18	542.6	16	D	60.68115942
3-C2_ap - 14.d	3.203	0.077	0.0871	0.0029	0.267	0.0069	-0.028223	0.53917	1456	19	538	17	D	63.04945055
3-C2_ap - 15.d	3.507	0.093	0.0896	0.003	0.2862	0.0085	0.14331	0.46576	1535	21	552.8	18	D	63.98697068
3-C2_ap - 16.d	3.541	0.091	0.0914	0.0029	0.2804	0.0078	0.17622	0.40242	1533	20	563.7	17	D	63.22896282
3-C2_ap - 17.d	3.504	0.079	0.0916	0.003	0.2779	0.008	0.083562	0.57373	1529	18	564.9	18	D	63.05428385
3-C2_ap - 18.d	3.443	0.076	0.0911	0.0031	0.2747	0.007	0.1852	0.48307	1514	17	561.9	18	D	62.88639366
3-C2_ap - 19.d	3.366	0.088	0.0897	0.003	0.2701	0.0066	0.30953	0.31061	1497	20	553.5	18	D	63.0260521
3-C2_ap - 20.d	3.381	0.066	0.0885	0.0029	0.2752	0.0058	0.20383	0.40668	1498	15	546.6	17	D	63.51134846
3-C3_ap - 1.d	3.843	0.082	0.0951	0.0031	0.2972	0.0072	0.063642	0.5298	1602	17	585.6	18	D	63.44569288
3-C3_ap - 2.d	4.148	0.097	0.0964	0.0031	0.3157	0.0091	0.067549	0.534	1669	19	593	18	D	64.46974236
3-C3_ap - 3.d	4.54	0.12	0.1008	0.0033	0.3296	0.0075	0.48026	0.13057	1743	22	619.2	19	D	64.47504303
3-C3_ap - 4.d	4.052	0.078	0.0963	0.0032	0.3023	0.0061	0.23689	0.47545	1643	16	592.7	19	D	63.92574559
3-C3_ap - 5.d	3.974	0.086	0.0961	0.0031	0.3009	0.0073	0.20247	0.39289	1629	17	592.8	18	D	63.60957643

Samantha Nicole March  
Ultrahigh-pressure metapelites in the WGR

3-C3_ap - 6.d	3.74	0.07	0.0942	0.0029	0.2903	0.0054	0.28971	0.34228	1583	15	580	17	D	63.36070752
3-C3_ap - 7.d	3.493	0.08	0.0911	0.0029	0.2765	0.0069	0.19363	0.37028	1526	17	562	17	D	63.17169069
3-C3_ap - 8.d	5.33	0.13	0.1068	0.0035	0.3622	0.0086	0.32838	0.25781	1874	21	654	21	D	65.10138741
3-C3_ap - 9.d	3.555	0.077	0.0922	0.003	0.2812	0.0063	0.25681	0.4095	1537	17	568.5	18	D	63.01236174
3-C3_ap - 10.d	3.238	0.063	0.08813	0.0027	0.2662	0.0059	0.02669	0.4751	1465	15	544.4	16	D	62.83959044
3-C3_ap - 11.d	3.462	0.088	0.0912	0.0029	0.2794	0.0076	0.16511	0.32139	1525	20	562.9	17	D	63.08852459
3-C3_ap - 12.d	3.219	0.083	0.08654	0.0027	0.2702	0.0067	0.29978	0.16929	1464	21	535	16	D	63.45628415
3-C3_ap - 13.d	3.214	0.073	0.0872	0.0028	0.2672	0.0065	0.26332	0.30449	1463	18	538.6	16	D	63.18523582
3-C3_ap - 14.d	3.101	0.08	0.0849	0.0027	0.263	0.007	0.074384	0.35964	1430	20	525	16	D	63.28671329
3-C3_ap - 15.d	3.254	0.078	0.0889	0.0028	0.2659	0.0058	0.39752	0.046119	1471	18	548.8	17	D	62.69204623
3-C3_ap - 16.d	3.079	0.067	0.0867	0.0027	0.2581	0.0061	0.20571	0.3302	1433	17	536.1	16	D	62.58897418
3-C3_ap - 17.d	3.174	0.056	0.0887	0.0028	0.2603	0.0057	0.061635	0.46046	1452	14	548	17	D	62.25895317
3-C3_ap - 18.d	3.538	0.083	0.0904	0.0029	0.2869	0.0073	0.22925	0.34234	1536	19	558	17	D	63.671875
3-C3_ap - 19.d	3.355	0.083	0.0896	0.0029	0.2688	0.0056	0.36631	0.18992	1496	19	552.9	17	D	63.04144385
3-C3_ap - 20.d	3.162	0.068	0.0871	0.0028	0.2646	0.0066	0.057225	0.51309	1446	17	538.6	17	D	62.75242047
3-C3_ap - 21.d	3.211	0.074	0.0876	0.0028	0.2676	0.0069	-0.019077	0.47973	1463	18	541	16	D	63.02118934
3-C3_ap - 22.d	3.46	0.093	0.0889	0.0029	0.2818	0.0085	0.21002	0.36525	1515	21	548.9	17	D	63.7689769
3-C3_ap - 23.d	3.288	0.064	0.0896	0.0028	0.2675	0.0061	0.19773	0.38903	1477	15	553.1	17	D	62.55247123
3-C3_ap - 24.d	3.207	0.088	0.0875	0.0028	0.2676	0.0065	0.31156	0.24982	1464	21	540.5	17	D	63.08060109
3-C3_ap - 25.d	2.845	0.05	0.08285	0.0026	0.2469	0.0047	0.14451	0.52355	1366	13	513.1	15	D	62.43777452
3-C3_ap - 26.d	2.942	0.068	0.0847	0.0027	0.2514	0.0062	0.079995	0.46	1390	17	523.9	16	D	62.30935252
3-C3_ap - 27.d	3.366	0.071	0.0889	0.003	0.2746	0.0072	0.25759	0.43328	1497	17	548.8	18	D	63.34001336
3-C3_ap - 28.d	3.202	0.079	0.0867	0.0029	0.2681	0.0058	0.43519	0.20836	1458	19	535.7	17	D	63.25788752
3-C3_ap - 29.d	3.031	0.068	0.0852	0.0027	0.2583	0.0054	0.40435	0.24093	1416	18	528	16	D	62.71186441
3-C3_ap - 30.d	3.049	0.076	0.0842	0.0027	0.2617	0.007	0.10777	0.42953	1420	18	521.2	16	D	63.29577465
3-C3_ap - 31.d	2.866	0.067	0.0828	0.0026	0.2503	0.0063	0.17694	0.42425	1375	17	512.6	16	D	62.72
3-C3_ap - 32.d	2.901	0.069	0.0854	0.0028	0.2428	0.0061	0.25892	0.27758	1383	18	528.3	16	D	61.80043384
3-C3_ap - 33.d	3.21	0.071	0.0862	0.0028	0.2685	0.0069	0.14007	0.38572	1460	17	533.2	16	D	63.47945205
3-C3_ap - 34.d	3.032	0.066	0.0853	0.0027	0.2576	0.0053	0.25644	0.34797	1414	17	527.5	16	D	62.69448373
3-C3_ap - 35.d	2.982	0.06	0.08304	0.0026	0.259	0.0055	0.30303	0.29879	1401	15	514.2	15	D	63.29764454
3-C3_ap - 36.d	2.708	0.064	0.0819	0.0026	0.2407	0.0057	0.27984	0.28385	1328	17	507.4	15	D	61.79216867

Samantha Nicole March  
Ultrahigh-pressure metapelites in the WGR

3-C3_ap - 37.d	2.947	0.064	0.0853	0.0027	0.2529	0.0055	0.11231	0.41625	1399	17	527.4	16	D	62.30164403
3-C3_ap - 38.d	2.944	0.072	0.0845	0.0027	0.2507	0.0061	0.12191	0.33132	1391	18	523	16	D	62.40115025
3-C3_ap - 39.d	2.767	0.062	0.0845	0.0027	0.2387	0.0054	0.11481	0.37505	1345	17	522.7	16	D	61.13754647
3-C3_ap - 40.d	2.829	0.059	0.08453	0.0026	0.2412	0.0054	0.21436	0.28861	1366	15	523.1	16	D	61.7057101
3-C3_ap - 41.d	2.78	0.063	0.08302	0.0026	0.2435	0.0063	0.095394	0.37286	1348	17	514.1	15	D	61.8620178
3-C3_ap - 42.d	3.018	0.063	0.0866	0.0027	0.2498	0.0056	0.16701	0.38602	1415	17	535.1	16	D	62.18374558
3-C3_ap - 43.d	2.808	0.064	0.0823	0.0026	0.2442	0.0052	0.30498	0.32504	1361	18	511	15	D	62.45407788
3-C3_ap - 44.d	2.896	0.076	0.08577	0.0027	0.2457	0.0061	0.11944	0.061899	1378	20	530.4	16	D	61.50943396
3-C3_ap - 45.d	2.705	0.057	0.0842	0.0027	0.2318	0.0056	0.098031	0.41993	1328	16	521.1	16	D	60.76054217
3-C3_ap - 46.d	2.631	0.063	0.0815	0.0026	0.2291	0.0054	0.33199	0.24593	1307	18	504.9	16	D	61.36954858
3-C3_ap - 47.d	2.673	0.055	0.0828	0.0027	0.2347	0.0055	0.23655	0.34492	1322	16	512.7	16	D	61.21785174
3-C3_ap - 48.d	2.629	0.057	0.0826	0.0026	0.2299	0.0056	-0.041374	0.49765	1310	15	511.3	16	D	60.96946565
3-C3_ap - 49.d	2.519	0.061	0.0825	0.0026	0.2214	0.0052	0.35144	0.17183	1275	18	511.2	15	D	59.90588235
3-C3_ap - 50.d	2.765	0.054	0.084	0.0026	0.2404	0.0055	0.087541	0.47318	1349	15	519.7	16	D	61.47516679
25B-3a-C1_ap - 1.d	5.06	0.25	0.1018	0.0043	0.353	0.021	-0.016869	0.53177	1831	42	625	25	D	65.86564719
25B-3a-C1_ap - 2.d	4.8	0.18	0.1007	0.0041	0.347	0.015	0.22288	0.45053	1787	31	618	24	D	65.41689983
25B-3a-C1_ap - 3.d	6.38	0.29	0.1167	0.0053	0.393	0.024	0.039323	0.60101	2022	40	711	30	D	64.83679525
25B-3a-C1_ap - 4.d	7.7	0.48	0.1306	0.0064	0.424	0.031	0.070934	0.55699	2184	58	791	36	D	63.78205128
25B-3a-C1_ap - 5.d	5	0.37	0.1002	0.006	0.348	0.029	-0.017613	0.5273	1809	64	615	35	D	66.00331675
25B-3a-C1_ap - 6.d	4.08	0.2	0.0971	0.0046	0.304	0.016	0.39733	0.43301	1663	38	597	27	D	64.10102225
25B-3a-C1_ap - 7.d	6.32	0.31	0.1097	0.005	0.426	0.017	0.43876	0.20017	2014	44	670	29	D	66.73286991
25B-3a-C1_ap - 8.d	4.2	0.25	0.0962	0.0047	0.312	0.017	0.4168	0.16827	1675	45	595	27	D	64.47761194
25B-3a-C1_ap - 9.d	4.48	0.19	0.0988	0.0038	0.331	0.015	0.31141	0.33901	1721	34	607	22	D	64.72980825
25B-3a-C1_ap - 10.d	4.68	0.26	0.0974	0.0042	0.335	0.016	0.65956	0.38097	1764	44	599	24	D	66.0430839
25B-3a-C1_ap - 11.d	5.02	0.2	0.1043	0.0046	0.35	0.018	0.19575	0.56001	1816	35	639	27	D	64.81277533
25B-3a-C1_ap - 12.d	4.95	0.24	0.1012	0.0047	0.362	0.022	0.15152	0.53701	1811	43	621	28	D	65.70955273
25B-3a-C1_ap - 14.d	4.11	0.19	0.0939	0.0049	0.328	0.02	0.11442	0.52485	1650	39	582	30	D	64.72727273
25B-3a-C2_ap1 - 1.d	1.85	0.12	0.076	0.003	0.172	0.011	0.19248	0.29477	1064	39	474	17	D	55.45112782
25B-3a-C2_ap1 - 2.d	2.06	0.13	0.0786	0.0036	0.191	0.013	0.23815	0.3041	1148	40	487	21	D	57.57839721
25B-3a-C2_ap1 - 3.d	1.94	0.12	0.075	0.003	0.191	0.012	0.14731	0.2768	1085	43	466	18	D	57.05069124
25B-3a-C2_ap1 - 4.d	2.12	0.14	0.0757	0.0032	0.207	0.014	-0.065741	0.53299	1157	45	470	19	D	59.37770095

Samantha Nicole March  
Ultrahigh-pressure metapelites in the WGR

25B-3a-C2_ap1 - 5.d	2.22	0.13	0.0795	0.0036	0.209	0.014	0.1965	0.35639	1192	41	493	22	D	58.6409396
25B-3a-C2_ap1 - 6.d	2.05	0.16	0.0771	0.0034	0.189	0.015	0.19481	0.26047	1133	52	479	21	D	57.72285966
25B-3a-C2_ap1 - 7.d	2.31	0.12	0.0794	0.0032	0.214	0.013	0.020207	0.51362	1223	35	492	19	D	59.77105478
25B-3a-C2_ap1 - 8.d	1.89	0.13	0.0757	0.0031	0.183	0.012	0.34917	0.01151	1075	44	470	18	D	56.27906977
25B-3a-C2_ap2 - 1.d	1.87	0.14	0.0745	0.0031	0.185	0.014	0.62925	0.065359	1059	49	463	19	D	56.27950897
25B-3a-C2_ap2 - 2.d	1.852	0.077	0.0755	0.0034	0.1782	0.0076	0.075295	0.57761	1060	27	469	21	D	55.75471698
25B-3a-C2_ap2 - 3.d	2.09	0.11	0.0779	0.0031	0.195	0.012	0.21963	0.27581	1138	37	483	19	D	57.55711775
25B-3a-C2_ap2 - 4.d	1.95	0.12	0.0765	0.0029	0.188	0.012	0.15174	0.26489	1112	36	475	17	D	57.28417266
25B-3a-C2_ap2 - 5.d	1.66	0.1	0.0754	0.0041	0.165	0.013	0.1888	0.53609	990	40	469	25	D	52.62626263
25B-3a-C2_ap2 - 6.d	2.05	0.12	0.0757	0.003	0.198	0.01	0.51466	-0.12702	1129	40	470	18	D	58.37023915
25B-3a-C3_ap1 - 1.d	6.11	0.86	0.116	0.011	0.365	0.037	0.63329	0.070373	1960	120	707	64	D	63.92857143
25B-3a-C3_ap1 - 3.d	5.26	0.56	0.1056	0.0076	0.356	0.029	0.33314	0.30706	1863	82	647	44	D	65.27106817
25B-3a-C3_ap1 - 4.d	7.2	1.3	0.141	0.033	0.38	0.098	0.1517	0.57159	2130	160	850	180	D	60.09389671
25B-3a-C3_ap1 - 6.d	3.51	0.2	0.0862	0.0058	0.293	0.019	0.58975	0.4488	1524	45	532	34	D	65.09186352
25B-3a-C3_ap1 - 7.d	3.9	0.34	0.0943	0.0062	0.29	0.026	0.32993	0.30789	1612	69	580	37	D	64.01985112
25B-3a-C3_ap2 - 1.d	3.13	0.2	0.092	0.0043	0.256	0.018	0.065019	0.49414	1436	47	567	25	D	60.51532033
25B-3a-C3_ap2 - 2.d	3.98	0.27	0.0905	0.0048	0.321	0.022	0.30981	0.3078	1626	54	558	28	D	65.68265683
25B-3a-C3_ap2 - 3.d	3.3	0.24	0.0875	0.0042	0.271	0.018	0.27207	0.26283	1466	58	540	25	D	63.16507503
25B-3a-C3_ap2 - 4.d	4.24	0.33	0.0948	0.0051	0.31	0.023	0.26735	0.46806	1679	63	584	30	D	65.2173913
25B-3a-C3_ap2 - 5.d	2.69	0.3	0.085	0.0045	0.236	0.025	0.24002	0.17327	1336	87	525	27	D	60.70359281
25B-3a-C3_ap2 - 6.d	2.91	0.26	0.0873	0.0047	0.239	0.02	0.52651	-0.062922	1364	64	539	28	D	60.48387097
25B-3a-C4_ap - 1.d	2.75	0.23	0.0885	0.0049	0.223	0.018	0.56475	0.1125	1334	63	547	29	D	58.99550225
25B-3a-C4_ap - 2.d	1.76	0.13	0.0748	0.0038	0.171	0.0078	0.84612	-0.091431	1014	40	465	23	D	54.14201183
25B-3a-C4_ap - 3.d	2.39	0.14	0.0815	0.0041	0.218	0.012	0.63308	0.1755	1234	40	505	24	D	59.07617504
25B-3a-C4_ap - 4.d	2.123	0.091	0.0766	0.003	0.1996	0.0094	0.46587	0.23229	1153	29	476	18	D	58.71639202
25B-3a-C4_ap - 5.d	1.866	0.099	0.0751	0.0029	0.178	0.011	0.3706	0.031452	1065	35	467	17	D	56.15023474
25B-3a-C4_ap - 6.d	2.33	0.12	0.079	0.004	0.215	0.013	0.49149	0.29083	1217	35	490	24	D	59.73705834
25B-3a-C4_ap - 7.d	1.88	0.11	0.0767	0.0039	0.177	0.013	0.25138	0.54712	1070	40	476	23	D	55.51401869
25B-3a-C4_ap - 8.d	2.1	0.12	0.0752	0.0027	0.201	0.013	0.3935	0.073608	1145	39	467.1	16	D	59.20524017
25B-3a-C4_ap - 9.d	2.16	0.12	0.0769	0.0032	0.205	0.011	0.3943	0.17861	1164	39	478	19	D	58.9347079
25B-3a-C4_ap - 10.d	2.034	0.098	0.079	0.0029	0.186	0.011	0.12088	0.31344	1124	33	490	17	D	56.40569395



Samantha Nicole March  
Ultrahigh-pressure metapelites in the WGR

25B-3a-C4_ap - 11.d	2.128	0.099	0.0773	0.0036	0.2015	0.0078	0.65508	0.11217	1162	29	480	21	D	58.6919105
25B-3a-C4_ap - 12.d	2.29	0.18	0.0798	0.0038	0.204	0.01	0.87878	-0.53145	1199	55	495	22	D	58.71559633
25B-3a-C4_ap - 13.d	2.16	0.12	0.0808	0.0035	0.1954	0.0094	0.22711	0.24045	1176	34	501	21	D	57.39795918
25B-3a-C4_ap - 14.d	2.76	0.14	0.0864	0.0036	0.228	0.012	0.40577	0.24405	1341	39	534	21	D	60.17897092
25B-3a-C4_ap - 15.d	2.137	0.093	0.0778	0.003	0.1977	0.0086	0.55005	0.093324	1158	30	483	18	D	58.29015544
25B-3a-C4_ap - 17.d	7.8	1.3	0.138	0.014	0.39	0.041	0.94158	-0.8203	2190	160	832	81	D	62.00913242
25B-3a-C4_ap - 19.d	3.51	0.37	0.1002	0.0076	0.251	0.016	0.84408	-0.36549	1514	77	615	44	D	59.37912814
25B-3a-C4_ap - 20.d	2.55	0.16	0.0801	0.0032	0.2233	0.0099	0.83957	-0.17869	1282	45	497	19	D	61.2324493
25B-3a-C4_ap - 21.d	2.37	0.11	0.0788	0.0037	0.217	0.012	0.43398	0.12567	1230	35	489	22	D	60.24390244
25B-3a-C4_ap - 22.d	2.6	0.1	0.0809	0.0034	0.2324	0.0092	0.50535	0.27766	1298	28	502	20	D	61.32511556
25B-3a-C4_ap - 23.d	2.33	0.15	0.0784	0.0032	0.21	0.012	0.24348	0.2148	1215	45	486	19	D	60
25B-3a-C4_ap - 25.d	2.35	0.1	0.0784	0.0032	0.2155	0.0099	0.7258	-0.19319	1225	31	486	19	D	60.32653061
25B-3a-C4_ap - 26.d	2.38	0.16	0.0799	0.003	0.209	0.015	-0.1331	0.44349	1230	49	495	18	D	59.75609756
25B-3a-C4_ap - 27.d	2.18	0.14	0.0768	0.0032	0.207	0.012	0.19247	0.19751	1170	46	477	19	D	59.23076923
25B-3a-C4_ap - 28.d	2.29	0.12	0.0768	0.0034	0.221	0.015	0.45344	-0.064402	1224	47	477	20	D	61.02941176
25B-3a-C4_ap - 29.d	2.99	0.23	0.0833	0.004	0.255	0.021	0.21681	0.26645	1397	59	521	21	D	62.70579814
25B-3a-C4_ap - 30.d	3.5	0.34	0.097	0.0083	0.279	0.026	0.76922	-0.26985	1580	110	596	48	D	62.27848101
25B-3a-C4_ap - 31.d	2.61	0.12	0.0794	0.0036	0.232	0.011	0.27924	0.55492	1302	32	492	22	D	62.21198157
25B-3a-C4_ap - 32.d	2.23	0.15	0.0798	0.0036	0.2	0.015	0.18417	0.33928	1185	47	495	21	D	58.2278481
25B-3a-C4_ap - 33.d	3.31	0.35	0.0963	0.0081	0.251	0.014	0.88416	-0.39061	1482	85	592	48	D	60.05398111
25B-3a-C4_ap - 34.d	2.48	0.17	0.0789	0.0034	0.22	0.011	0.7838	0.11911	1260	48	489	21	D	61.19047619
25B-3a-C4_ap - 35.d	5.09	0.51	0.1109	0.008	0.318	0.025	0.41505	0.24653	1843	76	677	46	D	63.26641346
25B-3b-C7_ap - 1.d	2.51	0.15	0.0796	0.0035	0.228	0.013	0.52155	0.020152	1279	42	494	21	D	61.37607506
25B-3b-C7_ap - 2.d	3.14	0.15	0.0865	0.0035	0.257	0.015	-0.13798	0.56197	1439	37	535	21	D	62.82140375
25B-3b-C7_ap - 3.d	2.94	0.15	0.084	0.0035	0.25	0.013	0.40165	0.49896	1405	39	520	21	D	62.98932384
25B-3b-C7_ap - 4.d	3.1	0.12	0.0857	0.0039	0.2662	0.0085	0.63511	0.30441	1430	32	530	23	D	62.93706294
25B-3b-C7_ap - 5.d	3.02	0.14	0.0835	0.0032	0.259	0.016	0.47466	0.31405	1409	36	517	19	D	63.30731015
25B-3b-C7_ap - 6.d	3.1	0.17	0.0867	0.0038	0.256	0.011	0.6163	-0.054138	1426	41	536	23	D	62.41234222
25B-3b-C7_ap - 7.d	3.29	0.17	0.0862	0.0037	0.278	0.012	0.67993	-0.13604	1485	35	533	22	D	64.10774411
25B-3b-C7_ap - 9.d	3.67	0.21	0.0902	0.0032	0.291	0.013	0.43762	0.020105	1558	44	557	19	D	64.24903723
25B-3b-C7_ap - 10.d	4.78	0.26	0.1011	0.0055	0.335	0.015	0.71932	0.097766	1774	45	621	32	D	64.99436302

Samantha Nicole March  
Ultrahigh-pressure metapelites in the WGR

25B-3b-C7_ap - 11.d	3.18	0.16	0.0852	0.0035	0.267	0.013	0.26946	0.33959	1456	42	527	21	D	63.80494505
25B-3b-C7_ap - 12.d	2.68	0.14	0.0821	0.0055	0.25	0.016	0.80961	0.080754	1319	39	508	32	D	61.48597422
25B-3b-C7_ap - 13.d	2.925	0.098	0.0816	0.0029	0.26	0.011	0.31886	0.27934	1394	23	506	17	D	63.70157819
25B-3b-C7_ap - 14.d	2.87	0.16	0.0848	0.0042	0.25	0.016	0.60035	-0.0048308	1369	42	524	25	D	61.72388605
25B-3b-C7_ap - 15.d	3.16	0.14	0.0846	0.003	0.267	0.013	-0.088606	0.52763	1450	32	523.4	18	D	63.90344828
25B-3b-C7_ap - 16.d	3.6	0.19	0.0885	0.0037	0.29	0.018	0.064628	0.59316	1543	42	546	22	D	64.61438756
25B-3b-C7_ap - 17.d	3.63	0.18	0.0893	0.0036	0.291	0.014	0.44185	0.25461	1550	40	551	21	D	64.4516129
25B-3b-C7_ap - 18.d	3.67	0.16	0.0914	0.004	0.284	0.012	0.31105	0.56176	1561	33	564	24	D	63.86931454
25B-3b-C7_ap - 19.d	3.52	0.24	0.0876	0.0035	0.283	0.016	0.55695	-0.052126	1523	53	541	21	D	64.47800394
25B-3b-C7_ap - 20.d	3.35	0.18	0.0857	0.004	0.279	0.012	0.70737	-0.010541	1487	43	530	24	D	64.35776732
25B-3b-C7_ap - 21.d	3.42	0.19	0.0845	0.0033	0.294	0.012	0.6567	-0.037241	1504	43	523	20	D	65.22606383
25B-3b-C7_ap - 22.d	3.13	0.14	0.086	0.0043	0.268	0.012	0.50084	0.37943	1435	35	532	25	D	62.92682927
25B-3b-C7_ap - 23.d	3.24	0.17	0.085	0.0039	0.274	0.016	0.1089	0.50964	1469	43	526	23	D	64.1933288
25B-3b-C7_ap - 24.d	2.74	0.14	0.0815	0.0041	0.243	0.01	0.82549	-0.32149	1335	37	505	24	D	62.17228464
25B-3b-C7_ap - 25.d	3.15	0.13	0.0849	0.0033	0.273	0.013	0.6469	0.046486	1442	31	525	19	D	63.59223301
25B-3b-C7_ap - 26.d	5.8	1.5	0.113	0.014	0.38	0.052	0.91548	-0.38816	1940	260	688	82	D	64.53608247
25B-3b-C7_ap - 27.d	3.57	0.18	0.0894	0.0035	0.293	0.017	0.10507	0.52016	1546	42	552	21	D	64.29495472
25B-3b-C7_ap - 28.d	3.66	0.25	0.0899	0.0042	0.289	0.017	0.66372	0.058888	1563	54	555	24	D	64.49136276
25B-3b-C7_ap - 29.d	3.51	0.19	0.0891	0.0038	0.28	0.015	0.28377	0.33082	1525	42	550	23	D	63.93442623
25B-3b-C7_ap - 30.d	3.5	0.14	0.0893	0.0037	0.284	0.013	0.29685	0.54504	1524	32	551	22	D	63.84514436
25B-3b-C7_ap - 32.d	3.58	0.19	0.0893	0.004	0.293	0.019	0.23393	0.42194	1540	42	551	24	D	64.22077922
25B-3b-C7_ap - 33.d	2.81	0.13	0.082	0.0039	0.245	0.01	0.52182	0.30271	1353	35	508	23	D	62.45380636
25B-3b-C7_ap - 34.d	3.49	0.28	0.0891	0.0047	0.275	0.016	0.71489	-0.051976	1513	58	550	28	D	63.6483807
25B-3b-C7_ap - 35.d	2.93	0.22	0.0811	0.0039	0.261	0.016	0.38457	0.13123	1397	53	503	23	D	63.99427344
25B-3b-C7_ap - 36.d	3.03	0.16	0.0841	0.0041	0.256	0.013	0.32824	0.39614	1411	41	520	24	D	63.14670446
25B-3b-C7_ap - 37.d	3.14	0.22	0.0844	0.005	0.261	0.013	0.66786	-0.019901	1435	54	522	30	D	63.62369338
25B-3b-C7_ap - 38.d	2.59	0.15	0.0799	0.0031	0.236	0.01	0.70162	-0.15347	1292	42	496	19	D	61.60990712
25B-3b-C7_ap - 39.d	2.58	0.15	0.0793	0.0033	0.234	0.012	0.43518	0.073859	1288	43	492	20	D	61.80124224
25B-3b-C7_ap - 40.d	2.71	0.15	0.0812	0.0033	0.246	0.014	0.48667	0.24638	1325	42	503	20	D	62.03773585
25B-3b-C7_ap - 41.d	3.58	0.23	0.0909	0.0052	0.284	0.015	0.27506	0.49073	1537	51	560	31	D	63.56538712
25B-3b-C7_ap - 42.d	3.45	0.16	0.0876	0.004	0.276	0.011	0.186	0.53688	1511	36	541	24	D	64.19589676

Samantha Nicole March  
Ultrahigh-pressure metapelites in the WGR

<b>25B-3b-C7_ap - 43.d</b>	3.29	0.14	0.0848	0.0033	0.284	0.014		0.14367	0.46879	1483	31	525	20	D	64.59878624
<b>25B-3b-C7_ap - 44.d</b>	2.5	0.17	0.0747	0.0041	0.241	0.012		0.75665	0.1013	1266	50	464	25	D	63.34913112
<b>25B-3b-C7_ap - 45.d</b>	2.35	0.16	0.0765	0.003	0.22	0.012		0.75719	0.18184	1220	46	475	18	D	61.06557377

C = concordant, NC = near concordant, D = discordant, RD = reversely discordant.

### Apatite geochronology standards

Standard	Type	207/235	2 $\sigma$	206/238	2 $\sigma$	207/206	2 $\sigma$	ErrorCorr 6/38vs7/35	ErrorCorr 38/6vs7/6	207/235 age	2 $\sigma$	206/238 age	2 $\sigma$	Concordant?	%discordance
<b>MAD - 1.d</b>	Primary	0.626	0.077	0.0775	0.0029	0.0582	0.0074	-0.01052	0.22355	497	55	481	18	C	3.219315895
<b>MAD - 2.d</b>	Primary	0.593	0.074	0.0762	0.0029	0.0564	0.0076	-0.24213	0.42168	468	46	473	18	C	-1.068376068
<b>MAD - 3.d</b>	Primary	0.594	0.071	0.0735	0.0026	0.0575	0.0073	-0.27514	0.42196	465	43	457	16	C	1.720430108
<b>MAD - 4.d</b>	Primary	0.571	0.074	0.0769	0.0027	0.0542	0.007	-0.12588	0.29687	455	49	477.3	16	C	-4.901098901
<b>MAD - 5.d</b>	Primary	0.593	0.092	0.0753	0.0028	0.0574	0.0091	0.063975	0.090343	445	63	468	17	C	-5.168539326
<b>MAD - 6.d</b>	Primary	0.636	0.09	0.0762	0.0028	0.0606	0.0086	-0.12548	0.28167	485	58	473	17	C	2.474226804
<b>MAD - 7.d</b>	Primary	0.613	0.069	0.0772	0.0028	0.0587	0.007	-0.37541	0.51492	471	44	479	17	C	-1.6985138
<b>MAD - 8.d</b>	Primary	0.604	0.08	0.0782	0.0028	0.0563	0.0073	-0.05846	0.16457	468	52	485	17	C	-3.632478632
<b>MAD - 9.d</b>	Primary	0.59	0.068	0.0749	0.0027	0.0552	0.0067	-0.14375	0.32744	457	44	465.6	16	C	-1.881838074
<b>MAD - 10.d</b>	Primary	0.629	0.087	0.0771	0.0028	0.0624	0.009	-0.21733	0.3735	490	57	478.9	17	C	2.265306122
<b>MAD - 11.d</b>	Primary	0.605	0.077	0.0761	0.0026	0.0591	0.0075	-0.01288	0.11439	468	51	472.6	16	C	-0.982905983
<b>MAD - 12.d</b>	Primary	0.601	0.077	0.0759	0.0031	0.0551	0.0078	-0.092	0.31609	475	47	471	18	C	0.842105263
<b>MAD - 13.d</b>	Primary	0.591	0.071	0.0762	0.0028	0.0564	0.0072	-0.06159	0.24256	492	47	473	17	C	3.861788618
<b>MAD - 14.d</b>	Primary	0.59	0.08	0.0766	0.0027	0.0569	0.0084	-0.11588	0.30371	460	50	475.8	16	C	-3.434782609
<b>MAD - 15.d</b>	Primary	0.607	0.075	0.0774	0.0028	0.0564	0.0069	0.1725	0.030963	480	46	481	17	C	-0.208333333
<b>MAD - 16.d</b>	Primary	0.582	0.06	0.0761	0.003	0.0572	0.006	0.056991	0.19498	466	39	473	18	C	-1.502145923
<b>MAD - 17.d</b>	Primary	0.613	0.08	0.0759	0.0027	0.0578	0.0076	0.038839	0.092386	473	52	472	16	C	0.21141649
<b>MAD - 18.d</b>	Primary	0.626	0.07	0.0781	0.0027	0.0569	0.0064	-0.28145	0.40895	486	45	484.7	16	C	0.267489712
<b>MAD - 19.d</b>	Primary	0.6	0.066	0.0776	0.0028	0.0568	0.007	-0.33083	0.49673	476	45	482	17	C	-1.260504202
<b>MAD - 20.d</b>	Primary	0.572	0.076	0.0743	0.0025	0.0563	0.0074	-0.19358	0.32635	440	51	462.2	15	C	-5.045454545
<b>MAD - 21.d</b>	Primary	0.592	0.087	0.0762	0.0027	0.0557	0.0081	-0.06873	0.22057	479	53	473.3	16	C	1.189979123
<b>MAD - 22.d</b>	Primary	0.628	0.079	0.0754	0.0027	0.0601	0.0076	0.098359	0.041346	476	50	468.8	16	C	1.512605042
<b>McClure - 1.d</b>	Secondary	3.8	0.24	0.1139	0.0055	0.246	0.017	0.21638	0.30143	1587	54	695	32	D	56.20667927

Samantha Nicole March  
Ultrahigh-pressure metapelites in the WGR

<b>McClure - 2.d</b>	Secondary	4.52	0.24	0.1209	0.0058	0.269	0.019	0.15194	0.45411	1728	46	735	33	D	57.46527778
<b>McClure - 3.d</b>	Secondary	4.17	0.32	0.1163	0.0057	0.264	0.023	-0.01307	0.23595	1637	64	708	33	D	56.75015272
<b>McClure - 4.d</b>	Secondary	2.55	0.13	0.105	0.0039	0.1732	0.009	0.086255	0.36257	1281	36	644	23	D	49.72677596
<b>McClure - 5.d</b>	Secondary	4.06	0.24	0.1151	0.0046	0.261	0.014	0.41402	0.13939	1643	48	702	27	D	57.27328058
<b>McClure - 6.d</b>	Secondary	2.99	0.13	0.1082	0.0039	0.2032	0.0096	0.19505	0.3179	1397	34	662	23	D	52.61274159
<b>McClure - 7.d</b>	Secondary	4.41	0.22	0.1178	0.005	0.269	0.015	0.09433	0.42995	1708	40	717	29	D	58.02107728
<b>McClure - 8.d</b>	Secondary	2.08	0.11	0.0985	0.0039	0.1562	0.0093	0.009003	0.45478	1148	38	605	23	D	47.29965157
<b>McClure - 9.d</b>	Secondary	2.56	0.17	0.1072	0.0043	0.178	0.013	0.017532	0.39488	1299	48	656	25	D	49.49961509
<b>McClure - 10.d</b>	Secondary	3.84	0.2	0.1139	0.0044	0.251	0.014	0.29899	0.30491	1606	43	695	25	D	56.72478207
<b>McClure - 11.d</b>	Secondary	3.98	0.2	0.1147	0.0049	0.251	0.011	0.29023	0.44262	1628	39	699	28	D	57.06388206
<b>McClure - 12.d</b>	Secondary	2.49	0.15	0.0996	0.004	0.183	0.011	0.14589	0.35718	1274	44	612	23	D	51.96232339
<b>McClure - 13.d</b>	Secondary	5.01	0.29	0.1194	0.0046	0.298	0.018	0.14303	0.36853	1810	49	727	27	D	59.83425414
<b>McClure - 14.d</b>	Secondary	2.45	0.17	0.102	0.0041	0.171	0.01	0.28663	0.16244	1247	47	626	24	D	49.79951885
<b>McClure - 15.d</b>	Secondary	3.48	0.18	0.1118	0.0042	0.225	0.012	0.20465	0.15624	1518	40	683	24	D	55.00658762
<b>McClure - 16.d</b>	Secondary	3.53	0.18	0.1101	0.0043	0.231	0.013	0.14896	0.37215	1526	42	673	25	D	55.89777195
<b>McClure - 17.d</b>	Secondary	3.27	0.16	0.1068	0.0043	0.223	0.012	0.13569	0.34891	1468	39	654	25	D	55.44959128
<b>McClure - 18.d</b>	Secondary	3.53	0.18	0.1091	0.0043	0.236	0.013	0.129	0.37062	1550	41	667	25	D	56.96774194
<b>McClure - 19.d</b>	Secondary	2.61	0.12	0.1008	0.0038	0.1884	0.0098	0.1205	0.37319	1309	37	619	22	D	52.71199389
<b>McClure - 20.d</b>	Secondary	2.74	0.2	0.1003	0.0042	0.196	0.012	0.35505	0.15834	1339	52	616	24	D	53.99551904
<b>McClure - 21.d</b>	Secondary	3.01	0.2	0.1038	0.0045	0.205	0.011	0.49938	0.058352	1392	49	636	26	D	54.31034483
<b>McClure - 22.d</b>	Secondary	5.03	0.27	0.1214	0.0047	0.303	0.015	0.48843	-0.00541	1815	47	738	27	D	59.33884298
<b>401 - 1.d</b>	Secondary	0.793	0.08	0.0871	0.0036	0.0658	0.0066	0.13892	0.1339	584	46	538	21	C	7.876712329
<b>401 - 2.d</b>	Secondary	0.71	0.082	0.0885	0.0035	0.0615	0.0062	0.16537	0.099332	565	46	546	21	C	3.362831858
<b>401 - 3.d</b>	Secondary	0.84	0.091	0.088	0.0035	0.065	0.0075	-0.09617	0.39674	606	51	544	21	C	10.2310231
<b>401 - 4.d</b>	Secondary	0.765	0.069	0.0896	0.004	0.0635	0.0056	0.15172	0.15303	586	39	553	23	C	5.631399317
<b>401 - 5.d</b>	Secondary	0.781	0.082	0.0894	0.0039	0.0636	0.0065	0.25505	-0.03473	582	49	552	23	C	5.154639175
<b>401 - 6.d</b>	Secondary	0.725	0.078	0.0887	0.0038	0.0583	0.0064	0.16411	0.15019	546	43	547	23	C	-0.183150183
<b>401 - 7.d</b>	Secondary	0.713	0.095	0.0884	0.004	0.0593	0.0082	-0.09956	0.3467	530	57	546	23	C	-3.018867925
<b>401 - 8.d</b>	Secondary	0.71	0.08	0.0906	0.0035	0.0572	0.0064	0.091367	0.11839	548	48	559	21	C	-2.00729927
<b>401 - 9.d</b>	Secondary	0.635	0.076	0.0874	0.0035	0.055	0.0068	0.04687	0.16224	518	48	540	21	C	-4.247104247
<b>401 - 10.d</b>	Secondary	0.788	0.079	0.0848	0.0034	0.0674	0.007	-0.06085	0.32186	601	43	524	20	D	12.81198003

Samantha Nicole March  
Ultrahigh-pressure metapelites in the WGR

401 - 11.d	Secondary	0.79	0.083	0.0882	0.0036	0.0659	0.0069		0.076044		0.16665	582	48	545	21	C	6.357388316
401 - 12.d	Secondary	0.831	0.073	0.0853	0.0032	0.0683	0.0064		0.058899		0.20377	609	39	527	19	D	13.46469622
401 - 13.d	Secondary	0.802	0.084	0.0837	0.0033	0.0684	0.0079		0.018059		0.20794	597	47	518	20	D	13.23283082
401 - 14.d	Secondary	0.735	0.078	0.0835	0.003	0.063	0.0067		0.15472		0.07166	543	47	517	18	C	4.788213628
401 - 15.d	Secondary	0.752	0.074	0.0855	0.0037	0.0614	0.0062		0.098307		0.29629	561	42	531	22	C	5.347593583
401 - 16.d	Secondary	0.79	0.12	0.0861	0.004	0.0652	0.0094		0.23484		-0.01088	567	70	532	24	C	6.172839506
401 - 17.d	Secondary	0.738	0.075	0.0835	0.0036	0.0625	0.0068		0.04037		0.26552	547	44	517	21	C	5.484460695
401 - 18.d	Secondary	0.779	0.072	0.0845	0.0035	0.0657	0.0071		-0.07232		0.32157	572	42	523	21	C	8.566433566
401 - 19.d	Secondary	0.832	0.088	0.0867	0.0041	0.0707	0.0074		0.30087		0.065756	610	50	538	24	D	11.80327869
401 - 20.d	Secondary	0.846	0.085	0.0909	0.0039	0.07	0.0069		0.22314		0.051197	621	47	560	23	D	9.822866345
401 - 21.d	Secondary	0.715	0.074	0.0849	0.0037	0.0623	0.0073		-0.05213		0.41459	551	44	525	22	C	4.718693285
401 - 22.d	Secondary	0.759	0.092	0.0857	0.0035	0.0646	0.008		0.129		0.26067	584	50	530	21	C	9.246575342

C = concordant, NC = near concordant, D = discordant, RD = reversely discordant.

## Apatite trace elements

Sample	Chondrite normalised REEs + Y																Total HREEs	Eu anomaly
	La	Ce	Pr	Nd	Sm	Eu	Gd	Tb	Dy	Y	Ho	Er	Tm	Yb	Lu			
3-C2_ap - 1.d	462.447	892.822	1292.02	1687.08	2399.32	727.531	2221.60	1654.29	1310.56	136	946.520	731.2	494.331	360.248	265.447	7130.66	0.31511	
	2574	186	5862	9716	4324	0835	804	3629	9106	8	1465	5	9838	4472	1545	0467	8104	
3-C2_ap - 2.d	475.949	922.675	1322.19	1722.53	2450.67	728.419	2223.11	1669.80	1295.52	135	945.970	723.1	492.712	350.931	272.357	7101.43	0.31207	
	3671	367	8276	8293	5676	1829	5578	6094	8455	1	696	25	5506	677	7236	2197	3889	
3-C2_ap - 3.d	489.873	953.833	1377.15	1787.30	2487.83	749.023	2268.84	1679.77	1328.86	137	958.424	735.6	498.785	365.838	273.983	7213.29	0.31526	
	4177	6052	5172	8534	7838	0906	4221	8393	1789	2	9084	25	4251	5093	7398	7765	9409	
3-C2_ap - 4.d	508.860	978.140	1391.16	1827.35	2505.40	745.115	2261.30	1668.69	1296.34	135	939.560	726.2	493.927	357.763	265.447	7102.98	0.31304	
	7595	2936	3793	2298	5405	4529	6533	8061	1463	5	4396	5	1255	9752	1545	8219	3612	
3-C2_ap - 5.d	529.113	1014.19	1418.10	1844.42	2560.81	765.541	2247.23	1680.05	1328.45	135	957.326	735.6	509.716	357.763	269.105	7193.04	0.31912	
	9241	2496	3448	0131	0811	7407	6181	5402	5285	5	0073	25	5992	9752	6911	7959	1283	
3-C2_ap - 6.d	518.143	997.553	1422.41	1840.26	2549.32	760.568	2260.80	1700	1327.23	137	953.113	740	501.214	365.217	264.227	7222.00	0.31680	
	4599	0179	3793	2582	4324	3837	402		5772	1	5531		5749	3913	6423	8934	6632	
3-C2_ap - 7.d	515.611	995.106	1417.02	1829.32	2555.40	762.699	2242.21	1693.90	1331.70	137	948.717	735	499.190	364.596	275.609	7225.72	0.31862	
	8143	0359	5862	1663	5405	8224	1055	5817	7317	7	9487		2834	2733	7561	7396	9143	
3-C2_ap - 8.d	506.329	967.862	1379.31	1778.99	2489.18	757.548	2259.79	1687.81	1319.51	138	954.578	746.2	503.643	372.049	272.764	7237.61	0.31940	
	1139	969	0345	3435	9189	8455	8995	1634	2195	1	7546	5	7247	6894	2276	0226	873	
3-C2_ap - 9.d	464.556	907.504	1294.18	1711.15	2481.08	711.190	2216.08	1652.07	1300	135	941.575	728.1	497.165	363.354	273.577	7113.87	0.30330	
	962	0783	1034	9737	1081	0533	0402	7562		8	0916	25	9919	0373	2358	4919	002	
3-C2_ap - 10.d	405.485	828.058	1212.28	1619.25	2359.45	715.275	2210.05	1673.13	1314.22	137	964.285	749.3	513.765	362.111	264.227	7217.12	0.31323	
	2321	7276	4483	6018	9459	3108	0251	0194	7642	6	7143	75	1822	8012	6423	3176	1839	

Samantha Nicole March  
Ultrahigh-pressure metapelites in the WGR

3-C2_ap - 11.d	502.953	962.642	1365.30	1759.29	2455.40	715.808	2197.98	1653.73	1278.45	134	936.630	712.5	490.283	354.658	268.699	7039.96	0.30812
	5865	7406	1724	9781	5405	1705	995	9612	5285	5	0366		4008	3851	187	5906	1637
3-C2_ap - 12.d	508.860	975.530	1383.62	1806.12	2529.05	742.451	2261.80	1706.64	1338.61	138	961.355	735.6	493.117	365.217	271.544	7260.12	0.31042
	7595	1794	069	6915	4054	1545	9045	8199	7886	8	3114	25	4089	3913	7154	5913	7983
3-C2_ap - 13.d	515.189	995.432	1411.63	1835.88	2544.59	742.451	2277.38	1709.14	1342.68	138	970.512	741.8	491.093	371.428	266.666	7275.40	0.30841
	8734	3002	7931	6214	4595	1545	6935	1274	2927	2	8205	75	1174	5714	6667	0377	8325
3-C2_ap - 14.d	459.071	889.885	1280.17	1678.33	2364.18	701.776	2183.41	1642.65	1285.77	134	943.406	725.6	492.712	357.142	273.170	7063.48	0.30887
	73	8075	2414	698	9189	1989	7085	928	2358	3	5934	25	5506	8571	7317	937	9559
3-C2_ap - 15.d	400.421	777.324	1117.45	1484.90	2130.40	657.015	2030.15	1571.74	1259.34	133	918.864	713.7	489.878	367.080	276.016	6933.68	0.31592
	9409	633	6897	1532	5405	9858	0754	5152	9593	7	4689	5	5425	7453	2602	4763	2578
3-C2_ap - 16.d	410.970	800.489	1149.78	1514.22	2181.08	658.792	2054.27	1574.79	1240.65	131	923.626	713.7	478.542	355.279	265.853	6871.49	0.31123
	4641	3964	4483	3195	1081	1847	1357	2244	0407	9	3736	5	5101	5031	6585	4696	1559
3-C2_ap - 17.d	446.835	859.216	1223.06	1611.59	2295.27	680.106	2102.51	1596.95	1262.19	132	907.692	708.1	479.757	354.658	268.699	6904.07	0.30959
	443	9657	0345	7374	027	5719	2563	2909	5122	6	3077	25	085	3851	187	9995	2732
3-C2_ap - 18.d	476.793	912.234	1295.25	1696.06	2350	708.348	2162.31	1637.67	1267.47	133	934.432	713.7	488.663	357.142	268.292	7005.43	0.31423
	2489	9103	8621	1269	135	1558	313	9675	8	2344	5	9676	8571	6829	4547	4373	
3-C2_ap - 19.d	452.742	893.800	1281.25	1680.52	2337.16	688.454	2150.75	1591.41	1247.96	132	925.641	709.3	463.967	342.857	255.691	6856.91	0.30706
	616	9788	5164	2162	7069	3769	2742	748	0	0256	75	6113	1429	0569	2059	8738	
3-C2_ap - 20.d	448.945	877.487	1248.92	1640.04	2356.08	687.566	2136.68	1603.04	1274.39	133	926.923	723.7	479.352	359.006	270.731	6976.20	0.30644
	1477	7651	2414	3764	1081	6075	3417	7091	0244	9	0769	5	2267	2112	7073	0557	2905
3-C3_ap - 1.d	532.489	1067.21	1553.87	1995.62	2577.02	738.721	1844.72	1111.08	768.699	798	532.967	414.3	316.194	265.217	205.284	4412.51	0.33880
	4515	044	931	3632	7027	1368	3618	0332	187	.7	033	75	332	3913	5528	7829	9348
3-C3_ap - 2.d	442.194	914.681	1368.53	1789.93	2464.86	722.024	1797.48	1124.93	775.203	816	549.267	425	334.817	266.459	211.788	4503.76	0.34302
	0928	8923	4483	4354	4865	8668	7437	0748	252	.3	3993		8138	6273	6179	7458	2546
3-C3_ap - 3.d	365.400	768.515	1159.48	1568.92	2276.35	695.737	1716.58	1096.39	757.317	812	534.432	426.2	327.935	265.838	209.349	4429.62	0.35195
	8439	4976	2759	779	1351	1226	2915	8892	0732	.1	2344	5	2227	5093	5935	1525	986
3-C3_ap - 4.d	448.523	941.598	1413.79	1838.07	2518.91	754.529	1861.30	1137.39	806.910	841	561.721	446.2	341.700	273.913	217.073	4625.96	0.34846
	2068	6949	3103	4398	8919	3073	6533	6122	5691		6117	5	4049	0435	1707	4922	5726
3-C3_ap - 5.d	517.721	1044.20	1540.94	1986.87	2599.32	738.543	1893.46	1138.78	794.715	822	543.406	426.8	320.242	263.975	204.065	4514.36	0.33290
	519	8809	8276	0897	4324	5169	7337	1163	4472	.3	5934	75	915	1553	0407	1315	2415
3-C3_ap - 6.d	562.869	1130.34	1617.45	2098.46	2653.37	765.186	1902.01	1141.27	800.813	832	550.549	444.3	321.052	265.838	209.349	4565.25	0.34061
	1983	2577	6897	8271	8378	5009	005	4238	0081		4505	75	6316	5093	5935	2431	3066
3-C3_ap - 7.d	606.329	1212.07	1731.68	2196.93	2713.51	763.232	1920.10	1152.90	793.902	812	547.069	424.3	320.242	263.478	201.626	4516.50	0.33437
	1139	1778	1034	6543	3514	6821	0503	8587	439	.9	5971	75	915	2609	0163	2815	1292
3-C3_ap - 8.d	304.219	686.460	1084.05	1481.18	2192.56	668.916	1700.50	1073.96	773.983	818	534.798	430.6	324.696	270.807	215.040	4441.91	0.34642
	4093	0326	1724	1619	7568	5187	2513	1219	7398		5348	25	3563	4534	6504	2954	3056
3-C3_ap - 9.d	542.194	1093.96	1588.36	2077.02	2676.35	782.238	1922.11	1171.46	804.471	845	559.890	448.1	329.959	267.701	215.040	4641.75	0.34488
	0928	4111	2069	407	1351	0107	0553	8144	5447	.1	1099	25	5142	8634	6504	6827	8069
3-C3_ap - 10.d	558.649	1141.27	1655.17	2131.29	2743.24	780.994	1948.24	1192.24	828.861	860	563.003	451.2	342.510	278.881	221.951	4739.00	0.33782
	789	2431	2414	1028	3243	6714	1206	3767	7886	.3	663	5	1215	9876	2195	2547	715
3-C3_ap - 11.d	579.324	1155.95	1663.79	2126.91	2705.40	777.264	1902.51	1160.94	799.186	836	554.212	441.8	327.935	271.242	212.601	4604.19	0.34260
	8945	4323	3103	4661	5405	6536	2563	1828	9919	.2	4542	75	2227	236	626	5359	1275
3-C3_ap - 12.d	618.143	1223.98	1778.01	2266.95	2807.43	803.197	1982.91	1196.95	825.609	844	565.384	442.5	341.295	272.049	208.943	4697.23	0.34042
	4599	0424	7241	8425	2432	1581	4573	2909	7561	.5	6154		5466	6894	0894	5606	0343
3-C3_ap - 13.d	627.848	1236.05	1785.56	2266.95	2812.16	790.586	1991.95	1194.45	824.796	853	562.271	448.7	334.008	280.745	214.634	4713.06	0.33403
	1013	2202	0345	8425	2162	1456	9799	9834	748	.4	0623	5	0972	3416	1463	5229	2508
3-C3_ap - 14.d	642.616	1256.93	1786.63	2275.71	2783.10	787.744	1978.39	1190.58	819.105	854	568.131	444.3	330.364	274.534	216.260	4697.35	0.33570
	0338	3116	7931	116	8108	2274	196	1717	6911		8681	75	3725	1615	1626	2973	9802
3-C3_ap - 15.d	595.358	1198.69	1726.29	2223.19	2775	794.671	1960.80	1190.85	832.113	851	558.974	447.5	332.388	271.428	217.073	4701.33	0.34067
	6498	4943	3103	4748		4032	402	8726	8211		359		664	5714	1707	7312	4006

Samantha Nicole March  
Ultrahigh-pressure metapelites in the WGR

3-C3_ap-16.d	629.113	1254.15	1782.32	2266.95	2822.97	768.206	1966.33	1175.06	833.333	845	568.681	447.5	340.080	273.291	213.414	4696.37	0.32605
	9241	9869	7586	8425	2973	0391	1658	9252	3333		3187		9717	9255	6341	1435	8834
3-C3_ap-17.d	644.303	1280.26	1828.66	2304.15	2860.13	782.415	1992.46	1203.60	828.861	866	587.179	451.2	331.174	272.049	218.699	4759.41	0.32775
	7975	1011	3793	7549	5135	6306	2312	1108	7886	.6	4872	5	0891	6894	187	5349	4893
3-C3_ap-18.d	614.767	1222.83	1773.70	2234.13	2753.37	772.113	1952.76	1176.17	812.195	853	563.003	443.7	323.076	267.080	212.195	4650.47	0.33298
	9325	8499	6897	5667	8378	6767	3819	7285	122		663	5	9231	7453	122	8861	4054
3-C3_ap-19.d	567.510	1153.01	1676.72	2146.60	2739.18	762.344	1936.18	1157.06	815.040	851	556.776	453.1	335.627	273.913	217.073	4659.91	0.33102
	5485	7945	4138	8315	9189	5826	0905	3712	6504	.3	5568	25	5304	0435	1707	9664	9988
3-C3_ap-20.d	599.156	1218.27	1768.31	2264.77	2836.48	801.953	2012.06	1209.41	852.845	892	583.882	468.7	350.202	281.987	219.512	4858.59	0.33569
	1181	0799	8966	0241	6486	8188	0302	8283	5285		7839	5	4291	5776	1951	8797	0077
3-C3_ap-21.d	624.050	1236.21	1776.93	2242.88	2786.48	774.422	1990.95	1183.37	828.048	859	565.018	449.3	331.578	273.291	216.666	4706.55	0.32879
	6329	5334	9655	8403	6486	7353	4774	9501	7805	.2	315	75	9474	9255	6667	9136	0247
3-C3_ap-22.d	579.746	1170.14	1715.51	2199.12	2743.24	760.035	1971.85	1183.65	832.113	865	570.879	450.6	324.696	272.670	211.382	4711.32	0.32678
	8354	6819	7241	4726	3243	524	9296	651	8211	.3	1209	25	3563	8075	1138	3729	6248
3-C3_ap-23.d	637.974	1265.41	1811.42	2293.21	2778.37	777.975	1995.47	1227.42	843.902	881	582.051	456.8	339.676	277.018	215.853	4823.80	0.33040
	6835	5987	2414	663	8378	1332	7387	3823	439		2821	75	1134	6335	6585	0949	5003
3-C3_ap-24.d	695.780	1350.89	1904.09	2404.81	2900.67	791.651	1999.49	1218.28	839.430	863	582.783	453.7	344.534	273.291	209.756	4785.62	0.32871
	5907	7227	4828	4004	5676	865	7487	2548	8943	.8	8828	5	413	9255	0976	9762	8557
3-C3_ap-25.d	701.687	1384.99	1963.36	2463.89	2984.45	810.657	2084.42	1248.19	865.853	892	590.109	470	349.797	282.608	223.983	4922.55	0.32502
	7637	1843	2069	4967	9459	1936	2111	9446	6585		8901		5709	6957	7398	3001	1106
3-C3_ap-26.d	676.371	1327.73	1894.39	2374.17	2900	801.420	2049.24	1219.39	843.495	890	586.630	468.1	355.465	281.925	215.447	4860.47	0.32874
	308	2463	6552	9431		9591	6231	0582	935		0366	25	587	4658	1545	9761	9139
3-C3_ap-27.d	489.451	1011.09	1503.23	1978.11	2547.29	683.481	1812.06	1136.84	793.089	841	556.959	441.2	332.388	267.701	215.447	4585.17	0.31812
	4768	2985	2759	8162	7297	3499	0302	2105	4309	.5	707	5	664	8634	1545	8925	6999
3-C3_ap-28.d	581.012	1154.32	1697.19	2179.43	2766.89	762.344	1943.21	1195.01	836.178	869	579.120	455	337.246	275.155	219.105	4765.82	0.32877
	6582	3002	8276	1072	1892	5826	608	385	8618		8791		9636	2795	6911	1525	1888
3-C3_ap-29.d	523.628	1083.84	1623.92	2076.58	2688.51	734.991	1928.14	1178.39	806.097	859	574.542	446.8	340.080	280.124	216.666	4701.77	0.32281
	692	9918	2414	6433	3514	119	0704	3352	561		1245	75	9717	2236	6667	9899	7164
3-C3_ap-30.d	657.805	1308.31	1869.61	2369.80	2850	781.349	2019.09	1244.87	863.821	897	600.549	468.7	344.939	282.608	225.203	4927.74	0.32572
	9072	9739	2069	3063		9112	5477	5346	1382		4505	5	2713	6957	252	7154	0212
3-C3_ap-31.d	667.510	1306.03	1871.76	2376.36	2858.78	791.296	2022.61	1217.45	848.780	881	587.179	470.6	342.105	280.745	214.634	4842.92	0.32907
	5485	5889	7241	7615	3784	6252	3065	1524	4878	.4	4872	25	2632	3416	1463	125	3003
3-C3_ap-32.d	702.109	1355.62	1911.63	2404.81	2870.94	781.527	2022.11	1235.45	863.821	881	592.490	468.7	346.153	272.049	215.853	4875.57	0.32436
	7046	8059	7931	4004	5946	5311	0553	7064	1382		8425	5	8462	6894	6585	6239	1519
3-C3_ap-33.d	616.033	1246.32	1783.40	2275.71	2736.48	745.293	1975.87	1213.29	832.113	873	585.714	464.3	333.603	278.881	211.788	4792.77	0.32051
	7553	9527	5172	116	6486	0728	9397	6399	8211		2857	75	2389	9876	6179	335	6369
3-C3_ap-34.d	682.278	1338.82	1911.63	2411.37	2905.40	778.863	2044.72	1226.59	852.439	903	603.113	473.7	346.153	277.018	220.731	4902.79	0.31955
	481	5449	7931	8556	5405	2327	3618	2798	0244		5531	5	8462	6335	7073	9562	1254
3-C3_ap-35.d	701.687	1353.99	1898.70	2407.00	2873.64	790.053	2069.84	1244.87	876.829	906	602.197	478.7	354.251	282.608	224.390	4969.90	0.32394
	7637	6737	6897	2188	8649	286	9246	5346	2683		8022	5	0121	6957	2439	2368	4188
3-C3_ap-36.d	711.814	1375.20	1932.11	2413.56	2918.91	765.008	2050.25	1229.63	848.780	898	592.673	470	355.465	284.472	226.016	4905.04	0.31271
	346	3915	2069	674	8919	881	1256	9889	4878		9927		587	0497	2602	8267	7307
3-C3_ap-37.d	691.139	1320.88	1869.61	2328.22	2806.08	728.241	1946.73	1175.90	826.829	852	573.992	453.1	341.700	273.291	220.325	4717.16	0.31158
	2405	0914	2069	7571	1081	5631	3668	0277	2683		674	25	4049	9255	2033	4753	1802
3-C3_ap-38.d	716.455	1375.53	1945.04	2444.20	2910.81	764.120	2041.70	1236.84	873.170	903	601.648	472.5	353.846	275.776	217.073	4933.85	0.31344
	6962	0179	3103	1313	0811	7815	8543	2105	7317		3516		1538	3975	1707	6911	2692
3-C3_ap-39.d	763.713	1415.98	1960.12	2452.95	2885.81	779.573	2031.15	1222.99	868.699	893	605.128	476.8	353.036	283.229	215.447	4919.10	0.32199
	0802	6949	931	4048	0811	7123	5779	169	187	.7	2051	75	4372	8137	1545	7487	6864
3-C3_ap-40.d	741.772	1409.46	1947.19	2459.51	2886.48	763.232	2046.73	1222.16	865.040	901	604.945	473.7	354.251	278.260	221.544	4921.85	0.31400
	1519	1664	8276	86	6486	6821	3668	0665	6504	.9	0549	5	0121	8696	7154	2967	8589

Samantha Nicole March  
Ultrahigh-pressure metapelites in the WGR

3-C3_ap - 41.d	747.257	1419.24	1985.99	2461.70	2909.45	772.113	2072.86	1240.44	891.869	925	619.597	491.8	357.085	288.819	228.455	5043.14	0.31440
3-C3_ap - 42.d	747.679	1420.88	1994.61	2470.45	2921.62	777.087	2086.93	1270.63	886.991	927	624.908	488.1	365.587	283.229	221.138	5067.61	0.31470
3-C3_ap - 43.d	756.962	1438.82	1980.60	2485.77	2971.62	772.646	2031.65	1249.30	888.617	926	621.245	477.5	357.085	285.093	222.764	5027.61	0.31445
3-C3_ap - 44.d	779.324	1432.30	2006.46	2468.27	2921.62	766.429	2059.79	1260.94	882.113	907	618.681	476.2	352.226	275.155	226.422	4998.79	0.31242
3-C3_ap - 45.d	751.898	1414.02	1970.90	2477.02	2909.45	763.765	2073.36	1241.27	886.585	927	613.369	493.7	359.514	284.472	221.138	5027.10	0.31096
3-C3_ap - 46.d	770.042	1449.75	2006.46	2538.29	2968.91	770.692	2093.46	1283.37	900.813	937	632.783	488.1	365.991	292.546	227.235	5128.47	0.30913
3-C3_ap - 47.d	752.320	1403.09	1969.82	2466.08	2895.94	746.536	2033.16	1232.68	865.040	908	607.142	486.2	361.943	284.472	223.983	4970.11	0.30765
3-C3_ap - 48.d	747.257	1404.73	1964.43	2470.45	2900.67	755.772	2067.33	1256.78	876.422	925	618.864	487.5	357.085	286.335	218.292	5026.58	0.30862
3-C3_ap - 49.d	743.881	1420.71	1966.59	2472.64	2938.51	731.971	2069.34	1263.43	876.016	914	614.285	475.6	347.368	278.944	224.796	4994.47	0.29683
3-C3_ap - 50.d	764.556	1438.82	2031.25	2516.41	2969.59	791.829	2110.55	1281.44	900	935	632.234	508.7	368.421	295.155	231.300	5152.30	0.31628
25B-3a-C1_ap - 1.d	370.886	919.249	1422.41	1827.13	1977.70	1083.48	1058.79	438.781	184.959	108	76.3736	37.25	18.6234	11.1180	7.92682	883.232	0.74874
25B-3a-C1_ap - 2.d	359.493	911.908	1425.64	1861.48	2104.05	1097.69	1095.97	452.908	186.585	113	82.9670	40.18	20	10.7453	5.81300	912.906	0.72285
25B-3a-C1_ap - 3.d	341.350	857.911	1340.51	1748.35	1927.02	1044.40	1058.79	425.484	175.203	104	73.0769	35.81	16.1943	8.44720	6.01626	844.935	0.73117
25B-3a-C1_ap - 4.d	399.156	907.014	1411.63	1781.18	1997.29	1078.15	1065.82	442.382	191.869	112	78.9377	35.62	18.0971	10.3726	6.58536	896.270	0.73895
25B-3a-C1_ap - 5.d	392.405	990.212	1536.63	1925.60	2124.32	1133.21	1158.79	453.462	190.243	115	82.2344	37.56	20.4048	9.25465	8.78048	917.543	0.72226
25B-3a-C1_ap - 6.d	425.316	1053.01	1613.14	2080.96	2238.51	1227.35	1235.17	495.844	205.284	119	89.0109	41.68	18.4615	11.0559	6.62601	987.871	0.73811
25B-3a-C1_ap - 7.d	403.797	983.686	1489.22	1932.16	2058.10	1119.00	1116.58	448.199	189.430	111	76.9230	38.12	16.4372	10.5590	6.26016	897.034	0.73816
25B-3a-C1_ap - 8.d	373.839	902.120	1414.87	1824.94	2090.54	1161.63	1139.69	475.069	206.097	127	95.4212	47	26.9635	19.3788	17.8455	1015.17	0.75256
25B-3a-C1_ap - 9.d	415.611	1023.00	1563.57	2010.94	2180.40	1149.20	1186.93	476.177	189.430	114	85.5311	41.87	19.9595	10.4968	6.50406	944.474	0.71435
25B-3a-C1_ap - 10.d	395.358	978.792	1517.24	1943.10	2116.21	1158.08	1143.71	461.772	188.617	109	84.4322	40.25	19.5951	10.2484	5.73170	920.448	0.74438
25B-3a-C1_ap - 11.d	381.856	955.791	1503.23	1936.54	2127.02	1158.08	1166.83	471.745	197.154	116	85.1648	41.62	20.0809	11.4906	7.11382	950.874	0.73510
25B-3a-C1_ap - 12.d	381.856	963.784	1506.46	1973.74	2197.29	1236.23	1211.55	493.351	201.626	121	86.6300	43.5	17.4898	12.4223	7.39837	984.218	0.75767
25B-3a-C1_ap - 14.d	346.413	881.239	1397.62	1853.39	2041.89	1134.99	1136.68	451.523	190.650	113	83.8827	37.18	19.6356	10.6211	7.52032	914.021	0.74500
25B-3a-C2_ap1 - 1.d	328.691	715.986	1088.36	1486.21	1773.64	998.934	965.326	355.955	135.040	74.	54.0293	25.37	13.5222	9.37888	7.27642	674.878	0.76342
25B-3a-C2_ap1 - 2.d	376.793	752.039	1119.61	1507.65	1742.56	987.566	938.190	353.462	137.398	77.	59.5238	29.93	15.3036	10	7.23577	690.061	0.77237
	2489	1517	2069	8643	7568	6075	9548	6039	374	2	0952	75	4372	2358	7035	1006	



Samantha Nicole March  
Ultrahigh-pressure metapelites in the WGR

25B-3a-	364.135	749.102	1123.92	1531.94	1739.18	966.252	928.140	357.617	134.796	71.	50.1831	25.75	13.7246	8.81987	7.92682	670.619	0.76051
C2_ap1 - 3.d	0211	7732	2414	7484	9189	2202	7035	7285	748	8	5018		9636	5776	9268	0281	9198
25B-3a-	311.814	680.750	1064.65	1450.76	1672.29	941.385	922.110	340.997	130.487	71.	51.6483	26.56	14.3724	8.69565	6.82926	650.693	0.75808
C2_ap1 - 4.d	346	4078	5172	5864	7297	4352	5528	2299	8049	1	5165	25	6964	2174	8293	2765	7324
25B-3a-	272.194	611.745	956.896	1346.38	1604.05	888.099	887.939	325.761	123.252	70	50.5494	25	11.7813	8.81987	4.02439	619.188	0.74414
C2_ap1 - 5.d	0928	5139	5517	9497	4054	4671	6985	7729	0325		5055		7652	5776	0244	8985	9807
25B-3a-	300.843	661.174	1035.56	1418.16	1623.64	917.761	883.417	324.376	127.235	70.	48.7179	26.5	11.2145	8.94409	6.70731	624.096	0.76630
C2_ap1 - 6.d	8819	5514	0345	1926	8649	9893	0854	7313	7724	4	4872		749	9379	7073	4437	4087
25B-3a-	318.565	673.898	1042.02	1402.62	1636.48	904.085	861.306	324.376	124.430	67.	48.1684	24.43	12.0242	7.63975	4.30894	612.986	0.76150
C2_ap1 - 7.d	4008	8581	5862	5821	6486	2575	5327	7313	8943	6	9817	75	915	1553	3089	6099	7711
25B-3a-	368.354	742.740	1133.62	1527.35	1723.64	982.238	954.773	347.091	134.065	74.	54.5787	25.68	17.4089	9.44099	6.34146	668.714	0.76567
C2_ap1 - 8.d	4304	6199	069	2298	8649	0107	8693	4127	0407	1	5458	75	0688	3789	3415	0721	0831
25B-3a-	258.649	577.487	903.017	1229.75	1432.43	866.785	780.904	281.440	108.536	58.	41.0256	19.62	9.63562	4.59627	2.84552	526.205	0.81954
C2_ap2 - 1.d	789	7651	2414	93	2432	0799	5226	4432	5854	5	4103	5	753	3292	8455	0989	9869
25B-3a-	318.143	659.543	977.370	1284.02	1406.08	849.378	749.246	277.285	104.390	54.	41.3919	18.18	7.89473	4.16149	2.07317	510.334	0.82752
C2_ap2 - 2.d	4599	23	6897	6258	1081	3304	2312	3186	2439	95	4139	75	6842	0683	0732	4021	9931
25B-3a-	324.050	655.791	963.362	1247.26	1383.10	811.722	722.613	263.988	99.2682	52.	37.3626	15.37	7.12550	4.40993	3.53658	483.736	0.81194
C2_ap2 - 3.d	6329	1909	069	477	8108	913	0653	9197	9268	67	3736	5	6073	7888	5366	879	5421
25B-3a-	344.303	691.843	1007.54	1300.65	1425.67	829.484	738.190	266.759	101.829	56.	42.3076	18.06	8.50202	4.90683	2.60162	501.108	0.80856
C2_ap2 - 4.d	7975	3931	3103	6455	5676	9023	9548	0028	2683	14	9231	25	4291	2298	6016	946	2799
25B-3a-	321.518	684.991	998.922	1310.72	1485.81	893.428	788.442	289.196	110.975	58.	39.7435	19.37	9.19028	4.40993	1.91056	532.901	0.82545
C2_ap2 - 5.d	9873	8434	4138	2101	0811	0639	2111	6759	6098	1	8974	5	3401	7888	9106	6658	4044
25B-3a-	242.194	545.350	842.672	1169.58	1331.75	804.618	719.597	259.833	99.2276	53.	40.2930	17.75	8.34008	4.65838	2.84552	486.698	0.82192
C2_ap2 - 6.d	0928	7341	4138	4245	6757	1172	9899	795	4228	75	4029		0972	5093	8455	4721	5363
25B-3a-	123.628	281.566	485.991	759.299	1056.08	635.879	658.291	248.199	103.252	56.	40.8424	15.93	6.76113	2.67080	1.58536	475.748	0.76263
C3_ap1 - 1.d	692	0685	3793	7812	1081	2185	4573	446	0325	5	9084	75	3603	7453	5854	7763	5278
25B-3a-	118.438	280.587	475.215	754.923	1052.02	634.103	649.246	251.800	102.845	57.	41.2087	18.56	7.61133	3.41614	3.13008	485.674	0.76725
C3_ap1 - 3.d	8186	2757	5172	4136	7027	0195	2312	554	5285	1	9121	25	6032	9068	1301	9401	8404
25B-3a-	121.518	292.006	506.465	792.122	1182.43	676.731	663.316	271.468	107.723	60.	46.1538	17.43	6.47773	5.83850	4.02439	519.923	0.76413
C3_ap1 - 4.d	9873	5253	5172	5383	2432	794	5829	144	5772	8	4615	75	2794	9317	0244	6998	1295
25B-3a-	106.835	272.593	488.146	784.245	1175	679.928	727.135	291.412	116.260	63.	44.5054	21.06	6.51821	4.16149	2.07317	549.393	0.73559
C3_ap1 - 6.d	443	801	5517	0766	952	6784	7424	1626	4	9451	25	8623	0683	0732	7795	179	
25B-3a-	101.308	251.712	450.431	715.973	1039.18	609.946	673.869	250.692	98.3739	57.	40.8424	19.62	7.97570	3.60248	1.34146	480.353	0.72888
C3_ap1 - 7.d	0169	8874	0345	7418	9189	714	3467	5208	8374	9	9084	5	8502	4472	3415	6517	1177
25B-3a-	98.9029	250.570	478.448	798.687	1202.70	693.783	760.804	284.487	102.601	52.	36.0805	15.12	4.81781	2.54658	1.50406	499.503	0.72528
C3_ap2 - 1.d	5359	9625	2759	0897	2703	3037	0201	5346	626	34	8608	5	3765	3851	5041	2094	4341
25B-3a-	94.5569	237.683	447.413	746.170	1142.56	659.502	721.608	268.144	94.9593	48.	38.6446	16.62	4.29149	3.04347	2.47967	476.997	0.72631
C3_ap2 - 2.d	6203	5237	7931	6783	7568	6643	0402	0443	4959	81	8864	5	7976	8261	4797	7336	4855
25B-3a-	91.3080	238.825	450.431	758.205	1131.08	692.717	753.266	260.664	97.1951	49.	38.6446	15.75	5.58704	3.16770	1.09756	471.806	0.75047
C3_ap2 - 3.d	1688	4486	0345	6893	1081	5844	3317	8199	2195	7	8864		4534	1863	0976	9379	2987
25B-3a-	94.0928	232.952	424.784	705.251	1029.05	596.269	644.723	231.578	91.0569	43.	32.2344	12.25	5.22267	2.91925	2.72357	421.085	0.73204
C3_ap2 - 4.d	27	6917	4828	6411	4054	9822	6181	9474	1057	1	3223		2065	4658	7236	7941	3793
25B-3a-	244.725	384.991	629.310	956.236	1404.05	811.722	854.271	321.329	118.699	58.	43.5897	17.68	6.76113	3.72670	3.08943	573.683	0.74117
C3_ap2 - 5.d	7384	8434	3448	3239	4054	913	3568	6399	187	8	4359	75	3603	8075	0894	343	0233
25B-3a-	119.240	292.006	540.948	900.656	1327.70	786.856	836.180	319.944	117.479	60.	43.2234	17.31	5.70850	4.96894	1.95121	570.688	0.74678
C3_ap2 - 6.d	5063	5253	2759	4551	2703	1279	9045	5983	6748	1	4322	25	2024	4099	9512	882	3629
25B-3a-	385.654	944.535	1480.60	1934.35	2222.97	555.950	1316.58	603.878	329.268	260	180.402	126.8	79.7570	62.1118	51.2195	1693.91	0.32497
C4_ap - 1.d	0084	0734	3448	4486	2973	2664	2915	1163	2927	.4	9304	75	8502	0124	122	2738	1103
25B-3a-	418.565	995.106	1526.93	1997.81	2218.24	571.225	1271.35	618.836	319.105	251	174.358	119.0	87.0445	62.9813	48.7804	1681.47	0.34014
C4_ap - 2.d	4008	0359	9655	1816	3243	5773	6784	5651	6911	.3	9744	625	3441	6646	878	0119	911

Samantha Nicole March  
Ultrahigh-pressure metapelites in the WGR

25B-3a-	404.641	986.949	1493.53	1936.54	2137.83	603.907	1226.63	547.368	284.552	213	153.479	91.25	63.5627	54.6583	42.5203	1451.29	0.37292
C4_ap - 3.d	3502	429	4483	267	7838	6377	3166	4211	8455	.9	8535		5304	8509	252	2583	8686
25B-3a-	434.177	1022.83	1547.41	1995.62	2220.27	632.326	1234.17	576.177	293.495	224	153.663	95.06	64.3724	55.6521	41.9918	1504.81	0.38198
C4_ap - 4.d	2152	8499	3793	3632	027	8206	0854	2853	935	.4	0037	25	6964	7391	6992	5237	916
25B-3a-	429.957	1047.30	1602.37	2045.95	2289.86	656.305	1308.04	586.149	301.219	237	167.216	109.7	70.4453	65.0310	42.6829	1579.69	0.37921
C4_ap - 5.d	8059	832	069	186	4865	5062	0201	5845	5122	.2	1172	5	4413	559	2683	4541	9425
25B-3a-	332.067	850.897	1331.89	1746.17	2054.72	609.236	1209.54	554.847	281.300	211	150	93.75	62.7530	45.8385	37.9268	1437.71	0.38645
C4_ap - 6.d	5105	2268	6552	0678	973	2345	7739	6454	813	.3			3644	0932	2927	6833	3163
25B-3a-	438.818	1053.83	1616.37	2074.39	2285.13	644.760	1297.98	597.229	304.065	234	169.597	105.4	73.2793	62.1118	47.5609	1593.88	0.37437
C4_ap - 7.d	5654	3605	931	8249	5135	2131	995	9169	0407	.6	0696	375	5223	0124	7561	1656	4812
25B-3a-	422.362	1030.99	1572.19	2002.18	2310.81	648.312	1264.32	589.750	307.317	225	155.128	98.25	62.7530	49.6273	41.8699	1530.59	0.37929
C4_ap - 8.d	8692	5106	8276	8184	0811	611	1608	6925	0732	.9	2051		3644	2919	187	6255	1835
25B-3a-	437.552	1040.78	1603.44	2043.76	2253.37	653.641	1296.98	572.022	296.747	220	152.380	102.7	58.7044	47.3913	38.1707	1488.16	0.38234
C4_ap - 9.d	7426	3034	8276	3676	8378	2078	4925	1607	9675		9524	5	5344	0435	3171	757	4545
25B-3a-	437.552	1047.30	1592.67	2102.84	2346.62	648.667	1286.93	604.155	304.471	224	157.692	98.37	63.1578	52.1739	40.2439	1544.96	0.37326
C4_ap - 10.d	7426	832	2414	4639	1622	8508	4673	1247	5447	.7	3077	5	9474	1304	0244	9687	9572
25B-3a-	431.645	1026.10	1592.67	2041.57	2302.70	660.746	1316.08	593.905	309.349	228	163.736	99.56	60.7287	52.7950	43.0894	1551.76	0.37955
C4_ap - 11.d	5696	1142	2414	5492	2703	0036	0402	8172	5935	.6	2637	25	4494	3106	3089	7381	4722
25B-3a-	422.784	1009.78	1551.72	2010.94	2254.05	632.504	1275.37	603.878	294.715	224	152.197	105.2	74.4939	49.5652	42.2764	1547.17	0.37304
C4_ap - 12.d	8101	7928	4138	0919	4054	4405	6884	1163	4472	.8	8022	5	2713	1739	2276	6933	5791
25B-3a-	431.645	1034.25	1574.35	2063.45	2279.05	628.774	1309.54	600.831	305.691	228	160.439	100.8	64.7773	53.1055	39.8373	1554.05	0.36396
C4_ap - 13.d	5696	7749	3448	733	4054	4227	7739	0249	0569	.5	5604	75	2794	9006	9837	6959	2707
25B-3a-	424.472	1024.46	1591.59	2059.08	2344.59	584.369	1307.03	607.479	297.154	223	151.648	99.75	58.2995	47.1428	36.9918	1521.46	0.33381
C4_ap - 14.d	5738	9821	4828	0963	4595	4494	5176	2244	4715		3516		9514	5714	6992	637	818
25B-3a-	436.708	1047.30	1598.06	2074.39	2293.91	632.326	1312.06	618.005	290.243	223	158.791	101.1	62.1457	49.7515	42.2764	1545.73	0.36448
C4_ap - 15.d	8608	832	0345	8249	8919	8206	0302	5402	9024	.4	2088	25	4899	528	2276	9376	1654
25B-3a-	268.354	716.150	1118.53	1520.78	1851.35	509.769	1090.45	495.844	261.788	195	140.659	80.62	65.5870	44.7204	32.5203	1316.74	0.35877
C4_ap - 17.d	4304	0816	4483	7746	1351	0941	2261	8753	6179		3407	5	4453	9689	252	5701	7954
25B-3a-	445.991	1066.88	1659.48	2070.02	2222.97	666.074	1236.18	554.016	281.300	207	138.461	84.18	51.4170	46.2732	30.8943	1394.35	0.40180
C4_ap - 19.d	5612	4176	2759	1882	2973	6004	0905	6205	813	.8	5385	75	0405	9193	0894	1077	4472
25B-3a-	449.367	1078.30	1593.75	2070.02	2238.51	650.088	1222.61	557.063	269.918	201	134.981	88.43	55.0607	41.4285	34.6747	1382.96	0.39295
C4_ap - 20.d	0886	3426	1882	3514	8099	3065	7119	6992	.4	685	75	2874	7143	9675	5693	9972	
25B-3a-	512.236	1182.70	1735.99	2253.82	2433.10	719.360	1332.16	600.831	292.682	217	147.802	86.5	54.6558	39.7515	32.5203	1471.74	0.39956
C4_ap - 21.d	2869	7993	1379	9322	8108	5684	0804	0249	9268		1978		7045	528	252	3898	5148
25B-3a-	448.101	1053.83	1576.50	2002.18	2280.40	669.626	1229.14	565.650	268.292	204	148.168	86.62	51.8218	41.1801	35.3658	1401.50	0.39996
C4_ap - 22.d	2658	3605	8621	8184	5405	9982	5729	9695	6829	.4	4982	5	6235	2422	5366	4991	7991
25B-3a-	395.358	975.530	1539.87	1949.67	2218.91	641.207	1214.07	550.692	271.951	205	142.673	90.18	56.9230	46.7080	32.5203	1396.75	0.39066
C4_ap - 23.d	6498	1794	069	1772	8919	8153	0352	5208	2195	.1	9927	75	7692	7453	252	671	6493
25B-3a-	453.164	1054.64	1599.13	2048.14	2264.86	641.385	1248.24	562.880	284.552	210	151.098	90.75	62.3481	48.3850	35.3658	1445.48	0.38145
C4_ap - 25.d	557	9266	7931	0044	4865	4352	1206	8864	8455	.1	9011		7814	9317	5366	1758	9723
25B-3a-	468.354	1089.72	1643.31	2087.52	2237.16	660.746	1265.82	575.069	284.146	215	143.956	93.31	60.3238	45.2173	35.7723	1452.79	0.39264
C4_ap - 26.d	4304	2675	8966	7352	2162	0036	9146	2521	3415		044	25	8664	913	5772	7773	3368
25B-3a-	396.624	973.898	1539.87	2032.82	2295.27	626.998	1303.01	587.257	300.406	220	154.578	96.87	59.1093	56.0248	36.0162	1510.46	0.36255
C4_ap - 27.d	4726	8581	069	2757	027	2238	5075	6177	5041	.2	7546	5	1174	4472	6016	8293	5648
25B-3a-	388.607	969.004	1516.16	2052.51	2383.10	623.445	1321.60	593.905	295.528	222	153.296	94.37	64.3724	50.1242	38.2113	1512.71	0.35129
C4_ap - 28.d	5949	894	3793	6411	8108	8259	804	8172	4553	.9	7033	5	6964	236	8211	4051	7867
25B-3a-	485.232	1107.66	1669.18	2153.17	2302.70	682.060	1301.00	589.473	299.593	226	150.366	91.31	57.8947	50.4347	34.9593	1500.33	0.39406
C4_ap - 29.d	0675	721	1034	2867	2703	3908	5025	6842	4959	.3	3004	25	3684	8261	4959	485	1864
25B-3a-	473.417	1081.56	1610.99	2050.32	2263.51	666.074	1211.55	534.626	268.699	205	133.150	82.5	45.7489	42.2981	32.3170	1344.63	0.40221
C4_ap - 30.d	7215	6069	1379	8228	3514	6004	7789	0388	187	.3	1832		8785	3665	7317	9607	5923

Samantha Nicole March  
Ultrahigh-pressure metapelites in the WGR

25B-3a-	451.476	1071.77	1590.51	2063.45	2245.94	667.850	1241.70	558.448	272.764	197	139.926	82.75	55.0607	36.9565	34.1463	1377.15	0.39991
C4_ap - 31.d	7932	814	7241	733	5946	7993	8543	7535	2276	.1	7399		2874	2174	4146	3313	7092
25B-3a-	374.683	946.166	1452.58	1910.28	2081.08	653.641	1208.04	544.598	257.723	202	132.783	85.75	51.8218	45.2173	36.1788	1356.57	0.41224
C4_ap - 32.d	5443	3948	6207	4464	1081	2078	0201	338	5772	.5	8828		6235	913	6179	3913	3892
25B-3a-	439.662	1019.57	1526.93	1929.97	2162.16	623.445	1198.99	528.808	258.536	198	124.542	80.81	47.7732	39.4409	26.0162	1304.33	0.38720
C4_ap - 33.d	4473	5856	9655	8118	2162	8259	4975	8643	5854	.4	1245		7935	9379	6016	0607	9415
25B-3a-	450.210	1057.09	1607.75	2054.70	2191.89	655.417	1214.57	558.171	273.170	199	137.362	83.81	52.6315	42.2360	36.1788	1382.96	0.40169
C4_ap - 34.d	9705	6248	8621	4595	1892	4067	2864	7452	7317	.4	6374		7895	2484	6179	408	5179
25B-3a-	441.772	1017.94	1496.76	1914.66	2027.02	658.969	1095.47	534.626	249.593	190	119.963	75	46.9635	45.9627	36.9918	1299.10	0.44221
C4_ap - 35.d	1519	4535	7241	0832	7027	8046	7387	0388	4959		37		6275	3292	6992	107	5577
25B-3b-	364.978	924.469	1438.57	1916.84	2237.83	804.618	1265.82	607.479	324.796	254	177.472	113.5	76.5182	63.7267	49.5934	1667.64	0.47806
C7_ap - 1.d	903	8206	7586	9015	7838	1172	9146	2244	748	.5	5275		625	1862	0807	9593	9422
25B-3b-	367.088	910.277	1438.57	1912.47	2177.02	820.603	1247.73	582.271	295.934	231	157.692	106.2	61.1336	48.9440	38.2113	1521.83	0.49789
C7_ap - 2.d	6076	3246	7586	2648	7027	9076	8693	4681	9593	.4	3077		5	0324	9938	8211	782
25B-3b-	360.759	910.440	1460.12	1929.97	2197.97	808.170	1272.86	596.121	313.008	231	160.256	100.3	61.5384	52.9813	43.4959	1559.47	0.48317
C7_ap - 3.d	4937	4568	931	8118	2973	5151	4322	8837	1301	.7	4103		75	6154	6646	3496	7187
25B-3b-	321.940	829.690	1324.35	1739.60	2114.18	815.275	1200.50	594.459	295.934	228	156.593	96.87	67.2064	50.4968	40.8130	1530.67	0.51174
C7_ap - 4.d	9283	0489	3448	6127	9189	3108	2513	8338	9593	.3	4066		5	7773	9441	0813	958
25B-3b-	272.151	719.412	1174.56	1634.57	2027.02	770.870	1165.82	570.914	296.341	227	158.424	99.37	67.2064	47.6397	43.7398	1511.44	0.50145
C7_ap - 5.d	8987	7243	8966	3304	7027	3375	9146	1274	4634	.8	9084		5	7773	5155	374	1566
25B-3b-	406.329	985.318	1522.62	1986.87	2261.48	854.351	1250.75	562.049	297.560	222	157.142	94.37	61.3765	50.0621	34.4308	1479.09	0.50798
C7_ap - 6.d	1139	1077	931	0897	6486	6874	3769	8615	9756	.1	8571		5	1822	118	9431	8219
25B-3b-	465.822	1078.30	1600.21	2085.33	2285.13	880.994	1275.37	578.116	286.585	214	148.717	89	59.5141	40.7453	34.9593	1452.13	0.51605
C7_ap - 7.d	7848	3426	5517	9168	5135	6714	6884	3435	3659	.5	9487		7004	4161	4959	8519	7468
25B-3b-	241.772	684.176	1162.71	1623.63	2043.24	838.365	1233.66	561.772	291.463	221	150.915	91.56	59.1093	47.5776	33.2113	1456.81	0.52804
C7_ap - 9.d	1519	1827	5517	2385	3243	897	8342	8532	4146	.2	7509		25	1174	3975	8211	2852
25B-3b-	191.983	560.848	953.663	1365.42	1845.27	744.227	1115.07	537.119	271.951	214	146.703	93	53.4412	43.4782	39.5934	1400.08	0.51882
C7_ap - 10.d	1224	2871	7931	6696	027	3535	5377	1136	2195	.8	2967		9555	6087	9593	6682	814
25B-3b-	371.729	924.959	1454.74	1940.91	2217.56	849.023	1232.66	568.698	284.146	216	150.549	91.56	58.7044	42.8571	35	1447.91	0.51352
C7_ap - 11.d	9578	217	1379	9037	7568	0906	3317	0609	3415	.4	4505		25	5344	4286	7949	1741
25B-3b-	217.130	658.238	1148.70	1621.44	1964.18	792.184	1149.74	543.213	279.674	213	141.575	92.56	58.0566	46.6459	36.7479	1411.97	0.52714
C7_ap - 12.d	8017	1729	6897	4201	9189	7247	8744	2964	7967	.5	0916		25	8016	6273	6748	6295
25B-3b-	399.578	982.055	1494.61	2002.18	2222.29	843.694	1216.08	573.407	287.398	217	146.153	94	53.0364	44.4099	35.2032	1451.40	0.51321
C7_ap - 13.d	0591	4649	2069	8184	7297	4938	0402	2022	374	.8	8462		3725	3789	5203	905	9313
25B-3b-	235.864	650.897	1120.68	1557.98	1959.45	761.989	1132.66	532.963	271.138	216	151.831	95.56	53.4412	46.3975	34.6341	1402.26	0.51148
C7_ap - 14.d	9789	2268	9655	6871	9459	3428	3317	9889	2114	.3	5018		25	9555	1553	4634	916
25B-3b-	398.312	951.060	1487.06	1943.10	2187.16	841.918	1210.05	547.922	291.869	213	142.124	93.56	54.1700	44.9068	32.7235	1420.87	0.51752
C7_ap - 15.d	2363	3589	8966	7221	2162	2948	0251	4377	9187	.6	5421		25	4049	323	7724	9849
25B-3b-	512.236	1148.45	1672.41	2113.78	2299.32	859.680	1270.35	564.819	280.894	219	147.435	88.37	62.7530	42.6086	33.2926	1439.27	0.50300
C7_ap - 16.d	2869	0245	3793	5558	4324	2842	1759	9446	3089	.1	8974		5	3644	9565	8293	9566
25B-3b-	528.691	1153.34	1687.5	2157.54	2307.43	877.442	1277.38	589.196	289.837	219	145.054	91.68	55.8704	40.4347	38.2113	1469.89	0.51108
C7_ap - 17.d	9831	4209	9234	2432	2735	6935	6759	3984	3984	.6	9451		75	4534	8261	8211	3129
25B-3b-	487.763	1101.14	1628.23	2067.83	2243.91	865.541	1228.14	560.110	283.739	209	141.758	85.93	49.7975	41.3664	33.7398	1406.15	0.52138
C7_ap - 18.d	7131	1925	2759	3698	8919	7407	0704	8033	8374	.7	2418		75	7085	5963	374	025
25B-3b-	486.919	1099.51	1619.61	2059.08	2212.16	863.232	1233.66	582.271	276.829	211	143.772	90	51.0121	40.6832	31.9105	1428.37	0.52254
C7_ap - 19.d	8312	0604	2069	0963	2162	6821	8342	4681	2683	.9	8938		4575	2981	6911	9575	0774
25B-3b-	399.156	949.429	1441.81	1927.78	2165.54	833.037	1216.58	555.678	273.577	212	150.549	85.5	56.2753	41.4906	31.3414	1407.11	0.51322
C7_ap - 20.d	1181	0375	0345	9934	0541	3002	2915	6704	2358	.7	4505		0364	8323	6341	2807	8106
25B-3b-	378.902	924.959	1454.74	1954.04	2204.72	857.904	1248.24	565.096	280.487	217	142.673	91.93	60.3238	46.6459	34.9186	1439.38	0.51714
C7_ap - 21.d	9536	217	1379	814	973	0853	1206	9529	8049	.3	9927		75	8664	6273	9919	4799

Samantha Nicole March  
Ultrahigh-pressure metapelites in the WGR

25B-3b-	246.413	687.112	1157.32	1630.19	2027.70	785.079	1185.92	575.623	296.341	224	152.564	94.12	59.1093	49.6894	38.2113	1490.26	0.50627
C7_ap - 22.d	5021	5612	7586	6937	2703	929	9648	2687	4634	.6	1026	5	1174	4099	8211	397	0091
25B-3b-	478.481	1120.71	1659.48	2164.11	2305.40	822.380	1257.28	586.426	297.967	225	156.043	99.87	65.5870	46.2732	34.8780	1512.45	0.48303
C7_ap - 23.d	0127	7781	2759	3786	5405	1066	6432	5928	4797	.4	956	5	4453	9193	4478	1414	859
25B-3b-	894.514	1696.57	2327.58	2781.18	2709.45	934.280	1427.13	648.753	323.170	247	170.329	111.3	71.6599	53.0434	38.1300	1664.19	0.47512
C7_ap - 24.d	7679	4225	6207	1619	9459	6394	5678	4626	7317	.8	6703	125	1903	7826	813	9843	0084
25B-3b-	377.637	944.535	1462.28	1899.34	2196.62	776.198	1217.58	555.678	293.089	222	148.717	96.18	64.7773	44.0993	36.1788	1461.12	0.47461
C7_ap - 25.d	1308	0734	4483	3545	1622	9343	794	6704	4309	.4	9487	75	2794	7888	6179	9119	9138
25B-3b-	309.282	781.402	1267.24	1708.97	1891.89	701.598	1075.37	512.465	266.666	213	128.937	93.75	46.9635	43.4782	23.5772	1328.83	0.49188
C7_ap - 26.d	7004	9364	1379	1554	1892	579	6884	374	6667		7289		6275	6087	3577	8829	1167
25B-3b-	372.151	923.654	1480.60	1910.28	2154.05	809.946	1239.19	575.623	288.211	225	144.505	97.62	61.1336	44.3478	32.1544	1468.60	0.49574
C7_ap - 27.d	8987	1599	3448	4464	4054	714	598	2687	3821		4945	5	0324	2609	7154	1046	4781
25B-3b-	414.767	996.737	1495.68	1993.43	2223.64	843.694	1206.53	558.448	284.552	223	146.336	89.93	59.9190	44.7204	36.3414	1443.25	0.51508
C7_ap - 28.d	9325	3573	9655	5449	8649	4938	2663	7535	8455		9963	75	2834	9689	6341	7084	9373
25B-3b-	509.704	1127.24	1650.86	2113.78	2279.05	856.127	1268.84	587.811	300	228	153.296	96.5	61.1336	47.2049	37.0325	1511.07	0.50345
C7_ap - 29.d	6414	3067	2069	5558	4054	8863	4221	6343		.1	7033		0324	6894	2033	943	0965
25B-3b-	477.637	1096.24	1616.37	2076.58	2254.05	827.708	1237.18	573.961	293.495	226	151.831	91.25	67.2064	45.2795	38.4959	1487.82	0.49565
C7_ap - 30.d	1308	7961	931	6433	4054	7034	593	2188	935	.3	5018		7773	0311	3496	0571	3152
25B-3b-	477.215	1075.04	1587.28	2052.51	2233.78	891.651	1250.75	572.576	288.617	219	150.366	92.56	59.1093	36.8322	40.9349	1460.09	0.53344
C7_ap - 32.d	1899	0783	4483	6411	3784	865	3769	1773	8862	.1	3004	25	1174	9814	5935	9433	4013
25B-3b-	481.434	1109.29	1658.40	2096.28	2314.86	776.198	1271.85	599.722	312.195	247	168.131	110.5	70.0404	47.6397	45.1219	1601.21	0.45236
C7_ap - 33.d	5992	8532	5172	0088	4865	9343	9296	9917	122	.8	8681	625	8583	5155	5122	467	6761
25B-3b-	422.784	1004.89	1504.31	1936.54	2155.40	754.884	1196.48	560.387	289.024	231	153.663	102.5	58.7044	47.5155	34.9593	1477.95	0.47007
C7_ap - 34.d	8101	3964	0345	267	5405	5471	2412	8116	3902	.2	0037		5344	2795	4959	4537	0386
25B-3b-	419.831	982.707	1490.30	1927.78	2170.27	751.332	1226.13	584.764	312.601	248	178.571	111.8	76.1133	54.3478	42.2764	1608.85	0.46058
C7_ap - 35.d	2236	9935	1724	9934	027	1492	0653	5429	626	.3	4286	75	6032	2609	2276	0207	1709
25B-3b-	378.059	934.747	1450.43	1910.28	2168.91	735.346	1274.87	597.506	334.146	269	184.065	120.6	72.4696	56.4596	46.3414	1681.21	0.44221
C7_ap - 36.d	0717	1452	1034	4464	8919	3588	4372	9252	3415	.6	9341	25	3563	2733	6341	4927	8179
25B-3b-	396.624	952.691	1473.06	1899.34	2139.18	706.927	1227.13	604.155	320.325	260	172.344	113.0	75.3036	61.3664	49.5934	1656.75	0.43631
C7_ap - 37.d	4726	6803	0345	3545	9189	1758	5678	1247	2033	.6	3223	625	4372	5963	9593	075	8661
25B-3b-	382.278	936.378	1410.56	1888.40	2131.75	693.605	1305.02	648.476	377.235	313	214.652	149	101.214	72.4223	58.5365	1935.33	0.41584
C7_ap - 38.d	481	4666	0345	2626	6757	6838	5126	4543	7724	.8	0147		5749	6025	8537	7762	7776
25B-3b-	354.430	876.508	1373.92	1827.13	2133.78	668.383	1300	665.373	387.804	324	224.175	155.1	101.619	82.9192	61.7886	2003.16	0.40130
C7_ap - 39.d	3797	9723	2414	3479	3784	659	9612	878	.3	8242	875	4332	5466	1789	9469	9039	
25B-3b-	423.206	972.267	1487.06	1925.60	2214.18	673.001	1342.71	704.986	398.373	340	239.194	155.6	105.668	85.7142	73.9837	2104.14	0.39031
C7_ap - 40.d	7511	5367	8966	1751	9189	7762	3568	1496	9837	.6	1392	25	0162	8571	3984	5314	6723
25B-3b-	264.978	694.616	1134.69	1540.48	1829.72	625.222	1140.70	544.875	301.219	252	171.978	115.7	72.0647	56.2732	48.7804	1563.54	0.43276
C7_ap - 41.d	903	6395	8276	14	973	0249	3518	3463	5122	.6	022	5	7733	9193	878	1437	7268
25B-3b-	297.046	752.854	1191.81	1617.06	1892.56	637.477	1185.42	604.432	330.487	269	182.234	126.3	74.4939	67.7018	49.1869	1704.04	0.42560
C7_ap - 42.d	4135	8124	0345	7834	7568	7975	7136	133	8049	.2	4322	125	2713	6335	9187	9652	0309
25B-3b-	308.438	750.570	1198.27	1628.00	1911.48	632.326	1141.20	575.900	319.105	263	184.065	122.1	85.0202	62.6708	48.3739	1660.72	0.42812
C7_ap - 43.d	8186	9625	5862	8753	6486	8206	603	277	6911	.4	9341	875	4291	0745	8374	4436	8321
25B-3b-	2531.64	2691.68	2780.17	2735.22	2385.13	726.465	1412.06	768.975	447.154	377	271.428	192.5	122.672	92.5465	82.1138	2355.19	0.39585
C7_ap - 44.d	557	0261	2414	9759	5135	3641	0302	0693	4715	.8	5714		0648	8385	2114	0582	1046
25B-3b-	313.080	766.721	1228.44	1680.52	2043.91	609.236	1288.44	687.257	404.065	349	243.406	173.7	113.360	91.9254	71.9512	2135.01	0.37542
C7_ap - 45.d	1688	044	8276	5164	8919	2345	2211	6177	0407	.3	5934	5	3239	6584	1951	6261	3471

**Apatite trace element standards**

Standard	La	Ce	Pr	Nd	Sm	Eu	Gd	Tb	Dy	Ho	Er	Tm	Yb	Lu
<b>NIST610 - 27.d</b>	2075	2146	2111	2036	2146	2100	2123	2066	2064	2125	2147	2053	2118	2070
<b>NIST610 - 28.d</b>	2079	2131	2121	2032	2137	2116	2125	2065	2068	2122	2163	2064	2141	2074
<b>NIST610 - 29.d</b>	2126	2196	2162	2080	2200	2159	2148	2112	2110	2170	2193	2097	2146	2116
<b>NIST610 - 30.d</b>	2105	2162	2137	2043	2140	2127	2153	2071	2075	2136	2160	2067	2136	2081
<b>NIST610 - 31.d</b>	2226	2295	2267	2170	2282	2276	2295	2236	2217	2294	2327	2228	2318	2252
<b>NIST610 - 32.d</b>	2196	2262	2231	2150	2241	2231	2247	2197	2187	2246	2284	2178	2248	2190
<b>NIST610 - 33.d</b>	2163	2220	2206	2119	2232	2190	2200	2146	2143	2209	2239	2138	2209	2153
<b>NIST610 - 34.d</b>	2133	2191	2159	2063	2186	2165	2176	2110	2112	2167	2183	2105	2171	2121
<b>NIST610 - 35.d</b>	2165	2227	2197	2107	2193	2184	2214	2130	2147	2200	2220	2128	2199	2148
<b>NIST610 - 36.d</b>	2103	2190	2138	2059	2173	2131	2147	2079	2077	2150	2182	2078	2145	2092
<b>NIST610 - 37.d</b>	2073	2131	2104	2024	2119	2098	2109	2060	2052	2109	2142	2043	2115	2062

## APPENDIX 3E: LA-ICP-MS RUTILE RESULTS

### Rutile morphology

Sample	Textural location	Size (long axis)	Crystal Habit	Spot location	Comments
WGC2019J-25B-C2_rut - 1.d	Garnet inclusion	~250µm	Elongate	core	
WGC2019J-25B-C2_rut - 2.d	Garnet edge	~250µm	Tabular	core	
WGC2019J-25B-C2_rut - 3.d	Garnet edge			rim	
WGC2019J-25B-C2_rut - 4.d	Garnet edge			rim	
WGC2019J-25B-C3_rut - 1.d	Garnet inclusion	~250µm	Elongate	core	
WGC2019J-25B-C3_rut - 2.d	Garnet inclusion	~150µm	Elongate	core	
WGC2019J-25B-C3_rut - 3.d	Garnet inclusion	~100µm	Tabular	core	
WGC2019J-25B-C3_rut - 4.d	Garnet inclusion	~250µm	Elongate	rim	Located in rounded end of grain
WGC2019J-25B-C3_rut - 5.d	Garnet inclusion			core	Located in elongate part of grain
WGC2019J-25B-C3_rut - 6.d	Garnet inclusion	~300µm	Tabular	rim	
WGC2019J-25B-C3_rut - 7.d	Garnet inclusion			rim	
WGC2019J-25B-C3_rut - 8.d	Garnet inclusion			core	
WGC2019J-25B-C8_rut - 1.d	Garnet inclusion	~400µm	Elongate	core	
WGC2019J-25B-C8_rut - 2.d	Garnet inclusion			rim	
WGC2019J-25B-C9_rut - 1.d	Garnet inclusion	~250µm	Elongate	rim	
WGC2019J-25B-C9_rut - 2.d	Garnet inclusion			core	
WGC2019J-25B-C10_rut - 1.d	Garnet inclusion - within fracture?	~250µm	Triangular	rim	
WGC2019J-25B-C10_rut - 2.d	Garnet inclusion - within fracture?			core	
WGC2019J-25B-C10_rut - 3.d	Garnet inclusion - within fracture?			rim	
WGC2019J-25B-C10_rut - 4.d	Garnet inclusion - within fracture?	~100µm	Tabular	core	broken off fragment
WGC2019J-25B-C10_rut - 5.d	Matrix	~100µm	Equant	core	
WGC2019J-25B-C11_rut - 1.d	Garnet inclusion	~300µm	Asymmetric	rim	Angular, asymmetric shape
WGC2019J-25B-C11_rut - 2.d	Garnet inclusion			rim	
WGC2019J-25B-C11_rut - 3.d	Garnet inclusion			core	

WGC2019J-25B-C11_rut - 4.d	Garnet inclusion			rim	
WGC2019J-25B-C11_rut - 5.d	Garnet inclusion	~200µm	Tabular	core	
WGC2019J-25B-C11_rut - 6.d	Garnet inclusion			core	
WGC2019J-25B-C11_rut - 7.d	Garnet inclusion	~100µm	Elongate	core	
WGC2019J-25B-C12_rut - 1.d	Garnet inclusion	~150µm	Tabular	core	
WGC2019J-25B-C12_rut - 2.d	Garnet inclusion	~400µm	Tabular	rim	
WGC2019J-25B-C12_rut - 3.d	Garnet inclusion			rim	
WGC2019J-25B-C12_rut - 5.d	Garnet inclusion			core	
WGC2019J-25B-C12_rut - 6.d	Garnet inclusion			core	
WGC2019J-25B-C12_rut - 7.d	Garnet inclusion	~300µm	Equant	rim	
WGC2019J-25B-C12_rut - 8.d	Garnet inclusion			core	
WGC2019J-25B-C12_rut - 9.d	Garnet inclusion			rim	
WGC2019J-25B-C13_rut - 1.d	Garnet inclusion	~250µm	Tabular	rim	
WGC2019J-25B-C13_rut - 2.d	Garnet inclusion			core	
WGC2019J-25B-C13_rut - 3.d	Garnet inclusion	~50µm	Equant	core	
WGC2019J-25B-C13_rut - 4.d	Garnet inclusion	~300µm	Tabular	rim	
WGC2019J-25B-C13_rut - 5.d	Garnet inclusion			core	
WGC2019J-25B-C13_rut - 6.d	Garnet inclusion			rim	
WGC2019J-25B-C13_rut - 7.d	Garnet inclusion	~200µm	Tabular	rim	
WGC2019J-25B-C13_rut - 8.d	Garnet inclusion	~100µm	Tabular	core	
WGC2019J-25B-C13_rut - 9.d	Garnet inclusion	~250µm	Tabular	rim	
WGC2019J-25B-C13_rut - 10.d	Garnet inclusion			rim	
WGC2019J-25B-C13_rut - 11.d	Garnet inclusion	~50µm	Equant	core	
WGC2019J-25B-C13_rut - 12.d	Garnet inclusion	~250µm	Tabular	core	part of grain 23
WGC2019J-25B-C14_rut - 1.d	Garnet inclusion	~250µm	Triangular	core	
WGC2019J-31A-2-C2_rut - 1.d	Matrix	~200µm	Tabular	core	
WGC2019J-31A-2-C3_rut - 1.d	Garnet inclusion	~300µm	Tabular	rim	
WGC2019J-31A-2-C3_rut - 2.d	Garnet inclusion			core	
WGC2019J-31A-2-C3_rut - 3.d	Garnet inclusion	~100µm	Tabular	core	Don't have a reflected light image for this grain
WGC2019J-31A-2-C3_rut - 4.d	Garnet inclusion	~50µm	Equant	core	
WGC2019J-31A-2-C4_rut - 1.d	Matrix	~200µm	Elongate	core	

WGC2019J-31A-2-C4_rut - 2.d	Matrix	~250µm	Tabular	rim	
WGC2019J-31A-2-C4_rut - 3.d	Matrix			rim	
WGC2019J-31A-2-C8_rut - 1.d	Edge of garnet	~400µm	Tabular	rim	
WGC2019J-31A-2-C8_rut - 2.d	Edge of garnet			rim	
WGC2019J-31A-2-C8_rut - 3.d	Edge of garnet			rim	
WGC2019J-31A-2-C8_rut - 4.d	Edge of garnet			rim	
WGC2019J-31A-2-C8_rut - 5.d	Edge of garnet			core	
WGC2019J-31A-2-C10_rut - 1.d	Matrix	~150µm	Tabular	core	Inclusion at edge of kyanite maybe?
WGC2019J-31A-3-C3_rut - 1.d	Matrix	~125µm	Tabular	core	
WGC2019J-31A-3-C4_rut - 1.d	Matrix	~175µm	Equant	rim	Equant grain with elongate tail
WGC2019J-31A-3-C5_rut - 1.d	Edge of garnet	~150µm	Triangular	rim	
WGC2019J-31A-3-C5_rut - 2.d	Edge of garnet			core	
WGC2019J-31A-3-C6_rut - 1.d	Edge of garnet	~200µm	Diamond	core	Diamond-shaped grain with circle eaten out
WGC2019J-31A-3-C12_rut - 1.d	Garnet inclusion	~75µm	Equant	core	
WGC2019J-31A-3-C19_rut - 1.d	Garnet inclusion	~150µm	Elongate	core	
WGC2019J-31A-3-C19_rut - 2.d	Garnet inclusion			core	
WGC2019J-31A-3-C20_rut - 1.d	Matrix	~650µm	Asymmetric	rim	Analyses all located within an equant section of the grain
WGC2019J-31A-3-C20_rut - 2.d	Matrix			core	
WGC2019J-31A-3-C20_rut - 3.d	Matrix			core	
WGC2019J-31A-3-C20_rut - 4.d	Matrix			core	
WGC2019J-31A-3-C20_rut - 5.d	Matrix			rim	
WGC2019J-31A-3-C20_rut - 6.d	Matrix			core	
WGC2019J-31A-3-C20_rut - 7.d	Matrix			rim	
WGC2019J-31A-3-C21_rut - 1.d	Matrix	~250µm	Elongate	core	
WGC2019J-31A-3-C21_rut - 2.d	Matrix	~200µm	Tabular	core	



### Rutile geochronology

Sample	207/235	2 $\sigma$	206/238	2 $\sigma$	207/206	2 $\sigma$	ErrCorr 6/38vs7/35	ErrCorr 38/6vs7/6	207/235 age	2 $\sigma$	206/238 age	2 $\sigma$	Concordant?	% discordance
WGC2019J-25B-C2_rut - 1.d	0.67	0.02	0.06592	0.0014	0.0733	0.0019	0.45392	0.07999	519	12	411.5	8.4	D	20.71290944
WGC2019J-25B-C2_rut - 2.d	0.546	0.022	0.068	0.0016	0.0585	0.0022	0.34399	0.14569	440	14	424.1	9.8	D	3.613636364
WGC2019J-25B-C2_rut - 3.d	0.572	0.021	0.07	0.0017	0.059	0.0019	0.33781	0.1604	456	13	435.8	10	NC - old Caledonian	4.429824561
WGC2019J-25B-C2_rut - 4.d	0.54	0.025	0.0699	0.0016	0.0567	0.0024	0.51133	-0.15958	435	16	435.4	9.5	C - old Caledonian	-0.09195402
WGC2019J-25B-C3_rut - 1.d	0.708	0.024	0.06529	0.0014	0.0791	0.0027	0.15791	0.22405	542	14	407.6	8.4	D	24.79704797
WGC2019J-25B-C3_rut - 2.d	1.07	0.15	0.0697	0.0031	0.114	0.014	0.49015	-0.4738	712	67	434	19	D	39.04494382
WGC2019J-25B-C3_rut - 3.d	0.494	0.017	0.06423	0.0013	0.0559	0.002	-0.044848	0.41934	407	11	401.2	8	C - old Caledonian	1.425061425
WGC2019J-25B-C3_rut - 4.d	0.522	0.019	0.06253	0.0012	0.0606	0.0022	0.10775	0.2203	426	13	391.4	7.4	NC - old Caledonian	8.122065728
WGC2019J-25B-C3_rut - 5.d	0.493	0.015	0.06564	0.0013	0.0545	0.0016	0.13649	0.25286	407.7	9.9	409.8	7.8	C - old Caledonian	-0.51508462
WGC2019J-25B-C3_rut - 6.d	0.529	0.018	0.06446	0.0013	0.059	0.0019	0.28825	0.070578	432	12	402.6	7.8	NC - old Caledonian	6.805555556
WGC2019J-25B-C3_rut - 7.d	0.487	0.015	0.06482	0.0013	0.0544	0.0018	0.078021	0.26399	402	10	404.8	7.7	C - old Caledonian	-0.69651741
WGC2019J-25B-C3_rut - 8.d	0.498	0.016	0.06687	0.0013	0.0544	0.0018	0.022895	0.37043	409	11	417.2	8.1	C - old Caledonian	-2.00488998
WGC2019J-25B-C8_rut - 1.d	0.562	0.022	0.0648	0.0018	0.0626	0.0026	0.15384	0.39061	452	14	404.6	11	NC - old Caledonian	10.48672566
WGC2019J-25B-C8_rut - 2.d	0.585	0.025	0.0672	0.0018	0.0632	0.0028	0.18546	0.28068	463	16	419.1	11	NC - old Caledonian	9.481641469
WGC2019J-25B-C9_rut - 1.d	1.242	0.068	0.0807	0.0024	0.1112	0.0049	0.61564	-0.16728	808	30	500	14	D	38.11881188
WGC2019J-25B-C9_rut - 2.d	0.574	0.029	0.0727	0.002	0.0571	0.0028	0.20629	0.23937	458	19	453.3	12	C - old Caledonian	1.026200873
WGC2019J-25B-C10_rut - 1.d	0.491	0.016	0.0643	0.0016	0.056	0.0018	0.36638	0.23164	405	11	401.4	9.5	C - old Caledonian	0.888888889
WGC2019J-25B-C10_rut - 2.d	0.502	0.017	0.0674	0.0017	0.0548	0.0017	0.35896	0.22104	414	11	420.4	10	C - old Caledonian	-1.54589372
WGC2019J-25B-C10_rut - 3.d	0.906	0.028	0.0803	0.0019	0.082	0.0021	0.50362	0.12931	654	15	498	11	D	23.85321101
WGC2019J-25B-C10_rut - 4.d	0.47	0.018	0.0631	0.0015	0.0543	0.0019	0.21565	0.20672	393	12	394.1	9.1	C - old Caledonian	-0.27989822
WGC2019J-25B-C10_rut - 5.d	0.558	0.033	0.0704	0.0019	0.0579	0.0035	0.16745	-0.060148	443	22	439.3	12	C - old Caledonian	0.835214447
WGC2019J-25B-C11_rut - 1.d	0.508	0.017	0.0682	0.0017	0.0541	0.0016	0.42831	0.18675	415	11	425.4	10	C - old Caledonian	-2.5060241
WGC2019J-25B-C11_rut - 2.d	0.495	0.018	0.0656	0.0017	0.0551	0.0018	0.3801	0.17379	408	12	409.7	10	C - old Caledonian	-0.41666667
WGC2019J-25B-C11_rut - 3.d	0.514	0.018	0.0676	0.0018	0.0558	0.0018	0.3406	0.23809	423	12	421.6	11	C - old Caledonian	0.330969267
WGC2019J-25B-C11_rut - 4.d	0.472	0.018	0.0651	0.0017	0.0531	0.0019	0.31547	0.20126	392	12	406.3	10	C - old Caledonian	-3.64795918
WGC2019J-25B-C11_rut - 5.d	0.496	0.02	0.066	0.0017	0.0557	0.0022	0.36429	0.16035	409	13	412	10	C - old Caledonian	-0.73349633
WGC2019J-25B-C11_rut - 6.d	0.563	0.024	0.0641	0.0015	0.0633	0.0029	0.045161	0.32088	453	16	400.3	8.9	NC - old Caledonian	11.63355408
WGC2019J-25B-C11_rut - 7.d	1.921	0.05	0.0801	0.0018	0.1699	0.0051	0.13627	0.36458	1089	18	496.6	11	D	54.39853076

Samantha Nicole March  
Ultrahigh-pressure metapelites in the WGR

WGC2019J-25B-C12_rut - 1.d	0.524	0.017	0.0685	0.0017	0.0564	0.0019	0.2625	0.30322	428	11	426.8	10	C - old Caledonian	0.280373832
WGC2019J-25B-C12_rut - 2.d	0.683	0.022	0.0672	0.0018	0.0756	0.0018	0.60153	-0.06159	526	13	419	11	D	20.34220532
WGC2019J-25B-C12_rut - 3.d	0.567	0.014	0.0694	0.0015	0.0593	0.0015	0.23537	0.33087	456	9.3	432.3	9.3	NC - old Caledonian	5.197368421
WGC2019J-25B-C12_rut - 5.d	0.535	0.015	0.0693	0.0016	0.0568	0.0015	0.33682	0.28396	436	10	431.9	9.6	C - old Caledonian	0.940366972
WGC2019J-25B-C12_rut - 6.d	0.737	0.056	0.07423	0.0015	0.072	0.0055	0.057285	0.030418	546	29	461.5	9.2	D	15.47619048
WGC2019J-25B-C12_rut - 7.d	0.522	0.018	0.0697	0.0018	0.0546	0.0019	0.35692	0.18187	425	12	434.4	11	C - old Caledonian	-2.21176471
WGC2019J-25B-C12_rut - 8.d	0.555	0.022	0.0719	0.0021	0.0568	0.002	0.41924	0.20739	449	15	448	13	C - old Caledonian	0.222717149
WGC2019J-25B-C12_rut - 9.d	0.524	0.02	0.0708	0.0017	0.0537	0.0019	0.32152	0.18003	426	13	440.6	10	C - old Caledonian	-3.42723005
WGC2019J-25B-C13_rut - 1.d	0.607	0.023	0.0705	0.0018	0.0632	0.002	0.46947	0.0028485	481	15	439	11	NC - old Caledonian	8.731808732
WGC2019J-25B-C13_rut - 2.d	0.505	0.015	0.0672	0.0015	0.0549	0.0016	0.22631	0.31968	416	10	419.2	9.3	C - old Caledonian	-0.76923077
WGC2019J-25B-C13_rut - 3.d	0.563	0.014	0.068	0.0016	0.0609	0.0014	0.36456	0.33326	452.8	9.3	424.3	9.5	NC - old Caledonian	6.294169611
WGC2019J-25B-C13_rut - 4.d	0.504	0.018	0.061	0.0014	0.0606	0.0023	-0.031981	0.40716	416	12	381.9	8.7	NC - young Caledonian	8.197115385
WGC2019J-25B-C13_rut - 5.d	0.884	0.033	0.084	0.0029	0.0772	0.0024	0.5357	0.36061	645	18	520	17	D	19.37984496
WGC2019J-25B-C13_rut - 6.d	0.516	0.023	0.0706	0.0017	0.0532	0.0024	0.16535	0.24652	425	15	439.7	10	C - old Caledonian	-3.45882353
WGC2019J-25B-C13_rut - 7.d	0.484	0.021	0.066	0.0017	0.0531	0.002	0.32506	0.189	403	14	412	10	C - old Caledonian	-2.23325062
WGC2019J-25B-C13_rut - 8.d	0.827	0.031	0.068	0.0017	0.0879	0.0027	0.59053	0.041155	612	17	423.8	11	D	30.75163399
WGC2019J-25B-C13_rut - 9.d	0.504	0.024	0.0647	0.0018	0.0573	0.0026	0.26616	0.19818	415	17	403.7	11	C - old Caledonian	2.722891566
WGC2019J-25B-C13_rut - 10.d	0.64	0.022	0.0706	0.002	0.0669	0.0021	0.49311	0.18824	502	14	439	12	NC - old Caledonian	12.5498008
WGC2019J-25B-C13_rut - 11.d	0.439	0.019	0.0591	0.0014	0.0545	0.0024	0.050972	0.31048	369	13	370.1	8.2	C - young Caledonian	-0.29810298
WGC2019J-25B-C13_rut - 12.d	0.531	0.024	0.07	0.0018	0.0546	0.0023	0.37794	0.082227	428	16	436	11	C - old Caledonian	-1.86915888
WGC2019J-25B-C14_rut - 1.d	0.598	0.045	0.0704	0.0023	0.0625	0.005	0.014571	0.11973	463	27	438	14	D	5.399568035
WGC2019J-31A-2-C2_rut - 1.d	2.46	0.27	0.0837	0.0042	0.195	0.016	0.6953	-0.34975	1183	83	519	25	D	56.1284869
WGC2019J-31A-2-C3_rut - 1.d	0.48	0.04	0.0679	0.0022	0.0514	0.0041	0.16293	0.2204	394	27	423	13	C - young Caledonian	-7.36040609
WGC2019J-31A-2-C3_rut - 2.d	0.512	0.041	0.0667	0.0021	0.0563	0.0047	0.03224	0.31766	410	28	416	13	C - young Caledonian	-1.46341463
WGC2019J-31A-2-C3_rut - 3.d	0.484	0.038	0.0606	0.0022	0.0577	0.005	0.016448	0.37882	390	26	379	13	C - young Caledonian	2.820512821
WGC2019J-31A-2-C3_rut - 4.d	0.715	0.063	0.0708	0.0029	0.0747	0.0063	0.27013	0.087419	543	38	441	18	D	18.78453039
WGC2019J-31A-2-C4_rut - 1.d	0.532	0.043	0.063	0.0021	0.0608	0.005	0.074139	0.30433	423	29	393	13	D	7.092198582
WGC2019J-31A-2-C4_rut - 2.d	0.454	0.044	0.0643	0.0023	0.0507	0.0049	0.10686	0.24585	378	31	402	14	C - young Caledonian	-6.34920635
WGC2019J-31A-2-C4_rut - 3.d	0.498	0.048	0.066	0.0024	0.0564	0.0057	0.052524	0.27443	424	31	412	15	C - young Caledonian	2.830188679
WGC2019J-31A-2-C8_rut - 1.d	0.49	0.039	0.0615	0.0024	0.0571	0.0047	0.12781	0.31232	396	27	384	14	C - young Caledonian	3.03030303
WGC2019J-31A-2-C8_rut - 2.d	0.449	0.041	0.0608	0.0022	0.0535	0.005	0.072172	0.24826	373	28	381	13	C - young Caledonian	-2.14477212

Samantha Nicole March  
Ultrahigh-pressure metapelites in the WGR

WGC2019J-31A-2-C8_rut - 3.d	0.511	0.045	0.0622	0.0019	0.0598	0.0054	0.071972	0.050641	404	30	389.1	11	C - young Caledonian	3.688118812
WGC2019J-31A-2-C8_rut - 4.d	0.476	0.041	0.0612	0.0023	0.0562	0.0051	0.14756	0.41536	394	28	382	14	C - young Caledonian	3.045685279
WGC2019J-31A-2-C8_rut - 5.d	0.464	0.041	0.0644	0.0025	0.0531	0.0048	0.12048	0.26675	392	30	403	15	C - young Caledonian	-2.80612245
WGC2019J-31A-2-C10_rut - 1.d	22.28	0.57	0.2533	0.0072	0.637	0.012	0.65513	0.25973	3191	25	1453	37	D	54.46568474
WGC2019J-31A-3-C3_rut - 1.d	0.468	0.037	0.0633	0.0022	0.0554	0.0045	0.20152	0.10256	391	26	395	13	C - young Caledonian	-1.0230179
WGC2019J-31A-3-C4_rut - 1.d	1.014	0.068	0.0709	0.0025	0.1064	0.0076	0.088709	0.34438	699	34	443	15	D	36.62374821
WGC2019J-31A-3-C5_rut - 1.d	0.943	0.084	0.0675	0.0029	0.1023	0.0095	-0.083695	0.33052	649	41	421	17	D	35.13097072
WGC2019J-31A-3-C5_rut - 2.d	0.585	0.054	0.0721	0.0029	0.0596	0.0059	0.11406	0.29595	457	35	449	17	C - old Caledonian	1.750547046
WGC2019J-31A-3-C6_rut - 1.d	0.613	0.055	0.0667	0.0027	0.068	0.0063	0.091126	0.43781	467	35	416	16	D	10.92077088
WGC2019J-31A-3-C12_rut - 1.d	0.436	0.04	0.0604	0.0021	0.0525	0.005	0.13628	0.24677	364	28	378	13	C - young Caledonian	-3.84615385
WGC2019J-31A-3-C19_rut - 1.d	0.409	0.04	0.0616	0.0024	0.0475	0.0047	0.11854	0.33087	349	29	385	15	D - under concordia?	-10.3151862
WGC2019J-31A-3-C19_rut - 2.d	0.501	0.04	0.0629	0.0022	0.0571	0.0047	0.11621	0.31247	406	27	393	13	C - young Caledonian	3.201970443
WGC2019J-31A-3-C20_rut - 1.d	0.474	0.038	0.062	0.0019	0.0544	0.0044	-0.076741	0.45679	390	26	389	12	C - young Caledonian	0.256410256
WGC2019J-31A-3-C20_rut - 2.d	0.481	0.035	0.0651	0.0019	0.0537	0.0041	0.043777	0.37418	402	23	406.1	12	C - young Caledonian	-1.0199005
WGC2019J-31A-3-C20_rut - 3.d	0.494	0.038	0.0637	0.0021	0.0566	0.0045	0.095851	0.31853	410	26	399	12	C - young Caledonian	2.682926829
WGC2019J-31A-3-C20_rut - 4.d	0.495	0.04	0.0638	0.0022	0.0569	0.0049	0.079976	0.27871	407	28	399	13	C - young Caledonian	1.965601966
WGC2019J-31A-3-C20_rut - 5.d	0.585	0.043	0.0711	0.0023	0.0594	0.0044	0.06276	0.2441	467	26	442	14	C - old Caledonian	5.353319058
WGC2019J-31A-3-C20_rut - 6.d	0.422	0.031	0.0634	0.002	0.0498	0.0039	-0.025681	0.33832	355	22	396	12	C - young Caledonian	-11.5492958
WGC2019J-31A-3-C20_rut - 7.d	0.491	0.03	0.0639	0.002	0.0554	0.0034	0.025468	0.41604	411	20	399	12	C - young Caledonian	2.919708029
WGC2019J-31A-3-C21_rut - 1.d	0.47	0.04	0.063	0.002	0.0552	0.0046	0.19219	0.16521	382	27	394	12	C - young Caledonian	-3.14136126
WGC2019J-31A-3-C21_rut - 2.d	0.553	0.053	0.0633	0.0025	0.067	0.0066	0.15488	0.18461	437	34	395	15	D	9.610983982

Crossed-out = discordant, C = concordant, NC = near concordant, D = discordant, RD = reversely discordant.

### Rutile geochronology standards

Standard	Type	207/23 5	2σ	206/23 8	2σ	207/20 6	2σ	ErrorCorr 6/38vs7/35	ErrorCorr 38/6vs7/6	207/235 age	2 σ	206/23 8	2 σ	Concordant ?	%discordanc e
R10 - 1.d	Primary	1.935	0.04	0.1831	0.003 5	0.0773	0.001 6	0.13529	0.29149	1090	14	1083.5	19	C	0.59633
R10 - 2.d	Primary	1.917	0.04 3	0.1835	0.003 5	0.0756	0.001 7	0.19835	0.29195	1088	15	1086	19	C	0.183824
R10 - 3.d	Primary	1.925	0.04 2	0.1848	0.003 6	0.0752	0.001 5	0.2751	0.23626	1090	15	1093	19	C	-0.27523

Samantha Nicole March  
Ultrahigh-pressure metapelites in the WGR

<b>R10 - 4.d</b>	Primary	1.936	0.04 1	0.1868	0.003 7	0.0753	0.001 8	0.17065	0.36397	1091	14	1104	20	C	-1.19157
<b>R10 - 5.d</b>	Primary	1.906	0.03 5	0.182	0.003 6	0.0757	0.001 6	0.053938	0.46206	1087	12	1078	19	C	0.827967
<b>R10 - 6.d</b>	Primary	1.963	0.03 9	0.186	0.003 5	0.0766	0.001 4	0.15806	0.29765	1104	13	1099.7	19	C	0.389493
<b>R10 - 7.d</b>	Primary	1.925	0.03 6	0.187	0.003 7	0.075	0.001 5	-0.06523	0.60079	1089	12	1105	20	C	-1.46924
<b>R10 - 8.d</b>	Primary	1.91	0.03 9	0.1848	0.003 7	0.0746	0.001 7	0.14296	0.39101	1082	14	1093	20	C	-1.01664
<b>R10 - 9.d</b>	Primary	1.942	0.04 2	0.1847	0.003 6	0.0761	0.001 8	-0.03304	0.29847	1093	13	1092	19	C	0.091491
<b>R10 - 10.d</b>	Primary	1.935	0.04	0.1844	0.003 6	0.0757	0.001 6	0.18311	0.42164	1090	14	1091	20	C	-0.09174
<b>R10 - 11.d</b>	Primary	1.934	0.04	0.1849	0.003 6	0.0752	0.001 7	0.009938	0.4182	1096	14	1096	19	C	0
<b>R10 - 12.d</b>	Primary	1.928	0.03 8	0.1854	0.003 7	0.0756	0.001 6	0.10749	0.42868	1088	13	1097	21	C	-0.82721
<b>R10 - 13.d</b>	Primary	1.901	0.03 7	0.1816	0.003 6	0.0764	0.001 6	0.19288	0.37506	1085	13	1077	20	C	0.737327
<b>R10 - 14.d</b>	Primary	1.925	0.03 4	0.1856	0.003 6	0.0751	0.001 4	0.11281	0.45255	1088	12	1097	20	C	-0.82721
<b>R10 - 15.d</b>	Primary	1.959	0.04 1	0.1837	0.003 5	0.0774	0.001 6	0.17313	0.27141	1100	14	1086.7	19	C	1.209091
<b>R19 - 1.d</b>	Secondary	0.645	0.08 9	0.08	0.003 4	0.0628	0.009 4	0.028538	0.041773	452	51	495	20	C	-9.51327
<b>R19 - 2.d</b>	Secondary	0.609	0.06 2	0.08	0.003 2	0.0565	0.006	0.053472	0.29259	484	39	497	19	C	-2.68595
<b>R19 - 3.d</b>	Secondary	0.663	0.07 5	0.0841	0.003 1	0.0588	0.006 9	0.02353	0.34624	496	47	520	19	C	-4.83871
<b>R19 - 4.d</b>	Secondary	0.565	0.06 5	0.0833	0.003 2	0.054	0.006 5	-0.09272	0.34619	479	43	517	19	C	-7.93319
<b>R19 - 5.d</b>	Secondary	0.608	0.06 5	0.0827	0.003	0.0534	0.005 9	0.074996	0.23923	496	40	512	18	C	-3.22581
<b>R19 - 6.d</b>	Secondary	0.629	0.05 6	0.0791	0.003 3	0.0579	0.005 7	-0.00126	0.34378	489	34	490	20	C	-0.2045
<b>R19 - 7.d</b>	Secondary	0.671	0.06 9	0.08	0.003 4	0.0618	0.006 9	0.12495	0.23054	528	40	495	20	C	6.25
<b>R19 - 8.d</b>	Secondary	0.579	0.04 4	0.0765	0.002 4	0.0538	0.004 5	-0.02444	0.38228	459	29	475	14	C	-3.48584
<b>R19 - 9.d</b>	Secondary	0.648	0.06 7	0.081	0.003 1	0.0596	0.006 4	-0.00174	0.36687	512	40	502	18	C	1.953125
<b>R19 - 10.d</b>	Secondary	0.611	0.06 6	0.0796	0.003	0.0543	0.006 1	0.009795	0.34401	494	40	493	18	C	0.202429

## Zr-rutile thermometry

Sample	Concordant?	Zr (ppm)	±	Pressure (kbar)	±	T (Tomkins et al. 2007)	±
WGC2019J-25B-C2_rut - 3.d	NC - old Caledonian	474.2	4.4	25		5	755.1779691 151.7802717
WGC2019J-25B-C2_rut - 4.d	C - old Caledonian	376.5	3.7	25		5	734.0813921 147.547847
WGC2019J-25B-C3_rut - 3.d	C - old Caledonian	649	3.6	25		5	785.3329491 157.7975535
WGC2019J-25B-C3_rut - 4.d	NC - old Caledonian	555.7	3.6	25		5	770.2006798 154.7656408
WGC2019J-25B-C3_rut - 5.d	C - old Caledonian	549.4	3.3	25		5	769.1060582 154.5411554
WGC2019J-25B-C3_rut - 6.d	NC - old Caledonian	412.3	3.3	25		5	742.2831495 149.172237
WGC2019J-25B-C3_rut - 7.d	C - old Caledonian	473.7	2.4	25		5	755.0794903 151.714852
WGC2019J-25B-C3_rut - 8.d	C - old Caledonian	445.4	3.6	25		5	749.3616397 150.5957083
WGC2019J-25B-C8_rut - 1.d	NC - old Caledonian	673.3	5.5	25		5	788.9813703 158.5590044
WGC2019J-25B-C8_rut - 2.d	NC - old Caledonian	729	11	25		5	796.9570304 160.2901208
WGC2019J-25B-C9_rut - 2.d	C - old Caledonian	390.9	4.1	25		5	737.4543704 148.2357112
WGC2019J-25B-C10_rut - 1.d	C - old Caledonian	620.6	5.4	25		5	780.9254051 156.9470392
WGC2019J-25B-C10_rut - 2.d	C - old Caledonian	624.9	5.6	25		5	781.6031495 157.0868412
WGC2019J-25B-C10_rut - 4.d	C - old Caledonian	709.5	5.2	25		5	794.2229365 159.6020502
WGC2019J-25B-C10_rut - 5.d	C - old Caledonian	590.2	5.4	25		5	776.0216658 155.9677152
WGC2019J-25B-C11_rut - 1.d	C - old Caledonian	517	4.4	25		5	763.3090972 153.4040848
WGC2019J-25B-C11_rut - 2.d	C - old Caledonian	494.9	5.3	25		5	759.1823291 152.6067988
WGC2019J-25B-C11_rut - 3.d	C - old Caledonian	550.1	5.7	25		5	769.228187 154.6205317
WGC2019J-25B-C11_rut - 4.d	C - old Caledonian	475.7	5.6	25		5	755.4728968 151.8792006
WGC2019J-25B-C11_rut - 5.d	C - old Caledonian	480.5	4.8	25		5	756.4115791 152.0385701
WGC2019J-25B-C11_rut - 6.d	NC - old Caledonian	543.7	6.4	25		5	768.1068253 154.4190909
WGC2019J-25B-C12_rut - 1.d	C - old Caledonian	597.1	5.4	25		5	777.152427 156.1934849
WGC2019J-25B-C12_rut - 3.d	NC - old Caledonian	603.4	5	25		5	778.1756036 156.3889114
WGC2019J-25B-C12_rut - 5.d	C - old Caledonian	618	6.8	25		5	780.5137499 156.8997101
WGC2019J-25B-C12_rut - 7.d	C - old Caledonian	460	3.9	25		5	752.3474775 151.2006876
WGC2019J-25B-C12_rut - 8.d	C - old Caledonian	492.1	4.2	25		5	758.6487843 152.4678035
WGC2019J-25B-C12_rut - 9.d	C - old Caledonian	505.1	5.1	25		5	761.1053191 152.983653
WGC2019J-25B-C13_rut - 1.d	NC - old Caledonian	514.5	5.2	25		5	762.8495837 153.334406

Samantha Nicole March  
Ultrahigh-pressure metapelites in the WGR

WGC2019J-25B-C13_rut - 2.d	C - old Caledonian	514	4.6	25	5	762.7574622	153.299065
WGC2019J-25B-C13_rut - 3.d	NC - old Caledonian	548.5	5.4	25	5	768.9488487	154.5563538
WGC2019J-25B-C13_rut - 4.d	NC - young Caledonian	703.8	6	25	5	793.4122299	159.4541807
WGC2019J-25B-C13_rut - 6.d	C - old Caledonian	703.1	5.3	25	5	793.3123024	159.4215193
WGC2019J-25B-C13_rut - 7.d	C - old Caledonian	597.7	5	25	5	777.2502502	156.2039672
WGC2019J-25B-C13_rut - 9.d	C - old Caledonian	584.5	9.9	25	5	775.0794063	155.9358081
WGC2019J-25B-C13_rut - 10.d	NC - old Caledonian	564.8	7.5	25	5	771.7640642	155.1834878
WGC2019J-25B-C13_rut - 11.d	C - young Caledonian	554.1	5.1	25	5	769.9236436	154.7428846
WGC2019J-25B-C13_rut - 12.d	C - old Caledonian	529.1	5.1	25	5	765.5078237	153.8616455
<b>C &amp; NC weighted mean</b>						<b>767.96</b>	<b>5.21</b>
<b>C weighted mean</b>						<b>768.32</b>	<b>5.31</b>
WGC2019J-31A-2-C3_rut - 1.d	C - young Caledonian	656.7	5.7	25	5	786.5008785	158.0672801
WGC2019J-31A-2-C3_rut - 2.d	C - young Caledonian	660.2	4.8	25	5	787.0280786	158.1555437
WGC2019J-31A-2-C3_rut - 3.d	C - young Caledonian	846.8	6.7	25	5	812.3180166	163.2455422
WGC2019J-31A-2-C4_rut - 2.d	C - young Caledonian	684.4	5.1	25	5	790.6124295	158.8779391
WGC2019J-31A-2-C4_rut - 3.d	C - young Caledonian	730.1	6.7	25	5	797.1094858	160.2064236
WGC2019J-31A-2-C8_rut - 1.d	C - young Caledonian	954.7	8.3	25	5	824.9387038	165.7925367
WGC2019J-31A-2-C8_rut - 2.d	C - young Caledonian	1025.1	9.9	25	5	832.5654205	167.3400456
WGC2019J-31A-2-C8_rut - 3.d	C - young Caledonian	936.4	7.5	25	5	822.882185	165.3698192
WGC2019J-31A-2-C8_rut - 4.d	C - young Caledonian	801	7.4	25	5	806.5646888	162.1076855
WGC2019J-31A-2-C8_rut - 5.d	C - young Caledonian	925.1	8.6	25	5	821.5960721	165.1296541
WGC2019J-31A-3-C3_rut - 1.d	C - young Caledonian	767.9	6.8	25	5	802.2386411	161.2326519
WGC2019J-31A-3-C5_rut - 2.d	C - old Caledonian	767.9	7.5	25	5	802.2386411	161.2462704
WGC2019J-31A-3-C12_rut - 1.d	C - young Caledonian	741.3	6.1	25	5	798.6512499	160.5031151
WGC2019J-31A-3-C19_rut - 2.d	C - young Caledonian	486.3	5.3	25	5	757.5356384	152.2788898
WGC2019J-31A-3-C20_rut - 1.d	C - young Caledonian	714.8	5.2	25	5	794.9720231	159.7519511
WGC2019J-31A-3-C20_rut - 2.d	C - young Caledonian	718.9	5.8	25	5	795.5484197	159.8774603
WGC2019J-31A-3-C20_rut - 3.d	C - young Caledonian	722.3	5.6	25	5	796.0243878	159.9691479
WGC2019J-31A-3-C20_rut - 4.d	C - young Caledonian	692.1	5.8	25	5	791.7313083	159.1144226
WGC2019J-31A-3-C20_rut - 5.d	C - old Caledonian	696.9	5	25	5	792.423687	159.238709

Samantha Nicole March  
 Ultrahigh-pressure metapelites in the WGR

<b>WGC2019J-31A-3-C20_rut - 6.d</b>	C - young Caledonian	698.6	5.6	25	5	792.6679761	159.2979307
<b>WGC2019J-31A-3-C20_rut - 7.d</b>	C - young Caledonian	707.2	5.5	25	5	793.8964477	159.5418144
<b>WGC2019J-31A-3-C21_rut - 1.d</b>	C - young Caledonian	710.8	6.3	25	5	794.4070939	159.6587916
<b>C weighted mean</b>						<b>799.13</b>	<b>7.15</b>

C = concordant, NC = near concordant

**APPENDIX 3F: LA-ICP-MS BIOTITE AND K-FELDSPAR RESULTS**

**Biotite:**

Source file	Pb207_204_Fi nal	Pb207_204_Final_Prop 2SE	Pb206_204_Fi nal	Pb206_204_Final_Prop 2SE	Pb208_206_Fi nal	Pb208_206_Final_Prop 2SE	Pb207_206_Fi nal	Pb207_206_Final_Prop 2SE	
25B-3b-C8_bio - 1.d	20.5	4.3	24.1	4.9	2.037	0.064	0.866	0.02	
25B-3b-C8_bio - 2.d	13.7	6.8	15.8	8.1	2.09	0.069	0.856	0.021	
25B-3b-C8_bio - 3.d	19.6	3.4	22.5	3.9	2.108	0.056	0.876	0.018	
25B-3b-C8_bio - 4.d	21.5	4.7	25.2	5.5	2.049	0.054	0.88	0.021	
25B-3b-C8_bio - 5.d	20	4.6	21.5	7.1	2.041	0.049	0.839	0.016	
25B-3b-C8_bio - 6.d	20.7	4.5	24.9	5.8	2.071	0.066	0.864	0.021	
25B-3b-C8_bio - 7.d	15.7	4	18.6	4.8	2.131	0.051	0.847	0.017	
25B-3b-C8_bio - 8.d	19.3	3.5	22.5	4.1	2.137	0.044	0.866	0.016	
25B-3b-C8_bio - 9.d	23	3.2	27.2	3.8	2.088	0.043	0.845	0.015	
25B-3b-C8_bio - 10.d	18.3	3.3	20.4	3.4	2.113	0.072	0.875	0.023	
25B-3b-C8_bio - 11.d	24.8	5.1	29.4	6.2	2.066	0.073	0.861	0.02	
25B-3b-C8_bio - 12.d	18.3	7	21.6	8.1	2.039	0.073	0.855	0.02	
25B-3b-C8_bio - 13.d	20.2	5	22.7	5.7	2.134	0.077	0.863	0.023	
25B-3b-C8_bio - 14.d	15.5	4.1	18.6	4.4	2.094	0.052	0.859	0.016	
25B-3b-C8_bio - 15.d	16.1	9.5	18	11	2.134	0.081	0.88	0.024	
25B-3b-C8_bio - 16.d	19.7	4.8	23.5	5.9	2.064	0.078	0.849	0.02	
<b>Weighted mean:</b>							<b>0.8593</b>	<b>± 0.0068</b>	

Source file	Pb207_204_Fi nal	Pb207_204_Final_Prop 2SE	Pb206_204_Fi nal	Pb206_204_Final_Prop 2SE	Pb208_206_Fi nal	Pb208_206_Final_Prop 2SE	Pb207_206_Fi nal	Pb207_206_Final_Prop 2SE
31A-3-C2_bio - 1.d	2	11	3	13	2.094	0.043	0.838	0.012



Samantha Nicole March  
Ultrahigh-pressure metapelites in the WGR

31A-3-C2_bio - 2.d	18.6		3.5	22.3	4.1	2.051	0.042	0.834	0.014	
31A-3-C2_bio - 3.d	19		3.3	24.8	4.5	2.009	0.045	0.785	0.016	
31A-3-C2_bio - 4.d	17		1.2	19.9	1.4	2.111	0.031	0.8435	0.0084	
31A-3-C2_bio - 5.d	21.1		3.1	24.6	3.6	2.135	0.047	0.86	0.016	
31A-3-C2_bio - 6.d	21.9		3.9	25.6	4.6	2.07	0.035	0.852	0.014	
31A-3-C4_bio - 1.d	21.9		3.8	25.6	4.3	2.126	0.044	0.854	0.015	
31A-3-C4_bio - 2.d	21.1		3.2	25	3.8	2.043	0.04	0.847	0.013	
31A-3-C4_bio - 3.d	16.6		1.1	19.5	1.2	2.087	0.025	0.8466	0.0086	
31A-3-C4_bio - 4.d	18.4		4.7	19.8	6.4	2.067	0.045	0.848	0.014	
31A-3-C4_bio - 5.d	19.6		3.5	23.5	4.2	2.092	0.051	0.843	0.014	
31A-3-C4_bio - 6.d	19.9		2.9	23.8	3.4	2.066	0.039	0.837	0.012	
31A-3-C5_bio - 1.d	no value	NAN	no value	NAN	no value	NAN	no value	NAN		
31A-3-C5_bio - 2.d	no value	NAN	no value	NAN	no value	NAN	no value	NAN		
31A-3-C5_bio - 3.d	no value	NAN	no value	NAN	no value	NAN	no value	NAN		
31A-3-C5_bio - 4.d	no value	NAN	no value	NAN	no value	NAN	no value	NAN		
31A-3-C5_bio - 5.d	0.63		0.62	-2.9	3.3	1.8	1.7	-0.11	0.25	
31A-3-C7_bio - 1.d	15.8		4	18.7	5	2.104	0.049	0.83	0.019	
31A-3-C7_bio - 2.d	16.7		4.2	20	5	2.124	0.045	0.83	0.015	
31A-3-C7_bio - 3.d	20.6		3.4	24.7	4.2	2.147	0.061	0.848	0.017	
31A-3-C7_bio - 4.d	20.6		3.1	24.1	3.6	2.082	0.047	0.847	0.015	
31A-3-C7_bio - 5.d	21.3		3.7	24.2	4.1	2.131	0.048	0.863	0.014	
31A-3-C7_bio - 6.d	19.1		3.9	22.8	4.6	2.094	0.046	0.831	0.015	
<b>Weighted mean:</b>								<b>0.8443</b>	<b>± 0.0045</b>	

**K-feldspar:**

Source file	Pb207_204_Final_Prop 2SE	Pb207_204_Final_Prop 2SE	Pb206_204_Final_Prop 2SE	Pb206_204_Final_Prop 2SE	Pb208_206_Final_Prop 2SE	Pb208_206_Final_Prop 2SE	Pb207_206_Final_Prop 2SE	Pb207_206_Final_Prop 2SE
31A-3-C1_kspar - 1.d	15.6	0.55	18.7	0.65	2.065	0.03	0.8355	0.0099
31A-3-C1_kspar - 2.d	15.67	0.29	18.65	0.33	2.09	0.02	0.8393	0.0039
31A-3-C1_kspar - 3.d	16.19	0.55	19.31	0.66	2.073	0.02	0.8403	0.006
31A-3-C1_kspar - 4.d	17.9	1.4	20.7	1.5	2.03	0.027	0.853	0.011
31A-3-C1_kspar - 5.d	17.7	1.4	20.6	1.6	2.079	0.03	0.851	0.012
31A-3-C1_kspar - 6.d	16.13	0.59	19.14	0.72	2.05	0.033	0.844	0.012
31A-3-C1_kspar - 7.d	17	1.5	19.9	1.6	2.047	0.024	0.841	0.011
31A-3-C1_kspar - 8.d	17.9	1.2	20.9	1.4	2.058	0.031	0.852	0.011
31A-3-C1_kspar - 9.d	20.9	2.5	24.5	2.8	2.085	0.03	0.8505	0.0098
31A-3-C1_kspar - 10.d	17.6	1.6	20.3	1.8	2.093	0.035	0.853	0.012
31A-3-C6_kspar - 1.d	17.3	1.3	20.4	1.6	2.101	0.03	0.8432	0.0099
31A-3-C6_kspar - 2.d	17.3	1.1	20.9	1.4	2.078	0.03	0.8397	0.0099
31A-3-C6_kspar - 3.d	18.5	1.6	21.5	1.8	2.063	0.03	0.8455	0.0097
31A-3-C6_kspar - 4.d	17.2	1.1	20	1.3	2.083	0.026	0.8508	0.0077
<b>Weighted mean:</b>							<b>0.8434</b>	<b>± 0.0032</b>

**31A combined ksp + bi weighted mean = 0.84370 ± 0.00245**

## APPENDIX 4A: EXTENDED MINERAL EQUILIBRIA FORWARD MODELLING METHODS

### Modelling oxidation state

Iron (Fe) has two oxidation states: FeO (Fe<sup>2+</sup>) which is reduced, and Fe<sub>2</sub>O<sub>3</sub> (Fe<sup>3+</sup>) which is oxidised. Oxidation state has a large impact on how a rock will react when subject to evolving *P-T* conditions. Thus, it is essential to differentiate between these oxidation states in order to calculate meaningful and accurate *P-T* diagrams.

Oxidation state is estimated in WGC2019J-25B by creating a 'PMo' (also known as a *P-X*). A PMo can be calculated by modelling pressure versus oxidation state at a fixed temperature, in this instance temperature was fixed at 790°C. The calculation of a PMo using THERMOCALC follows the same steps as will be detailed below, but without the ability to calculate points. Users are instead required to manually estimate point data by monitoring mineral abundances along lines, recording when a second phase reaches <10<sup>-6</sup>. The completed diagram is then imported into THERMOCALC Investigator (TCI) (Pearce et al., 2016), and calculated mineral composition and abundance contours are compared with the known composition of the rock to constrain oxidation state.

In WGC2019J-31A, oxidation state was estimated by finding the volume percentage of garnet and biotite in thin section, and then converting these values to wt% by multiplying by mineral volume % by mineral density and dividing by rock density. These values were then converted to Fe<sup>3+</sup> and Fe<sup>2+</sup> cations and used to calculate FeO and Fe<sub>2</sub>O<sub>3</sub> wt% based on the assumption that FeO/Fe<sub>2</sub>O<sub>3</sub> = 1.112.

### Calculating *P-T* diagrams

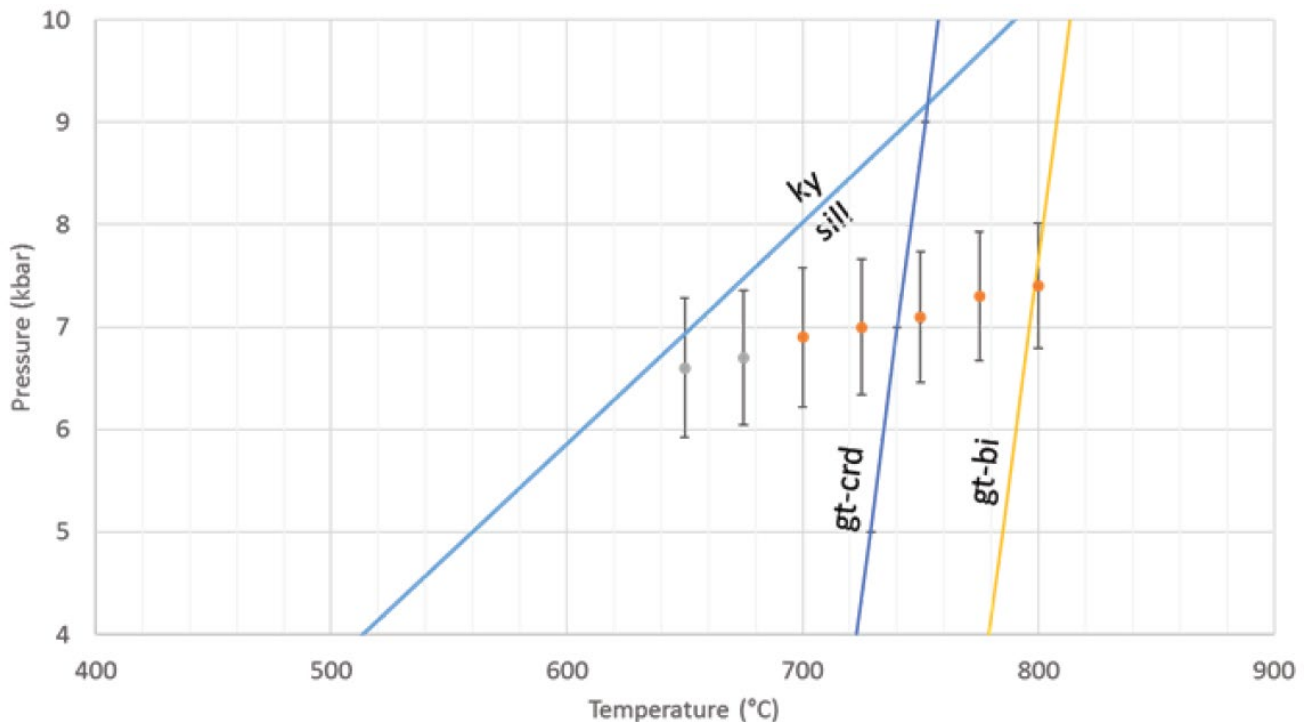
After calculating relevant preliminary diagrams, *P<sub>3</sub>T* diagrams can be modelled using THERMOCALC. THERMOCALC v.3.40 was used in this study. Prior to commencing phase diagram calculations, the user must first study the petrographic relationships within their rock and identify the stable mineral assemblage. This provides the user with a starting point for their phase diagram calculations. The location of this initial stable assemblage in *P-T* space is then estimated using a Gibb's free energy minimisation calculation (also known as a 'dogmin'). Dogmins are a useful tool but are dependent on the user accurately inputting all phases present for a set *P-T* interval. They are also susceptible to erroneous results, so should not be too heavily relied upon. The phase equilibria model is then progressively built up from the initial assemblage through the trial and error calculation of lines and points. Lines represent the zero abundance of a singular phase within an assemblage (as specified by the user), whilst points signify the exact position at which two phases within an assemblage are zero and four lines intersect. In order to accurately calculate these points and lines, the assemblage that they are included within must also be input correctly. Phase equilibria calculations require an advanced understanding of the stability of different minerals across *P-T* space in order to predict the subtle addition of accessory phases. Missing a phase can be difficult to notice, and often only causes issues after significant progress in the diagram, ultimately resulting in the loss of many calculations. THERMOCALC software also requires the frequent updating of 'starting guesses'; compositional variables of phases that

THERMOCALC uses during its least-squares calculation for the output. The choice of starting guesses not only impacts how a line or point plots, but also THERMOCALC's ability to run a specific calculation at all.

The principal uncertainties on bulk composition when calculating phase diagrams are H<sub>2</sub>O and oxidation. H<sub>2</sub>O was calculated based on biotite abundance, however oxidation required the separate modelling of a *PMo* prior to calculation of a *P-T*.

Phase equilibria models are contoured using the Matlab-based, automated software TCIInvestigator v2.0 (Pearce et al., 2016). Input into TCI requires THERMOCALC input files, executable (.exe) files, and the finished *P-T* model (.eps).

### Calculating a *P-T* point



Garnet-cordierite and garnet-biotite thermometer calculations were performed based on several assumptions:

1. The most Ca-rich plagioclase and Ca-poor garnet was considered representative.
2. Average compositions of cordierite, spinel and biotite were used.
3. It was assumed that biotite occurred in chemical equilibrium with garnet rims, spinel, cordierite, ilmenite, rutile, quartz and plagioclase rims.
4. It was assumed that the rock didn't have fluid (i.e. that the fluid was existing within a melt).
5. Grossular content in garnet was arbitrarily changed by a small degree so that calculations passed a statistical test.

Average *P* calculations (grey and orange circles) were calculated following Powell and Holland, 1994. Average *P* calculations fit an optimised result to a series of calculated mineral reactions based on the activities of the mineral endmembers. Calculations were performed every 25 °C between 650-800 °C. Orange circles pass a Chi-squared test, grey circles fail. Failed results may be indicative of compositional dispersion within the minerals.

The final calculated retrograde  $P$ - $T$  point was defined based on the intersect between the garnet-cordierite thermometry line and the average  $P$  calculations (740 °C, 7 kbar). The garnet-cordierite thermometer is preferred over the garnet-biotite thermometer due to cordierite being a newly formed mineral.

**APPENDIX 4B: EXTENDED MINERAL EQUILIBRIA FORWARD MODELLING RESULTS**

